APPENDIX A

ACOUSTIC PROPAGATION AND MARINE MAMMAL EXPOSURE MODELING OF GEOLOGICAL AND GEOPHYSICAL SOURCES IN THE GULF OF MEXICO

2016–2025 Annual Acoustic Exposure Estimates for Marine Mammals

Submitted to:

Kimberly Skrupky Warshaw
Bureau of Ocean Energy Management (BOEM)

Authors:
David Zeddies
Mikhail Zykov
Harald Yurk
Terry Deveau
Loren Bailey
Isabelle Gaboury
Roberto Racca
David Hannay
Scott Carr

JASCO Applied Sciences
Suite 202, 32 Troop Ave.
Dartmouth, NS B3B 1Z1 Canada
Phone: +1-902-405-3336
Fax: +1-902-405-3337
www.jasco.com

6 Nov 2015
P001253-001
Document 00976
Version 3.0

Statement of Disclaimer

This draft report was reviewed by the BOEM. Approval does not signify that the contents necessarily reflect the views and policies of the Bureau, nor does mention of trade names or commercial products constitute endorsement or recommendation for use.

Acknowledgement of Sponsorship

Study concept, oversight, and funding were provided by the US Department of the Interior, Bureau of Ocean Energy Management, Environmental Studies Program, Washington, DC under Contract Number M14PC00004.

Suggested citation:

Zeddies, D.G., M. Zykov, H. Yurk, T. Deveau, L. Bailey, I. Gaboury, R. Racca, D. Hannay, and S. Carr. 2015. *Acoustic Propagation and Marine Mammal Exposure Modeling of Geological and Geophysical Sources in the Gulf of Mexico: 2016–2025 Annual Acoustic Exposure Estimates for Marine Mammals*. JASCO Document 00976, Version 3.0. Technical report by JASCO Applied Sciences for Bureau of Ocean Energy Management (BOEM).

Contents

1. EXECUTIVE SUMMARY 1
1.1. Overview 1
1.2. Sounds and Marine Mammals 1
1.3. Acoustic Modeling 2
1.4. Marine Mammals in the Gulf of Mexico 3
1.5. Animal Movement Modeling 3
1.6. Phase I 4
1.7. Phase II: Annual Acoustic Exposure Estimates 4
2. PROJECT OVERVIEW 5
3. INTRODUCTION 6
3.1. The Ocean Soundscape 6
3.1.1. Seismic Sources 6
3.1.1.1. Airguns 6
3.1.2. High-resolution Sources 6
3.1.2.1. Side-scan Sonar Systems 6
3.1.2.2. Multibeam Echosounders Sonar Systems 7
3.1.2.3. Sub-bottom Profiler Sonar Systems 7
3.1.2.4. Boomer Sources 7
3.1.3. Pulsed Versus Non-Pulsed Sounds 7
3.2. Acoustic Metrics 8
3.3. Use of Sounds by Marine Species 9
3.3.1. Cetacean Hearing 10
3.3.1.1. Classification of Cetacean Hearing 10
3.4. Potential Effects of Sounds on Marine Mammals 11
3.4.1. Auditory Signal Masking 11
3.4.2. Behavioral Disturbance 12
3.4.3. Temporary and Permanent Hearing Loss 14
3.4.4. Non-Auditory Health Effects 15
3.4.5. Reduction of Prey Availability 15
4. MARINE MAMMALS IN THE GULF OF MEXICO 17
5. MODELING METHODOLOGY 19
5.1. Acoustic Source Model 19
5.1.1. Airgun and Airgun Array Modeling Methodology 19
5.1.2. Electromechanical Source Modeling—Transducer Beam Theory 20
5.1.2.1. Circular Transducers 21
5.1.2.2. Rectangular Transducers 22
5.1.2.3. Multibeam Systems 23
5.2. Acoustic Propagation Modeling 24
5.2.1. Two Frequency Regimes: RAM vs. BELLHOP 24
5.2.2. N×2-D Volume Approximation 25
5.2.3. Frequency Dependence: Summing Over 1/3-Octave-Bands 25

5.2.4. Converting Modeled SEL to rms SPL 26
5.2.4.1. Background 26
5.2.4.2. Fixed Integration Time Window 27
5.3. Animal Movement Modeling for Impact Assessment 27
5.4. Acoustic Exposure Criteria 28
5.4.1. Marine Mammal Frequency Weighting Functions 29
5.4.2. Injury Exposure Criteria Selection 32
5.4.3. Behavioral Exposure Criteria Selection 34
5.4.4. Exposure Estimation 35
5.4.4.1. Injury Exposure Estimates—cumulative SEL 35
5.4.4.2. Injury Exposure Estimates—peak SPL 35
5.4.4.3. Behavior Exposure Estimates—rms SPL 35
5.4.4.4. NMFS Criteria for Injury and Behavior Exposure Estimates—rms SPL 35
6. PHASE I: TEST CASE AND TEST SCENARIOS 36
6.1. Test Case Acoustic Source Parameters 37
6.2. Test Case Environmental Parameters 40
6.2.1. Modeling Sites 40
6.2.2. Bathymetry 40
6.2.3. Multi-Layer Geoacoustic Profile 40
6.2.4. Sound Speed Profile 42
6.2.5. Marine Mammals Density Estimates 43
6.2.6. Animal Movement Modeling 46
6.3. Test Case Results 46
6.3.1. Acoustic Sources: Levels and Directivity 46
6.3.1.1. 8000 in³ Airgun Array 46
6.3.1.2. Per-Pulse Acoustic Field for Input to ESME 49
6.3.1.3. Range to Zero-to-Peak SPL Isopleths 49
6.3.2. Simulation Exposure Estimates 50
6.3.3. Real-world Individual Exposure Estimates 53
6.4. Test Case Exposure Summary 55
6.5. Test Scenarios 56
6.5.1. Test Scenario 1: Scaling Modeled Acoustic Exposure Estimates 56
6.5.1.1. Large-scale Animal Movement 56
6.5.1.1.1. Scaling Methods 57
6.5.1.1.2. Assumptions 57
6.5.1.1.3. Prey Distribution as an Environmental Attractor 57
6.5.1.1.4. Distribution and Movement Behavior of Modeled Species 57
6.5.1.2. Potential Biases in the Modeling Procedure 59
6.5.1.2.1. Methods 59
6.5.1.2.2. Results 60
6.5.1.3. Summary of Scaling Modeled Acoustic Exposure Results 68
6.5.1.3.1. Large-scale Animal Movement 68
6.5.1.3.2. Potential Biases in the Modeling Procedure 68
6.5.1.3.3. Scaling Short-duration Simulations for Long-duration Operations 70

6.5.2. Test Scenario 2: Analysis of Uncertainty in Acoustic and Animal Modeling 70
6.5.2.1. Acoustic Modeling Uncertainty 71
6.5.2.1.1. Source Characterization Modeling Uncertainty 71
6.5.2.1.2. Acoustic Propagation Modeling Uncertainty 72
6.5.2.1.3. Sound Speed Profiles 72
6.5.2.1.4. Sound Speed Profile Results 78
6.5.2.1.5. Geoacoustics 84
6.5.2.1.6. Geoacoustic Results 86
6.5.2.1.7. Bathymetry 91
6.5.2.1.8. Bathymetry Results 92
6.5.2.1.9. Sea State 99
6.5.2.1.10. Summary of Acoustic Uncertainty 100
6.5.2.2. Animal Modeling Uncertainty 101
6.5.2.2.1. Animal Movement Parameters Uncertainty 101
6.5.2.2.2. Summary of Animal Movement Parameter Uncertainty 102
6.5.2.2.3. Animal Density Estimates Uncertainty 102
6.5.2.2.4. Animal Density Estimates Uncertainty Results 103
6.5.2.2.5. Summary of Animal Density Estimate Uncertainty 107
6.5.2.2.6. Impact of Social Group Size on Exposure Estimates 107
6.5.2.2.7. Impact of Social Group Size on Exposure Estimates: Methods 108
6.5.2.2.8. Impact of Social Group Size on Exposure Estimates: Results 109
6.5.2.2.9. Summary of Impact of Social Group Size on Exposure Estimates 112
6.5.2.3. Exposure Estimate Uncertainty 113
6.5.2.3.1. Exposure Estimate Uncertainty: Results 113
6.5.2.3.2. Summary of Exposure Estimate Uncertainty 118
6.5.3. Test Scenario 3: Mitigation Effectiveness 118
6.5.3.1. Mitigation Effectiveness Methods 118
6.5.3.1.1. Bootstrap Resampling 119
6.5.3.1.2. Detection Probability 120
6.5.3.2. Mitigation Effectiveness Results 121
6.5.3.3. Summary of Mitigation Effectiveness 129
6.5.4. Test Scenario 4: Effects of Aversion on Acoustic Exposure Estimates 129
6.5.4.1. Effects of Aversion on Acoustic Exposure Estimates Methods 130
6.5.4.2. Exposure History with Aversion 130
6.5.4.3. Effects of Aversion on Acoustic Exposure Estimates: Results 131
6.5.4.4. Summary of Effects of Aversion on Acoustic Exposure Estimates 138
6.5.5. Test Scenarios 5 and 6: Stand-off Distance and Simultaneous Firing 139
6.5.5.1. Stand-off Distance 139
6.5.5.2. Simultaneous Firing 142
6.5.5.3. Summary of Stand-off Distance and Simultaneous Firing 145
6.6. Cumulative and Chronic Effects Assessment Framework 146
6.6.1. Overview 146

6.6.2. Method of Use 147
6.6.3. Calculator Output 148
6.6.4. Discussion 150
7. PHASE II: MARINE MAMMAL EXPOSURE ESTIMATES 151
7.1. Assumptions 151
7.2. Phase II Modeling Methods 153
7.2.1. Acoustic Source Parameters 153
7.2.1.1. Airgun Array—8000 in³ 153
7.2.1.2. Single Airgun—90 in³ 153
7.2.1.3. Boomer 153
7.2.1.4. High Resolution Survey Sources 153
7.2.1.4.1. Multibeam Echosounder—Simrad EM2000 154
7.2.1.4.2. Side-scan Sonar—EdgeTech 2200 IM 154
7.2.1.4.3. Sub-bottom Profiler—EdgeTech 2200 IM with DW−424 154
7.2.2. Survey Patterns 154
7.2.2.1. 2-D Seismic Survey 155
7.2.2.2. 3-D Narrow Azimuth Seismic Survey 156
7.2.2.3. 3-D Wide Azimuth Seismic Survey 156
7.2.2.4. Coil Seismic Survey 157
7.2.2.5. High Resolution Geotechnical Survey 158
7.2.3. Choice of Zone Boundaries 158
7.2.3.1. Survey Extents 159
7.2.3.2. Acoustic Modeling Sites 159
7.2.4. Environmental Parameters 161
7.2.4.1. Bathymetry 161
7.2.4.2. Multi-Layer Geoacoustic Profile 161
7.2.4.3. Sound Speed Profiles 163
7.2.4.3.1. Sound Speed Profiles for Box Centers 165
7.2.4.3.2. Sound Speed Profiles for Acoustic Modeling Sites along Transects 166
7.2.5. 3MB Simulation Areas 169
7.2.5.1. Large Seismic Surveys 169
7.2.5.2. High-resolution Surveys 170
7.2.6. Animal Densities 171
7.2.6.1. Marine Mammal Density Estimates in Modeling Zones 179
7.2.7. Animal Movement: JEMS 179
7.2.7.1. Depth-restricted Density Adjustment 179
7.2.7.2. Evaluation Time Period 179
7.2.7.3. Annual Aggregate Estimates 180
7.3. Phase II Modeling Results 180
7.3.1. Acoustic Sources: Levels and Directivity 180
7.3.1.1. Airgun Sources 180
7.3.1.1.1. Airgun Array—8000 in³ 180
7.3.1.1.2. Single Airgun—90 in³ 182
7.3.1.2. Boomer 183
7.3.1.3. High-resolution Acoustic Sources 185

7.3.1.3.1. Multibeam Echosounder—Simrad EM2000 185
7.3.1.3.2. Side-scan Sonar—EdgeTech 2200 IM 185
7.3.1.3.3. Sub-bottom Profiler—EdgeTech 2200 IM, DW−424 186
7.3.2. Per-Pulse Acoustic Field 187
7.3.2.1. Per-Pulse Acoustic Field for Input to JEMS 187
7.3.2.1.1. Seismic Survey (8000 in³ Airgun Array) 187
7.3.2.1.2. Geotechnical Surveys with High-resolution sources 188
7.3.2.2. Range to Zero-to-Peak SPL Isopleths 189
7.3.2.3. Per-Pulse Acoustic Field for Threshold Ranges 190
7.3.3. 24-hour Exposure Estimates 190
7.3.4. Annual Exposure Estimates 192
8. DISCUSSION 202
9. LITERATURE CITED 205
APPENDIX A. PER-PULSE ACOUSTIC FIELD EXAMPLE RADII TABLES AND MAPS 221
APPENDIX B. TEST CASE SIMULATION RECEIVED LEVELS 228
APPENDIX C. MARINE MAMMAL DISTRIBUTION IN THE GULF OF MEXICO 234
APPENDIX D. 3MB ANIMAL MOVEMENT PARAMETERS 252
APPENDIX E. PER-PULSE ACOUSTIC FIELD MAPS AND RADII 275
APPENDIX F. ANNUAL EXPOSURE ESTIMATES 288

Figures

Figure 1. Typical 3-D beam pattern for a circular transducer 21
Figure 2. Vertical cross section of a beam pattern measured in situ from a transducer 21
Figure 3. Calculated beam pattern for a circular transducer 22
Figure 4. Calculated beam pattern for a rectangular transducer 23
Figure 5. Calculated beam pattern for two rectangular transducers 23
Figure 6. The *N*×2-D and maximum-over-depth modeling approach 25
Figure 7. Cartoon animats in a moving sound field. 28
Figure 8. Standard M-weighting functions for the four underwater functional marine mammal hearing groups 30
Figure 9. Frequency weighting functions for the cetacean functional hearing groups. 32
Figure 10. Locations of the Survey site A (purple box) and Survey site B (red box) and acoustic field modeling sites. 37
Figure 11. Layout of the modeled airgun array 39
Figure 12. Sound speed profiles 43
Figure 13. Density estimates for sperm whales near Survey site A 44
Figure 14. Density estimates for sperm whales near Survey site B 45
Figure 15. The 8000 in^3 array: 46
Figure 16. Maximum directional source level (SL) in the horizontal plane 47
Figure 17. Horizontal directivity of the 8000 in^3 array. 48
Figure 18. An example of per-pulse received SEL field 49
Figure 19. Vessel track locations for behavioral response analysis at Survey sites A and B. 51
Figure 20. Vessel track locations for injury analysis at Survey sites A and B 52
Figure 21. Bryde's whales: Behavioral exposure estimates for (a) Survey sites A and (b) B. 60
Figure 22. Common bottlenose dolphins: Behavioral exposure estimates for (a) Survey sites A and (b) B. 61
Figure 23. Cuvier's beaked whales: Behavioral exposure estimates for (a) Survey sites A and (b) B. 61
Figure 24. Short-finned pilot whales: Behavioral exposure estimates for (a) Survey sites A and (b) B62
Figure 25. Sperm whales: Behavioral exposure estimates for (a) Survey sites A and (b) B. 62
Figure 26. Dwarf sperm whales: Behavioral exposure estimates for (a) Survey sites A and (b) B. 63
Figure 27. Behavioral exposure estimates for (a) short-finned pilot whales and (b) sperm whales, both with reversed vessel tracks at Survey site A. 63
Figure 28. Behavioral exposure estimates for (a) short-finned pilot whales and (b) sperm whales, with stationary source in deep water near Survey site B. 64
Figure 29. The Shelf zone (28.5° N, 90° W): Mean monthly sound speed profiles, separated into Seasons 1 (left) and 2 (right) 74
Figure 30. The Slope zone (27.25° N, 90° W): Mean monthly sound speed profiles, separated into Seasons 1 (left) and 2 (right) 75
Figure 31. Deep zone (25.5° N, 90° W): Mean monthly sound speed profiles. 75
Figure 32. Shelf zone: Modeled average and worst-case sound speed profiles based on variations in CTD cast data for Seasons 1 (left) and 2 (right). 77

Figure 33. Slope zone: Modeled average and worst-case sound profiles based on variations in CTD cast data for Seasons 1 (left) and 2 (right). 77
Figure 34. Deep zone: Modeled average and worst-case sound speed profiles based on variations in CTD cast data. 78
Figure 35. Shelf zone, Dec–Mar: Received SEL acoustic field using conservative (enhanced propagation) sound speed profile and median reflectivity geoacoustic parameters. 78
Figure 36. Shelf zone, Dec–Mar: Received SEL acoustic field using median sound speed profile and median reflectivity geoacoustic parameters. 79
Figure 37. Shelf zone, Dec–Mar: Differential acoustic field due to variation in the sound speed profile. 79
Figure 38. Shelf zone, Apr–Nov: Received SEL acoustic field using conservative sound (enhanced propagation) speed profile and median reflectivity geoacoustic parameters. 79
Figure 39. Shelf zone, Apr–Nov: Received SEL acoustic field using median sound speed profile and median reflectivity geoacoustic parameters. 80
Figure 40. Shelf zone, Apr–Nov: Differential acoustic field due to variation in the sound speed profile. 80
Figure 41. Slope zone, Jul–Sep: Received SEL acoustic field using conservative sound speed profile and median reflectivity geoacoustic parameters. 80
Figure 42. Slope zone, Jul–Sep: Received SEL acoustic field using median sound speed profile and median reflectivity geoacoustic parameters. 81
Figure 43. Slope zone, Jul–Sep: Differential acoustic field due to variation in the sound speed profile. 81
Figure 44. Slope zone: Received SEL acoustic field sing conservative sound speed profile and median reflectivity geoacoustic parameters. 81
Figure 45. Slope zone, Oct–Jun: Received SEL acoustic field using median sound speed profile and median reflectivity geoacoustic parameters. 82
Figure 46. Slope zone, Oct–Jun: Differential acoustic field due to variation in the sound speed profile. 82
Figure 47. Deep zone: Received SEL acoustic field using conservative sound speed profile and median reflectivity geoacoustic parameters. 82
Figure 48. Deep zone: Received SEL acoustic field using median sound speed profile and median reflectivity geoacoustic parameters. 83
Figure 49. Deep zone: Differential acoustic field due to variation in the sound speed profile. 83
Figure 50. The map of dominant type for the surficial sediments (NOS 2013) and location of the drill wells in the Gulf of Mexico. 84
Figure 51. Shelf zone, Dec–Mar: Received SEL acoustic field using median sound speed profile and high reflectivity geoacoustic parameters. 86
Figure 52. Shelf zone, Dec–Mar: Received SEL acoustic field using median sound speed profile and median reflectivity geoacoustic parameters. 86
Figure 53. Shelf zone, Dec–Mar: Differential acoustic field due to variation in the bottom geoacoustic parameters. 87
Figure 54. Shelf zone, Apr–Nov: Received SEL acoustic field using median sound speed profile and high reflectivity geoacoustic parameters. 87
Figure 55. Shelf zone, Apr–Nov: Received SEL acoustic field using median sound speed profile and median reflectivity geoacoustic parameters. 87

Figure 56. Shelf zone, Apr–Nov: Differential acoustic field due to variation in the bottom geoacoustic parameters. 88
Figure 57. Slope zone, Jul–Sep: Received SEL acoustic field using median sound speed profile and high reflectivity geoacoustic parameters. 88
Figure 58. Slope zone, Jul–Sep: Received SEL acoustic field using median sound speed profile and median reflectivity geoacoustic parameters. 88
Figure 59. Slope zone, Jul–Sep: Differential acoustic field due to variation in the bottom geoacoustic parameters. 89
Figure 60. Slope zone, Oct–Jun: Received SEL acoustic field using median speed profile and high reflectivity geoacoustic parameters. 89
Figure 61. Slope zone, Oct–Jun: Received SEL acoustic field using median sound speed profile and median reflectivity geoacoustic parameters. 89
Figure 62. Slope zone, Oct–Jun: Differential acoustic field due to variation in the bottom geoacoustic parameters. 90
Figure 63. Deep zone: Received SEL acoustic field using median sound speed profile and high reflectivity geoacoustic parameters. 90
Figure 64. Deep zone: Received SEL acoustic field using median sound speed profile and median reflectivity geoacoustic parameters. 90
Figure 65. Deep zone: Differential acoustic field due to variation in the bottom geoacoustic parameters. 91
Figure 66. Shelf zone: The source when positioned at water column depth of 25 m: Received SEL acoustic field using Season 1 sound speed profile and median reflectivity geoacoustic parameters.92
Figure 67. Shelf zone: The source when positioned at water column depth of 75 m: Received SEL acoustic field using Season 1 sound speed profile and median reflectivity geoacoustic parameters.93
Figure 68. Shelf zone: The source when positioned at water column depth of 150 m: Received SEL acoustic field using Season 1 sound speed profile and median reflectivity geoacoustic parameters.93
Figure 69. Shelf zone: Differential acoustic field for the source when positioned at water column depths of 25 and 75 m: Differential acoustic field due to variation of the water depth at the source. 93
Figure 70. Shelf zone: Differential acoustic field for the source when positioned at water column depths of 75 and 150 m: Differential acoustic field due to variation of the water depth at the source. 94
Figure 71. Slope zone: The source when positioned at water column depth of 300 m: Received SEL acoustic field using Season 1 sound speed profile and median reflectivity geoacoustic parameters.94
Figure 72. Slope zone: The source when positioned at water column depth of 500 m: Received SEL acoustic field using Season 1 sound speed profile and median reflectivity geoacoustic parameters.94
Figure 73. Slope zone: The source when positioned at water column depth of 750 m: Received SEL acoustic field using Season 1 sound speed profile and median reflectivity geoacoustic parameters.95
Figure 74. Slope zone: The source when positioned at water column depth of 1000 m: Received SEL acoustic field using Season 1 sound speed profile and median reflectivity geoacoustic parameters.95
Figure 75. Slope zone: The source when positioned at water column depth of 1500 m: Received SEL acoustic field using Season 1 sound speed profile and median reflectivity geoacoustic parameters.95
Figure 76. Slope zone: Differential acoustic field for the source when positioned at water column depths of 300 and 500 m. 96
Figure 77. Slope zone: Differential acoustic field for the source when positioned at water column depths of 500 and 750 m. 96

Figure 78. Slope zone: Differential acoustic field for the source when positioned at water column depths of 750 and 1000 m. 96
Figure 79. Slope zone: Differential acoustic field for the source when positioned at water column depths of 1000 and 1500 m. 97
Figure 80. Deep zone: The source when positioned at water column depth of 2000 m: Received SEL acoustic field using Season 1 sound speed profile and median reflectivity geoacoustic parameters.97
Figure 81. Deep zone: The source when positioned at water column depth of 2500 m: Received SEL acoustic field using Season 1 sound speed profile and median reflectivity geoacoustic parameters.97
Figure 82. Deep zone: Differential acoustic field for the source when positioned at water column depths of 2000 and 2500 m 98
Figure 83. Bootstrap resampling and SEL injury and behavioral response exposure estimation for Bryde's whales and dwarf sperm whales. 105
Figure 84. Bootstrap resampled behavioral disruption exposure estimate distribution for modeled results and adjusted for real-world density estimate mean ± standard deviation at Survey site A 106
Figure 85. SEL Injury and behavioral disruption exposure estimate distributions for Bryde's whales and dwarf sperm whales at Survey site A. 111
Figure 86. Behavioral disruption exposure estimate distributions with social group size at Survey site A 112
Figure 87. Bootstrap resampling with acoustic uncertainty for SEL injury potential behavioral response for Bryde's whales and dwarf sperm whales at Survey site A 115
Figure 88. Bootstrap resampling for SEL injury 116
Figure 89. Potential behavioral response exposure estimates of species at Survey site A from bootstrap resampling 117
Figure 90. Cuvier's beaked whales: Probability of exposure above injury thresholds at Survey site A without (left panels) and with mitigation (right panels) for peak SPL (top panels) and rms SPL (bottom panels). 124
Figure 91. Common bottlenose dolphins: Probability of exposure at or above injury thresholds at Survey site A without (left panels) and with mitigation (right panels) for peak SPL (top panels) and rms SPL (bottom panels) 125
Figure 92. Short-finned pilot whales: Probability of exposure at or above injury thresholds at Survey site A without (left panels) and with mitigation (right panels) for peak SPL (top panels) and rms SPL (bottom panels). 126
Figure 93. Sperm whales: Probability of exposure at or above injury thresholds at Survey site A without (left panels) and with mitigation (right panels) for peak SPL (top panels) and rms SPL (bottom panels). 127
Figure 94. Dwarf sperm whales: Probability of exposure at or above injury thresholds at Survey site A without (left panels) and with mitigation (right panels) for SEL (top panels), peak SPL (middle panels), and rms SPL (bottom panels) 128
Figure 95. Probability of exposure at or above rms SPL injury thresholds for Bryde's whales at Survey site A, (left) without and (right) with aversion. 132
Figure 96. Probability of exposure at or above peak SPL (top panels) and rms SPL (bottom panels) injury thresholds for Cuvier's beaked whales at Survey site A, without (left panels) and with aversion (right panels). 133
Figure 97. Probability of exposure at or above peak SPL (top panels) and rms SPL (bottom panels) injury thresholds for common bottlenose dolphins at Survey site A, without (left panels) and with (right panels) aversion. 134

Figure 98. Probability of exposure at or above peak SPL (top panels) and rms SPL (bottom panels) injury thresholds for short-finned pilot whales at Survey site A, without (left panels) and with (right panels) aversion. 135
Figure 99. Probability of exposure at or above peak SPL (top panels) and rms SPL (bottom panels) thresholds for sperm whales at Survey site A, without (left panels) and with (right panels) aversion. 136
Figure 100. Probability of exposure at or above (top panels) SEL, (middle panels) peak SPL, rms SPL (bottom panels) injury thresholds for dwarf sperm whales at Survey site A, without (left panels) and with (right panels) aversion. 137
Figure 101. Waveforms predicted by FWRAM for the 8000 in^3 array at Survey site A, for a 10 m receiver depth. 141
Figure 102. Sound exposure level for four 8000 in^3 arrays at the start of a 3-D wide azimuth seismic survey at Survey site A, S01 modeling province. 142
Figure 103. SPL for (top) one 8000 in^3 array and (bottom) two 8000 in^3 arrays fired simultaneously with an across-track separation of 350 m and an along-track separation of 2700 m. 144
Figure 104. Map automatically produced by the cumulative and chronic effects calculator, showing seismic survey positions and receiver locations. 148
Figure 105. Simulated portion of the track for the 2-D seismic survey. 156
Figure 106. Simulated portion of the track for the 3-D NAZ seismic survey. 156
Figure 107. Simulated portion of the track for the 3-D WAZ seismic survey. 157
Figure 108. Simulated portion of the track for the Coil seismic survey. 157
Figure 109. Simulated portion of the track for the geotechnical survey. 158
Figure 110. Gulf of Mexico project area. 159
Figure 111. Sound speed profiles at the (left) Shelf, (center) Slope, and (right) Deep zones 164
Figure 112. Sound speed profiles at modeling boxes, Season 1 165
Figure 113. Sound speed profiles at modeling boxes, Season 3 166
Figure 114. Sound speed profiles along the West transect 167
Figure 115. Sound speed profiles along Central transect 168
Figure 116. Sound speed profiles along East transect 169
Figure 117. Predicted (a) overpressure signature and (b) power spectrum in the broadside and endfire (horizontal) directions, for a generic 8000 in^3 airgun array towed at a depth of 8 m. 181
Figure 118. Maximum 1/3-octave-band source level in the horizontal plane for a generic 8000 in^3 airgun array. 181
Figure 119. Directionality of predicted horizontal source levels for a generic 8000 in^3 airgun array. 182
Figure 120. Predicted (a) overpressure signature and (b) power spectrum in the broadside and endfire (horizontal) directions for a single 90 in^3 airgun. 183
Figure 121. Maximum 1/3-octave-band source level in the horizontal plane for a single 90 in^3 airgun. 183
Figure 122. Vertical beam pattern calculated for the Simrad EM2000 multibeam 88° × 17° width in the (left) along- and (right) across-track directions. 185
Figure 123. Vertical beam pattern calculated for the EdgeTech 2200 IM side-scan sonar 70° × 0.8° width and 20° declination angle. Slices (left) at 20° declination angle and (right) across-track directions. 186
Figure 124. Vertical beam pattern calculated for the EdgeTech 2200 IM sub-bottom with 20° beamwidth. 187

Figure 125. Probability density function of received levels shown as a histogram. 191
Figure 126. Broadband (10–5000 Hz) maximum-over-depth sound pressure levels for 8000 in³ airgun array, in August at the Survey site A, S01 modeling province..... 225
Figure 127. Broadband (10–5000 Hz) maximum-over-depth sound pressure levels for 8000 in³ airgun array, in August at the Survey site A, S02 modeling province..... 226
Figure 128. Broadband (10–5000 Hz) maximum-over-depth sound pressure levels for 8000 in³ airgun array, in August at the Survey site B, D01 modeling province. 227

Tables

Table 1. Marine mammal functional hearing groups 11
Table 2. Marine mammal species considered in the acoustic exposure analysis. 18
Table 3. Low and high frequency cut-off parameters of M-weighting functions for the cetacean functional hearing groups 30
Table 4. Frequency weighting parameters for the cetacean functional hearing groups 31
Table 5. Injury exposure criteria for pulsed sounds. 34
Table 6. Behavioral exposure criteria. 34
Table 7. Relative airgun positions within each of the six sub-arrays. 38
Table 8. Geoacoustic properties of the sub-bottom sediments as a function of depth for the S01 modeling province. 41
Table 9. Geoacoustic properties of the sub-bottom sediments as a function of depth for the S02 modeling province. 41
Table 10. Geoacoustic properties of the sub-bottom sediments as a function of depth for the D01 modeling province. 42
Table 11. Summer regional statistics of marine mammal density near Survey site A 45
Table 12. Summer regional statistics of marine mammal density near Survey site B 45
Table 13. Horizontal source level specifications (10–5000 Hz) for the seismic airgun array 47
Table 14. Number of modeled cetaceans above exposure criteria for Survey site A for entire duration of the simulations. 53
Table 15. Number of modeled cetaceans above exposure criteria for Survey site B for entire duration of the simulations. 53
Table 16. Real-world number of cetaceans above injury exposure criteria for summer for Survey site A. 54
Table 17. Real-world number of cetaceans above injury exposure criteria for summer for Survey site B. 54
Table 18. Real-world number of cetaceans above behavioral exposure criteria for summer for Survey site A. 54
Table 19. Real-world number of cetaceans above behavioral exposure criteria for summer for Survey site B. 55
Table 20. Average number of modeled cetaceans above exposure criteria at Survey site A for 24 h sliding windows. 65
Table 21. Average number of modeled cetaceans above exposure criteria at Survey site B for 24 h sliding windows. 66
Table 22. Number of modeled cetaceans above exposure criteria at Survey site A for average 24 h sliding windows estimate scaled to full duration (5 or 30 days). 66
Table 23. Number of modeled cetacean animats above exposure criteria at Survey site B for average 24 h sliding windows estimate scaled to full duration (5 or 30 days). 66
Table 24. Percentage difference in number of modeled cetaceans above exposure criteria at Survey site A for 24 h sliding windows scaled to 4 day evaluation window. 67
Table 25. Percentage difference in number of modeled cetaceans above exposure criteria at Survey site B for 24 h sliding windows scaled to 4 day evaluation window. 67

Table 26. Amount of time that animats exceed NMFS threshold criteria at Survey site A for 30 days and 24 h. 67
Table 27. Amount of time that animats exceed NMFS threshold criteria at Survey site B for 30 days and 24 h. 68
Table 28. Depth zones along the study line. 73
Table 29. Modeled seasons and their characteristics. 73
Table 30. Acoustic field differences between worst-case and average sound speed profile conditions.84
Table 31. Shelf zone: Median and higher reflectivity geoacoustic profiles. 85
Table 32. Slope zone: Lower, median, and higher reflectivity geoacoustic profiles. 85
Table 33. Deep zone: Lower, median, and higher reflectivity geoacoustic profiles. 86
Table 34. Acoustic field differences between reflective and average geoacoustic conditions. 91
Table 35. Acoustic field uncertainty due to variations in the water depth at the source. 99
Table 36. Real-world density estimates for summer at Survey sites A and B. 103
Table 37. Published (social) group size statistics for Test Case species. 108
Table 38. Social group size (number of individuals ± standard deviation) used to evaluate effects on exposure estimates. 110
Table 39. Estimates of trackline detection probability, *g*(0), coefficients of variation (CV) for *g*(0), and mean group size. 120
Table 40. Cuvier's beaked whales: Modeled Level A exposure estimates and mitigation efficiency for peak SPL and rms SPL. 121
Table 41. Common bottlenose dolphins: Modeled Level A exposure estimates and mitigation efficiency for peak SPL and rms SPL. 122
Table 42. Short-finned pilot whales: Modeled Level A exposure estimates and mitigation efficiency for peak SPL and rms SPL. 122
Table 43. Sperm whales: Modeled Level A exposure estimates and mitigation efficiency for peak SPL and rms SPL. 123
Table 44. Dwarf-sperm whales: Modeled Level A exposure estimates and mitigation efficiency for 5-day SEL, peak SPL, and rms SPL. 123
Table 45. Modeled Level A exposures, with and without aversion. 132
Table 46. Receiver site locations and water depths. 146
Table 47. Summary of the Phase II surveys considered to determine the exposure estimates. 155
Table 48. Modeling sites along the West transect. 160
Table 49. Modeling sites along Central transect. 160
Table 50. Modeling sites along East transect. 161
Table 51. Center coordinates of survey boxes. 161
Table 52. Shelf zone Center and West: Geoacoustic properties of the sub-bottom sediments 162
Table 53. Shelf zone East: Geoacoustic properties of the sub-bottom sediments 162
Table 54. Slope zone: Geoacoustic properties of the sub-bottom sediments 163
Table 55. Deep zone: Geoacoustic properties of the sub-bottom sediments 163
Table 56. Representative months for each season and modeling zone. 164
Table 57. Modeling seasons for each box. 165
Table 58. Modeling seasons for the sites along transects. 166

Table 59. Geographic extent of the animat movement boxes for behavior simulation with the large seismic surveys. 170
Table 60. Geographic extent of the animat movement boxes for injury simulation with the large seismic surveys. 170
Table 61. Geographic extent of the animat movement boxes for both behavior and injury simulation with the high-resolution surveys. 171
Table 62. Zone 1 Marine mammal density estimates. 172
Table 63. Zone 2 Marine mammal density estimates. 173
Table 64. Zone 3 Marine mammal density estimates. 174
Table 65. Zone 4 Marine mammal density estimates. 175
Table 66. Zone 5 Marine mammal density estimates. 176
Table 67. Zone 6 Marine mammal density estimates. 177
Table 68. Zone 7 Marine mammal density estimates. 178
Table 69. Horizontal source level specifications for a generic 8000 in^3 airgun array. 181
Table 70. Estimated source levels (SELs) and beamwidths from the AA301 boomer plate 184
Table 71. Boomer and 90 in^3 airgun broadband source levels after M-weighting filters were applied. 185
Table 72. Modeling parameters for the geotechnical sources. 189
Table 73. Angle step configuration of profiles around side-scan sonar. 189
Table 74. Ranges to specific threshold levels for all sources. 190
Table 75. Projected level of effort in days (24 h) for survey types in years 2016 to 2025. 192
Table 76. Decade exposure estimates totals for 2-D survey (8000 in3 airgun array, 1 vessel). 195
Table 77. Decade exposure estimates totals for 3-D NAZ survey (8000 in^3 airgun array, 2 vessels). 196
Table 78. Decade exposure estimates totals for 3-D WAZ survey (8000 in^3 airgun array, 4 vessels). 197
Table 79. Decade exposure estimates totals for Coil survey (8000 in^3 airgun array, 4 vessels). 198
Table 80. Decade exposure estimates totals for 90 in^3 airgun. 199
Table 81. Decade exposure estimates totals for boomer. 200
Table 82. Decade exposure estimate totals for the high resolution sources (side-scan sonar, sub-bottom profiler, and multibeam scanner). 201
Table 83. 8000 in^3 airgun array at the Survey site A, S01 modeling province: maximum (R_{max}, m) and 95% ($R_{95\%}$, m) horizontal distance 222
Table 84. 8000 in^3 airgun array at the Survey site A, S02 modeling province: maximum (R_{max}, m) and 95% ($R_{95\%}$, m) horizontal distance 223
Table 85. 8000 in^3 airgun array at the Survey site B, D01 modeling province: maximum (R_{max}, m) and 95% ($R_{95\%}$, m) horizontal distance 224

1. Executive Summary

1.1. Overview

This report provides estimates of the annual marine mammal acoustic exposure caused by sounds from geological and geophysical exploration activity in the Gulf of Mexico for years 2016 to 2025. Exposure estimates were computed from modeled sound levels as received by simulated animals (animats) in the area for several exploration survey types performed at multiple locations. Because animals and noise sources move relative to the environment and each other, and the sound fields generated by the sound sources are shaped by various physical parameters, the sound levels received by an animal are a complex function of location and time. We used acoustic modeling to compute three-dimensional (3-D) sound fields that varied with time, and we simulated realistic movements of animats within these fields to sample the sound levels in a manner representing how real animals would experience this sound. From the time history of the received sound levels, the number of animats exposed to levels exceeding threshold criteria (thresholds used in this report are described in **Section 5.4**) were determined and then adjusted by the number of animals in the area to estimate the potential number of animals impacted.

The project was divided into two phases. In Phase I, a typical wide azimuth geophysical survey using an airgun array source was simulated at two locations within the Mississippi Canyon. This was done to establish the basic methodological approach and to evaluate the sensitivities of results to uncertainties in input parameters. Results from the Test Scenarios were then used to guide the main modeling effort of Phase II. In Phase II, we divided the Gulf into seven modeling zones and simulated six survey types within each zone to estimate the potential effects of each survey. The results from each zone were summed to provide Gulf-wide estimates of effects on each marine mammal species for each survey type for each year based on specific assumed levels of survey activities.

1.2. Sounds and Marine Mammals

The Marine Mammal Protection Act defines harassment as activities that can potentially injure marine mammals or disrupt their behavioral patterns (MMPA 2007); loud sounds produced by geophysical survey equipment are possible sources of such harassment. National Marine Fisheries Service (NMFS) adopted threshold criteria thought to represent cautionary lower limits for pulsed sound levels that could injure marine mammals or disrupt their activities. The thresholds for cetaceans exposed to impulsive noise were set at 180 dB re 1 µPa rms sound pressure level (rms SPL) for potential injury (Level A harassment) and 160 dB re 1 µPa rms SPL for potential behavioral disruption (Level B harassment; NFMS 1995, NMFS 2000). Animals exceeding these thresholds were considered exposed at their respective harassment level. As further knowledge on injury from sound became available, an expert group reviewed the available evidence and published suggestions for marine mammal sound exposure criteria (Southall et al. 2007). The present study has considered, in the exposure estimates, the NMFS criteria and adaptations of the Southall et al. (2007) criteria based on additional studies.

Injury to marine mammals' anatomical, morphological, and physiological hearing structures (hereafter called hearing structures) can be caused by the fatiguing effect of accumulated sound energy. This energy, measured in terms of the sound exposure level (SEL) [1], depends on the position of the animal in the sound

[1] Sound Exposure Level (SEL) is numerically proportional to acoustic energy flux density only when the acoustic impedance is constant and purely resistive. That is not the case when surface or seabed reflections are present or in refractive environments. SEL is not expressed in energy density units.

field. It changes as the animal and the sound source move, and continues to accumulate as long as the animal is exposed to the sound. Because intense sounds of short duration can also damage an animal's hearing structures, an additional metric of peak sound pressure level (peak SPL) is also used to assess acoustic exposure risk. The exposure duration is not a factor in determining potential injury due to peak SPL; only the proximity of an animal to a source is relevant for estimating this metric.

Defining sound levels that disrupt behavioral patterns is difficult because responses depend on the context in which the animal receives the sound. The environmental context and responses depend on many factors, including an animal's behavioral mode when it hears sounds (e.g., feeding, resting, or migrating), and on biological factors (e.g., age and sex). Available data are consistent with the notion that louder sounds evoke greater responses, but the levels at which responses occur are not necessarily consistent. To predict the probability of behavioral response, we used a step function based on the received rms SPL. Some species, beaked whales in particular, are known to be more behaviorally sensitive to sounds than other species, so the function was adjusted as warranted for such species. To evaluate the potential for behavioral disruption, the maximum sound pressure level each simulated animal received was identified and the step function used to determine the number of simulated animals with the potential to respond.

In developing the exposure effects criteria, a 24 h reset period was chosen. A 24 h reset period is commonly used and means that acoustic energy accumulation and the maximum values of the other metrics were reset after 24 h. Individual animats were eligible to be re-exposed in subsequent 24 h periods.

The NMFS exposure criteria for injury (180 dB re 1 µPa rms SPL) and behavioral disruption (160 dB re 1 µPa rms SPL) uses unfiltered (unweighted) sound fields when determining the number of animals exposed to levels exceeding threshold. The Southall et al. (2007) criteria attempt to account for the hearing ability of the animals. Southall et al. (2007) propose weighting functions for species groups based on their hearing range. These M-weighting filters, based on known and assumed species hearing ranges (audiograms) divide the cetaceans into three hearing groups low-, mid-, and high- frequency specialists (Southall et al. 2007) . Later, Finneran and Jenkins (2012) developed a weighting function based on perceptual measure of subjective loudness. Equal-loudness contours better match the onset of hearing impairment (temporary threshold shift) than the original M-weighting functions. Data for the equal-loudness contours do not, however, cover the full frequency range of the M-weighting filters. Finneran and Jenkins (2012) propose a hybrid filter based on the equal-loudness contours in their measured frequency band and, outside of this range, the original M-weighting function was discounted to match the end points of the equal-loudness functions. Finneran and Jenkins (2012) term the hybrid filters Type II M-weighting to distinguish them from the original M-weighting, which they term Type I M-weighting.

Because Type II filtering was designed to better-predict the onset of injury, it is used in the current report to evaluate exposure for potential injury when using the SEL metric for mid- and high-frequency species. For low-frequency species, Type I filtering is used. No filtering is used when evaluating potential injury with the peak SPL metric. Although the Type II filtering is based on perceptual measures and, therefore, could be an appropriate indicator of behavioral response, as a conservative measure, Type I filtering is used to evaluate potential behavioral disruption using rms SPL criteria with a step function. The current report uses the step function from Wood et al. (2012), which sets out a graded step of increasing probability of behavioral response with increasing received level. Additionally, following Wood et al. (2012), the step function is modified for behaviorally sensitive species (beaked whales).

1.3. Acoustic Modeling

Acoustic source emission levels of a single airgun and an airgun array are calculated using the Airgun Array Source Model (AASM; JASCO Applied Sciences). Source levels of high-resolution survey sources are obtained from manufacturer's specifications for representative sources. Acoustic transmission loss as

a function of range from each source is calculated using the Marine Operations Noise Model (MONM; JASCO Applied Sciences) for multiple propagation radials centered at the source to yield 3-D transmission loss fields in the surrounding area. The primary seasonal influence on transmission loss is the presence of a sound channel, or duct, near the surface in winter. To account for seasonal variability in propagation, winter (most conservative) and summer (least conservative) were modeled. The modeled sound fields were also filtered for the hearing ability of the animals as described above.

To account for both the geospatial dependence of acoustic fields and the geographic variations of animal distributions, the project area of the Gulf was divided into seven zones. The selected zone boundaries, patterned to conform to BOEM's planning areas where possible, also considered sound propagation conditions and species distribution to create regions of optimized uniformity in both acoustic environment and animal density. This approach allows the calculation of generalized sound exposure estimates for each species for a representative survey type, season, and zone in which the survey occurs. Modeling was performed for each of the six different acoustic survey types that are assessed in this study: 2-D, 3-D narrow azimuth (NAZ), 3-D wide-azimuth (WAZ), Coil, Shallow Hazard (using a single airgun or boomer), and high resolution surveys (using side-scan sonar, sub-bottom profiler, and multibeam echosounder). The 2-D, 3-D NAZ, 3-D WAZ, and Coil represent large seismic exploration surveys using 8000 in^3 towed airgun array(s) as the sound source(s).

1.4. Marine Mammals in the Gulf of Mexico

Twenty-one cetacean species have been sighted in surveys since 1991 (Waring et al. 2013). Eighteen are mid-frequency hearing specialists—Atlantic spotted dolphins (*Stenella frontalis*), beaked whales spp. (Cuvier's (*Ziphius cavirostris*), Blainville's (*Mesoplodon densirostris*), Gervais' (*Mesoplodon europaeus*)), common bottlenose dolphins (*Tursiops truncatus*), clymene dolphins (*Stenella clymene*), false killer whales (*Pseudorca crassidens*), Fraser's dolphins (*Lagenodelphis hosei*), killer whales (*Orcinus orca*), melon-headed whales (*Peponocephala electra*), pantropical spotted dolphins (*Stenella attenuata*), pygmy killer whales (*Feresa attenuata*), Risso's dolphins (*Grampus griseus*), rough-toothed dolphins (*Steno bredanesis*), short-finned pilot whales (*Globicephala melas*), sperm whales (*Physeter macrocephalus*), spinner dolphins (*Stenella longirostris*), and striped dolphins (*Stenella coeruleoalba*). Bryde's whales (*Balaenoptera brydei/edeni*) are the only low-frequency species, and dwarf and pygmy sperm whales (*Kogia sima, Kogia breviceps*) comprise the only high-frequency hearing specialist group.

In Phase I, the Navy's U.S. Navy OPAREA Density Estimate (NODE; DoN 2007) model was used to obtain animal density estimates (animals/km^2). In Phase II, more current density estimates were obtained from the Marine Geospatial Ecology Laboratory at Duke University preliminary results (Roberts et al., in preparation). In part, distribution information was used to inform boundary choices when establishing modeling zones. Density information was obtained for each of the zones and used when determining exposure estimates.

1.5. Animal Movement Modeling

This analysis uses the Marine Mammal Movement and Behavior (3MB) model developed by Houser (2006). Parameter values to control animat movement are determined using behavioral observations of the species members and reviewing behavior reported by tagging studies. The amount and quality of data varies by species, but often provides a detailed description of the proximate behavior expected for real individual animals. Because there are few or no data available for some species included in this study, surrogate species with more available information are used: Pantropical spotted dolphins are used as a surrogate for Clymene, spinner, and striped dolphins; short-finned pilot whales are surrogates for Fraser's dolphins, the *Kogia* species, and melon-headed whales; and rough-toothed dolphins are surrogates for

false killer whales and pygmy killer whales. Observational data for all remaining species in the study were sufficient to determine animat movement. The use of surrogate species is a reasonable assumption for the simulation of proximate or observable behavior, and it is unlikely that this choice adds more uncertainty about location preference.

1.6. Phase I

A Test Case simulating a typical WAZ survey at two locations was performed as a demonstration of the basic modeling approach and as an investigation tool to establish methods used in the full modeling approach of Phase II. Test Scenarios were undertaken using, primarily, the results of the Test Case to investigate the effects of methodological choices on exposure estimates. Surveys vary in duration and some can be months long. In Test Scenario 1, a method for scaling up simulation results to account for long-duration surveys was suggested. In Test Scenario 2, sources of uncertainty and their effects on exposures estimates were investigated. In general, the finding of Test Scenario 2 was that uncertainty affects the distribution of the number of animals projected to exceed threshold levels, but the mean number remains the same. Test Scenario 3 found that mitigation procedures involving shut-downs for animals observed within an exclusion zone may reduce the number of animals exposed, but the effectiveness depends on the probability of detecting animals near the source. Detection probability varies with species and weather. Similarly, in Test Scenario 4, it was shown that animals avoiding high sound levels (aversion) potentially reduces the number of animals exposed to levels exceeding a threshold, but there is little information available upon which to define such behavior. Mitigation and aversion were not suggested for use in the Phase II modeling. Test Scenarios 5 and 6 investigated the effects of overlapping surveys and the impact of simultaneous firing. In neither case were these occurrences found to have a practical impact on exposure estimates. In other words, the exposure estimates from closely-spaced surveys analyzed separately and summed were as high as or higher than if the two surveys were evaluated as a single, combined survey.

1.7. Phase II: Annual Acoustic Exposure Estimates

The top-level results of the Phase II analysis are estimates of the number of exposures for each species and each year from 2016 to 2025 for the entire Gulf of Mexico. To get these annual aggregate exposure estimates, 24 h average exposure estimates from each survey type were scaled by the number of expected survey days from BOEM's regulatory planning projections. Because these projections are not season-specific, surveys are assumed to be equally likely to occur at any time of the year and at any location within a given zone. The exposure estimates from the zones are summed to provide an annual exposure estimate for each species for the entire Gulf.

2. Project Overview

The overall goal of this project is to estimate the yearly acoustic exposures received by marine mammals due to geological and geophysical survey activities in the Gulf of Mexico for the coming decade. This information will be used in developing a Programmatic Environmental Impact Statement, pursuant to the Marine Mammal Protection Act petition for rule making and the consultation under Section 7 of the Endangered Species Act. Six different seismic survey types will be assessed: 2-D, 3-D narrow azimuth (NAZ), 3-D wide azimuth (WAZ), Coil, Shallow Hazard (using single airgun or boomer), and high resolution (using side-scan sonar, sub-bottom profiler, and multibeam echosounder). The exact number, type, and location of future surveys are not known, but yearly level-of-effort projections are available.

The project was divided into two phases. In Phase I, a typical WAZ survey was simulated at two locations. This was done to establish the basic methodological approach and the results used to evaluate scenarios that may influence exposure estimates. Results from the Test Scenarios were then used to guide the main modeling effort of Phase II. In Phase II, we divided the Gulf into modeling zones and simulated each survey type in each zone to estimate the potential effects of each survey. The results from each zone were summed to provide Gulf-wide estimates of effects on each marine mammal species for each survey type for each year.

A modeling workshop was held in January 2014 (in Silver Spring, MD) as a collaborative effort between the American Petroleum Institute (API) and the International Association of Geophysical Contractors (IAGC), the National Marine Fisheries Service (NMFS), and Bureau of Ocean Energy Management (BOEM). The objectives of the workshop were to identify 1) gaps in modeling sound fields from airgun arrays and other active acoustic sources, including data requirements and performance in various contexts, 2) gaps in approaches to integration of modeled sound fields with biological data to estimate marine mammal exposures, and 3) assumptions and uncertainties in approaches and resultant effects on exposure estimates. This workshop aided BOEM and NOAA’s development of the Request for Proposals, Statement of Work, and by extension the methodologies undertaken in this modeling project.

3. Introduction

3.1. The Ocean Soundscape

Human-generated (anthropogenic) contributions to the ocean's soundscape have steadily increased in the past several decades largely driven by a worldwide increase in oil and gas exploration and in shipping (Hildebrand 2009). Some anthropogenic sources, such as vessel noise, are a chronic contribution to local and global soundscapes. Other anthropogenic sources affect marine life on a more restricted temporal and spatial scale, but often produce high sound energies and may pose immediate health risks to marine wildlife. Many anthropogenic sounds are produced intentionally as part of active data gathering effort using sonar, depth sounding, and seismic surveys. When seismic surveys expanded into deep water, their sound footprints increased markedly and these signals are detectable across ocean basins (Nieukirk et al. 2004).

3.1.1. Seismic Sources

3.1.1.1. Airguns

Seismic airguns generate pulsed acoustic energy by releasing into the water highly compressed air, which forms air bubbles that undergo a damped volume oscillation and emit an acoustic pressure wave that follows the bubble's oscillating internal pressure. Seismic airguns produce sounds primarily at frequencies from a few hertz to a few kilohertz, but also produce lower level sounds at higher frequencies. Larger airguns, with larger internal air volume, produce higher broadband sound levels with sound energy spectrum shifted toward the lower frequencies. Single airguns or multiple airguns arranged in a spatial pattern (referred to as an airgun array) are typically towed by a survey vessel, with shots or impulses typically generated every 5 to 30 s along survey track lines.

A single airgun produces an approximately omnidirectional sound field—the acoustic energy is initially emitted equally in all directions. The sound signal that reflects from the water's surface, however, interacts with sounds that travel directly from the airgun. The result of this interaction is that, on average, more sound energy is focused downwardly than horizontally, an effect that is more prominent for lower frequencies. Larger 2-D and 3-D seismic surveys usually use multiple airguns arranged in arrays; this configuration emits higher overall sound levels, specifically more highly downward directed. The arrays are configured with most of the airguns in a horizontal plane. This configuration, combined with the effect of the surface reflection, focuses more sound energy downwardly, while emitting lower levels of sound horizontally. Airgun arrays generally show significant horizontal directionality patterns due to the phase delay between pulses from horizontally separated lines of airguns.

3.1.2. High-resolution Sources

3.1.2.1. Side-scan Sonar Systems

Side-scan sonar systems produce shaded relief images of the ocean bottom by recording the intensity and timing of signals reflected off the seafloor. Side-scan sonars consist of two transducers on the sides of the sonar body that are oriented orthogonally to the towing direction. The projected acoustic beams are usually wide in the vertical plane (50°−70°) and very narrow in the horizontal plane (less than a few degrees). The declination of the beam axis is small: 10°−20° below the horizon. Side-scan sonars can be

mounted on a survey vessel, towed behind it, or be part of a survey complex installed on an autonomous underwater vehicle (AUV).

3.1.2.2. Multibeam Echosounders Sonar Systems

Multibeam echosounder sonar systems use an array of transducers that project a fan-shaped beam under the hull of a survey ship and orthogonal to the direction of motion. The system measures the time for the acoustic signal to travel to the ocean floor and back to the receiver. The multibeam echosounder produces a swath of depth measurements to ensure full coverage of an area. The coverage area on the seafloor is typically two to four times the water depth. Many multibeam echosounder systems can record acoustic backscatter data. Multibeam backscatter is intensity data that, when processed, creates a low-resolution image which often helps interpret and post-process the bathymetric data. Instead of deploying the multibeam echosounder under the hull of the survey ship, it can alternatively be deployed on an AUV.

3.1.2.3. Sub-bottom Profiler Sonar Systems

Sub-bottom profiler sonar systems are used to generate vertical cross-section plots of the layers of sediment under the ocean floor. To make measurements, the sub-bottom profiler is towed behind a survey vessel or deployed on an AUV. The towed body of the sub-bottom profiles system contains the acoustic source and receiver elements. The source transducer projects a chirp pulse that spans an operator-selectable frequency band. The lower and upper limits of the sonar's frequency band are usually between ~ 1 to 20 kHz. The system projects a single beam directed vertically down. The projected beamwidth depends on the operating frequency, but is approximately 10°−30°.

3.1.2.4. Boomer Sources

Some sub-bottom profiler systems use a boomer source, which consists of an insulated metal plate paired with an adjacent electromagnetic Coil. A powerful electrical discharge pulse generated by a shipboard power supply and capacitor bank is applied to the Coil, generating an abrupt and strong magnetic field that repels the metal plate. The resulting mechanical impulse generates a high-amplitude broadband acoustic pulse in the water, with high downward directivity (Verbeek and McGee 1995). The boomer source functions as a circular piston surrounded by a rigid baffle; it is not a point-like source (Verbeek and McGee 1995) because the beam pattern of a boomer plate shows some directivity for frequencies above 1 kHz, where acoustic wavelength is on the same order of magnitude as the baffle size.

3.1.3. Pulsed Versus Non-Pulsed Sounds

Anthropogenic sounds can affect marine life in a variety of ways. Numerous scientific reviews and workshops over the past 40 years have investigated these effects (Payne and Webb 1971, Fletcher and Busnel 1978, Richardson et al. 1995, MMC 2007, Nowacek et al. 2007, Southall et al. 2007, Weilgart 2007, Tyack 2008). Anthropogenic sounds that could affect marine life are generally divided into two main categories when they are investigated—pulsed divided into single and multiple, and non-pulsed sounds (Southall et al. 2007). Pulsed or impulsive sounds include pile driving and airgun shots as well as some sonar; non-pulsed, continuous-types of sounds include certain sonar and vessel propulsion sounds and machinery sounds. Numerous definitions and mathematical distinctions distinguish pulsed from non-pulsed sounds (Burdic 2003). Southall et al. (2007) adopted a measurement-based distinction originally proposed by Harris (1998) that if measurements between the continuous and impulse sound level meter settings differ by ≥ 3 dB, a sound is pulsed, whereas if the difference is < 3 dB the sound is non-pulsed. The distinction between these two sound types, however, is not always obvious. Certain signals, for example those from acoustic deterrent or harassment devices, share properties of both pulsed and non-

pulsed sounds. A signal near a source could be categorized as a pulse, but due to propagation effects as it moves farther from the source, it could be categorized as non-pulsed (e.g., Greene and Richardson 1988).

3.2. Acoustic Metrics

Underwater sound pressure amplitude is commonly measured in decibels (dB) relative to a fixed reference pressure of p_o = 1 μPa. Because the loudness and other exposure effects of impulsive (pulsed) noise, e.g., shots from seismic airguns, are not generally proportional to the instantaneous acoustic pressure, several sound level metrics are commonly used to evaluate impulsive sound effects on marine life.

The zero-to-peak sound pressure level (SPL), or peak SPL (L_{pk}, dB re 1 μPa), is the maximum instantaneous sound pressure level in a stated frequency band attained by an impulse, $p(t)$:

$$L_{\mathrm{pk}} = 10\log_{10}\left[\frac{\max\left(\left|p^2(t)\right|\right)}{p_{\mathrm{o}}^2}\right] \tag{1}$$

The peak-to-peak SPL ($L_{pk\text{-}pk}$, dB re 1 μPa) is the difference between the maximum and minimum instantaneous sound pressure level in a stated frequency band attained by an impulse, $p(t)$:

$$L_{\mathrm{pk-pk}} = 10\log_{10}\left\{\frac{\left[\max\left(p(t)\right)-\min\left(p(t)\right)\right]^2}{p_{\mathrm{o}}^2}\right\} \tag{2}$$

The root-mean square (rms) SPL (L_p, dB re 1 μPa) is the rms pressure level in a stated frequency band over a time window (T, s) containing the pulse:

$$L_p = 10\log_{10}\left(\frac{1}{T}\int_T p^2(t)dt \Big/ p_{\mathrm{o}}^2\right) \tag{3}$$

The rms SPL can be thought of as a measure related to the average sound intensity or as the effective pressure intensity over the duration of an acoustic event, such as the emission of one acoustic pulse. Because the time window length, T, is a divisor, pulses having the same total acoustic energy, but more spread out in time, will have a lower rms SPL. The value of T for the purpose of the rms SPL calculation can be selected using different approaches. According to one, T is defined as the 90% energy pulse duration, containing the central 90% (from 5% to 95% of the total) of the cumulative square pressure (or sound exposure level) of the pulse, rather than over a fixed time window (Malme et al. 1986, Greene 1997, McCauley et al. 1998). The 90% rms SPL (L_{p90}, dB re 1 μPa) in a stated frequency band is calculated over this 90% energy time window, T_{90}:

$$L_{p90} = 10\log_{10}\left(\frac{1}{T_{90}}\int_{T_{90}} p^2(t)dt \Big/ p_{\mathrm{o}}^2\right) \tag{4}$$

The other approach for rms SPL calculation of a pulse is to use fixed time window. In this case, a sliding window was used to calculate rms SPL values for a series of fixed window lengths within the pulse. The maximum value of rms SPL over all time window positions is taken to represent the rms SPL of the pulse.

The sound exposure level (SEL) (L_E, dB re 1 μPa^2·s) is the time integral of the squared pressure in a stated frequency band over a stated time interval or event. The per-pulse SEL is calculated over the time window containing the entire pulse (i.e., 100% of the acoustic energy), T_{100}:

$$L_E = 10\log_{10}\left(\int_{T_{100}} p^2(t)dt \Big/ T_o p_o^2\right) \tag{5}$$

where T_o is a reference time interval of 1 s by convention. The per-pulse SEL, with units of dB re 1 μPa·√s, or equivalently dB re 1 μPa^2·s, is related, at least numerically, to the total acoustic energy flux density delivered over the duration of the acoustic event at a receiver location. SEL, unlike energy flux density, neglects the acoustic impedance of the medium (here water), which depends on density and sound speed and also on proximity to reflective surfaces and position within refractive environments. SEL is a measure of sound exposure through time rather than just sound pressure.

SEL is a cumulative metric; it can be accumulated over a single pulse, or calculated over periods containing multiple pulses. To accumulate multiple pulse cumulative SEL (L_{Ec}), the single pulse SELs are summed. If there are N such pulses having individual SELs of (L_{Ei}), then:

$$L_{Ec} = 10\log_{10}\left(\sum_{i=1}^{N} 10^{\frac{L_{Ei}}{10}}\right) \tag{6}$$

The SEL is related to the total acoustic energy flux density delivered over the duration of the set period of time, i.e., 24 h. It is a representation of the accumulated SEL delivered by multiple acoustic events, e.g., multiple pulses of a single acoustic source.

Because the rms SPL and SEL of a single pulse are computed from the same time integral of square pressure, these metrics are related numerically by a simple expression, which depends only on the duration of the 90% energy time window T_{90}:

$$L_E = L_{p90} + 10\log_{10}(T_{90}) + 0.458 \tag{7}$$

where the factor of 0.458 dB accounts for the missing 10% of SEL due to consideration of just 90% of the cumulative square pressure in the L_{p90} calculation. It is important to note that the decibel reference units of L_E and L_{p90} are not the same, so this expression must be interpreted only in a numerical sense. No similar relationship exists when SPL is calculated using fixed time windows shorter than the full pulse duration, T_{100}; however, if the window length T is equal to or greater than T_{100} then the relationship is simply:

$$L_E = L_p + 10\log_{10}(T) \tag{8}$$

3.3. Use of Sounds by Marine Species

Sounds tend to travel farther than light in water. Many marine species use underwater acoustic signals as their principal mode of information transfer. Cetaceans (whales, dolphins, and porpoises) and sirenians (manatees and dugongs) use sounds passively, when listening to the environment, and actively, when communicating or foraging. Cetaceans in particular are heavily dependent on sounds for communicating, avoiding predators, foraging, and likely for navigating. Anthropogenic sounds in the ocean might interfere with basic life functions of marine species, especially marine mammals.

3.3.1. Cetacean Hearing

Marine mammals have broader hearing frequency ranges than terrestrial mammals, an indication of how important sounds are to them. Because marine mammals evolved from terrestrial mammals, their basic hearing anatomy and physiology resembles that of their terrestrial ancestors. Divergence between terrestrial and marine mammals is primarily apparent in their outer ear structures—absent in cetacean species—and in the middle ear—modified in marine mammals (Mooney et al. 2012).

The majority of detailed data on hearing ranges come from a subset of trained small cetaceans housed in captive settings who are amenable to training (see Southall et al. 2007 for review). Direct hearing data are not available for most of the cetacean species, particularly larger whales, but biophysical procedures and mathematical models have been developed to try to derive audiograms (e.g. Tubelli et al. 2012, Cranford and Krysl 2015) for many mysticete species. In addition, measurements of auditory evoked potentials (AEP) to determine hearing ranges have been successful when applied to some stranded animals (reviewed by Mooney et al. 2012).

3.3.1.1. Classification of Cetacean Hearing

Southall et al. (2007) categorized cetaceans into three functional hearing groups: low-, mid-, and high-frequency cetaceans (Table 1). These groups were defined based on similarities in their known or assumed hearing capabilities rather than their taxonomy.

All low-frequency hearing specialists among cetaceans are mysticetes (baleen whales), which consist of seven species in five genera. Wartzok and Ketten (1999) found mysticetes to be most sensitive to sounds with frequencies in the tens of hertz to lower tens of kilohertz. Some findings, however, suggest that humpback whales (*Megaptera novaeangliae*) produce signals with harmonics extending above 24 kHz (Au et al. 2006). Computational models of the minke whale (*Balaenoptera acutorostrata*) middle ear predicted that their hearing frequency range is between 100 Hz and 30 kHz (Tubelli et al. 2012). Modeling based on computer tomography scans of a juvenile fin whale (*Balaenoptera physalus)* ear predicted their best hearing range is between 20 Hz and 20 kHz (Cranford and Krysl 2015). All of these findings suggest mysticete body size and hearing range are related, with larger whales being sensitive to very low frequencies (< 100 Hz) and smaller mysticetes hearing higher frequencies (> 20 kHz) better than their larger counterparts. From a functional perspective, all cetaceans should be able to hear the important frequencies in signals they produce and to hear predators well. For most cetaceans, including all mysticetes, killer whales are their primary predator. Killer whales produce broadband signals (calls and clicks) with a large portion of signal energy between 1 and 25 kHz. This frequency range is detectable by all cetaceans including low frequency specialists.

Mid- and high-frequency cetaceans are all odontocetes (toothed whales) who have a broad (150 Hz to 180 kHz) functional hearing frequency range. They use echolocation (biosonar) at intermediate to high frequencies (tens of hertz to tens of kilohertz), and produce social sounds in the lower frequency range (one kHz to tens of kHz).

Mid-frequency cetacean adults have a large range in size. This group includes dolphins, larger toothed whales, such as sperm whales, and beaked whales and bottlenose whales (*Hyperoodon ampullatus*; Southall et al. 2007). Mid-frequency cetaceans are estimated to have lower and upper frequency limits of nominal hearing at approximately 150 Hz and 160 kHz, respectively (Table 1).

High-frequency cetaceans are typically characterized by a smaller body size and include, notably, porpoises, but also dwarf and pygmy sperm whales (*Kogia* sp.; Southall et al. 2007). High-frequency cetaceans produce echolocation clicks in a wide range of frequencies, which correspond well with the estimated lower and upper frequency limits of nominal hearing at approximately 200 Hz and 180 kHz, respectively (Table 1).

Table 1. Marine mammal functional hearing groups, auditory bandwidth (estimated lower to upper frequency hearing cut-off), and genera represented in each group. Modified from Southall et al. (2007).

Functional hearing group	Estimated auditory bandwidth	Genera represented in the Gulf of Mexico	Number of species/subspecies
Low-frequency cetaceans	7 Hz to 22 kHz	*Balaenoptera*	1
Mid-frequency cetaceans	150 Hz to 160 kHz	*Steno, Tursiops, Stenella, Lagenodelphis, Grampus, Peponocephala, Feresa, Pseudorca, Orcinus, Globicephala, Physeter, Ziphius, Mesoplodon*	18
High-frequency cetaceans	200 Hz to 180 kHz	*Kogia*	2

3.4. Potential Effects of Sounds on Marine Mammals

The sounds that marine mammals hear and generate vary in characteristics such as dominant frequency, bandwidth, energy, temporal pattern, and directivity. The environment often contains multiple co-occurring sounds and, like all animals, marine mammals must be able to discriminate signals (meaningful sounds) from background sounds. Just as terrestrial animals integrate multiple stimuli from their visual landscape, marine mammals tend to discriminate among multiple stimuli in their acoustic seascape.

Responses of marine mammals exposed to underwater anthropogenic sounds are variable and range from no effect to injury. The magnitude of the effect appears to depend on a combination of various factors, such as spatial relationships between a sound source and the animal, hearing sensitivity of the animal, received sound exposure, duration of exposure, duty cycle, and ambient sound level. Among other ecological factors, the animal's activity at time of exposure and its history of exposure and familiarity with the noise signal are important influences.

The potential effects of sounds on individual marine mammals can be broadly categorized as follows (based on Richardson et al. 1995, Southall et al. 2007):

- Trauma and death
- Temporary and permanent hearing loss
- Non-auditory health effects
- Self-stranding
- Auditory signal masking
- Behavioral disturbance
- Reduced availability of prey

All of these effects can lead to potential removal of individuals and subsequent population consequences. Sections 3.4.1–3.4.5 briefly discuss several of these effects.

3.4.1. Auditory Signal Masking

Auditory signal masking is the reduction in an animal's ability to perceive, recognize or decode biologically relevant sounds because of interfering sounds. Masking may lead to altered communications

and, potentially, increased metabolic costs (for example, due to increased call amplitude and repetition). The amplitude, timing, and spectral content of the interfering sounds determine the amount of masking an animal experiences. Masking can decrease the range over which an animal communicates, detects predators, or finds food.

The study of masking in the ocean has traditionally focused on interactions between shipping sounds and mysticetes because these whales communicate using low-frequency calls in the same frequency bands as shipping sounds (Payne and Webb 1971). Over the past 50 years commercial shipping, the largest contributor of masking noise (McDonald et al. 2008), has increased the ambient sound levels in the deep ocean at low frequencies by 10–15 dB (Hatch and Wright 2007). Hatch et al. (2012) estimate that calling North Atlantic right whales (*Eubalaena glacialis*) might have lost, on average, 63–67% of their active acoustic or communication space due to shipping noise.

Sounds from seismic surveys contribute to ocean-wide masking (Hildebrand 2009). Impulse sounds produced during pile driving operations in particular in connection with wind farm installations have been found to mask the calls of marine mammals at great distances (Madsen et al. 2006). Gordon et al. (2003) listed a range of possible effects of seismic impulses on cetacean behavior and communication including masking of sounds used during foraging, such as echolocation.

Cumulative effects of seismic operations and other anthropogenic sound on marine mammals is poorly understood, but there is increasing concerns about masking by ship sounds at higher frequency ranges (e.g., up to 30 kHz; Arveson and Vendittis 2000); (up to 44.8 kHz; Aguilar Soto et al. 2006) at distances up to at least 700 m from the source (Aguilar Soto et al. 2006). Aguilar Soto et al. (2006) recorded a passing vessel on a Digital Acoustic Recording Tag (DTAG) attached to a Cuvier's beaked whale. This recording demonstrated that vessel sounds masked the whale's ultrasonic vocalizations and reduced its maximum communication range by 82% when ambient sound levels increased 15 dB in the vocalization frequencies. The study also determined that the effective detection distance of Cuvier's beaked whales' echolocation clicks was reduced by 58%. It is important to note, however, that these calculations are based on observed noise increases at high frequencies from a single passing vessel at close range, and that noise profiles from ships are highly variable, and high-frequency components attenuate more rapidly than do low frequencies (Hatch and Wright 2007). The reduction in communication space Cuvier's beaked whales would experience at greater distance from the source is much lower.

3.4.2. Behavioral Disturbance

The extent by which an animal's behavior changes in response to underwater sounds can vary greatly, even within the same species (Nowacek et al. 2004). The extent of an individual's response to a stimulus is influenced largely by the context in which the stimulus is received and the relevance that an individual attributes to the acoustic stimulus. The perceived relevance depends on a number of biological and environmental factors, such as age, sex, and behavioral state at the time of exposure (e.g., resting, foraging, or socializing), the origin of the sounds, and the proximity of the sound source. An immediate response to anthropogenic sounds is that animals temporarily avoid or move away from an ensonified area; however, they might also respond more conspicuously based on how close the sound sources are. For instance, their vigilance, defined as scanning for the source of the stimulus, could increase. The more time an animal invests in addressing noise means less time they can spend foraging (Purser and Radford 2011), but this is not always easy to detect.

Marine mammals have reduced their vocalization rates in response to anthropogenic sounds, sometimes not calling for weeks or months (IWC 2007). Some cetaceans might compensate for masking, to a limited degree, by increasing the amplitude of their calls (the Lombard effect, a known response of humans to noise) or by changing vocalization properties such as frequency content (Parks et al. 2010, Hotchkin and Parks 2013). As ambient noise levels increase, killer whales have been known to increase the amplitude

of their calls (Holt et al. 2009). North Atlantic right whales produced calls with a higher average fundamental frequency and lowered their call rates in high noise conditions (Parks et al. 2007, Parks et al. 2009), whereas blue whales (*Balaenoptera musculus*) increased the frequency of their discrete, audible calls during a seismic survey (Di Iorio and Clark 2010) or when nearby ships made sounds (Melcon et al. 2012). A long signal or one that repeats could reduce an animal's ability to perceive biologically relevant sounds in a noisy environment. Whales seem most reactive at the onset of a sound and when the sound levels are increasing rapidly. All of these responses increase an animal's metabolic costs and, depending on the animal's metabolic state and the duration of its response, can negatively affect its health.

Although limited, some data suggest that stationary industrial activities that produce continuous sounds such as dredging, drilling, and oil-production-related activities, cause cetaceans to react less than sounds produced by moving sources, particularly ships. Some cetaceans might behaviorally habituate to reliably occurring continuous sounds (Richardson et al. 1995), a response that has also been observed in humans where some physiological habituation (lower endocrine stress responses) to prolonged noise exposure can occur. However, the act of responding could indirectly affect health through related physiological responses, such as cardiovascular stress responses (e.g., increased blood pressure; Christal and Whitehead 2001).

Stone and Tasker (2006) reported that airgun sounds elicited strong reactions—moving away from or avoiding an ensonified area—by small odontocetes. Mysticetes and killer whales responded by diverting paths and long-finned pilot whales changed their orientation. Controlled exposure experiments were conducted with eight tagged sperm whales over a series of 30-min intervals during pre-exposure, ramp-up, and full-array airgun firing (Miller et al. 2009). Results showed seven whales did not avoid airgun sounds. They did not change their buzz rates; however, oscillations in pitch were affected. Following the final airgun transmission, only one individual rested at the surface during the sound exposure and dove immediately thereafter. Miller et al. (2009) concluded that sperm whales in the highly exposed Gulf of Mexico habitat do not show any significant avoidance response to airguns, a lack of reaction that Rankin and Evans (1998) also noticed, but exhibited subtle effects on their foraging behavior.

Others suggested some mysticetes might change their habitat usage considerably after they are exposed to seismic sounds. During the first 72 h of a 10-day seismic survey, fin whales appeared to move away from the airgun array; this displacement persisted well beyond the 10 days of seismic airgun activity (Castellote et al. 2012). It was unknown, however, if the whales were avoiding the sound or following another cue such as a prey. McDonald et al. (1995) observed blue whales' responses to airgun firing. They stopped singing within a 10 km radius of the source, although this could have been a direct response to avoid their sounds being masked.

For reactions to pulsed sounds specifically, there is evidence that the behavioral state (traveling/migrating, foraging, resting, or socializing) of baleen whales exposed to seismic sounds (McCauley et al. 1998, Gordon et al. 2003), combined with their proximity to the airguns, affects how the whales react to the sounds. Several species of baleen whales showed avoidance behavior to sounds from seismic surveys (Richardson et al. 1995); bowhead whales (*Balaena mysticetus*) avoided distant seismic airguns at received levels of rms SPL of 120–130 dB re 1 µPa during their fall migration (Richardson et al. 1999). Feeding bowhead whales in the summer were more tolerant to airgun sounds avoiding airguns only when received levels reached 152–178 dB re 1 µPa, which is roughly 10,000 times louder than avoidance levels of the migrating whales (Richardson et al. 1995). Different sexes might also react differently when exposed to seismic signals. Resting female humpback whales avoided seismic surveys by diverting their travel paths to remain 7–12 km away, while males were occasionally attracted to the sounds (McCauley et al. 2000b).

For other pulsed sound sources, Brandt et al. (2011) and (Dähne et al. 2013) reported that harbor porpoises (*Phocoena phocoena*) were displaced from an area by pile driving noises, a repeating impulsive sound, while male humpback whales either moved out of a study area or sang less when exposed to

frequency-modulated pulses that were 200 km away (Risch et al. 2012). Humpback whales also lengthened their mating songs when they were exposed to low-frequency active (LFA) sonar (Miller et al. 2000). Long-finned pilot whales whistled more in response to military mid-frequency sonar (Rendell and Gordon 1999). Castellote et al. (2012) noted that in response to shipping and airgun noise, fin whale calls were of shorter duration, lower frequency ranges, and lowered center and peak frequencies.

In their review of the effect of non-pulsed (continuous) sounds on cetaceans, Southall et al. (2007) reported that low-frequency cetaceans exhibited no or limited responses with received levels up to 120 dB re 1 µPa, but an increasing probability of avoidance (and other behavioral responses) beginning at received levels between 120 to 160 dB re 1 µPa. Reports of possible behavioral responses to non-pulsed sounds include harbor porpoises (high-frequency cetaceans) that generally swam away from approaching vessels (Polacheck and Thorpe 1990) or moved rapidly out of the way of an approaching survey vessel when the vessel was 1 km away (Barlow 1988). In both studies, however, it was unclear whether it was the approaching vessel or its sound that elicited the response, although reacting at 1 km suggests the animal was reacting to the sound.

Aguilar Soto et al. (2006) noted a Cuvier's beaked whale responding to ship sounds by decreasing the vocalizations they normally make when trying to catch prey. Blainville's beaked whales changed their foraging after they were exposed to vessel noise (Pirotta et al. 2012). Groups of Pacific humpback dolphins (*Sousa chinensis*) that contained mother-calf pairs increased their whistling rate after a boat had transited the area (Van Parijs and Corkeron 2001). The authors postulated that vessel sounds disrupted group cohesion, especially between mother-calf pairs, requiring the group to re-establish vocal contact after signal masking from boat noise. In responses to high levels of boat traffic, the duration (Foote et al. 2004) or the amplitude (Holt et al. 2009) of killer whale calls increased. Common bottlenose dolphins produced more whistles when boats approached (Buckstaff 2004).

3.4.3. Temporary and Permanent Hearing Loss

Physical impacts to an animal's auditory system can occur from exposure to intense sounds and can result in the animal losing hearing sensitivity. A temporary threshold shift (TTS) is hearing loss that persists only for minutes or hours, whereas a permanent threshold shift (PTS) is indefinite. The severity of TTS is expressed as the duration of hearing impairment (lowered sensitivity in the bandwidths in which the noise was centered) and the magnitude of the shift in hearing sensitivity relative to pre-exposure sensitivity. TTS generally occurs at lower sound levels than PTS. Repeated TTS, especially if the animal is receiving another loud sound exposure before recovering from the previous TTS, is thought to cause PTS (Lin et al. 2011). If the sound is intense enough, however, an animal can succumb to PTS without first experiencing TTS (Weilgart 2007). Though the relationship between the onset of TTS and the onset of PTS is not fully understood, TTS onset is used to predict sound levels that are likely to result in PTS.

Recent studies have modeled the potential impacts (TTS: Kremser et al. 2005; PTS: Lurton and DeRuiter 2011) of echosounders on marine mammals. The results from the studies suggest that TTS and PTS occur generally at distances of 100 m or less and most important, only apply in the cone ensonified by the modeled echosounders, meaning only animals below the ship are exposed to these levels. Animals at the same distances but to the sides of the vessel will be exposed to lower levels.

Experiments with captive common bottlenose dolphins have shown that loud, short (1 s) tonal sounds can cause TTS (Schlundt et al. 2000), as can lower sound level exposures for periods up to 50 min (Finneran et al. 2005, Nachtigall et al 2005, Nachtigall et al. 2004). Impulsive sounds from a watergun (Finneran et al. 2002) or an airgun (Lucke et al. 2009) have also been shown to cause TTS in beluga whales and harbor porpoises, respectively. Cook (2006) found that captive odontocetes typically experienced more hearing loss than similar-aged free-ranging dolphins. Older captive common bottlenose dolphins are known to have reduced hearing sensitivity, especially at higher frequencies, but whether the cause of this hearing

loss is related to captivity is unknown (Ridgway and Carder 1997); it could simply be the phenomenon of reduced high frequency sensitivity with age that occurs in humans.

3.4.4. Non-Auditory Health Effects

Scientists have studied the physiological stress response of captive marine mammals to noise. When Thomas et al. (1990) played drilling noise to four captive beluga whales, they measured their stress hormone levels (blood adrenaline/epinephrine and noradrenaline/norepinephrine) immediately after playback and found no changes in them. After exposing a captive common bottlenose dolphin and a captive beluga whale to sounds from a seismic watergun, Romano et al. (2004) found changes in some hormones and blood cell counts—from the common bottlenose dolphin, with aldosterone and monocytes levels; from the beluga, epinephrine, norepinephrine, and dopamine levels. Miksis et al. (2001) found that the heart rate in a captive common bottlenose dolphin increased in response to threat sounds produced by other dolphins. Rolland et al. (2012) demonstrated that exposing right whales to low-frequency ship noise might be associated with chronic stress.

Crum and Mao (1996) hypothesized that when marine mammals are exposed to high-intensity low-frequency sounds, gas bubbles might form in their tissues, a process called rectified diffusion. The physiological state of a diving cetacean when it is exposed to sounds determines its susceptibility to rectified diffusion. Diving speed and depth of diving are the primary determinants of the amount of nitrogen that can accumulate in tissues, with slower rates of ascent/descent and deeper dives increasing gas supersaturation (accumulation of higher levels of nitrogen than would be possible at atmospheric pressure). Acoustic activation or generation of bubble nuclei before the animal surfaces or when it is just at the surface, can theoretically drive bubbles to grow rapidly by the degree of supersaturation and the animal's continued exposure to sounds (Houser et al. 2001). Bubble growth can damage tissue and block blood vessels. In deep-diving marine mammals, such as beaked whales, Fernández et al. (2005) calculated supersaturation at over 300%, and found bubbles in some stranded beaked whales' tissues.

Animals that change their behavior in response to sounds could injure themselves. Although the sound characteristics and behavioral and physiological mechanisms behind strandings are not fully understood, some scientists believe acoustic exposure might be a culprit, noting particularly the association between military mid-frequency sonar and strandings of melon-headed whales (Southall et al. 2006, 2013), beaked whales (D'Amico et al. 2009) and common dolphins (Jepson et al. 2013). Because beaked whales are extreme divers that undergo gas supersaturation, exposure to sounds that induces them to ascend more rapidly might put them at risk of tissue-damaging nitrogen bubbles forming, similar to decompression sickness that human divers experience (Cox et al. 2006). Alternatively, if beaked whales remain submerged longer because of acoustic exposure, hypoxia could damage their tissues (Cox et al. 2006).

3.4.5. Reduction of Prey Availability

Sound might indirectly affect marine mammals by altering prey abundance, behavior, and distribution. Rising sound levels could affect fish populations (McCauley et al. 2003, Popper and Hastings 2009, Slabbekoorn et al. 2010). Marine fish are typically sensitive to the 100–500 Hz range, where most seismic sounds are produced.

Several studies have demonstrated that anthropogenic sounds might affect the behavior of at least some species of fish. For example, field studies by Engås et al. (1996) and Whitlock and Schluter (2009) showed that when seismic airguns were operating the catch rate of haddock (*Melanogrammus aeglefinus*) and Atlantic cod (*Gadus morhua*) significantly declined over the five days following, after which the catch rate returned to normal. Engås et al. (1996) and Whitlock and Schluter (2009) suggested that the catch rate declined because fish were responding to the sounds of the airguns by avoiding the area of

ensonification. Slotte et al. (2004) showed parallel results for several other pelagic species. Fish near the airguns appeared to move to greater depths after being exposed to airguns. Moreover, because the number of fish 30–50 km away from the ensonification area increased, it seems likely that migrating fish avoided the seismic activity zone. Other studies found only minor responses by fish to noise created during or following seismic surveys, such as a small decline in lesser sandeel (*Ammodytes marinus*) abundance that quickly returned to pre-seismic levels (Hassel et al. 2004), or no permanent changes in the behavior of marine reef fishes (Wardle et al. 2001). Both Hassel et al. (2004) and Wardle et al. (2001), however, noted that when fish saw the airgun firing they performed a startle response and sometimes fled.

Squid (*Sepioteuthis australis*) are an extremely important food chain component for many higher order predators, including sperm whales. McCauley et al. (2000b) recorded caged squid responding to airgun signals. They exhibited strong startle responses to a nearby airgun starting up: they fired their ink sacs and/or jetted away from the airgun source. Squid also avoided the airgun by staying close to the water surface near the cage end farthest from the airgun.

The effects of sounds on fish and squid are still poorly understand. Although some fish additionally sense pressure, all fish and squid sense particle motion, and particle motion is not always directly related to pressure measurements. While no studies have investigated the indirect effects of seismic airguns on marine mammals' prey availability, it is possible that seismic surveys could change the feeding opportunities available to marine mammals, especially in cases of restricted foraging locations.

4. Marine Mammals in the Gulf of Mexico

Twenty-one cetacean species have been sighted in marine mammal surveys since 1991(Waring et al. 2013). Eighteen are mid-frequency hearing specialists. Bryde's whales are the only low-frequency species. Dwarf and pygmy sperm whales comprise the only high-frequency hearing specialist group.

Table 2 lists these species, their functional hearing group, and preferred habitat. Determining the risk of acoustic exposure to a population of animals requires an estimate of the number of animals in that area. Occurrence and abundance estimates are determined from surveys that identify, count, and log the position of species in various waters. From these data, models have been created to provide estimates of likely densities) along transect lines and between lines. In Phase I, the Navy's U.S. Navy OPAREA Density Estimate (NODE; DoN 2007) model was used to obtain animal density estimates (see Section 6.2.5). In Phase II, density estimates were obtained from the Marine Geospatial Ecology Laboratory at Duke University preliminary results (Roberts et al. In preparation; see Section 7.2.6).

Table 2. Marine mammal species considered in the acoustic exposure analysis.

Common name	Latin binomial	Functional hearing group	Preferred habitat
Atlantic spotted dolphins	*Stenella frontalis*	MFC	Primarily coastal (< 200 m)
Beaked whales spp. (Cuvier's, Blainville's, Gervais')	*Mesoplodon densirostris, Ziphius cavirostris, Mesoplodon europaeus*	MFC	Oceanic
Common bottlenose dolphins	*Tursiops truncatus*	MFC	Primarily coastal (< 200 m), occasionally oceanic
Bryde's whales	*Balaenoptera brydei/edeni*	LFC	Oceanic
Clymene dolphins	*Stenella clymene*	MFC	Oceanic
False killer whales	*Pseudorca crassidens*	MFC	Oceanic
Fraser's dolphins	*Lagenodelphis hosei*	MFC	Oceanic
Killer whales	*Orcinus orca*	MFC	Various
Kogia spp. (Dwarf sperm whales, Pygmy sperm whales)	*Kogia sima, Kogia breviceps*	HFC	Oceanic
Melon-headed whales	*Peponocephala electra*	MFC	Oceanic
Pantropical spotted dolphins	*Stenella attenuata*	MFC	Oceanic
Pygmy killer whales	*Feresa attentuata*	MFC	Oceanic
Risso's dolphins	*Grampus griseus*	MFC	Oceanic
Rough-toothed dolphins	*Steno bredanesis*	MFC	Oceanic
Short-finned pilot whales	*Globicephala macrorhyncus*	MFC	Various
Sperm whales	*Physeter macrocephalus*	MFC	Oceanic
Spinner dolphins	*Stenella longirostris*	MFC	Oceanic
Striped dolphins	*Stenella coeruleoalba*	MFC	Oceanic

LFC=Low-frequency cetacean; MFC=Mid-frequency cetacean; HFC=High-frequency cetacean.

5. Modeling Methodology

5.1. Acoustic Source Model

5.1.1. Airgun and Airgun Array Modeling Methodology

The source levels and directivity of the airgun array were predicted with JASCO's Airgun Array Source Model (AASM; Austin et al. 2010). This model is based on the physics of oscillation and radiation of airgun bubbles described by Ziolkowski (1970). The model solves the set of parallel differential equations that govern bubble oscillations. AASM also accounts for nonlinear pressure interactions between airguns, port throttling, bubble damping, and generator-injector gun behavior that are discussed by Dragoset (1984), Laws et al. (1990), and Landro (1992). AASM includes four empirical parameters that were tuned so that model output matches observed airgun behavior. The model was originally fit to a large library of empirical airgun data using a simulated annealing global optimization algorithm. These airgun data consisted of measured signatures of Bolt 600/B airguns ranging in volume from 5 to 185 in^3 (Racca and Scrimger 1986).

While airgun signatures are highly repeatable at the low frequencies used for seismic imaging, their sound emissions have a random component at higher frequencies that cannot be predicted using a deterministic model. Therefore, AASM uses a stochastic simulation to predict the high-frequency (560−25,000 Hz) sound emissions of individual airguns, using a data-driven multiple-regression model. The multiple-regression model is based on a statistical analysis of a large collection of high quality seismic source signature data recently obtained from the Joint Industry Program (JIP) on Sound and Marine Life (Mattsson and Jenkerson 2008). The stochastic model uses a Monte-Carlo simulation to simulate the random component of the high-frequency spectrum of each airgun in an array. The mean high-frequency spectra from the stochastic model augment the low-frequency signatures from the physical model, making AASM capable of predicting airgun source levels at frequencies up to 25,000 Hz.

AASM produces a set of notional signatures for each airgun element based on:

- Array layout
- Volume, tow depth, and firing pressure of each airgun
- Interactions between different airguns in the array

These notional signatures are the pressure waveforms of the individual airguns at a standard reference distance of 1 m; they account for the interactions with the other airguns in the array. The signatures are summed with the appropriate phase delays to obtain the far-field[2] source signature of the entire array in the horizontal plane. This far-field array signature is filtered into 1/3-octave passbands to compute the source levels of the array as a function of frequency band and azimuthal angle in the horizontal plane (at the source depth), after which it is considered to be an azimuth-dependent directional point source in the far field.

[2] The far field is the zone where, to an observer, sound originating from a spatially-distributed source appears to radiate from a single point. The distance to the acoustic far field increases with frequency.

A seismic array consists of many sources. The point-source assumption is invalid in the near field where the array elements add incoherently. The maximum extent of the near field of an array (R_{nf}) is:

$$R_{nf} < \frac{l^2}{4\lambda} \tag{9}$$

where λ is the sound wavelength and l is the longest dimension of the array (Lurton 2002 Section 5.2.4). For example, an airgun array length of $l \approx 16$ m yields a near-field range of 85 m at 2 kHz and 17 m at 100 Hz. Beyond R_{nf} range, the array is assumed to radiate like a directional point source and is treated as such for propagation modeling.

The AASM accurately predicts the source level of the complete array as a point source for acoustic propagation modeling in the far field; however, predicted source levels for zero-to-peak SPL and sound exposure level (SEL) metrics might be higher than the possible maximum levels during the array operation even within the array.

The interactions between individual elements of the array create directionality in the overall acoustic emission. Generally, this directionality is prominent mainly at frequencies in the mid-range between tens of hertz to several hundred hertz. At lower frequencies, with acoustic wavelengths much larger than the inter-airgun separation distances, the directionality is small. At higher frequencies, the pattern of lobes is too finely spaced to be resolved and there is less effective directivity.

5.1.2. Electromechanical Source Modeling—Transducer Beam Theory

Mid- and high-frequency underwater acoustic sources for geophysical measurements create an oscillatory overpressure by either electromagnetic forces or the piezoelectric effect rapidly vibrating the surface of the source. A vibratory source based on the piezoelectric effect is commonly referred to as a transducer, and piezo transducers are often able to receive and emit signals. Transducers are usually designed to produce an acoustic wave of a specific frequency, often in a highly directive beam. The directional capability increases with increasing operating frequency. The main parameter characterizing directivity is beamwidth, defined as the angle subtended by diametrically opposite half power (−3 dB) points of the main lobe (Massa 2003). Depending on the frequency and size of the transducer, the beamwidth can vary from 180° (almost omnidirectional) to less than 1 degree.

Transducers are commonly designed with either circular or rectangular active surfaces. For circular transducers, the beamwidth in the horizontal plane (assuming a downward pointing main beam) is equal in all directions. Rectangular transducers produce more complex beam patterns with variable beamwidth in the horizontal plane; two beamwidth values are usually specified for orthogonal axes.

The acoustic radiation pattern, or beam pattern, of a transducer is the relative measure of acoustic transmitting or receiving power as a function of spatial angle. Directionality is generally measured in decibels relative to the maximum radiation level along the central axis perpendicular to the transducer surface. The pattern is defined largely by the operating frequency of the device and the size and shape of the transducer. Beam patterns generally consist of a main lobe, extending along the central axis of the transducer, and multiple secondary lobes separated by nulls. The width of the main lobe depends on the size of the active surface relative to the sound wavelength in the medium, with larger transducers producing narrower beams. Figure 1 presents a 3-dimensional (3-D) visualization of a generic beam pattern of a circular transducer.

The true beam pattern of a transducer can be obtained only by measuring the emitted energy around the device when it is in place. Such data, however, are not always available. For propagation modeling, estimating the beam pattern of the source based on transducer beam theory often suffices. An example of a measured beam pattern is shown in Figure 2.

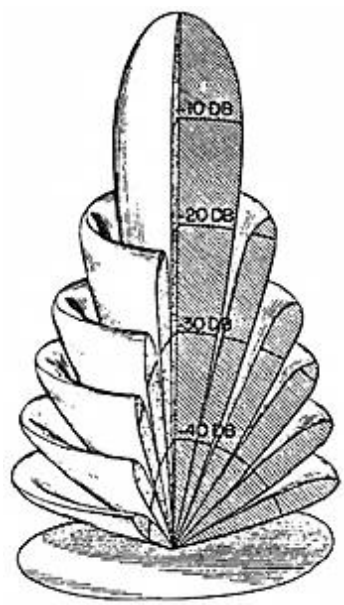

Figure 1. Typical 3-D beam pattern for a circular transducer (Massa 2003).

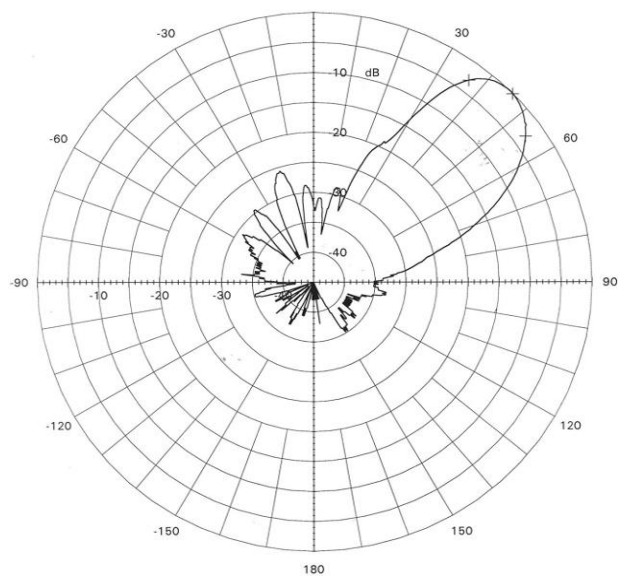

Figure 2. Vertical cross section of a beam pattern measured in situ from a transducer used by Kongsberg (pers. comm. with the manufacturer).

5.1.2.1. Circular Transducers

The beam of an ideal circular transducer is symmetric about the main axis; the radiated level depends only on the depression angle. In this study, beam directivities were calculated from the standard formula for the beam pattern of a circular transducer (ITC 1993, Kinsler et al. 2000). The directivity function of a conical beam relative to the on-axis pressure amplitude is:

$$R(\phi) = \frac{2 \cdot J_1\left(\pi\, D_\lambda \sin(\phi)\right)}{\pi\, D_\lambda \sin(\phi)} \text{ and } D_\lambda = \frac{60}{\theta_{bw}}, \tag{10}$$

where $J_1(\phi)$ is the first-order Bessel function, D_λ is the transducer dimension in wavelengths of sound in the medium, θ_{bw} is the beamwidth in degrees, and ϕ is the beam angle from the transducer axis. The beam pattern of a circular transducer can be calculated from the transducer's specified beamwidth or from the diameter of the active surface and the operating frequency. The calculated beam pattern for a circular transducer with a beamwidth of 20° is shown in Figure 3. The grayscale represents the source level (dB re 1 µPa @ 1 m) and the declination angle is relative to a central vector (0°, 0°) pointing down.

Although some acoustic energy is emitted at the back of the transducer, the theory accounts for the beam power in only the front half-space ($\phi < 90°$) and assumes no energy directed into the back half-space. The relative power at these rearward angles is significantly lower, generally by more than 30 dB, and consequently the emission in the back half-space can be estimated by applying a simple decay rate, in decibels per angular degree, which gives a beam power at $\phi = 90°$ of 30 dB less than that at $\phi = 0°$. This is a conservative estimate of the beam power in the back half-space.

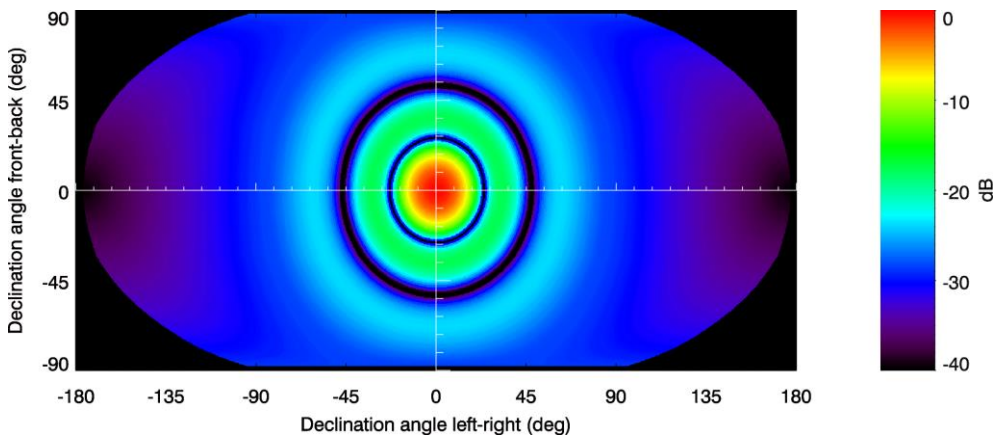

Figure 3. Calculated beam pattern for a circular transducer with a beamwidth of 20°. The beam power function is shown relative to the on-axis level.

5.1.2.2. Rectangular Transducers

Rectangular transducer beam directivities were calculated from the standard formula for the beam pattern of a rectangular acoustic array (ITC 1993, Kinsler et al. 2000). The directivity function is the product of the toroidal beam patterns of two line arrays, where the directional characteristics in the along- and across-track directions are computed from the respective beamwidths. The directivity function of a toroidal beam relative to the on-axis pressure amplitude is:

$$R(\phi) = \frac{\sin\left(\pi\, L_\lambda \sin(\phi)\right)}{\pi\, L_\lambda \sin(\phi)} \text{ and } L_\lambda = \frac{50}{\theta_{bw}}, \tag{11}$$

where L_λ is the transducer dimension in wavelengths, θ_{bw} is the beamwidth in degrees, and ϕ is the angle from the transducer axis. The beam pattern of a transducer can be calculated using either the specified beamwidth in each plane or the dimensions of the active surface and the operating frequency of the transducer. The calculated beam pattern for a rectangular transducer with along- and across-track beamwidths of 4° and 10°, respectively, is shown in Figure 4.

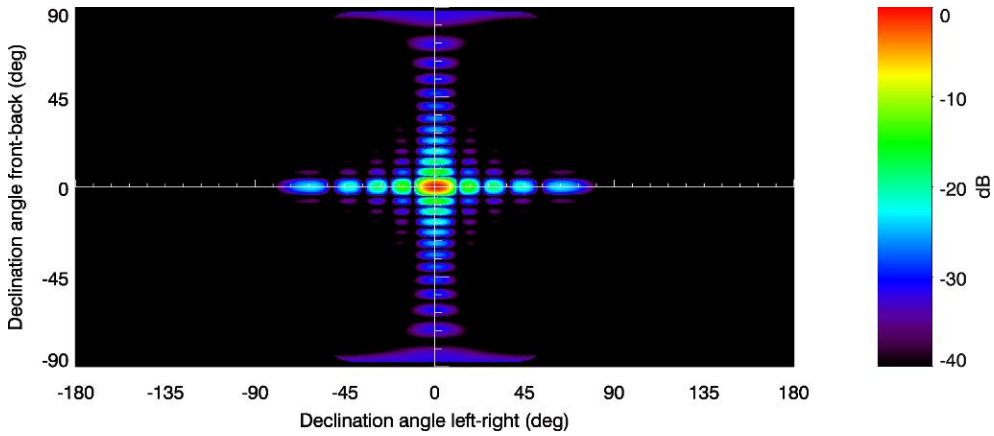

Figure 4. Calculated beam pattern for a rectangular transducer with a 4° × 10° beamwidth. The beam power function is shown relative to the on-axis level using the Robinson projection.

5.1.2.3. Multibeam Systems

High-frequency systems often have two or more transducers, e.g., side-scan and multibeam sonar. Typical side-scan sonar use two transducers, with the central axes directed perpendicular to the survey track and at some depression angle below the horizontal. In contrast, multibeam bathymetry systems can have upward of 100 transducers. Such systems generally consist of rectangular transducers and have a narrow beamwidth in the horizontal (along-track) plane (0.2–3°) and a wide beamwidth in the vertical (across-track) plane.

For multibeam systems, the beam patterns of individual transducers are calculated separately and then combined into the overall pattern of the system based on beam engagement types, which can be broadcast simultaneously or successively. If the beams are engaged successively, the source level of the system in a given direction is assumed to be the maximum source level realized from the individual transducers; if the beams are engaged simultaneously, the system beam pattern is the sum of all beam patterns. Figure 5 shows the predicted beam pattern for two rectangular transducers engaged simultaneously. These transducers have along- and across-track beamwidths of 1.5° and 50°, respectively.

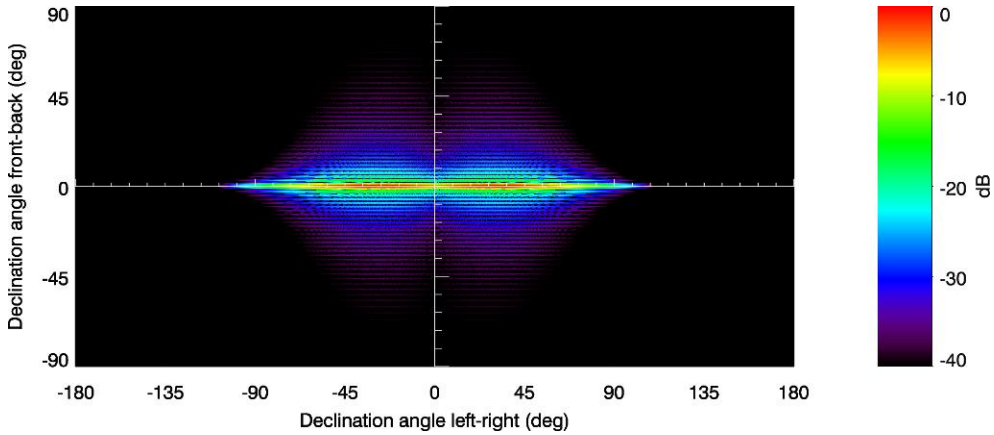

Figure 5. Calculated beam pattern for two rectangular transducers engaged simultaneously, with individual beamwidths of 1.5° × 50°, and a declination angle of 25°. The beam power function is shown relative to the on-axis level using the Robinson projection.

5.2. Acoustic Propagation Modeling

The underwater sound propagation (i.e., transmission loss) was predicted with JASCO's Marine Operations Noise Model (MONM). This model computes received per-pulse SEL for directional sources at a specified depth.

5.2.1. Two Frequency Regimes: RAM vs. BELLHOP

In order to achieve the greatest accuracy and computational efficiency, MONM uses two separate models to estimate transmission loss. At frequencies ≤ 2 kHz, MONM computes acoustic propagation via a wide-angle parabolic equation solution to the acoustic wave equation (Collins 1993) based on a version of the U.S. Naval Research Laboratory's Range-dependent Acoustic Model (RAM), which has been modified to account for an elastic seabed (Zhang and Tindle 1995). The parabolic equation method has been extensively benchmarked and is widely employed in the underwater acoustics community (Collins et al. 1996). The RAM-based component of MONM (MONM-RAM) accounts for the additional reflection loss at the seabed due to partial conversion of incident compressional waves to shear waves at the seabed and sub-bottom interfaces, and it includes wave attenuations in all layers. MONM-RAM's predictions have been validated against experimental data in several underwater acoustic measurement programs conducted by JASCO (Hannay and Racca 2005, Aerts et al. 2008, Funk et al. 2008, Ireland et al. 2009, O'Neill et al. 2010, Warner et al. 2010). MONM-RAM incorporates the following site-specific environmental properties: a modeled area bathymetric grid, underwater sound speed as a function of depth, and a geoacoustic profile based on the overall stratified composition of the seafloor. MONM-RAM accounts for source horizontal directivity.

At frequencies ≥ 2 kHz, MONM employs the widely-used BELLHOP Gaussian beam ray-trace propagation model (Porter and Liu 1994), which accounts for increased sound attenuation due to volume absorption at these higher frequencies following Fisher and Simmons (1977). This type of attenuation is significant for frequencies higher than 5 kHz and cannot be neglected or model results far from the source will noticeably suffer. The BELLHOP component of MONM (MONM-BELLHOP) accounts for the source directivity, specified as a function of both azimuthal angle and depression angle. MONM-BELLHOP incorporates the following site-specific environmental properties: a bathymetric grid of the modeled area and underwater sound speed as a function of depth. In addition to horizontal directivity of the source, MONM-BELLHOP accounts for the vertical variation of the source beam pattern.

In contrast to MONM-RAM, the geoacoustic input for MONM-BELLHOP consists of only one interface: the sea bottom. This is an acceptable limitation because the influence of the sub-bottom layers on the propagation of acoustic waves with frequencies above 1 kHz is negligible. Both propagation models account for full exposure from a direct acoustic wave, as well as exposure from acoustic wave reflections and refractions (i.e., multi-path arrivals at the receiver).

These propagation models effectively assume a continuous wave source. That is an acceptable approximation for a pulse in the case of the SEL metric because the energy in the various multi-path arrivals will be summed. When significant multi-path arrivals cause broadening of the pulse, the continuous wave assumption breaks down for pressure metrics such as rms SPL. For this reason, a subset of the modeling sites were selected to have acoustic propagation from the airgun array modeled using a full-wave RAM PE model (FWRAM), with which broadband SEL to SPL conversion factors could be calculated using a sliding 100 ms integration window. The modeling time required to perform these calculations (often several days for each site) made it prohibitive to perform them at any more than a representative subset of the modeling sites. These azimuth-, range- and depth-dependent conversion factors were then used to calculate the broadband rms SPL from the broadband SEL prediction at all the modeling sites. Conversion factors were calculated for each modeling location.

For geotechnical source propagation modeling, a fixed +10 dB factor was used to convert SEL to rms SPL. A fixed correction factor was used for simplicity because there was little variability over the range of propagation for the geotechnical sources. It is noted that 10 dB assumes the pulse length is 100 ms. Pulse lengths less than 100 ms would have greater than 10 dB conversion factors, but the minimal integration time for the mammalian ear is ~100 ms. Additional details about source directivity and propagation modeling are provided in Sections 5.1.1, 5.1.2, 5.2.2, 5.2.3, and 5.2.4.

5.2.2. *N*×2-D Volume Approximation

MONM computes acoustic fields in three dimensions by modeling transmission loss within two-dimensional (2-D) vertical planes aligned along radials covering a 360° swath from the source, an approach commonly referred to as *N*×2-D. These vertical radial planes are separated by an angular step size of Δθ, yielding $N = 360°/\Delta\theta$ number of planes (Figure 6).

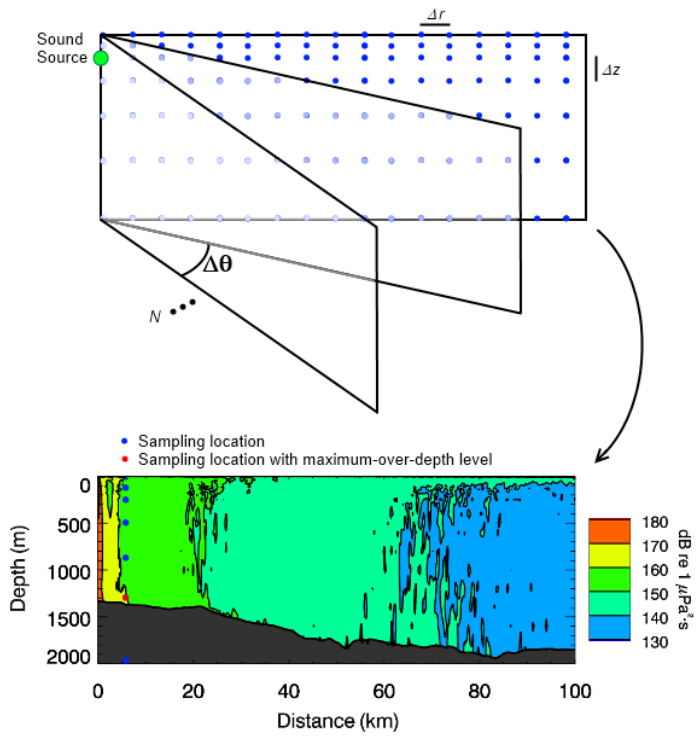

Figure 6. The *N*×2-D and maximum-over-depth modeling approach.

5.2.3. Frequency Dependence: Summing Over 1/3-Octave-Bands

MONM treats frequency dependence by computing acoustic transmission loss at the center frequencies of 1/3-octave-bands. Sufficiently many 1/3-octave-bands, starting at 10 Hz, are modeled to include the majority of acoustic energy emitted by the source. At each center frequency, the transmission loss is modeled within each of the *N* vertical planes as a function of depth and range from the source. The 1/3-octave-band received per-pulse SELs are computed by subtracting the band transmission loss values from the SL in that frequency band.

Composite broadband received SELs are computed by combining the transmission loss (TL) values obtained from propagation modeling with MONM and source levels (SL) obtained from source modeling (see Section 5.1) in each 1/3-octave-band and summing the band levels:

$$\mathrm{RL} = 10 \cdot \log_{10} \sum_{i=1}^{n} 10^{(\mathrm{SL}_i - \mathrm{TL}_i)/10} \tag{12}$$

where n is the number of modeled 1/3-octave-bands, SL_i and TL_i are the source level and transmission loss in the respective 1/3-octave-band.

The frequency weighted received levels ($\mathrm{RL}_{\mathrm{MW}}$) were obtained by adding the relative levels (MW) (see Section 5.4.1) to the above equation:

$$\mathrm{RL}_{\mathrm{MW}} = 10 \cdot \log_{10} \sum_{i=1}^{N} 10^{(\mathrm{SL}_i - \mathrm{TL}_i + \mathrm{MW}_i)/10} . \tag{13}$$

MONM's predictions have been validated against experimental data from several underwater acoustic measurement programs conducted by JASCO (Hannay and Racca 2005, Aerts et al. 2008, Funk et al. 2008, Ireland et al. 2009, O'Neill et al. 2010, Warner et al. 2010, Racca et al. 2012a, Racca et al. 2012b).

5.2.4. Converting Modeled SEL to rms SPL

5.2.4.1. Background

Current National Marine Fisheries Service (NMFS) exposure criteria for impulsive sound sources are based largely on the rms SPL metric. As shown in Equations 7 and 8 in Section 3.2, the rms SPL metric is numerically related to the single pulse SEL and the integration time window for the cases of the commonly-used 90% window, T_{90}, and for fixed integration windows greater than T_{100}. These relationships are important because models are more efficient at estimating SEL than rms SPL. Therefore, in some cases models can be used to calculate the SEL of impulsive acoustic events, after which the aforementioned equations can be used to derive the corresponding rms SPL.

Unfortunately, T_{90} is sensitive to the specific acoustic multipath arrival time of signals. Multipath arrival time varies greatly with source and receiver depths, distance of the receiver from the source, and the water depth profile between source and receiver. Water column refractive effects in deep waters, such as those within deeper regions of the study area, can strongly influence the multipath arrival structure and consequently affect T_{90}. Another problem arises when considering fixed time windows of duration shorter than T_{100}; in these cases Equations 7 and 8 are not valid and cannot be used directly.

Two methods are available to deal with the problems identified above: if field measurements in a similar environment are available, they can be analyzed to directly calculate differences between SEL and rms SPL. Those differences can then be applied to modeled SEL values to derive the corresponding rms SPL. The approach is limited to applications where measurements are available in a suitably similar environment and where the actual measurement source-receiver geometry spans the ranges and depths of interest. The second approach is to apply full-waveform models to calculate synthetic data from which the numeric differences between SEL and corresponding rms SPL can be predicted. This approach can address a much larger variety of ocean environments and source-receiver geometries.

Various empirical measurements of airgun pulses have shown that differences between rms SPL and SEL typically range from +15 to −5 dB (Greene 1997, McCauley et al. 1998, Blackwell et al. 2007, MacGillivray et al. 2007). The difference is highly sensitive to multipath arrival timing and reverberation, but it is generally larger at closer distances, where the airgun pulse duration is short ($\ll$ 1 s), and smaller

at farther distances, where pulse duration tends to increase due to increased reverberation and larger differences in the arrival times of different propagation paths.

5.2.4.2. Fixed Integration Time Window

For individual acoustic pulses, we used a fixed integration time window of 100 ms, the shortest expected temporal integration time for the mammalian ear (Plomp and Bouman 1959, MacGillivray et al. 2014). At this window length, the maximum numerical difference between SEL and rms SPL for an impulsive acoustic event is 10 dB. This maximum difference occurs when all of the pulse's acoustic energy is received in less than 100 ms. As the pulse length increases beyond 100 ms, the difference decreases. A difference value of 0 dB (SEL = rms SPL), occurs when the acoustic energy is received evenly distributed over 1 s.

We applied a nominal conversion difference of +10 dB from SEL to rms SPL at all receiver positions for all single airgun and geotechnical source types. The +10 dB results from the assumption that the shortest temporal integration time of the mammalian ear is 100 ms (as mentioned above). This approach is accurate at distances where the pulse duration is less than 100 ms, and conservative for longer distances. Most of the effects of these smaller sources occur at relatively short distances where the pulse durations are short so this approach is not expected to be overly conservative even for lower-level effects.

Conversion values for the larger airgun array source were determined with the Full-Waveform Range-dependent Acoustic Model (FWRAM) (JASCO Applied Sciences). This model was applied at a representative shallow (Shelf), mid-depth (Slope), and deep-water location along each of the three acoustic modeling transects (see Section 7.2.3.2). At each of these locations, the model was run along 16 evenly spaced azimuths to examine the effect of source directivity and direction-dependent bathymetric variation. The synthetic data from the model were processed to compute SEL and rms SPL using 100 ms time windows. These results were computed as a function of distance, receiver depth, and receiver direction from each full-waveform modeling site. Conversion tables were then used to extract representative SEL to rms SPL conversions at all 30 sites modeled using MONM. The optimal conversion values were selected from the tables based on the closest full-waveform model source location and the nearest azimuthal direction, using bilinear interpolation over receiver range and depth.

5.3. Animal Movement Modeling for Impact Assessment

The sounds animals receive when near one or more sound sources are a function of where the animal is at any given time relative to the source(s), which may themselves be moving (Figure 7). To a reasonable approximation, the location of the sound source(s) is known and acoustic modeling can be used to predict the three dimensional (3-D) sound field (Section 5.1 and 5.2). The location of animals within the sound field, however, is unknown. Realistic animal movement within the sound field can be simulated, and repeated random sampling (Monte Carlo)—achieved by simulating many animals within the operations area—used to estimate the sound exposure history of animals during the operation. Monte Carlo methods provide a heuristic approach to determine the probability distribution function (PDF) of complex situations, such as animals moving in a sound field. A greater number of random samples, in this case more simulated animals (animats), better approximates the PDF. Animats are randomly placed, or seeded, within the simulation boundary at a specified density (animats/km^2), and to maintain constant modeling density any animat exiting across a border is replaced with a new animat at the opposite border. Higher densities provide a finer PDF estimate resolution, but require greater computational resources. To ensure good representation of the PDF, the animat density is set as high as practical allowing for computation time. The resulting PDF is then scaled using the real-world animal density to obtain the real-world number of individuals affected. The probability of an event's occurrence is determined by the frequency

with which it occurs in the simulation. The Monte Carlo method works well for assessing the probability of common events, its weakness is in accurately determining the probability of rare events.

Several models for marine mammal movement have been developed (Ellison et al. 1987, Frankel et al. 2002, Houser 2006). These models use an underlying Markov chain to transition from one state to another based on probabilities determined from measured swimming behavior. The parameters may represent simple states, such as the speed or heading of the animal, or complex states, such as likelihood of an animal foraging, playing, resting, or traveling. This analysis uses the Marine Mammal Movement and Behavior (3MB) model developed by (Houser 2006). The parameters used for forecasting realistic movement are detailed in Appendix C.

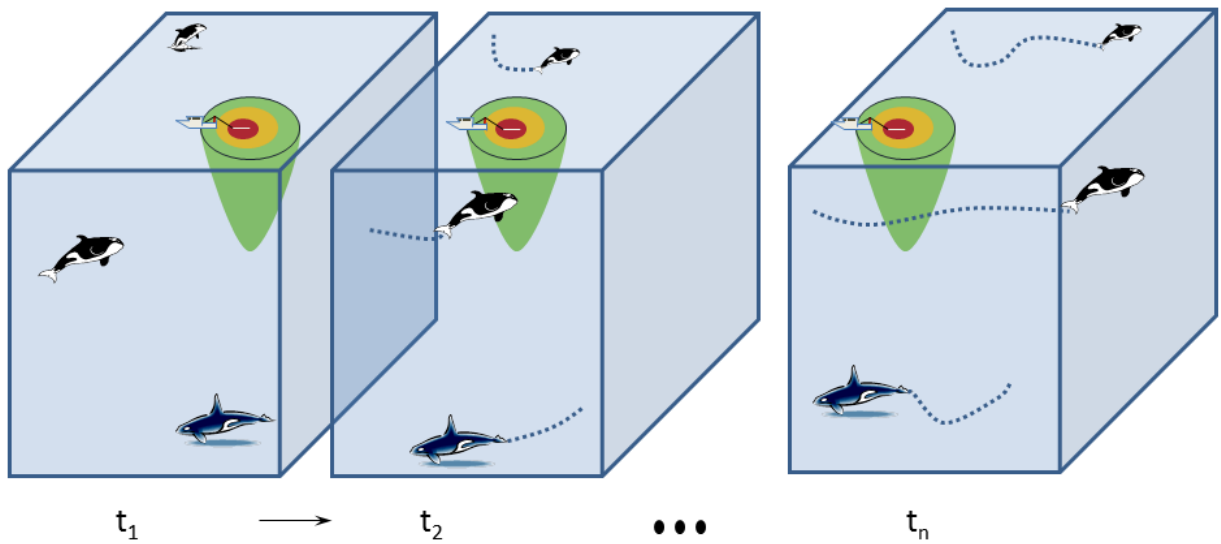

Figure 7. Cartoon animats in a moving sound field. The acoustic exposure of each animat is determined by where it is in the sound field, and its exposure history is accumulated as the simulation progresses. In this cartoon, the vessel and sound source are moving right to left, as is the lowest animat. The two upper animats move from left to right. Because the upper and lower animats are far from the source, low levels of sound exposure are expected. The middle animat is nearer the sound source so its acoustic exposure would be expected to be higher than the other two animats, and its highest exposure occurs when it is closest to the sound sources at the second time step (t_2).

5.4. Acoustic Exposure Criteria

The Marine Mammal Protection Act (MMPA 2007) defines harassment as any act of pursuit, torment, or annoyance that (i) has the potential to injure a marine mammal, or (ii) has the potential to disturb a marine mammal by disrupting its behavioral patterns, including but not limited to, migration, breathing, nursing, breeding, feeding, or sheltering.

Harassment with the potential for injury is termed Level A harassment, and harassment with the potential to disrupt behavior is termed Level B harassment. Loud sounds can potentially damage the hearing of marine mammals or disrupt their behavior. In the 1990s, NMFS adopted received levels for pulsed sounds that should not be exceeded for marine mammals. The rms SPL thresholds for marine mammals exposed to impulsive sound are 180 dB re 1 µPa for Level A and 160 dB re 1 µPa for Level B (NMFS 1995, NMFS 2000).

These criteria were set before there was adequate data about the received levels that could injure marine mammals. Since then, more data have become available. In 1998, a group of experts was convened to update and establish methods for determining acoustic exposure criteria (Gentry et al. 2004). The results of the expert group were published as Southall et al. (2007) and are commonly referred to as the Southall criteria. In this report, the Southall criteria were used as the basis for developing additional exposure criteria to evaluate potential impacts of the modeling results described in this study.

5.4.1. Marine Mammal Frequency Weighting Functions

The potential for anthropogenic sounds to impact marine animals depends on how well the animal detects the sounds. Sounds are less likely to injure or disturb animals if it occurs at frequencies that an animal cannot hear well, except when the sound pressure level is so high that it could physically injure tissue. Based on a review of marine mammal hearing and on physiological and behavioral responses to anthropogenic sounds, Southall et al. (2007) proposed standard frequency weighting functions—referred to as M-weighting functions—for three functional hearing groups of cetaceans (Table 1):

- Low-frequency cetaceans (LFCs)—mysticetes (baleen whales)
- Mid-frequency cetaceans (MFCs)—some odontocetes (toothed whales)
- High-frequency cetaceans (HFCs)—odontocetes specialized for using high-frequencies

The discount applied by the M-weighting functions for less-audible frequencies is less than that indicated by the corresponding audiograms (where available) for member species of these hearing groups. The rationale for applying a smaller discount than suggested by the audiograms measured at low sound levels is due in part to an observed characteristic of mammalian hearing that, as sound levels increase, perceived equal loudness curves increasingly have less rapid roll-off outside of the most sensitive hearing frequency range. This is why, for example, C-weighting curves for humans, used for assessing loud sounds such as blasts, are flatter than A-weighting curves, used for quiet to mid-level sounds. The M-weighting functions are, therefore, usually applied at high sound levels where impacts such as temporary or permanent hearing threshold shifts might occur. The use of M-weighting is considered precautionary (in the sense of overestimating the potential for impact) when applied to lower level impacts such as the onset of behavioral response. Figure 8 shows the decibel frequency weighting of the cetacean underwater M-weighting functions.

The M-weighting functions have unity gain (0 dB) through the passband and their high and low frequency roll-offs are approximately –12 dB per octave. The amplitude response in the frequency domain is defined by:

$$G(f) = K - 20\log_{10}\left[\left(1+\frac{f_{low}{}^{2}}{f^{2}}\right)\left(1+\frac{f^{2}}{f_{hi}}\right)\right] \tag{14}$$

where K is a constant used to normalize the function at a reference frequency, and the roll-off and passband of these functions are controlled by the parameters f_{lo} and f_{hi}, the estimated upper and lower hearing limits specific to each functional hearing group (Table 3).

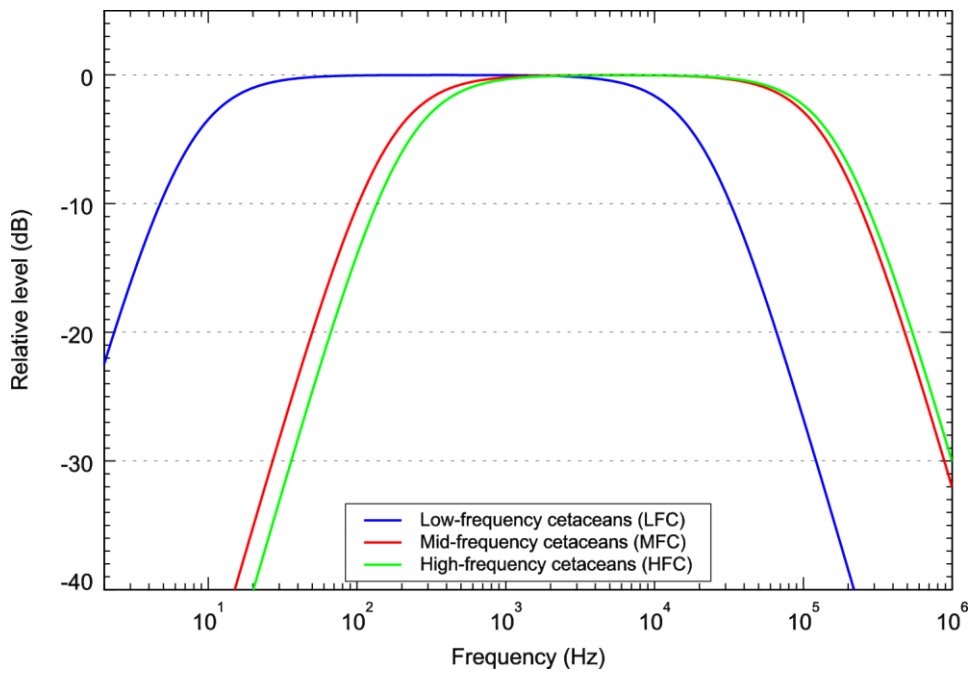

Figure 8. Standard M-weighting functions for the four underwater functional marine mammal hearing groups (Southall et al. 2007).

Table 3. Low and high frequency cut-off parameters of M-weighting functions for the cetacean functional hearing groups (Southall et al. 2007).

Functional hearing group	K	f_{low} (Hz)	f_{hi} (Hz)
Low-frequency cetaceans	0	7	22,000
Mid-frequency cetaceans	0	150	160,000
High-frequency cetaceans	0	200	180,000

Subjective loudness measurements for a common bottlenose dolphins have provided information to help develop equal-loudness contours for this animal (Finneran and Schlundt 2011). Equal loudness contours (also called Fletcher-Munson curves) are the sound levels over the frequency spectrum for which a listener perceives constant loudness. These curves are the basis of the Occupational Safety and Health Administration (OSHA) noise regulation 1910.95. The equal-loudness contours determined by Finneran and Schlundt (2011) better match the frequency dependence of TTS onset data (Schlundt et al. 2000) than audiograms or the M-weighting curves. For this reason, the dolphin equal-loudness contours were used to develop marine mammal frequency weighting functions (Finneran and Jenkins 2012).

The (inverse) equal-loudness contours were fit with equations of the same form as the M-weighting function (Equation 14). The fits suggest steeper roll-off at lower frequencies than the mid-frequency M-weighting curve. Because data for the equal-loudness contours did not cover the entire spectral range of the M-weighting functions, the M-weighting curves were modified. The lowest frequency for which subjective loudness data were obtained was 3 kHz, therefore Finneran and Jenkins (2012) took a conservative approach and set the mid-frequency M-weighting curve and the inverted equal loudness contour equal at 3 kHz. The result is that below 3 kHz the overall function is identical to the M-weighting curves, while above 3 kHz the overall function is equal to the fitted (inverse) equal-loudness contour. A similar procedure was used for low- and high-frequency animals, but the fitting parameters for the inverted equal-loudness contours were adjusted appropriately for each of those groups.

Frequency weighting functions for cetaceans are calculated as:

$$G_1(f) = K_1 - 20\log_{10}\left[\left(1+\frac{f_{low1}^{\ 2}}{f^2}\right)\left(1+\frac{f^2}{f_{hi1}^{\ 2}}\right)\right] \tag{15}$$

$$G_2(f) = K_2 - 20\log_{10}\left[\left(1+\frac{f_{low2}^{\ 2}}{f^2}\right)\left(1+\frac{f^2}{f_{hi2}^{\ 2}}\right)\right] \tag{16}$$

$$G_2(f) = \max[G_1(f), G_2(f)] \tag{17}$$

where f_{low1} and f_{hi1} are the same parameter values for M-weighting, and $f_{low\,2}$ and f_{hi2} are the fitted parameters for the inverted equal-loudness contour adjusted for hearing groups. K_2 is used to normalize the G_2 equation to zero at 10 kHz (the reference frequency for the subjective loudness studies) and K_1 is used to set the G_1 equation equal to the G_2 equation at 3 kHz for mid-frequency and high-frequency species. For low-frequency species, K_1 was adjusted so that the flat portion of the G_2 was 16.5 dB below the peak level of G_2 (as it was for the mid-frequency cetaceans). G_1 and G_2 are equal at 267 Hz for low-frequency species. Parameters for each of the cetacean groups are shown in Table 4, and the resulting frequency weight curves are shown in Figure 9.

Finneran and Jenkins (2012) termed their frequency weighting functions Type II M-weighting and referred to the original Southall et al. (2007) M-weighting as Type I M-weighting. We adopt the Finneran and Jenkins (2012) nomenclature in this study.

Table 4. Frequency weighting parameters for the cetacean functional hearing groups. Modified from Finneran and Jenkins (2012).

Functional hearing group	K_1 (dB)	f_{low1} (Hz)	f_{hi1} (Hz)	K_2 (dB)	f_{low2} (Hz)	f_{hi2} (Hz)	Inflection point (Hz)
Low-frequency cetaceans	−16.5	7	22,000	0.9	674	12,130	267
Mid-frequency cetaceans	−16.5	150	160,000	1.4	7,829	95,520	3,000
High-frequency cetaceans	−19.4	200	180,000	1.4	9,480	108,820	3,000

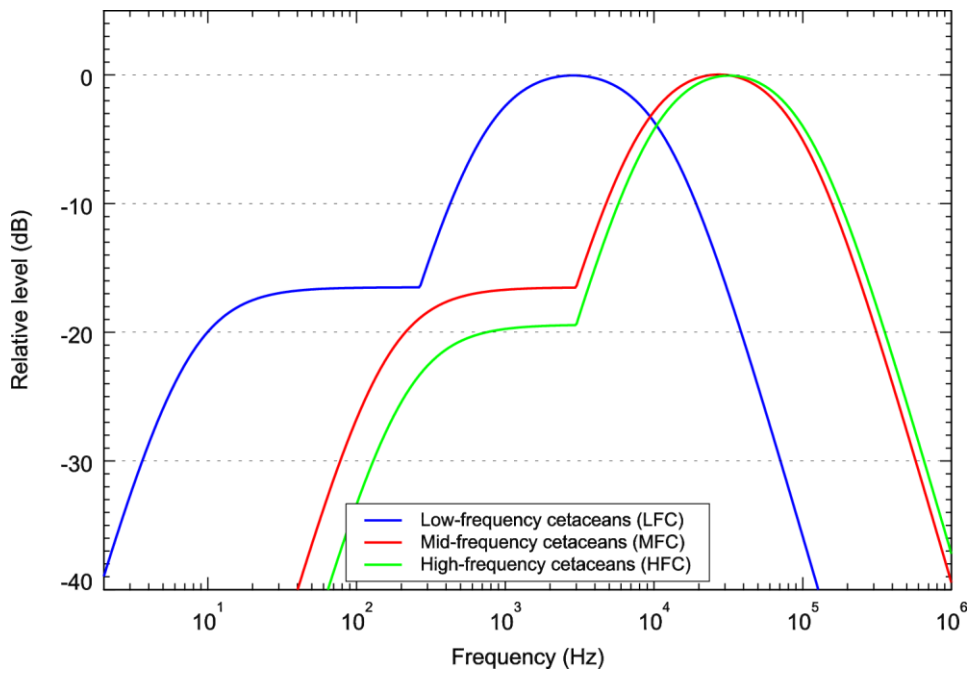

Figure 9. Frequency weighting functions for the cetacean functional hearing groups. Adapted from Finneran and Jenkins (2012).

5.4.2. Injury Exposure Criteria Selection

Loud or sustained sounds can injure an animal's hearing structures, resulting in a permanent shift in hearing thresholds (PTS; see Section 3.4.3). There are no data on the sound levels that cause PTS in marine mammals. There are, however, data that indicate the received sound levels at which temporary threshold shifts (TTS) occur. PTS onset can be hypothetically extrapolated from TTS onset and growth.

Sound level and duration are key determinants in TTS. The SEL metric includes amplitude, duration, and TTS magnitude. TTS is best correlated with SEL (rather than SPL) in dolphins exposed to sounds of < 8 s long (Finneran et al. 2005). Although limited, these findings are consistent with an equal acoustic energy hypothesis for TTS prediction (see Southall et al. 2007). Data from terrestrial mammals indicate that TTS of 40–50 dB could be induced without causing PTS (e.g., Ward et al. 1958, Ward et al. 1959, Ward 1960, Miller 1963, Kryter et al. 1966). Southall et al. (2007) chose 40 dB of TTS as a conservative onset limit of PTS. In humans, Ward et al. (1958) found a linear relationship between TTS and SEL of 1.5–1.6 dB TTS per 1 dB increase in SEL. TTS onset is defined as the sound level that produces 6 dB of TTS. The TTS growth rates from Ward et al. (1958) predict the onset PTS SEL at about 21 dB greater than the onset of TTS SEL ($34/1.6 \approx 21$). This TTS growth rate appears to be conservative for cetaceans, as Finneran and Schlundt (2010) measured a TTS growth rate in a dolphin exposed to 16 s tones from 3 and 20 kHz, to be somewhat less than the values found in humans by Ward et al. (1958). For non-pulsed stimuli, both Southall et al. (2007) and Finneran and Jenkins (2012) rounded down and used a conservative value of 20 dB + TTS SEL onset as the PTS SEL onset level. For pulsed sounds, Henderson and Hamernik (1986) reported that the TTS growth rate for chinchillas was between 0.5 and 3 dB TTS per dB SEL, with higher growth rates at higher SELs. Southall et al. (2007) used 2.3 dB TTS per dB SEL as a conservative growth rate to predict PTS SEL onset for marine mammals, and thus calculated 15 dB + TTS SEL onset as the PTS SEL onset. Because TTS is related to hearing sensitivity, the signal levels for determining TTS and PTS should be filtered using an appropriate auditory frequency weighting function (see Section 5.4.1).

Particularly loud sounds could induce TTS regardless of whether a cumulative sound energy (SEL) threshold has been exceeded or how long they last. Rather than the sensory system fatiguing, tissue damage might occur, which would violate the equal-energy assumption of TTS prediction. In this case, SPL is the appropriate metric and no auditory frequency weighting is applied. In assessing the potential for injury due to these sounds, Southall et al. (2007) began with 40 dB of TTS as the onset of PTS. They used a conservative extrapolation of chinchilla data to argue that sounds 6 dB above the TTS SPL threshold could cause PTS.

Injury exposure criteria for each cetacean functional hearing group is determined from TTS onset data as explained below, and the results are shown in Table 5.

Low-Frequency Cetaceans

There are no TTS data for low-frequency species. As a conservative measure, the Type I M-weighting function described by Southall et al. (2007; Section 5.4.1) was used for low-frequency species. Extrapolating current data from mid-frequency animals, we subtracted 6 dB from the Southall et al. (2007) SEL injury criteria of 198 dB re 1 $\mu Pa^2 \cdot s$ to obtain 192 dB re 1 $\mu Pa^2 \cdot s$ for use in this study (Wood et al. 2012).

Mid-Frequency Cetaceans

For pulsed sounds, TTS data are available for common bottlenose dolphins and beluga whales exposed to single impulse from a seismic watergun (Finneran et al. 2002). The beluga whales were found to have a TTS onset at a SEL of 186 dB re 1 $\mu Pa^2 \cdot s$ or peak SPL of 224 dB re 1 μPa (measured at 0.4 and 30 kHz). The dolphins showed no TTS up to a SEL of 186 dB re 1 $\mu Pa^2 \cdot s$ or peak SPL of 226 dB re 1 μPa. As a precaution, the TTS onset levels for the beluga are taken to represent all mid-frequency cetaceans (Southall et al. 2007, Finneran and Jenkins 2012). Using the auditory frequency weighting, TTS onset occurs at an SEL of 172 dB 1 $\mu Pa^2 \cdot s$. Adding 15 dB results in a PTS SEL threshold of 187 dB 1 $\mu Pa^2 \cdot s$.

We used the unweighted peak SPL of 224 dB re 1 μPa for TTS in beluga to predict PTS onset for particularly loud sounds that violate the equal energy hypothesis for TTS prediction (Southall et al. 2007, Finneran and Jenkins 2012). Adding 6 dB to the TTS onset results in a PTS SPL onset threshold of 230 dB re 1 μPa. We used this hypothetical exposure value as SPL PTS threshold for all mid-frequency cetaceans and for all types of sounds.

High-Frequency Cetaceans

Lucke et al. (2009) found a TTS SEL onset of 164 dB re 1 $\mu Pa^2 \cdot s$ at 4 kHz for a harbor porpoise exposed to a seismic airgun impulse. When auditory frequency weighting is applied to the airgun signal, the SEL TTS exposure threshold is 146 dB re 1 $\mu Pa^2 \cdot s$ (see Finneran and Jenkins 2012); adding 15 dB to the TTS onset results in an SEL threshold of 161 dB re 1 $\mu Pa^2 \cdot s$ as the PTS exposure criteria for pulsed sounds.

Lucke et al. (2009) also found that 194 dB re 1 μPa was the peak SPL that resulted in TTS. Adding 6 dB to the peak SPL results in a peak SPL PTS onset of 200 dB re 1 μPa, which will be used in this report as the peak sound pressure level exposure criteria for high-frequency cetaceans for all types of sounds.

Table 5. Injury exposure criteria for pulsed sounds. Cumulative sound exposure level (SEL) is weighted for hearing sensitivity; peak sound pressure level (peak SPL) is unweighted.

Functional hearing group	SEL (dB re 1 μPa^2·s)	peak SPL (dB re 1 μPa)
Low-frequency cetaceans	192	230
Mid-frequency cetaceans	187	230
High-frequency cetaceans	161	200

5.4.3. Behavioral Exposure Criteria Selection

NMFS currently uses a step function at an unweighted rms SPL of 160 dB re 1 μPa to assess behavioral impacts (NMFS and NOAA1995). This threshold is based on observations of migrating mysticete whales responding to an airgun (Malme et al. 1984, Malme et al. 1988). Although animals' behaviors in response to sounds might happen at lower levels, significant responses were only likely to occur above an rms SPL of 140 dB re 1 μPa; animals began avoiding pulsed sounds when rms SPL neared 160 dB re 1 μPa (Malme et al. 1988).

Southall et al. (2007, Appendix B) extensively reviews behavioral responses to sounds, and finds that most marine mammals exhibited varying responses between rms SPLs of 140 and 180 dB re 1 μPa—consistent with the NMFS threshold—but lack of convergence in the data prevents them from suggesting explicit step functions. Lack of controls, precise measurements, appropriate metrics, and context dependency of responses (including the activity state of the animal) all contribute to variability. Southall et al. (2007) propose a severity scale that increases with increased sound level as a qualitative scaling paradigm.

For pulsed sounds, Wood et al. (2012) proposed a graded probability of response with 10% response likelihood at an rms SPL of 140 dB re 1 μPa, 50% at an rms SPL of 160 dB re 1 μPa, and 90% at an rms SPL of 180 dB re 1 μPa for most marine mammals. Wood et al. (2012) also designated behavioral response categories for migrating mysticetes and sensitive species, such as harbor porpoises and beaked whales. For the sensitive species, the likelihood of a 50% response was set to an rms SPL of 120 dB re 1 μPa; 90% response probability was set at an rms SPL of 140 dB re 1 μPa (Wood et al. 2012). No migrating mysticetes were modeled in our study.

The NMFS step function, (unweighted) rms SPL of 160 dB re 1 μPa, and the Wood et al. (2012) graded functions (Table 6) were used to determine the number of behavioral responses. Following Wood et al. (2012), Type I weighting was used to filter the source signals when behavioral responses were evaluated with the graded functions (see Section 5.4.1).

Table 6. Behavioral exposure criteria. Probability of behavioral response frequency-weighted sound pressure level (rms SPL dB re 1 μPa). Probabilities are not additive. Adapted from Wood et al. (2012).

Marine mammal group	Probability of response to frequency-weighted rms SPL (dB re 1 μPa)			
	120	140	160	180
Beaked whales	50%	90%		
All other species		10%	50%	90%

5.4.4. Exposure Estimation

5.4.4.1. Injury Exposure Estimates—cumulative SEL

To evaluate the likelihood an animal might be injured from accumulated sound energy, the cumulative SEL for each animat in the simulation was calculated. To obtain that animat's cumulative SEL, the SEL an animat received from each source over the integration window was summed. The number of animats whose cumulative SEL exceeded the specified thresholds (Table 5) during the integration window was counted.

5.4.4.2. Injury Exposure Estimates—peak SPL

To evaluate the likelihood an animal might be injured by being exposed to peak SPL, we estimated the range at which the specific peak SPL threshold occurs (Table 5) for each source based on the broadband peak SPL source level. For each integration window, the number of animats that came within this range of the source was counted.

5.4.4.3. Behavior Exposure Estimates—rms SPL

To evaluate the likelihood an animal might have its behavior disrupted based on the step function criteria, we calculated the number of animats that received a maximum rms SPL exposure within the specified step ranges (Table 6). The number of animats with a maximum rms SPL received level categorized into each bin of the step function was scaled by the probability of the behavioral response specific to that range (Table 6). These scaled values were then summed as the estimated number of behavioral exposures. This process was repeated for each integration window.

5.4.4.4. NMFS Criteria for Injury and Behavior Exposure Estimates—rms SPL

To evaluate the likelihood an animal might be injured or its behavior disrupted based on NMFS's criteria (180 and 160 dB rms SPL, respectively), we set the exposure simulation to use un-weighted rms SPL acoustic fields. The number of animats receiving an exposure greater than 180 dB was counted as the number of injurious exposures. The number of animats that received an exposure between 160 dB and 180 dB was counted as the number of behavioral exposures. An animat counted as an injurious exposure is not counted as a behavioral disruption exposure. As with the other criteria, animat received level was reset at the beginning of each integration window.

6. Phase I: Test Case and Test Scenarios

A seismic survey Test Case was defined and evaluated using acoustic and animal movement models as an initial evaluation of potential impacts on marine mammals and to establish the use of various modeling methodologies prior to the Phase II modeling. The Test Case was a typical WAZ seismic survey conducted at two locations near the Mississippi Canyon of the Gulf of Mexico (Figure 10). Survey site A was centered on the slope of the continental shelf break and Survey site B was centered on the deep ocean plain. The WAZ surveys consisted of four vessels sailing in parallel with staggered sail directions. Each vessel towed two 8000 in^3 arrays. Six species (Bryde's whales, Cuvier's beaked whales, common bottlenose dolphins, dwarf sperm whales, short-finned pilot whales, and sperm whales) were evaluated in the Test Case as representative Gulf of Mexico species that may be near the survey sites. Bryde's whales were chosen because they are the only low-frequency species in the Gulf. Dwarf sperm whales were chosen as the representative high-frequency *Kogia* species. The four mid-frequency species were chosen to represent various other aspects of diving and hearing sensitivity. Cuvier's beaked whales are deep-diving and behaviorally sensitive to sounds, sperm whales are also deep-diving and are the only endangered species listed in the Gulf. Short-fin pilot whales and common bottlenose dolphins both represent the swimming behavior of smaller cetaceans with different preferred water depth. Sound exposure estimates were determined by first using computational models to calculate sound fields generated by the airgun arrays, and then by sampling those sound fields using computational models of animal movement during each survey. Risk for each species was evaluated based on the predetermined exposure criteria (see Section 5.4).

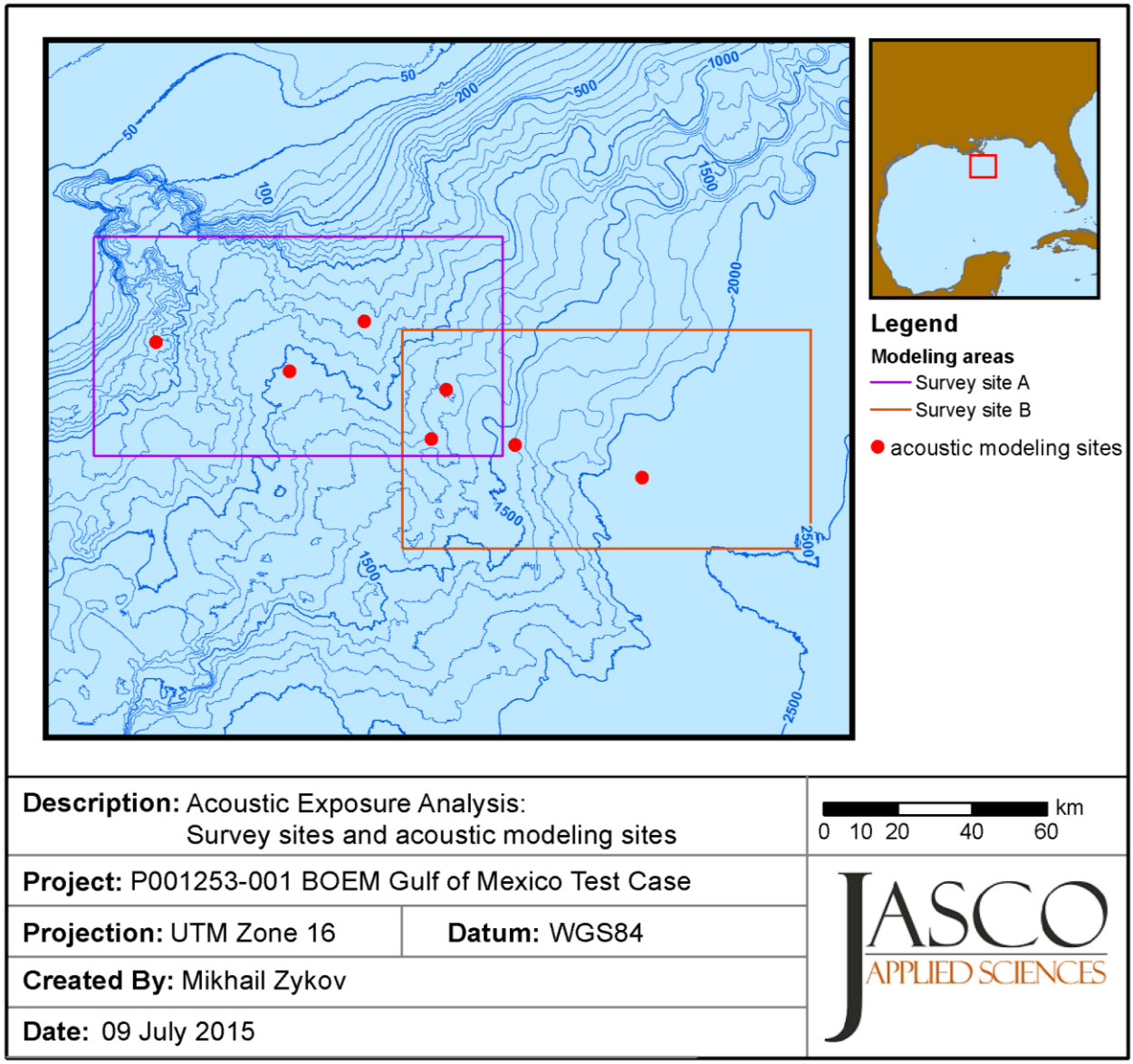

Figure 10. Locations of the Survey site A (purple box) and Survey site B (red box) and acoustic field modeling sites.

6.1. Test Case Acoustic Source Parameters

The WAZ surveys consist of four vessels, each towing two 8000 in^3 airgun arrays fired in flip-flop mode with a shot interval of ~ 14 s.

Acoustic source levels were modeled for the Bolt 1900 LLXT 8000 in^3 airgun array, which was used for the 3-D WAZ survey. The array consisted of six sub-arrays with 9 m in-line separations. The airguns fired simultaneously at 2,000 psi air pressure. The airgun array was modeled at a tow depth of 8 m (the center of the array). Table 7 describes the horizontal layout of each sub-array. Figure 11 presents the airgun distribution in the horizontal plane and gives the volume of each airgun within the sub-array.

Table 7. Relative airgun positions within each of the six sub-arrays. The center of each sub-array is aligned at the same position in *x* (fore-aft, where the array is towed in the positive *x* direction), and spaced 9 m apart in *y* (port-starboard, where port is in the positive *y* direction). All airguns are at 8 m depth. The volume of the airgun at each position varies among the sub-arrays.

Gun	*x* (m)	*y* (m)	Volume (in^3)	
			Strings 1 and 6	Strings 2–5
1	−7.0	0.4	150	150
2	−7.0	−0.4	150	150
3	−4.0	0.4	70	60
4	−4.0	−0.4	70	60
5	−2.0	0	50	40
6	0.0	0	90	70
7	2.0	0.4	70	60
8	2.0	−0.4	70	60
9	4.0	0.4	60	90
10	4.0	−0.4	60	90
11	7.0	0.4	250	250
12	7.0	−0.4	250	250

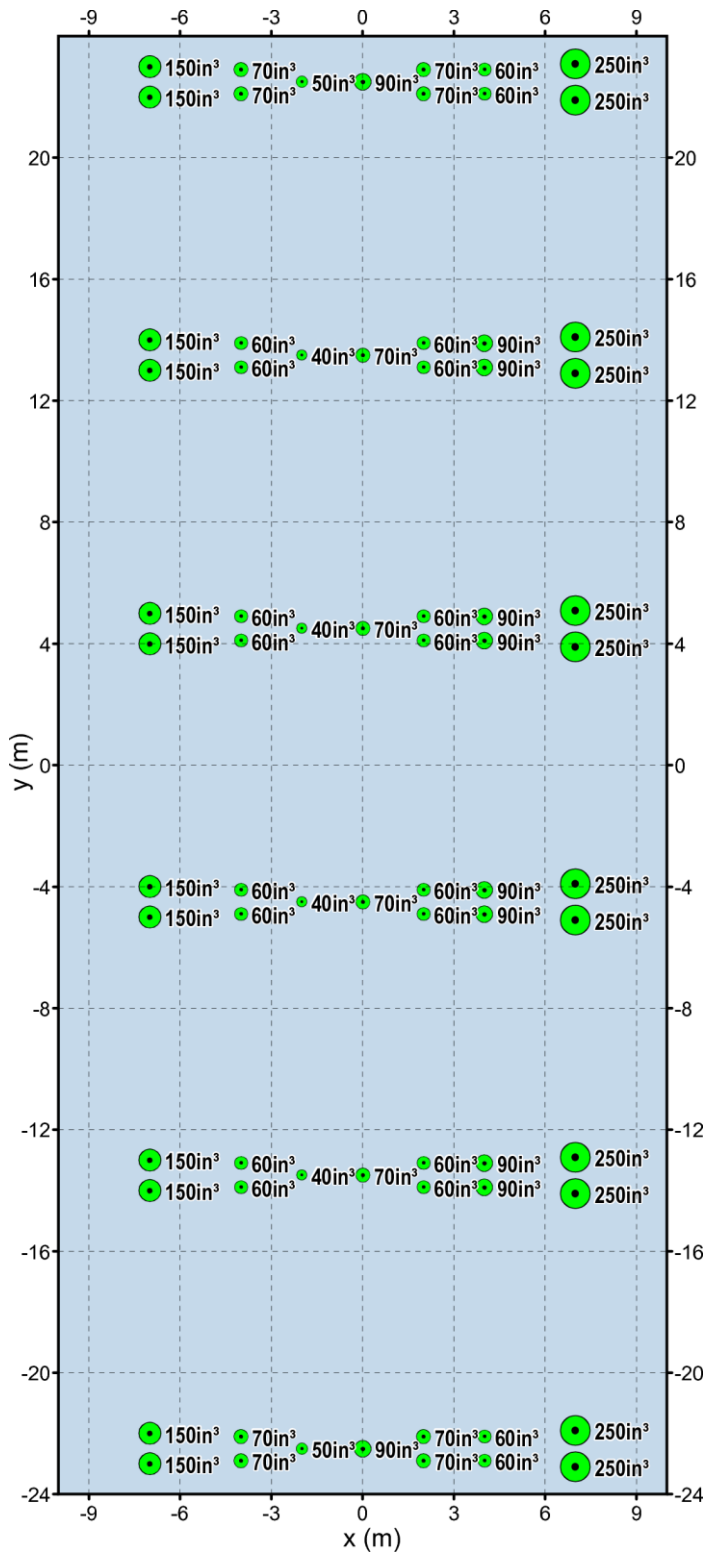

Figure 11. Layout of the modeled airgun array (8000 in³ total firing volume, 8 m depth), which is composed of 6 sub-arrays of 12 airguns each (72 airguns in total). The relative size of green circles and the numbers next to each indicate airgun firing volume.

6.2. Test Case Environmental Parameters

6.2.1. Modeling Sites

Survey site A and Survey site B around Mississippi Canyon (rectangular zones in Figure 10) were selected to be representative of locations for typical shallow (Survey site A) and deep (Survey site B) 3-D wide azimuth surveys conducted in the Gulf. Survey site A was placed so that the shallowest portion would remain at a depth of at least ~ 100 m to ensure that the survey could be safely conducted. The location for Survey site B was chosen to include the deepest water where a seismic survey could reasonably be expected to occur. Acoustic fields were computed at four locations in each survey area (Figure 10), with one location common to both areas. As examples, Appendix A shows per-pulse acoustic fields from a single 8000 in^3 array as field maps and tables of propagation radii for three of the acoustic propagation modeling sites.

6.2.2. Bathymetry

Water depths throughout the modeled area were obtained from the National Geophysical Data Center's U.S. Coastal Relief Model (NGDC 2003) that extends up to about 200 km from the U.S. coast. These bathymetry data have a resolution of 3 arc-seconds (~ 80 × 90 m at the studied latitude). Bathymetry data for an area were extracted and re-gridded, using minimum curvature method, onto a Universal Transverse Mercator (UTM) zone 15 coordinate projection with a horizontal resolution of 50 × 50 m.

6.2.3. Multi-Layer Geoacoustic Profile

MONM assumes a single geoacoustic profile of the seafloor for the entire modeled area. MONM requires these acoustic properties:

- Sediment density
- Compressional-wave (or P-wave) speed
- P-wave attenuation in decibels per wavelength
- Shear-wave (or S-wave) speed
- S-wave attenuation, also in decibels per wavelength

The geoacoustic parameters were estimated based on typical values expected within the Mississippi Canyon, in accordance with our experience in modeling this area. Survey site A was in the vicinity of latitude 28 N and longitude 89 W, and Survey site B was centered approximately 72 km farther southeast (Figure 10). Modeling at Survey site A required two geoacoustic provinces, one consisting of surficial clay, designated S01, and a second consisting of surficial sand, designated S02. Modeling at Survey site B required only one geoacoustic province, designated as D01. The geoacoustic profile assumed for these three modeling provinces is shown in Tables 8 through 10, respectively.

Table 8. Geoacoustic properties of the sub-bottom sediments as a function of depth for the S01 modeling province. Within each depth range, each parameter varies linearly within the stated range.

Depth below seafloor (m)	Material	Density (g/cm^3)	P-wave speed (m/s)	P-wave attenuation (dB/λ)	S-wave speed (m/s)	S-wave attenuation (dB/λ)
0–10	Clay	1.44–1.61	1480–1522	0.21–0.37	100	0.1
10–50		1.61–1.78	1522–1610	0.37–0.56		
50–100		1.78–1.87	1610–1670	0.56–0.67		
100–300		1.87–2.0	1670–1800	0.67–0.9		
300–1000	Compacted/ consolidated sediments	2.0–2.5	1800–3000	0.9–0.2		
> 1000	Compacted/ consolidated sediments	2.5	3000	0.2		

Table 9. Geoacoustic properties of the sub-bottom sediments as a function of depth for the S02 modeling province. Within each depth range, each parameter varies linearly within the stated range.

Depth below seafloor (m)	Material	Density (g/cm^3)	P-wave speed (m/s)	P-wave attenuation (dB/λ)	S-wave speed (m/s)	S-wave attenuation (dB/λ)
0–10	Silt	1.44–1.61	1505–1570	0.34–0.55	150	0.2
10–50		1.61–1.78	1570–1695	0.55–0.86		
50–100		1.78–1.87	1695–1775	0.86–1.02		
100–300		1.87–2.0	1775–1950	1.02–1.3		
300–1000	Compacted/ consolidated sediments	2.0–2.5	1950–3000	1.3–0.2		
> 1000	Compacted/ consolidated sediments	2.5	3000	0.2		

Table 10. Geoacoustic properties of the sub-bottom sediments as a function of depth for the D01 modeling province. Within each depth range, each parameter varies linearly within the stated range.

Depth below seafloor (m)	Material	Density (g/cm^3)	P-wave speed (m/s)	P-wave attenuation (dB/λ)	S-wave speed (m/s)	S-wave attenuation (dB/λ)
0–12	Soft clay	1.35–1.68	1460–1518	0.14–0.55	100	0.1
12–45	Clay	1.68–1.87	1518–1601	0.55–0.86		
45–90	Stiff clay	1.87–1.95	1601–1660	0.86–1.02		
90–200		1.95–2.0	1660–2200	1.02–1.3		
200–1000	Compacted/ consolidated sediments	2.0–2.5	2200–3000	1.3–0.2		
> 1000	Compacted/ consolidated sediments	2.5	3000	0.2		

6.2.4. Sound Speed Profile

The sound speed profiles for the modeled sites were derived from temperature and salinity profiles from the U.S. Naval Oceanographic Office's *Generalized Digital Environmental Model V 3.0* (GDEM; Teague et al. 1990, Carnes 2009). GDEM provides an ocean climatology of temperature and salinity for the world's oceans on a latitude-longitude grid with 0.25° resolution, with a temporal resolution of one month, based on global historical observations from the U.S. Navy's Master Oceanographic Observational Data Set (MOODS). The climatology profiles include 78 fixed depth points to a maximum depth of 6800 m (where the ocean is that deep), including 55 standard depths between 0 and 2000 m. The GDEM temperature-salinity profiles were converted to sound speed profiles according to the equations of Coppens (1981):

$$\begin{aligned} c(z,T,S,\phi) &= 1449.05 + 45.7t - 5.21t^2 - 0.23t^3 \\ &\quad + \left(1.333 - 0.126t + 0.009t^2\right)(S-35) + \Delta \\ \Delta &= 16.3Z + 0.18Z^2 \\ Z &= \frac{z}{1000}\left[1 - 0.0026\cos(2\phi)\right] \\ t &= \frac{T}{10} \end{aligned} \tag{18}$$

where z is water depth (m), T is water temperature (°C), S is salinity (psu), and ϕ is latitude (radians).

The sound speed profile for August at Survey site A indicates a strong, downward-refracting environment with a very weak surface sound channel (Figure 12). The surface channel is essentially absent in the Survey site B profile, which is also strongly downward refracting for a sound source near the surface. For a source near the surface, long-range acoustic propagation at both sites is mainly dependent on bottom-interacting pathways (despite a weak surface channel at Survey site A). As discussed in Section 6.2.3, the bottom composition is unfavorable for long-range propagation.

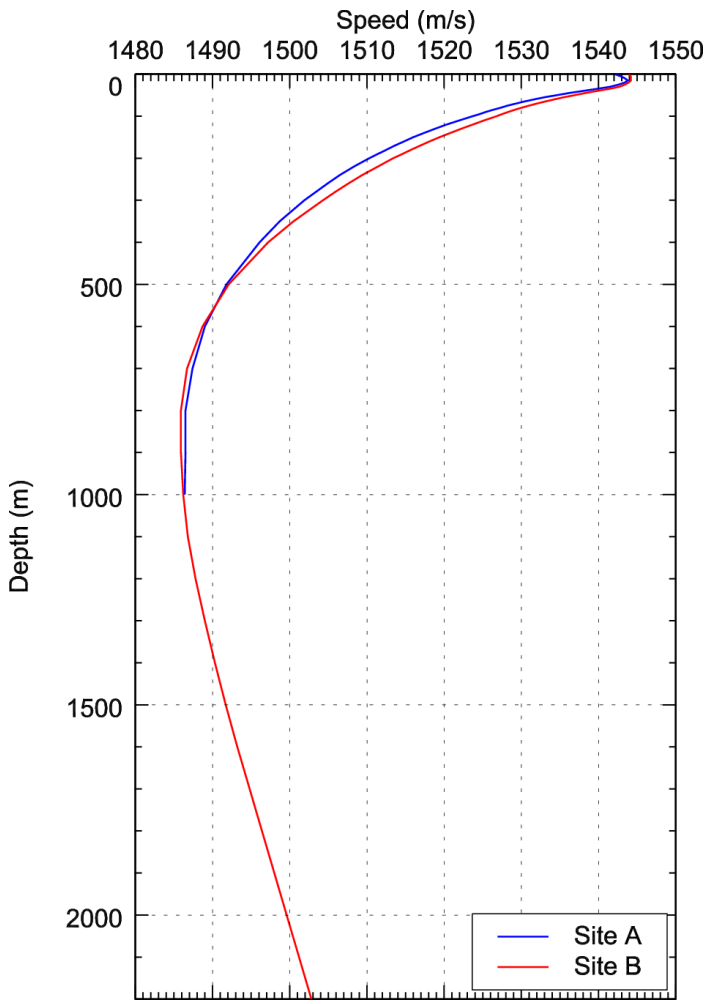

Figure 12. Sound speed profiles for August in the Mississippi Canyon, Gulf of Mexico at Survey sites A and B, derived from data obtained from GDEM V 3.0 (Teague et al. 1990, Carnes 2009).

6.2.5. Marine Mammals Density Estimates

Density estimates, animals/km^2, for marine mammal species from survey data can be obtained from the online Strategic Environmental Research and Development Program (SERDP) Spatial Decision Support System (SDSS) hosted by Ocean Biogeographic Information System Spatial Ecological Analysis of Megavertebrate Populations (OBIS SEAMAP) at Duke University. For the Gulf of Mexico, the U.S. Navy OPAREA Density Estimate (NODE; DoN 2007) model is available. The NODE data for the Gulf of Mexico are based on shipboard surveys conducted between 1994 and 2004 by the National Marine Fisheries Service-Southeast Fisheries Science Center (NMFS-SEFSC). Surveys conducted before 2003 were in conjunction with Southeast Area Monitoring and Assessment Program (SEAMAP) as adjuncts to cruises designed as ichthyoplankton sampling surveys. The NODE database generates seasonal density estimates for each species based on a statistical analysis of the survey data. For species with adequate sighting data, the DISTANCE model (Buckland et al. 2001) was used to generate density estimates. For species with too few sightings for the DISTANCE model to create a density, NOAA's stock assessment report (SAR; Waring et al. 2013) data were used to generate density by dividing abundance by the regional area.

Seasons were defined by the mean sea surface temperature (DoN 2007) as:

- Winter: 23 Dec through 2 Apr
- Spring: 3 Apr through 1 Jul
- Summer: 2 Jul through 28 Sep
- Fall: 29 Sep through 22 Dec

The DISTANCE model is a regression model (as opposed to a habitat suitability model), and, as with any model, a number of assumptions and simplifications are required. A notable assumption when generating the NODE database was that the estimating bias—the probability of detecting an object on a transect line, $g(0)$—was set to 1. That is, no correction is made to the density estimates to account for animals missed during the survey. Animals can be missed for a variety of reasons, including deep or long diving times for species including sperm whales and beaked whales. With no correction for the estimation bias, the density estimates should be regarded as floor estimates. Figures 13 and 14 are examples of density estimates for sperm whales obtained at Survey sites A and B, respectively. Tables 11 and 12 list the marine mammal density estimates for the species evaluated. The minimum, maximum, and mean density estimates for the region of interest are shown.

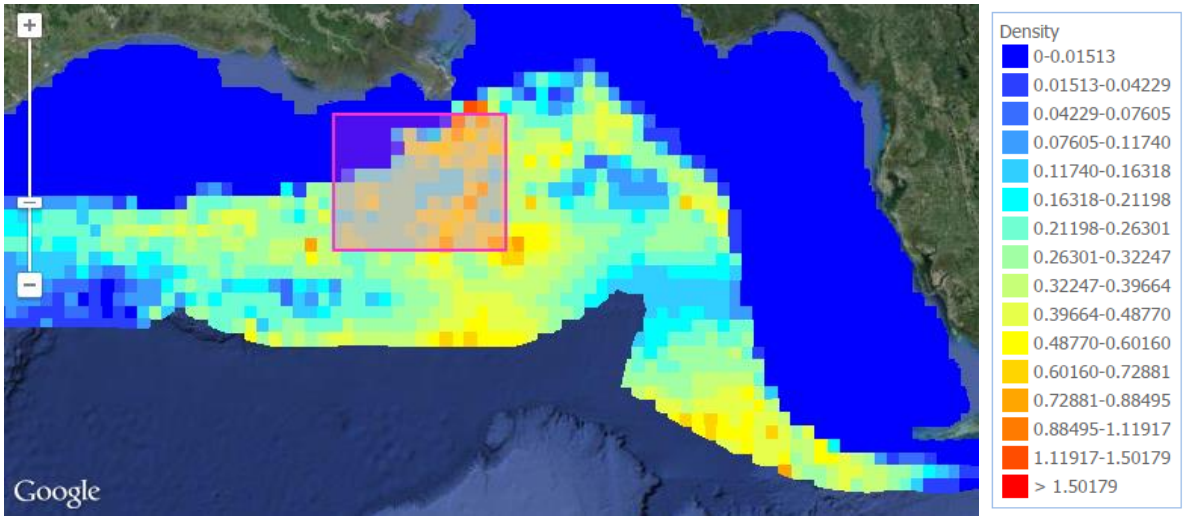

Figure 13. Density estimates for sperm whales near Survey site A in the Gulf of Mexico from NODES model. Density is animals/km^2. The red rectangle represents the area around the survey site for which density estimates were obtained.

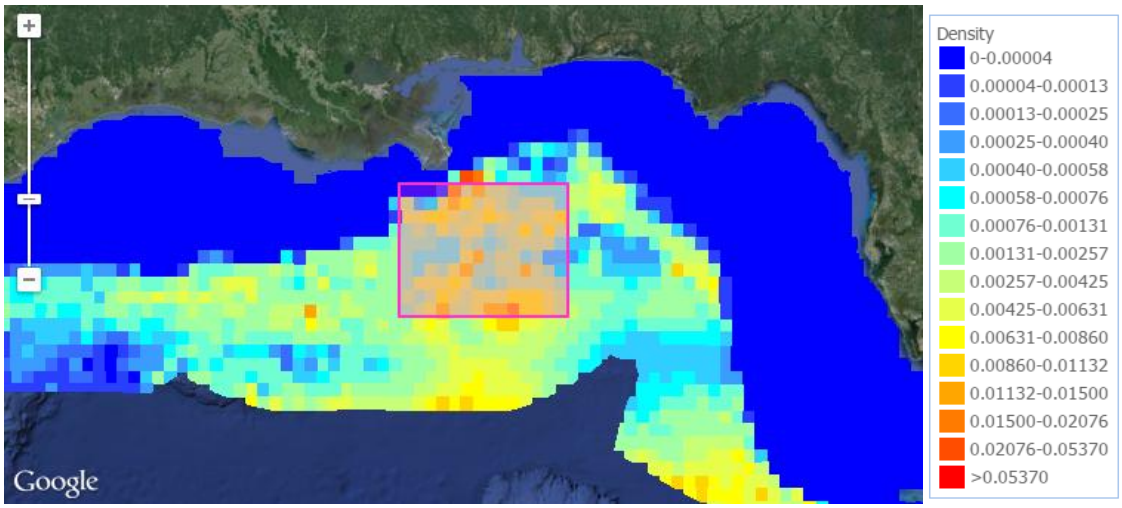

Figure 14. Density estimates for sperm whales near Survey site B in the Gulf of Mexico from NODES model. Density is animals/km^2. The red rectangle represents the area around the survey site for which density estimates were obtained.

Table 11. Summer regional statistics of marine mammal density near Survey site A for the Gulf of Mexico.

Common name	Regional Density (animals/km^2)		
	Minimum	Maximum	Mean
Bryde's whales	0	0.000105	0.000081
Cuvier's beaked whales	0.000003	0.004121	0.000676
Common bottlenose dolphins†	0	0.107	0.01387
Short-finned pilot whales†	0	0.006277	0.004845
Sperm whales†	0.000036	0.008154	0.002761
Dwarf sperm whales	0	0.004605	0.000673

† Density estimates from SERDP-SDSS NODES database derived from NMFS-SEFSC survey data.

Table 12. Summer regional statistics of marine mammal density near Survey site B for the Gulf of Mexico.

Common name	Regional Density (animals/km^2)		
	Minimum	Maximum	Mean
Bryde's whales	0	0.000105	0.000097
Cuvier's beaked whales	0	0.004121	0.000809
Common bottlenose dolphins†	0	0.08429	0.001525
Short-finned pilot whales†	0	0.006277	0.005785
Sperm whales†	0.000365	0.005395	0.002311
Dwarf sperm whales	0.000002	0.01558	0.001589

† Density estimates from SERDP-SDSS NODES database derived from NMFS-SEFSC survey data.

6.2.6. Animal Movement Modeling

In in Phase I analysis, the Marine Mammal Movement and Behavior (3MB) model developed by Houser (2006) was used. 3MB is included in the Effects of Sound on the Marine Environment (ESME) interface developed by the Office of Naval Research (ONR) and Boston University (Gisiner et al. 2006, Shyu and Hillison 2006). ESME is an open-source software program conveniently combines animal movement models and computed sound fields. For the current application, ESME was modified so that it used the sound fields from the study area. 3MB uses a number of parameters to simulate realistic animal movement. It was necessary to determine these parameters from published studies for the simulated species (see Appendix D).

6.3. Test Case Results

6.3.1. Acoustic Sources: Levels and Directivity

The pressure signatures of the individual airguns and the composite 1/3-octave-band source levels of the array, as functions of azimuthal angle (in the horizontal plan), were computed with AASM as described in Section 5.1. While effects of source depth on bubble interactions are accounted for in the AASM source model, the surface-reflected signal (i.e., surface ghost) is not included in the far-field source signatures. The surface reflections, a property of the medium rather than the source, are accounted for by the acoustic propagation models.

6.3.1.1. 8000 in³ Airgun Array

The horizontal overpressure signatures and corresponding power spectrum levels for the 8000 in^3 array, when stationary at a depth of 8 m (to the vertical center of the gun clusters), are shown in Figure 15 and Table 13 for the broadside (perpendicular to the tow direction) and endfire (parallel to the tow direction) directions. The signatures consist of a strong primary peak related to the initial firing of the airguns, followed by a series of pulses associated with bubble oscillations. Most energy is produced at frequencies below 200 Hz (Figure 15b). The spectrum contains peaks and nulls resulting from interference among airguns in the array, where the frequencies at which they occur depend on the volumes of the airguns and their locations within the array. The maximum (horizontal) 1/3-octave-band sound levels over all directions are plotted in Figure 16. The horizontal 1/3-octave-band directivities are shown in Figure 17.

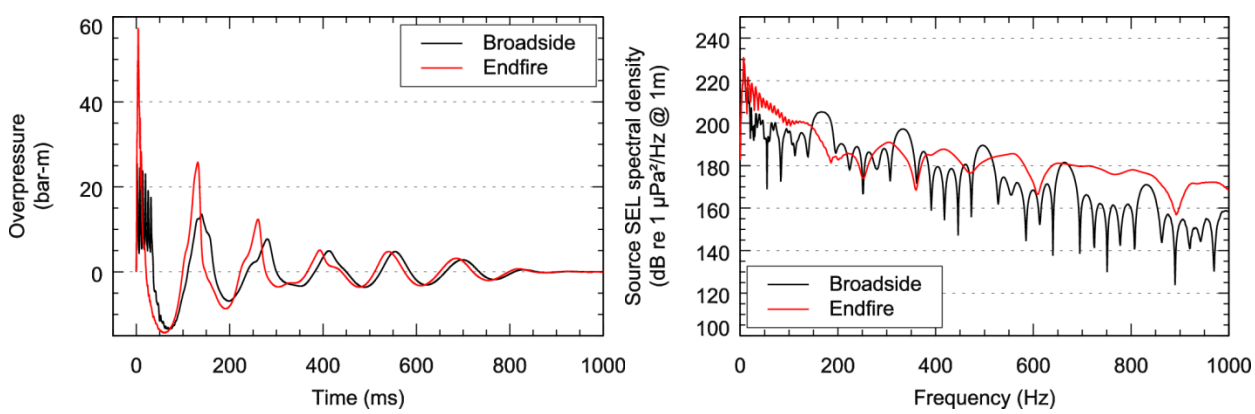

(a) (b)

Figure 15. The 8000 in^3 array: Predicted (a) overpressure signature and (b) power spectrum in the broadside and endfire (horizontal) directions. Surface ghosts (effects of the pulse reflection at

the water surface) are not included in these signatures as they are accounted for by the MONM propagation model.

Table 13. Horizontal source level specifications (10–5000 Hz) for the seismic airgun array (8000 in^3) at 8 m depth, computed with AASM in the broadside and endfire directions. Surface ghost effects are not included as they are accounted for by the MONM propagation model.

Direction	Zero-to-peak SPL (dB re 1 µPa @ 1 m)	SEL (dB re 1 µPa^2 @ 1 m)		
		0.01–2 kHz	0.01–1 kHz	1–2 kHz
Broadside	248.1	225.7	225.7	182.2
Endfire	255.2	231.8	231.8	189.6

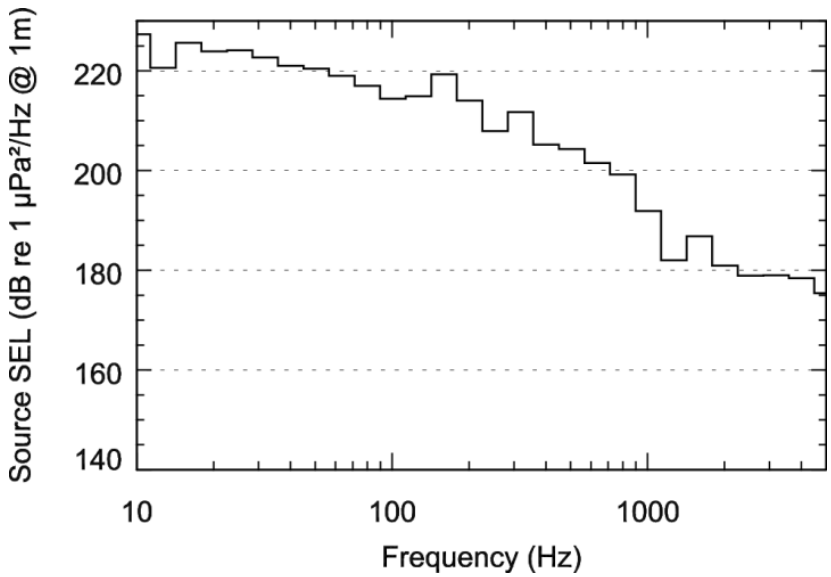

Figure 16. Maximum directional source level (SL) in the horizontal plane, in each 1/3-octave-band, for the 8000 in^3 airgun array (10–5000 Hz).

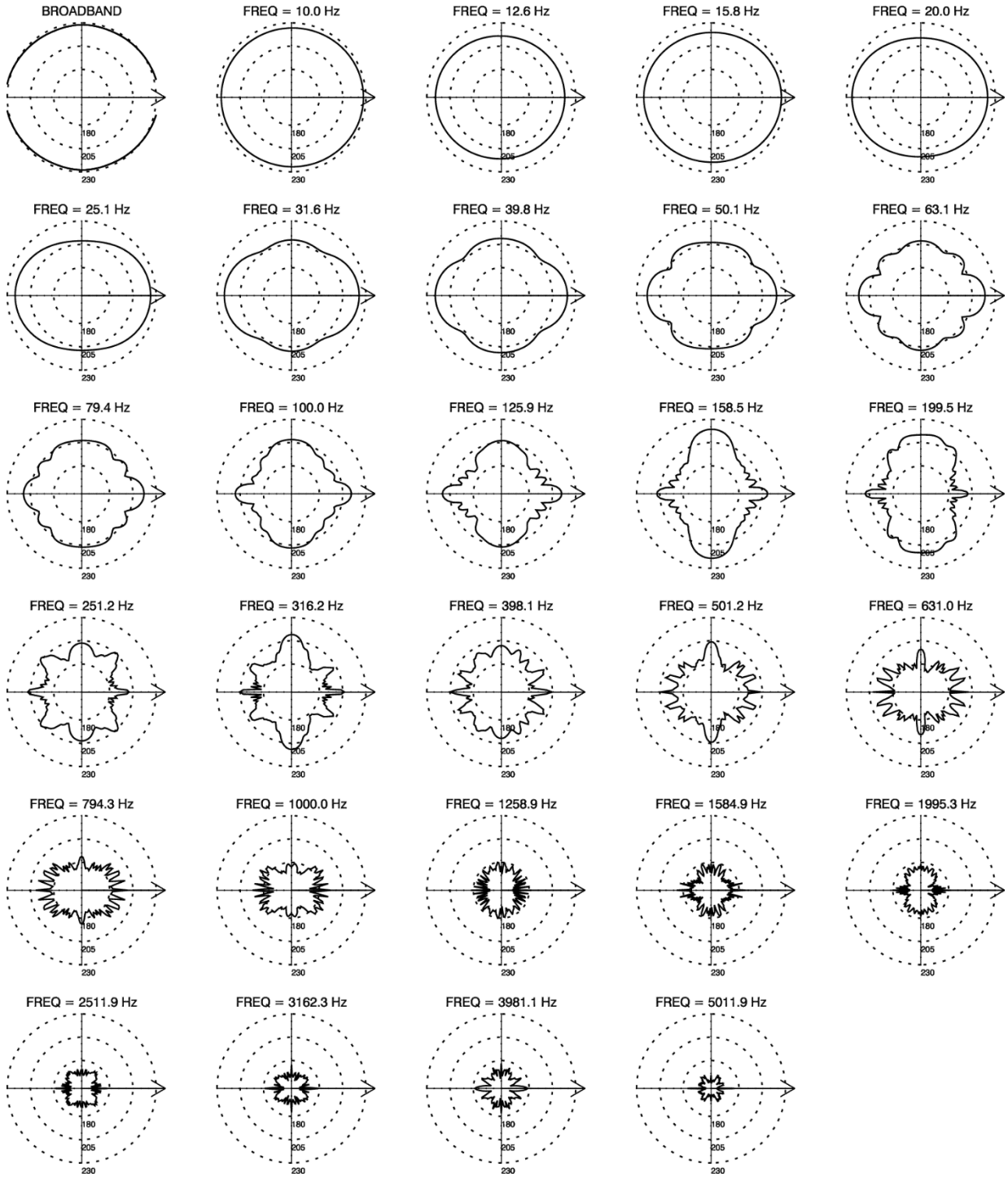

Figure 17. Horizontal directivity of the 8000 in^3 array. Source levels (SLs, dB re 1 μPa^2·s) in 1/3-octave-bands. The 1/3-octave-band center frequencies are indicated above each plot.

6.3.1.2. Per-Pulse Acoustic Field for Input to ESME

The per-pulse acoustic field propagation modeling for input to ESME was computed for the Survey site A and Survey site B modeling locations. Transmission loss for the purpose of exposure simulation was modeled along 16 radial profiles (angular step 22.5°) to the range of up to 50 km from the source location. The horizontal step along the radials was 10 m. At each surface sampling location, the sound field was sampled at multiple depths with equal vertical steps of 10 m down to the maximum water depth along the profile.

The frequencies up to 5 kHz for the airgun array source were considered in the calculations of the broadband received levels. All 1/3-octave-band frequencies from 10 Hz to 5 kHz were used for the airgun array source level modeling (Section 7.3.1). For the transmission loss calculations, frequencies higher than 2 kHz are computationally intensive, so it was assumed that the transmission loss field for higher frequencies (up to 5 kHz) was identical to that at 2 kHz.

The broadband acoustic field passed as input to ESME was in SEL metrics and was both range and depth dependent (Figure 18).

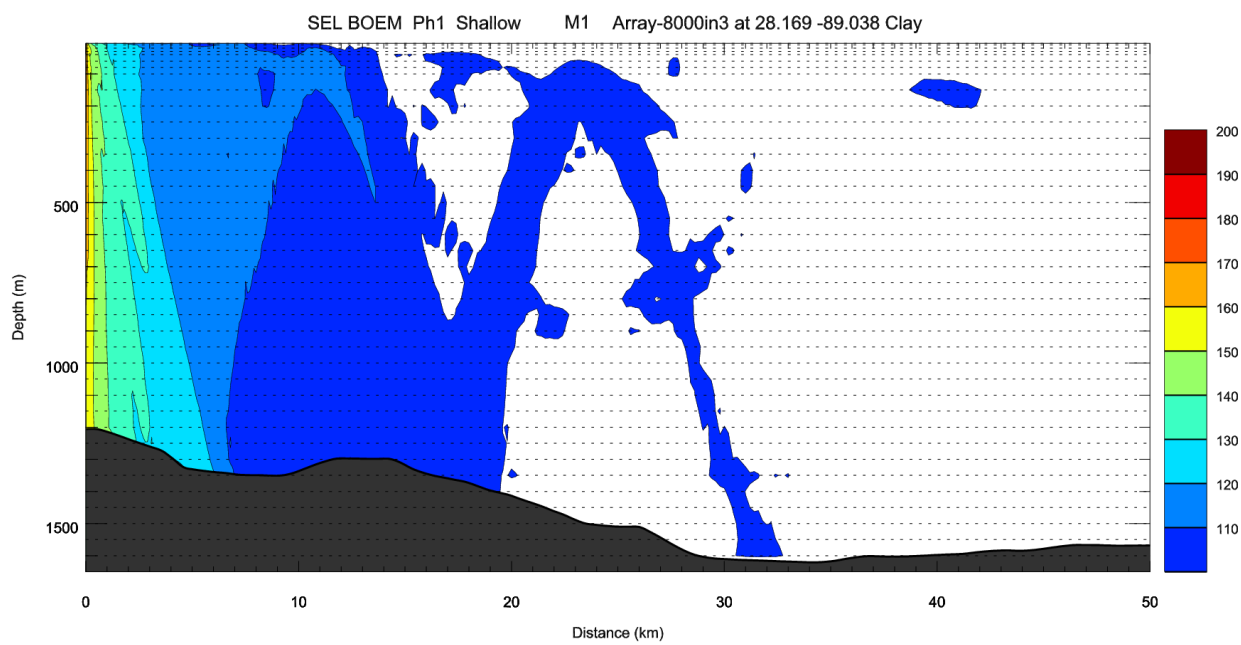

Figure 18. An example of per-pulse received SEL field (with mid-frequency cetacean auditory frequency weighting applied) from the 8000 in³ airgun array at the S01 modeling province.

6.3.1.3. Range to Zero-to-Peak SPL Isopleths

To evaluate the risk of acoustic injury, the range to the unweighted, zero-to-peak SPL (dB re 1µPa) was needed to the 200 dB isopleth (high-frequency cetaceans) and 230 dB isopleth (low- and mid-frequency cetaceans). The ranges were calculated assuming spherical spreading from a point source starting with the maximum source level of the airgun arrays being considered. The maximum zero-to-peak source level for the 8000 in^3 array was 255.2 dB re 1µPa in the endfire direction (Table 13; the broadside source level was lower). The range to 200 dB zero-to-peak SPL re 1µPa was 575.4 m and the range to 230 dB zero-to-peak SPL re 1µPa was 18.2 m. The source level of the array is a theoretical definition assuming a point source and measurement in the far field of the source. The 230 dB isopleth was within the near field of the array where the definition of source level breaks down, so actual locations within the 18.2 m of the array center

(or near any one airgun) where the sound level exceeds 230 dB zero-to-peak SPL re 1µPa did not necessarily exist. The 200 dB isopleth, however, was in the far field and sound levels within 575.4 m of the center of the array did experience sound levels exceeding 200 dB zero-to-peak SPL re 1µPa. The number of animals expected to come within the 200 dB and 230 dB isopleths were determined for the high-frequency, and low-frequency and mid-frequency cetaceans, respectively.

6.3.2. Simulation Exposure Estimates

The amount of acoustic energy received depends on where in the sound field, both horizontally and vertically, an animal is when the sound source is active. Animal movement was simulated using the Marine Mammal Movement and Behavior (3MB) model, and ESME was used to sample the sound field produced by the airgun array. Sampling the sound field(s) produced during an operation using a simulated animal (animat) provided a history of acoustic exposure for that animat. The acoustic exposure history of many animats yields the probability, or risk, of exposure due to operations.

Two sites were chosen near the Mississippi Canyon to conduct hypothetical, though typical, WAZ surveys. Survey site A was centered on the slope of the continental shelf break with the survey extending into shallow waters on the continental shelf. Survey site B was centered in deeper water though the survey also included the slope of the continental shelf break. The longitudinal tow direction of the vessels was selected for computational efficiency.

The WAZ survey area was covered in a racetrack fashion using four seismic vessels, each towing a single airgun array. Production segments were 100 km long and the overall survey width was 60 km. Each production segment included 5 km run-in and run-off segments, and the turning segment to the next track line in the opposite direction was 30 km. For the first vessel, the lateral offset to the track in the opposite direction was 30 km. The other vessels had identical track geometries, but laterally shifted by 350 m relative to their neighbors. There was also a 2700 m shift along the track for each vessel, so the vessels were not moving side-by-side (inset Figure 19). Each vessel delivered a seismic pulse every 60 s (15 s for the vessel group), and vessel speed was 4 kts.

To account for variability of sound propagation due to changing water depth, the acoustic field was pre-computed at four locations for each of the survey areas. For each location, the 2-D acoustic field was calculated for 16 radials emanating from the source (airgun array). For each shot during the simulation, an acoustic field was selected from the pre-computed set based on the nearest neighborhood method.

To evaluate potential behavioral response, 30 day simulations of hypothetical WAZ surveys (Survey sites A and B) were run for each of the species evaluated (Figure 19). The boundaries of the simulation were determined from transmission loss calculations by finding the maximum range at which an animat could receive an rms SPL ≥ 120 dB re 1µPa (the lowest exposure levels at which impacts are expected). The maximum range was estimated at 50 km. To evaluate potential behavioral disruption, the simulation area was defined based on the perimeter of the survey tracks with an extension of 50 km on each side with the exception for the north side at Survey site A, where the extension was 35 km due to proximity of the shore. The simulation areas for Survey sites A and B were 214 × 144 km (30,800 km^2) and \212 × 161 km (34,100 km^2), respectively. To evaluate potential injury, the width of the survey was reduced to 11 km (Figure 20), and duration of 5 days. The boundaries of the simulation were extended by 5 km on each side of the survey area for 214 × 21 km (5061 km^2) areas at both Survey site A and Survey site B (Figure 20). The animat density for simulations were 0.1 and 2 animats/km^2 for behavior and injury, respectively.

Exposure levels were determined for the combined effect of the sources. Results for each of the marine mammal species are shown in Table 14 for Survey site A and Table 15 for Survey site B. Appendix A shows the frequency of exposure level for each simulation.

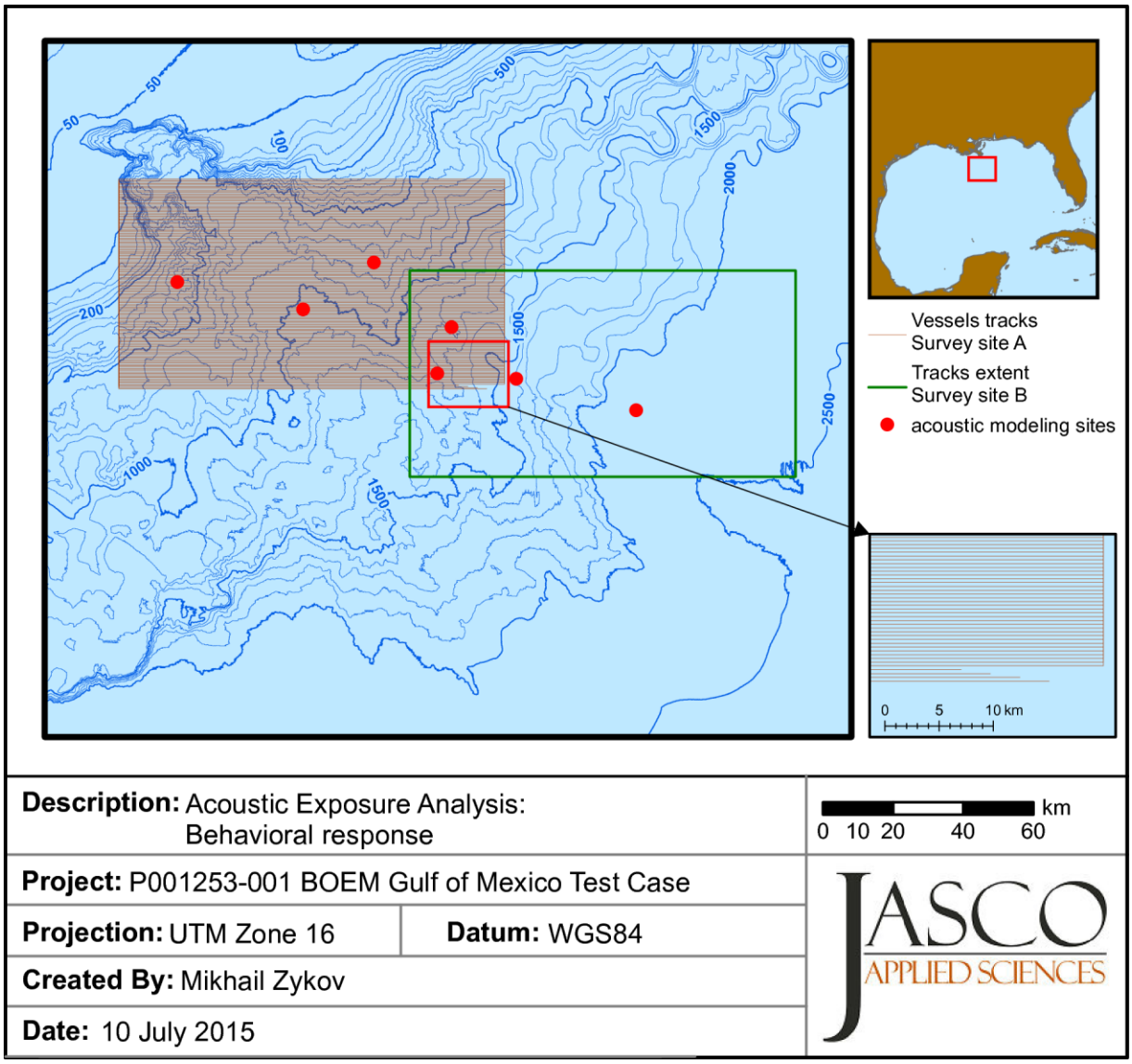

Figure 19. Vessel track locations for behavioral response analysis at Survey sites A and B. Inset shows the starting point in the southeast corner.

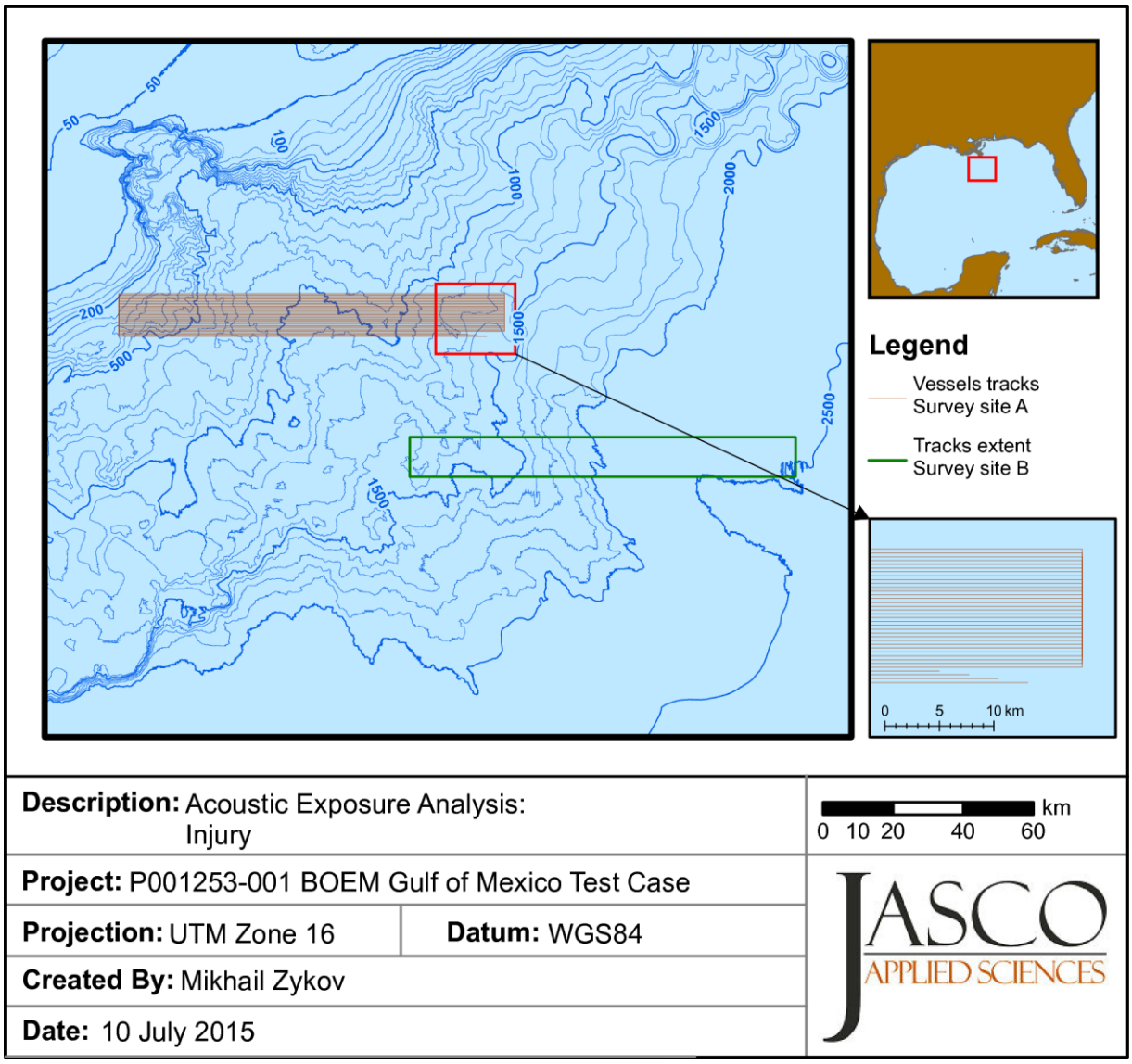

Figure 20. Vessel track locations for injury analysis at Survey sites A and B. Inset shows the starting point in the southeast corner.

Table 14. Number of modeled cetaceans above exposure criteria for Survey site A for entire duration of the simulations. Simulations for zero-to-peak SPL and SEL injury metrics were 5 day duration with animat density of 2.0 animats/km^2. Simulations for rms SPL metrics were 30 day duration with animat density of 0.1 animats/km^2.

Marine mammal species	Injury			Behavior	
	zero-to-peak SPL	SEL	180 dB rms SPL	160 dB rms SPL	Step fxn. rms SPL
Bryde's whales	47	534	348	571	637
Cuvier's beaked whales	45	0	276	577	1941.4
Common bottlenose dolphins	105	0	246	342	439.2
Short-finned pilot whales	106	1	240	330	425
Sperm whales	15	1	166	349	386.5
Dwarf sperm whales	7060	1053	209	343	405

SPL=sound pressure level; SEL=sound exposure level; rms=root-mean-square.

Table 15. Number of modeled cetaceans above exposure criteria for Survey site B for entire duration of the simulations. Simulations for zero-to-Peak SPL and SEL injury metrics were 5 day duration with animat density of 2.0 animats/km^2. Simulations for rms SPL metrics were 30 day duration with animat density of 0.1 animats/km^2.

Marine mammal species	Injury			Behavior	
	zero-to-peak SPL	SEL	180 dB rms SPL	160 dB rms SPL	Step fxn. rms SPL
Bryde's whales	51	485	313	357	529.8
Cuvier's beaked whales	38	0	300	491	1829.2
Common bottlenose dolphins	99	0	254	285	411
Short-finned pilot whales	102	0	263	315	426.6
Sperm whales	35	0	381	701	789.9
Dwarf sperm whales	7246	893	242	337	417.7

SPL=sound pressure level; SEL=sound exposure level; rms=root-mean-square

6.3.3. Real-world Individual Exposure Estimates

Simulations were run with animat densities (animats/km^2) greater than are typically found in the real world in order to generate reliable exposure probability density functions for each species. The numbers of exposures, therefore, must be adjusted for the species real-world density. Minimum, maximum, and mean regional real-world densities estimates were obtained from the U.S. Navy OPAREA Density Estimate (NODE) model for the Gulf of Mexico (DoN 2007, as shown in Section 6.2.5 and Table 11). The real-world number of cetacean individuals expected to exceed the injury exposure criteria is shown for Survey sites A and B in Tables 16 and 17, respectively. Likewise, the real-world number of cetacean individuals expected to exceed the behavioral disruption exposure criteria is shown for Survey sites A and B in Tables 18 and21, respectively.

Table 16. Real-world number of cetaceans above injury exposure criteria for summer for Survey site A.

Marine mammal species	peak SPL			SEL			180 dB rms SPL		
	Min	Max	Mean	Min	Max	Mean	Min	Max	Mean
Bryde's whales	< 0.01	< 0.01	< 0.01	< 0.01	0.03	0.02	< 0.01	0.37	0.28
Cuvier's beaked whales	< 0.01	0.03	< 0.01	< 0.01	< 0.01	< 0.01	< 0.01	59.56	5.43
Common bottlenose dolphins	< 0.01	5.62	0.73	< 0.01	0.05	0.01	< 0.01	714.63	53.65
Short-finned pilot whales	< 0.01	0.14	0.11	< 0.01	< 0.01	< 0.01	< 0.01	15.06	11.63
Sperm whales	< 0.01	0.42	0.14	< 0.01	< 0.01	< 0.01	< 0.01	45.68	4.73
Dwarf sperm whales	< 0.01	16.30	2.38	< 0.01	2.42	0.35	< 0.01	11.59	1.29

SPL=sound pressure level; SEL=sound exposure level; rms=root-mean-square; min=minimum; max=maximum

Table 17. Real-world number of cetaceans above injury exposure criteria for summer for Survey site B.

Marine mammal species	peak SPL			SEL			180 dB rms SPL		
	Min	Max	Mean	Min	Max	Mean	Min	Max	Mean
Bryde's whales	< 0.01	< 0.01	< 0.01	< 0.01	0.03	0.02	< 0.01	0.33	0.30
Cuvier's beaked whales	< 0.01	0.07	0.01	< 0.01	< 0.01	< 0.01	< 0.01	52.26	5.49
Common bottlenose dolphins	< 0.01	4.21	0.08	< 0.01	< 0.01	< 0.01	< 0.01	250.42	8.20
Short-finned pilot whales	< 0.01	0.12	0.11	< 0.01	< 0.01	< 0.01	< 0.01	16.51	15.21
Sperm whales	< 0.01	0.27	0.11	< 0.01	< 0.01	< 0.01	< 0.01	104.85	13.57
Dwarf sperm whales	< 0.01	56.45	5.76	< 0.01	6.95	0.71	< 0.01	33.15	3.33

SPL=sound pressure level; SEL=sound exposure level; rms=root-mean-square; min=minimum; max=maximum

Table 18. Real-world number of cetaceans above behavioral exposure criteria for summer for Survey site A.

Marine mammal species	Step fxn. max. rms SPL			160 dB rms SPL		
	Min	Min	Min	Min	Max	Mean
Bryde's whales	< 0.01	0.76	0.59	< 0.01	0.60	0.46
Cuvier's beaked whales	0.10	140.57	23.06	< 0.01	124.52	11.34
Common bottlenose dolphins	< 0.01	522.16	67.69	< 0.01	993.51	74.59
Short-finned pilot whales	< 0.01	30.18	23.29	< 0.01	20.71	15.99
Sperm whales	0.16	35.96	12.18	< 0.01	96.04	9.95
Dwarf sperm whales	< 0.01	20.75	3.03	< 0.01	19.03	2.12

SPL=sound pressure level; rms=root-mean-square; min=minimum; max=maximum

Table 19. Real-world number of cetaceans above behavioral exposure criteria for summer for Survey site B.

Marine mammal species	Step fxn. max. rms SPL			160 dB rms SPL		
	Min	Min	Min	Min	Max	Mean
Bryde's whales	< 0.01	0.75	0.69	< 0.01	0.37	0.35
Cuvier's beaked whales	< 0.01	99.11	19.46	< 0.01	85.53	8.98
Common bottlenose dolphins	< 0.01	383.18	6.93	< 0.01	280.98	9.20
Short-finned pilot whales	< 0.01	29.41	27.10	< 0.01	19.77	18.22
Sperm whales	3.31	48.99	20.98	< 0.01	192.92	24.97
Dwarf sperm whales	0.01	71.12	7.25	0.01	46.17	4.64

SPL=sound pressure level; rms=root-mean-square; min=minimum; max=maximum

6.4. Test Case Exposure Summary

The estimated number of animals exposed to levels exceeding the acoustic exposure thresholds was determined for the two WAZ survey sites. For injury, it was found that relative to the other species, a large number of dwarf sperm whales may be exposed to levels exceeding both the SEL and zero-to-peak SPL thresholds. It was also found that a relatively high number of Bryde's whales may be exposed to levels exceeding the SEL injury threshold. Dwarf sperm whales are a high-frequency species with greater susceptibility to injury than the other species. For this reason, injury thresholds were lower for dwarf sperm whales and as a result the number of animats exposed to levels exceeding threshold was higher. Bryde's whales are low frequency animals and most of the acoustic energy emanating from an airgun is low frequency. Because less restrictive filtering (Type I M weighting) was used to calculate the sound field for the low-frequency species, the ensonified area above threshold was much greater than for mid-frequency species and therefore the number of animats exposed to levels exceeding threshold is higher. For Bryde's whales, the estimated real-world density is low so the predicted real-world number of animals exposed to levels exceeding injury criteria is less than one animal. The estimated real-world density of dwarf sperm whales is higher and, therefore, the predicted number of real-world animals exposed to levels exceeding injury threshold was up to 56.5 animals (Survey site B and maximum density estimate).

The volume over which behavioral disturbance may occur is greater than the volume over which injury may occur. Animats for all species were found to exceed thresholds for potential behavioral disturbance. Cuvier's beaked whales had the greatest number of exceedances because, as a behaviorally sensitive species, the step function used to assess their potential for behavioral disturbance starts at lower sound levels (120 dB rms SPL versus 140 dB rms SPL for the remaining species). It was also found that Bryde's whales and sperm whales had higher exceedance than the common bottlenose dolphins, short-finned pilot whales, and dwarf sperm whales. Because the majority of acoustic energy from the airguns is in the low frequency band (< 1500 Hz) and the low-frequency weighting function permits more low-frequency energy to propagate, the ensonified volume above threshold was larger for low frequency species and results in more animats exposed to sounds above the thresholds. Sperm whales are deep-diving animals and in the downward-refracting acoustic environment are more consistently exposed to sound levels above threshold when diving. This is apparent at Survey site B where a behavioral response was predicted for approximately twice as many sperm whale animats (908) as common bottlenose dolphin, short-finned pilot whale, and dwarf sperm whale animats (all ~ 450). At Survey site A, the number behavioral responses predicted for sperm whales was about the same as the predictions for common bottlenose dolphin, short-finned pilot whale, and dwarf sperm whale animats (all ~ 450). The reason for the difference in the number of behavioral responses predicted for sperm whales at the two sites is that

Survey site A is shallower than Survey site B. Sperm whales generally do not enter water shallower than 1000 m, so during the simulation the animats changed swimming direction to avoid depths < 1000 m. In addition, because much of the area at Survey site A is < 1000 m, a smaller number of animats were used during the simulation (animats are not seeded in depth-restricted areas) so that the animat density remained consistent for all simulations.

6.5. Test Scenarios

Primarily using the results of the Test Case, several scenarios were investigated to determine their potential effects on exposure estimates and to inform the main modeling effort.

Scenarios investigated were:

- Long-duration surveys (Section 6.5.1),
- Sources and effects of uncertainty (Section 6.5.2),
- Mitigation (Section 6.5.3),
- Aversion (Section 6.5.4),
- Stand-off distance (Section 6.5.5.1), and
- Simultaneous firing of sources (Section 6.5.5.2).

6.5.1. Test Scenario 1: Scaling Modeled Acoustic Exposure Estimates

Some seismic surveys operate (nearly) continuously for several months. Evaluating the potential impacts due to underwater sound exposures from these extended operations is challenging because assumptions about parameters that are valid for short-duration simulations may become less valid, or more varied, as the time period increases. For example, the average sound velocity profile changes as the surface layer temperature changes. Also large-scale animal movement, such as migrations or prey movement, may change the density estimate of animals in the simulation area. Treating such parameters as constant, as is typically done in shorter duration simulations, could lead to errors. Systematic bias in modeling processes may also lead to increasing error as the simulation time is increased. Simulated animals (animats) may settle into unrealistic behaviors such as following an arbitrary boundary, or, if animats are allowed to leave the simulation area without a replacement method, a diffusion process will systematically decrease the density.

This Test Scenario investigates the potential impacts of large-scale animal movement and possible systematic bias in the modeling process. Methods for scaling results from shorter-duration simulations to longer duration operations are suggested.

6.5.1.1. Large-scale Animal Movement

Current agent-based animal movement models, such as the Marine Mammal Movement and Behavior (3MB) model (Houser 2006), estimate movement from the current disposition of a simulated animal. Limited, or no, memory of prior states is considered when generating movement changes, such as change of direction or swim speed. These models generate realistic behavior (using swimming and diving parameters) over short durations (days to weeks). They become increasingly less valid as durations are extended because they may not include the effects of long-term behaviors. The models do not account for animal movements on large temporal or spatial scales, and this also may lead to errors. Large-scale

marine mammal movement in the Gulf of Mexico and its potential as a source of error in the acoustic exposure estimates is discussed in the subsections below, and further in section 6.5.1.3.1.

6.5.1.1.1. Scaling Methods

The available literature on cetacean distribution and behavior for the six Gulf of Mexico species studied in the Test Case were examined for information on large-scale movement and seasonality. The majority of the Test Case species prefer deeper water (> 200 m), which makes it difficult to obtain detailed information on their distribution and movements. If no quantitative information could be found, knowledge of behavioral and feeding ecology for the species was used to infer possible movement patterns and large-scale movement behavior.

6.5.1.1.2. Assumptions

Potential movement patterns were based on available information regarding the general behavioral and feeding ecologies of the species in question and observed interactions of the species/populations with the environment. The patterns do not account for evolved programs, such as adaptive predator responses (spatial and temporal movement patterns due to behavioral programming to reduce predation risks) or intra- and interspecies competition for resources, as the available information is insufficient to discuss their relevance.

6.5.1.1.3. Prey Distribution as an Environmental Attractor

The distribution of plankton in the deeper waters of the Gulf of Mexico, especially the northern and eastern parts of the Gulf, is controlled by the loop current (Mullin and Fulling 2004). The temporal movement of all organisms, including marine mammals and their prey, may be effected by upwelling of nutrient rich cold water eddies (Davis et al. 2001); however, habitat use appears to be more directly correlated with static features such as water depth, bottom gradient, and longitude (Mullin and Fulling 2004). Temporal fluctuation near the surface can cause changes in diurnal movement patterns in squid, which prefer colder water, but does not substantially affect cetaceans feeding on squid in deeper waters. As a result, the occurrences of the four Test Case odontocetes that rely on squid as a main food source are only affected by water temperature when deeper layers are affected, which is rarely the case. A more critical consequence of feeding on squid that may cause the whales to leave an area may be that squid may learn to avoid the whales by moving to different areas (Long et al. 1989).

6.5.1.1.4. Distribution and Movement Behavior of Modeled Species

Common Bottlenose Dolphins

Common bottlenose dolphins travel and forage in close association with short-finned pilot whales and other species that feed on squid (NOAA Fisheries 2012a), but since common bottlenose dolphins do not regularly perform deep foraging dives, large-scale movements are likely driven by fish movement in the upper ocean layers. The one offshore common bottlenose dolphin population that feeds primarily on schooling fish, but also on squid, is less driven by the vertical diurnal movements of squid (Barros and Odell 1990, Barros and Wells 1998). Other oceanic delphinids, such as some spotted dolphins travel 55–90 km/day (Mullin and Fulling 2004) possibly following fish schools, such as tuna. Common bottlenose dolphin density in a given area is likely to fluctuate because they travel at high speed and in groups of more than 100 individuals (NOAA Fisheries 2015a).

Sperm Whales

Most sperm whales are found in very deep waters (> 3,000 m), but can be encountered in waters as shallow as 300 m. Male and female sperm whales are not usually encountered together, and females are rarely found in waters less than 1000 m deep (Taylor et al. 2008a).

In the northern Gulf of Mexico, sperm whales occur year round, but at higher densities during the summer. There are no discernable seasonal migrations, but Gulf-wide movements occur primarily along the northern Gulf slope. Tracks show that whales exhibit a range of movement patterns within the Gulf, including movement into the southern Gulf in a few cases (Waring et al. 2013, NOAA Fisheries 2015b).

Kingsley and Stirling (1991) reported movements of groups of female sperm whales from different vocal clans ranging from less than 10 km to over 100 km in 24 h. The movements appeared to be driven by differences in dominance rankings between clans; more dominant groups often displace lower ranking clans. This likely causes rapid displacement movement patterns in areas of high prey concentrations. These rapid movements of groups of females due to displacement may show short-term changes in density, but are not likely considerable in magnitude.

Dwarf Sperm Whales

Dwarf sperm whales prefer warm tropical, subtropical, and temperate waters worldwide. They are most common along the waters of the continental shelf edge and the slope; dwarf sperm whales are thought to be more "coastal" than pygmy sperm whales (NOAA Fisheries 2012b).

There is very little information on dwarf sperm whales feeding habits, other than a preference for squid. Information on movement behaviors is practically absent. The density of dwarf sperm whales in the Gulf is considered very low, and members of the species either travel alone or groups of 6–10 animals (NOAA Fisheries 2012b). Würsig et al. (1998) notes that dwarf sperm whales are difficult to survey because they avoid ships and airplanes. This could mean that their density is generally underestimated.

Short-finned Pilot Whales

These whales occur in tropical to cool temperate waters. Sightings in the northern Gulf of Mexico (i.e., U.S. Gulf of Mexico) occur primarily on the continental slope west of 89˚W. There appears to be a year round aggregation of short-finned pilot whales in nutrient rich waters off the Mississippi River outflow. In other areas, pilot whales travel constantly (Mullin and Fulling 2004).

Short-finned pilot whales often occur in groups of 25–50 animals and often co-occur with common bottlenose dolphins and other delphinids. This species feeds on vertically migrating prey, with deep dives at dusk and dawn following vertically migrating prey and near-surface foraging at night (Baird et al. 2003). When they are swimming and probably looking for food, pilot whales form ranks that can be over a kilometer long (Taylor et al. 2011).

Based on food preference and group size information, it appears that short-finned pilot whales may need to travel over large distances to sustain groups of the reported sizes. This will lead to fluctuating densities in any given area as groups of 25–50 animals are possibly widely dispersed in order to avoid competition for patchy food sources. Squid abundance in any given area will be affected by groups of that size and the fact that pilot whales often occur together with odontocetes feeding on the same prey would underline the need for large-scale movement in this species.

Cuvier's Beaked Whales

Beaked whales were seen in all seasons during GulfCet aerial surveys of the northern Gulf of Mexico (Waring et al. 2013). Like many beaked whales, Cuvier's beaked whales eat mostly deep water squid and octopus near the bottom, but will eat fish and crustaceans in the water column. They prefer deep waters (depths usually greater than 1,000 m) of the continental slope, as well as steep underwater geologic

features like banks, seamounts, and submarine canyons. Recent surveys suggest that beaked whales, like this species, may favor oceanographic features such as currents, current boundaries, and core ring features (Taylor et al. 2008b).

Cuvier's beaked whales occur individually or in small groups of 2–12 animals (NOAA Fisheries 2012c). Like most beaked whales, information on behavior is sparse, and movements are not well understood. Given their small group sizes, but highly specialized foraging on squid, these whales probably remain in the same area longer than pilot whales. Information on aggregations is not available, which means density fluctuation in a given area is unknown and cannot be accurately assessed. The reported foraging locations over steep topographical structures may indicate avoidance of competition with other odontocetes foraging on the same prey. This may allow Cuvier's beaked whales to remain longer in a specific area.

Bryde's Whales

Bryde's whales are often characterized as displaying erratic and strange behavior relative to other baleen whales because they surface for irregularly spaced time intervals and can unexpectedly change directions (NOAA Fisheries 2014). These large baleen whales are usually sighted individually or in pairs, but there are reports of loose aggregations of up to twenty animals associated with feeding areas. These whales feed opportunistically on plankton, crustaceans, and schooling fish. They regularly dive for about 5–15 min (maximum of 20 min) after 4–7 blows at the surface. Bryde's whales are capable of reaching depths up to 300 m during dives (NOAA Fisheries 2014).

Given the information about feeding behavior and grouping, it appears unlikely that animals move rapidly between feeding areas. There is no information on large-scale movements, but aggregations could be the result of animals moving synchronously toward a certain area of high primary productivity. Bryde's whale distribution and movements are affected by plankton occurrence, which can be patchy due to the presence of large, warm-water eddies in the Gulf of Mexico.

6.5.1.2. Potential Biases in the Modeling Procedure

Underlying, and perhaps unknown, systematic biases in model procedures may lead to errors that could increase with modeling run duration.

6.5.1.2.1. Methods

Exposure estimates from 30 day (0.1 animats/km^2) and 5 day (2.0 animats/km^2) wide azimuth survey simulations from the Test Case (Section 6.3.2) were determined in subsets using a 'sliding window' to find the number of exposures as a function of time. The length of the sliding window was 24 h, advanced by 4 h, resulting in 174 samples from the 30 day simulation and 25 samples from the 5 day simulation. A sliding window of 7 days advancing by 1 day for the 30 day simulation was also be evaluated. Exposures were calculated using the behavioral threshold criteria indicated in the Test Case (Section 5.4.3). Bias in the model was expected to manifest itself as a trend in the exposure levels as a function of time.

The survey vessel paths in the simulations begin in the south east corner of the survey area, proceed on a westward longitudinal production line, step north at the end of the survey area, and then start on an eastward longitudinal production line (Figures 19 and 20). Simulations with 'reversed' track lines at Survey site A (starting in the northwest corner of the survey area, initially proceeding eastward on a longitudinal production line, and then stepping south) were also analyzed for short-finned pilot whales and sperm whales. To eliminate trends and variance due to changing sound fields (as the vessels move) and depth constraints, simulations were run with a stationary source in deep water (2000 m) and a flat bottom.

During all simulations in this project, any animat that left the simulation area as it crossed the simulation boundary was replaced by a new animat traveling in the same direction and entering at the opposite boundary. For example, an animat heading north and crossing the northern boundary of the simulation was replaced by a new animat heading north and entering at the southern boundary. By replacing animats in this manner, the animat modeling density remained constant.

Also common to all analysis in this project was that animats were only allowed to be 'taken' once during an evaluation period. That is, an animat whose received level exceeds the peak SPL threshold more than once during an evaluation period (i.e., 24 h, 7 day, or 30 day) was only counted once. Energy accumulation for SEL occurred throughout the evaluation period and was reset at the beginning of each period. Similarly, the maximum received rms SPL was determined for the entirety of the evaluation period and reset at the beginning of each period. The consequences of using a short time-period, such as 24 h, was evaluated.

6.5.1.2.2. Results

The number of animats exposed to levels exceeding the behavioral step function criteria in 30 day simulations evaluated using a 24 h sliding window are shown in Figure 21 for the low-frequency Bryde's whales at Survey sites A and B. In Figure 21, least-squares fitted trend lines show a positive trend at Survey site A indicating increasing exposures as function of simulation time, and a negative trend at Survey site B indicating decreasing exposures as a function of simulation time, but residual analysis did not find either trend to be significant. For the other species, the trend lines at Survey site A, though not necessarily significant, were negative, indicating decreasing exposures as a function of simulation time: common bottlenose dolphins (Figure 22a), Cuvier's beaked whales (Figure 23a), short-finned pilot whales (Figure 24a), sperm whales (Figure 25a), and dwarf sperm whales (Figure 26a). The trend lines at Survey site B for these species (Figure 22b–26b) were less pronounced, positive for common bottlenose dolphins and sperm whales, and negative for Cuvier's beaked whales, short-finned pilot whales, and dwarf sperm whales.

The exposure estimates as a function of simulation time and trend lines for 'reversed' track lines are shown in Figure 27. For short-finned pilot whales and sperm whales, the trend lines were positive. Figure 28 shows that the variability in the exposure estimates decreased, and there was no significant trend as a function of simulation time when the source was stationary and there were no depth constraints on the animats.

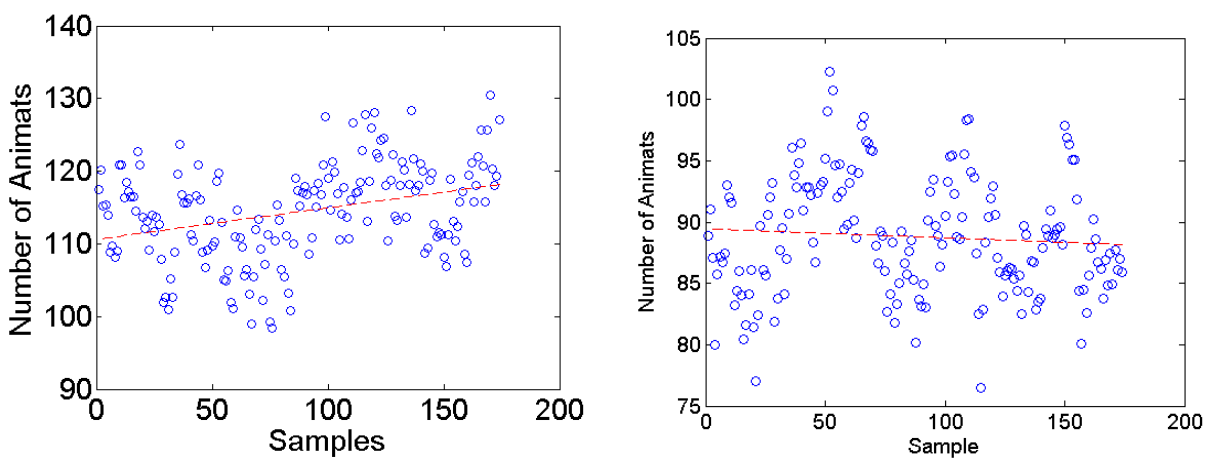

(a) (b)

Figure 21. Bryde's whales: Behavioral exposure estimates for (a) Survey sites A and (b) B. Exposure estimates are for 24 h sliding windows (samples), which advance in 4 h increments during 30

day simulations. Circle markers indicate exposure estimates during each 24 h sample period, dashed red line is a least-squares fit.

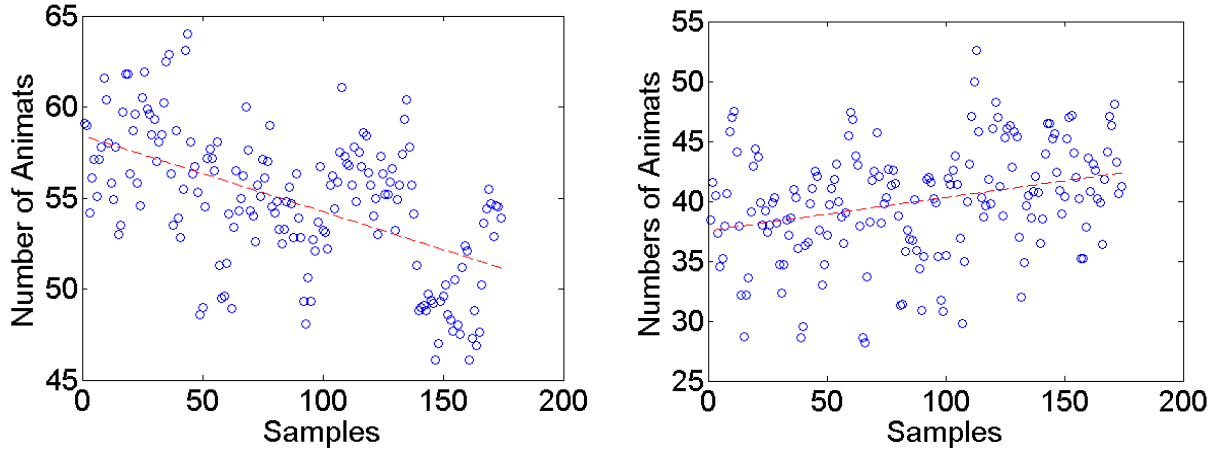

(a) (b)

Figure 22. Common bottlenose dolphins: Behavioral exposure estimates for (a) Survey sites A and (b) B. Exposure estimates are for 24 h sliding windows (samples), which advance in 4 h increments during 30 day simulations. Circle markers indicate exposure estimates during each 24 h sample period, dashed red line is a least-squares fit.

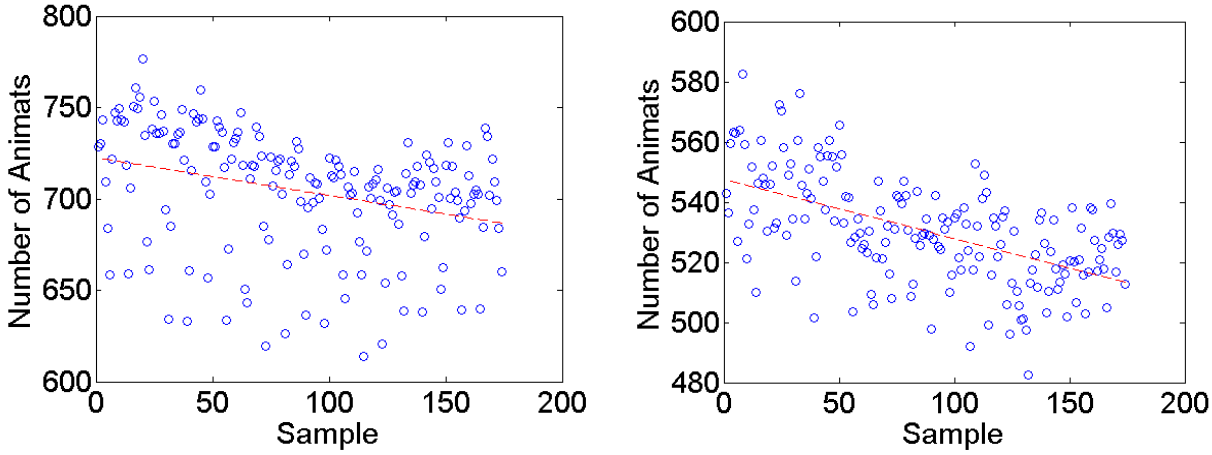

(a) (b)

Figure 23. Cuvier's beaked whales: Behavioral exposure estimates for (a) Survey sites A and (b) B. Exposure estimates are for 24 h sliding windows (samples), which advance in 4 h increments during 30 day simulations. Circle markers indicate exposure estimates during each 24 h sample period, dashed red line is a least-squares fit.

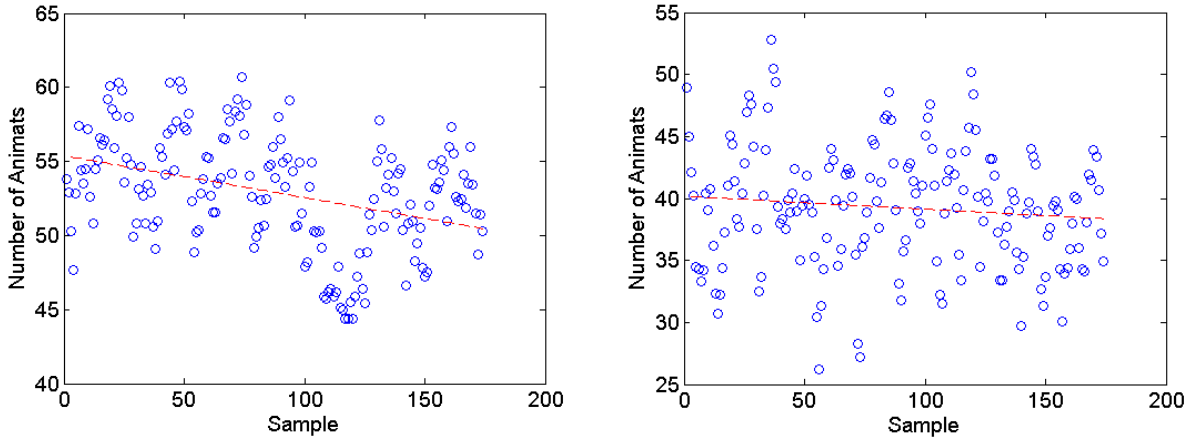

(a) (b)

Figure 24. Short-finned pilot whales: Behavioral exposure estimates for (a) Survey sites A and (b) B. Exposure estimates are for 24 h sliding windows (samples), which advance in 4 h increments during 30 day simulations. Circle markers indicate exposure estimates during each 24 h sample period, dashed red line is a least-squares fit.

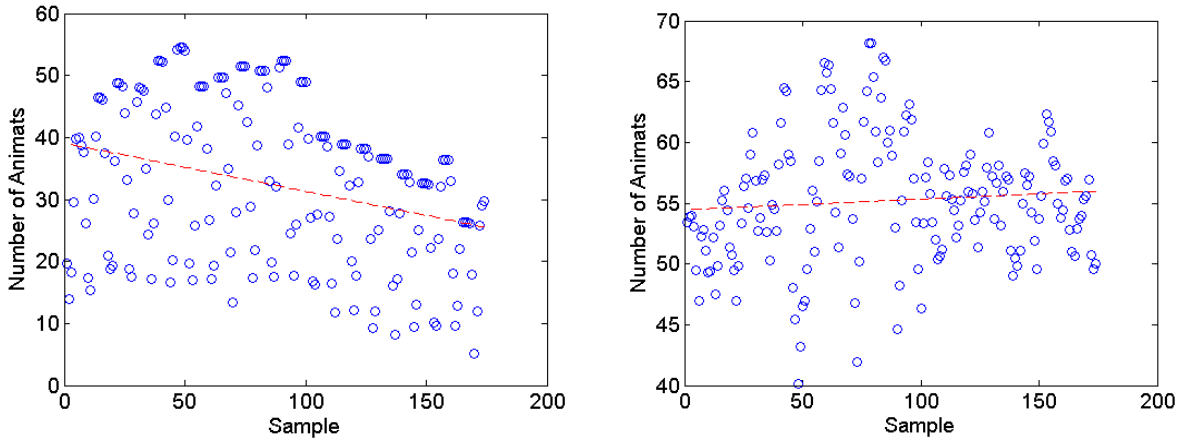

(a) (b)

Figure 25. Sperm whales: Behavioral exposure estimates for (a) Survey sites A and (b) B. Exposure estimates are for 24 h sliding windows (samples), which advance in 4 h increments during 30 day simulations. Circle markers indicate exposure estimates during each 24 h sample period, dashed red line is a least-squares fit.

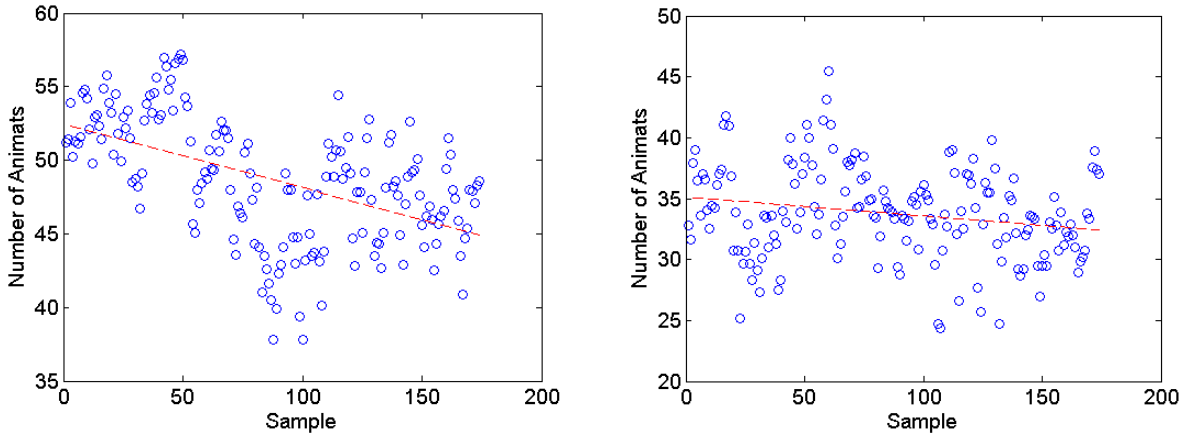

(a) (b)

Figure 26. Dwarf sperm whales: Behavioral exposure estimates for (a) Survey sites A and (b) B. Exposure estimates are for 24 h sliding windows (samples), which advance in 4 h increments during 30 day simulations. Circle markers indicate exposure estimates during each 24 h sample period, dashed red line is a least-squares fit.

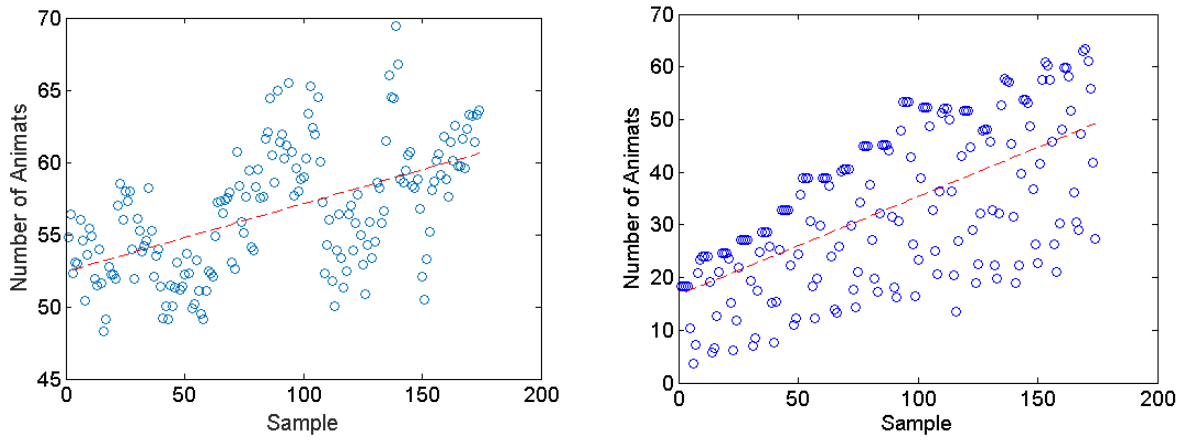

(a) (b)

Figure 27. Behavioral exposure estimates for (a) short-finned pilot whales and (b) sperm whales, both with reversed vessel tracks at Survey site A. Exposure estimates are for 24 h sliding windows (samples), which advance in 4 h increments during 30-day simulations. Circle markers indicate exposure estimates during each 24 h sample period, dashed red line is a least-squares fit.

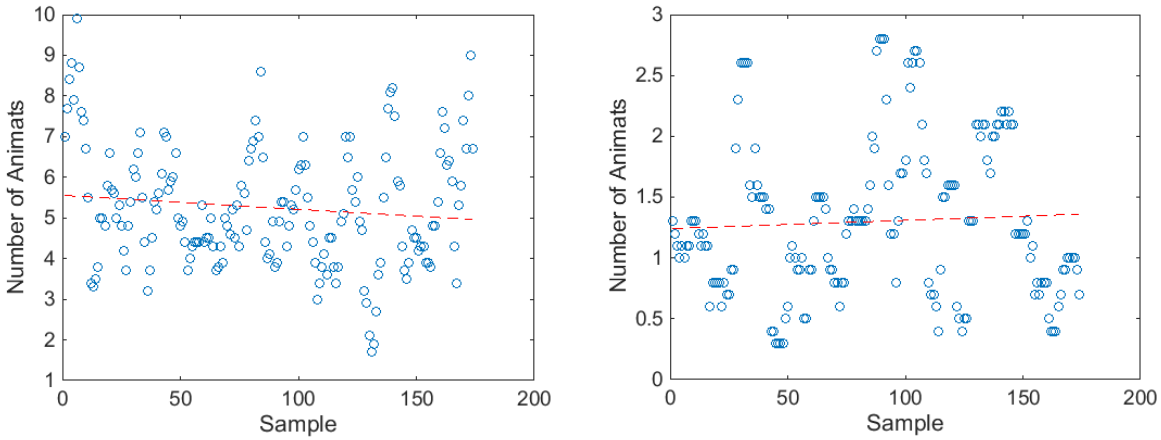

(a) (b)

Figure 28. Behavioral exposure estimates for (a) short-finned pilot whales and (b) sperm whales, with stationary source in deep water near Survey site B. Exposure estimates are for 24 h sliding windows (samples), which advance in 4 h increments during 30 day simulations. Circle markers indicate exposure estimates during each 24 h sample period, dashed red line is a least-squares fit.

The Test Case preliminary results found the number of animats exposed to levels exceeding threshold criteria for the entire duration of the simulations—5 days for the zero-to-peak SPL and SEL and 30 days for the criteria based on rms SPL (Table 14 and Table 15). It is often impractical or unwarranted to integrate exposures for an entire survey and an integration window is defined. A 24 h time-period for determining potential impacts is commonly used. Table 20 and Table 21 show the average number of animats receiving levels exceeding exposure criteria in the 24 h sliding windows at Survey sites A and B, respectively. To estimate the number of animats receiving levels exceeding threshold for a longer duration survey, the 24 h average was scaled by the survey duration in days. Table 22 and Table 23 show the 24 h averages scaled to the simulation length (5 days for zero-to-peak SPL and SEL, and 30 days for the criteria based on rms SPL) and the percentage of the full-duration estimates that the scaled values represent (shown in parenthesis). It can be seen in Tables 22 and 23 that when scaling the 24 h averages for the rms SPL-based criteria, the percentages were uniformly positive, indicating that scaling resulted in a greater number of animats predicted to received levels exceed these criteria. The increased number of animats estimated to exceed threshold could be quite large, several times the estimate for the full duration (100% is twice the full duration estimate). For the zero-to-peak and SEL metrics the difference between the scaled estimates and the full-duration estimates was smaller and the scaled values may be less than the full duration values (indicated by a negative percentage). Because SEL accumulates throughout the evaluation period, it is possible that some animats' received level SELs would not exceed threshold in 24 h, but would when integrated over the full duration of the simulation. The zero-to-peak SPL criteria does not accumulate and animats were only counted once per evaluation period, so a reduced number of estimated exceedances for the scaled values compared to the full-duration values was not expected. To investigate, the 24 h estimates were scaled (by 4) and compared to a 4 day evaluation period starting 12 h into the 5 day simulation. Tables 26 and 27 shows that the percentage difference between the scaled estimates and the 4 day estimates were positive, except for SEL for short-finned pilot whales and zero-to-peak SPL for sperm whales, which are very rare events, and the negative percentage results from a rounding error (e.g., there was one short-finned pilot whale above the zero-to-peak SPL threshold for the entire simulation, but the 24 h average was ~ 0.23 and rounded to 0.2).

Knowing the amount of time that animals are exposed to levels exceeding the threshold criteria can provide additional information about the potential impacts. Tables 26 and 27 show the mean time that

levels exceeded the NMFS criteria of 180 dB rms SPL re 1 µPa (Level A Harassment) and 160 dB rms SPL re 1 µPa (Level B Harassment) for the entire duration of the 30 day simulation and the averaged mean time in the 24 h sliding windows. The times only consider animats exposed to levels that exceed the criteria and the distributions of exceedance times are not normally distributed. The exceedance-time distributions are better fit by a Poisson model (not shown), but it is improper to fit these distributions because the animats whose received levels are below threshold are not considered (i.e., the number of animats with zero time above threshold exposure is indefinable because it changes with the arbitrary choice of simulation boundaries). For this reason, we report the mean value (equivalent to lambda for a Poison distribution) and the maxim time that an animat was exposed leveling exceeding threshold. Other criteria, such as SEL and zero-to-peak SPL injury criteria were not considered. SEL was not considered because it only positively accumulates; once the SEL threshold is reached it does not decrease even though the animal may have moved away from the source. Zero-to-peak SPL is meant for evaluating one-time exposures to very loud sounds that may do mechanical damage to the ear, once damage has occurred it is not expected to regain function.

The amounts of time that animats were exposed to levels exceeding the 160 dB rms SPL re 1 µPa threshold over the 30 day duration were approximately twice as long as the average times in a 24 h window. Whereas, the amounts of time that exposure levels exceeded the 180 dB rms SPL re 1 µPa threshold over the 30 day duration were closer to the average times in a 24 h window. The exceedance times of the 180 dB rms SPL re 1 µPa threshold were similar because threshold exceedance was a relatively rare event and was not usually repeated (an individual animat was not often exposed to levels exceeding this threshold in multiple separated events). There were more opportunities for animats to be exposed to levels exceeding the 160 dB rms SPL re 1 µPa threshold, so there were more instances when this threshold was reached and it was more common for the threshold to be exceeded on multiple separate occasions. Exceedance on multiple occasions accounts for the increased exceedance times for the 30 day duration relative to the 24 h average. The amount of time when either threshold was exceeded was short relative to the evaluation period (24 h or 30 days). Two factors contributed to the total time thresholds were exceeded—the amount of time per occasion (i.e., how long an animat was near the source) and the number of occasions that occur (i.e., how many times an animat was near a source). The number of occasions was, essentially, the same item determined when finding the number of animats with exposures exceeding threshold criteria (the typical use of the threshold criteria). As was investigated above, the number of occasions scales with the duration of the evaluation period, but the time per occasion does not. The time per occasion is specific to how an individual animat interacted with a source. It is, therefore, inappropriate to scale the 24 h exceedance times to estimate the exceedance times for longer durations.

Table 20. Average number of modeled cetaceans above exposure criteria at Survey site A for 24 h sliding windows. Simulations for zero-to-Peak SPL and SEL injury were 5 day duration with animat density of 2.0 animats/km^2. Simulations for rms SPL metrics were 30 day duration with animat density of 0.1 animats/km^2.

Marine mammal species	Injury			Behavior	
	zero-to-peak SPL	SEL	180 dB rms SPL	160 dB rms SPL	Step fxn. rms SPL
Bryde's whales	8.1	105.5	15.6	113	115.4
Cuvier's beaked whales	8.6	0	10.5	38.1	715.3
Common bottlenose dolphins	20.3	0	10.9	32.2	57.3
Short-finned pilot whales	21.1	0.2	10.2	29.5	55.1
Sperm whales	2.9	0.2	6	19.3	32.4
Dwarf sperm whales	1871.7	207.7	8.7	26	49.8

SPL=sound pressure level; SEL=sound exposure level; rms=root-mean-square

Table 21. Average number of modeled cetaceans above exposure criteria at Survey site B for 24 h sliding windows. Simulations for zero-to-Peak SPL and SEL injury were 5 day duration with animat density of 2.0 animats/km^2. Simulations for rms SPL metrics were 30 day duration with animat density of 0.1 animats/km^2.

Marine mammal species	Injury			Behavior	
	zero-to-peak SPL	SEL	180 dB rms SPL	160 dB rms SPL	Step fxn. rms SPL
Bryde's whales	10.6	93.7	14.3	41.6	90.5
Cuvier's beaked whales	8.6	0	11.3	30.9	538
Common bottlenose dolphins	18.9	0	11	24.9	42.1
Short-finned pilot whales	19.9	0	10.7	24.5	41
Sperm whales	6.5	0	14.3	40.53	58.1
Dwarf sperm whales	1892.2	193.2	9.8	25.4	35.5

SPL=sound pressure level; SEL=sound exposure level; rms=root-mean-square

Table 22. Number of modeled cetaceans above exposure criteria at Survey site A for average 24 h sliding windows estimate scaled to full duration (5 or 30 days). Numbers in parenthesis represent the percentage change relative to the full duration estimate. Positive numbers indicate the scaled value is greater than full duration estimate. +100% is a doubling of the full duration estimate.

Marine mammal species	Injury			Behavior	
	zero-to-peak SPL	SEL	180 dB rms SPL	160 dB rms SPL	Step fxn. rms SPL
Bryde's whales	40.5 (−14)	527.5 (−1)	468.0 (35)	3390.0 (494)	3462.0 (444)
Cuvier's beaked whales	43 (−4)	0 (0)	315.0 (14)	1143.0 (98)	21459.0 (1006)
Common bottlenose dolphins	101.5 (−3)	0 (0)	327.0 (33)	966.0 (183)	1719.0 (291)
Short-finned pilot whales	105.5 (0)	1 (0)	306.0 (28)	885.0 (168)	1653.0 (289)
Sperm whales	14.5 (−3)	1 (0)	180.0 (8)	579.0 (66)	972.0 (152)
Dwarf sperm whales	9358.5 (33)	1038.5 (−1)	261.0 (25)	780.0 (127)	1494.0 (269)

SPL=sound pressure level; SEL=sound exposure level; rms=root-mean-square

Table 23. Number of modeled cetacean animats above exposure criteria at Survey site B for average 24 h sliding windows estimate scaled to full duration (5 or 30 days). Numbers in parenthesis represent the percentage change relative to the full duration estimate. Positive numbers indicate the scaled value is greater than full duration estimate. +100% is a doubling of the full duration estimate.

Marine mammal species	Injury			Behavior	
	zero-to-peak SPL	SEL	180 dB rms SPL	160 dB rms SPL	Step fxn. rms SPL
Bryde's whales	53 (4)	468.5 (−3)	429.0 (37)	1248.0 (250)	2715.0 (412)
Cuvier's beaked whales	43 (13)	0 (0)	339.0 (13)	927.0 (89)	16140.0 (782)
Common bottlenose dolphins	94.5 (−5)	0 (0)	330.0 (30)	747.0 (162)	1263.0 (207)
Short-finned pilot whales	99.5 (−2)	0 (0)	321.0 (22)	735.0 (133)	1230.0 (188)
Sperm whales	32.5 (−7)	0 (0)	429.0 (13)	1215.9 (74)	1743.0 (121)
Dwarf sperm whales	9461 (31)	966 (8)	294.0 (22)	762.0 (126)	1065.0 (155)

SPL=sound pressure level; SEL=sound exposure level; rms=root-mean-square

Table 24. Percentage difference in number of modeled cetaceans above exposure criteria at Survey site A for 24 h sliding windows scaled to 4 day evaluation window.Positive numbers indicate the scaled value is greater than 4 day estimate. +100% is a doubling of the 4 day estimate.

Marine mammal species	Injury	
	zero-to-peak SPL	SEL
Bryde's whales	8	12
Cuvier's beaked whales	23	0
Common bottlenose dolphins	25	0
Short-finned pilot whales	13	−20
Sperm whales	−17	0
Dwarf sperm whales	43	10

SPL=sound pressure level; SEL=sound exposure level

Table 25. Percentage difference in number of modeled cetaceans above exposure criteria at Survey site B for 24 h sliding windows scaled to 4 day evaluation window. Positive numbers indicate the scaled value is greater than 4 day estimate. +100% is a doubling of the 4 day estimate.

Marine mammal species	Injury	
	zero-to-peak SPL	SEL
Bryde's whales	9	12
Cuvier's beaked whales	50	0
Common bottlenose dolphins	16	0
Short-finned pilot whales	15	0
Sperm whales	30	0
Dwarf sperm whales	39	21

SPL=sound pressure level; SEL=sound exposure level

Table 26. Amount of time that animats exceed NMFS threshold criteria at Survey site A for 30 days and 24 h. The average amount of time, in minutes, that animats exposed to levels exceeding the criteria remain above the criteria is shown. The maximum amount of time an animat exceeded the threshold is shown in parentheses. 30 days show the results for the entire duration of the simulation, 24 h show the average values from the 24-h sliding windows.

Marine mammal species	30 day		24 h	
	180 dB rms SPL	160 dB rms SPL	180 dB rms SPL	160 dB rms SPL
Bryde's whales	2.2 (10)	75.6 (554)	1.6 (3.4)	18 (83)
Cuvier's beaked whales	1.5 (4)	8.2 (48)	1.3 (2.4)	4.8 (16)
Common bottlenose dolphins	1.9 (8)	12.6 (115)	1.4 (2.7)	5.7 (17.8)
Short-finned pilot whales	1.8 (8)	12 (73)	1.4 (2.4)	5.7 (18.3)
Sperm whales	1.5 (6)	5.2 (35)	1.3 (2.1)	3.7 (10.5)
Dwarf sperm whales	1.5 (6)	8.6 (63)	1.3 (2.2)	4.6 (14.3)

SPL=sound pressure level; rms=root-mean-square

Table 27. Amount of time that animats exceed NMFS threshold criteria at Survey site B for 30 days and 24 h.The average amount of time, in minutes, that animats exposed to levels exceeding the criteria remain above the criteria is shown. The maximum amount of time an animat exceeded the threshold is shown in parentheses. 30 days show the results for the entire duration of the simulation, 24 h show the average values from the 24-h sliding windows.

Marine mammal species	30 day		24 h	
	180 dB rms SPL	160 dB rms SPL	180 dB rms SPL	160 dB rms SPL
Bryde's whales	2.2 (10)	20.5 (131)	1.6 (3.5)	8.1 (38)
Cuvier's beaked whales	1.5 (5)	6.2 (30)	1.3 (2.4)	3.9 (12.4)
Common bottlenose dolphins	1.8 (6)	8.8 (45)	1.4 (2.7)	4.4 (13.3)
Short-finned pilot whales	1.7 (7)	8.2 (58)	1.4 (2.7)	4.4 (13.5)
Sperm whales	1.4 (5)	5.3 (33)	1.3 (2.6)	3.5 (11.5)
Dwarf sperm whales	1.5 (6)	7.3 (52)	1.3 (2.4)	4.0 (11.7)

SPL=sound pressure level; rms=root-mean-square

6.5.1.3. Summary of Scaling Modeled Acoustic Exposure Results

6.5.1.3.1. Large-scale Animal Movement

Large-scale movements of cetaceans are driven primarily by migrations and temporally-varying prey concentrations (Hastie et al. 2004). Prey availability is ultimately driven by changes in production in the oceanic food web (Davis et al. 2001). These changes influence directly the availability of marine mammal prey, as is the case for plankton feeders such as Bryde's whales. The changes also cause a delayed, but often amplified, abundance of larger invertebrates (e.g., squid) and/or vertebrates (e.g., fish), the food source of most odontocetes, such as sperm and pilot whales and smaller dolphins (e.g., Davis et al. 2001).

The acoustically-modeled seismic surveys usually occur in deeper water (> 200 m). Five of the six representative cetacean species typically only occur in deeper water. Common bottlenose dolphins, however, have several distinct populations. One of these inhabits water deeper than 200 m and is the most likely population affected by seismic surveys of this Test Case. Most cetacean movement data is from inshore populations that have been studied more intensely and from migrating species, since information on movements of offshore species is sparse. None of the Test Case species is distributed evenly across the Gulf (Davis et al. 2001). All cetaceans surveyed in Davis et al. (2001) were found primarily in water depths ranging between 1200–2300 m, with the exception of common bottlenose dolphins, which also occurred in slightly shallower waters. There is no information indicating that any of the six modeled species migrate regularly on a large-scale in the Gulf; thus, large-scale movement was not integrated into the animal movement model.

6.5.1.3.2. Potential Biases in the Modeling Procedure

To investigate potential systematic, and possibly unknown, biases in the modeling procedure, behavioral exposure estimates were determined for subsets of the Test Case simulations (see Section 6.3.2). Behavioral exposure estimates were determined as a function of time by finding the number of exposures occurring in 24 h subsets using a sliding window that advanced in 4 h increments. Trends were evident, particularly at Survey site A, but the trends appeared to be the consequence of survey design, such as changing sound fields as the vessels move into different acoustic zones. The negative trend for most species at Survey site A reflected the survey design in that the survey vessels start operations in deeper water and proceed to shallower water toward the end of the simulation. Because the acoustic propagation

range is generally longer in deeper water than at intermediate depths (see Tables 83–85 and Figures 126–128), the ensonified volume was larger at the beginning of the simulation than at the end and more exposures are registered per 24 h period earlier in the simulation. This was borne out in simulations with the vessel tracks reversed (starting in intermediate water depths and proceeding toward deeper water). Fewer exposures were registered at the beginning of the simulation and more toward the end of the simulation as the vessels proceeded into deeper water (Figure 27). For sperm whales, there was an additional bias due to their general avoidance of water depths < 1000 m. The area of Survey site A began at a location with water depth ~ 1500 m, but proceeds to depths < 200 m. Therefore, fewer sperm whale animats were within exposure range of the source later in the simulation. As expected, reversing the track lines of the vessels (starting in shallow water and proceeding to deeper water) lead to increased behavioral exposure estimate rates for sperm whales over time (Figure 27b). To determine if undesired, and unknown, systematic biases exist in the modeling procedure, simulations were run with the source stationary and with no limiting bathymetric constraints (depth > 1300 m). No clear trends were found (Figure 28), indicating that undesired systematic biases in the modeling procedure, if present, were small relative to the survey design and would not affect scaling up the results in time, if applied.

The results of the Test Case were presented as the number of animats (and animals) that were exposed to levels that exceed the threshold criteria for the entire simulation. SEL was accumulated throughout the simulation (5 days) and the maximum rms SPL exposure values were found for the whole simulation (30 days). Animats receiving levels exceeding threshold were only counted once, but there was no mechanism to account for potential recovery of hearing. For this reason a smaller time period for evaluating exposure risk was used and the animats' received levels were reset at the beginning of each period. The time period for evaluating exposure risk has not been standardized, but 24 h is often used. We compared the number of animats exposed to levels exceeding threshold for 24 h time periods scaled up by the number of days in the simulations to the number of animats exposed to levels exceeding threshold for the entire duration of the simulations. For metrics based on rms SPL (the NMFS criteria and the behavioral step function), scaling up the 24 h average estimates to 30 days (vastly) overestimates the number of animats exposed to levels exceeding threshold when determined over the entire simulation. This is an expected finding. It results because animats were commonly exposed to levels exceeding these thresholds and the relatively short reset period of 24 h means that individual animats were, in effect, counted several times during the scale up that would only have been counted once when evaluating over the entire simulation. SEL is an accumulation of energy, so unlike the SPL metrics evaluating over a longer period could result in more animats exposed to levels exceeding SEL threshold that would not when evaluated over a shorter period. The med-frequency species had only one or no animats above SEL threshold, so scaling trends could not be established for such rare events. Only Bryde's whales (low frequency) and dwarf sperm whales (high frequency) had significant numbers of animats exposed to levels exceeding SEL threshold. For Bryde's whales and dwarf sperm whales, scaling the 24 h average by 5 resulted in fewer animats exposed to levels exceeding threshold than the number of animats exposed to levels exceeding threshold for the entire simulation. The percentage shortfall, however, was much less than the overestimates seen in the NMFS criteria and behavioral step function in the 30 day simulations. In addition, it was observed that scaling the 24 h zero-to-peak SPL exceedance estimates could also result in a modest shortfall. Animats exceeding zero-to-peak SPL were only counted once per evaluation period and energy did not accumulate, so scaling up from a short reset period should overestimate the number of animats exposed to levels exceeding threshold. When using an overlap, the sliding window approach under-samples the edge time periods compared to the central time periods. When the number of animats exposed to levels exceeding the zero-to-peak SPL and SEL thresholds for 24 h was scaled up by 4 and compared to number of animats exposed to levels exceeding these thresholds during a 4 day period in the middle of the 5 day simulation, the scaled estimates again overestimated the longer time window results. (Except in the case of the sperm whales, which was an artifact of rounding a small number.) These edge effects of the sliding window sampling were small and exaggerated in the Test Case because the surveys start an end at extreme locations of the sound field and animal locations. Starting and ending surveys at the extremes of

sound fields and animal depth restrictions is not typical, so the edge effects were not expected to significantly affect results.

6.5.1.3.3. Scaling Short-duration Simulations for Long-duration Operations

As discussed previously, large-scale animal movements can affect the real-world densities that are used to adjust model (animat) exposure estimates. If the simulation is short relative to the large-scale movement (or behavioral change), there is little effect on the estimated exposures (i.e., provided the behavioral states and acoustic fields remain relatively constant, exposure estimates from short-duration simulations can be adjusted for different seasonal density estimates).

Systematic trends in the modeling procedure were evident, indicating that survey design can affect exposure estimates when scaling is used. The minimum duration of a simulation should, therefore, include all of the acoustic environments likely to be encountered during the operation. For example, if a survey will range from deep to shallow water, then it is not sufficient to only simulate operations in deep water (unless it is known that exposures in deep water are always greater than in shallow water and a conservative estimate of the exposures is desired). When the evaluation period (or reset time) is short, e.g., 24 h, the simulation should still include all acoustic environments, and exposures should be presented as a function of time or averaged to get an expected value during the evaluation period.

Our suggested procedure for estimating exposures for long-duration surveys (i.e., three months):

1. Identify the shortest large-scale animal movement time-period (e.g., seasonal migration).
2. Identify acoustic environments over which the survey will occur (e.g., shallow, slope, deep, and associated geoacoustic parameters).
3. Identify the minimum period of validity for the acoustic model (e.g., month due to changing sound velocity profile).
4. Break the survey into parts that are shorter in duration than both large-scale animal movement times and the period of acoustic model validity.
5. Create animal movement simulations for acoustic exposure with adequate duration to meaningfully sample the exposure-estimating parameter (e.g., if a 24 h reset period is used then enough samples should be obtained to get a reliable mean value given the various acoustic environments).
6. If the simulation time is less than the duration of the survey parts determined in Step 4, then scale the results by the ratio of survey duration to simulation time (e.g., if the simulation time is one week, but the survey division is 28 days, then multiply the simulation exposure results by four).
7. Sum, or aggregate, the results from the survey parts to calculate exposures for the entire survey.

6.5.2. Test Scenario 2: Analysis of Uncertainty in Acoustic and Animal Modeling

The process of using computer models to predict acoustic effects on marine mammals requires making simplifying assumptions about oceanographic parameters, seabed parameters, and animal behaviors. These assumptions carry some uncertainty, which may lead to uncertainty in the form of variance or error in individual model outputs and in the final estimates of marine mammal acoustic exposures. For example, acoustic propagation models assume a specific shape of the sound speed profile in the ocean (speed of sound versus depth) for each season. We know, however, that the real sound speed profile regularly changes and that substantial variation within a season is possible. The assumption that a single profile represents the environment through a full season approximates real-world cases, but can, to some degree, cause errors. The uncertainty in model outputs caused by approximations like this can be

investigated by examining how much the outputs change when the inputs are purposely offset. This type of investigation, referred to as parametric uncertainty analysis, provides a means to characterize the accuracy, or uncertainty, of the model results in light of errors in model inputs. It can also be used to characterize the expected variability in model results due to natural variations in some of the input parameters.

The exposure calculations used for biological effects assessment are performed using an animal movement model that simulates and tracks individual animals in space and time through the sound field. As with the acoustic model, the animat movement model requires inputs that approximate real-world values. In fact, the acoustic model results are one of the inputs to the animat model, and those inherently have uncertainty, as described above. The animat model outputs consequently also include uncertainty. By using a resampling technique, we can quantify the effects of uncertainty in exposure estimates due to uncertainty in acoustic and animal movement models.

6.5.2.1. Acoustic Modeling Uncertainty

Acoustic exposure estimates require knowledge of the sound fields to which marine mammals are exposed. Here we are concerned with estimating exposures from geotechnical and geophysical survey operations. Sound field modeling consists of two major stages: source characterization and acoustic propagation modeling. The uncertainty that arises in both of these stages is considered in the following sections.

6.5.2.1.1. Source Characterization Modeling Uncertainty

Characteristics of sound sources, such as the sound levels in different frequency bands and the directivity of the sources, were used with acoustic propagation modeling to determine quantify the received sound levels to which marine mammals are exposed. There were uncertainties associated with the source, such as variations in source level during operation, and uncertainty associated with a source model's predicted levels. Field measurements of an operating source that has been modeled can be used to determine the overall uncertainty associated with the source level modeling.

The sound source used in the Test Case (Section 6.3.1.1) was a generic 8000 in³ airgun array. JASCO's airgun array source model (AASM) was used to characterize the far-field emission levels and directivity of the source. AASM is a numerical model that simulates the fluid dynamics and sound radiation of a collection of high-pressure air bubbles. As with other airgun models, AASM incorporates a number of simplifying assumptions about the underlying physics to make the numerical calculation tractable. Among these assumptions are that the bubbles are perfectly spherical and that the sound field radiated by each airgun is isotropic and point-like, which are only approximately true in practice. Furthermore, the physical model employed by AASM includes free parameters, which govern the rate of air injected into the bubble and the rate of heat transfer between the bubble and the surrounding water. The values of these free parameters are determined by fitting model predictions to the measured signatures for a large collection of airguns (MacGillivray 2006). Errors in AASM thus originate from two different sources: the approximations employed in the underlying physical model, and the experimental uncertainties in the model parameterization of the specific airguns.

Uncertainty associated with these errors can be estimated by comparing model predictions to acoustic field measurements of airgun arrays. Such comparisons are complicated because the source levels computed by the model must, by definition, be measured in the far field of the array. Since a model of sound propagation must be used to calculate received levels in the far field, it is thus impossible to completely decouple uncertainties in the source model from uncertainties in the sound propagation model. Nonetheless, uncertainties can be estimated from field data by comparing model predictions with sound level measurements at relatively short range, where propagation loss is reasonably well constrained.

Studies comparing AASM predictions with seismic array measurements have been carried at a number of sites, including in the Chukchi Sea (McPherson et al. 2005), the Beaufort Sea (Matthews and MacGillivray 2013), and offshore British Columbia (Austin et al. 2012). These studies have shown that the modeled SELs are typically within 3 dB of the measured values.

6.5.2.1.2. Acoustic Propagation Modeling Uncertainty

Transmission of sound is determined by the characteristics of the media (e.g., air, water, and seafloor sediments) in which that sound propagates. The acoustics model used here accepts several parameters describing the ocean environment in which sound propagation is modeled. The key inputs are sound speed variation with depth (sound speed profile), seabed composition and layering, and bathymetric variation between each sound source and receiver.

Uncertainty in acoustic environmental parameters leads to uncertainty in model outputs. The relationship between the input parameters and the output is complex and cannot be expressed with a simple rule. An empirical approach was taken to investigate how uncertainty in the inputs affects the modeled acoustic field. Sound fields were modeled using typical and worst-case conditions. These sound fields were subtracted to determine the difference, which indicates the range of errors due to uncertainty in inputs. Three acoustic zones were analyzed: Shelf, Slope, and Deep. Each zone was modeled for three propagation directions: downslope, upslope, and along-slope. The upslope and downslope directions led respectively from the source into shallower and deeper waters. The along-slope direction followed a path of (approximate) constant depth (bathymetric contour) away from the source.

6.5.2.1.3. Sound Speed Profiles

A sound speed profile represents the water sound speed as a function of depth. In general, sound speed increases with increasing temperature and salinity. It also increases with increased hydrostatic pressure, so there is a systematic increase with depth. Sound speed profiles for the modeled sites were derived from temperature and salinity profiles from the U.S. Naval Oceanographic Office's Generalized Digital Environmental Model V 3.0 (GDEM, Teague et al. 1990, Carnes 2009). GDEM provides an ocean climatology of temperature and salinity for the world's oceans on a latitude-longitude grid with 0.25° resolution, with a temporal resolution of one month, based on global historical observations from the U.S. Navy's Master Oceanographic Observational Data Set (MOODS). The climatology profiles include 78 fixed depth points to a maximum depth of 6800 m (where the ocean is that deep), including 55 standard depths between 0 and 2000 m. The GDEM temperature-salinity profiles were converted to sound speed profiles according to the equations of Coppens (1981).

$$
\begin{aligned}
c(z,T,S,\phi) &= 1449.05 + 45.7t - 5.21t^2 - 0.23t^3 \\
&\quad + \left(1.333 - 0.126t + 0.009t^2\right)(S - 35) + \Delta \\
\Delta &= 16.3Z + 0.18Z^2 \\
Z &= \frac{z}{1000}\left[1 - 0.0026\cos(2\phi)\right] \\
t &= \frac{T}{10}
\end{aligned}
\tag{19}
$$

where z is water depth (m), T is water temperature (°C), S is salinity (psu), and ϕ is latitude (radians).

Sound speed profiles were obtained for three depth zones (Table 28) along the study line, south of Louisiana (Figures 29–31). Surface sound ducts, or channels, occur when the sound speed increases with depth below the surface leading to a positive sound speed gradient. This can occur physically when

surface waters are cooler than underlying waters. Sounds propagating in the gradient are refracted upward and can become partially trapped near the surface, leading to enhanced sound propagation and higher near-surface sound levels. A weak surface sound channel is present during some months of the year in the Gulf of Mexico, with variations in the gradient and depth of the channel based on the month and zone. To account for varying sound speed profiles throughout the year, seasons were defined for each zone based on the sound speed at the surface and the gradient and depth of the sound channel in the top 200 m (Table 29). A negative gradient indicates a more downward refracting environment, whereas a positive gradient at the surface indicates a surface sound channel that can propagate sound to longer ranges.

Table 28. Depth zones along the study line.

Zone	Depths (m)	Range–Latitude (°N)	Range–Longitude (°W)
Shelf	25–200	28–28.75	89–91
Slope	200–2000	26.5–28	
Deep	> 2000	24.5–26.5	

Table 29. Modeled seasons and their characteristics.

Zone	Season	Period	Month used to acquire representative sound speed profile	Seasonal characteristics
Shelf	1	Dec–Mar	Feb	Strong sound channel at depths up to 50–75 m below surface
	2	Apr–Nov	Sep	Weak to no sound channel in top 20–40 m
Slope	1	Jul–Sep	Aug	Weak to no sound channel
	2	Oct–Jun	Mar	Downward refracting at surface
Deep	1	Jan–Dec	May	Very weak to no sound channel throughout year

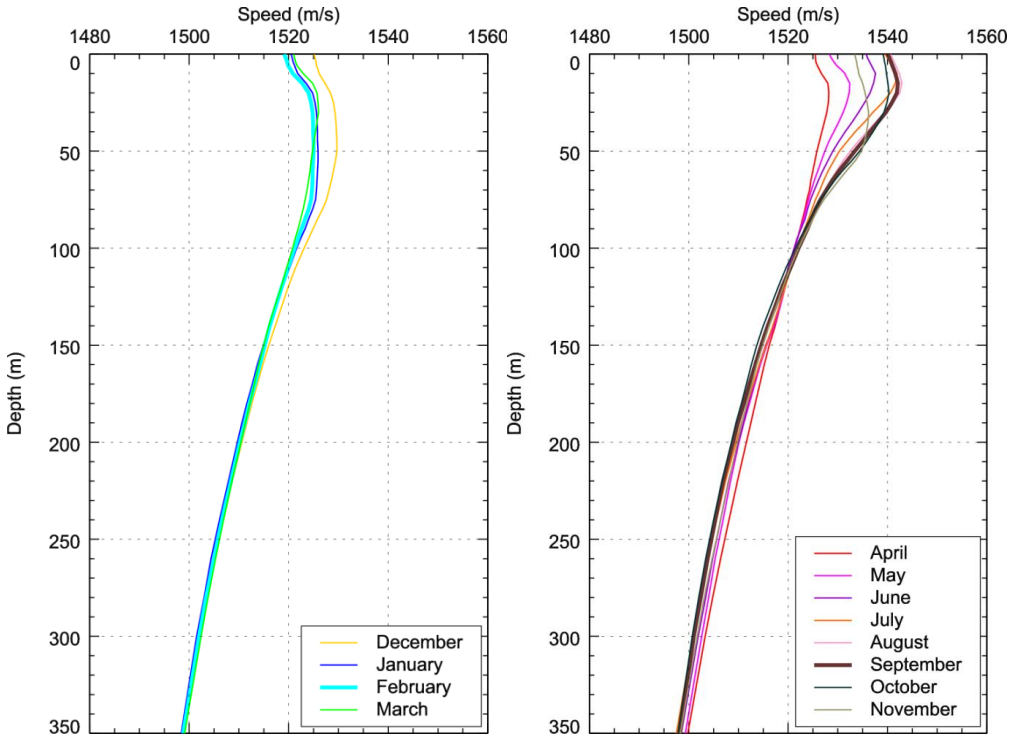

Figure 29. The Shelf zone (28.5° N, 90° W): Mean monthly sound speed profiles, separated into Seasons 1 (left) and 2 (right). Bolded profiles indicate average sound speed profile used for the season. Derived from data obtained from GDEM V 3.0 (Teague et al. 1990, Carnes 2009).

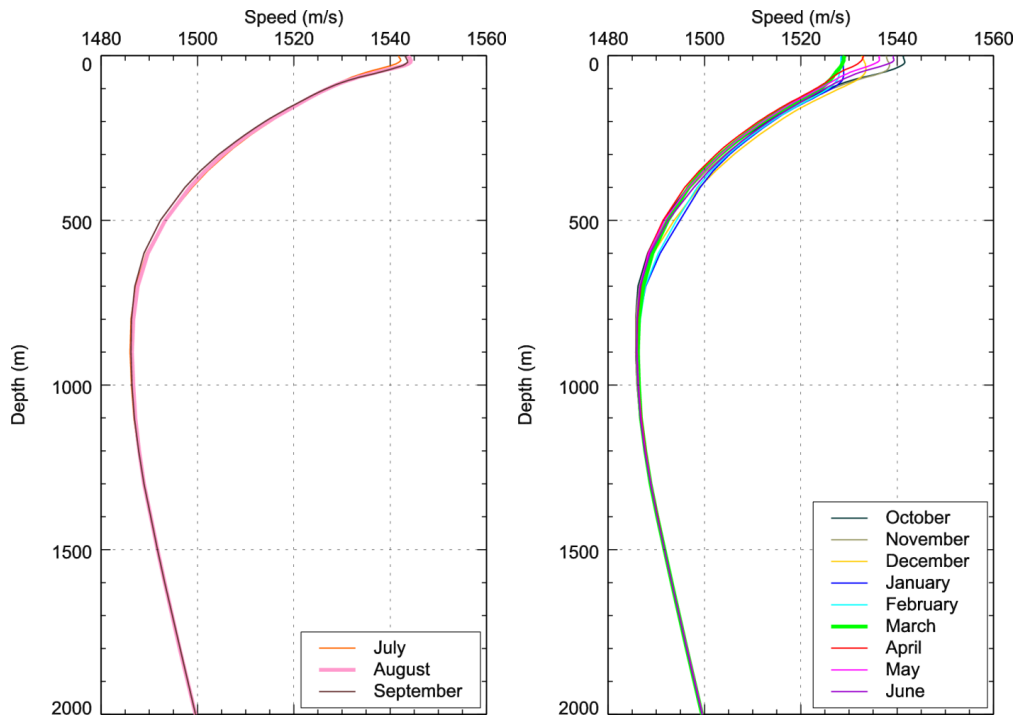

Figure 30. The Slope zone (27.25° N, 90° W): Mean monthly sound speed profiles, separated into Seasons 1 (left) and 2 (right). Bolded profiles indicate average sound speed profile used for the season. Derived from data obtained from GDEM V 3.0 (Teague et al. 1990, Carnes 2009).

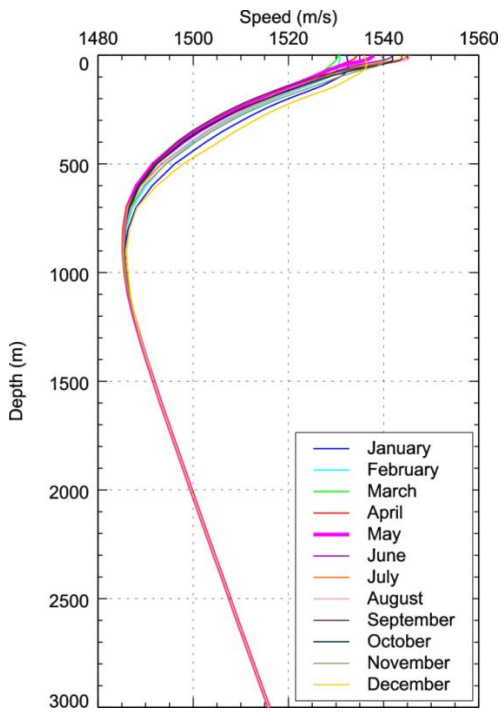

Figure 31. Deep zone (25.5° N, 90° W): Mean monthly sound speed profiles. Bolded profile indicates average sound speed profile used for the season. Derived from data obtained from GDEM V 3.0 (Teague et al. 1990, Carnes 2009).

To determine uncertainty in the acoustic field propagation due to variability of the sound speed profiles within in each season, original CTD casts, containing temperature and salinity information, were extracted from NOAA's database. Spatial limits from W89° to W91° were applied during database query. Temperature and salinity data were processed to obtain sound speed profiles using Equation 19.

All sound speed profiles were plotted by month separately for each zone: Shelf, Slope, and Deep. Monthly groups of sound speed profiles were combined into seasons based on similarity of the features: variability within each month and presence of the surface sound channel.

Two periods (seasons) were distinguished for the Shelf zone:

- Dec–Mar
- Apr–Nov

Two periods (seasons) were distinguished for the Slope zone:

- Jul–Sep
- Oct–Jun

In the Deep zone, we established that the separation into seasons is unwarranted because variability of the sound speed profiles throughout the year is not significantly larger than the variability within individual months.

In each group of sound speed profiles, 16% of the profiles with the highest gradient in the top 25 m (with the most pronounced sound channel) were removed to avoid the most extreme conditions, for which the probability of occurrence is low. This step was taken to omit profiles that may have been distorted by measurement system temperature settling. The remaining profiles are plotted together in Figures 32–34. A worst-case sound speed profile was chosen from the remaining profiles to reproduce the maximum gradient. The median sound speed profiles were obtained from GDEM profile of the central month of the season as identified in Table 29.

The worst-case scenario sound speed profiles for both seasons in the Shelf zone exhibit a surface sound channel extending to 40 m depth. The difference between the sound speed at the top (surface) and bottom (at 40 m depth) of the channel is 15 m/s during Season 1 and 10 m/s during Season 2. In the Slope zone, the occurrence of the surface sound channel exists only during Season 1. Season 2 in the Slope zone is characterized by a small negative gradient in the sound speed profile over the top 75 m of the water column, so no surface channel exists. Data for the Deep zone show little variability of the shape of the sound speed profile throughout the year. A single season was, therefore, defined and used for modeling in that zone.

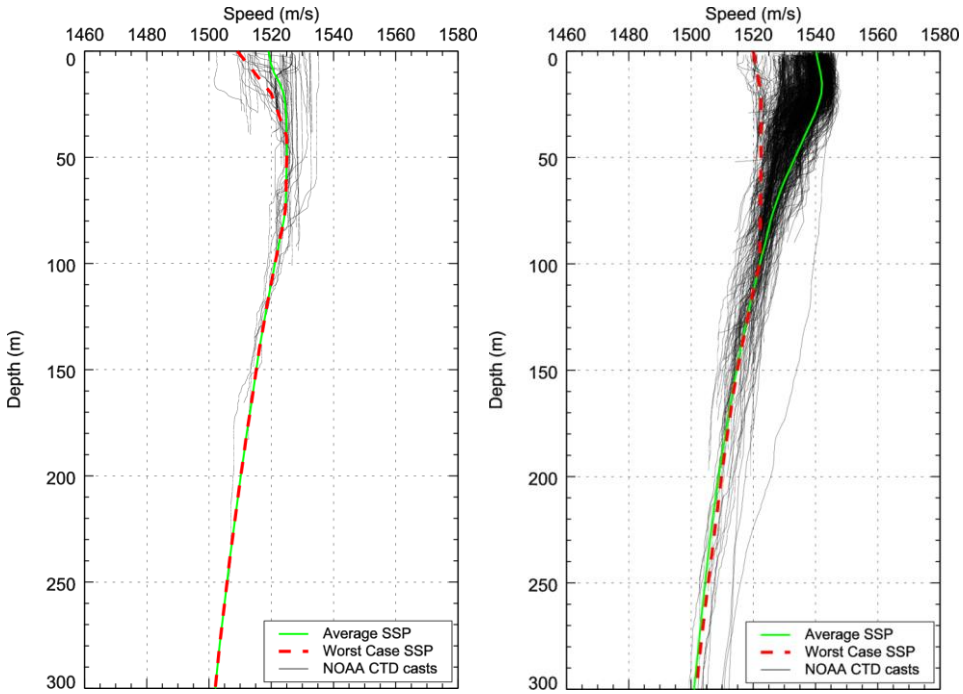

Figure 32. Shelf zone: Modeled average and worst-case sound speed profiles based on variations in CTD cast data for Seasons 1 (left) and 2 (right). Raw profiles are derived from NOAA Gulf of Mexico CTD cast data and mean monthly profiles are derived from GDEM V 3.0 (Teague et al. 1990, Carnes 2009).

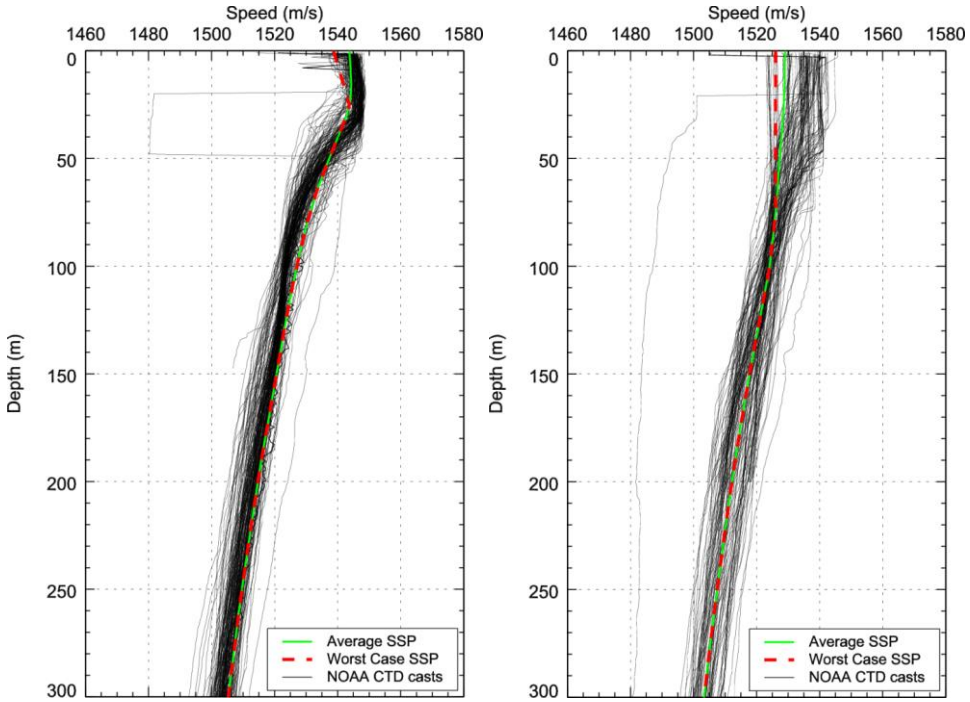

Figure 33. Slope zone: Modeled average and worst-case sound profiles based on variations in CTD cast data for Seasons 1 (left) and 2 (right). Raw profiles are derived from NOAA Gulf of Mexico CTD cast data and mean monthly profiles are derived from GDEM V 3.0 (Teague et al. 1990, Carnes 2009).

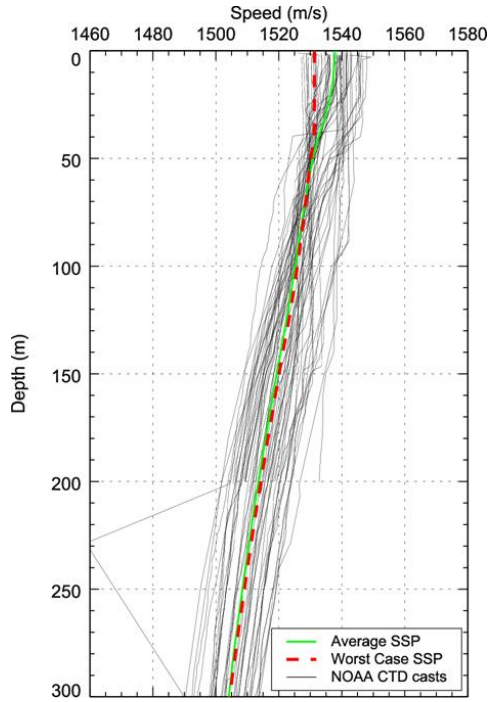

Figure 34. Deep zone: Modeled average and worst-case sound speed profiles based on variations in CTD cast data. Raw profiles are derived from NOAA Gulf of Mexico CTD cast data and mean monthly profiles are derived from GDEM (Teague et al. 1990, Carnes 2009).

6.5.2.1.4. Sound Speed Profile Results

The analysis of acoustic field uncertainty due to sound speed profile uncertainty was performed by calculating and examining the differences in acoustic fields between the worst-case and median case sound speed profiles. The source used for these runs was the 8000 in³ airgun array, at 8 m depth. All model runs for this analysis used geoacoustic (seabed parameter) profiles with median reflectivity at all three zones. The comparisons performed for the Shelf and Slope zones were made for both of the seasonal sound speed profiles of those zones. Only the one season and a single corresponding sound speed profile exist for the Deep zone.

Shelf zone: December–March

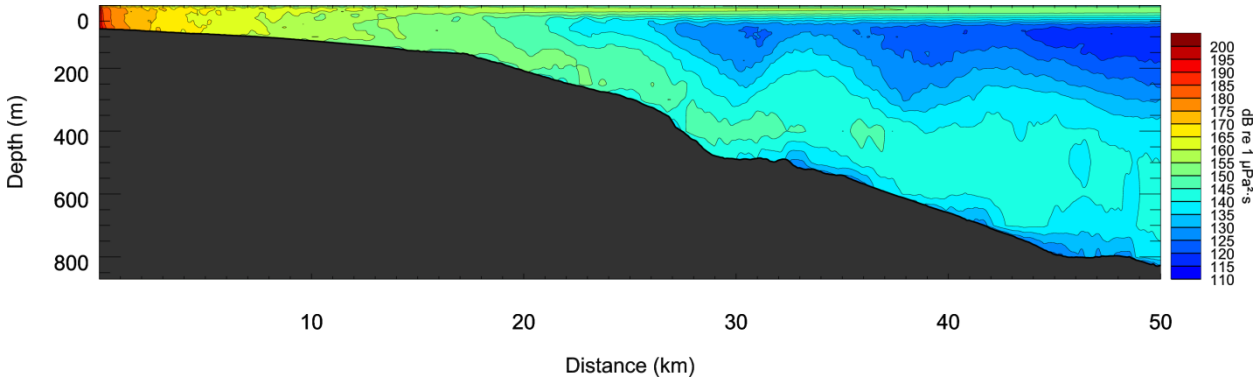

Figure 35. Shelf zone, Dec–Mar: Received SEL acoustic field using conservative (enhanced propagation) sound speed profile and median reflectivity geoacoustic parameters. Downslope direction.

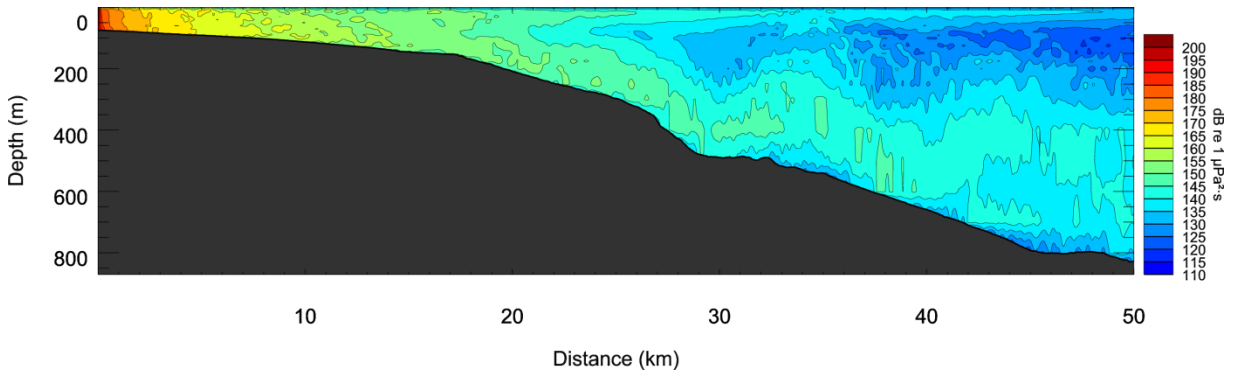

Figure 36. Shelf zone, Dec–Mar: Received SEL acoustic field using median sound speed profile and median reflectivity geoacoustic parameters. Downslope direction.

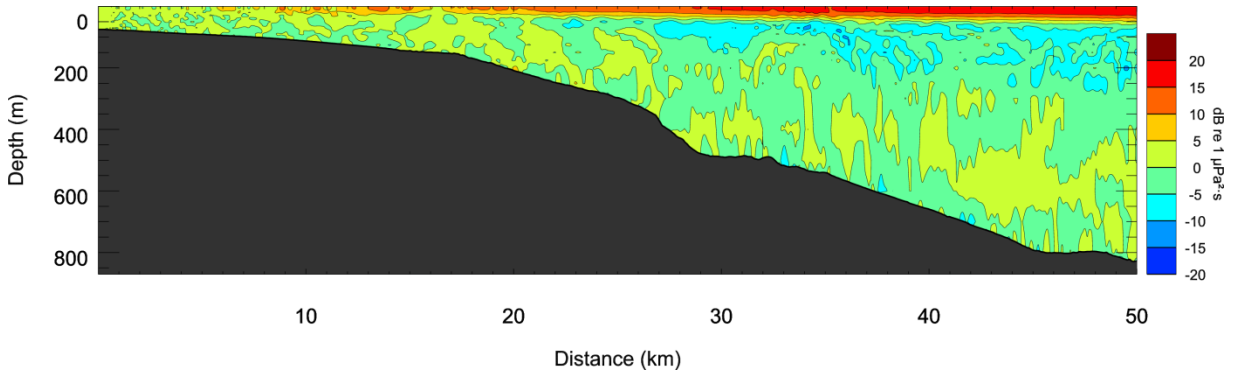

Figure 37. Shelf zone, Dec–Mar: Differential acoustic field due to variation in the sound speed profile. Downslope direction.

Shelf zone: April–November

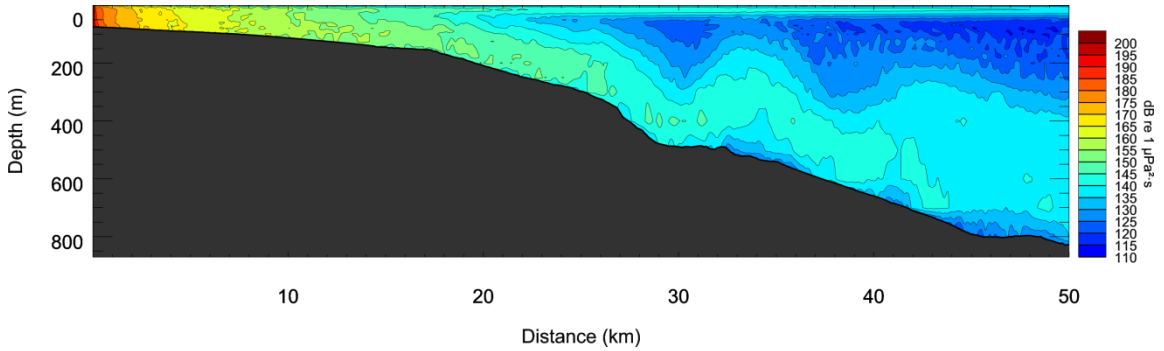

Figure 38. Shelf zone, Apr–Nov: Received SEL acoustic field using conservative sound (enhanced propagation) speed profile and median reflectivity geoacoustic parameters. Downslope direction.

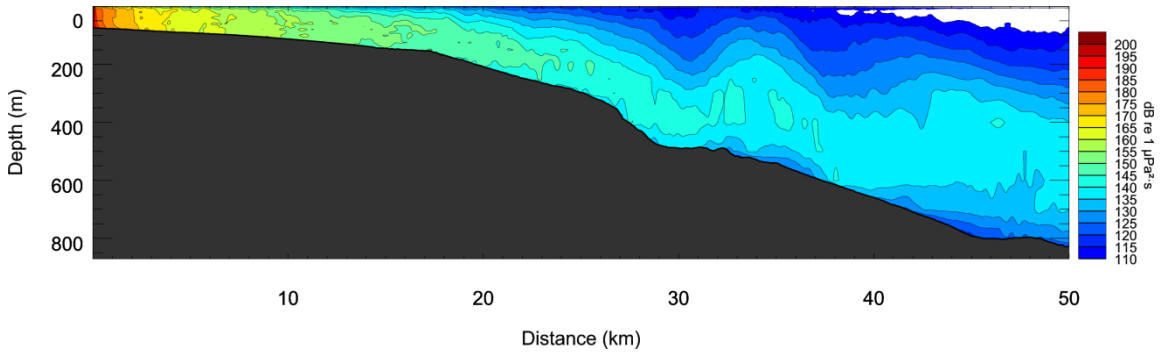

Figure 39. Shelf zone, Apr–Nov: Received SEL acoustic field using median sound speed profile and median reflectivity geoacoustic parameters. Downslope direction.

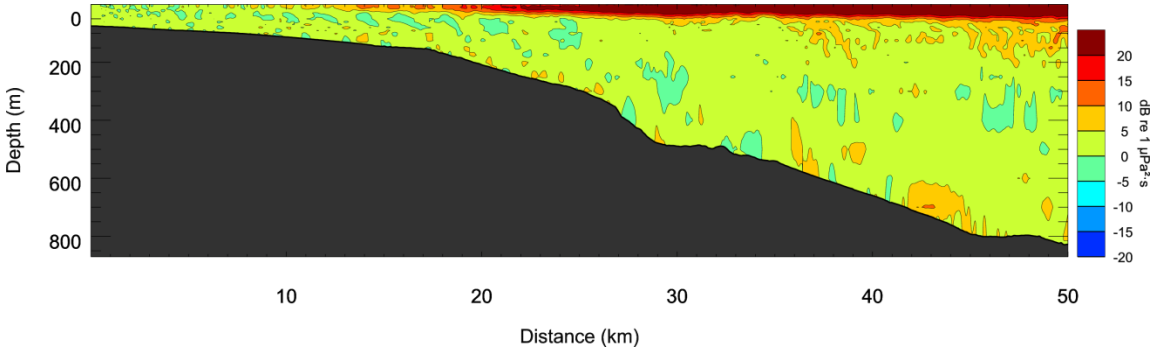

Figure 40. Shelf zone, Apr–Nov: Differential acoustic field due to variation in the sound speed profile. Downslope direction.

Slope zone: July–September

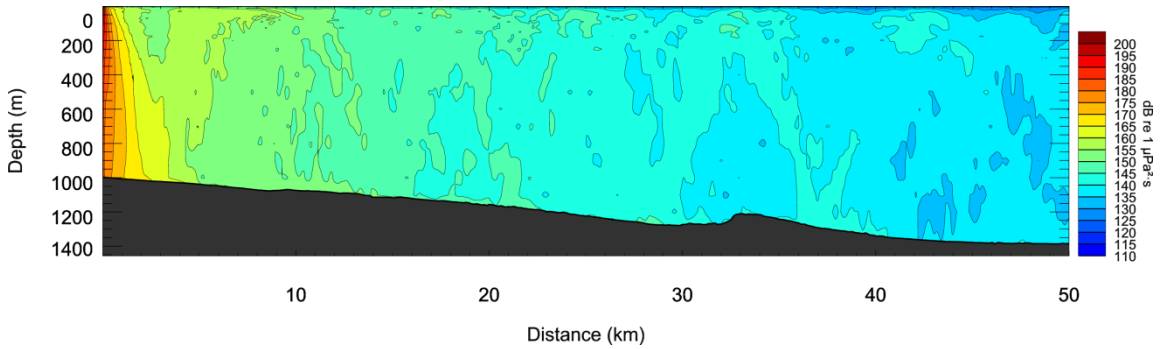

Figure 41. Slope zone, Jul–Sep: Received SEL acoustic field using conservative sound speed profile and median reflectivity geoacoustic parameters. Downslope direction.

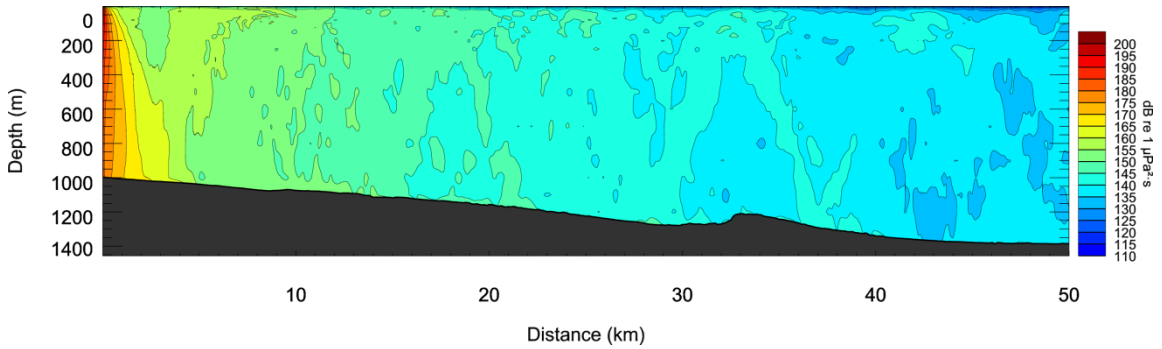

Figure 42. Slope zone, Jul–Sep: Received SEL acoustic field using median sound speed profile and median reflectivity geoacoustic parameters. Downslope direction.

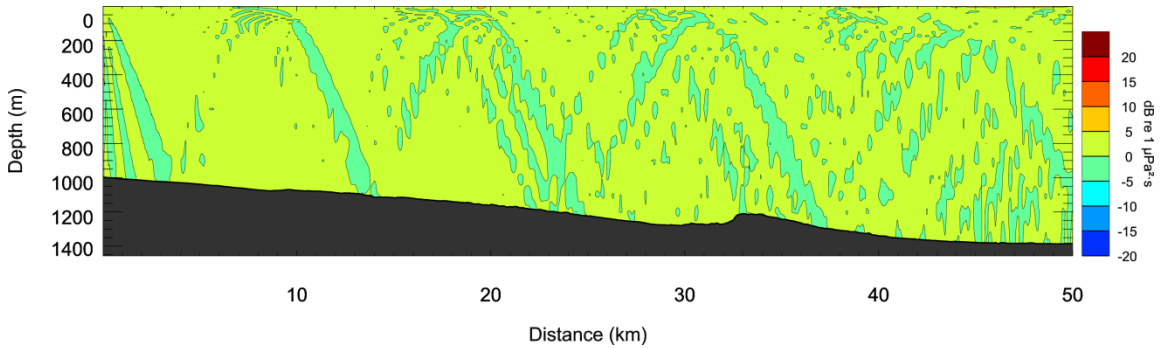

Figure 43. Slope zone, Jul–Sep: Differential acoustic field due to variation in the sound speed profile. Downslope direction.

Slope zone: October–June

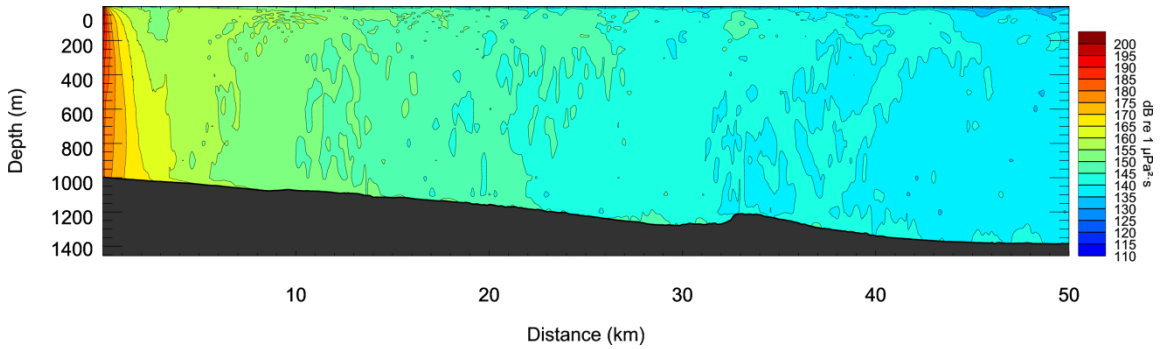

Figure 44. Slope zone: Received SEL acoustic field sing conservative sound speed profile and median reflectivity geoacoustic parameters. Downslope direction.

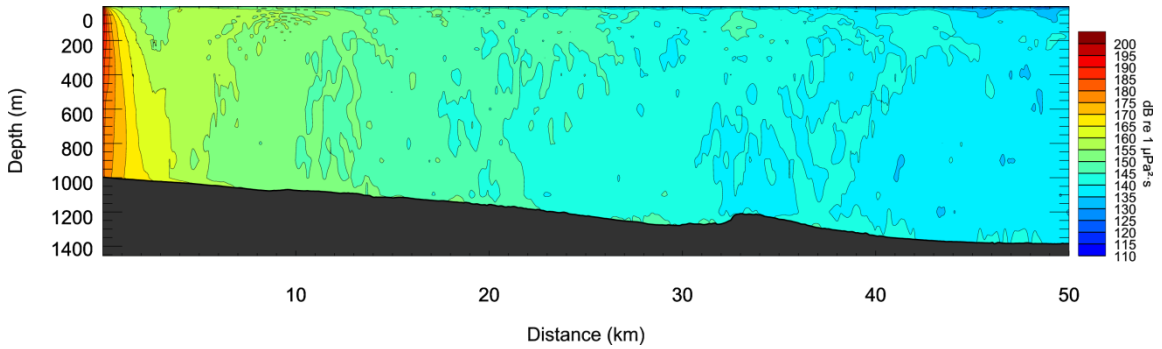

Figure 45. Slope zone, Oct–Jun: Received SEL acoustic field using median sound speed profile and median reflectivity geoacoustic parameters. Downslope direction.

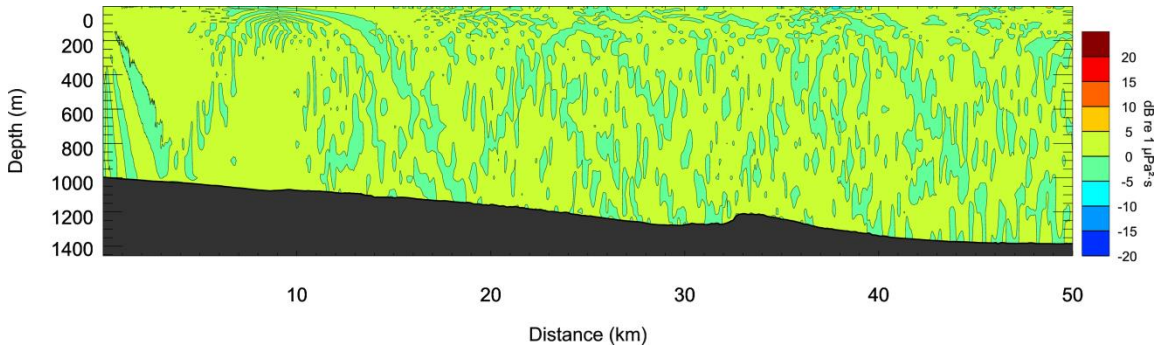

Figure 46. Slope zone, Oct–Jun: Differential acoustic field due to variation in the sound speed profile. Downslope direction.

Deep zone

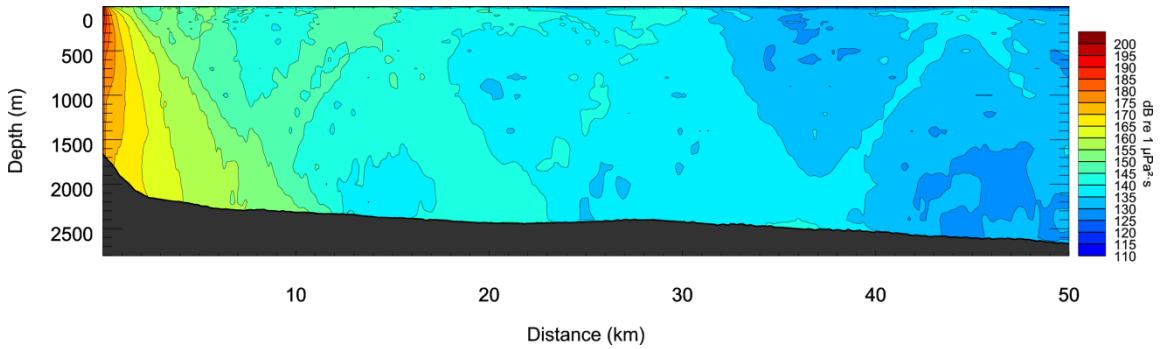

Figure 47. Deep zone: Received SEL acoustic field using conservative sound speed profile and median reflectivity geoacoustic parameters. Downslope direction.

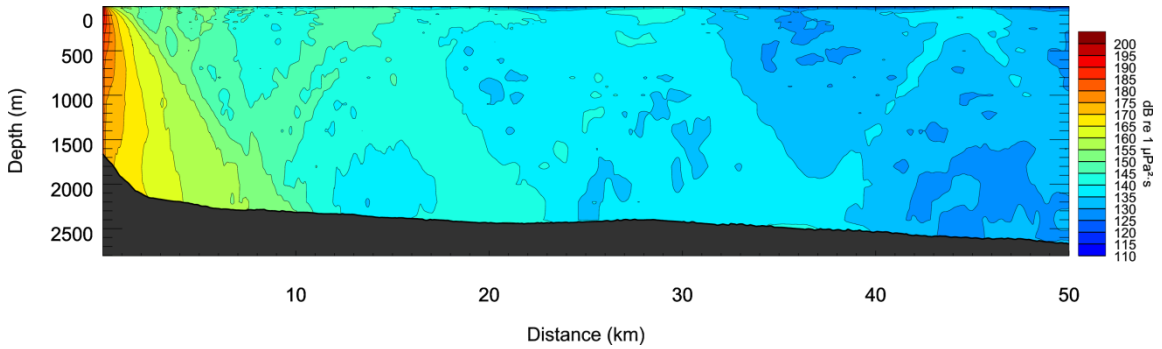

Figure 48. Deep zone: Received SEL acoustic field using median sound speed profile and median reflectivity geoacoustic parameters. Downslope direction.

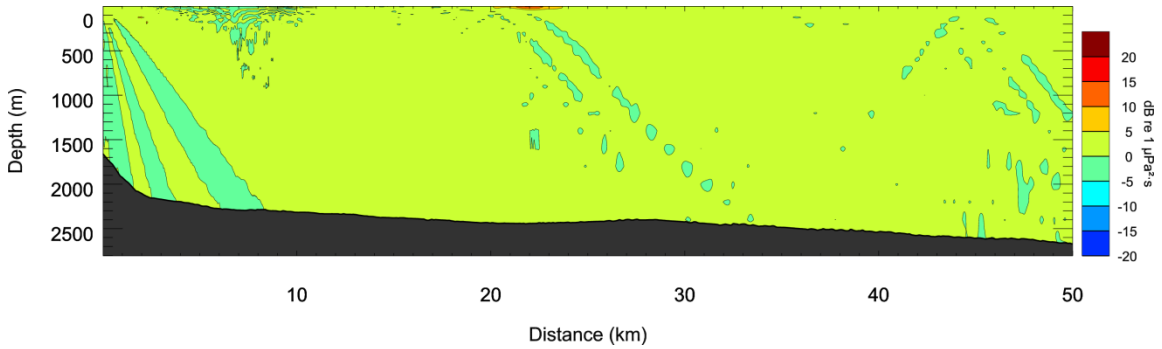

Figure 49. Deep zone: Differential acoustic field due to variation in the sound speed profile. Downslope direction.

In each zone, the acoustic field was propagated in three directions (downslope, upslope, and along slope). For each direction, the range to the rms SPL 160 dB re 1 µPa (153 dB re 1 µPa·s² SEL) threshold was estimated based on the worst-case scenario acoustic field in the comparison pair. The average difference and standard deviation were calculated based on the differences at locations within a 5 km horizontal × 20 m deep box along the radials starting at the threshold range. The 20 m vertical extent was selected to emphasize the depths at which the animals spend much of their time. Table 30 shows the calculated average differences between the worst-case and median case scenarios, and the distance at which the 160 dB re 1 µPa rms SPL threshold occurs.

Table 30. Acoustic field differences between worst-case and average sound speed profile conditions. Column "R" shows the maximum distance in kilometers of 160 dB re 1 µPa rms SPL threshold exceedance. The Median (σ) column shows the median difference and standard deviation in decibels, over a range-depth zone containing many receivers, near the 160 dB re 1 µPa threshold location.

Direction	Shelf zone				Slope zone				Deep zone	
	Dec-Mar		Apr-Nov		Jul-Sep		Oct-Jun		Jan-Dec	
	R (km)	Median (σ) (dB)	R (km)	Median (σ) (dB)	R (km)	Median (σ) (dB)	R (km)	Median (σ) (dB)	R (km)	Median (σ) (dB)
Downslope	30.6*	14.9 (1.0)	22.6	10.5 (2.7)	11.5	0.7 (0.6)	14.1	0.2 (0.5)	10	0.3 (0.3)
Along slope	23.5	7.0 (1.2)	12.2	5.7 (2.8)	8.8	2.0 (1.8)	8.3	0.7 (0.9)	6.7	−0.1 (0.3)
Upslope	14.3	5.0 (1.3)	9.2	6.5 (1.8)	7.7	1.2 (0.8)	8.9	0.4 (0.4)	9.4	3.8 (2.5)

* 163 dB re 1 µPa rms SPL threshold was used for this scenario since 160 dB re 1 µPa rms SPL threshold was beyond 50 km modeled range.

6.5.2.1.5. Geoacoustics

Geoacoustic parameters describe the acoustic properties of the seabed, including sound speeds in various layers. JASCO's MONM-RAM model, a parabolic-equation-based acoustic propagation model, was used to calculate transmission loss from the source to locations within a vertical plane in the water column. MONM-RAM assumes a single geoacoustic profile of the seafloor for the entire modeled area (see 6.2.3 for required input parameters).

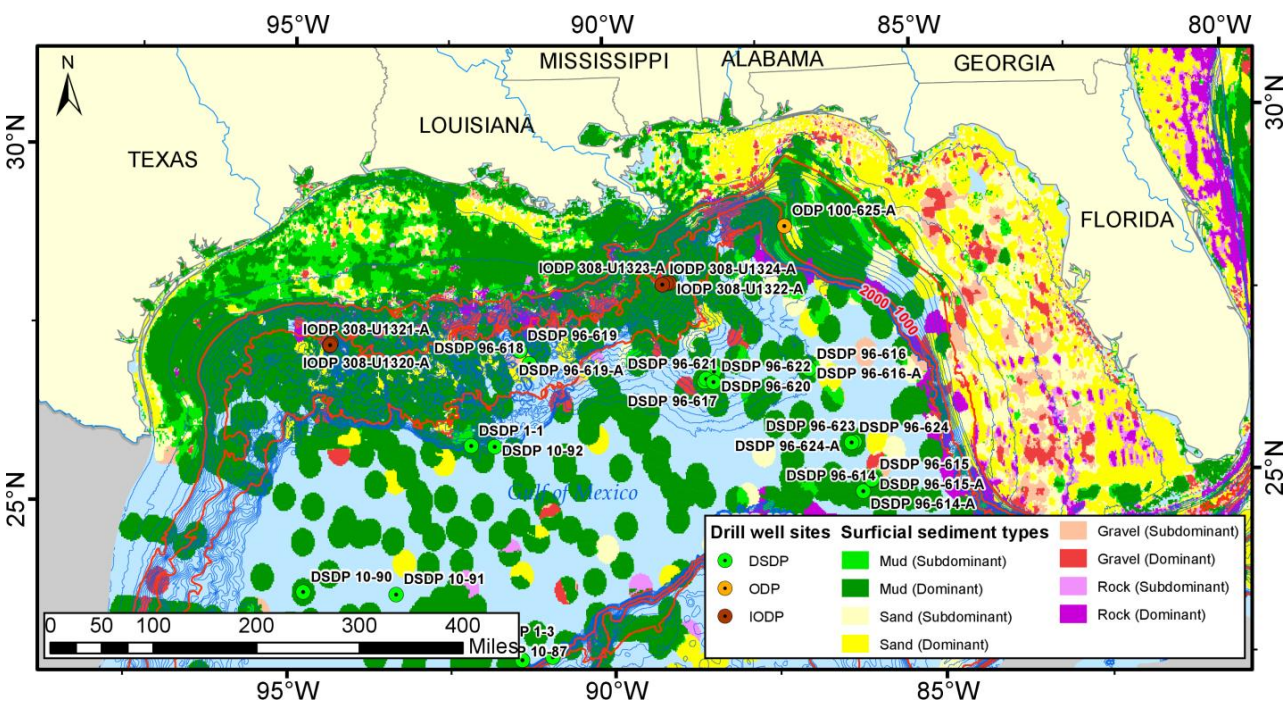

Figure 50. The map of dominant type for the surficial sediments (NOS 2013) and location of the drill wells in the Gulf of Mexico.

Two geoacoustic profiles—(1) the most likely (median) propagation conditions and (2) an extreme case of a more reflective bottom—were determined for each zone (Shelf, Slope, and Deep). The two profiles within each zone were based on similar sediment types, but the more-reflective variant was achieved by increasing the grain size and/or porosity of the sediment layers relative to the median case values.

The NOAA/NOS and USCGS Seabed Descriptions from Hydrographic Surveys (National Ocean Service 2013) were used to define the surficial sediment types for the specific zone (Figure 50). The well log data from DSDP/ODP/IODP legs were used to estimate the change of the porosity with depth. Sediment grain-shearing model (Buckingham 2005) was used to compute the acoustic properties of the sediments based on the porosity data and grain-size estimates. The grain size of the sediments is usually indicated by the parameter, φ, using an inverse logarithmic scale. From coarsest to finest, sand has φ from 0 to 4, for silt φ varies from 4 to 8, and for clay φ varies from 8 to 10.

The top layers of the seafloor in the Gulf of Mexico are represented by layers of unconsolidated sediments with the thickness of at least several hundred meters. The grain size of the surficial sediments follow the general trend for the sedimentary basins: the grain size of the deposited sediments decreases with the distance from the shore. The general surficial bottom type varies by zones: for the Shelf zone it was sand, for the Slope zone it was silt, and for the Deep zone it was clay.

The three sets of geoacoustic parameters for each zone, Shelf, Slope, and Deep, are presented in Tables 31, 32, and 33, respectively.

Table 31. Shelf zone: Median and higher reflectivity geoacoustic profiles. Sand is the dominant surficial sediment.

Depth below the seafloor (m)	Median reflectivity (φ=2)			Higher reflectivity (φ=1)		
	Porosity (%)	Rho (g/cm³)	V_P (m/s)	Porosity (%)	Rho (g/cm³)	V_P (m/s)
1	65	1.61	1610	60	1.70	1660
20	60	1.70	1900	55	1.78	2040
50	55	1.78	2090	50	1.87	2290
200	50	1.87	2500	45	1.96	2500
600	40	2.04	2500	40	2.04	2500

Table 32. Slope zone: Lower, median, and higher reflectivity geoacoustic profiles. Silt is the dominant surficial sediment.

Depth below the seafloor (m)	Lower reflectivity (φ=7)			Median reflectivity (φ=5)			Higher reflectivity (φ=4)		
	Porosity (%)	Rho (g/cm³)	V_P (m/s)	Porosity (%)	Rho (g/cm³)	V_P (m/s)	Porosity (%)	Rho (g/cm³)	V_P (m/s)
1	80	1.35	1490	75	1.44	1515	75	1.44	1530
20	65	1.61	1580	60	1.7	1670	60	1.7	1720
50	60	1.7	1640	60	1.7	1750	60	1.7	1830
200	50	1.87	1790	50	1.87	1970	50	1.87	1870
600	40	2.04	1980	40	2.04	2260	40	2.04	2040

Table 33. Deep zone: Lower, median, and higher reflectivity geoacoustic profiles. Clay is the dominant surficial sediment.

Depth below the seafloor (m)	Lower reflectivity (φ=9)			Median reflectivity (φ=8)			Higher reflectivity (φ=8)		
	Porosity (%)	Rho (g/cm³)	V_P (m/s)	Porosity (%)	Rho (g/cm³)	V_P (m/s)	Porosity (%)	Rho (g/cm³)	V_P (m/s)
1	75	1.44	1460	70	1.52	1472	60	1.70	1494
20	65	1.61	1520	60	1.70	1560	55	1.78	1570
50	60	1.70	1560	55	1.78	1610	50	1.87	1640
200	55	1.78	1650	50	1.87	1720	45	1.96	1750
600	45	1.96	1780	40	2.04	1890	40	2.04	1890

6.5.2.1.6. Geoacoustic Results

To analyze acoustic field uncertainty due to differences in the geoacoustic properties of the sea bottom, the respective median sound speed profiles were used to model in each zone. Sound fields were generated using the median and high reflectivity geoacoustic parameters (as defined above) and the resulting sound fields subtracted to determine the differences. The comparison was conducted separately for two seasons each in the Shelf and Slope zones and for the one season representing the entire year in the Deep zone.

Shelf zone: December–March

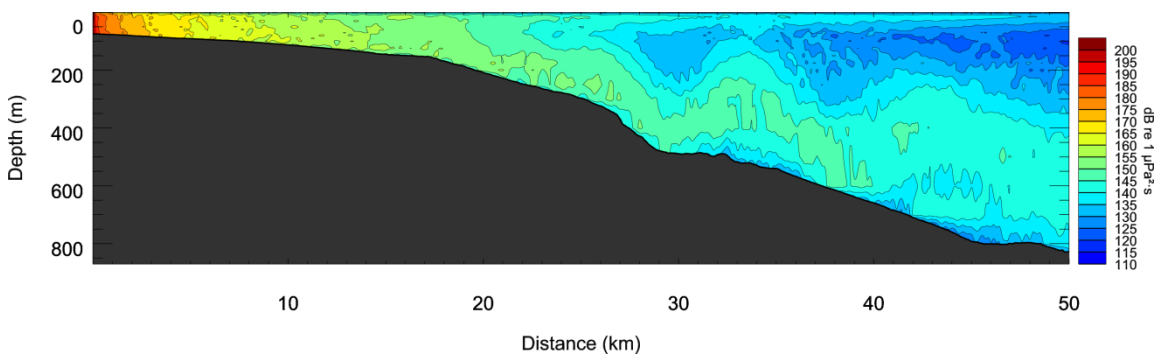

Figure 51. Shelf zone, Dec–Mar: Received SEL acoustic field using median sound speed profile and high reflectivity geoacoustic parameters. Downslope direction.

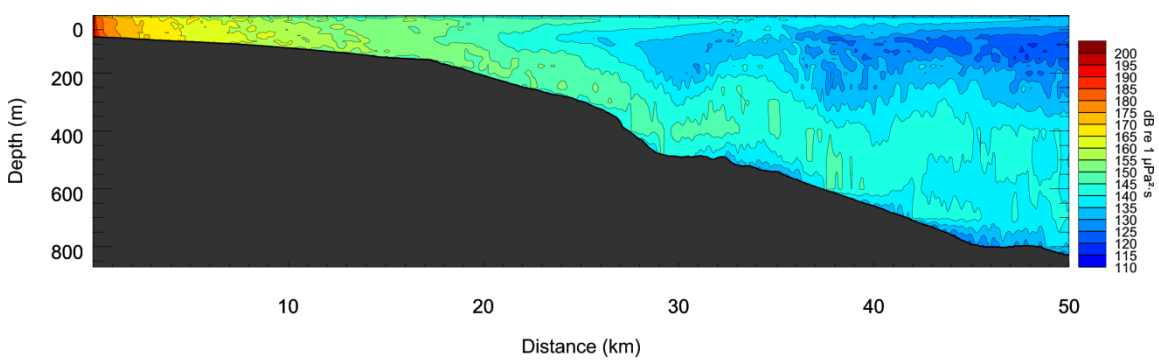

Figure 52. Shelf zone, Dec–Mar: Received SEL acoustic field using median sound speed profile and median reflectivity geoacoustic parameters. Downslope direction.

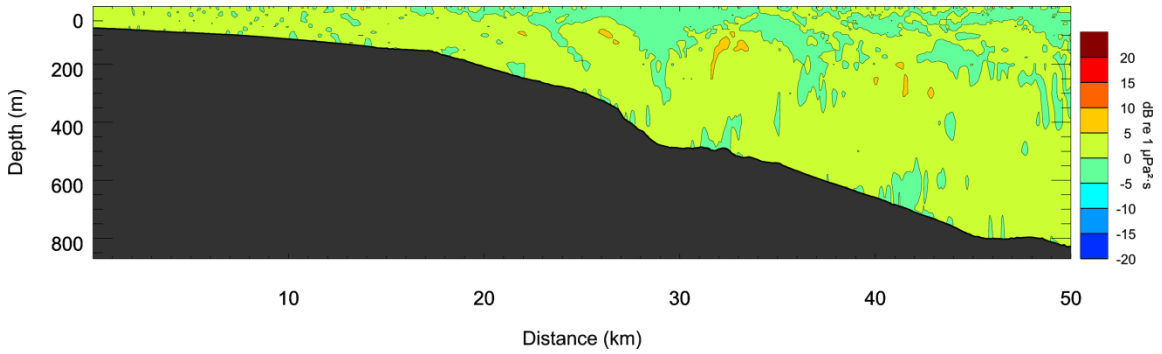

Figure 53. Shelf zone, Dec–Mar: Differential acoustic field due to variation in the bottom geoacoustic parameters. Downslope direction.

Shelf zone: April–November

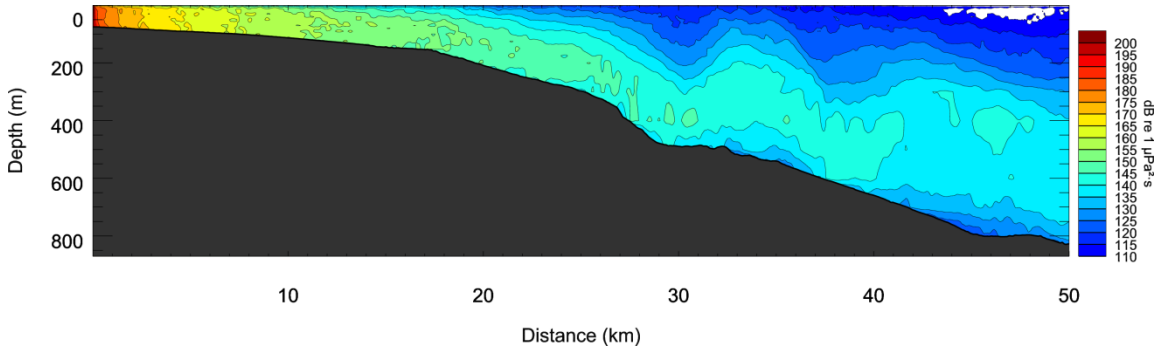

Figure 54. Shelf zone, Apr–Nov: Received SEL acoustic field using median sound speed profile and high reflectivity geoacoustic parameters. Downslope direction.

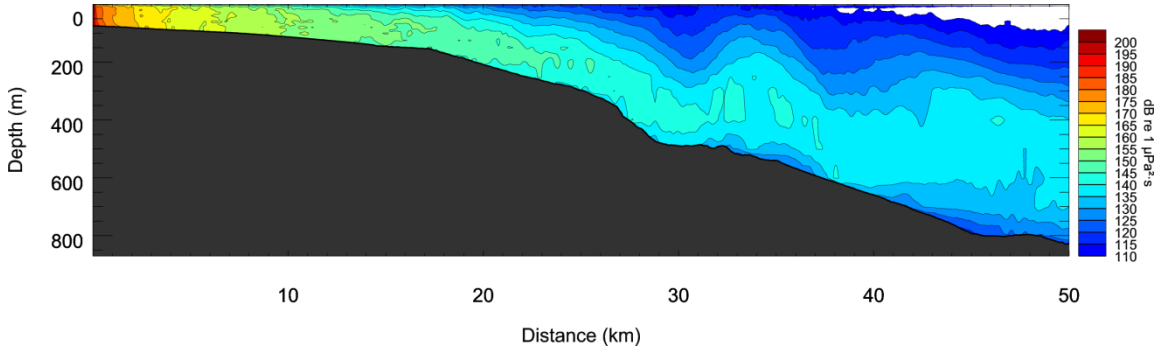

Figure 55. Shelf zone, Apr–Nov: Received SEL acoustic field using median sound speed profile and median reflectivity geoacoustic parameters. Downslope direction.

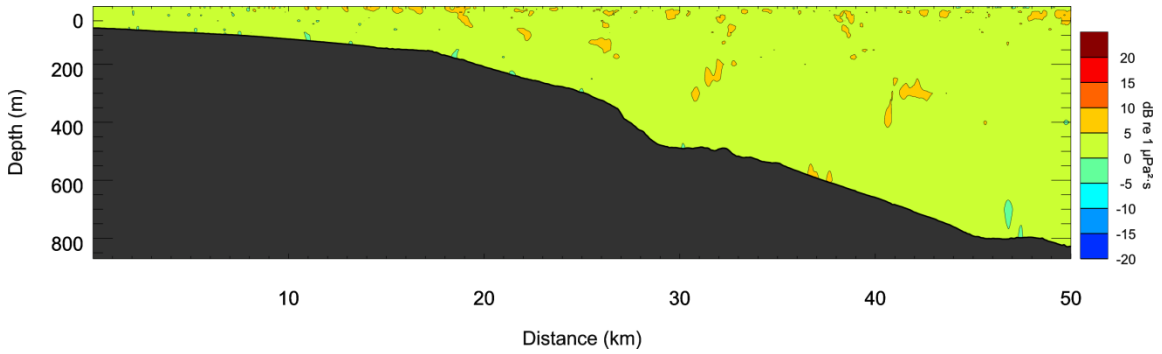

Figure 56. Shelf zone, Apr–Nov: Differential acoustic field due to variation in the bottom geoacoustic parameters. Downslope direction.

Slope zone: July–September

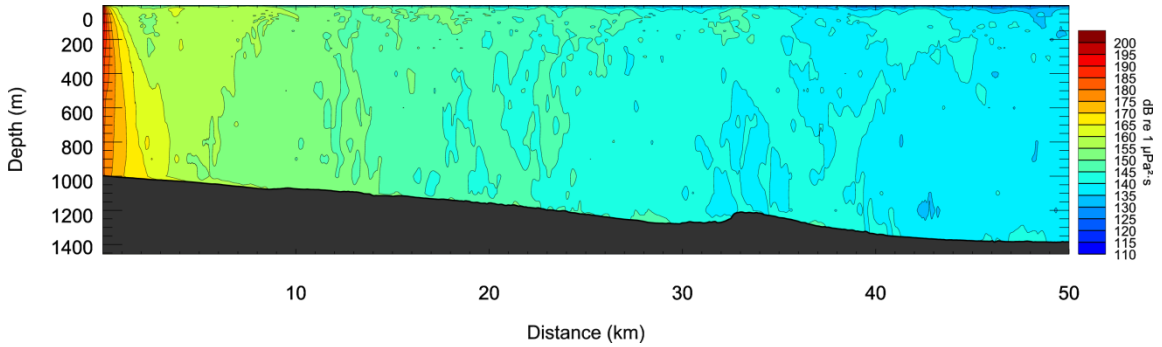

Figure 57. Slope zone, Jul–Sep: Received SEL acoustic field using median sound speed profile and high reflectivity geoacoustic parameters. Downslope direction.

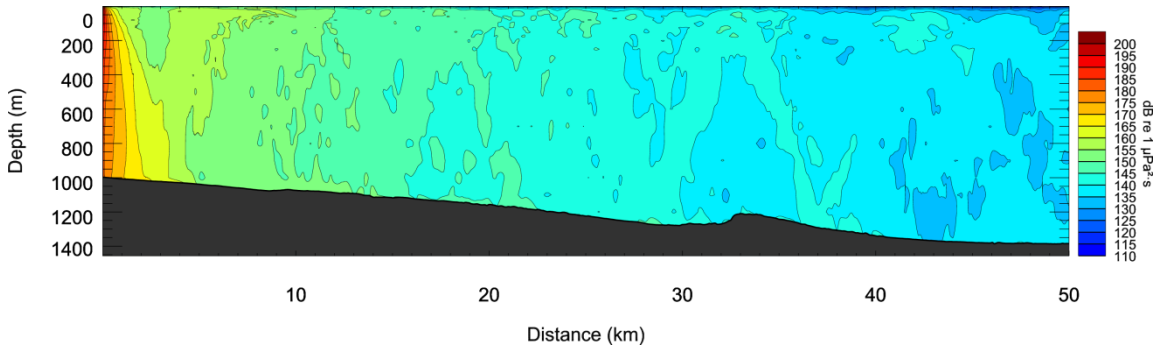

Figure 58. Slope zone, Jul–Sep: Received SEL acoustic field using median sound speed profile and median reflectivity geoacoustic parameters. Downslope direction.

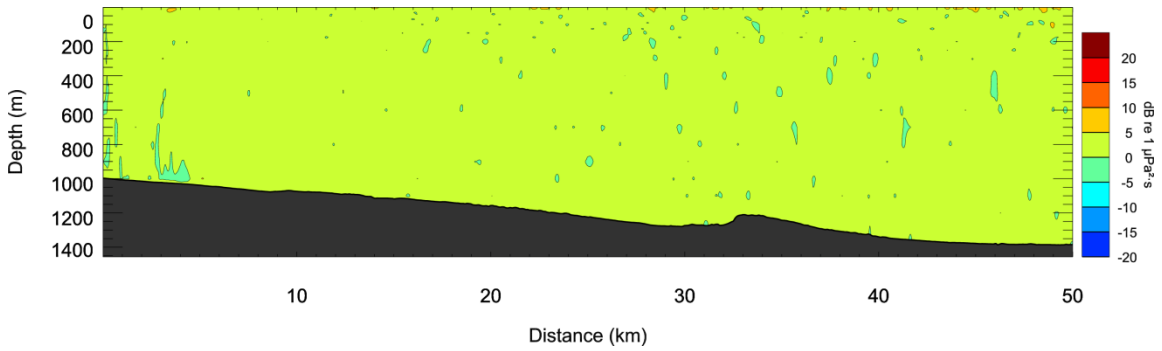

Figure 59. Slope zone, Jul–Sep: Differential acoustic field due to variation in the bottom geoacoustic parameters. Downslope direction.

Slope zone: October–June

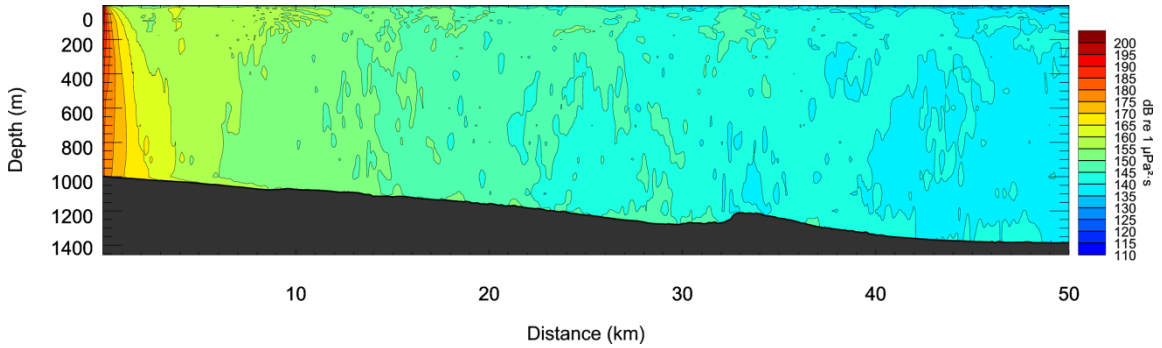

Figure 60. Slope zone, Oct–Jun: Received SEL acoustic field using median speed profile and high reflectivity geoacoustic parameters. Downslope direction.

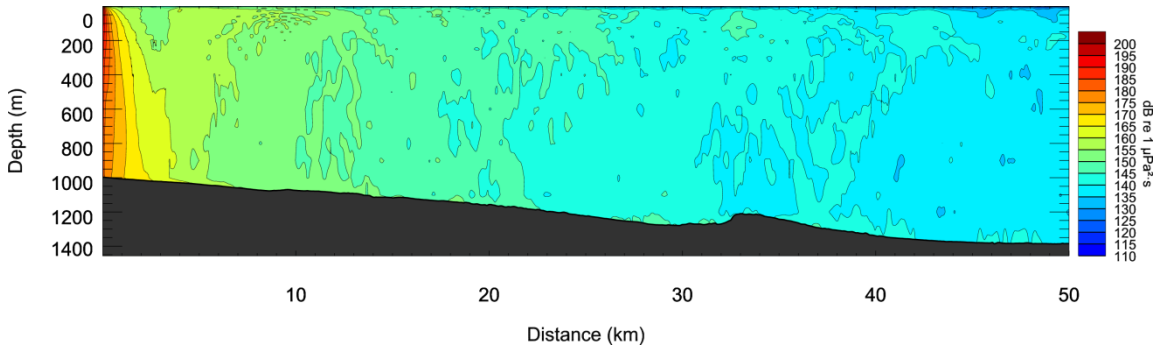

Figure 61. Slope zone, Oct–Jun: Received SEL acoustic field using median sound speed profile and median reflectivity geoacoustic parameters. Downslope direction.

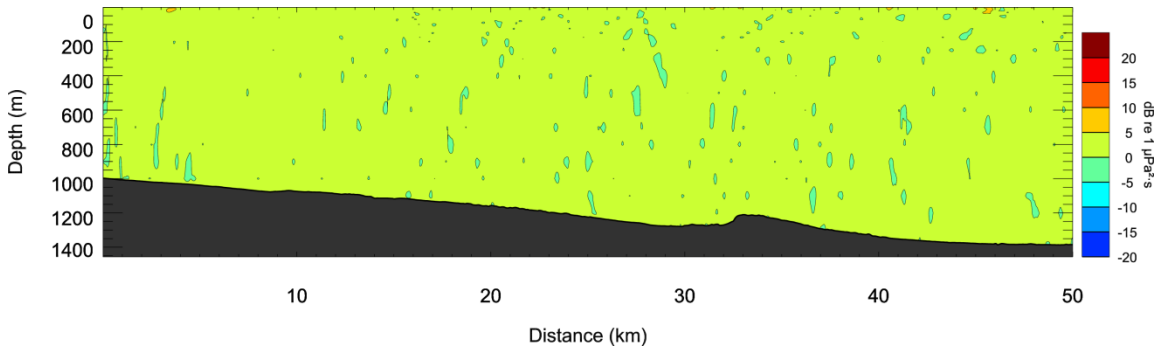

Figure 62. Slope zone, Oct–Jun: Differential acoustic field due to variation in the bottom geoacoustic parameters. Downslope direction.

Deep zone

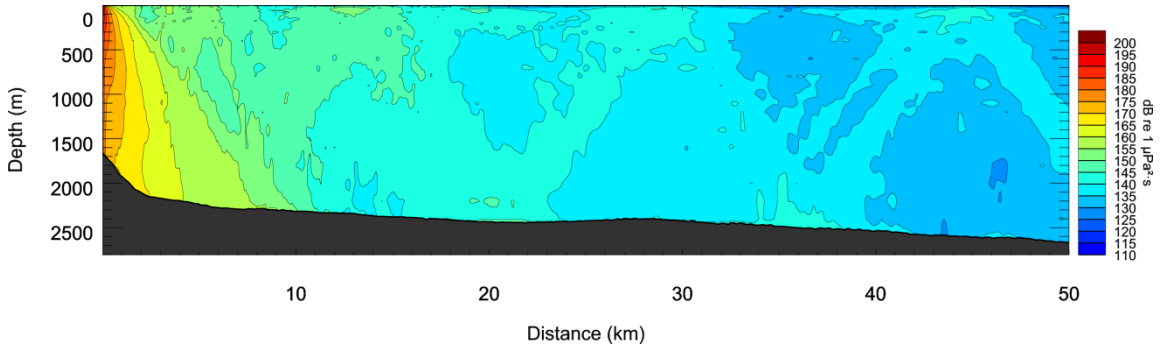

Figure 63. Deep zone: Received SEL acoustic field using median sound speed profile and high reflectivity geoacoustic parameters. Downslope direction.

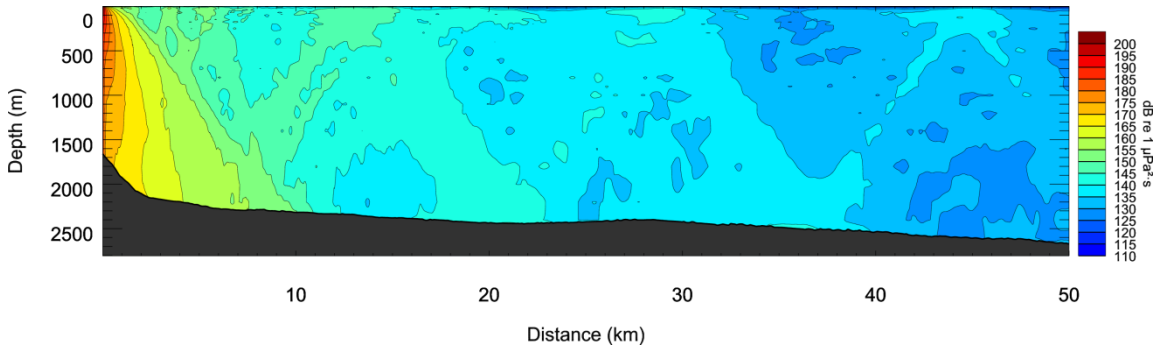

Figure 64. Deep zone: Received SEL acoustic field using median sound speed profile and median reflectivity geoacoustic parameters. Downslope direction.

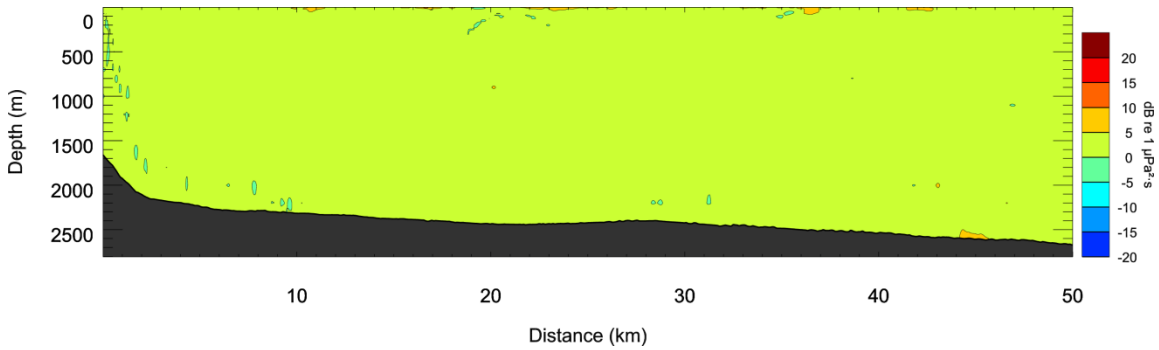

Figure 65. Deep zone: Differential acoustic field due to variation in the bottom geoacoustic parameters. Downslope direction.

As was done for the sound velocity profiles, the acoustic field in each zone was propagated in three directions (downslope, upslope, and along-slope), and for each direction the range to the 160 dB re 1 µPa rms SPL (153 dB re 1 µPa·s² SEL) threshold was estimated. The average difference and standard deviation were calculated based on the differences for individual receivers within a 5 km horizontal × 20 m deep box starting at the threshold range. The 20 m vertical extent was selected to emphasize the depths at which animals spend much of their time. Table 34 shows the calculated average differences between the worst-case and median case scenarios, and the distance at which the 160 dB re 1 µPa rms SPL threshold occurs.

Table 34. Acoustic field differences between reflective and average geoacoustic conditions. Column "R" shows the maximum distance in kilometers of 160 dB re 1 µPa rms SPL threshold exceedance. Median (σ) column shows the median difference and standard deviation in decibels, over a range-depth zone containing many receivers, near the 160 dB re 1 µPa threshold location.

Direction	Shelf zone				Slope zone				Deep zone	
	Dec-Mar		Apr-Nov		Jul-Sep		Oct-Jun		Jan-Dec	
	R (km)	Median (σ) (dB)	R (km)	Median (σ) (dB)	R (km)	Median (σ) (dB)	R (km)	Median (σ) (dB)	R (km)	Median (σ) (dB)
Downslope	24.1	−0.9 (0.7)	18.6	3.4 (1.7)	17.3	2.7 (1.1)	18.5	2.2 (1.2)	9.6	3.8 (1.5)
Along slope	16.5	1.3 (2.2)	11.6	3.5 (2.8)	8.5	3.4 (2.2)	10.9	1.8 (1.1)	6.8	4.0 (1.2)
Upslope	10.7	1.1 (1.3)	8.0	3.4 (1.3)	9.4	2.4 (1.0)	9.4	1.8 (0.9)	9.7	3.1 (1.9)

* 156 dB re 1 µPa rms SPL threshold was used for this scenario since 153 dB re 1 µPa rms SPL threshold was beyond 50 km modeled range.

6.5.2.1.7. Bathymetry

Water depth and local bathymetric features affect sound propagation. There is uncertainty associated with bathymetric accuracy and uncertainty in using sound fields generated for a specific location to represent a larger area. Here, a comparison is developed to show the variation in received levels with both the water depth at the source and with local features such as hills, troughs, and local slopes.

The purpose of this analysis was to delineate how acoustic propagation differences due to variations in bathymetry result in variations in the acoustic field in each of several water depth regimes (shallow, slope, deep vs. downslope, along-slope, upslope). The bathymetry variation in any one regime was represented as a pair of modeling sites at different, but nearby, water depths. The difference in the acoustic field modeled at these paired sites is reported as a mean and standard deviation over range and receiver depth. The bottom topography variation differences that exist between each paired site are included in the

analysis. This is different from a sensitivity analysis that would examine variations in the acoustic field based on small perturbations in modeling bathymetry at individual modeling sites. As such, the analysis reported here estimates the uncertainty in the acoustic field due to bathymetric variations that occur within a given acoustic regime. This is directly relevant to the Phase II study because modeling results from one site were used as a proxy for the acoustic field produced by a source at various locations within a given modeling regime represented by that site.

6.5.2.1.8. Bathymetry Results

To analyze acoustic field uncertainty due to bathymetry, the acoustic fields calculated for the exposure modeling were used. Modeling sites were selected at 25, 75, and 150 m depth (Shelf zone), 300, 500, 750, 1000, and 1500 m depth (Slope zone), and 2000 and 2500 m depth (Deep zone). The sound propagation modeling for the analysis was performed for Season 1 (winter) sound speed profile and median reflectivity geoacoustic profile.

Acoustic fields at pairs of water depths were compared:

- 25 and 75 m
- 75 and 150 m
- 300 and 500 m
- 500 and 750 m
- 750 and 1000 m
- 1000 and 1500 m
- 2000 and 2500 m

The differential field was calculated by subtracting the received levels of the acoustic field at deeper site from the received levels at shallower site. The positive values of the differential field indicate that the received level at specific distance from the source and depth from the sea surface was greater for the site with shallower water depth at the source.

Shelf zone: 25 m to 150 m

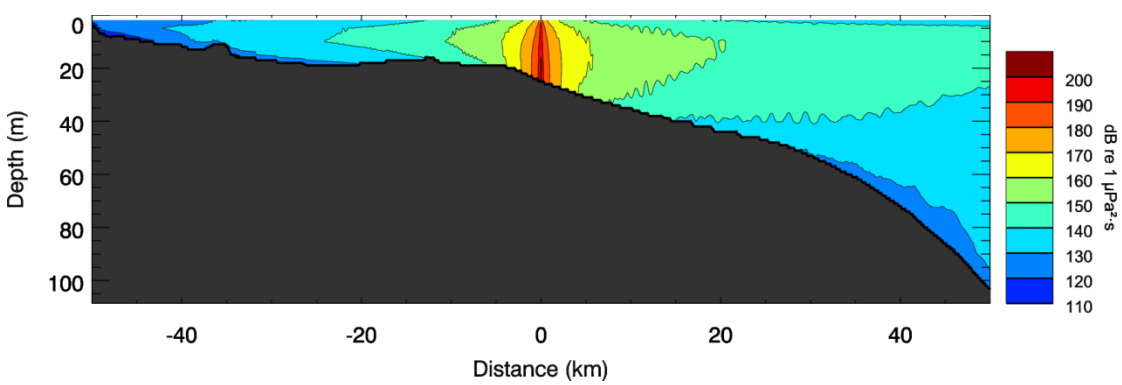

Figure 66. Shelf zone: The source when positioned at water column depth of 25 m: Received SEL acoustic field using Season 1 sound speed profile and median reflectivity geoacoustic parameters. Cross-slope direction.

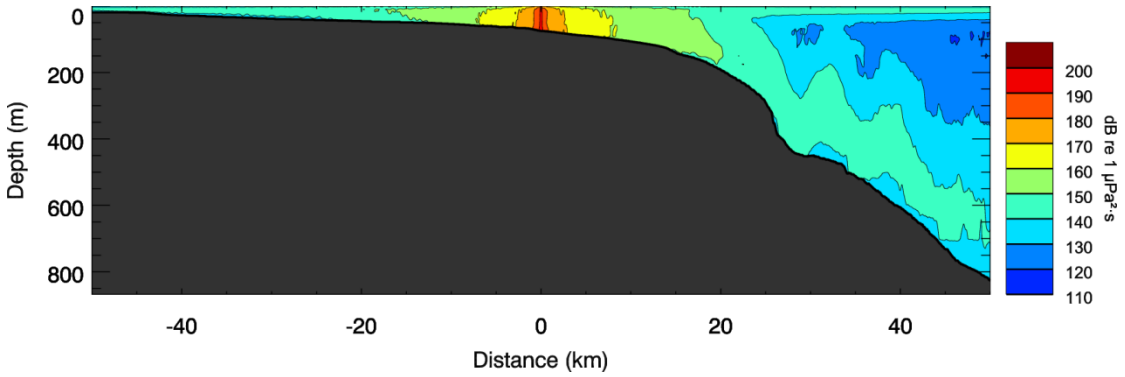

Figure 67. Shelf zone: The source when positioned at water column depth of 75 m: Received SEL acoustic field using Season 1 sound speed profile and median reflectivity geoacoustic parameters. Cross-slope direction.

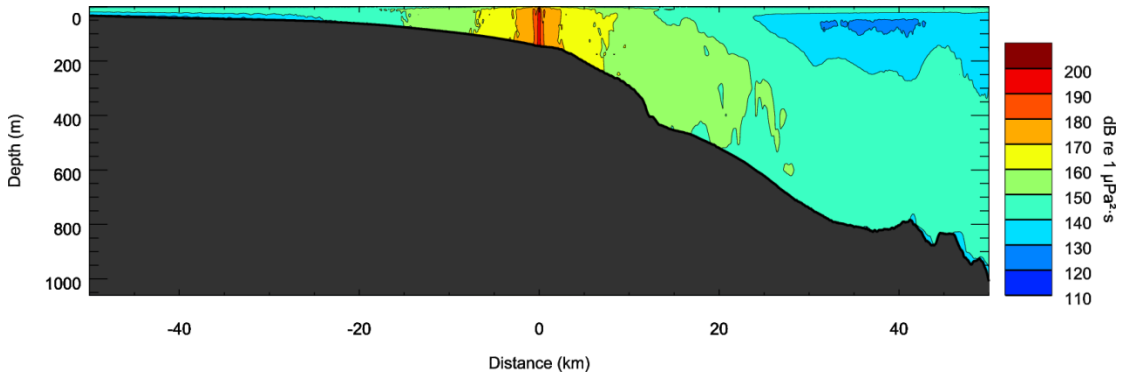

Figure 68. Shelf zone: The source when positioned at water column depth of 150 m: Received SEL acoustic field using Season 1 sound speed profile and median reflectivity geoacoustic parameters. Cross-slope direction.

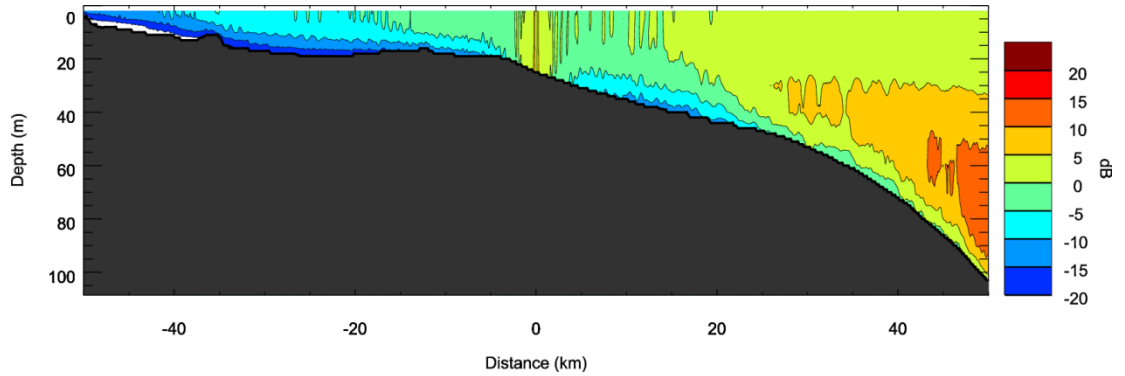

Figure 69. Shelf zone: Differential acoustic field for the source when positioned at water column depths of 25 and 75 m: Differential acoustic field due to variation of the water depth at the source. Cross-slope direction.

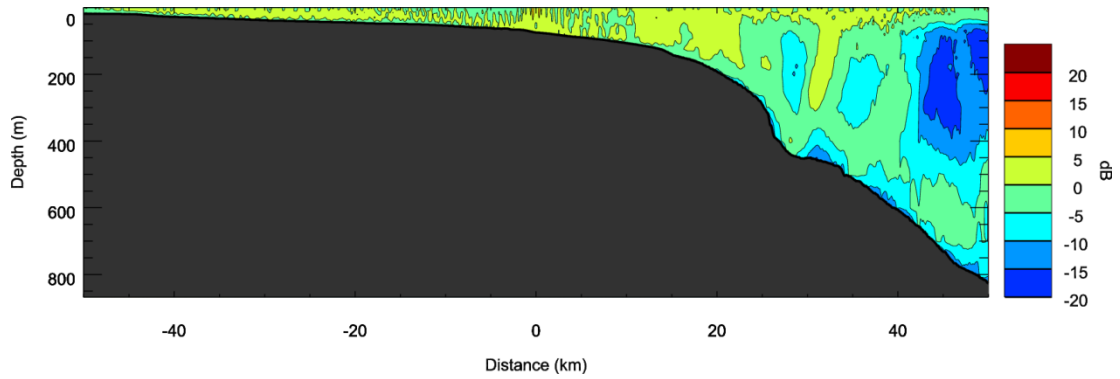

Figure 70. Shelf zone: Differential acoustic field for the source when positioned at water column depths of 75 and 150 m: Differential acoustic field due to variation of the water depth at the source. Cross-slope direction.

Slope zone: 300 m to 1500 m

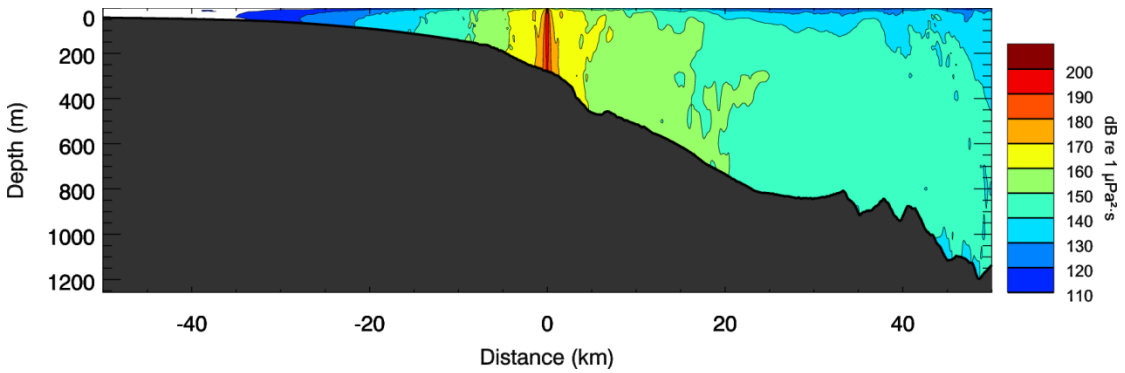

Figure 71. Slope zone: The source when positioned at water column depth of 300 m: Received SEL acoustic field using Season 1 sound speed profile and median reflectivity geoacoustic parameters. Cross-slope direction.

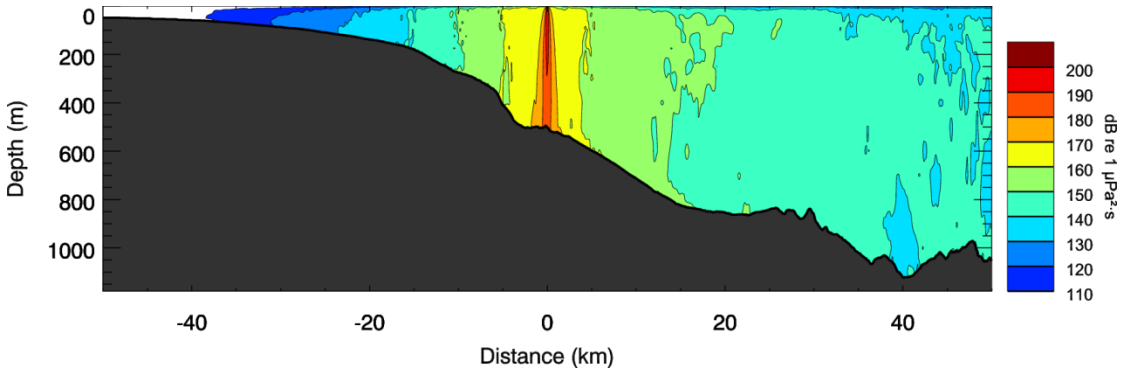

Figure 72. Slope zone: The source when positioned at water column depth of 500 m: Received SEL acoustic field using Season 1 sound speed profile and median reflectivity geoacoustic parameters. Cross-slope direction.

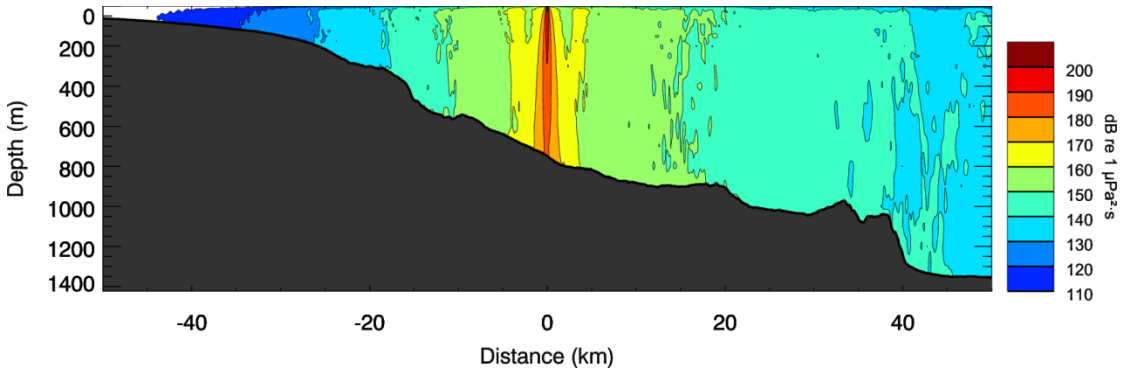

Figure 73. Slope zone: The source when positioned at water column depth of 750 m: Received SEL acoustic field using Season 1 sound speed profile and median reflectivity geoacoustic parameters. Cross-slope direction.

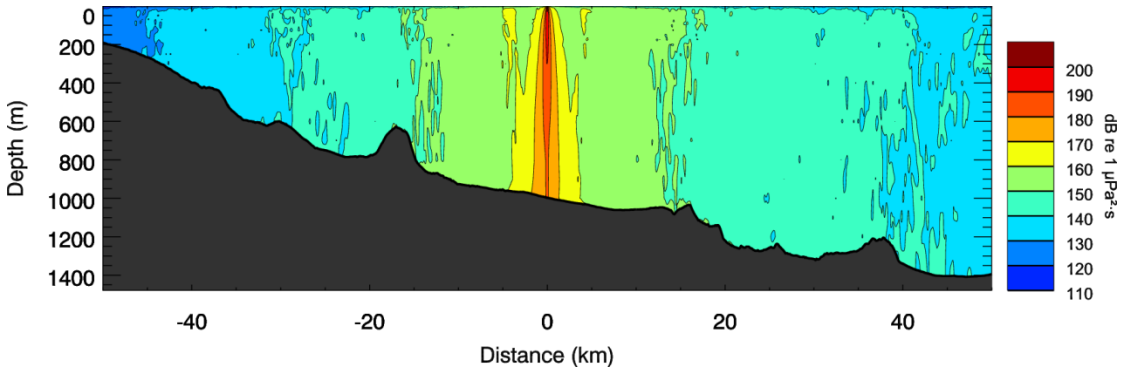

Figure 74. Slope zone: The source when positioned at water column depth of 1000 m: Received SEL acoustic field using Season 1 sound speed profile and median reflectivity geoacoustic parameters. Cross-slope direction.

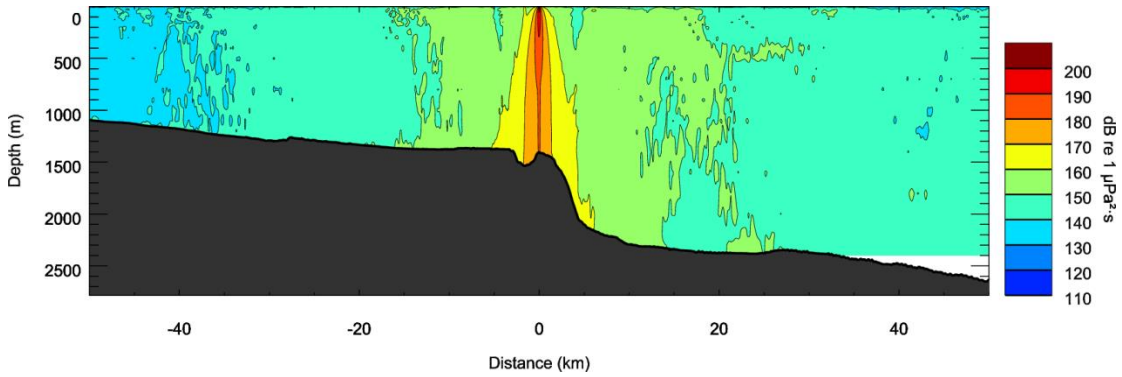

Figure 75. Slope zone: The source when positioned at water column depth of 1500 m: Received SEL acoustic field using Season 1 sound speed profile and median reflectivity geoacoustic parameters. Cross-slope direction.

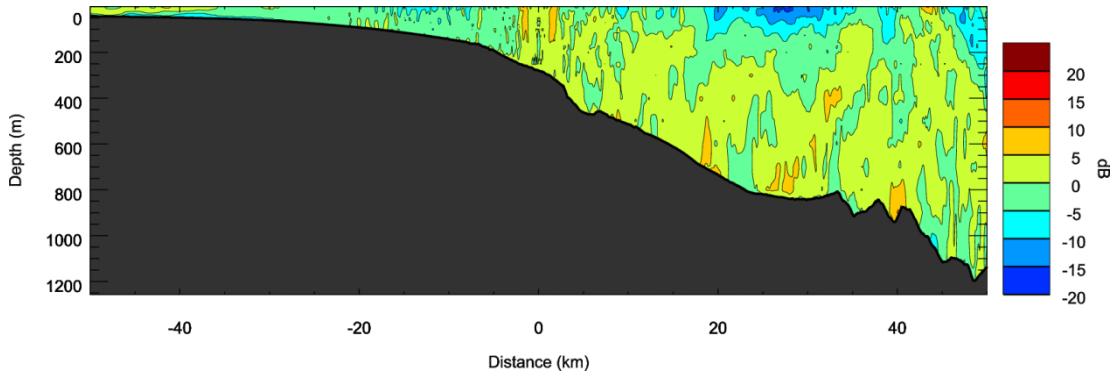

Figure 76. Slope zone: Differential acoustic field for the source when positioned at water column depths of 300 and 500 m. Cross-slope direction.

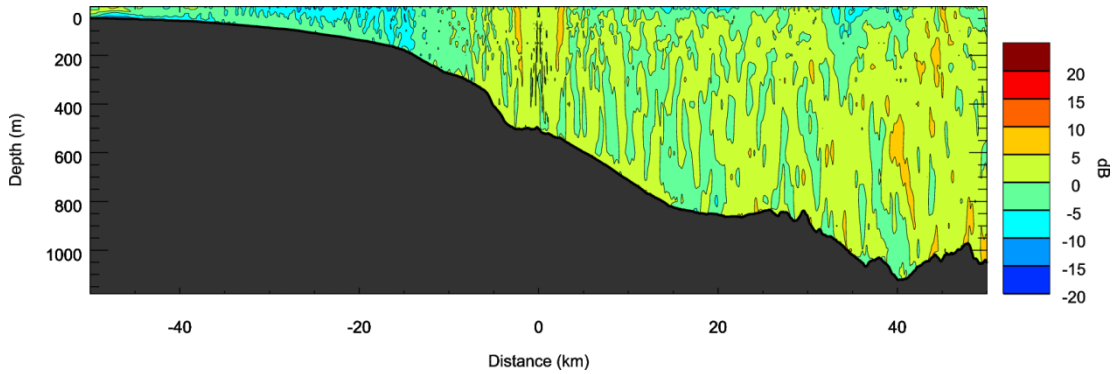

Figure 77. Slope zone: Differential acoustic field for the source when positioned at water column depths of 500 and 750 m. Cross-slope direction.

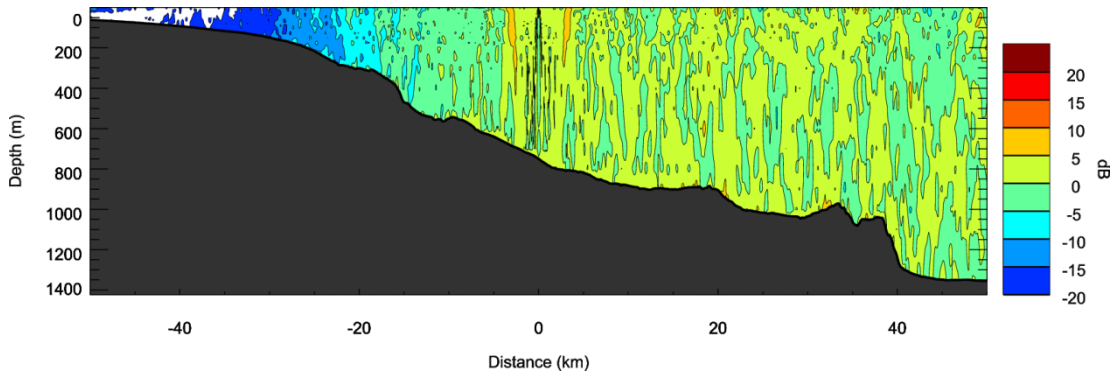

Figure 78. Slope zone: Differential acoustic field for the source when positioned at water column depths of 750 and 1000 m. Cross-slope direction.

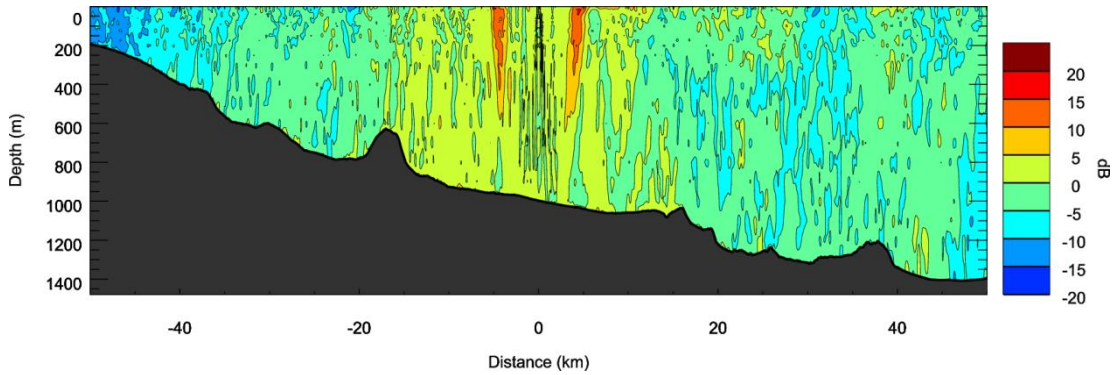

Figure 79. Slope zone: Differential acoustic field for the source when positioned at water column depths of 1000 and 1500 m. Cross-slope direction.

Deep zone: 2000 m to 2500 m

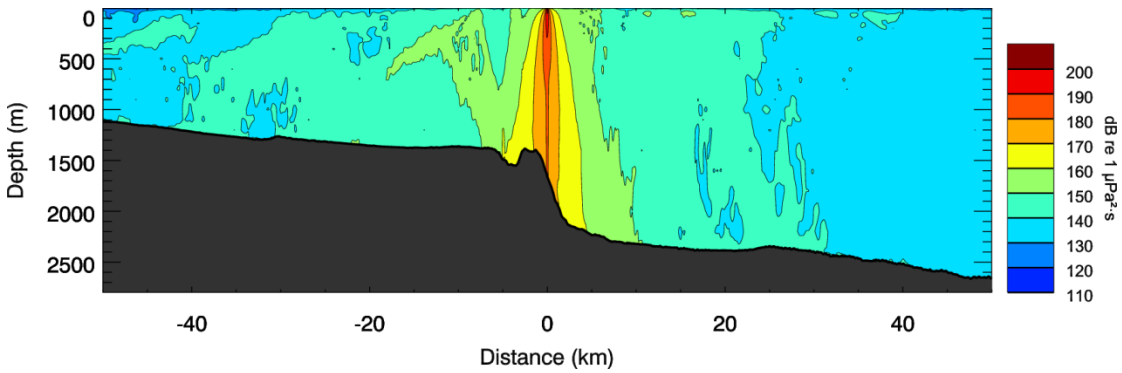

Figure 80. Deep zone: The source when positioned at water column depth of 2000 m: Received SEL acoustic field using Season 1 sound speed profile and median reflectivity geoacoustic parameters. Cross-slope direction.

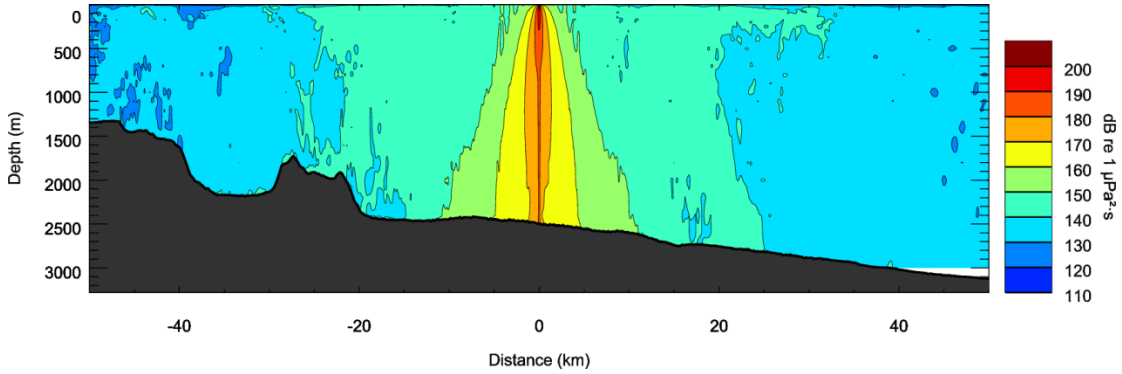

Figure 81. Deep zone: The source when positioned at water column depth of 2500 m: Received SEL acoustic field using Season 1 sound speed profile and median reflectivity geoacoustic parameters. Cross-slope direction.

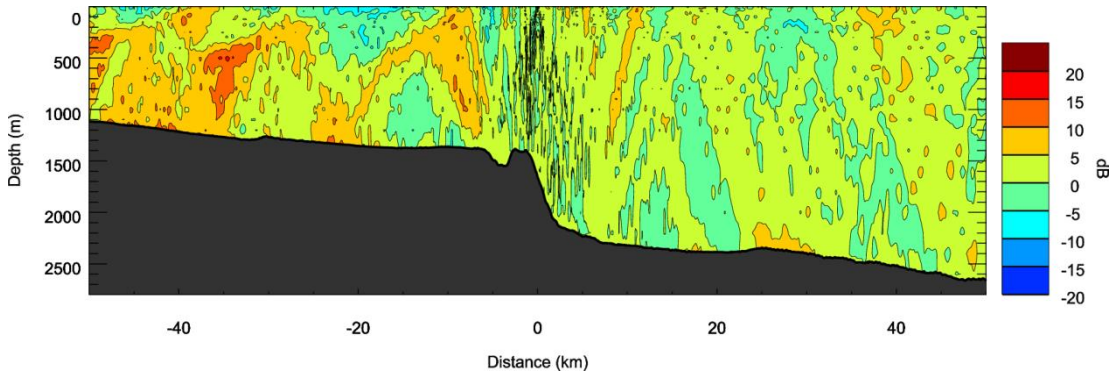

Figure 82. Deep zone: Differential acoustic field for the source when positioned at water column depths of 2000 and 2500 m Cross-slope direction.

For each scenario, the acoustic field was propagated in three directions: downslope, upslope, and along-slope. Two sites at adjacent water depths were compared. The average difference and standard deviation were calculated for a set of ranges from the source: 500, 1000, 2000, 5000, and 10,000 m. The received levels at the individual receivers within the selected ranges and the top 20 m were considered. The 20 m vertical extent was selected to emphasize the depths at which the animals spend much of their time. Table 35 provides the calculated average differences in the selected volume between the acoustic fields calculated for the adjacent sites.

Table 35. Acoustic field uncertainty due to variations in the water depth at the source. Median value and σ (number in brackets) are provided in dB for various averaging ranges from the source and direction of the propagation.

Range/ Direction	Shelf zone		Slope zone				Deep zone
	25–75 m	75–150 m	300–500 m	500–750 m	750–1000 m	1000–1500 m	2000–2500 m
500 m							
Downslope	3.8 (2.6)	3.6 (2.8)	1.2 (1.3)	0.6 (0.8)	0.4 (0.8)	0.1 (0.5)	0.3 (0.7)
Along slope	4.4 (4.1)	3.8 (4.5)	0.9 (1.7)	0.5 (1.3)	0.3 (1.1)	0.2 (0.8)	−0.0 (0.1)
Upslope	3.8 (2.9)	3.9 (3.1)	1.4 (1.3)	0.8 (1.0)	0.3 (0.7)	0.4 (0.9)	−0.1 (0.4)
1000 m							
Downslope	2.9 (2.2)	2.3 (2.6)	0.9 (1.3)	1.3 (1.0)	1.1 (1.1)	1.2 (1.4)	1.6 (1.9)
Along slope	3.4 (3.5)	3.0 (3.8)	0.6 (1.9)	0.8 (1.9)	0.8 (1.6)	0.6 (1.9)	0.3 (1.3)
Upslope	2.8 (2.5)	2.3 (2.9)	1.5 (1.3)	1.5 (1.2)	1.0 (1.1)	1.8 (1.8)	−0.1 (1.2)
2000 m							
Downslope	1.7 (2.2)	1.4 (2.2)	3.4 (3.3)	1.3 (1.0)	1.0 (1.0)	1.7 (1.8)	1.8 (3.2)
Along slope	2.4 (3.2)	1.9 (3.5)	4.2 (4.6)	0.9 (2.1)	0.6 (1.7)	0.8 (2.4)	−0.5 (2.2)
Upslope	1.7 (2.2)	1.0 (2.6)	3.7 (3.1)	1.5 (1.3)	1.0 (0.9)	2.3 (3.2)	1.0 (2.2)
5000 m							
Downslope	0.0 (2.2)	0.5 (2.0)	0.3 (3.8)	1.5 (2.7)	1.8 (2.4)	4.9 (5.2)	2.2 (3.3)
Along slope	1.0 (3.0)	0.8 (3.3)	2.1 (4.4)	2.9 (3.6)	2.8 (3.4)	3.5 (3.8)	1.0 (2.9)
Upslope	−0.8 (3.1)	−0.3 (2.2)	0.8 (3.5)	1.8 (2.4)	1.8 (2.7)	4.1 (5.0)	0.4 (4.0)
10000 m							
Downslope	−0.6 (1.9)	0.5 (1.7)	−1.2 (3.9)	−0.1 (2.8)	1.0 (2.2)	4.9 (4.2)	1.4 (3.6)
Along slope	−1.2 (3.8)	0.4 (3.5)	0.0 (4.2)	1.4 (3.8)	2.4 (3.6)	1.9 (5.4)	2.0 (4.3)
Upslope	−3.2 (4.3)	−0.6 (1.9)	−1.4 (3.8)	0.4 (2.6)	0.4 (2.5)	2.7 (4.2)	0.4 (4.6)

* 156 dB re 1 µPa rms SPL threshold was used for this scenario since 153 dB re 1 µPa rms SPL threshold was beyond 50 km modeled range.

6.5.2.1.9. Sea State

A smooth sea surface is a near-perfect reflector of sound waves incident from below. However, ocean waves at the sea surface, due to local winds or from distant weather disturbances, can scatter sound in a non-uniform way. The degree of scattering depends on the amplitude of the surface roughness (wave height and wave crest separation), the wavelength of the sound energy, and the angle at which the sound energy is incident onto the surface. In very rough seas, breaking waves can entrap air bubbles, blurring the actual position of the water-air interface. In general, scattering effects are small when the dimension of the surface roughness is small relative to the wavelength of the sound. Surface wave height is (typically) a function of wind speed, so higher frequency sounds are generally affected at lower wind speeds than lower frequency sounds. Sea-surface roughness generally has negligible effect on the propagation of sounds with frequencies < 50 Hz, where acoustic wavelengths are greater than 30 m. There can be a moderate effect on frequencies between 50 and 200 Hz, and a more significant effect on frequencies > 200 Hz in higher sea states. The additional coherent reflection losses at the air-sea interface due to the roughness of the boundary usually range from 0 to 2 dB per interaction and greatly depend on the grazing angle of the incoming wave (Long et al. 1989).

Scattered sound energy is not lost and does not reduce the total amount of acoustic energy in the water. Scattering, however, has the effect of randomizing the phase of reflected sounds, thereby blurring the

coherent interaction of reflected energy with sound that does not reflect. This results in a reduction of the strength of interference maxima and minima in the water column. The overall effect is to even out the otherwise more-variable spatial variations of sound levels in the water. In very rough conditions, when air is entrapped by breaking waves at the surface, high frequency sounds can be attenuated through absorption and high frequency levels can be reduced.

Surface roughness depends on weather conditions, duration of increased winds, proximity to land, and on distant sea state patterns. For the acoustic propagation modeling here, we assumed perfectly calm conditions and a flat air-sea interface. This scenario leads to near perfect acoustic reflections. Although such conditions are rarely observed exactly, it is an often realistic approximation. It should be noted, however, that propagation in sound speed profiles that cause surface sound channels can be quite strongly affected, as sound can be scattered out of the duct. In those cases, sound levels in the channel can be substantially reduced. In the absence of a surface sound channel, or when sea state is low or moderate, the effects will generally be small.

6.5.2.1.10. Summary of Acoustic Uncertainty

Uncertainties in the results of acoustic propagation modeling were estimated by examining the variation in model outputs when model inputs were offset by realistic errors. The environmental properties were selected so that the median, or expected, value could be compared to a worst-case outcome, which was generated by selecting extreme values for several input parameters. These comparisons represent the maximum errors in the predicted sound fields that result from incorrect specification of the parameters tested. Most of the comparisons were made at selected locations in the top 20 m of the water column, where marine mammals spend a substantial amount of time.

For uncertainty in the sound speed profile, a difference of > 10 dB between the median and worst-case scenarios was observed in the Shelf zone in both seasons (Table 30). The worst-case scenario for the December–March period exhibited a strong surface duct (30 m/s difference between speed at the surface and maximum speed) that trapped the acoustic energy and propagated it with lower transmission loss. A surface duct was present in the median sound speed profile for the same period, but the maximum difference in sound speed was only 5 m/s. The difference in the sound fields for the April–November season was primarily due to a difference in the negative gradient below the surface duct where the worst-case scenario sound speed profile was significantly less downward refracting. Surface ducts in the other zones were weaker, and variations in their sound speed profiles lead to less pronounced changes in sound propagation. The difference between the worst-case and median scenarios in the Slope and Deep zones was < 4.0 dB.

The greatest uncertainty due to geoacoustic parameters of the sea bottom is 4 dB, in the Deep zone (Table 34). The effect of the geoacoustic uncertainty increased when the sound speed profile was downwardly refracting. In the case of a surface channel (Slope zone, winter season), the average difference between the median and worst-case was only 0.5 dB, i.e., in this case the geoacoustic parameters had virtually no effect on the sound levels at the top of the water column. Because the interaction of sound waves with the ocean bottom is most important in downward refracting environments, the uncertainty in the sound speed profile and geoacoustic parameters are negatively correlated.

Unlike the geoacoustic parameters, bathymetry is better documented and, unlike the sound speed profile, it does not change with time. For seismic surveys with moving sources, however, it is not practical to model the acoustic field for every possible source position. The common practice is to model acoustic propagation in a limited number of source positions and to use these derived fields as representative of the source operating in similar bathymetric regions. With this approach, there is uncertainty in the acoustic fields due to the presence or absence of local bathymetric features. Local features of the sea bottom generally affect specific azimuths and/or ranges while differences in the water depth affect regions of the

sound field. The analysis of uncertainty due to bathymetry showed that uncertainty varies with range from the source and there is a dependence on the water depth—the greater the water depth, the greater the range at which the highest uncertainty occurs. Comparison of the two cases in the Shelf zone revealed an uncertainty of about 4.5 dB within 500 m from the source (Table 35). In the Deep zone, the highest uncertainty occurred 5–10 km from the source. On average, the received levels differed by about 1.6 dB between the source operating in 2500 m and 2000 m depths.

The weather-driven sea state also adds to the uncertainty in the acoustic field by changing the roughness at the air-sea interface. Scattering diminishes the extremes in the sound field, especially at higher frequencies. Sea-surface roughness negligibly affects the propagation of acoustic waves with frequencies < 50 Hz and moderately affects frequencies between 50 and 200 Hz, and can significantly affect higher frequency sounds. It is expected to have more effect when surface sound duct propagation is present. The acoustic propagation modeling assumed a flat air-sea interface, and because the airgun array was a low-frequency source minimally affected by sea state, little uncertainty was expected due to sea state changes.

Uncertainties in the acoustic field discussed here represent a multi-dimensional envelope that can be wrapped around the main modeling results. This envelope is meant to enclose the modeled acoustic field and the real world acoustic field. The uncertainties in the different dimensions of this envelope (sound speed profile, geoacoustics, bathymetry, and sea state) cannot be summed to yield a "total" uncertainty as this would be a meaningless quantity. The overall uncertainty is measured for the volume of the multi-dimensional uncertainty envelope, but this is a difficult concept to use in operational planning. The best way to visualize the overall uncertainty is in terms of the different dimensions of the uncertainty envelope, as discussed above.

6.5.2.2. Animal Modeling Uncertainty

The exact location, behavioral, and motivational state of animals during an operation are not known and, as such, are the main sources of uncertainty in this modeling project. Those uncertainties are best addressed with animal movement simulations and Monte Carlo sampling which combines simulated animal movement from the Marine Mammal Movement and Behavior Model (3MB, Houser 2006) with the modeled sound fields of geotechnical and geophysical operation. Each simulated animal (animat) acts as a receiver and samples the sound field in a way real animals are expected to experience the sound field. With multiple animats sampling the sound field (Monte Carlo sampling), the distribution of received levels for the operation can be estimated as a probability of exposure. Exposure estimates can then be calculated from the exposure probability.

6.5.2.2.1. Animal Movement Parameters Uncertainty

The movement parameters for 3MB are based on a two level process—a) preselected behavioral states and their temporal variation provide a framework for animat movements that b) follow a preselected stochastic processes for movement within the selected behavior states. The user-chosen parameters and preselected movement processes determine how simulated members of each species (animats) sample the sound fields. Uncertainty about the underlying motivation for any animal's location choice means there is uncertainty in the parameters chosen for the model, and consequently uncertainty in the sampled received levels. Because there are many variables and a large range of possible parameter values, and oftentimes there are few data to support the model parameter values chosen, the uncertainty level can be high. It is impractical to conduct a parametric sensitivity analysis (as was done for Acoustic Modeling Uncertainty), but the results from the six Test Case species (Section 6.3 and see Table 14 for species) can be compared. Because each species has distinct parameters that govern their movements, we were able to qualitatively compare how the different behavioral parameters might affect exposure estimates.

6.5.2.2.2. Summary of Animal Movement Parameter Uncertainty

Animal movement is simulated using an animal movement model, such as the 3MB (Houser 2006), and combined with the modeled sound fields of an operation. The 3MB incorporated many parameters to produce realistic animal movement. Each parameter could affect the estimated exposure levels independently or in association with each other. The results of the different modeled species are compared, giving a semi-quantitative indication of how different animal movement types affect exposure.

The primary differences in the modeled exposure estimates among species are due to differences in animal acoustic sensitivity (Tables 14–15):

- Beaked whales have lower behavioral response thresholds than other species
- High-frequency dwarf sperm whales have lower injury thresholds than other species
- There is a larger range for potential injury due to accumulated energy for low-frequency species relative to the other species because of the weighting functions used; the low-frequency weighting function admits more acoustic energy from the low-frequency airgun source to propagate.

When the same filtering and thresholds were applied, comparisons between animals resulted in similar exposure estimates. The exposure estimates for potential injury and exposure estimates for potential behavioral disruption for common bottlenose dolphins, short-finned pilot whales, and, to some extent sperm whales, were similar. For sperm whales, however, there was a marked difference in modeled exposure estimates between Survey sites A and B. This was due to a behavioral depth restriction for this species—sperm whales usually occur in water deeper than 1000 m. Because much of the survey area at Survey site A was shallower than 1000 m, few animats were near the source and the exposure levels were low through much of the modeling. Sperm whales also showed greater potential of behavioral response to noise exposure than other species with the same auditory thresholds. Sperm whales are deep divers; in this downward refracting environment they appear to be consistently exposed relative to the shallow divers such as Cuvier's beaked whales, also a deep diving species, but with lower behavioral thresholds.

Related to animal location and movement, but not currently captured by our animal movement modeling, are behavioral aspects that could increase uncertainty. Factors that affect the motivation of animals to remain at a certain location or to leave that location include the presence of prey and predators, which influence density. Another potential uncertainty is the socio-ecological need of animals to aggregate in groups. The sections below detail the effects of animal density and social group size on exposure estimates.

6.5.2.2.3. Animal Density Estimates Uncertainty

The Monte Carlo simulations are run using a fixed animat density. Real-world animal density estimates are used to adjust the modeled (animat) exposure estimates to get real-world exposure estimates. Real-world density estimates are, very likely, the second largest source of uncertainty in the modeling project. Density estimates come from visual surveys (aerial and shipboard) and acoustic surveys. They are expensive, time consuming, and typically only examine small portions of populations for short times and often miss longer term and seasonal distribution patterns The best available data currently are from the U.S. Navy OPAREA Density Estimate (NODE) for the Gulf of Mexico (Department of the Navy 2007). For one region, the density estimates include minimum, maximum, mean, and standard deviation per area, e.g., km^2, assuming animals are normally, if not uniformly, distributed across the region. We often incorporated the uncertainty into the density estimates by reporting the impacts for the minimum, maximum, and mean density estimates, which bracket the range of expected impacts. We also used a resampling technique (bootstrap resampling) to estimate exposures with sample sizes scaled for the real-world density estimate.

6.5.2.2.4. Animal Density Estimates Uncertainty Results

Estimates for the number of animats exposed to levels exceeding injury and behavioral response thresholds were determined in the 3-D WAZ survey of the Test Case (Section 6.3.2, Tables 14–15). Real-world exposure estimates were also determined and presented in the Test Case report (Tables 16–17). The real-world exposure estimates were obtained using the real-world density estimates (Table 36), which were used to adjust the modeled exposure estimates (Tables 14–15) to get the real-world exposure estimates (Tables 16–17).

Table 36. Real-world density estimates for summer at Survey sites A and B.

Modeled marine mammal species	Survey site A				Survey site B			
	Min	Max	Mean	σ	Min	Max	Mean	σ
Bryde's whales	0	0.000105	0.000081	0.000044	0	0.000105	0.000097	0.000029
Cuvier's beaked whales	0.000003	0.004121	0.000676	0.000918	0	0.004121	0.000809	0.00092
Common bottlenose dolphins	0	0.2905	0.02181	0.027384	0	0.09859	0.003227	0.007823
Short-finned pilot whales	0	0.006277	0.004845	0.002657	0	0.006277	0.005785	0.001704
Sperm whales	0.000036	0.008154	0.002761	0.001859	0.000365	0.005395	0.002311	0.001496
Dwarf sperm whales	0	0.004605	0.000673	0.000912	0.000002	0.01558	0.001589	0.002174

min=minimum; max=maximum; σ=standard deviation

Bootstrap resampling

Bootstrap resampling is a random re-sampling (with replacement) technique used to quantify distribution accuracy for a sample estimate (e.g., Whitlock and Schluter 2009). Bootstrap resampling was used in this project to quantify the distribution accuracy of exposure probabilities and real-world exposure estimates (the number of animals above threshold) obtained from the Monte Carlo simulations of the six Test Case species. The exposure probabilities were the received-level frequency of occurrence, which were expressed as histograms (Figure 83A). The exposure probability histograms were randomly resampled, with replacement, and the number of animats exposed to levels above threshold was found (as the sample estimate). This process was repeated many times to get an expected distribution of animats with exposures above threshold. One sample drawn from the exposure probability is one bootstrap sample, one group of samples drawn from the exposure probability to represent a sample population is a bootstrap replicate.

For example, there were 16,000 Bryde's whale animats in the simulation, to maintain the same density throughout the resampling process 16,000 bootstrap samples could be taken as one bootstrap replicate, and 10,000 bootstrap replicates (of 16,000 samples each) obtained and the sample estimate calculated for each replicate. The sample estimate distribution is the distribution of animats exposed to levels above threshold for the bootstrap replicates (Figure 83B). Without resampling, there were 534 simulated Bryde's whales at Survey site A with received levels above SEL 187 dB re 1 $\mu Pa^2 \cdot s$ (Table 14). Resampling obtained the range of animats above threshold and their probability of occurrence. In Figure 83B, the mean number of animats above threshold for the bootstrap replicates was also ~ 534, with a 5% likelihood of getting 495 or less animats and a 95% likelihood of 573 or less animats. There was 90% chance that the number of animats above threshold was between 496 and 573.

Without bootstrap resampling, the number of animats exposed to levels above threshold (Tables 14 and 15) was adjusted by the real-world density (Table 36) to calculate the number of animals expected to be exposed to levels exceeding threshold (Tables 16 and 17). For Bryde's whales at Survey site A, adjusting the 534 animats above threshold by the mean density estimate of 0.000081 resulted in 0.02 animals with above threshold exposures. When the minimum and maximum density estimates were used, the number of animals above threshold was < 0.01 and 0.03, respectively. With bootstrap resampling, changing the number of bootstrap samples in the bootstrap replicate is equivalent to changing the modeling density. To incorporate the uncertainty in the density estimates (standard deviation), the number of bootstrap samples in the bootstrap replicate was scaled by the ratio of the real-world density (± standard deviation) to the modeled density. The resulting distribution of real-world Bryde's whales exposed to sound levels above threshold after resampling had a mean value of 0.0195, with a 98% likelihood of no animals above threshold, a 99.8% likelihood of 1 animal or less above threshold, and a maximum of 2 animals above threshold (Figure 83C). Note that the mean values with or without bootstrap resampling were about the same at 0.02 animals receiving levels above threshold and the range was also comparable, but the resampling procedure provided a more complete description of the sample estimate distribution. Similar to the Bryde's whales, the number of dwarf sperm whale animats exposed to levels above SEL injury threshold without resampling was 1053 at Survey site A and the real-world exposure estimate was 0.35 animals. After bootstrap resampling was applied to the modeled animat exposure probability distribution and after the sample size for each bootstrap replicate was adjusted to reflect real-world animal density, the distribution of animals exposed to levels above threshold had a mean of 0.4019 with 71% of samples with no animals exposures above threshold. The number of animals receiving levels above threshold increased to 2 when 97.6% of replicates were considered while up to 7 animals could be exposed to levels above threshold when 99.5% of replicates were considered (Figure 83D). The remaining species (Cuvier's beaked whales, common bottlenose dolphins, short-finned pilot whales, and sperm whales) either had 1 or no animats receiving levels above SEL injury threshold, so the sample distribution was essentially zero mean with zero variance (not shown).

The same approach was used to obtain a distribution for potential behavioral responses. Figure 83E and F, show the real world behavioral disruption exposure estimate distributions for Bryde's whales and dwarf sperm whales. For Bryde's whales, the mean value matched the adjusted exposure estimate of 0.59 animals (Table 16) and distribution includes 60% of bootstrap samples with zero animals exposed to levels above threshold, 95% of samples with 2 or fewer animals, and a maximum of 5 animals. For dwarf sperm whales, the mean number of animals with a potential behavioral response was 3.5 (close to the exposure estimate without resampling of 3.03 in Table 16); 30% of bootstrap samples showed no animals with a behavioral response, 50% showed 3 or fewer animals, 95% showed 10 or fewer, and the maximum was 20 animals exhibiting a behavioral response. For the remaining Test Case species, Figure 84 shows the resampled behavioral disruption exposure estimates and resampled exposure estimates adjusted for real-world densities. All means matched the (unadjusted) modeled exposure estimates (Table 14) within ~ 2%. The means of the bootstrap resampled exposure estimates with bootstrap sample size were also close to the adjusted exposure estimate values (Table 16) for short-finned pilot whales and sperm whales, but were high for common bottlenose dolphins (120 versus 67) and Cuvier's beaked whales (27 versus 23 animals). Common bottlenose dolphins and Cuvier's beaked whales had larger standard deviation of the density estimate than the mean density estimate. The ranges of exposure estimates with resampling for the species also matched the adjusted exposure estimates (maximum density in Table 16) reasonably well.

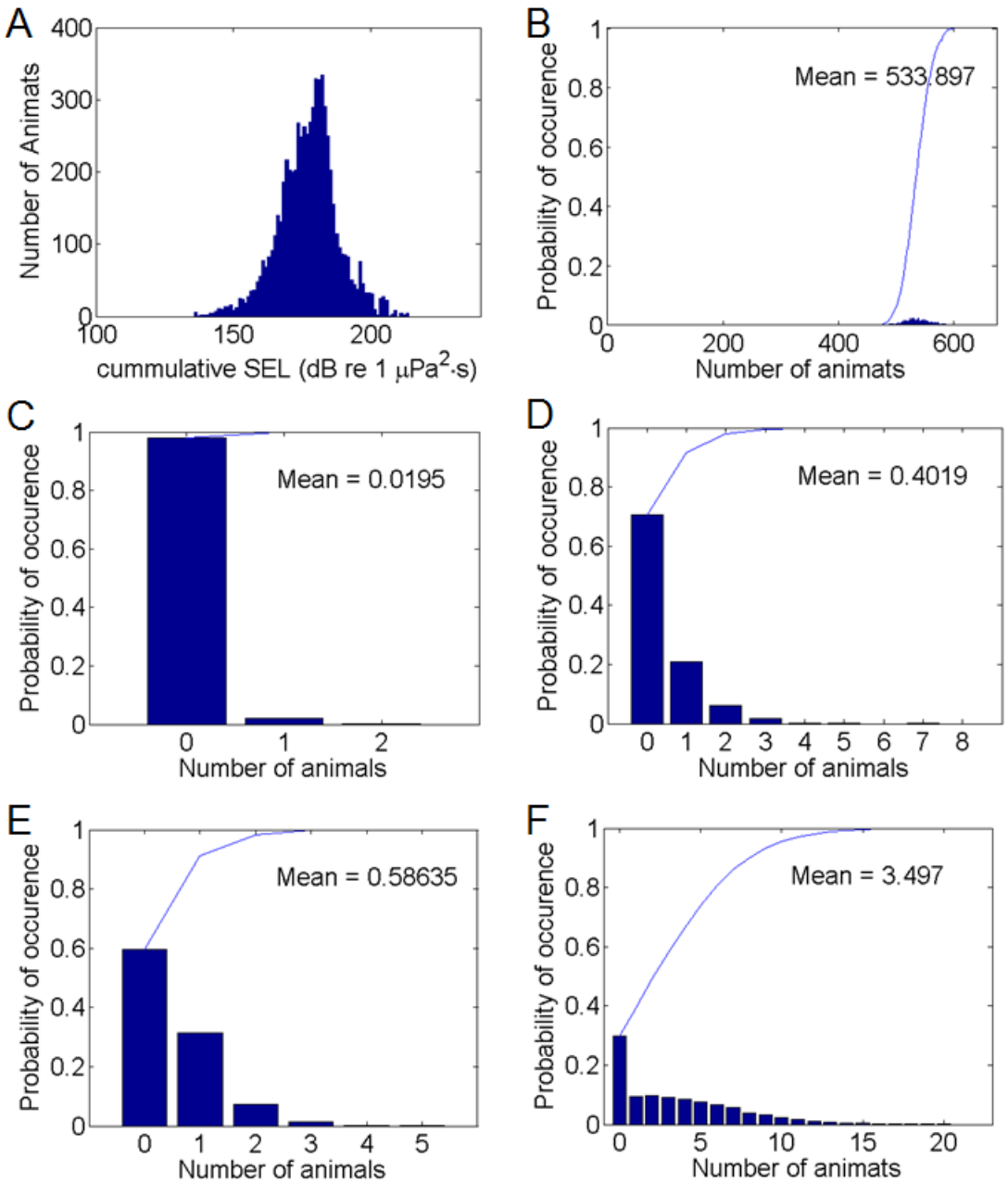

Figure 83. Bootstrap resampling and SEL injury and behavioral response exposure estimation for Bryde's whales and dwarf sperm whales. A) Exposure probability for Bryde's whales from modeling expressed as a histogram, B) Estimated number of Bryde's whale animats (modeled exposures) above SEL 187 dB re 1 μPa$^{2\cdot}$s using bootstrap resampling (10,000 bootstrap replicates, where each bootstrap replicate consisted of an equal number of bootstrap samples as the number of animats in simulation), and C) Estimated number Bryde's whales (real-world exposures) above 187 dB SEL (re 1 μPa$^{2\cdot}$s) using bootstrap resampling with sample size adjusted for real-world mean ± standard deviation density estimate (10,000 bootstrap replicates, where the number of bootstrap samples in the replicate was scaled for the real-world density; in this case, the number of animats in simulation × 0.0000405 ± 0.000022). D) Estimated number of dwarf sperm whales (real-world exposures) above SEL 161 dB re 1 μPa$^{2\cdot}$s using bootstrap resampling with bootstrap sample size adjusted for real-world mean ± standard deviation density estimate (10,000 bootstrap replicates). E) and F) Behavioral

disruption exposure estimate distribution for Bryde's and dwarf sperm whales, respectively (10,000 bootstrap replicates with number of bootstrap samples adjusted for real-world density). Blue line shows cumulative probability in each plot.

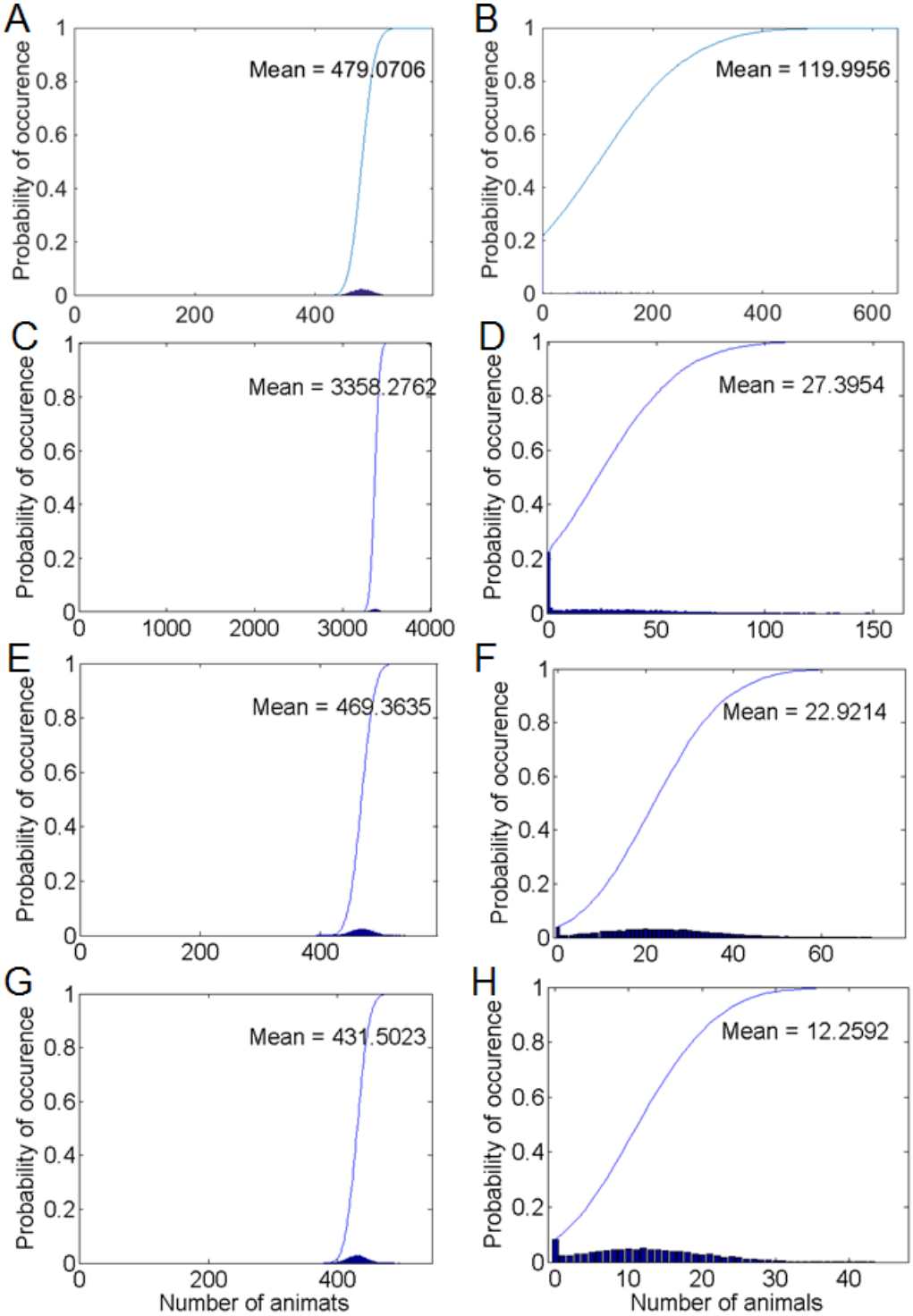

Figure 84. Bootstrap resampled behavioral disruption exposure estimate distribution for modeled results and adjusted for real-world density estimate mean ± standard deviation at Survey site A, A) model results and B) real-world exposure estimates for common bottlenose dolphins; C)

model results and D) real-world exposure estimates for Cuvier's beaked whales; E) model results and F) real-world exposure estimates for short-finned pilot whales; and G) model results and H) real-world exposure estimates for sperm whales. 10,000 bootstrap replicates were obtained with the number of bootstrap samples scaled for real-world density. Blue line shows the cumulative probability in each plot.

6.5.2.2.5. Summary of Animal Density Estimate Uncertainty

The 3MB was run using animat densities (animats/km^2) that are typically much higher than in the real-world densities. Higher modeling densities were used so the sound field of an operation could be thoroughly sampled and provide a good estimate of exposure probability.

To determine the expected number of real-world animals affected by an operation, the model results had to be adjusted by the real-world animal density estimates. There is uncertainty in the real-world density estimates, which can be quantified and presented as minimums, maximums, means, and standard deviations. As a way of bounding the range of potential impacts, the expected number of animals exposed to levels exceeding threshold can be determined for the minimum, maximum, and mean real-world density estimates. This method is most often used when presenting exposure estimates, i.e., the expected number of Level A or Level B exposures (see results in Section 6.3.2).

Another method that can be used to incorporate the uncertainty of real-world density estimates into exposure estimates is to use a resampling technique and include the mean and standard deviation of the real-world density estimate during the resampling process. We used a bootstrapping method (see Section 6.5.2.2.3) to resample the exposure probability distribution; the length of the bootstrap sample was adjusted by the mean and standard deviation of the real-world density estimate. The result of this bootstrap resampling was an exposure estimate distribution based on the number of potential real-world animals affected. Unlike the bracketing method, incorporating real-world density estimate standard deviation into the resampling process quantifies the probability of exposures as a range of potential exposures reflecting the variance of the density estimates. The mean value of the distribution essentially remains the same as the number of exposures calculated using the mean density estimate when bounding is used, but additional information is available in the shape of the distribution. The shape of the distribution could help evaluate the risk an operation poses. Knowing the likelihood that no animals will be exposed to levels exceeding threshold during an operation, or the number of animals exposed to levels exceeding threshold in 95% of the cases, gives a fuller picture of the risk due to the operation.

To illustrate how this information helps us better understand risk, consider the Bryde's whales for the 3-D WAZ survey at Survey site A, for which the real-world mean number of animals above the injury threshold (Level A exposure) was 0.0195. There is a 98% likelihood that none of these animals would exceed threshold during the operation, a 99.8% likelihood that one or no animal exceeds threshold, and no more than two animals above threshold (Figure 83C). For dwarf sperm whales, the real-world mean number of animals above the injury threshold was 0.4019 with a 71% likelihood that no animals would be above threshold, a 97.6% likelihood that two or fewer animals would be above threshold, and a 99.5% likelihood that seven or fewer animals would exceed threshold (Figure 83D).When incorporating the variability of the density estimates into the exposure estimate, we assumed that the uncertainty ascribed to the density estimates (i.e., minimum, maximum, mean, and standard deviation) reflects the real-world uncertainty in the density estimate for each of the modeled locations. In other words, we did not consider potential errors in the density estimates that were not captured by their own uncertainty estimates.

6.5.2.2.6. Impact of Social Group Size on Exposure Estimates

Many animals form temporary or permanent social groups. When animals move in groups, the likelihood of their exposure within the sample region decreases, but the effect when exposure occurs increases

proportionally with group size. Group size can affect how impacts should be interpreted, but this has not yet been quantified.

6.5.2.2.7. Impact of Social Group Size on Exposure Estimates: Methods

Bootstrap resampling was used to determine the distribution of exposure estimates assuming animats were in groups of animals, instead of a single animal. Group sizes might be large and disperse, but to more simply illustrate the effects of group sizes on exposure estimates, all members of a potential group were assumed to have the same received levels.

Table 37. Published (social) group size statistics for Test Case species. The comments column describes how we used the source information to determine the mean group sizes suitable for post-process modeling.

Mean	SE	Range	Reference and area	Comments
Common bottlenose dolphins				
21	2	1–154	Maze-Foley and Mullin (2006) Gulf of Mexico	NOAA separates Gulf animals into three ecotypes: inshore animals inhabiting bays and estuaries, coastal types mainly found on the shelf, and offshore types found on the shelf and upper slope (Waring et al. 2013). The three ecotypes support varying group sizes. Mean group sizes reported by Maze-Foley and Mullin (2006) likely include all three ecotypes. Toth et al. (2012) reported mean group size for coastal and offshore ecotypes in the Atlantic. Maximum value reported by Shane et al. (1986) represents offshore types off South Africa. Variations in observed group size are mainly due to whether the group was a feeding aggregate or if the group was traveling, etc. Deeper water groups are generally larger sizes.
42		31–53	Toth et al. (2012) Atlantic	
1000 (max.)			Shane et al. (1986) South Africa	
Cuvier's beaked whales				
2	< 1	1–4	Maze-Foley and Mullin (2006) Gulf of Mexico	The similar group sizes encountered around the Hawaiian Islands and in the Gulf would indicate these are typical group sizes for the species.
3	2	1–5	McSweeney et al. (2007) Hawaii	
Sperm whales				
12		3–24	Christal et al. (1998) Galapagos	Results from Maze-Foley and Mullin (2006) and Richter et al. (2008) were generated from some of the same survey data, but Richter et al. included newer survey data and used different detection probability method. Congruence of group sizes reported by Christal et al. (1998) in the Pacific and by Richter et al. (2008) in the Gulf indicates typical group size is ~ 11–15 animals. The higher mean in the Gulf data includes surveys performed in a year with unusual oceanographic conditions. These Gulf groups primarily consist of females, calves, and sub-adult males. Adult males temporarily joined groups. Stable female groups are based on long-term associations between individuals (Christal et al. 1998).
3	< 1	1–11	Maze-Foley and Mullin (2006) Gulf of Mexico	
11 or 15	3		Richter et al. (2008) Gulf of Mexico	
20			Whitehead and Arnbom (1987) Pacific	

Mean	SE	Range	Reference and area	Comments
Dwarf sperm whales				
2		1–10	Baird (2005) Hawaii	Groups around the Hawaiian Islands and in the Gulf are similar in size, which indicates these group sizes are likely typical for the species.
2	< 1	1–8	Maze-Foley and Mullin (2006) Gulf of Mexico	
Short-finned pilot whales				
31		14–52	Kasuya and Marsh (1984) Pacific	The different methods of assessment are the likely reason reported group sizes vary considerably. Kasuya and Marsh (1984) captured animals during whaling operations. (Heimlich-Boran 1993) used long-term photo-identification of social groups. Mullin and Fulling (2004) and Maze-Foley and Mullin (2006) used ship surveys.
12–16		2–33	Heimlich-Boran (1993) Canary Islands	
34			Mullin and Fulling (2004) Gulf of Mexico	
25	4	3–85	Maze-Foley and Mullin (2006) Gulf of Mexico	
Bryde's whales				
1		1–15	Tershy (1992) Gulf of California	More than 90% of the time Tershy (1992) encountered whales, they were alone. Given the similarity of the reported means in these references, we assumed a typical group size of two animals.
2			Barlow (2006) Hawaii	
2	<1	1–5	Maze-Foley and Mullin (2006) Gulf of Mexico	

SE = standard error

6.5.2.2.8. Impact of Social Group Size on Exposure Estimates: Results

For the species whose group size mean or median is similar across different regions and for which the measured variance or range was relatively small—such as Cuvier's beaked whales, dwarf sperm whales, and Bryde's whales—the reported mean or median and estimated standard deviation were used during the bootstrap resampling processing. For species with a much larger group size range, and for which normality of the size distribution could not be tested, the highest reported mean was used and a standard deviation was estimated from the range of reported group sizes. The social group sizes used to evaluate the effects of group size on the distribution of exposure estimates are shown in Table 38.

Table 38. Social group size (number of individuals ± standard deviation) used to evaluate effects on exposure estimates.

Species	Group size
Bryde's whales	2 ± 1
Cuvier's beaked whales	3 ± 1.5
Common bottlenose dolphins	42 ± 6
Short-finned pilot whales	34 ± 10
Sperm whales	15 ± 3
Dwarf sperm whales	2 ± 1

During bootstrap resampling, each animat was considered to be a group of animals with the species-specific group size listed in Table 38. In the Bryde's whales simulation at Survey site A, there were 534 animats exposed to SEL above 192 dB re 1 $\mu Pa^2 \cdot s$ and 727.3 animats predicted to incur a behavioral response (Table 14). Figure 84A and B show that after bootstrap resampling was applied to the modeled animat exposure probability distribution and social group size was included, the sample estimate distribution of animats above threshold had a mean of 535 and 732, respectively for SEL injury and behavior (nearly the same as predicted in Table 14), but ~ 50% of the bootstrap samples had no animats above exposure threshold. In addition, the potential number of animats above threshold was much greater than the mean value; 95% of bootstrap samples had 1752 and 2326 (or less) animats above threshold with maximum estimates of 3134 and 3646 animats above threshold for injury and behavior, respectively. The results were very similar for dwarf sperm whales, where the mean exposure estimates after resampling are 1058 and 442 (Figure 85C and D) versus 1053 and 451 (Table 14) for injury and behavior.

The social group size used for both Bryde's whales and dwarf sperm whales was 2 ± 1 animals. The effects of group size on the distribution of behavioral disruption exposure estimates for species with larger groups was even more pronounced. Nearly 98% of bootstrap samples indicate no animals with a behavioral response for common bottlenose dolphins (Figure 86A), 97% for short-finned pilot whales (Figure 86C), and 95% for sperm whales (Figure 86D), and in each case the number of potential animals impacted was much greater than the mean value.

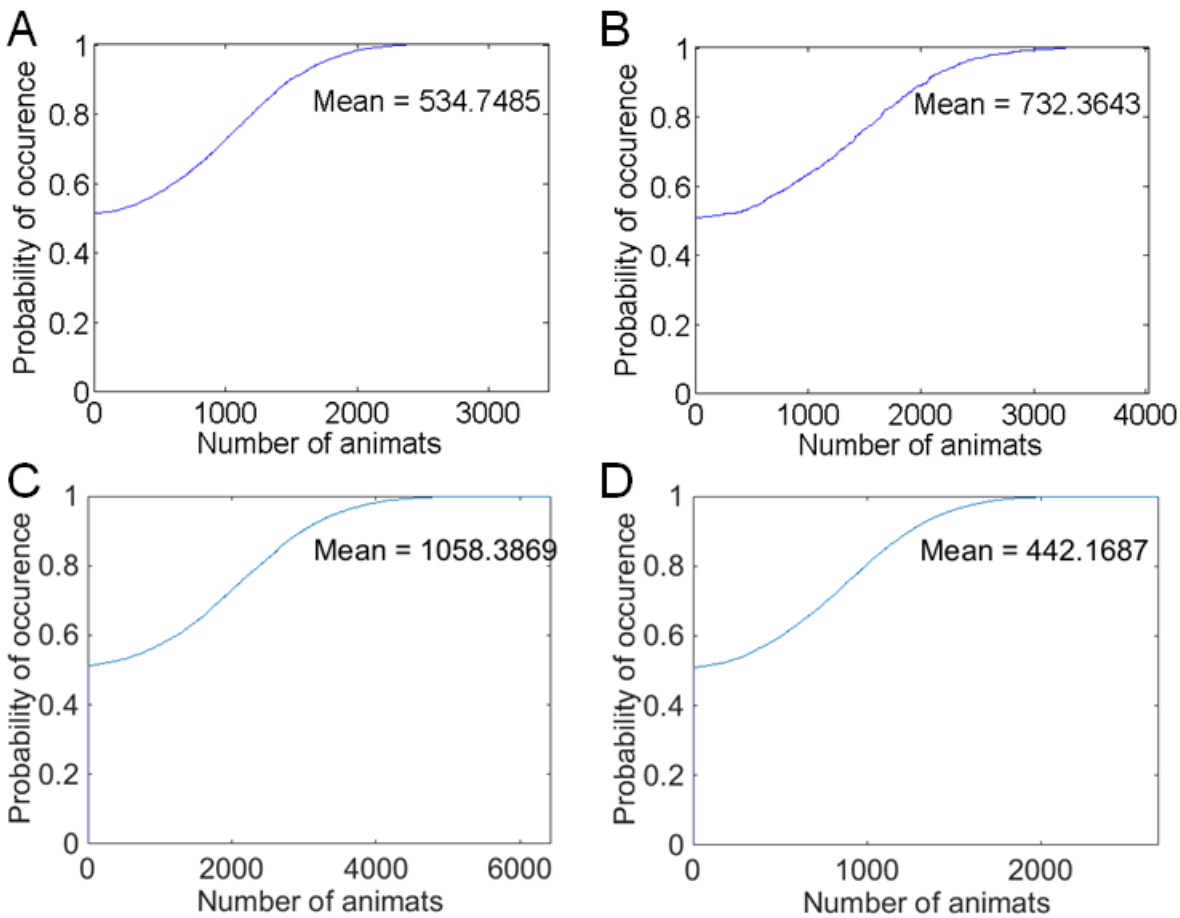

Figure 85. SEL Injury and behavioral disruption exposure estimate distributions for Bryde's whales and dwarf sperm whales at Survey site A. A) SEL injury SEL exposure estimate distribution for Bryde's whales. B) Behavioral response exposure estimate distribution for Bryde's whales. C) SEL injury exposure estimate distribution for dwarf sperm whales. D) Behavioral disruption exposure estimate for dwarf sperm whales. All exposure estimate distribution were determined with 10,000 bootstrap samples, each bootstrap sample size was equal to the total number of animats in the simulation, and each animat was treated as a social group of size 2 ± 1 animals (Table 38). Blue line shows the cumulative probability in each plot.

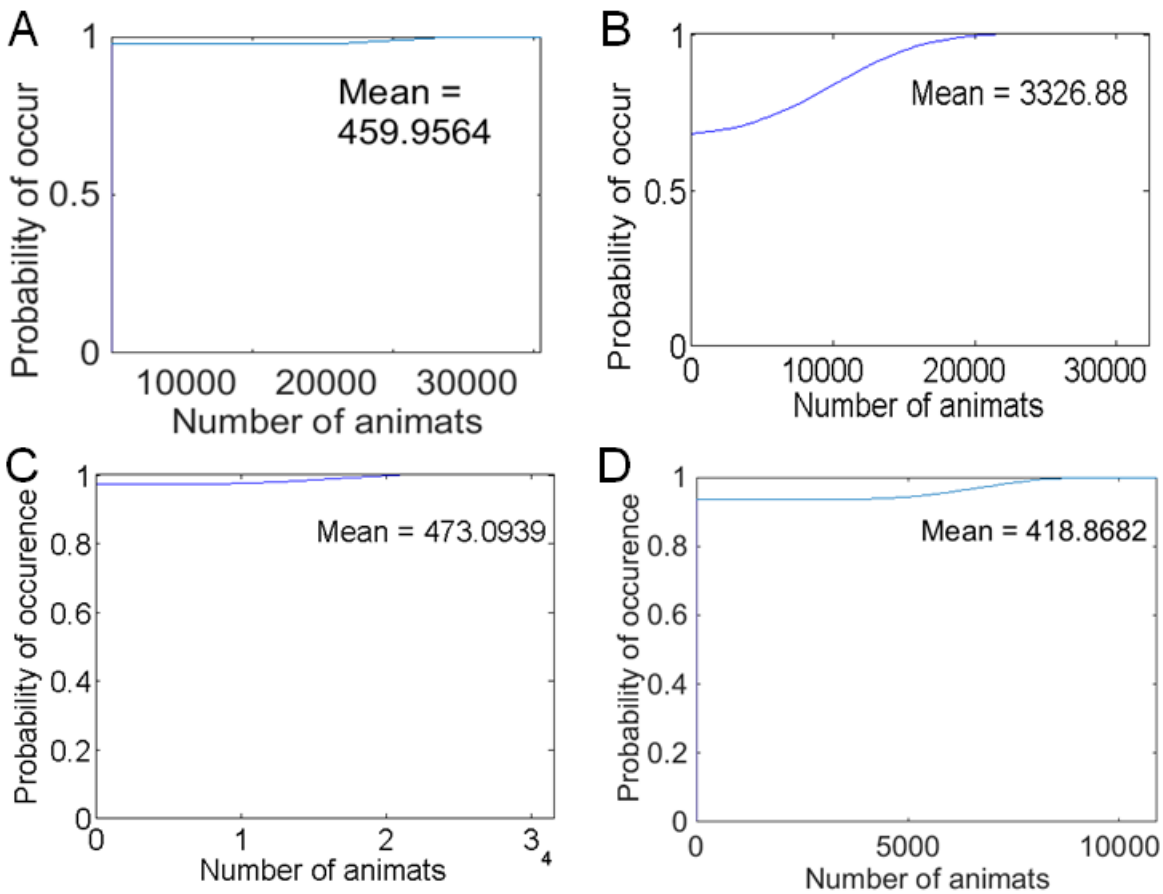

Figure 86. Behavioral disruption exposure estimate distributions with social group size at Survey site A for A) Common bottlenose dolphins, B) Cuvier's beaked whales, C) Short-finned pilot whales, D) Sperm whales. All exposure estimate distributions were determined with 10,000 bootstrap samples, each bootstrap sample size was equal to the total number of grouped animats in the simulation based on the group size listed in Table 38. Blue line shows the cumulative probability in each plot.

6.5.2.2.9. Summary of Impact of Social Group Size on Exposure Estimates

Most animals have some ecologically driven grouping behaviors. Many cetaceans aggregate due to patchy food distribution (e.g., Jaquet and Gendron 2002, Burkhardt and Lanfredi 2012). Stable groups and a distinct social organization are key elements of the population structures of many, if not all odontocete species (Connor et al. 1998, Toth et al. 2012). While feeding aggregations create temporal fluctuations in group sizes, social group sizes may remain stable for a number of years (e.g., sperm whales, Christal et al. 1998, Christal and Whitehead 2001) and possibly for their whole lives (e.g., pilot whales, Amos et al. 1993, and possibly some beaked whales Kasuya et al. 1997). Interactions between social groups are characterized by temporary associations or avoidance, perhaps to reduce inter-group competition for food, a behavior that spatially influences animal distributions in populations.

Group formation can affect exposure estimates in that grouping reduces the probability of exposure occurrence, but at the same time increases the number of impacted animals when exposures occur. Incorporating social groups into the animal movement modeling is difficult because temporary random associations and dissociations, such as group formation and dissolution, which could be related to patchy food availability, might form. Even long-term groupings might alter their makeup, move, or sample the

space differently than individuals. Social groups, by their very name, fulfil social functions, such as sharing care of young. Within social groups, individuals move in a more synchronized fashion than those in random feeding groups or groups of cooperative hunters that move in an even more coordinated fashion than other social groups. Allomothering, or babysitting, is an example of a group behavior seen in a number of cetaceans that directly affects group diving and swimming (Whitehead 1996, Hill and Campbell 2014). Allomothering creates groups of varying numbers of diving animals A number of animals remain at the surface or within the top 10 m of the water column at all times. Any acoustics effect that increases exposure in surface waters (e.g., surface ducting) will either increase the risk of animals staying at the surface and/or cause groups of animals to leave an area earlier than under quiet conditions, thus potentially affecting the amount of food required for optimal survival. Furthermore, higher exposure in surface waters will selectively affect younger animals because they do not dive to depth.

The effects of social grouping on exposure estimates can be shown by assuming that animats within the simulation are groups of animals instead of individuals. (As a note–groups can be simulated and the received level of individuals within the group can be tracked, but for simplicity in evaluating the effects of grouping, each animat was assumed to represent a group in which all individuals had the same exposure history.) During resampling, each animat was considered to be a population with a mean and standard deviation. Because each animat represents a group of animals, the effective modeling density was increased by the mean value of the group size, so the probability of exposure must be reduced by the same amount to account for the reduced likelihood of exposure. When group size was incorporated during the resampling process, the mean value of the exposure estimate distribution does not change relative to animats being considered as individuals, but the shape of the distribution can change markedly. For example, in the Bryde's whale simulation at Survey site A there were 534 animats above the SEL injury threshold and 727.3 animats predicted to incur a behavioral response (Table 14). After bootstrap resampling was applied with group size included, the exposure estimate distribution of animats above threshold had means of 535 and 732, respectively for SEL injury and behavior. There was, however, a 50% likelihood that no animats above threshold or predicted to have behavioral responses, and the potential number of animats above threshold was much greater than the mean value. The same group size (2 ± 1) was used for Bryde's whales and dwarf sperm whales and thus the results were similar for the two species. Species with larger group sizes showed more pronounced exposure estimate distributions. Common bottlenose dolphins exhibited a 98% likelihood that no animals would have a behavioral response, short-finned pilot whales a 97% likelihood, and sperm whales a 95% likelihood. In each case, the number of potential animals affected was much greater than the mean value (Figure 86).

6.5.2.3. Exposure Estimate Uncertainty

Both the uncertainty in acoustic modeling and uncertainty in the animal modeling contributed to the overall uncertainty in the exposure estimates. These uncertainties could be combined during the bootstrap resampling process to estimate exposure distributions that included the uncertainties from the various sources.

6.5.2.3.1. Exposure Estimate Uncertainty: Results

Acoustic uncertainty can be incorporated in the bootstrap resampling process by adding the uncertainty to the animats' received levels. For potential injury, the primary acoustic uncertainly was the source level variance. Airguns are designed to have low inter-shot variability and predicted source levels within 3 dB (Section 6.5.2.1.1). A conservative estimate of ±3 dB standard deviation was used to investigate the effects of source level variance on SEL injury exposure estimates. We did not investigate effects of peak SPL variance because these were calculated based on range to the source, which was only ~ 18 m for most species. The effects of small changes in a small volume would be difficult to determine. Figure 87A shows that the mean number of animats above SEL threshold increases relative to the expected value (938

vs. 534 for Bryde's whales, and 1134 vs. 1053 for dwarf sperm whales). The exposure estimate distributions, however, did not change much; for both species, the range from 5% to 95% was about 100 animats with or without acoustic variance. For potential behavioral disruption, propagation uncertainty also contributes to the uncertainty in the acoustic modeling predictions. Figure 87B shows the behavioral disruption exposure estimation distributions for Bryde's whales and dwarf sperm whales when 6 dB of acoustic uncertainty (standard deviation) was included in the received levels during bootstrap resampling. 6 dB was chosen as a test to include the ~ 4 dB uncertainty in propagation plus 3 dB in source variance. For behavior, the mean behavioral disruption exposure estimates (727 versus 727 for Bryde's whales and 459 versus 451 for dwarf sperm whales) and the distribution ranges (put ranges here) stay approximately the same when ± 6dB of acoustic variability was included.

During resampling, acoustic uncertainty (3 dB for injury, 6 dB for behavior), can be combined with real-world density (mean ± standard deviation), and social group size (mean ± standard deviation). Figure 88 shows the potential real-world number of animals above the SEL injury threshold for Bryde's whales (SEL > 192 dB re 1 $\mu Pa^2 \cdot s$) and dwarf sperm whales (SEL > 161 dB re 1 $\mu Pa^2 \cdot s$). In the exposure estimate distributions, about 70% of the bootstrap replicates predict no animals above threshold (73% for Bryde's and 64% for dwarf sperm whales). When 95% of the Bryde's whales replicates were considered 5 animals or less are above threshold and a maximum of 20 animals exceed the threshold in 100% of replicates. The corresponding values for dwarf sperm whales were 95% of the replicates have 49 animals or less above threshold with a maximum of 146 animals exposed to levels exceeding the threshold. For behavior, Bryde's whales had 76% of replicates with no behavioral response; when increased to 95% 3 or less animals were impacted, and a maximum of 15 animals were above behavioral response threshold for all of the replicates. Dwarf sperm whales had 65% of replicates with no behavioral response and up to 19 or less animals in 95% of replicates, up to a maximum of 78 animals for all replicates. For Cuvier's beaked whales, a species with lower behavioral thresholds, 75% of replicates showed no behavioral response of animals, while 3585 or less animals could potentially be affected when 95% of replicates were taken into account. Because of larger group sizes, common bottlenose dolphins, short-finned pilot, and sperm whales all showed no predicted behavioral responses in well over 90% of the replicates, but the potential number of animals impacted was much higher than the mean.

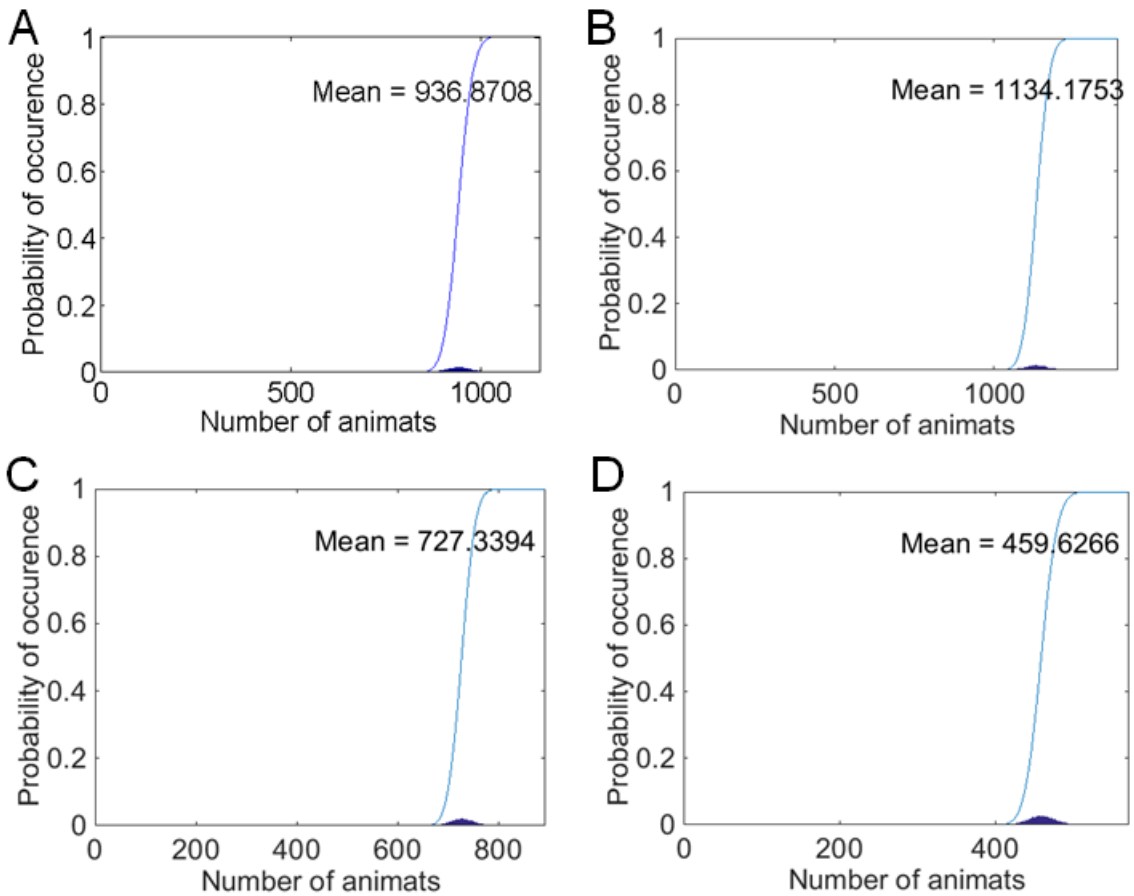

Figure 87. Bootstrap resampling with acoustic uncertainty for SEL injury potential behavioral response for Bryde's whales and dwarf sperm whales at Survey site A. A) Bryde's whales and B) Dwarf sperm whales potential SEL injury. The exposure estimate distributions are the number of animats above SEL 187 (Bryde's whales) and 161 (dwarf sperm whales) dB re 1 $\mu Pa^2 \cdot s$ with 10,000 bootstrap replicates where the number of bootstrap samples was equal to the number of animats in the simulation and the animat received level includes a standard deviation of 3 dB. C) Bryde's whales and D) Dwarf sperm whales potential behavioral response. The exposure estimate distributions are the number of animats above the rms SPL step function with 10,000 bootstrap replicates where the number of bootstrap samples was equal to the number of animats in the simulation and the animat received level includes a standard deviation of 6 dB. Blue line shows the cumulative probability in each plot.

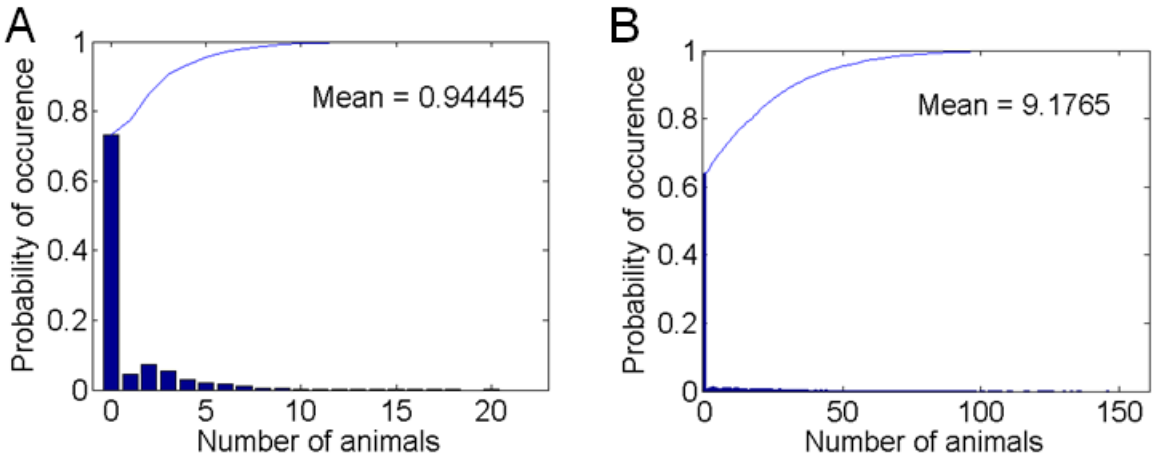

Figure 88. Bootstrap resampling for SEL injury for A) Bryde's and B) Dwarf sperm whales at Survey site A with 3 dB of acoustic uncertainty, bootstrap sample size adjusted for real-world mean density ± standard deviation, and social group size of 2 ± 1 for both species. The exposure estimate distributions are the number of animals with the potential to receive an injurious exposure; 10,000 bootstrap replicates were obtained, and the blue line shows the cumulative probability in each plot.

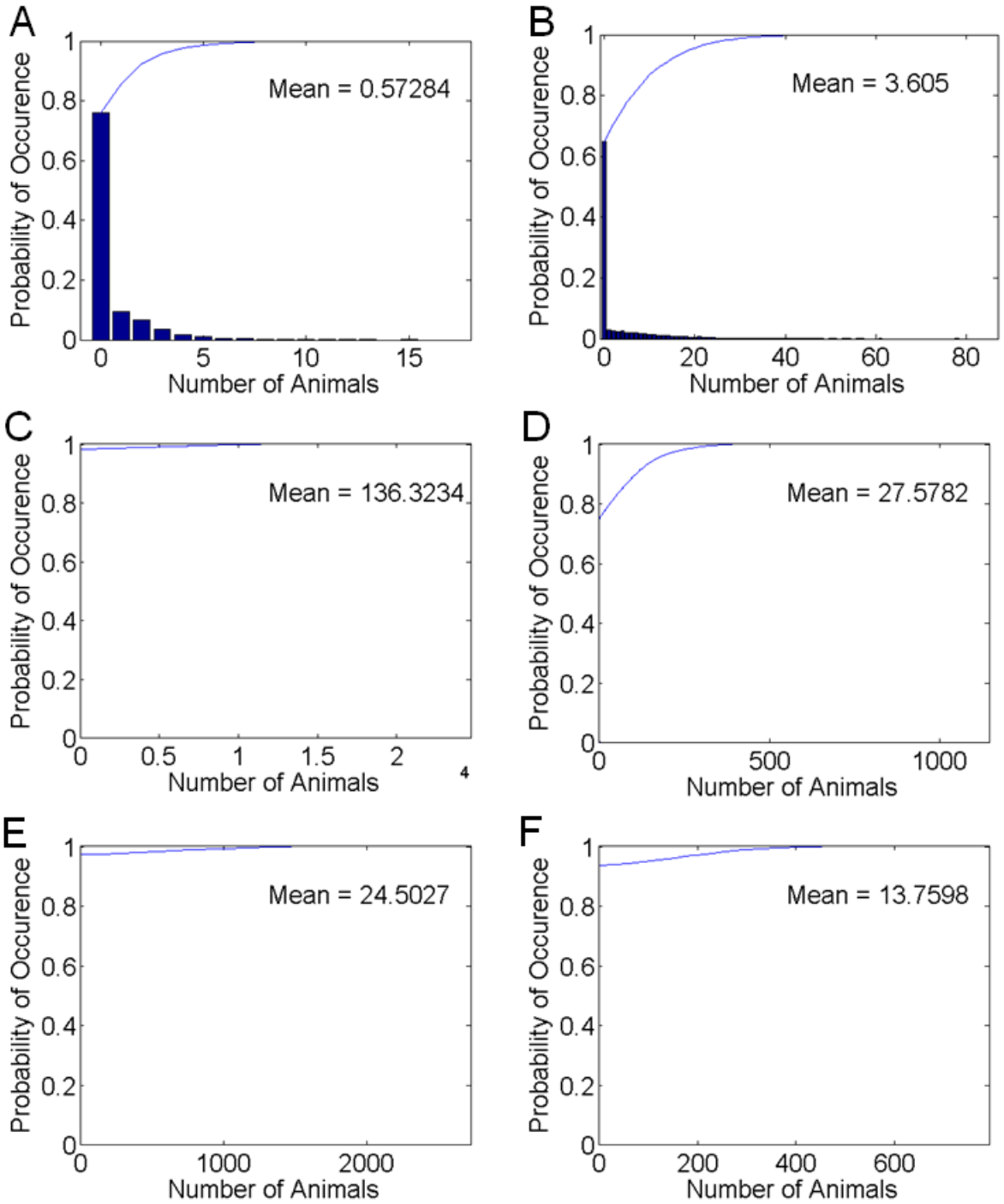

Figure 89. Potential behavioral response exposure estimates of species at Survey site A from bootstrap resampling with acoustic uncertainty (± 6 dB), real-world density (mean ± standard deviation; Table 36), and social group size (mean ± standard deviation). A) Bryde's whales, B) Dwarf sperm whales, C) Common bottlenose dolphins, D) Cuvier's beaked whales, E) Short-finned pilot whales, F) Sperm whales. The exposure estimate distributions are the potential number of animals predicted to have a behavioral response. 10,000 bootstrap replicates were obtained and the blue line shows the cumulative probability in each plot.

6.5.2.3.2. Summary of Exposure Estimate Uncertainty

Traditionally, only a limited indication of uncertainty is included when presenting exposure estimates. The exposure estimate is usually the number of animals expected to exceed a threshold. Presenting a single value as the exposure estimate does not allow for a quantitative description of the variance in the modeling process. By presenting the exposure estimate as a distribution, a measure of uncertainty can be included in the exposure estimate. The exposure estimate distribution gives the probability of certain events occurring, such as the probability that an operation would not result in any animals above a defined threshold.

Various sources of model uncertainty can be included in the resampling process to provide an exposure estimate distribution with uncertainty. In general, the uncertainty associated with the animals (density and group size) does not change the mean exposure estimate, but can profoundly affect the exposure estimate distribution. This phenomenon is especially pronounced when group size is included during the resampling process because the likelihood of exposure decreases by approximately the mean group size, concurrent with increasing consequences of the exposure (by approximately the mean group size). Uncertainty in the acoustic modeling can change the mean value of the exposure estimate because sampling near the tails of the exposure distribution is asymmetric, meaning more animats are typically slightly below threshold than slightly above it, so uncertainty in the received level results in relatively more animats exposed to levels exceeding threshold.

6.5.3. Test Scenario 3: Mitigation Effectiveness

Mitigation procedures to reduce adverse effects of sound exposures to marine mammals are often implemented during seismic surveys. The most common form of mitigation for injurious effects involves turning off the sound source (e.g., seismic array) when a protected animal is visually, or in some cases acoustically, detected within a pre-defined exclusion zone. Survey work resumes at a specified time interval after detection, allowing the animal to leave the exclusion zone. The effectiveness at reducing marine mammal exposure to potentially injurious sound levels with this commonly used approach is unknown. Mitigation effectiveness varies with the ability to detect an animal in the exclusion zone. Some species spend little time at the surface, so they are difficult to see. Others emerge frequently and visibly spout, so are easily seen. Detectability may decrease as the sea state increases as it is more difficult to visually-detect an animal in rough seas than in calm water. Detectability, and consequently mitigation efficacy, depends on the species, potentially individual animal characteristics, survey configuration, and environmental conditions.

This Test Scenario uses a modeling approach to quantify the potential reduction in the numbers of exposures at or above Level A thresholds for selected species by comparing acoustic exposure estimates with and without mitigation (array shutdown). Specifically, a 3-D wide azimuth seismic survey was simulated for six representative species at two sites within the Gulf of Mexico (Figure 10). For each species, a range of detection probabilities was considered.

6.5.3.1. Mitigation Effectiveness Methods

Level A exposure estimates associated with the 5-day wide-azimuth survey simulation described in the Test Case simulations (Figure 20) were calculated with and without a mitigation procedure. Exposure estimates were computed relative to SEL, peak SPL, and rms SPL (180 dB re 1 µPa) exposure criteria (Section 5.4). Airgun shutdown was modeled by zeroing all animat received levels when an animat was detected within an exclusion zone. The animat detection was registered when the horizontal range of an animat from the source was less than an exclusion zone radius of 500 m, its depth was < 50 m, and a

random draw indicated detection. The 500 m exclusion zone was chosen based on the BOEM JOINT Notice to Lessees No. 2012-G02 (Lydersen and Kovacs 1999).

To determine the effectiveness of mitigation, a measure of animal detection probability is needed. In cetacean surveys, the generally adopted methodology to determine animal abundance and density involves an assessment of the detection probability $g(0)$, which is estimated from visual or acoustic surveys for animals. Detection probability is the likelihood of detecting an animal within an area along a trackline (usually a circle around a survey vessel) and is biased by availability (detection is limited due to environmental factors) and perception (observers miss detecting an available animal). The estimated probability is based on the statistical correlation between two independent, but temporally correlated observations assumed to be those of the same animals (Buckland 2001). The metric include parts the vertical water column cylinder below the surface that can be surveyed simultaneously, so it depends on survey methodology. The accuracy of $g(0)$ is higher for simultaneously conducted visual and acoustic surveys than for two visual surveys due to lower availability bias, but accuracy varies with species and environmental conditions (e.g., sea state, wind, rain and resulting ambient noise level) and ultimately availability of animals for detection is limited for both survey methods (Barlow 2013). The $g(0)$ during visual surveys has been estimated for a number of species in a variety of conditions (see Section 6.5.3.1.2 below). The positions of animats in the simulation are known and reported in short time steps. The $g(0)$, however, is the probability of detecting an animal along the trackline as the survey passes through an area, rather than for an individual time step. For this Test Scenario, $g(0)$ is used as estimate of the detection probability for animats near the surface and close to the vessel.

Simulations typically use a much higher animat density than the real-world animal density. For these reasons, we reduced the number of animats (see Section 6.5.3.1.1 below) to that of the real-world density for each species and checked for detection only once for each animat that entered the exclusion zone. To assign detections, a random value from a uniform distribution between 0 and 1 was generated for each animat in the exclusion zone and whose depth was < 50 m. The value for each animat was thresholded against $g(0)$. If the random value was less than $g(0)$, the detection was registered, the time of the closest point of approach (CPA) was found, and the received levels for all animats were zeroed for 30 min before and after the CPA. Normally the true shutdown would occur for 1 h following the detection, but for our purposes the specific timing is not important as animats are independent, and the centered window conveniently allowed the detected animat to avoid being exposed.

For the purposes of the simulation, it was assumed that array shutdown was the only mitigation procedure performed, and it was assumed that portions of the survey line missed during shutdown were re-surveyed (i.e., shutdowns result in an increase in the overall survey duration in order to keep the distance surveyed the same as the unmitigated case). Shutdown was assumed to occur only for the source (array) around which the animat was detected. Other sources present in the simulation continued operating. Because it is impossible to accurately predict $g(0)$ for an operation, a likely range was used for each species (Section 6.5.3.1.2).

6.5.3.1.1. Bootstrap Resampling

We used bootstrap resampling (see *Bootstrap Resampling* in Section 6.5.2.2.4) to quantify the number of animals exposed to levels above Level A thresholds obtained from the Monte Carlo simulations of the six Test Case species, with and without mitigation. Again, the exposure probabilities are the received-level frequency of occurrence expressed as histograms. 10,000 bootstrap replicates were obtained, where the number of bootstrap samples in each replicate were adjusted by the ratio of the real-world density to the model density, and the number of animats exposed to levels above threshold (SEL or peak SPL) was found for each bootstrap replicate. Without mitigation, the resampling provides a baseline distribution of expected exposures, which is compared to the exposure estimate distribution with mitigation. The mean difference and the relative change between the two estimate distributions were calculated to quantify the

effect of mitigation on exposure estimates. Mitigation was incorporated into the bootstrap process during each replicate by testing if an animat was within the exclusion zone and detected. If a detection occurred the received levels for each animat in the replicate were zeroed for 30 min before and 30 min after the detection to simulate a shutdown.

6.5.3.1.2. Detection Probability

In surveys designed to determine animal presence or abundance, independent observations along different tracklines or temporally shifted observations along the same trackline (such as circling back in aerial surveys) provide an indication of all or a known fraction of detectable animals and can be used to estimate detection probability, typically *g*(0) (Buckland et al. 2001).

Detection probability varies with species, environmental conditions, and group size. Large whales that spend considerable time with portions of their body above the water surface and exhale a visible spout when resurfacing are more easily spotted than cryptic species that spend much of their time submerged and only break the surface for short breaths. Likewise, there are more opportunities to spot large groups than solitary animals. Detection probability decreases for all species as sea state increases, but the greatest decrease is for the difficult-to-detect species (MacIntyre et al. In Press). For example, Moore and Barlow (2013) noted a decrease in *g*(0) for Cuvier's beaked whales from 0.23 at Beaufort sea state 0 (calm) to 0.024 at sea state 5 (wave height 2–3 m). Table 39 shows *g*(0) reported for the six test species for a range of sea states (Beaufort sea states 0–5). These data are from surveys at locations around the world, as indicated in the table footnotes, but are good proxies for trackline detection probabilities of the Gulf of Mexico species.

Model simulations were run for detection probabilities of 0.05 to 0.45 simulate an assumed range of probabilities for animats in the upper 50 meters of the water column independent of the species. Simulations were run in increments of 0.05, to estimate the likely range of detection probabilities for beaked whales and dwarf sperm whales (for which Barlow (2006) noted low detection probabilities). Simulations for all other species were modeled with *g*(0) ranging from 0.5 to 0.9, in increments of 0.1.

Table 39. Estimates of trackline detection probability, *g*(0), coefficients of variation (CV) for *g*(0), and mean group size. The CV for each estimate of *g*(0) is shown in parentheses.

Species	*g*(0) Estimates for group size ranges*	
	1–20	> 20
Common bottlenose dolphins[a]	0.76 (0.14)	1.00 (n/a)
Short-finned pilot whales[a]	0.76 (0.14)	1.00 (n/a)
Sperm whales[b]	0.87 (0.09)	0.87 (0.09)
Dwarf sperm whales[c]	0.35 (0.29)	
Cuvier's beaked whales[c]	0.23 (0.35)	
Bryde's whales[a]	0.90 (0.07)	

* In Barlow (2006) Table 2, pg. 451.
[a] The *g*(0) estimates from Barlow (1995), based on his categories of small delphinids, large delphinids, and other large whales. Large and small delphinids are pooled based on the similarity in their *g*(0) values (0.74 and 0.77, respectively, for groups of less than 20).
[b] The *g*(0) estimates from Baird et al. (2006a) for sperm whales with 30-min dives.
[c] The *g*(0) estimates from Barlow (1999) based on his categories of *Kogia spp*., *Mesoplodon spp*., and *Ziphius cavirostris*.

6.5.3.2. Mitigation Effectiveness Results

The average number of cetaceans exposed to sounds above Level A exposure criteria was computed for Survey sites A (shallower water) and B (deeper water) for the six sample species. Exposure estimates were computed both with and without mitigation, producing an estimate of the mitigation effectiveness for each site and species modeled (Tables 40–44). For all species except the high-frequency dwarf sperm whales, no or a vanishing small number of SEL exposures were registered with and without mitigation. In the case of Bryde's whales, some animats were exposed to sound exceeding the SEL or SPL thresholds, however, their low real-world density meant only rarely was an animat exposed to levels above threshold chosen during bootstrap resampling.

Sample plots of the probability distribution of peak SPL and rms SPL exposure estimates, without and with mitigation, are shown in Figures 90–94 for five of the six species modeled at Survey site A (results for Bryde's whales were trivial, as noted above). Each figure shows the example for the mid-range detection probability.

Table 40. Cuvier's beaked whales: Modeled Level A exposure estimates and mitigation efficiency for peak SPL and rms SPL.

Metric	Detection probability	Average number of cetaceans above exposure criteria					
		Survey site A			Survey site B		
		Without mitigation	With mitigation	Mitigation effectiveness	Without mitigation	With mitigation	Mitigation effectiveness
peak SPL	0.05	0.032	0.032	0.001 (2%)	0.040	0.040	0.001 (2%)
	0.15	0.032	0.030	0.002 (5%)	0.038	0.036	0.002 (6%)
	0.25	0.030	0.028	0.003 (9%)	0.039	0.036	0.003 (8%)
	0.35	0.034	0.028	0.005 (16%)	0.036	0.031	0.005 (14%)
	0.45	0.031	0.024	0.007 (21%)	0.038	0.032	0.006 (16%)
rms SPL	0.05	0.123	0.120	0.003 (2%)	0.136	0.135	0.001 (1%)
	0.15	0.122	0.115	0.007 (6%)	0.138	0.130	0.008 (6%)
	0.25	0.126	0.113	0.013 (11%)	0.137	0.124	0.013 (10%)
	0.35	0.121	0.104	0.016 (14%)	0.144	0.129	0.015 (11%)
	0.45	0.122	0.099	0.023 (19%)	0.141	0.117	0.024 (17%)

Table 41. Common bottlenose dolphins: Modeled Level A exposure estimates and mitigation efficiency for peak SPL and rms SPL.

Metric	Detection probability	Average number of cetaceans above exposure criteria					
		Survey site A			Survey site B		
		Without mitigation	With mitigation	Mitigation effectiveness	Without mitigation	With mitigation	Mitigation effectiveness
peak SPL	0.5	1.364	0.778	0.586 (43%)	0.189	0.096	0.092 (49%)
	0.6	1.353	0.741	0.612 (45%)	0.203	0.089	0.114 (56%)
	0.7	1.329	0.654	0.675 (51%)	0.187	0.062	0.125 (67%)
	0.8	1.335	0.553	0.781 (59%)	0.188	0.051	0.137 (73%)
	0.9	1.354	0.398	0.956 (71%)	0.190	0.028	0.162 (85%)
rms SPL	0.5	4.510	2.561	1.949 (43%)	0.627	0.335	0.292 (47%)
	0.6	4.505	2.386	2.119 (47%)	0.630	0.281	0.349 (55%)
	0.7	4.528	2.128	2.400 (53%)	0.624	0.214	0.411 (66%)
	0.8	4.527	1.703	2.825 (62%)	0.623	0.153	0.470 (75%)
	0.9	4.520	1.104	3.416 (76%)	0.631	0.087	0.544 (86%)

Table 42. Short-finned pilot whales: Modeled Level A exposure estimates and mitigation efficiency for peak SPL and rms SPL.

Metric	Detection probability	Average number of cetaceans above exposure criteria					
		Survey site A			Survey site B		
		Without mitigation	With mitigation	Mitigation effectiveness	Without mitigation	With mitigation	Mitigation effectiveness
peak SPL	0.5	0.275	0.155	0.120 (44%)	0.334	0.186	0.148 (44%)
	0.6	0.284	0.143	0.141 (50%)	0.339	0.157	0.181 (54%)
	0.7	0.274	0.108	0.166 (61%)	0.341	0.135	0.205 (60%)
	0.8	0.281	0.085	0.196 (70%)	0.338	0.105	0.234 (69%)
	0.9	0.277	0.057	0.220 (80%)	0.339	0.064	0.275 (81%)
rms SPL	0.5	0.989	0.535	0.454 (46%)	1.225	0.663	0.562 (46%)
	0.6	0.993	0.454	0.539 (54%)	1.212	0.563	0.649 (54%)
	0.7	0.986	0.369	0.617 (63%)	1.216	0.456	0.760 (63%)
	0.8	0.991	0.271	0.720 (73%)	1.228	0.340	0.888 (72%)
	0.9	0.980	0.162	0.818 (83%)	1.224	0.206	1.017 (83%)

Table 43. Sperm whales: Modeled Level A exposure estimates and mitigation efficiency for peak SPL and rms SPL.

Metric	Detection probability	Average number of cetaceans above exposure criteria					
		Survey site A			Survey site B		
		Without mitigation	With mitigation	Mitigation effectiveness	Without mitigation	With mitigation	Mitigation effectiveness
peak SPL	0.5	0.086	0.072	0.013 (15%)	0.121	0.102	0.019 (16%)
	0.6	0.086	0.073	0.013 (15%)	0.119	0.098	0.021 (18%)
	0.7	0.084	0.064	0.020 (24%)	0.121	0.095	0.026 (21%)
	0.8	0.087	0.068	0.019 (22%)	0.124	0.095	0.029 (24%)
	0.9	0.081	0.058	0.022 (28%)	0.117	0.084	0.033 (29%)
rms SPL	0.5	0.344	0.295	0.049 (14%)	0.395	0.337	0.058 (15%)
	0.6	0.336	0.281	0.055 (16%)	0.399	0.332	0.067 (17%)
	0.7	0.337	0.267	0.069 (21%)	0.399	0.322	0.077 (19%)
	0.8	0.337	0.264	0.073 (22%)	0.399	0.315	0.084 (21%)
	0.9	0.330	0.249	0.082 (25%)	0.388	0.294	0.094 (24%)

Table 44. Dwarf-sperm whales: Modeled Level A exposure estimates and mitigation efficiency for 5-day SEL, peak SPL, and rms SPL.

Metric	Detection probability	Average number of cetaceans above exposure criteria					
		Survey site A			Survey site B		
		Without mitigation	With mitigation	Mitigation effectiveness	Without mitigation	With mitigation	Mitigation effectiveness
5-day SEL	0.05	0.320	0.311	0.009 (3%)	0.635	0.620	0.015 (2%)
	0.15	0.321	0.277	0.044 (14%)	0.632	0.557	0.076 (12%)
	0.25	0.326	0.253	0.072 (22%)	0.632	0.493	0.139 (22%)
	0.35	0.322	0.216	0.106 (33%)	0.630	0.424	0.206 (33%)
	0.45	0.304	0.177	0.127 (42%)	0.639	0.372	0.267 (42%)
peak SPL	0.05	0.865	0.869	−0.004 (0%)	1.955	1.989	−0.034 (−2%)
	0.15	0.871	0.859	0.012 (1%)	1.947	1.943	0.004 (0%)
	0.25	0.880	0.847	0.033 (4%)	1.932	1.886	0.047 (2%)
	0.35	0.865	0.814	0.051 (6%)	1.950	1.841	0.109 (6%)
	0.45	0.861	0.780	0.081 (9%)	1.935	1.769	0.166 (9%)
rms SPL	0.05	0.055	0.054	0.001 (1%)	0.130	0.127	0.003 (2%)
	0.15	0.055	0.047	0.008 (14%	0.127	0.114	0.014 (11%)
	0.25	0.055	0.043	0.012 (22%)	0.129	0.101	0.029 (22%)
	0.35	0.053	0.037	0.017 (31%)	0.130	0.089	0.040 (31%)
	0.45	0.055	0.033	0.023 (41%)	0.134	0.078	0.056 (42%)

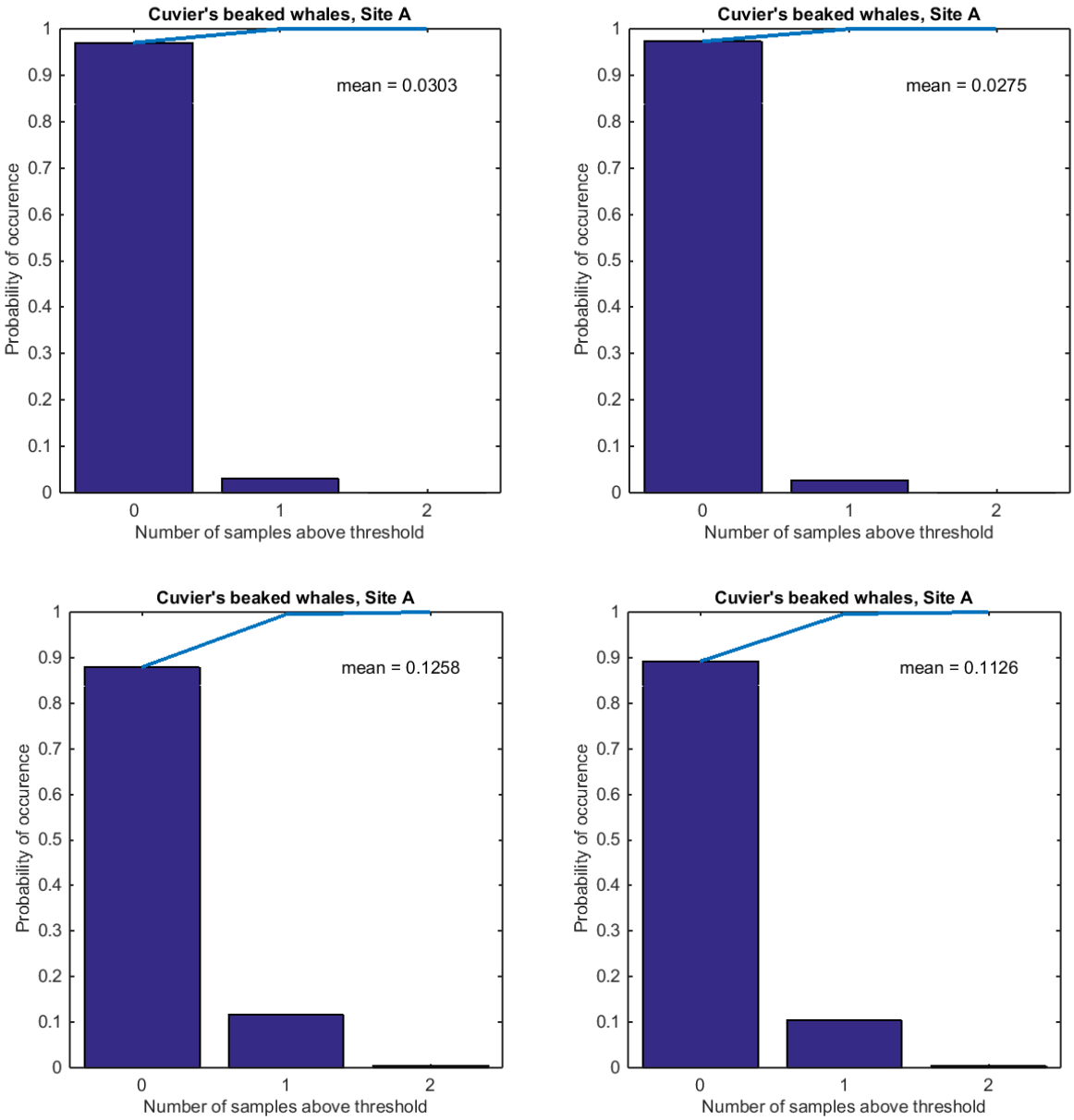

Figure 90. Cuvier's beaked whales: Probability of exposure above injury thresholds at Survey site A without (left panels) and with mitigation (right panels) for peak SPL (top panels) and rms SPL (bottom panels). Detection probability is 0.25. The blue line is the cumulative distribution.

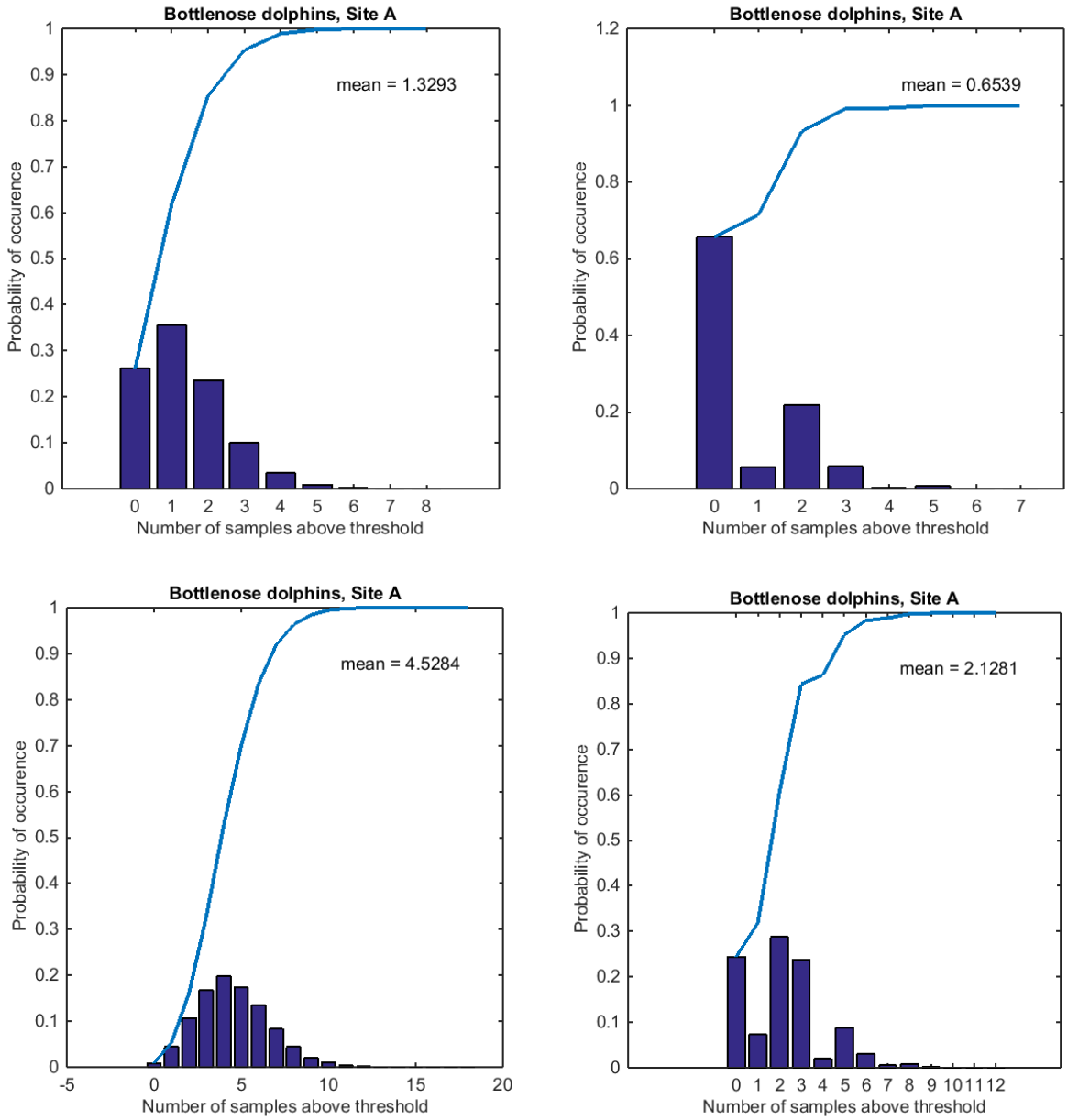

Figure 91. Common bottlenose dolphins: Probability of exposure at or above injury thresholds at Survey site A without (left panels) and with mitigation (right panels) for peak SPL (top panels) and rms SPL (bottom panels). Detection probability is 0.7. The blue line is the cumulative distribution.

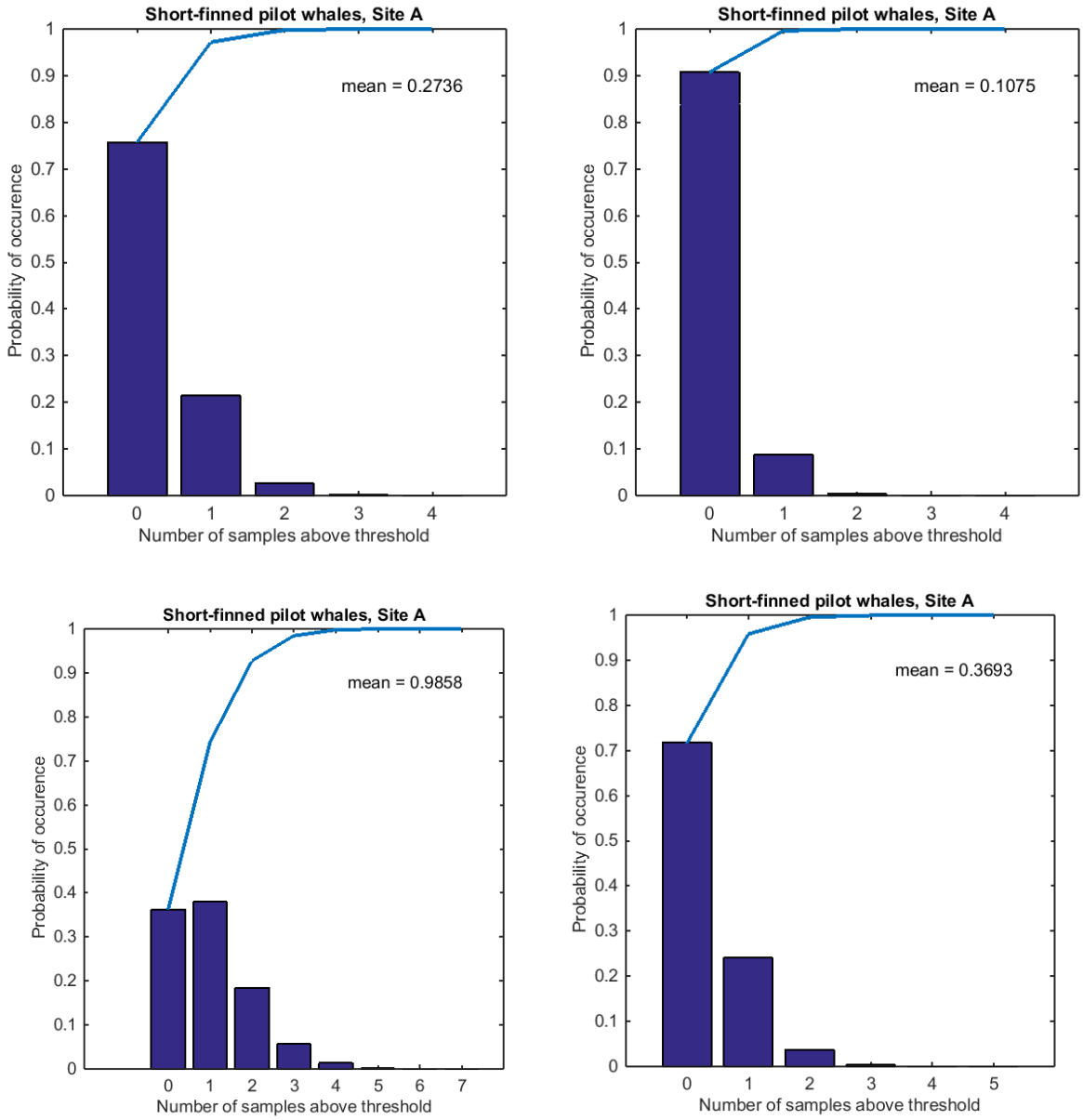

Figure 92. Short-finned pilot whales: Probability of exposure at or above injury thresholds at Survey site A without (left panels) and with mitigation (right panels) for peak SPL (top panels) and rms SPL (bottom panels). Detection probability is 0.7. The blue line is the cumulative distribution.

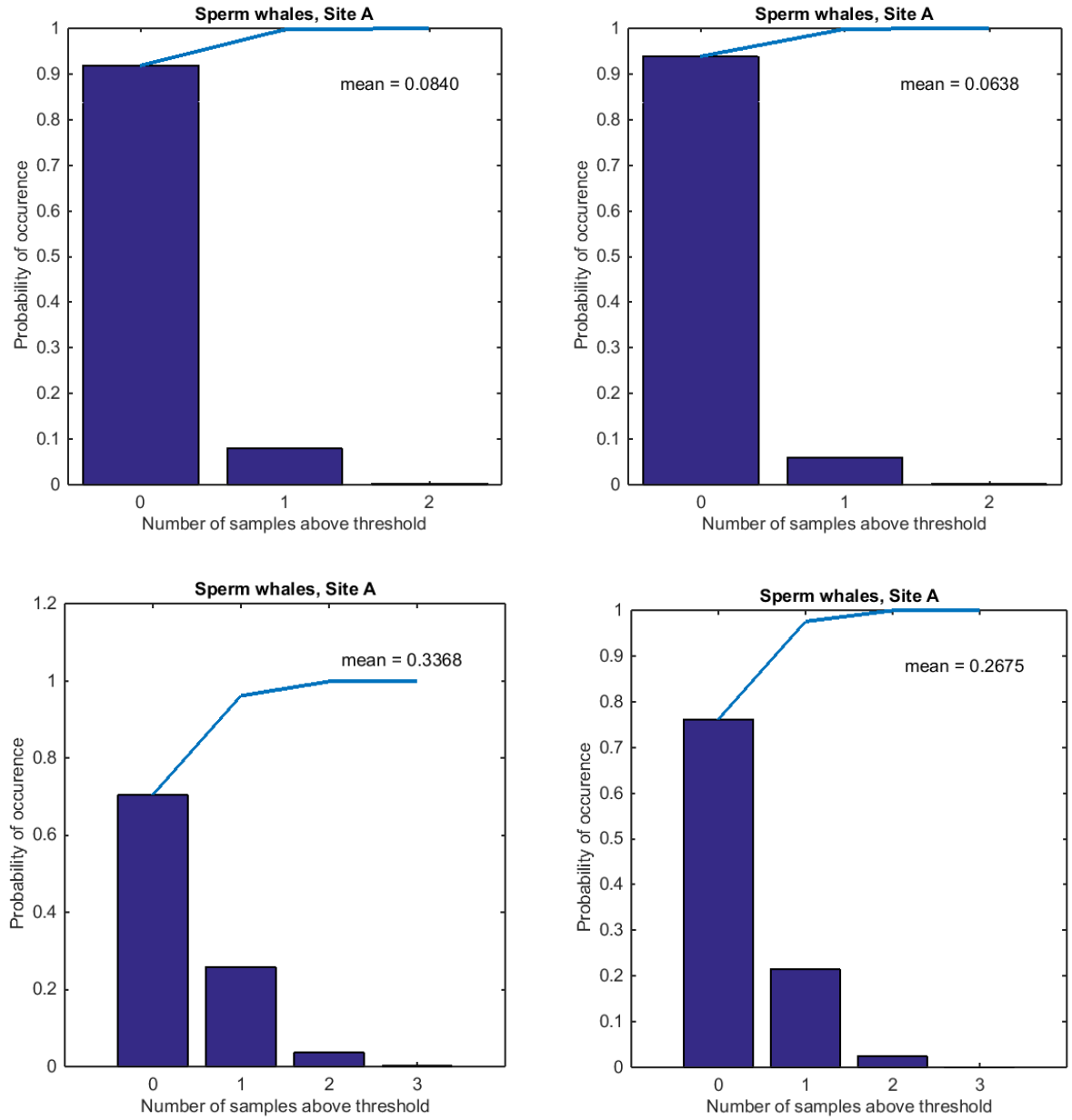

Figure 93. Sperm whales: Probability of exposure at or above injury thresholds at Survey site A without (left panels) and with mitigation (right panels) for peak SPL (top panels) and rms SPL (bottom panels). Detection probability is 0.7. The blue line is the cumulative distribution.

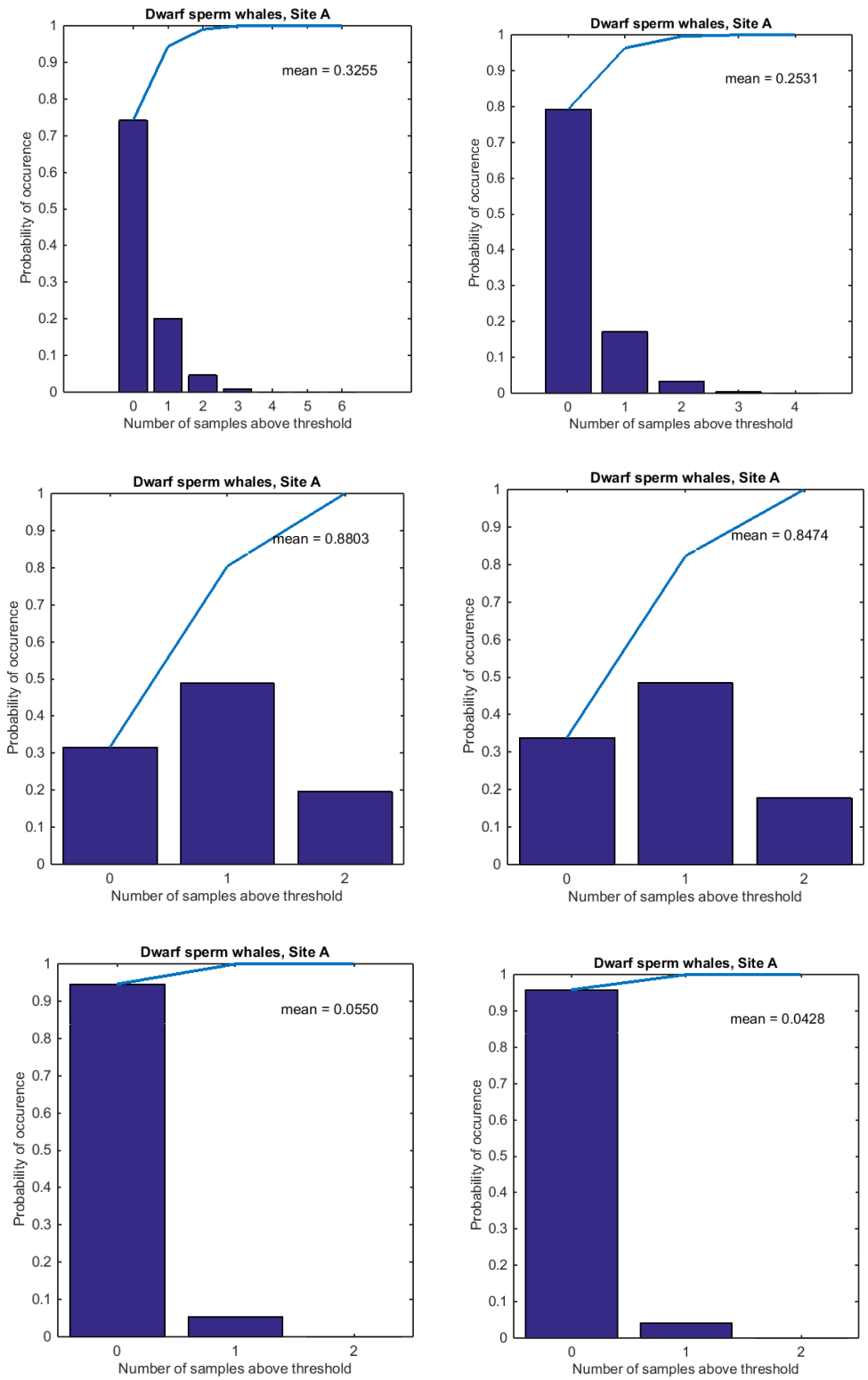

Figure 94. Dwarf sperm whales: Probability of exposure at or above injury thresholds at Survey site A without (left panels) and with mitigation (right panels) for SEL (top panels), peak SPL (middle panels), and rms SPL (bottom panels). Detection probability is 0.25. The blue line is the cumulative distribution.

6.5.3.3. Summary of Mitigation Effectiveness

The inclusion of mitigation procedures in the simulations reduced the numbers of exposures based on peak SPL and rms SPL criteria for five out of six species and detection probabilities considered, even though an extension in the survey period due to line re-shoot was taken into account. The exception was Bryde's whales, for which real-world densities were so low that no exposures were modeled even in the absence of mitigation. The numbers of exposures based on the SEL criteria were zero for most species (even without mitigation), except for dwarf sperm whales. For dwarf sperm whales, there was a reduction in SEL exposures with mitigation, but, as with the peak SPL criteria, the reduction amounted to fractions of an animal. Mitigation effectiveness, expressed as the reduction in the number of individual animals exposed, was generally related to animal densities; species with higher densities were more often exposed and the reduction in the number of exposures from mitigation was greater.

Mitigation effectiveness, as measured by the percentage reduction in the exposure estimates, is predominantly a function of animal detection probability during a seismic survey. The greater the detection probability, the greater the effectiveness of shutdown mitigation. The percentage reduction in exposures for species with relatively high detection probability (common bottlenose dolphins, short-finned pilot whales, and sperm whales) was higher than the percentage reduction for species with relatively low detection probability (Cuvier's beaked whales and dwarf sperm whales). Bryde's whales had no exposures with or without mitigation. In addition, the detection probability of beaked and dwarf sperm whales is potentially lower than reported from surveys due to uncertainty of detection availability. This also lead to a higher uncertainty in measuring mitigation effectiveness for these species using detection probability metrics. For deep diving species with unreliable vocal rates, a very conservative estimate of mitigation effectiveness should be used.

To summarize, the usefulness of mitigation depends on species characteristics and environmental conditions. Mitigation effectiveness, measured as percent reduction in exposures relative to no mitigation, tracks with detection probability and animal density. The absolute number of exposed animals reduced by mitigation is mainly dependent on how many animals were originally affected by the survey. The reduction due to mitigation for easily-detected, species with large populations, e.g., a large group of dolphins, may be high in terms of percentage decrease (perhaps ~ 70%) and absolute number of animals. For low-density species that are difficult to detect in rough seas (e.g., cryptic, deep-diving species like beaked whales), the efforts of mitigation may produce little mitigating effect.

6.5.4. Test Scenario 4: Effects of Aversion on Acoustic Exposure Estimates

Animals can display a range of behaviors in response to anthropogenic sounds, including increased respiration rates, increased or decreased vocalization rates, and changes in swimming speed (Nowacek et al. 2007). There can be substantial variation in individuals' responses to acoustic exposures; there are many examples where individuals of the same species exposed to the same sound reacted differently (Nowacek et al. 2004). If sounds are perceived as a threat or an annoyance, animals might temporarily or permanently avoid the area near the source (Stansfield and Matheson 2003, Southall et al. 2007, Ellison et al. 2012). Animals moving to avoid sound is called aversion.

Aversive responses to sounds are of particular interest because such behavior could decrease the number of injuries that result from acoustic exposure. If aversion occurs at a level less than that considered an exposure, a decrease in the corresponding exposure estimates can be assumed. The degree of aversion and level of onset for aversion, however, are poorly understood.

This Test Scenario uses a modeling approach to quantify the potential reduction in injury exposure estimates. Aversion is simulated as a reduction in received levels and, because little is known about the received levels at which animals begin to avert, the sound levels and probabilities used to evaluate potential behavioral disruption are used to implement aversion. This report only addresses the effects of

aversion on potential injury exposures; disturbance or behavioral exposures are not considered because the aversive thresholds used are the same as the current behavioral disruption exposure thresholds. Consequently, based on these thresholds, aversion itself represents a behavioral disruption exposure. It is important to note that, if aversion thresholds were lower than behavioral disruption exposure thresholds, then aversion could also reduce behavioral exposures.

6.5.4.1. Effects of Aversion on Acoustic Exposure Estimates Methods

Injury exposure estimates associated with the 5-day WAZ simulation (Section 6.3.2) were determined with and without aversion. For each site and species, distributions of expected exposures were calculated using bootstrap resampling (Section 6.5.3.1.1) of the animats' acoustic exposure histories generated in the course of the Test Case simulations. For computational efficiency, the number of animats per bootstrap replicate was scaled by the ratio of the real-word animal densities to the modeling density. To simulate aversion, a modified exposure history was generated as outlined in Section 6.5.4.2, and injury exposure estimates were computed relative to SEL, peak SPL, and rms SPL (180 dB re 1 µPa) exposure criteria (Sections 5.4.2 and 5.4.3). The difference in the mean value of the exposure estimate distributions with and without aversion indicates the effect of aversion on the injury exposure estimates.

6.5.4.2. Exposure History with Aversion

Each animat sampled during the bootstrap process (Section 6.5.3.1.1) has an associated exposure history, i.e., a time series of received sound levels arising from relative motion of the source and animat. These exposure histories were computed assuming the animats' behaviors were otherwise unaffected by their received sound levels. Each exposure history was then modified based on received-level dependent probabilities of averting:

1. For each bootstrap sample, the occurrence of aversion was determined probabilistically based on the exposure level and the probability of aversion using the step function defined in Section 5.4.3 for SEL and peak SPL, and 50% probability at 160 dB rms SPL for 180 dB rms SPL. An iteration-specific aversion efficacy was also chosen randomly from a uniform distribution in the range of 2–10 dB.
2. Animats for which aversion occurred in Step 1 had their received levels adjusted as described in the following steps. The received levels were unchanged for animats that did not avert.
3. For an animat entering an averted state, the aversion level excesses (the levels above the threshold that prompted aversion) until the end of the aversion episode were calculated from the difference between the received level at the start of aversion and the threshold level at which aversion began up to a maximum of 5 dB.
4. The adjusted received level during aversion was set to the greater of two quantities:
    - The received level minus the aversion efficacy (from Step 1), or
    - The threshold level plus the aversion level excess at the start of aversion (from Step 3)

Adjusted exposure histories were computed separately for each source, animat, and episode of aversion; each occurrence of aversive behavior was thus independent.

Although the probability of aversion was defined in terms of the rms SPL, exposure histories were recorded in terms of the per-pulse SEL. A nominal conversion offset of +10 dB from SEL to rms SPL, corresponding to a pulse arrival duration of ~ 100 ms (Section 5.2.4), was used so the two metrics could be compared. Additionally, 5-day SELs, used to compute injury exposure estimates, were weighted using Type I M-weighting for low-frequency cetaceans (Bryde's whales) and Type II M-weighting for mid- and high-frequency cetaceans, but behavioral effects were estimated using Type I M-weighting for all species

considered (Section 5.4.1). As such, the 5-day SEL exposure histories for mid- and high-frequency cetaceans were adjusted upward by an amount corresponding to the K_1 value of the Type II M-weighting functions (i.e., 16.5 dB for mid-frequency cetaceans and 19.4 dB for high-frequency cetaceans; Section 5.4.1) before they were compared to the aversion threshold levels (see Section 5.4 for exposure criteria levels developed for this study).

6.5.4.3. Effects of Aversion on Acoustic Exposure Estimates: Results

The average number of cetaceans exposed to sounds above the potential injury threshold was computed for Survey sites A (shallower water) and B (deeper water) for the six sample species. Exposure estimates were computed with and without aversion, producing an estimate of the aversion effectiveness for each site and species modeled (Table 45). For all species except the high-frequency dwarf sperm whales, no or a vanishingly small number of SEL exposures were registered with and without aversion. In the case of Bryde's whales, their very low real-world density led to a small number of bootstrap samples in each replicate and animats exposed to sound levels above SEL threshold were very rarely chosen during bootstrap resampling. Because the probability of exposure cannot truly be zero, and to keep our reporting convention consistent, the exposure estimates are listed as < 0.01 for these cases.

Sample plots of the probability distribution of injury exposure estimates, with and without aversion, are shown in Figures 95–100. In each case, the cumulative probability is shown as a blue line and the mean value (i.e., the expected number of exposures) is labeled. When the step function was used to determine aversion, the median amount of time common bottlenose dolphin, dwarf sperm whale, short-finned pilot whale, and sperm whale animats spent in an averted state was approximately 7 min at Survey site A and 2 min at Survey site B. The corresponding mean times were approximately 18 and 4 min, respectively. For beaked whales, the median was 45 min at Survey site A and 5 min at Survey site B and the corresponding means were 41 and 19 min. Too few Bryde's whale animats exceeded threshold to obtain a reliable statistical measure.

Table 45. Modeled Level A exposures, with and without aversion.

Species	Metric	Average number of cetaceans above exposure criteria					
		Survey site A			Survey site B		
		Without aversion	With aversion	Aversion effectiveness	Without aversion	With aversion	Aversion effectiveness
Bryde's whales	5-day SEL	< 0.01	< 0.01	N/A	< 0.01	< 0.01	N/A
	peak SPL	< 0.01	< 0.01	N/A	< 0.01	< 0.01	N/A
	rms SPL	0.341	0.299	0.043 (12%)	0.390	0.336	0.054 (14%)
Cuvier's beaked whales	5-day SEL	< 0.01	< 0.01	N/A	< 0.01	< 0.01	N/A
	peak SPL	0.033	0.006	0.028 (83%)	0.038	0.004	0.034 (89%)
	rms SPL	1.930	1.604	0.326 (17%)	2.662	2.237	0.425 (16%)
Common bottlenose dolphins	5-day SEL	< 0.01	< 0.01	N/A	< 0.01	< 0.01	N/A
	peak SPL	1.357	0.219	1.139 (84%)	0.191	0.033	0.159 (83%)
	rms SPL	68.701	57.940	0.761 (16%)	9.798	8.043	1.756 (18%)
Short-finned pilot whales	5-day SEL	< 0.01	< 0.01	N/A	< 0.01	< 0.01	N/A
	peak SPL	0.279	0.040	0.239 (86%)	0.346	0.052	0.294 (85%)
	rms SPL	13.287	11.410	1.877 (14%)	18.311	15.521	2.790 (15%)
Sperm whales	5-day SEL	< 0.01	< 0.01	N/A	< 0.01	< 0.01	N/A
	peak SPL	0.082	0.013	0.069 (84%)	0.126	0.020	0.106 (84%)
	rms SPL	4.744	3.819	0.925 (20%)	8.969	7.555	1.414 (16%)
Dwarf sperm whales	5-day SEL	0.318	0.191	0.127 (40%)	0.647	0.399	0.248 (38%)
	peak SPL	0.859	0.774	0.086 (10%)	1.958	1.756	0.202 (10%)
	rms SPL	1.756	1.421	0.335 (19%)	4.708	3.795	0.912 (19%)

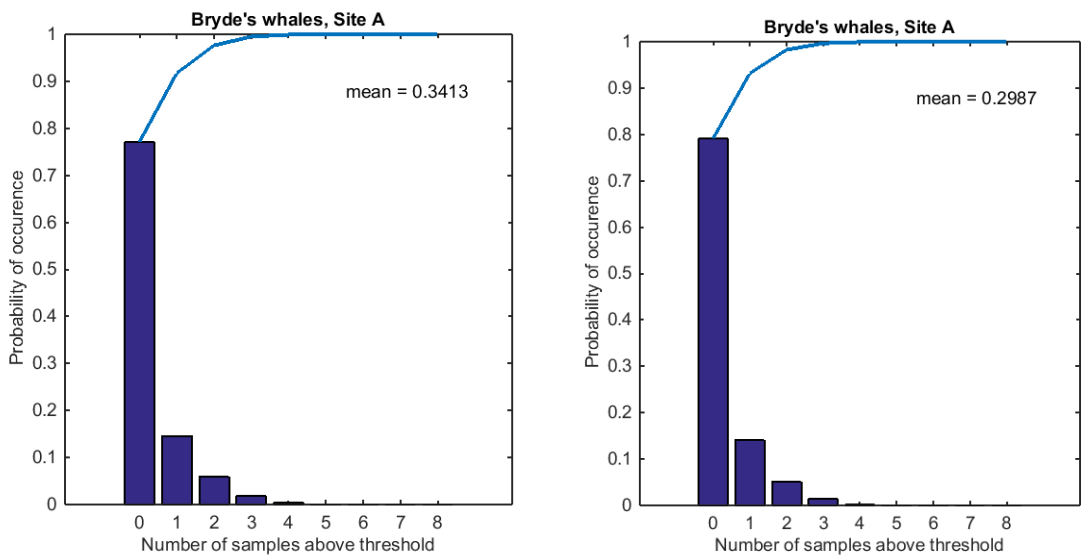

Figure 95. Probability of exposure at or above rms SPL injury thresholds for Bryde's whales at Survey site A, (left) without and (right) with aversion. The blue line is the cumulative distribution.

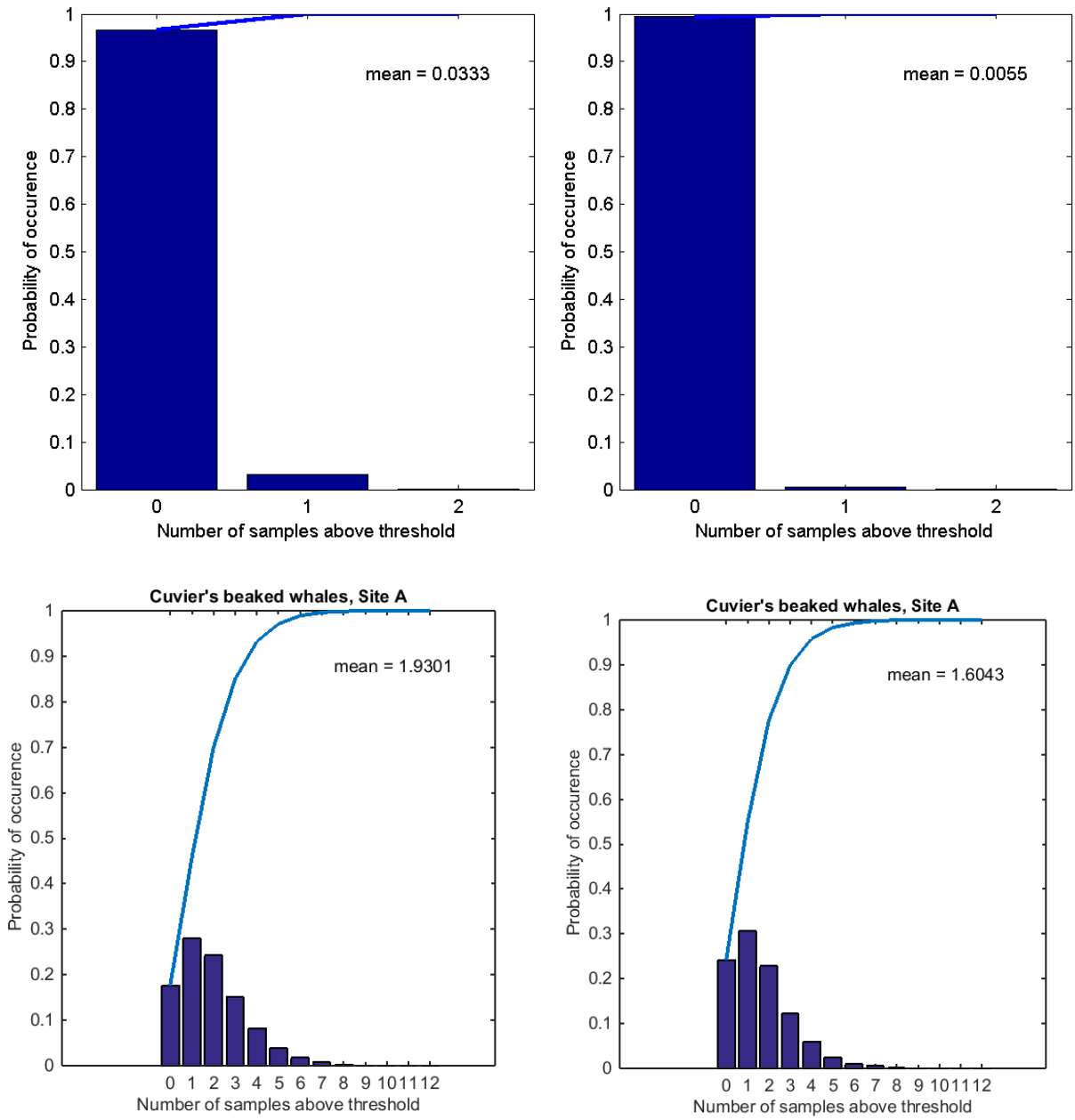

Figure 96. Probability of exposure at or above peak SPL (top panels) and rms SPL (bottom panels) injury thresholds for Cuvier's beaked whales at Survey site A, without (left panels) and with aversion (right panels). The blue line is the cumulative distribution.

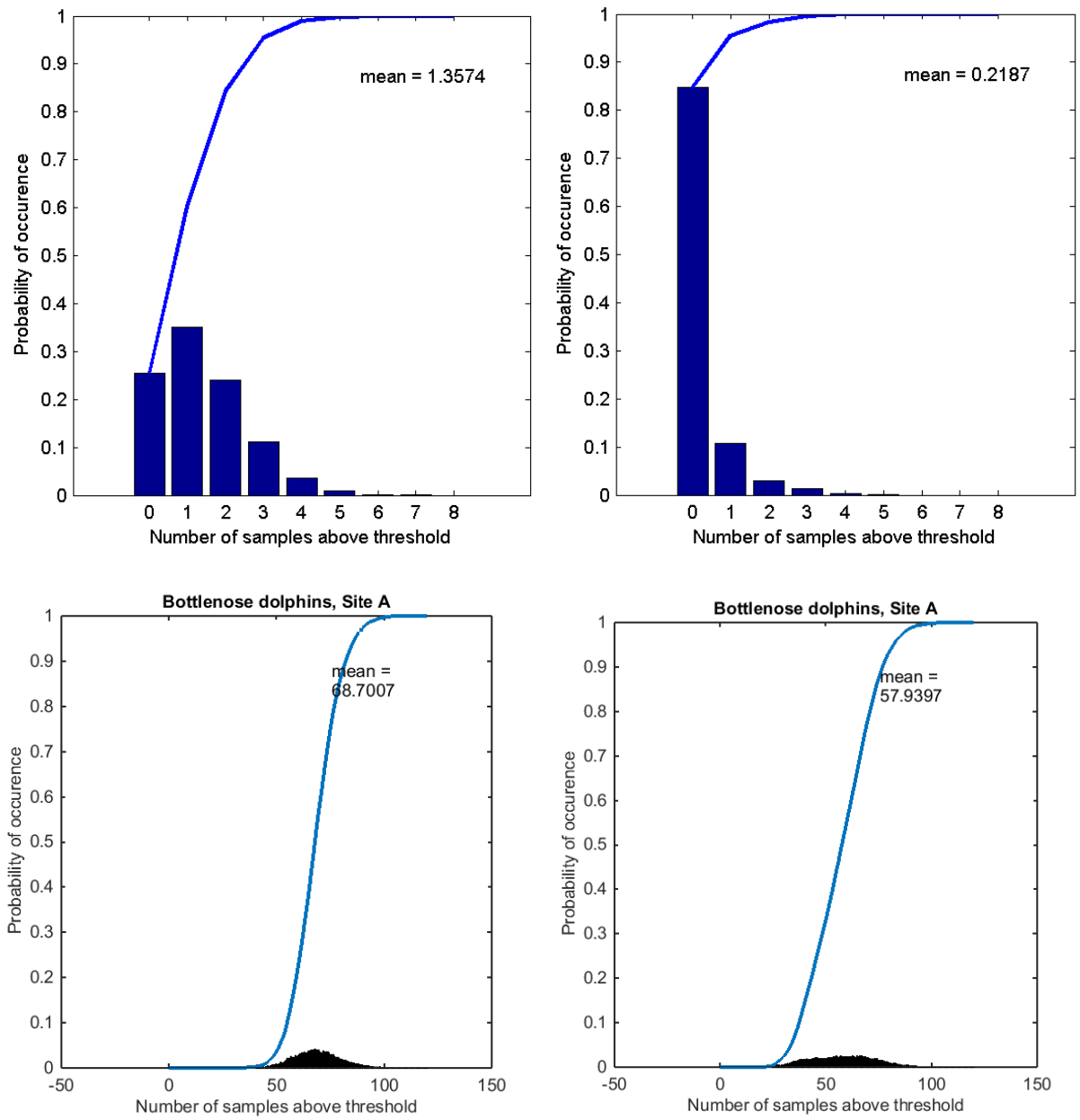

Figure 97. Probability of exposure at or above peak SPL (top panels) and rms SPL (bottom panels) injury thresholds for common bottlenose dolphins at Survey site A, without (left panels) and with (right panels) aversion. The blue line is the cumulative distribution.

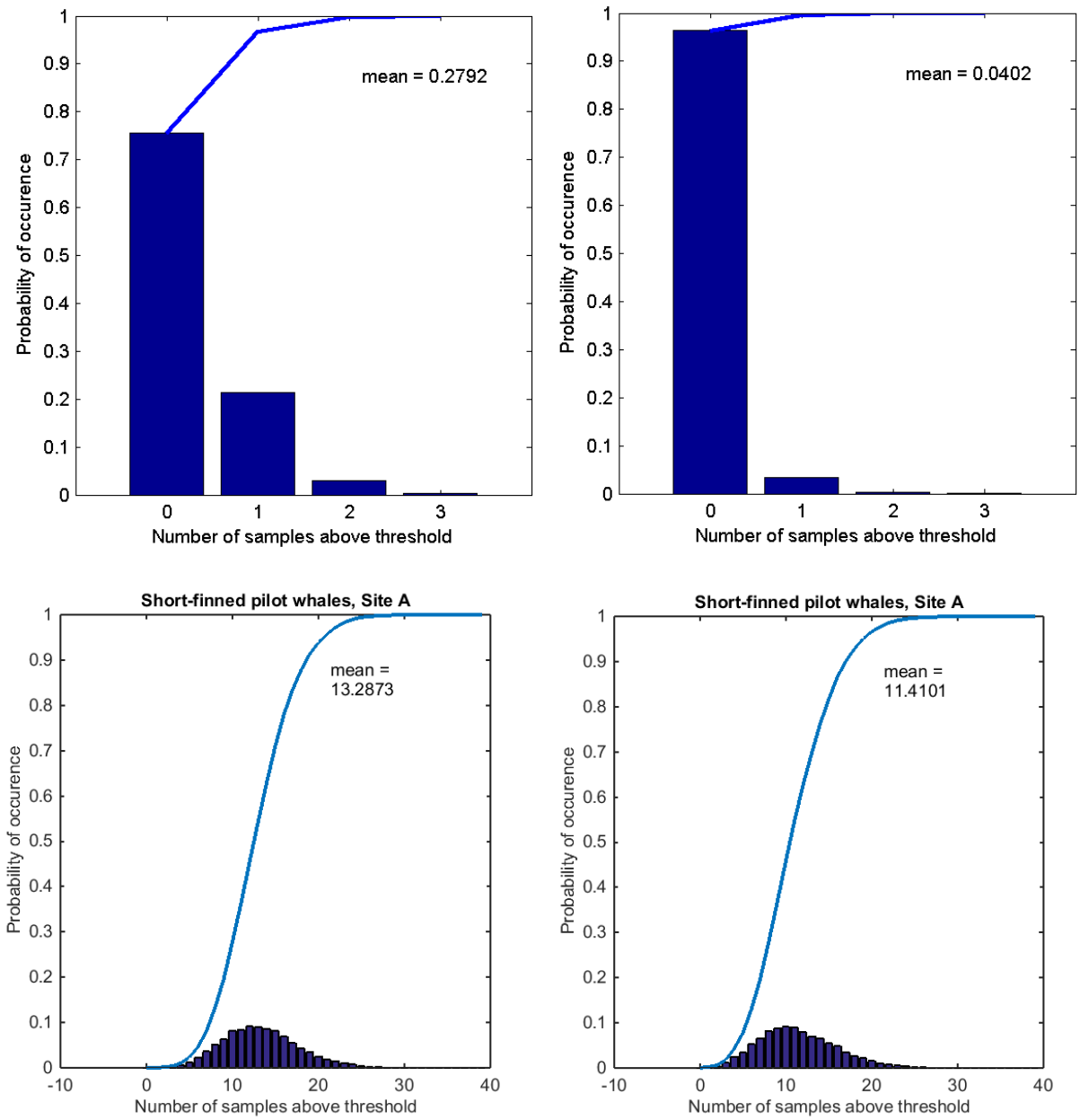

Figure 98. Probability of exposure at or above peak SPL (top panels) and rms SPL (bottom panels) injury thresholds for short-finned pilot whales at Survey site A, without (left panels) and with (right panels) aversion. The blue line is the cumulative distribution.

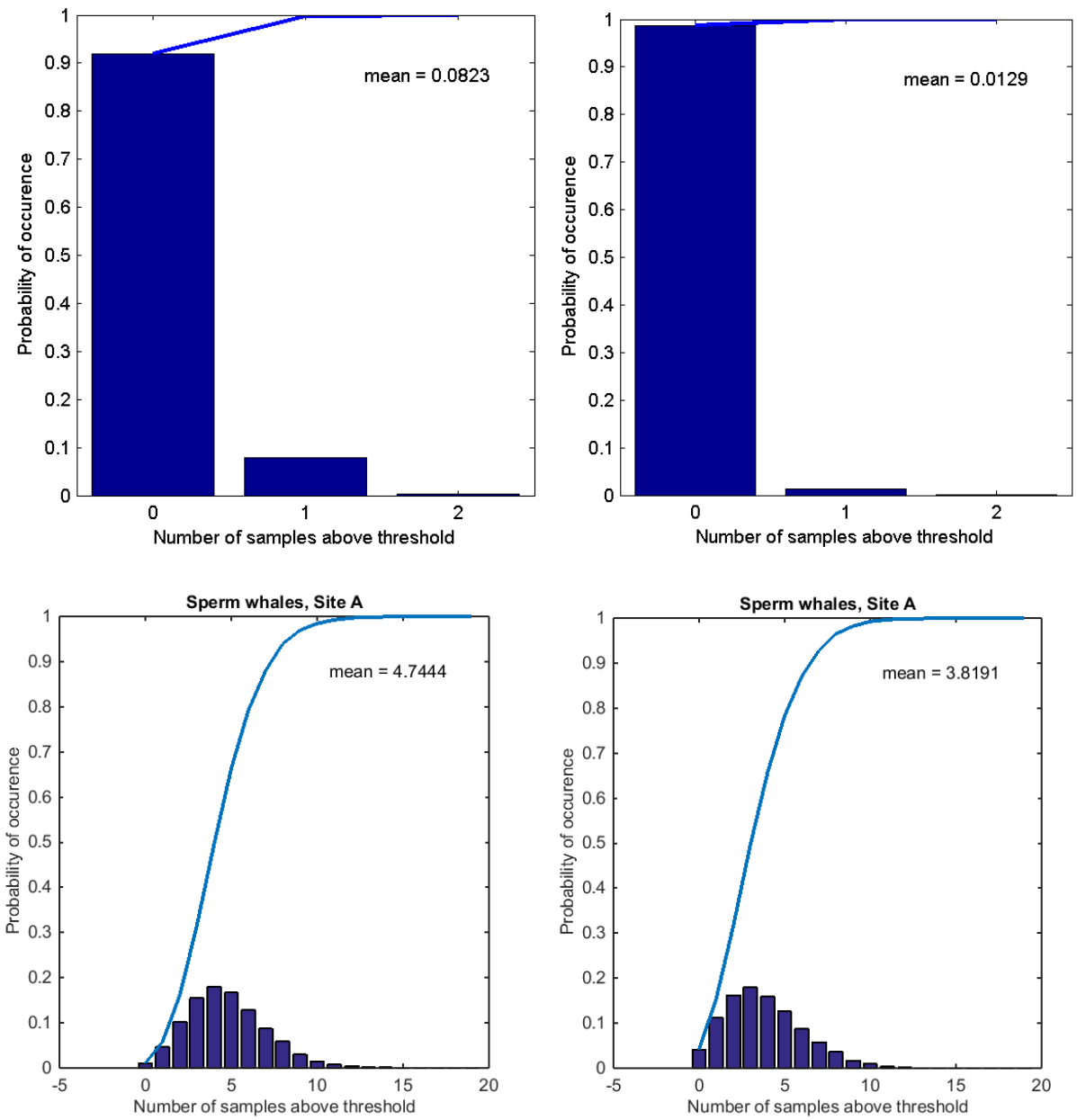

Figure 99. Probability of exposure at or above peak SPL (top panels) and rms SPL (bottom panels) thresholds for sperm whales at Survey site A, without (left panels) and with (right panels) aversion. The blue line is the cumulative distribution.

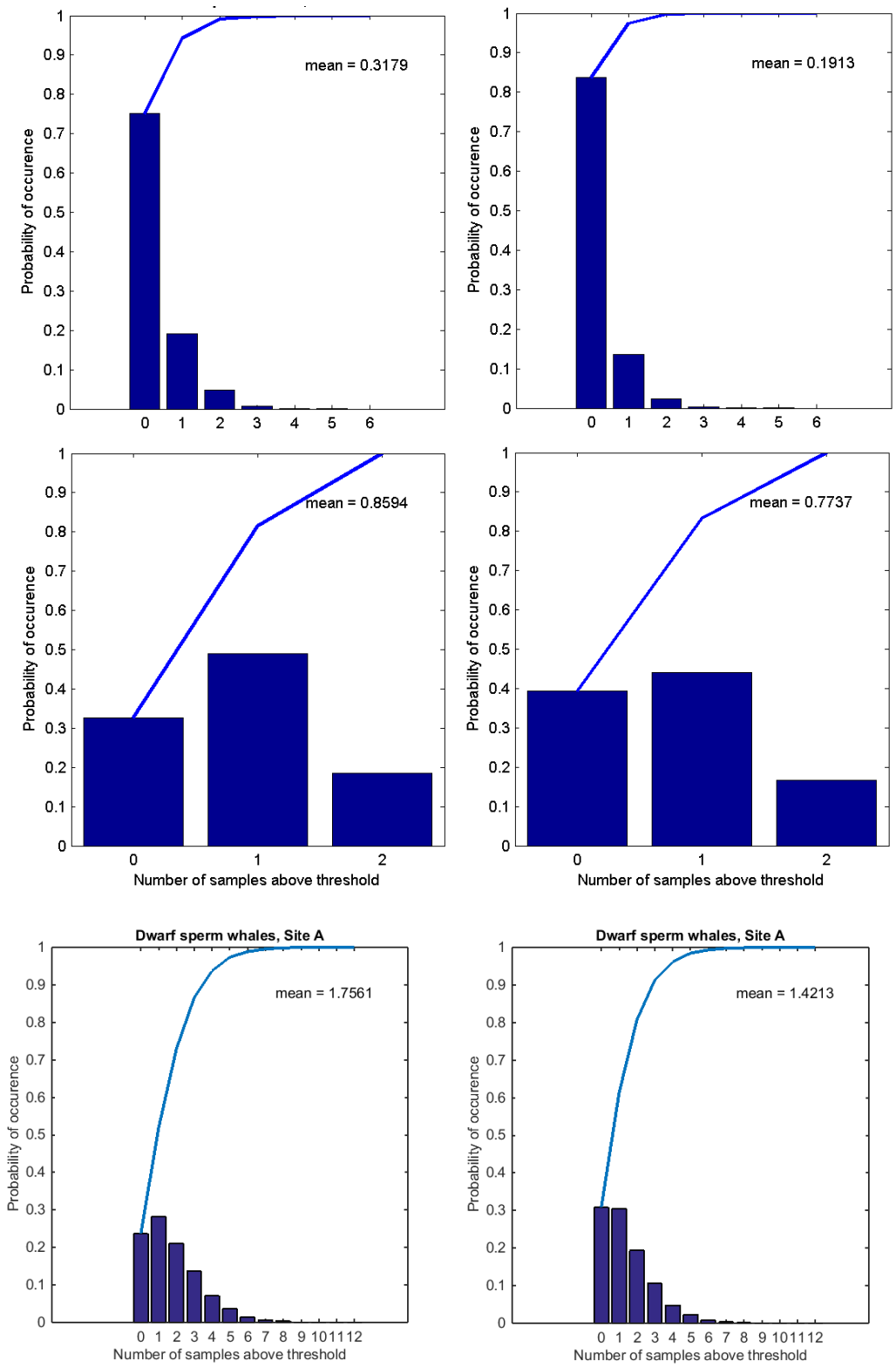

Figure 100. Probability of exposure at or above (top panels) SEL, (middle panels) peak SPL, rms SPL (bottom panels) injury thresholds for dwarf sperm whales at Survey site A, without (left panels) and with (right panels) aversion. The blue line in each plot is the cumulative distribution.

6.5.4.4. Summary of Effects of Aversion on Acoustic Exposure Estimates

Responses to sound carry potential health costs to animals. Hiding or retreating from an ensonified area could decrease their foraging time and/or increase the energy they spend searching for food (Bateson 2007). In most cases, animals likely expend less energy temporarily avoiding or averting noise by changing their travel or migratory routes, than they would if their foraging was interrupted. The circumstances under which aversion occurs depends on the context in which the animals receive sounds and on the animals' motivation. The decision to deviate from a path or avoid an ensonified area is likely driven by energetic and reproductive requirements (Croll et al. 2001). For example, bowhead whales who avoided distant seismic airguns at received levels of rms SPL of 120–130 dB re 1 µPa during fall migration (Richardson et al. 1999) were more tolerant of airgun sounds while feeding in the summer. The feeding whales avoided airguns only when received levels reached 152–178 dB re 1 µPa, roughly 30–50 dB higher than migrating avoidance levels (Richardson et al. 1995).

Stone and Tasker (2006) reported that small odontocetes showed the strongest reaction to airgun sounds by moving away from or avoiding an ensonified area. Mysticetes and killer whales showed more localized avoidance, with fewer sightings when the source was active; long-finned pilot whales only changed their orientation; and sperm whales showed no significant avoidance response (Stone and Tasker 2006). Others (e.g., Rankin and Evans 1998) also noted sperm whales' apparent lack of response to seismic operations. In controlled exposure experiments, eight tagged sperm whales over a series of 120 min intervals during pre-exposure, ramp-up, and full-array airgun firing did not avoid airgun sounds by adjusting their position horizontally; only one individual adjusted its diving and foraging rate by resting longer at the surface and diving immediately following the final airgun pulse (Miller et al. 2009). In contrast, during the first 72 h of a 10-day seismic survey, fin whales moved away from the airgun array. This displacement persisted well beyond the 10-day duration of seismic airgun activity (Castellote et al. 2012). Though consistent with aversion to airgun sounds, another possibility is that the animals were following a food source that was not tracked during the observations. Gender-specific responses were also observed. Resting female humpback whales avoided seismic surveys by distancing themselves from the source by 7–12 km, whereas males were occasionally attracted to the sounds (McCauley et al. 2000a).

To assess how aversion could reduce injury exposure estimates, a simple model was created that allowed for lower exposure levels for animats in the simulation, based probabilistically on their received level. Any animat that averted was considered to have a behavioral response so only the effects of aversion on injury exposures were considered.

Aversion in the simulations reduced the numbers of exposures based on peak SPL criteria for most species. Aversion effectiveness, as measured by the percentage reduction in the exposure estimates, could be high: ~ 85% for common bottlenose dolphins, Cuvier's beaked whales, short-finned pilot whales, and sperm whales, and ~ 40% for dwarf sperm whales. Bryde's whales, whose real-world densities were so low that no exposures were modeled even in the absence of aversion, were the exception. The numbers of exposures based on SEL criteria were near zero for most species even without aversion. For dwarf sperm whales, there was a reduction in SEL exposures with aversion, but as with the peak SPL criteria, the reduction amounted to a fraction of an animal. There was a consistent reduction of 14–20% in exposures above rms SPL 180 dB re µPa based on aversion starting at rms SPL 160 dB re µPa for all species. The reduction in the number of individuals above rms SPL 180 dB re µPa ranged from a fraction of an animal to more than ten individuals. Aversion effectiveness, expressed as the reduction in the number of exposures, was generally related to animal densities: species with higher densities were more often exposed, and the reduction in the number of exposures from aversion was greater. This reduction in exposures was also influenced by the criteria used to estimate exposures and by the assumptions made with respect to aversion probability. For example, although the real-world densities of dwarf sperm whales (a high-frequency cetacean) are similar to those for Cuvier's beaked whales (a mid-frequency cetacean), exposure estimates and the decrease in number of exposure estimates arising from aversion were different. The differences in aversion effectiveness reflect differences in injury threshold criteria and

aversion probability. The Cuvier's beaked whales' behavioral response thresholds are lower than other species, leading to potential aversion at lower received levels and greater reduction in injury exposures based on the SPL metric. Dwarf sperm whales had more absolute exposures and less reduction because of their lower behavioral response thresholds and larger ensonified area in which injury could occur.

6.5.5. Test Scenarios 5 and 6: Stand-off Distance and Simultaneous Firing

Modern geophysical seismic surveys employ a variety of seismic sources, including airgun arrays. Recent survey practices have included survey geometries that with multiple airgun arrays, separated by tens of meters to several kilometers, in a single survey. New technologies for analyzing seismic data are less sensitive to interference of noise between multiple surveys, and this has allowed for different surveys to be performed closer together than previously. There is concern that the combined sound pressure levels of multiple sources operated close-by can lead to increased noise effects than would occur with a single source. This Test Scenario report addresses the issue of the aggregate noise produced by multiple airgun arrays and the potential for those signals to combine and lead to larger effects.

Airgun arrays consist of multiple airguns that are fired almost simultaneously to increase the amplitude of the overall source pressure signal. The combined sound emission amplitude and directivity of an airgun array is dependent on the number and sizes of individual airguns and their geometric positions within the array. Airgun arrays are typically operated repetitively as the arrays are towed over a survey grid pattern. The time intervals between airgun shots are optimized for water depth and the distance of important geological features below seafloor; there must be enough time between shots for the sound signals to propagate down to and reflect from the feature of interest, and then to propagate upward to be received on hydrophones. Reverberation of sound from previous shots must also be given time to dissipate. The receiving hydrophones can be towed behind or in-front of the airgun array, or deployed on the seabed. These can be displaced several kilometers horizontally away from the source, so horizontal propagation time is also considered in setting the interval between shots.

Many 3-D surveys now use two or more airgun array sources to get different 'views' of geological features. A common approach for these surveys has been to tow two arrays spaced horizontally a few tens of meters away from each other, and to fire them alternately. This alternate firing of pairs of arrays is referred to as 'flip-flop' mode. More recently, wider offsets of the airgun arrays are achieved by towing the arrays from different vessels. Surveys of this type are referred to as wide azimuth, and they are be performed with multiple vessels spaced from hundreds or thousands of meters apart, with each vessel towing its own airgun array or arrays.

In these cases, a stand-off distance may be required for operational and data quality purposes. A minimum standoff distance may be desired, or required for permitting, to allow a corridor for animals to pass between adjacent work zones. Determining the underwater sound field of surveys involving multiple arrays with potential overlap is more complex than evaluating the impacts due to a single-array survey because relative locations and relative shot timing might have to be taken into account. The influence of stand-off distance and simultaneous firing on acoustic exposure estimates is explored here.

6.5.5.1. Stand-off Distance

Multiple seismic surveys may be conducted nearby one another at the same time. The sound emissions of the multiple sources from these surveys, operating in close proximity, can lead to increased received sound levels for nearby marine mammals. A minimum separation distance between the surveys, referred to as a stand-off distance, may be mandated to keep the noise exposures lower. If the stand-off distance keeps the surveys sufficiently separated, the estimates of marine mammal exposures for either survey, i.e., the number of animals exposed to sound levels above exposure thresholds, is largely independent of the presence of the other survey. If the surveys move closer together, nearby marine mammals can experience

sound exposure contributions from both surveys, potentially increasing their total exposures above effects thresholds and consequently causing additional exposures. In the case where a marine mammal approaches two surveys close enough to exceed the exposure threshold of both independently, it is only considered to have been exposed once (if the exposures occur within the reset period). In those cases, the number of exposures might actually be reduced by smaller stand-off distances. The issue of value of stand-off distance is therefore not straightforward. It is further complicated by the fact that the SPL and SEL sound metrics, all used for exposure assessments, vary differently in the presence of sound contributions from two or more surveys.

SPL is a metric used for both injurious and behavioral exposure assessments. SPL of impulsive airgun sounds is calculated over relatively short time windows, almost always less than 1 s and commonly approximately 100 ms, during which the highest amplitude parts of the pulse-like sounds occur (see Figure 15a, which shows the pressure waveform of the 8000 in^3 array from the Test Case). When two seismic surveys are operating nearby, marine mammal receivers can experience pulses from both surveys. However, unless those pulses happen to arrive near-simultaneously at the receiver, the SPLs do not sum and the SPL exposure will be that only of the louder survey (at the receiver position). Interpulse time intervals typically are 10 to 20 s, with 15 s being quite common. Using that as an example, with a SPL time window of 100 ms, only one in 75 pulses will have some degree of important overlap for a given receiver, and that will usually only be partial. This example neglects that signals in deep waters can have several discrete arrivals associated with multipaths (e.g., Figure 101, which shows pressure waveform shapes at several distances from the 8000 in^3 array source at Survey site A, from the Test Case, in 500 m water depth), but typically just one of those paths dominates. In the worst-case scenario of full overlap and signals from both arrays having the same SPLs, the SPL increase would be about 3 dB. Generally, one signal will have higher amplitude than the other and the potential increase will be less. For example, if the received SPL from one survey is 158 dB re 1 µPa, and the other is 155 dB re 1 µPa, the fully overlapped pulses would have a combined SPL of 159.8 dB re 1 µPa, an increase of less than 2 dB over the higher-amplitude pulse, assuming they have the same pulse duration.

While the expected SPL increases from multiple surveys are relatively small, and occur infrequently, SPL-based exposures occur on a single instance of an exposure above the threshold. The behavior-based threshold may be exceeded several kilometers from either source, so there is a chance an animal mid-way between two surveys, and receiving similar SPL levels from both, could experience an increase by up to 3 dB when exposed to overlapping sounds from both surveys. To avoid this effect entirely would require stand-off distances of twice the distance to the exposure threshold minus 3 dB. Under the assumption of 20 log R (spherical spreading) transmission loss, the stand-off distance would have to be more than 3 times the distance to the exposure threshold to ensure that summed levels always fall off to the exposure threshold mid-way between the two sources. However, this is probably the worst-case geometry, since the exposure zones of the individual surveys meet at the mid-point and it provides the largest combined exposure zone. In fact, much smaller stand-off distances reduce the size of the combined exposure zone.

The peak SPL metric is used to assess potential injury exposures close to a source. Peak SPLs occur over very short times, and the argument for rare overlaps of pulses, provided above for SPL, is even more pronounced for peak pressure. The likelihood of temporal overlaps of pressure peaks is very limited. Further, the peak pressure injury threshold exceedance zones are so small (typically a few hundred meters) that marine mammals would be extremely unlikely to experience an overlap that would lead to a peak pressure acoustic exposure that did not occur from a single survey source.

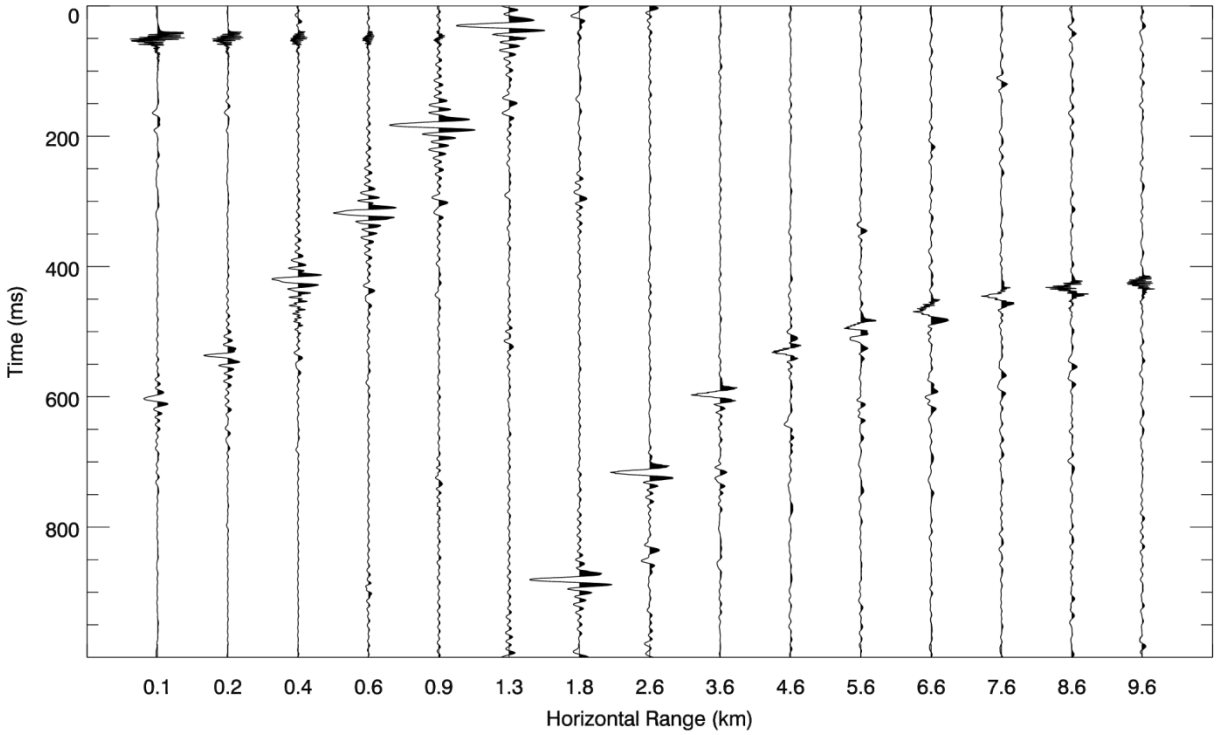

Figure 101. Waveforms predicted by FWRAM for the 8000 in^3 array at Survey site A, for a 10 m receiver depth. Waveforms are shown as a function of horizontal range from the receiver. Positive pressures are filled in black. The key feature is that pressure signals for individual multipaths are short in duration, here generally 50–100 ms.

SEL is a measure of accumulated sound energy. Unlike the previously described metrics of SPL and peak pressure, it does not depend on the structure (time and phase) of the received sound, and it increases throughout the reset period with each received pulse. For example, Figure 102 shows the unweighted SEL field for the start of a 3-D WAZ survey, assuming stationary receivers (as opposed to the moving animats used to compute exposure estimates). When surveys are close enough for animals to receive energy from two or more surveys, some animals that would have been below threshold in one survey could accumulate sufficient additional energy to exceed threshold in the aggregate of the surveys. In this case, an exposure would occur when no exposure would have been registered if the surveys did not overlap. For the current SEL criteria (Section 5.4.2), which apply only to potential injury, ranges for which injury may occur are on the order of a few hundred meters from the source. As such, overlap must occur over similarly short ranges to affect exposures. For example, even in high-density simulations (2 animats/km^2) of the 3-D WAZ surveys, no animats were exposed to levels exceeding the SEL threshold for mid-frequency species at Survey site B (deep) and only common bottlenose dolphin and Cuvier's beaked whale animats were exposed to levels exceeding the threshold at Survey site A. For Bryde's whales (low frequency) and dwarf sperm whales (high frequency), the number of acoustic exposures was much higher, but when real-world animal densities are considered, SEL exceedance is still rare and resulted from being near an individual source once rather than accumulating energy from multiple sources. Overall, exceeding the SEL threshold is a rare event and having four vessels close to each other (350 m between tracks) did not cause appreciable accumulation of energy at the ranges relevant for injury exposures, thus accumulation of energy from independent surveys is expected to be negligible.

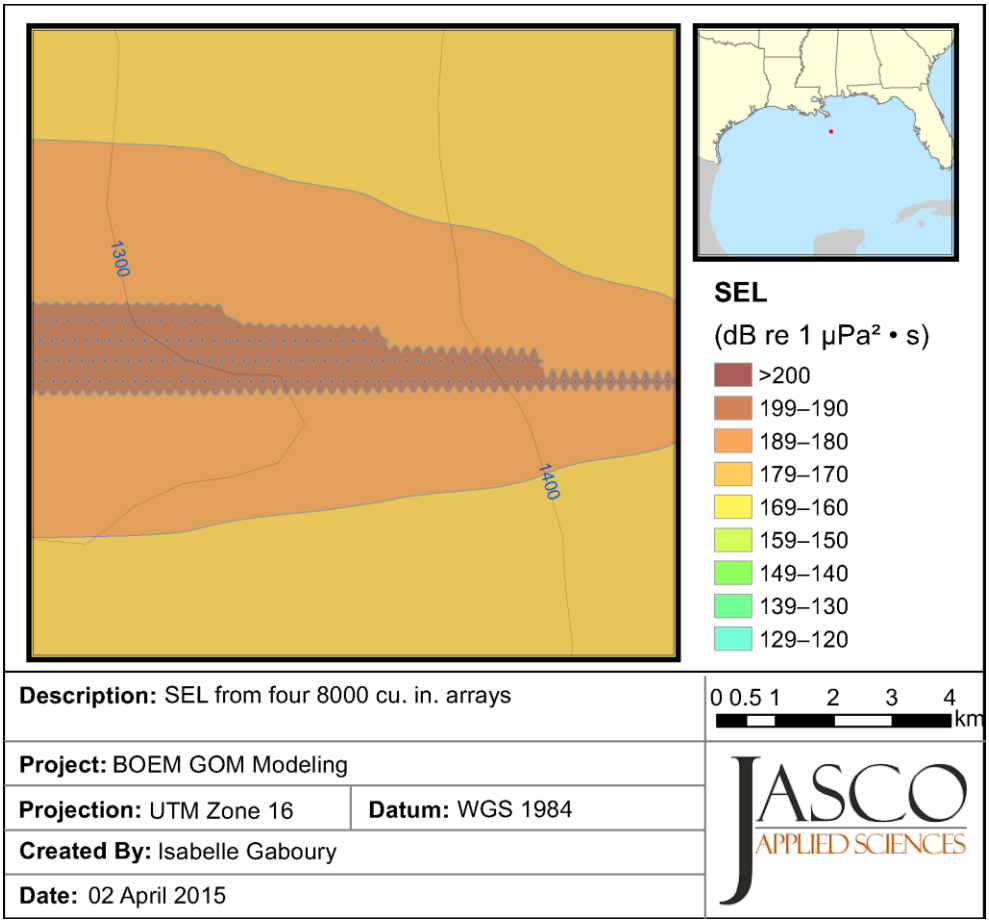

Figure 102. Sound exposure level for four 8000 in^3 arrays at the start of a 3-D wide azimuth seismic survey at Survey site A, S01 modeling province. Arrays are offset by an across-track distance of 350 m and an along-track distance of 2.7 km. Tow speed is 2.3 m/s, and shot interval for each vessel is 86.4 s.

6.5.5.2. Simultaneous Firing

Traditional large-scale surveys involving multiple airgun arrays towed from multiple vessels alternate, or distribute, the shots fired among the arrays. Some modern surveys now fire multiple arrays simultaneously. This simultaneous firing warrants special consideration for its potential to affect estimated exposures.

Coincidence of pulse arrival is only of concern for metrics based on sound pressure (the energy-related metric, SEL, is simply summed and does not rely on signal timing). As discussed in Section 6.5.5.1, the sound pressure at a location with multiple impinging sources is a function of the arrival time, shape, and phase of each arriving pulse. The "worst-case" is when two identical pulses arrive at the same time and in the same phase. These pulses sum coherently, doubling the sound pressure or, equivalently, increasing the SPL by 6 dB. Because phase varies with time, location, and frequency as sound propagates away from a source, coherent summing occurs only with nearly-coincident synchronized sources such as those within a single array. For separate arrays the pressure signals combine incoherently, with a maximum SPL

increase of 3 dB, as described previously. More precisely, the incoherent sum of the rms SPLs from two arriving pulses in regions of overlap may be estimated as follows:

$$L_p = 10\log\left(\frac{T_1 \times \log^{-1}(L_{p1}/10) + T_2 \times \log^{-1}(L_{p2}/10)}{T_2 + \Delta t}\right), \qquad \Delta t < T_1 \tag{20}$$

where L_{p1} and L_{p2} are the rms SPLs of the two pulses (dB re 1 µPa), T_1 and T_2 are time windows for computation of rms SPL (s), $\log^{-1}$ is the antilog function, and Δt is the difference in arrival time of the two pulses. The sum of more than two pulses is computed similarly. Where pulses do not overlap, the received SPL is taken to be the maximum SPL of the two individual pulses. For example, Figure 103 shows the maximum-over-depth rms SPL sound fields for one 8000 in^3 array and for two identical arrays fired simultaneously with an across-track separation of 350 m and an along-track separation of 2700 m (as in Figure 102 showing SEL). While there are some regions where the combined sound field is louder than the individual sound fields (e.g., the small extensions to the isopleths visible in the across-track direction in the bottom panel of Figure 103), the individual and combined sound fields are nearly identical. Similar results would be expected for simultaneous firing of three or four arrays.

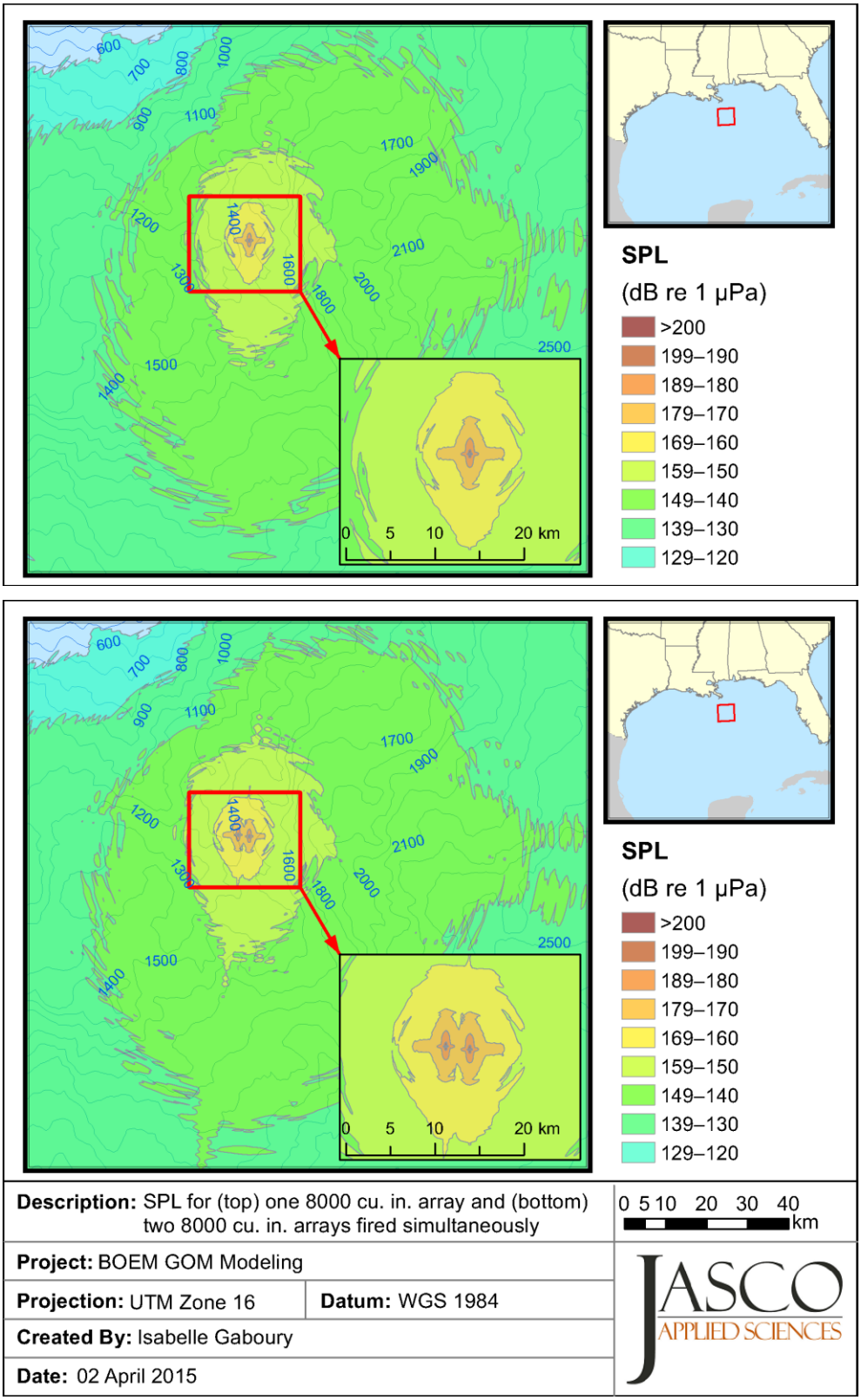

Figure 103. SPL for (top) one 8000 in^3 array and (bottom) two 8000 in^3 arrays fired simultaneously with an across-track separation of 350 m and an along-track separation of 2700 m.

6.5.5.3. Summary of Stand-off Distance and Simultaneous Firing

It was found that while SEL increases for overlapping surveys, injury due to accumulated energy is a rare event, and exceeding threshold resulted from a few high-level exposures near a source, not an accumulation of many lower-level exposures. The range to injury assessed by peak SPL is up to a few hundred meters and does not accumulate. Injury in typical seismic surveys, therefore, occurs mainly because of a close encounter with a single airgun array. There are practical limits to how close two acquisition lines can be without one survey source interfering with the other survey's recordings. Depending on the survey type and the propagation environment of the area, the stand-off distance between fully concurrent surveys operating independently may be several tens of kilometers. If two surveys are conducted in closer proximity, then the operators will generally agree to "time-sharing" strategies whereby, for example, one survey acquires a line while the other completes a line turn with the source inactive, or similar ways of minimizing the amount of missed effort. Effects of overlapping surveys on injury exposure estimates are unlikely.

For potential behavioral disruption, overlapping surveys may affect exposure estimates, but the effect is either small or potentially negative (reducing the overall number of estimated exposures). Because coincident reception in which the sound level increases appreciably only occurs in small portions of the ensonified volume, overlapping survey sound fields do not generally result in higher maximum received sound pressure levels. And, because animals may only be exposed once, animals exposed in more than one survey are only counted once in the aggregate of the surveys. This does not preclude possible behavioral effects of animals spending more time above threshold, but such effects are not addressed by existing criteria.

From an energetic perspective, the relative firing pattern of different arrays does not matter. The same SEL will be registered when two arrays are alternated or fired simultaneously. For the pressure-based metrics, peak SPL and rms SPL, simultaneous firing can increase the received levels, but in only a small portion the ensonified volume. Because the maximum received levels are rarely increased, the exposure estimates based on SPL are rarely increased. The most likely place for meaningful summation to occur is very near the source, and in that case the firing pattern would be included in the simulation and therefore in the exposure estimates.

In sum, neither stand-off distance nor simultaneous firing are of significant concern when estimating exposures using the current criteria.

6.6. Cumulative and Chronic Effects Assessment Framework

6.6.1. Overview

A cumulative sound exposure calculation framework was developed to assist with assessing chronic seismic exploration noise received by marine mammals at a set of ten pre-defined receiver locations (Table 46) in the Gulf of Mexico. This framework is implemented as Excel spreadsheets with scripting to provide a flexible tool for evaluating potential effects of scenarios representing different levels of seismic exploration activity over wide areas of the Gulf of Mexico. The spreadsheets incorporate the results of acoustic modeling of the same 8000 in^3 seismic array and single 90 in^3 airgun that were considered in the broader environmental assessment. Source directivity is accounted for with an azimuthal resolution of 22.5°. Model results are currently available for winter and summer seasons and at three possible receiver depths: 5 m, 30 m and 500 m.

Table 46. Receiver site locations and water depths.

Site #	Receiver Site Name	Latitude	Longitude	Water Depth
1	Western Gulf	27.01606	-95.7405	842
2	Florid Escarpment	25.95807	-84.6956	693
3	Midwestern Gulf	27.43300	-92.1200	830
4	Sperm Whale site	24.34771	-83.7727	1053
5	Deep offshore	27.64026	-87.0285	3050
6	Mississippi Canyon	28.15455	-89.3971	1106
7	Bryde's Whale site	28.74043	-85.7302	212
8	De Soto Canyon	29.14145	-87.1762	919
9	FGBNMS*	27.86713	-93.8259	88
10	Bottlenose Dolphin Site	29.40526	-93.3247	12

*Flower Garden Banks National Marine Sanctuary

Spreadsheets store the acoustic transmission loss results generated by the parabolic equation model (MONM) used in the broader assessment. The model was used to generate range and direction-dependent transmission loss along radials 150 km long that converge on the receiver sites. The radials are in azimuthal steps of 22.5° and the transmission loss results along each were modeled at the center frequencies of all consecutive 1/3-octave-bands from 10 Hz to 5 kHz. The modeling geometry was implemented using acoustic reciprocity, whereby the model was run with the source and receiver positions interchanged—an efficient approach when there are more potential source sites than receiver sites.

The spreadsheets also contain several sets of frequency weighting coefficients that can be applied to the received levels. Currently the framework supports the Low-Frequency Cetacean (LF1), Mid-Frequency Cetacean (MF1), and High-Frequency Cetacean (HF1) filters as defined by Southall et al. (2007), and the equal-loudness weightings for Low-Frequency Cetaceans (LF2), Mid-Frequency Cetaceans (MF2), and High-Frequency Cetaceans (HF2) as defined by Finneran and Jenkins (2012). It is straightforward to add other weightings by including them in the weighting table spreadsheet.

6.6.2. Method of Use

The spreadsheet scripting initially displays a data entry screen with two panes to the user: one for entering receiver-based and general information, and the other for entering information related to multiple seismic surveys.

The general information pane has four fields:

- Select Frequency Filter: displays a drop-down list of filter types that include unweighted, LFC1, MFC1, HFC1, LFC2, MFC2, HFC2 as described above.
- Select Site: displays a drop-down list of the ten receiver sites (Table 46).
- Receiver Depth: displays a list of the possible depths: 5 m, 30 m, and 500 m. If water depth is less than 30 m or 500 m then those options are listed as n/a.
- Month: current choices are July or December.

The spreadsheet displays information based on the choices made, as shown in this example of the general information pane:

Select Frequency Filter:	**LFC1**	N 28.155	East: 853873	Water depth	Description
Select site:	**Site 6**	W 89.397	North: 3119577	1100 m	Mississippi Canyon - Sperm whales, cryptic deep divers
Receiver depth:	**5 m**				
Month:	**July**	Season:	S3		

The seismic survey entry pane is a multi-line data entry area in which the user can enter information associated with each of the surveys considered. These are the primary inputs for each seismic survey:

- Location: Entered in latitude and longitude in WGS-83 coordinates. The current version of the framework assumes the source is fixed at this location for the duration of the survey, although a single survey can be divided into multiple sub-parts at different locations.
- Array type and operating depth: Selected from a drop-down list. Currently the framework includes an 8000 in^3 airgun array operating at 8 m depth and a 90 in^3 single airgun operating at 4 m depth.
- Duration: The total operating time in seconds. The total cumulative operating time does not include break times. It is used with shot interval to calculate the total number of seismic shots or pulses.
- Shot interval: The time in seconds between each seismic shot or pulse. That typically ranges from 10-20 seconds, but can be shorter in shallow waters. This value is used with survey duration to calculate the number of pulses accounted for in the cumulative sound exposure level calculation.
- Azimuth: The direction, in degrees, relative to true North that the seismic array is towed. 90° is due east. The value is used to select the appropriate direction-dependent source levels.

Up to 50 separate seismic surveys can be entered in the survey entry pane. The spreadsheet automatically computes and displays several other fields in the greyed-out “control numbers” section:

Surveys						Source:		Control numbers:				
#	Active	Lat	Lon	Duration (seconds)	Shot interval (seconds)	Type	Tow azimuth	Number of shots	East	North	Range	Azimuth
1	yes	29.000	-89.500	864000	30.00	8000 in³ at 8 m	90	28800	841013	3213039	94343	352.2
2	yes	28.000	-89.600	864000	10.00	90 in³ at 4 m	90	86400	834407	3101864	26318	227.7
3	yes	29.000	-91.000	864000	30.00	8000 in³ at 8 m	10	28800	694821	3209635	182778	109.5
4	yes	29.000	-91.500	864000	15.00	90 in³ at 4 m	350	57600	646109	3208913	226156	123.3
5	yes	27.000	-89.700	864000	10.00	90 in³ at 4 m	350	86400	827517	2990720	131524	21.6
6	yes	27.000	-89.800	864000	30.00	8000 in³ at 8 m	350	28800	817586	2990464	134115	25.7

The framework contains a separate sheet that displays a map of the first ten survey locations with the receiver locations. The map also shows the currently-selected receiver position, which is displayed using a different symbol than the other receiver positions. This map is help for reviewing survey location values relative to a chosen receiver. An example map is shown in Figure 104.

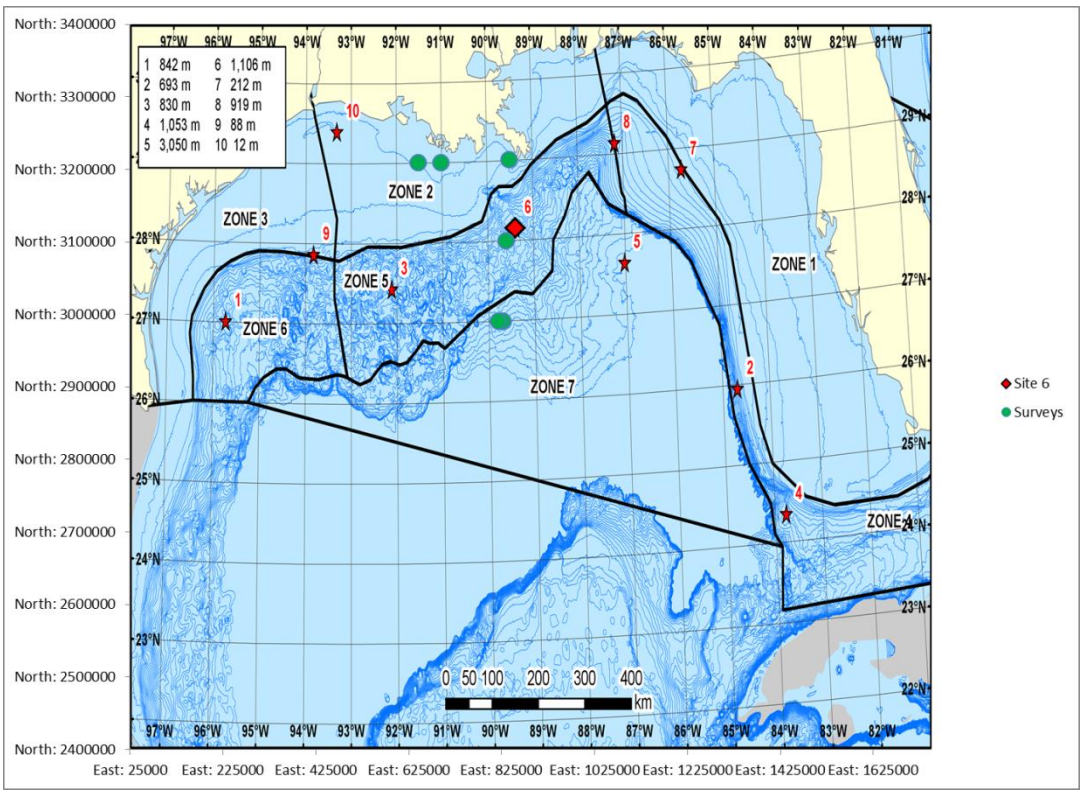

Figure 104. Map automatically produced by the cumulative and chronic effects calculator, showing seismic survey positions and receiver locations. The seismic survey locations are shown as green dots. Receiver stations are shown as red stars, except for the selected receiver which is shown as a red diamond.

6.6.3. Calculator Output

The calculator computes cumulative frequency-weighted sound exposure level (SEL) at a selected receiver location and depth from all shots from all seismic surveys specified. The modeled radial lengths

are 150 km, so surveys more distant than that from a receiver will not contribute to the calculated received SEL. The calculator computes the SEL contribution of each survey separately as follows:

5. Looks up the 1/3-octave band per-pulse SEL source levels based on the selected source type and depth, and the calculated direction to the receiver that depends on source and receiver locations and source tow direction.
6. Extracts the appropriate 1/3-octave band transmission loss levels based on the selected source depth and receiver depth and closest modeled radial passing by the source position.
7. Subtracts the transmission losses from the source levels in each frequency band to compute unweighted received per-pulse band levels.
8. Calculates the number of pulses in the survey based on the survey duration and pulse interval, and sums this number of received per-pulse SELs to calculate the unweighted band SEL for the entire survey.
9. Applies the 1/3-octave filter coefficients for the selected filter to the corresponding received band levels for the entire survey.
10. Sums the filtered 1/3-octave band received levels to compute a broadband filtered SEL for the survey as a single number.

The final cumulative frequency-weighted SEL at the receiver from all surveys is the sum of the results of individual surveys. The calculator displays the individual survey SELs and the total exposure. An example of this output is given in the screen capture below (note only the first 13 of 50 surveys is captured in the figure so the total exposure doesn't match the sum of those displayed):

Total exposure:
161.0 dB re 1 µPa·s²

Individual survey Exposures		
	Per-pulse	Per-survey
1	81.6	126.2
2	103.7	153.1
3	100.8	145.3
4	63.7	111.3
5	75.5	124.9
6	100.2	144.8
7	99.6	147.2
8	100.8	148.4
9	100.8	150.1
10	100.8	148.4
11	100.8	148.4
12	100.8	148.4
13	100.8	148.4

6.6.4. Discussion

Few studies of cumulative and chronic effects have involved quantitative assessments of the type this framework provides. There are no generally accepted methods for interpreting cumulative SEL in terms of chronic effects, and there are no thresholds defined for this use. In the Gulf of Mexico, seismic surveys continue year-round and, at least in deeper locations, the sounds from distant surveys contribute to a relatively continuous background noise field that is above natural ambient. Superimposed on this background field are the contributions of closer-range seismic surveys that have shorter durations, typically of a few weeks, but those surveys lead to substantially higher sound levels. Initial tests with the framework have shown that seismic surveys close to receivers dominate the received cumulative SEL, which raises questions about how to interpret the results, such as:

- Should chronic effects assessments neglect close-range surveys that produce higher received sound levels, but occur for limited periods, and if so, which surveys should be excluded?
- What errors are introduced by assuming fixed seismic survey locations for surveys that in reality can have large spatial extents that lead to significant received sound level variations?

The cumulative and chronic effects calculator framework developed here is being used to investigate such questions with a goal of developing systematic methods to deal with the issues. The framework will then be applied to assess potential chronic effects from seismic survey noise in the Gulf of Mexico.

7. Phase II: Marine Mammal Exposure Estimates

The goal of Phase II of this study was to estimate the yearly acoustic exposures received by marine mammals to geological and geophysical survey activities in the Gulf of Mexico for the coming decade. Phase I demonstrated and explored the basic methodological approach using agent-based animal movement in simulated sound fields as a Monte Carlo simulation to determine the probability of exposure. The results are specific to the survey simulated. The exact number, location, and configuration of future surveys are unknown, but yearly level-of-effort projections within planning areas for several survey types (including different sources) were provided by BOEM (Table 75). To evaluate the impact of exposure, a 24 h resetting time was chosen such that the received level of each animat was reset to zero after each 24 h evaluation period. In Test Scenario 1, it was found that location-specific characteristics of a survey, such as the acoustic propagation regime (e.g., shelf versus slope) or depth restrictions of animals had the greatest influence on the 24 h exposure estimates (as opposed to inherent modeling constraints, such as replacing animats as they move across the boundaries of the simulation). In Test Scenario 1, a method for scaling up simulation results to account for long-duration surveys was suggested. When using a resetting period (e.g., 24 h) the primary objective was to accurately estimate the average exposure within the reset period by ensuring that the simulation covered the various location-specific environments. The surveys may be conducted at any location within the planning area and occur at any time of the year, so the requirement was to adequately cover each area during the simulations. All survey simulations in Phase II are for 7 days and a sliding window approach was used to get the average 24 h exposure. The 24 h exposure levels were then be scaled by the level of effort for each survey type to calculate the yearly exposure levels.

7.1. Assumptions

In Phase II, the annual marine mammal acoustic exposure associated with geological and geophysical activity in the Gulf for the upcoming decade (2016–2025) used agent-based animal movement in simulated sound fields as Monte Carlo simulations to estimate the probability of exposure. The average number of animals exposed to levels exceeding threshold criteria in 24 h periods was scaled by the level of survey effort to determine the yearly number of potential individuals exceeding threshold for each species. The threshold criteria included the current NMFS criteria for potential injury (Level A harassment) and potential behavioral disruption (Level B harassment), and criteria for potentially injurious exposure based on Southall et al. (2007) and step-function criteria based on Wood et al. (2012) to evaluate potential behavioral disruption.

The situations simulated are complex and evolving. The time period evaluated was 10 years of future survey efforts using representative surveys whose precise design, location, and time of performance are not known. There is presently a great of variety in survey and source configurations, and new configurations, sources, or use of sources are likely to be developed. The details of marine mammal density, distributions, and behavior patterns are imprecisely known and change as animal populations vary from year to year and location to location.

When modeling complex situations with imperfect and incomplete data, assumptions must be made. When possible, the most representative data or methods were used. When necessary, the choices were made to be conservative, i.e., were expected to produce an overestimate. Conservative assumptions in the Phase II modeling procedures include:

- Environment parameters for acoustic propagation modeling: The environmental input parameters used for transmission loss modeling were from databases that provide averaged values with limited spatial and temporal resolution. Sound speed profiles are averaged seasonal values taken from many sample locations. Geoacoustic parameters (including sediment type, thickness, and reflectivity

coefficients) and bathymetric grids are smoothed and averaged to characterize large regions of the seafloor. Local variability, which can be effected by weather, daily temperature cycles, and small-scale surface and sediment details, generally increases signal transmission loss, but was removed by these averaging processes. As a result, the transmission loss could in some cases be underestimated and, therefore, the received levels would be overestimated.

- Acoustic propagation modeling: The acoustic propagation model, MONM, used the horizontal-direction source level for all vertical angles. This may slightly underestimate the true sound levels in the vertical directional beam of the array that ensonifies a zone directly under the array. This is expected to be a minor effect given the small volume over which the reduction occurs. Additionally, there is a steep angle limitation in the parabolic equation (PE) model used in MONM that also leads to slightly reduced levels directly under the array. The wide-angle PE that is used in MONMN is accurate to at least 70 degrees. The reduced-level zone is a cone within a cone few degrees of vertical, which represents a relatively small water volume that should not significantly affect results.
- Acoustic filtering: Auditory weighting functions were used to filter the SEL and rms SPL sound fields. Type II M-weighting based on equal loudness perception (Finneran and Jenkins 2012) was used to filter the SEL sound field used to evaluate potential injury. Type I M-weighting (Southall et al. 2007) was used to filter the rms SPL sound fields that, primarily, were used to evaluate behavior. Type I and Type II M-weighting are approximations of the hearing ability of different species groups. As approximations, they do not necessarily represent any one individual animal. Type I M-weighting was meant as a conservative filter to account for the expected hearing range of the species groups (Southall et al. 2007). The use of Type I filtering is a conservative choice because these filter roll-off at high and low frequencies admit more sound energy than the corresponding audiograms would suggest.
- Seasons modeled: To account for seasonal variation in propagation, winter (most conservative) and summer (least conservative) were both used to calculate exposure estimates. Propagation during spring and fall was found to be almost identical to the results for summer, so those seasons were represented with the summer results.
- Social grouping: Marine mammals often form social groups, or pods, that may number in the hundreds of animals. Although it was found that group size effects the distribution of the exposure estimates, the mean value of the exposure estimate was, generally, unchanged. Because the annual exposure estimates are meant to represent the aggregate of many surveys conducted in many locations at various times throughout the year, it is the mean exposure estimates that are most relevant. For this reason, social group size was not included in the exposure estimates.
- Mitigation: Mitigation procedures, such as shutting down an airgun array when animals are detected within an established exclusion zone, can reduce the injury exposure estimates. Mitigation effectiveness was found to be influenced by several factors, most importantly the ability to detect the animals within the exclusion zone. Some species are more easily detected than others, and detection probability varies with weather and observational set up. Weather during any seismic survey is unknown beforehand and detection probabilities are difficult to predict, so the effects of mitigation were not included in the exposure estimates.
- Aversion: Aversion is a context-dependent behavioral response affected by biological factors, including energetic and reproductive state, sociality, and health status of individual animals. Animals may avoid loud or annoying sounds, which could reduce exposure levels. Currently, too little is known about the factors that lead to avoidance (or attraction) of sounds to include aversive behavior in the exposure estimates.

7.2. Phase II Modeling Methods

7.2.1. Acoustic Source Parameters

7.2.1.1. Airgun Array—8000 in³

The airgun array parameters Phase II were the same as those used in the Test Case (Section 6.1).

7.2.1.2. Single Airgun—90 in³

This acoustic source consists of a single Sercel airgun with a working firing volume of 90 in³. This source was used in a high-resolution geotechnical survey. The modeling assumed a tow depth of 4 m for the airgun, which was typical for this source type. The model assumed an operating pressure of 2000 psi.

7.2.1.3. Boomer

The representative boomer system for geotechnical survey operations was the Applied Acoustics AA301, based on a single plate with ~ 40 cm baffle diameter. Since the boomer plate has a circular piston surrounded by a rigid baffle, it has acoustic directivity and cannot be considered a point-like source (Verbeek and McGee 1995). The beam pattern of a boomer plate shows directivity for frequencies above 1 kHz. The input energy for the AA301 boomer plate was up to 350 J per pulse or 1,000 J per second. The width of the pulse was 0.15–0.4 ms.

Source: Applied Acoustic Engineering Limited. Accessed January 2015

A source verification study was performed on a system similar to the AA301, the AP3000 system (Martin et al. 2012), which has a double-plate configuration operating at maximum input energy of 1,000 J. During the Martin et al. (2012) study, acoustic data were collected as close as 8 m to the source and directly below it. The data showed that the broadband source level for the system was 203.3 dB 1 µPa @ 1 m rms SPL over a 0.2 ms window length and 172.6 dB re 1 $\mu Pa^2 \cdot s$ @ 1 m SEL. Data from the AP3000 were used in this study for modeling the boomer source.

7.2.1.4. High Resolution Survey Sources

An autonomous underwater vehicle (AUV) may be used when performing high-resolution geotechnical surveys. Three types of survey equipment may be installed on the AUV:

- Multibeam echosounder
- Side-scan sonar
- Sub-bottom profiler

All three sources can operate concurrently, and typically do, although there may be times when one or two of the three is off. In our modeling, we assume that all three were operated concurrently. When sources were towed, the towing depth of the AUV was 4 m below the sea surface when the water depth was less than 100 m, and 40 m above the seafloor where water depth was more than 100 m. High resolution geophysical surveys are not always towed by an AUV, but in this modeling effort, the sources were assumed to be towed by an AUV.

7.2.1.4.1. Multibeam Echosounder—Simrad EM2000

The representative multibeam echosounder system for geotechnical survey operations was the Simrad EM2000 (manufactured by Kongsberg Maritime AS). This device operates at 200 kHz (Kongsberg 2004). The system is equipped with an SM2000 transducer head that produces a single beam 17°× 88° wide. The multibeam forming occurs through receiving head and processing software. The nominal source level was 204 dB re 1 µPa @ 1 m. The per-pulse SEL depends on the pulse length.

Operational parameters of the Simrad EM2000 multibeam echosounder system (Kongsberg 2004) are:

- Operating frequency: 200 kHz
- Beam width: 17°× 88°
- Beam: 1 (straight down)
- rms SPL: 203 dB re 1 µPa @ 1 m
- Pulse length: 0.04–1.3 ms
- Per pulse SEL: 160–175 dB re 1 $\mu Pa^2 \cdot s$ @ 1 m

7.2.1.4.2. Side-scan Sonar—EdgeTech 2200 IM

EdgeTech 2200 IM was a representative modular system designed for installation on an AUV. The system features full spectrum chirp side-scan capabilities that work at two frequencies concurrently, 120 and 410 kHz. The side-scan sonar uses two side-mounted rectangular transducers, whose declination angle can be adjusted from 10° to 20° below the horizontal plain. The produced beam angle was 70° × 0.8° at 120 kHz and 70° × 0.5° at 410 kHz. At 120 kHz, we estimated the peak level at 210 dB re 1 µPa @ 1 m; at 410 kHz, we estimated the peak level at 216 dB re 1 µPa @ 1 m (EdgeTech 2007). The pulse length was 8.3 ms at 120 kHz and 2.4 ms at 410 kHz.

7.2.1.4.3. Sub-bottom Profiler—EdgeTech 2200 IM with DW−424

EdgeTech 2200 IM was a representative modular system designed for installation on an AUV. The system features DW−424, a full spectrum chirp sub-bottom profiler that produces a sweep signal in the frequency range from 4 to 24 kHz. The transmitter is a circular transducer directed straight down. The projected beamwidth varies from 15° to 25° depending on the emitted frequency. The source level was 200 dB re 1 µPa @ 1 m (EdgeTech 2007). The pulse length was 10 ms.

7.2.2. Survey Patterns

To estimate exposures, we considered two major survey types:

- Large area seismic
- Small-area, high-resolution geotechnical study

The primary differences between each survey were the energy of the sources, the size of the areas, and the density of the tracks.

Large area seismic surveys cover more than 1,000 square miles and include 2-D, 3-D NAZ, 3-D WAZ, and Coil types. An 8000 in^3 airgun array was the primary source for the large area seismic surveys. The large surveys use a survey vessel with an average speed of 4.5–5 knots; it travels 200–220 linear km per day. No mitigation airguns were modeled, and airgun arrays were off during turns.

Geotechnical study surveys cover an area less than 100 mi^2 and use small airgun arrays (20–90 in^3) and/or high-frequency electromechanical sources (sonars) installed on an AUV. The high resolution sources included a side-scan sonar, a sub-bottom profiler, and a multibeam echosounder. The survey vessel used in the large surveys travels at an average speed of 4 kts; it transits 180 km per day.

Although parameters of the actual surveys could vary from one survey to the other, we selected specific parameters to model based on specifications provided by BOEM. The subsections herein describe the parameters of each survey type as they were modeled for Phase II.

Table 47. Summary of the Phase II surveys considered to determine the exposure estimates. The high resolution sources were modeled independently.

Survey type	Area	Source	Production lines lateral offset (km)
2-D	10 × 30 blocks 48 × 145 km 2700 mi^2	1 × 8000 in^3	4.8
3-D NAZ		2 × 8000 in^3	1
3-D WAZ		4 × 8000 in^3	1.2
Coil	12 × 12 blocks 58 × 58 km 1300 mi^2	4 × 8000 in^3	not applicable
Geotechnical	1 × 3 blocks 5 × 14.5 km 27 mi^2	1 × 90 in^3 high resolution sources	0.03

The survey schematics indicate the survey area (black rectangle) and vessel tracks. The tracks for different vessel are shown with different colors. To simplify the track design for the surveys using a racetrack fill-in method, the actual circular turn track was substituted with three straight legs: run-out, offset, and run-in sections. The run-in and run-out sections were 1 km long and extend beyond the survey area.

7.2.2.1. 2-D Seismic Survey

The 2-D seismic survey was performed with a single vessel towing a single large seismic array. The lateral spacing of the production lines was 4.8 km (Figure 105). The production lines were filled in with a racetrack fill-in method, skipping two tracks on the left side turn (15 km wide turn) and transitioning on to the adjacent line on the right side turn (5 km wide turn). Seven days of survey were simulated. The vessel speed was 4.5 kts (2.3 m/s). The shot interval was 21.6 s (50 m). The total length of the simulated track was ~ 1400 km. The number of simulated pulses was ~ 28,000. Constant towing azimuth, parallel to the long side of the survey box, was modeled for all shots.

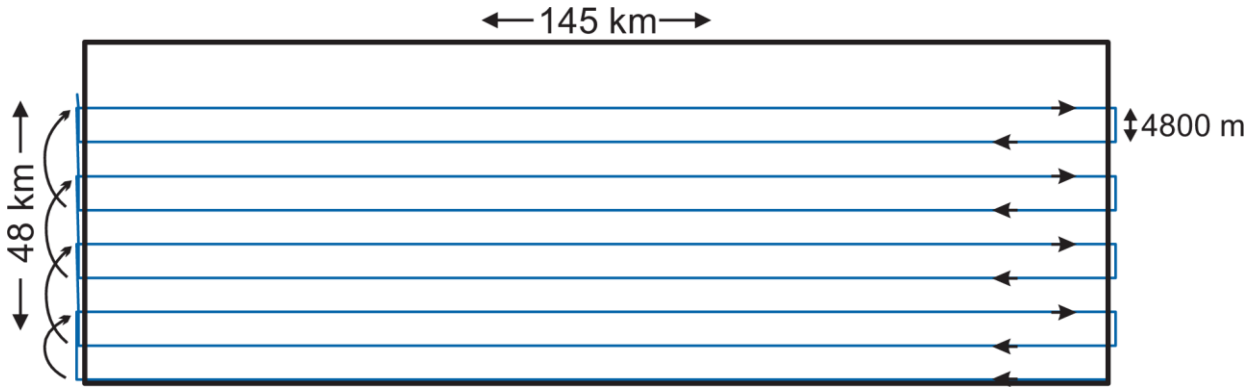

Figure 105. Simulated portion of the track for the 2-D seismic survey.

7.2.2.2. 3-D Narrow Azimuth Seismic Survey

The 3-D NAZ seismic survey was performed with one or two vessels towing two identical large seismic arrays. The sources towed by the same vessel were operated in a flip-flop mode, i.e., for each shot position only one of the two produces a seismic pulse. In the two-vessel option, sources at each vessel produce seismic pulses simultaneously. The two-vessel option was simulated. Both vessels follow the same track, but were separated along the track by 6,000 m. The production lines were laterally spaced by 1 km (Figure 106). The production lines were filled via a racetrack fill-in method with eight loops in each racetrack (7–8 km wide turn). Forty-nine lines were required to fully cover the survey area. The 7-day simulation covered ~ 20% of the complete survey. The vessel speed was 4.9 kts (2.5 m/s). The shot interval was 15 s (37.5 m) for each vessel. The total length of the simulated track was ~ 1500 km. The number of simulated pulses was ~ 80,000.

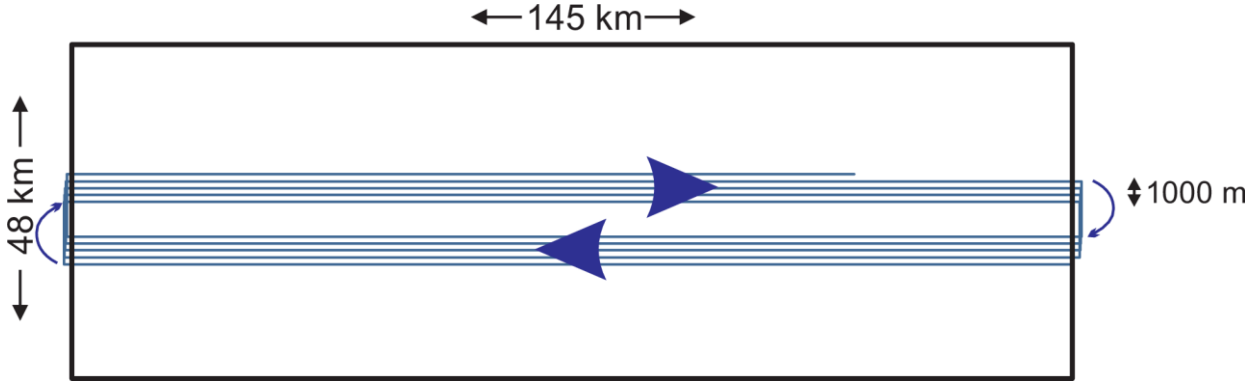

Figure 106. Simulated portion of the track for the 3-D NAZ seismic survey.

7.2.2.3. 3-D Wide Azimuth Seismic Survey

The3-D WAZ seismic survey was performed with multiple vessels traveling along parallel tracks with some lateral and along the track offsets. The four-vessel option with seismic sources firing sequentially was simulated. The tracks of each vessel had the same geometry and had 1,200 m lateral offset. The vessels also had 500 m offset along the track. The lateral spacing of the same vessel's production lines was 4.8 km and 1.2 km for the group (Figure 107). The production lines were filled in with a racetrack fill-in method with two loops in each racetrack (9.6 km wide turn). Forty lines were required to fully cover the survey area. The 7-day simulation covered ~ 85% of the complete survey. The vessel speed was

4.5 kts (2.3 m/s). The shot interval was 86.4 s (200 m) for each vessel or 21.6 for the group. The total length of the simulated track was ~ 1400 km. The number of simulated pulses was ~ 28,000.

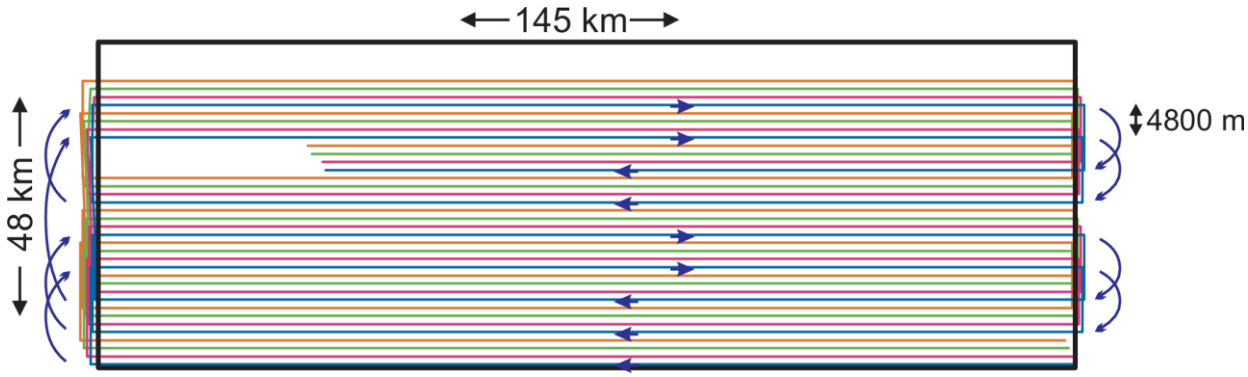

Figure 107. Simulated portion of the track for the 3-D WAZ seismic survey.

7.2.2.4. Coil Seismic Survey

The Coil seismic survey was performed by multiple vessels that sailed a series of circular tracks with some angular separation while towing sources. The four-vessel option was simulated assuming simultaneous firing, and the track consisted of a series of circles with 12.5 km diameter (Figure 108). Once the vessel completes a full circle, it advanced to the next one along a tangential connection segment. The offset between the center of one circle and the next, either along-swath or between swaths, was 5 km. The full survey geometry consisted of two tracks with identical configuration with 1,200 m and 600 m offsets along X and Y directions, respectively. Two of the four vessels followed the first track with 180° separation; the other two vessels followed the second track with 180° separation relative to each other and 90° separation relative to the first pair. One hundred circles per vessel pair were required to fully cover the survey area. The 7-day simulation covered ~ 30% of the complete survey. The vessel speed was 4.9 kts (2.5 m/s). The shot interval was 20 s (50 m) for each vessel. The total length of the simulated track was ~ 1,500 km. The number of simulated pulses was ~ 120,000.

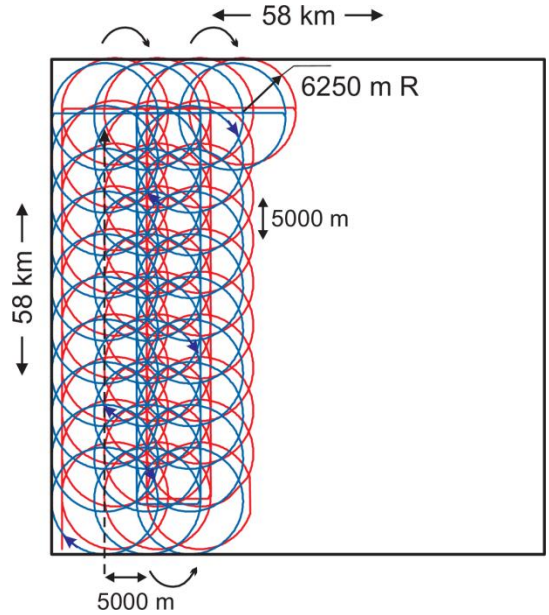

Figure 108. Simulated portion of the track for the Coil seismic survey.

7.2.2.5. High Resolution Geotechnical Survey

The geotechnical survey was performed in a similar fashion as the 2-D and 3-D surveys, only on significantly smaller survey areas and with denser production lines.

A single vessel survey was considered for the simulation, towing either a 90 in³ airgun or a high resolution source equipped with a side-scan sonar, a sub-bottom profiler, and a multibeam echosounder. Production lines were laterally spaced 30 m (Figure 109) then filled in with a racetrack fill-in method where each racetrack has 20 loops (1.2 km wide turn). One hundred and sixty lines were required to fully cover the survey area. The 7-day simulation covered ~ 50% of the complete survey. The vessel speed was 4 kts (2 m/s). The shot interval was 10 s (20 m). The total length of the simulated track was ~ 1260 km. The number of simulated pulses was ~ 60,000.

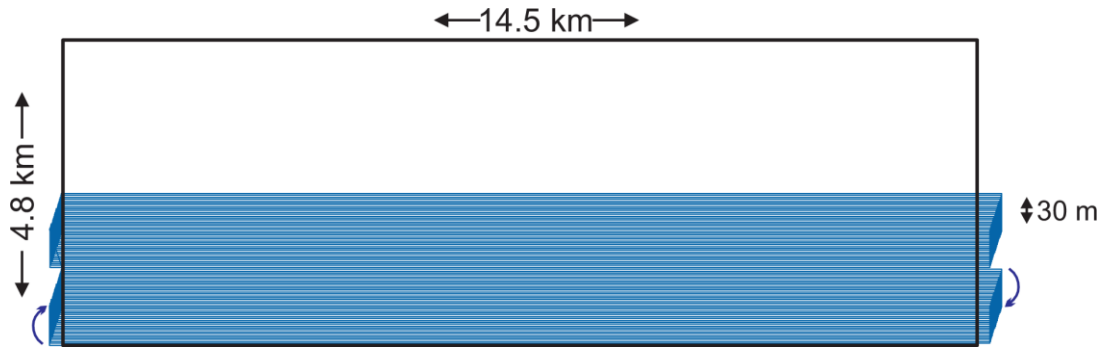

Figure 109. Simulated portion of the track for the geotechnical survey.

7.2.3. Choice of Zone Boundaries

The size and shape of acoustic footprints from exploration surveys in the Gulf of Mexico are influenced by many parameters, but the strongest influencers are water depth and seabed slope. We divided the project area into three main bathymetric areas Shelf, Slope, and Deep. The Shelf extend from shore to 100–200 m depths, where bathymetric relief is gradual; water depths on the continental shelf off Florida's eastern coast are less than 200 m deep out to ~ 150 km from shore. The Slope starts at the Shelf's outer boundary and extends into deeper water where the seabed relief is steeper and water deepens from 100–200 m to 1500–2500 m over as little as a 50 km horizontal distance. The Slope ends at the Deep area, where, although water depths are more consistent than in the other areas, depths can vary from 2000–3300 m. The subdivision depth definitions are Shelf: 0–200 m, Slope 200–2000 m, and Deep: > 2000 m.

Water depth influences species distribution in that there are distinctions from Shelf to Slope and from Slope to Deep. The maps in Appendix A show marine mammal distribution information from the Marine Geospatial Ecology Laboratory (Duke University) model (Roberts et al. In preparation; Section 7.2.6) and the subdivision depth boundary contours. The subdivision depths were chosen so that nominal marine mammal densities remain relatively constant over the resulting depth intervals. While different species prefer different depths, there are optimal depth breaks based on density distribution for the majority of species considered. The density of several species varies within the Shelf and Slope areas, but less so within the Deep area. Interestingly, the variation in animal density within the Shelf and Slope areas seems correlated with the orientation and differences in the widths of these areas over the east-west extent of the project area. The western region is characterized by a relatively narrow shelf and moderate-width slope. The central region has a moderate-width shelf and moderate-width slope, and the eastern region has a wide shelf and a very narrow slope. Because of these differences, areas were further division into lateral regions, which align with the previously defined BOEM Planning Area boundaries: West, Central, and East, was made in the Shelf and Slope areas.

Based on the physical properties of the project area and the distribution of its marine inhabitants, we divided the Gulf into 7 zones: 3 Shelf zones, 3 Slope zones, and 1 Deep zone. The southern edge of the Deep zone is defined by the U.S. Exclusive Economic Zone (EEZ) boundary. The zones boundaries were defined by the 200 and 2000 m depth contours and the east-west boundary lines of BOEM's Planning Areas (except for the Deep zone 7, which included portions of all three Planning Areas). The seven modeling zones, labelled "zones" are shown in Figure 110 along with the seven representative simulation locations—the numbered rectangles—which are discussed in the next section.

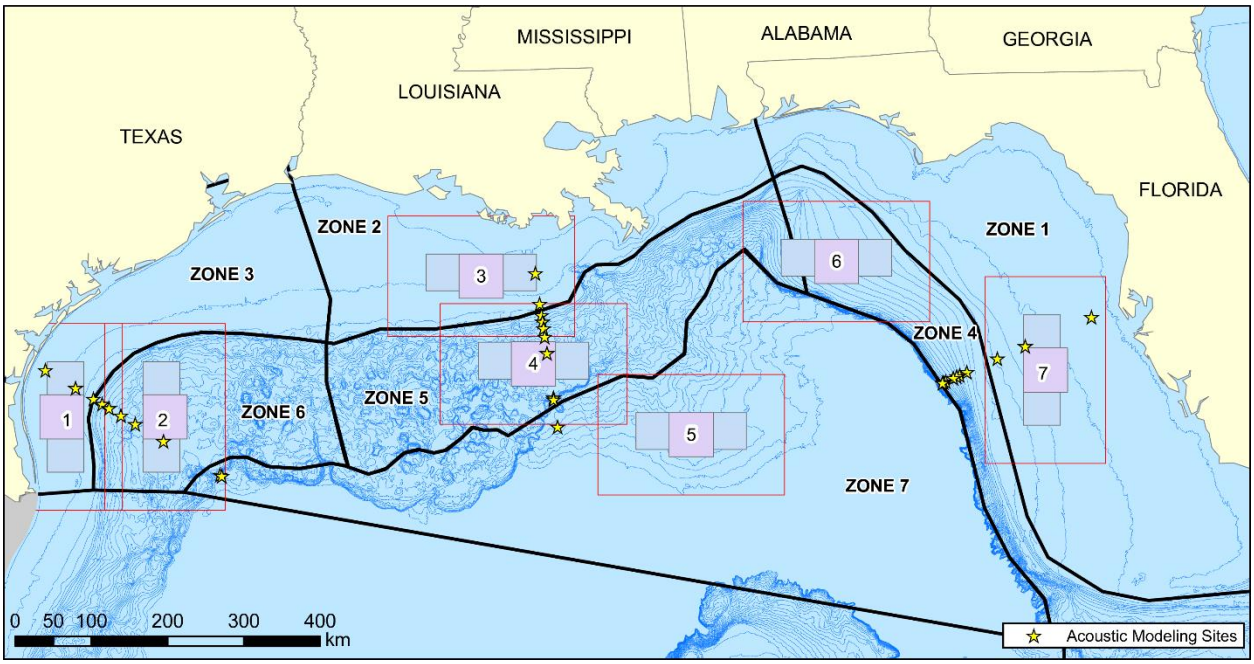

Figure 110. Gulf of Mexico project area. Black lines delineate the zones. Large, red rectangular boxes show the animal simulation extents for seismic surveys. Gray rectangles are the survey area extents for the 2-D and 3-D surveys. Pink squares are the survey extents of Coil surveys. Yellow stars show the acoustic modeling sites are along West, Central, and East transects.

7.2.3.1. Survey Extents

Within each of the seven zones, we defined a set of representative survey-simulation rectangles for each of the survey types discussed in Section 7.2.2. To avoid clutter in the diagram, Figure 110 shows the rectangles for the largest area surveys (2-D, 3-D, and Coil). Smaller area surveys (geotechnical surveys) were modeled near the center of the larger area surveys. During the seismic survey simulation, the source was moved within these rectangles. The sound produced, however, would ensonify an area larger than the rectangle. The corresponding animat simulation extents are shown as large, red boxes (Figure 110) and are discussed in more detail in Section 7.2.5.

7.2.3.2. Acoustic Modeling Sites

As the acoustic energy from a source propagates, it is subject to a number of marine acoustic effects that depend on the ocean and bottom environment (see Section 5.2). We selected a set of 30 sites to calculate acoustic propagation loss grids as functions of source, range from the source, azimuth from the source, and receiver depth. We then used these grids as inputs to the acoustic exposure model. The 30 modeling sites (yellow stars in Figure 110) were grouped into three transects—Western, Central, and Eastern. The detailed geographic coordinates and water column depth of each acoustic modeling site are listed in

Tables 48–51 for each transect. The coordinates of the center of survey locations are shown in Table 51. Even though these 30 modeling sites were not all located within the survey extents (boxes) discussed in the previous section, and Boxes 5 and 6 do not contain any individual modeling sites, the environmental parameters and acoustic propagation conditions represented by these 30 modeling sites were chosen to be representative of the prevalent acoustic propagation conditions within the survey extents (boxes).

Table 48. Modeling sites along the West transect.

Region	Site	Geographic coordinates	UTM Zone 15 coordinates		Water depth at source (m)
West-Shelf	WS1	27° 24.77′ N 97° 5.78′ W	3038833 N	94877 E	25
	WS2	27° 12.59′ N 96° 41.28′ W	3015053 N	134623 E	75
	WS3	27° 5.40′ N 96° 26.93′ W	3001087 N	157967 E	150
West-Slope	WM1	27° 1.94′ N 96° 20.06′ W	2994389 N	169162 E	300
	WM2	26° 59.07′ N 96° 14.39′ W	2988854 N	178414 E	500
	WM3	26° 54.23′ N 96° 4.82′ W	2979509 N	194032 E	750
	WM4	26° 48.37′ N 95° 53.29′ W	2968231 N	212884 E	1000
	WM5	26° 36.82′ N 95° 30.73′ W	2946105 N	249866 E	1500
West-Deep	WD1	26° 13.56′ N 94° 45.86′ W	2901905 N	323744 E	2000
	WD2	26° 12.73′ N 94° 44.29′ W	2900349 N	326344 E	2500

In the site names, S denotes a Shelf site, M a Slope (middle) site, and D a deep site.

Table 49. Modeling sites along Central transect.

Region	Site	Geographic coordinates	UTM Zone 15 coordinates		Water depth at source (m)
Central-Shelf	CS1	28° 35.84′ N 90° 34.27′ W	3165787 N	737510 E	25
	CS2	28° 14.08′ N 90° 31.20′ W	3125696 N	743350 E	75
	CS3	28° 6.06′ N 90° 30.07′ W	3110922 N	745502 E	150
Central-Slope	CM1	28° 1.19′ N 90° 29.39′ W	3101933 N	746812 E	300
	CM2	27° 56.60′ N 90° 28.74′ W	3093482 N	748043 E	500
	CM3	27° 50.68′ N 90° 27.91′ W	3082567 N	749633 E	750
	CM4	27° 39.14′ N 90° 26.30′ W	3061316 N	752729 E	1000
	CM5	27° 7.28′ N 90° 21.85′ W	3002614 N	761280 E	1500
Central-Deep	CD1	27° 5.87′ N 90° 21.66′ W	3000015 N	761658 E	2000
	CD2	26° 46.56′ N 90° 18.98′ W	2964438 N	766841 E	2500

In the site names, S denotes a Shelf site, M a Slope (middle) site, and D a deep site.

Table 50. Modeling sites along East transect.

Region	Site	Geographic coordinates	UTM Zone 15 coordinates		Water depth at source (m)
East-Shelf	ES1	27° 45.04′ N 83° 12.99′ W	3108253 N	1466813 E	25
	ES2	27° 28.13′ N 84° 6.79′ W	3070008 N	1380052 E	75
	ES3	27° 20.87′ N 84° 29.42′ W	3053885 N	1343477 E	150
East-Slope	EM1	27° 12.89′ N 84° 54.04′ W	3036311 N	1303609 E	300
	EM2	27° 10.97′ N 84° 59.89′ W	3032133 N	1294132 E	500
	EM3	27° 10.13′ N 85° 2.47′ W	3030284 N	1289936 E	750
	EM4	27° 9.30′ N 85° 5.00′ W	3028478 N	1285839 E	1000
	EM5	27° 7.24′ N 85° 11.27′ W	3023996 N	1275672 E	1500
East-Deep	ED1	27° 6.69′ N 85° 12.93′ W	3022805 N	1272969 E	2000
	ED2	27° 6.40′ N 85° 13.79′ W	3022193 N	1271580 E	2500

In the site names, S denotes a Shelf site, M a Slope (middle) site, and D a deep site.

Table 51. Center coordinates of survey boxes.

Box	Geographic coordinates	UTM Zone 15 coordinates		Water depth at source (m)
1	26° 51.96′ N 96° 47.61′ W	2977239 N	123022 E	70
2	26° 53.66′ N 95° 31.78′ W	2977239 N	248731 E	1400
3	28° 36.94′ N 91° 17.84′ W	3166579 N	666464 E	30
4	27° 34.03′ N 90° 37.10′ W	3051524 N	735128 E	1000
5	26° 40.82′ N 88° 33.67′ W	2958720 N	941905 E	2400
6	28° 38.72′ N 86° 32.18′ W	3185841 N	1132432 E	500
7	27° 10.49′ N 83° 54.20′ W	3038730 N	1403352 E	70

7.2.4. Environmental Parameters

7.2.4.1. Bathymetry

Water depths throughout the modeled area were obtained from the National Geophysical Data Center's U.S. Coastal Relief Model l (NGDC 2014) that extends up to about 200 km from the U.S. coast. These bathymetry data have a resolution of 3 arc-seconds (~ 80 × 90 m at the studied latitude). Bathymetry data for an area were extracted and re-gridded, using the minimum curvature method, onto a Universal Transverse Mercator (UTM) Zone 15 coordinate projection with a horizontal resolution of 50 × 50 m.

Two bathymetry grids were used for modeling. The first covered the West region (Boxes 1 and 2 in Figure 110); the second covered Central and East regions (Boxes 3–7 in Figure 110).

7.2.4.2. Multi-Layer Geoacoustic Profile

The top sections of the sediment cover in the Gulf of Mexico are represented by layers of unconsolidated sediments at least several hundred meters thick. The grain size of the surficial sediments follows the general trend for the sedimentary basins: the grain size of the deposited sediments decreases with the distance from the shore. For the Shelf zone, the general surficial bottom type was assumed to be sand, for

the Slope zone silt, and for the Deep zone clay. In constructing a geoacoustic model for input to MONM (see 6.5.2.1.5 for required input parameters), a median value of φ was selected for each sediment type with the exception of the geoacoustic profile for the East-Shelf area. Because the grain size of the surficial sediment offshore Florida is consistently larger than in other shelf areas (Figure 50), we assumed φ equal to 1 for the sand in this zone.

Four sets of geoacoustic parameters were used in the acoustic propagation modeling:

- Center-West Shelf (Table 52)
- East Shelf (Table 53)
- Slope (Table 54)
- Deep (Table 55)

Table 52. Shelf zone Center and West: Geoacoustic properties of the sub-bottom sediments as a function of depth, in meters below the seafloor (mbsf), for fine sand. Within each depth range, each parameter varies linearly within the stated range.

Depth below seafloor (m)	Material	Density (g/cm^3)	P-wave speed (m/s)	P-wave attenuation (dB/λ)	S-wave speed (m/s)	S-wave attenuation (dB/λ)
0–20	Sand $\varphi=2$	1.61	1610	0.62	200	0.76
20–50		1.7	1900	1.44		
50–200		1.78	2090	1.77		
200–600		1.87	2500	2.31		
> 600		2.04	2500	2.67		

Table 53. Shelf zone East: Geoacoustic properties of the sub-bottom sediments as a function of depth, in meters below the seafloor (mbsf), for medium-sand. Within each depth range, each parameter varies linearly within the stated range.

Depth below seafloor (m)	Material	Density (g/cm^3)	P-wave speed (m/s)	P-wave attenuation (dB/λ)	S-wave speed (m/s)	S-wave attenuation (dB/λ)
0–20	Sand $\varphi=1$	1.7	1660	0.76	200	1.13
20–50		1.78	2040	1.68		
50–200		1.87	2290	2.03		
200–600		1.96	2500	2.56		
> 600		2.04	2500	2.91		

Table 54. Slope zone: Geoacoustic properties of the sub-bottom sediments as a function of depth, in meters below the seafloor (mbsf), for medium silt. Within each depth range, each parameter varies linearly within the stated range.

Depth below seafloor (m)	Material	Density (g/cm^3)	P-wave speed (m/s)	P-wave attenuation (dB/λ)	S-wave speed (m/s)	S-wave attenuation (dB/λ)
0–20	Silt $\varphi=6$	1.44	1515	0.33	150	0.22
20–50		1.7	1670	0.82		
50–200		1.7	1750	1.07		
200–600		1.87	1970	1.48		
> 600		2.04	2260	1.82		

Table 55. Deep zone: Geoacoustic properties of the sub-bottom sediments as a function of depth, in meters below the seafloor (mbsf), for medium clay. Within each depth range, each parameter varies linearly within the stated range.

Depth below seafloor (m)	Material	Density (g/cm^3)	P-wave speed (m/s)	P-wave attenuation (dB/λ)	S-wave speed (m/s)	S-wave attenuation (dB/λ)
0–20	Clay $\varphi=9$	1.52	1472	0.17	100	0.06
20–50		1.7	1560	0.43		
50–200		1.78	1610	0.56		
200–600		1.87	1720	0.83		
> 600		2.04	1890	1.05		

7.2.4.3. Sound Speed Profiles

The sound speed profiles for the modeled sites were derived using the same source and method as described in Section 6.2.4.

We investigated variation in the sound speed profile throughout the year and produced a set of 12 sound speed profiles, each representing one month, in the Shelf, Slope, and Deep zones (Figure 111). The set was divided into four seasons:

- Season 1: January, February, and March
- Season 2: April, May, and June
- Season 3: July, August, and September
- Season 4: October, November, and December

For each zone, a month was selected to represent the propagation conditions in the water column in each season (Table 56).

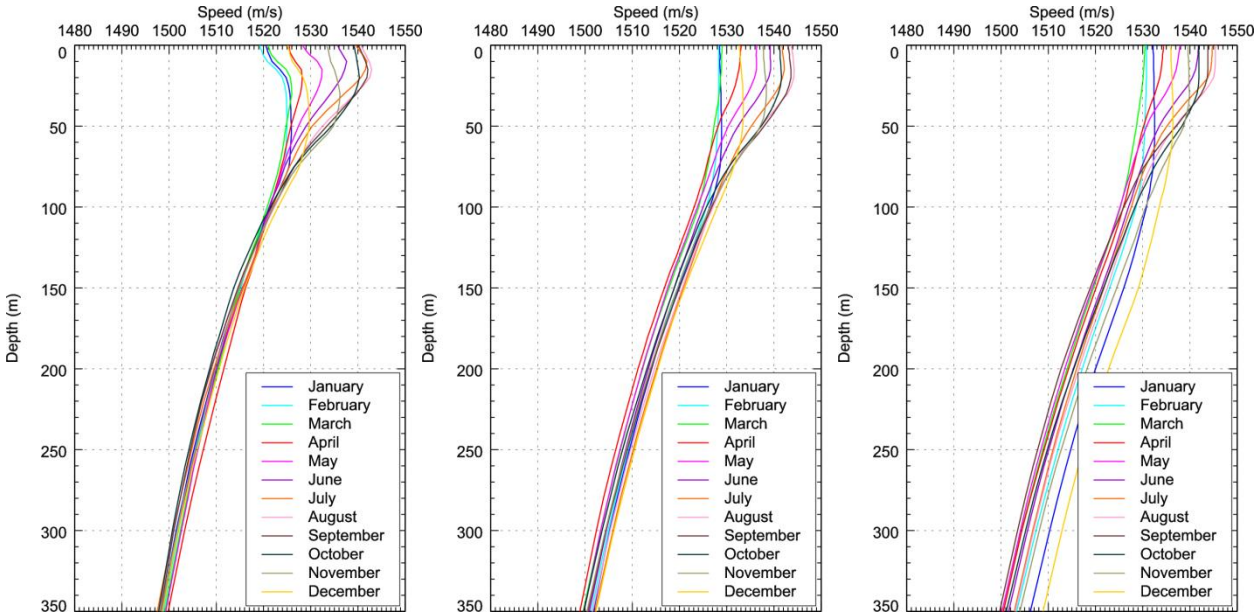

Figure 111. Sound speed profiles at the (left) Shelf, (center) Slope, and (right) Deep zones, derived from data obtained from GDEM V 3.0 (Teague et al. 1990, Carnes 2009).

Table 56. Representative months for each season and modeling zone.

Zone	SSP GDEM location	Season 1 (Jan-Mar)	Season 2 (Apr-Jun)	Season 3 (Jul-Sep)	Season 4 (Oct-Dec)
Shelf	25.5° N 90° W	Feb	May	Aug	Oct
Slope	27.25° N 90° W			Sep	Nov
Deep	28.5° N 90° W			Aug	Dec

ssp=sound speed profile

Acoustic fields were modeled using sound speed profiles for Season 1 and Season 3, and all three regions—East, Central, and West—used the same month. Profiles for Season 1 (February) provided the most conservative propagation environment because a surface duct, caused by upward refraction in the top 50–75 m, was present. Although a surface duct of this depth will not be able to prevent leakage of frequencies below 500–250 Hz (respectively), the ducting of frequencies above this cut off is important because these are the frequencies to which most marine mammals are most sensitive and the horizontal far-field acoustic projection from the airgun array seismic sources do have significant energy in this part of the spectrum. The modeling results obtained when the duct was present, therefore, represent the most precautionary propagation environment. Profiles for Season 3 (August or September) provided the least conservative results because they have weak to no sound channels at the surface and are strongly downward refracting in the top 200 m. Only the top 100 m of the water column are affected by the seasonal variation in the sound speed.

The possibility of separately modeling the spring and fall seasons was investigated; however, the results for spring and fall are almost identical to the results for summer, which were used as a proxy for the spring and fall results.

7.2.4.3.1. Sound Speed Profiles for Box Centers

Sound speed profiles were gathered from the center of each modeling box for Seasons 1 and 3. Table 57 presents the months modeled for each of these seasons. Figures 112 and 113 show the sound speed profiles for Seasons 1 and 3, respectively.

Table 57. Modeling seasons for each box.

Box	Region	Zone	Season 1	Season 3
1	West	Shelf	Feb	Aug
2		Slope		Sep
3	Central	Shelf		Aug
4		Slope		Sep
5		Deep		Aug
6	East	Slope		Sep
7		Shelf		Aug

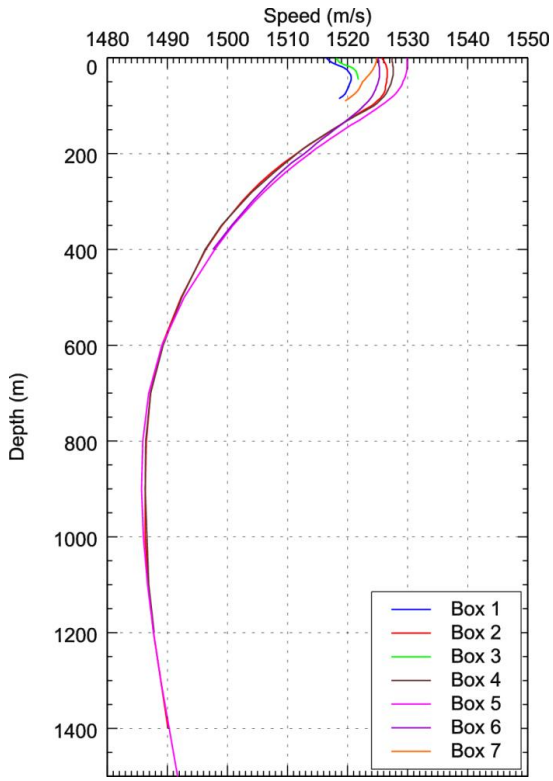

Figure 112. Sound speed profiles at modeling boxes, Season 1, derived from data obtained from GDEM V 3.0 (Teague et al. 1990, Carnes 2009).

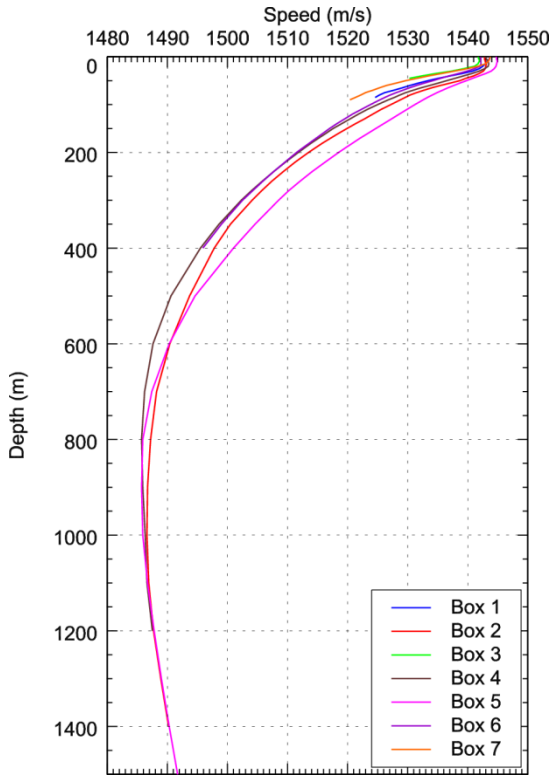

Figure 113. Sound speed profiles at modeling boxes, Season 3, derived from data obtained from GDEM V 3.0 (Teague et al. 1990, Carnes 2009).

7.2.4.3.2. Sound Speed Profiles for Acoustic Modeling Sites along Transects

Sound speed profiles were obtained at three locations along each transect. Profiles were selected for Season 1 and Season 3. The months modeled for each season are presented in Table 58. Figures 114–116, show the sound speed profiles for transects in the West, Central, and East regions respectively.

Table 58. Modeling seasons for the sites along transects.

Region	Zone	Season 1	Season 3
West	Shelf	Feb	Aug
	Slope		Sep
	Shelf		Aug
Central	Shelf		Aug
	Slope		Sep
	Shelf		Aug
East	Shelf		Aug
	Slope		Sep
	Deep		Aug

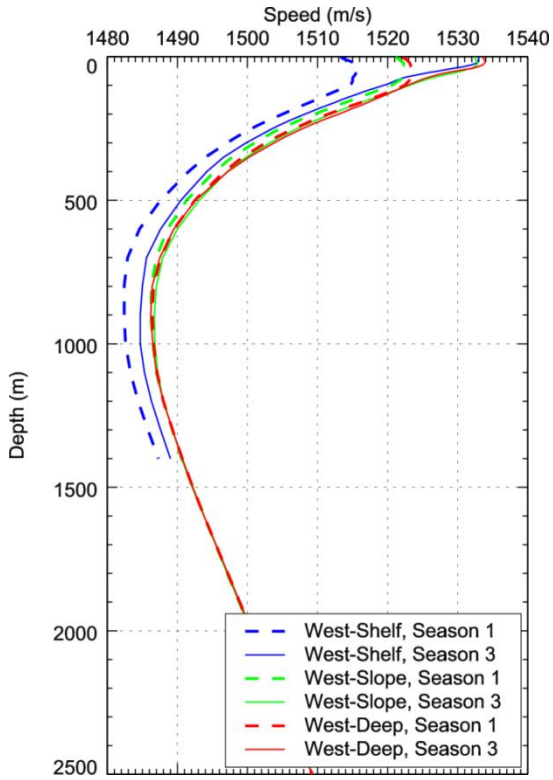

Figure 114. Sound speed profiles along the West transect, derived from data obtained from GDEM V 3.0 (Teague et al. 1990, Carnes 2009).

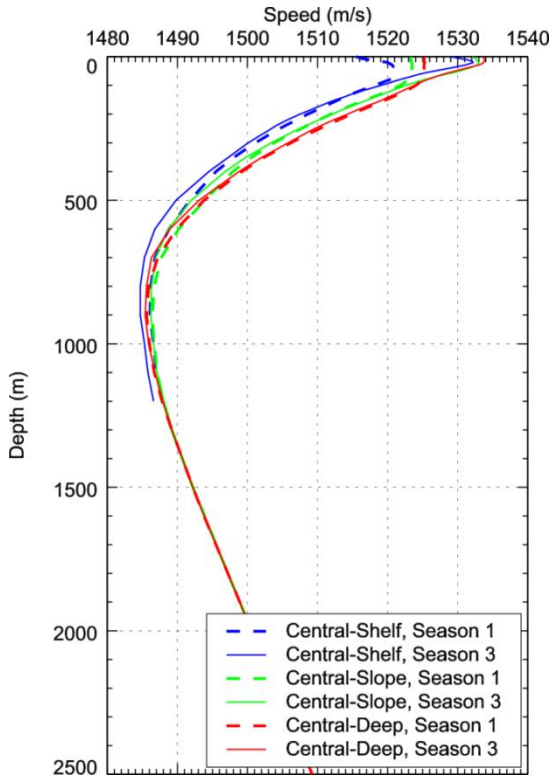

Figure 115. Sound speed profiles along Central transect, derived from data obtained from GDEM V 3.0 (Teague et al. 1990, Carnes 2009).

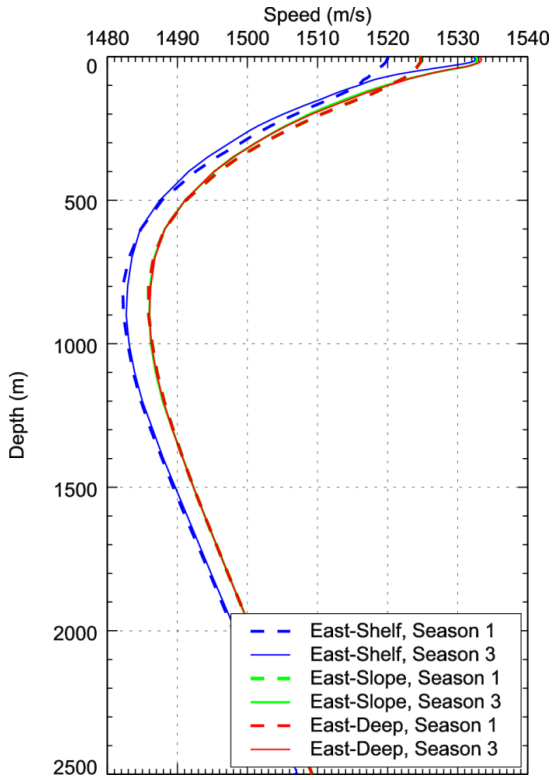

Figure 116. Sound speed profiles along East transect, derived from data obtained from GDEM V 3.0 (Teague et al. 1990, Carnes 2009).

7.2.5. 3MB Simulation Areas

The extents of the surveys were determined (Section 7.2.3.1), and the boxes surrounding the surveys for animat movement simulation were introduced (Figure 110, large red rectangles). These animat simulation boxes set the geographic limits of the 3MB simulation defined by the 3MB bathymetry file input. For large seismic surveys, potential behavioral disruption and NMFS criteria (for injury and behavior) were evaluated using the boxes shown Figure 110. Because potential injury assessed with SEL and peak SPL exposure criteria occurs at higher received levels (i.e., closer to the source) than those used to assess behavioral disruption and the NMFS criteria, the injury exposure boxes can be smaller than the behavioral disruption boxes. The extents of the simulation boxes for the surveys are described below.

7.2.5.1. Large Seismic Surveys

For the large seismic surveys, the injury simulation boxes extend outward (north, south, east, and west) by 10 km from the survey limits (Table 59), a distance over which the unweighted received levels drop below 160 dB re 1 µPa²·s SEL for a single shot. This injury simulation box was therefore much larger than the area that would enclose received levels less than the high frequency-weighted 161 dB re 1 µPa²·s SEL criterion, even for multiple shot accumulation. The behavior simulation boxes, on the other hand, extend outward by 50 km from the survey limits (Table 60), a distance necessary to ensure that the animat movement modeling extends out to where the M-weighted received levels drop to 120 dB re 1 µPa rms SPL or lower, and below 160 dB re 1 µPa²·s SEL for unweighted received levels.

Since injury events are intrinsically rare, improved statistical assessment was achieved by using a higher animat modeling density, and prorating the final exposure estimates by the real-world species density in

the final stage of the statistical analysis. The smaller injury simulation boxes, relative to the behavior simulation boxes, allows for higher modeling density to be used for injury without incurring a corresponding additional cost in computation time because the geographical area was smaller.

Because the 3MB modeling of animat movement requires significant computer resources, and lengthy computer run times, the same 3MB animat movement model results files were reused for the different large seismic surveys (although different for injury and behavior simulations), i.e., the 2-D, 3-D, and Coil surveys. Based on range to the received level limits, the animal simulation areas were large enough to satisfy the geographical extent requirements in each of the four cardinal directions.

Table 59. Geographic extent of the animat movement boxes for behavior simulation with the large seismic surveys.

Box	South latitude limit (degrees)	North latitude limit (degrees)	West longitude limit (degrees)	East longitude limit (degrees)
1	25.7385828	27.9873227	−97.697267	−96.035589
2	25.7750253	28.0114215	−96.324378	−94.686512
3	27.8386100	29.2946720	−92.552590	−90.027197
4	26.7853837	28.2521000	−91.865786	−89.357844
5	25.8836263	27.3817193	−89.809799	−87.302241
6	27.8304152	29.3656712	−87.819438	−85.244178
7	26.0299683	28.3155107	−84.739032	−82.985553

Table 60. Geographic extent of the animat movement boxes for injury simulation with the large seismic surveys.

Box	South latitude limit (degrees)	North latitude limit (degrees)	West longitude limit (degrees)	East longitude limit (degrees)
1	26.0989428	27.6269627	−97.29331627	−96.43953973
2	26.1353853	27.6510615	−95.92031909	−95.09057091
3	28.1989700	28.9343120	−92.14227901	−90.43750799
4	27.1457437	27.8917400	−91.45945302	−89.76417698
5	26.2439863	27.0213593	−89.40666570	−87.70537430
6	28.1907752	29.0053112	−87.40900447	−85.65461153
7	26.3903283	27.9551507	−84.33396603	−83.39061897

7.2.5.2. High-resolution Surveys

The received levels for the sources used in the high-resolution surveys drop off much more quickly with range than for the seismic survey sources discussed above. If we used the same approach for high-resolution sources as was used for large seismic surveys, very small boxes would result, which would prevent the animat movements from realistically behaving. Consequently, the 3MB simulation boxes to the high-resolution surveys were extended to 10 km from the center of the survey in each cardinal direction (Table 61), a much larger distance than that required for the received level conditions, but one that supports more realistic animal movements. Consequently, the behavior and injury simulations for high-resolution surveys used the same boxes, although, as discussed in the section above, a higher animat modeling density was used to simulate injury.

Table 61. Geographic extent of the animat movement boxes for both behavior and injury simulation with the high-resolution surveys.

Box	South latitude limit (degrees)	North latitude limit (degrees)	West longitude limit (degrees)	East longitude limit (degrees)
1	26.77588	26.95606	−96.8939	−96.6930
2	26.80408	26.98447	−95.6303	−95.4292
3	28.52530	28.70575	−91.3996	−91.1951
4	27.47697	27.65738	−90.7197	−90.5173
5	26.59023	26.77026	−88.6614	−88.4610
6	28.55562	28.73499	−86.6380	−86.4346
7	27.08567	27.26396	−84.0030	−83.8037

7.2.6. Animal Densities

Cetacean density estimates (animals/km^2) were obtained using the Marine Geospatial Ecology Laboratory (Duke University) model Roberts et al. (In preparation), preliminary results. These estimates were produced with distance sampling methodology (Buckland et al. 2001) from 195,000 linear km of shipboard and aerial surveys conducted by NOAA's Southeast Fisheries Science Center (SEFSC) in the Gulf of Mexico from 1992–2009. For each species, the count of animals per 10 km survey segment was modeled using a Horvitz-Thompson-like estimator (Marques and Buckland 2004, Miller et al. 2013). Species-specific detection functions were fitted using observation-level covariates such as Beaufort sea state, sun glare, and group size. When possible, availability and perception bias were estimated on a per-species basis using results from the scientific literature. After the sightings were corrected for detectability, availability, and perception bias, statistical regressions were used to model counts of animals per segment.

The density of frequently-sighted species were modeled with generalized additive models based on a collection of physiographic, physical oceanographic, and biological productivity predictor variables that plausibly relate to cetacean habitat. Both contemporaneous and climatological predictors were tested. Models were fitted to survey data and insignificant predictors were dropped from the models (Wood 2006). Final models were predicted across a time series of grids at 10 km resolution and averaged to produce a single surface representing mean density at each 10 km × 10 km grid square or cell.

There was insufficient data for infrequently seen species to model density from habitat variables. Instead, the geographic area of probable habitat was delineated from the scientific literature; patterns in the available sightings and density were estimated from the survey segments that occurred there using a statistical model that had no covariates. This model ran over the entire extent of the habitat area, yielding a uniform density estimate for the area.

Marine mammal density estimates for each species in the modeling zones are shown in Tables 62–68.

Table 62. Zone 1 Marine mammal density estimates.

Species	Movement surrogate	Seeding adjustment		Density estimate			
		Injury	Behavior	Min	Max	Mean	STD
Atlantic spotted dolphins		1.0	0.9988	0.000002	65.932686	19.561691	17.154286
Beaked whales		1.0	0.9879	0.000000	0.004306	0.000107	0.000402
Common bottlenose dolphins		1.0	0.9988	10.718610	143.330322	37.130025	20.297288
Bryde's whales		0.1661	0.2849	0.000000	0.167721	0.012267	0.035798
Clymene dolphins	Pantropical spotted dolphins	1.0	0.9988	0.000000	0.080756	0.000785	0.004739
False killer whales	Rough-toothed dolphins	1.0	0.9988	0.000000	0.748148	0.123816	0.278033
Fraser's dolphins	Short-finned pilot whales	1.0	0.9988	0.000000	0.388778	0.064342	0.144481
Killer whales		1.0	0.9988	0.000003	0.002641	0.000392	0.000507
Kogia	Short-finned pilot whales	1.0	0.9988	0.000000	0.381413	0.016379	0.046385
Melon-headed whales	Short-finned pilot whales	1.0	0.9988	0.000000	0.071767	0.002691	0.008428
Pantropical spotted dolphins		1.0	0.9988	0.000000	2.683713	0.111202	0.350165
Pygmy killer whales	Rough-toothed dolphins	1.0	0.9988	0.000000	0.026950	0.001253	0.003460
Risso's dolphins		1.0	0.9634	0.000000	0.489424	0.017854	0.055393
Rough-toothed dolphins		1.0	0.9988	0.000000	0.857693	0.406426	0.109876
Short-finned pilot whales		1.0	0.9988	0.078137	0.017168	0.000262	0.001151
Sperm whales*		0.1	0.1	0.000000	0.004952	0.000150	0.000473
Spinner dolphins	Pantropical spotted dolphins	1.0	0.9988	0.000000	2.888299	0.018491	0.124570
Striped dolphins	Pantropical spotted dolphins	1.0	0.9988	0.000000	0.180768	0.002602	0.012559

* Due to depth restrictions, in Zone 1 no sperm whale animats were seeded (placed in the model area) for injury and behavior. For this case, it was necessary to make a seeding adjustment = 0.1 to avoid a division by 0 error, but the dummy value did not contribute to the overall exposure estimate. See Section 7.2.7.1 for more information about seeding.

Table 63. Zone 2 Marine mammal density estimates.

Species	Movement surrogate	Seeding adjustment		Density estimate			
		Injury	Behavior	Min	Max	Mean	STD
Atlantic spotted dolphins		0.9532	0.8597	0.000001	30.319336	7.456256	9.462431
Beaked whales		0.9149	0.82	0.000000	0.000281	0.000003	0.000018
Common bottlenose dolphins		0.9532	0.8597	8.439063	113.845413	53.082960	22.977138
Bryde's whales*		0.1	0.2103	0.000000	0.028985	0.000164	0.001293
Clymene dolphins	Pantropical spotted dolphins	0.9532	0.8597	0.000000	0.000935	0.000002	0.000035
False killer whales	Rough-toothed dolphins	0.9532	0.8597	0.000000	0.748148	0.028735	0.143780
Fraser's dolphins	Short-finned pilot whales	0.9532	0.8597	0.000000	0.388778	0.014932	0.074716
Killer whales		0.9532	0.8597	0.000004	0.001135	0.000177	0.000192
Kogia	Short-finned pilot whales	0.9532	0.8597	0.000000	0.043914	0.000937	0.004897
Melon-headed whales	Short-finned pilot whales	0.9532	0.8597	0.000000	0.011606	0.000181	0.000979
Pantropical spotted dolphins		0.9532	0.8597	0.000000	0.131169	0.002317	0.012380
Pygmy killer whales	Rough-toothed dolphins	0.9532	0.8597	0.000000	0.004356	0.000078	0.000413
Risso's dolphins		0.7538	0.7252	0.000000	0.071479	0.000835	0.004760
Rough-toothed dolphins		0.9532	0.8597	0.154323	0.887101	0.394670	0.083382
Short-finned pilot whales		0.9532	0.8597	0.000000	0.002055	0.000010	0.000086
Sperm whales*		0.1	0.1	0.000000	0.000350	0.000007	0.000035
Spinner dolphins	Pantropical spotted dolphins	0.9532	0.8597	0.000000	0.000022	0.000000	0.000001
Striped dolphins	Pantropical spotted dolphins	0.9532	0.8597	0.000000	0.001711	0.000025	0.000141

* Due to depth restrictions, in Zone 2 no sperm whale animats were seeded (placed in the model area) for injury and behavior and no Bryde's whale animats were seeded for injury. For these cases, it was necessary to make a seeding adjustment = 0.1 to avoid a division by 0 error, but the dummy values did not contribute to the overall exposure estimates. See Section 7.2.7.1 for more information about seeding.

Table 64. Zone 3 Marine mammal density estimates.

Species	Movement surrogate	Seeding adjustment		Density estimate			
		Injury	Behavior	Min	Max	Mean	STD
Atlantic spotted dolphins		0.9916	0.9696	0.000071	27.600784	8.191627	7.035238
Beaked whales		0.9795	0.9522	0.000000	0.000140	0.000001	0.000012
Common bottlenose dolphins		0.9916	0.9522	8.936208	79.201904	39.405915	14.535437
Bryde's whales		0.0759	0.2908	0.000000	0.007863	0.000041	0.000375
Clymene dolphins	Pantropical spotted dolphins	0.9916	0.9696	0.000000	0.000152	0.000000	0.000007
False killer whales	Rough-toothed dolphins	0.9916	0.9696	0.000000	0.748148	0.013218	0.098562
Fraser's dolphins	Short-finned pilot whales	0.9916	0.9696	0.000000	0.388778	0.006869	0.051218
Killer whales		0.9916	0.9696	0.000006	0.000913	0.000191	0.000162
Kogia	Short-finned pilot whales	0.9916	0.9696	0.000000	0.024987	0.000187	0.001645
Melon-headed whales	Short-finned pilot whales	0.9916	0.9696	0.000000	0.006796	0.000062	0.000496
Pantropical spotted dolphins		0.9916	0.9696	0.000000	0.069956	0.000597	0.004851
Pygmy killer whales	Rough-toothed dolphins	0.9916	0.9696	0.000000	0.002749	0.000029	0.000223
Risso's dolphins		0.9073	0.895	0.000000	0.043172	0.000297	0.002568
Rough-toothed dolphins		0.9916	0.9696	0.277675	0.765203	0.396268	0.060134
Short-finned pilot whales		0.9916	0.9696	0.000000	0.001161	0.000005	0.000054
Sperm whales*		0.1	0.1	0.000000	0.000212	0.000002	0.000018
Spinner dolphins	Pantropical spotted dolphins	0.9916	0.9696	0.000000	0.000001	0.000000	0.000000
Striped dolphins	Pantropical spotted dolphins	0.9916	0.9696	0.000000	0.003908	0.000030	0.000310

* Due to depth restrictions, in Zone 3 no sperm whale animats were seeded (placed in the model area) for injury and behavior. For this case, it was necessary to make a seeding adjustment = 0.1 to avoid a division by 0 error, but the dummy value did not contribute to the overall exposure estimate. See Section 7.2.7.1 for more information about seeding.

Table 65. Zone 4 Marine mammal density estimates.

Species	Movement surrogate	Seeding adjustment		Density estimate			
		Injury	Behavior	Min	Max	Mean	STD
Atlantic spotted dolphins		1.0	1.0	0.000002	40.318748	2.781758	6.191489
Beaked whales		1.0	1.0	0.000000	4.682173	0.725775	1.107739
Common bottlenose dolphins		1.0	1.0	0.003873	66.720116	11.553444	12.482596
Bryde's whales		1.0	0.9502	0.000000	0.167727	0.035179	0.055666
Clymene dolphins	Pantropical spotted dolphins	1.0	1.0	0.000000	7.119437	0.914148	1.012023
False killer whales	Rough-toothed dolphins	1.0	1.0	0.000000	0.748148	0.727735	0.121883
Fraser's dolphins	Short-finned pilot whales	1.0	1.0	0.000000	0.388778	0.378170	0.063337
Killer whales		1.0	1.0	0.000090	0.094036	0.013264	0.015548
Kogia	Short-finned pilot whales	1.0	1.0	0.000000	2.564462	0.958299	0.613179
Melon-headed whales	Short-finned pilot whales	1.0	1.0	0.000000	4.612887	1.181967	1.227168
Pantropical spotted dolphins		1.0	1.0	0.000000	88.489113	21.767563	19.221821
Pygmy killer whales	Rough-toothed dolphins	1.0	1.0	0.000000	0.691082	0.296539	0.253896
Risso's dolphins		1.0	1.0	0.000000	10.243490	1.419280	1.445694
Rough-toothed dolphins		1.0	1.0	0.501328	1.931466	0.961959	0.308922
Short-finned pilot whales		1.0	1.0	0.000000	5.891473	0.685525	0.842500
Sperm whales		0.184	0.3378	0.000000	2.049208	0.482223	0.480525
Spinner dolphins	Pantropical spotted dolphins	1.0	1.0	0.000000	145.747696	11.762649	17.414109
Striped dolphins	Pantropical spotted dolphins	1.0	1.0	0.000000	5.765086	0.799246	0.882350

Table 66. Zone 5 Marine mammal density estimates.

Species	Movement surrogate	Seeding adjustment		Density estimate			
		Injury	Behavior	Min	Max	Mean	STD
Atlantic spotted dolphins		1.0	1.0	0.000013	26.744694	2.031142	4.981907
Beaked whales		1.0	1.0	0.000000	3.432981	1.080930	0.851019
Common bottlenose dolphins		1.0	1.0	0.025899	46.434166	5.728691	8.809752
Bryde's whales		1.0	0.9525	0.000000	0.167701	0.014526	0.039290
Clymene dolphins	Pantropical spotted dolphins	1.0	1.0	0.000000	15.461932	3.416620	3.148363
False killer whales	Rough-toothed dolphins	1.0	1.0	0.000000	0.748148	0.726846	0.124434
Fraser's dolphins	Short-finned pilot whales	1.0	1.0	0.000000	0.388778	0.377708	0.064662
Killer whales		1.0	1.0	0.000159	0.056221	0.020153	0.014145
Kogia	Short-finned pilot whales	1.0	1.0	0.000000	1.972867	0.726706	0.450570
Melon-headed whales	Short-finned pilot whales	1.0	1.0	0.000000	3.859135	2.209811	1.321709
Pantropical spotted dolphins		1.0	1.0	0.000000	31.898088	15.504281	9.582240
Pygmy killer whales	Rough-toothed dolphins	1.0	1.0	0.000000	0.691082	0.456866	0.269419
Risso's dolphins		1.0	1.0	0.000000	7.244700	0.972485	1.026923
Rough-toothed dolphins		1.0	1.0	0.484941	1.574484	1.050021	0.185273
Short-finned pilot whales		1.0	1.0	0.000000	3.430244	0.639206	0.665957
Sperm whales		0.6644	0.6107	0.000000	2.049208	0.725159	0.527590
Spinner dolphins	Pantropical spotted dolphins	1.0	1.0	0.000000	66.322189	4.154421	8.152655
Striped dolphins	Pantropical spotted dolphins	1.0	1.0	0.000000	4.547289	1.334442	0.985099

Table 67. Zone 6 Marine mammal density estimates.

Species	Movement surrogate	Seeding adjustment		Density estimate			
		Injury	Behavior	Min	Max	Mean	STD
Atlantic spotted dolphins		1.0	1.0	0.000007	17.078234	1.273500	3.317500
Beaked whales		1.0	1.0	0.000000	2.336602	0.832344	0.536911
Common bottlenose dolphins		1.0	1.0	0.030806	24.043407	3.342733	5.111497
Bryde's whales		1.0	0.9034	0.000000	0.167480	0.013691	0.037372
Clymene dolphins	Pantropical spotted dolphins	1.0	1.0	0.000000	16.132580	4.262516	3.869130
False killer whales	Rough-toothed dolphins	1.0	1.0	0.000000	0.748148	0.735816	0.095258
Fraser's dolphins	Short-finned pilot whales	1.0	1.0	0.000000	0.388778	0.382369	0.049501
Killer whales		1.0	1.0	0.000358	0.053226	0.019773	0.012304
Kogia	Short-finned pilot whales	1.0	1.0	0.000000	1.100742	0.411093	0.228572
Melon-headed whales	Short-finned pilot whales	1.0	1.0	0.000000	3.280858	1.890231	1.024283
Pantropical spotted dolphins		1.0	1.0	0.000000	16.103422	9.864202	5.300093
Pygmy killer whales	Rough-toothed dolphins	1.0	1.0	0.000000	0.691080	0.476313	0.254439
Risso's dolphins		1.0	1.0	0.000000	3.041948	0.794562	0.616821
Rough-toothed dolphins		1.0	1.0	0.420462	1.595734	0.997906	0.183769
Short-finned pilot whales		1.0	1.0	0.000000	5.996468	1.249850	1.434598
Sperm whales		0.7368	0.5215	0.000000	1.356392	0.486587	0.286136
Spinner dolphins	Pantropical spotted dolphins	1.0	1.0	0.000000	2.337054	0.236570	0.284845
Striped dolphins	Pantropical spotted dolphins	1.0	1.0	0.000000	1.833318	1.091651	0.565132

Table 68. Zone 7 Marine mammal density estimates.

Species	Movement surrogate	Seeding adjustment		Density estimate			
		Injury	Behavior	Min	Max	Mean	STD
Atlantic spotted dolphins		1.0	1.0	0.000000	0.001134	0.000004	0.000027
Beaked whales		1.0	1.0	0.222212	3.113844	0.519543	0.286857
Common bottlenose dolphins		1.0	1.0	0.001245	1.554906	0.027482	0.067843
Bryde's whales		1.0	1.0	0.000000	0.000004	0.000000	0.000000
Clymene dolphins	Pantropical spotted dolphins	1.0	1.0	0.005837	16.310186	2.627719	3.204962
False killer whales	Rough-toothed dolphins	1.0	1.0	0.748148	0.748148	0.748148	0.000000
Fraser's dolphins	Short-finned pilot whales	1.0	1.0	0.388778	0.388778	0.388778	0.000000
Killer whales		1.0	1.0	0.023988	0.101078	0.077865	0.016385
Kogia	Short-finned pilot whales	1.0	1.0	0.151227	0.825459	0.342218	0.062230
Melon-headed whales	Short-finned pilot whales	1.0	1.0	0.618728	4.204332	1.533612	0.671281
Pantropical spotted dolphins		1.0	1.0	10.890163	46.524502	26.087947	6.013833
Pygmy killer whales	Rough-toothed dolphins	1.0	1.0	0.643905	0.691082	0.661113	0.013441
Risso's dolphins		1.0	1.0	0.083161	2.332364	0.419790	0.237456
Rough-toothed dolphins		1.0	1.0	0.385164	1.895322	0.798816	0.276520
Short-finned pilot whales		1.0	1.0	0.003767	0.771689	0.121555	0.104179
Sperm whales		1.0	1.0	0.354441	1.140214	0.467025	0.131315
Spinner dolphins	Pantropical spotted dolphins	1.0	1.0	0.043222	24.800802	0.612156	1.245325
Striped dolphins	Pantropical spotted dolphins	1.0	1.0	0.541343	2.608293	1.365036	0.429627

7.2.6.1. Marine Mammal Density Estimates in Modeling Zones

The Marine Geospatial Ecology Laboratory (Duke University) model (Roberts et al. In preparation) is a GIS-compatible raster of density estimates in 10 km^2 × 10 km^2 squares. The minimum, maximum, mean, and the standard deviation of the mean were obtained for each species in each zone. These density estimates and depth-restricted density adjustments (Section 7.2.7.1) are shown in Tables 62–68; Appendix A shows distribution maps.

7.2.7. Animal Movement: JEMS

The JASCO Exposure Modeling System (JEMS) combines animal movement data, the output from 3MB (Section 5.3), with pre-computed acoustic fields (Sections 5.1–5.2). The JEMS output was the time-history of received levels and slant ranges (the three dimensional distance between the animat and the source) for all animats of the 3MB simulation. Animat received levels and slant ranges are used to determine the risk of acoustic exposure. JEMS can use any acoustic field data provided as a 3-D radial grid (e.g., *N*×2-D MONM output). Source movement and shooting patterns can be defined, and multiple sources and sound fields used. For impulsive sources, a shooting pattern based on movement can be defined for each source, with shots distributed along the vessel track by location (or time). Because the acoustic environment varies with location, acoustic fields are pre-computed at selected sites in the simulation area and JEMS chooses the closest modeled site to the source at each time step.

7.2.7.1. Depth-restricted Density Adjustment

The number of animats that 3MB initially places, or seeds, in a simulation was based on the specified animat density (in units of animats per km^2) and simulation area. The model establishes a grid to cover the simulation area, then examines the bathymetry in the simulation area and determines the number of grid points where the water depth is greater than zero. The number of grid points where the water depth is greater than zero provides an estimate of the working area and the number of animats to seed is calculated from the working area and the animat's specified density. 3MB randomly selects grid points and evaluates the points based on the suitability for the animat species. For example, a depth restriction may be set that eliminates grid points too shallow for seeding a particular species. If the grid point is accepted, an animat is placed at that grid point (at a random depth location within the species-defined depth range) and 3MB decreases its animat seeding quota by one. The loop continues until the predetermined number animats is successfully seeded. For species whose definition accepts seeding locations in all water depths greater than zero, a uniform animat seeding density equal to the specified density is achieved in the simulation area. For species with depth restrictions, such as sperm whales that are restricted to water deeper than 1000 m, the number of animats determined by the working area and specified density will be concentrated within the area of the simulation that meets the restriction and their density effectively increased in that portion. The animat modeling density is a key value when calculating the exposure estimates, so exposure estimates are skewed if concentrating the animats increases the density. To avoid this problem, we calculated separately the number of acceptable grid points (based on the percentage of the working area that meets the depth restriction) and used this information to calculate an adjustment factor to pro-rate the exposure estimates.

7.2.7.2. Evaluation Time Period

Animat exposure histories were processed to calculate the number of animats exposed to levels exceeding threshold (the number of exposures). The time interval over which the counting was done must be defined. While there is no consensus on the time interval (see time interval effects in Section 6.5.1: Test Scenario 1), a 24 h period is often used (Southall et al. 2007). For this analysis, seven-day simulations

were run and the exposures estimated in 24 h windows within the seven days. The first 24 h window begins at the start of the simulation and each subsequent window is advanced by 4 h. In this sliding-windows approach, 42 exposure estimate samples are obtained for each seven-day simulation. The mean value is then used as the 24 h exposure estimate for that survey.

7.2.7.3. Annual Aggregate Estimates

This analysis estimated the annual number of exposures for each species for each year for each type of source for the entire Gulf. To get these annual exposure estimates, the 24 h exposure estimates were scaled by the number of expected survey days. BOEM provided projections of survey level of effort (shown in Table 75) for each survey type in each year (2016–2025) in BOEM's Gulf of Mexico Planning Areas (eastern, central, and western; divided into shallow and deep zones). These survey projections were used to scale the 24 h exposure estimates from simulations in the appropriate locations.

7.3. Phase II Modeling Results

7.3.1. Acoustic Sources: Levels and Directivity

7.3.1.1. Airgun Sources

We used the Airgun Array Source Model (AASM) to model the pressure signatures of the individual airguns and the composite 1/3-octave-band source levels of the arrays, as functions of azimuthal angle in the horizontal plane (Section 5.1.1). While AASM accounts for effects of source depth on bubble interactions, the surface-reflected signal (i.e., surface ghost) was not included in the far-field source signatures. The acoustic propagation models account for surface reflections, which are a property of the medium, not the source.

7.3.1.1.1. Airgun Array—8000 in³

The broadside (perpendicular to the tow direction) and endfire (parallel to the tow direction) horizontal overpressure signatures (Figure 117a) consist of a strong primary peak, related to the initial firing of the airguns, followed by a series of pulses associated with the bubble oscillations. The broadside and endfire power spectrum levels were highest at frequencies below 500 Hz (Figure 117b). Frequency-dependent peaks and nulls in the spectrum were caused by interference among airguns in the array; they reflect the volumes and relative locations of the airguns. The broadband horizontal source levels are shown in Table 69.

As discussed in Section 5.1.1, directivity in the sound field was most noticeable at mid-frequencies. Maximum (horizontal) 1/3-octave-band source levels over all azimuths are shown in Figure 118. Horizontal 1/3-octave-band source levels are shown as a function of band center frequency and azimuth in Figure 119.

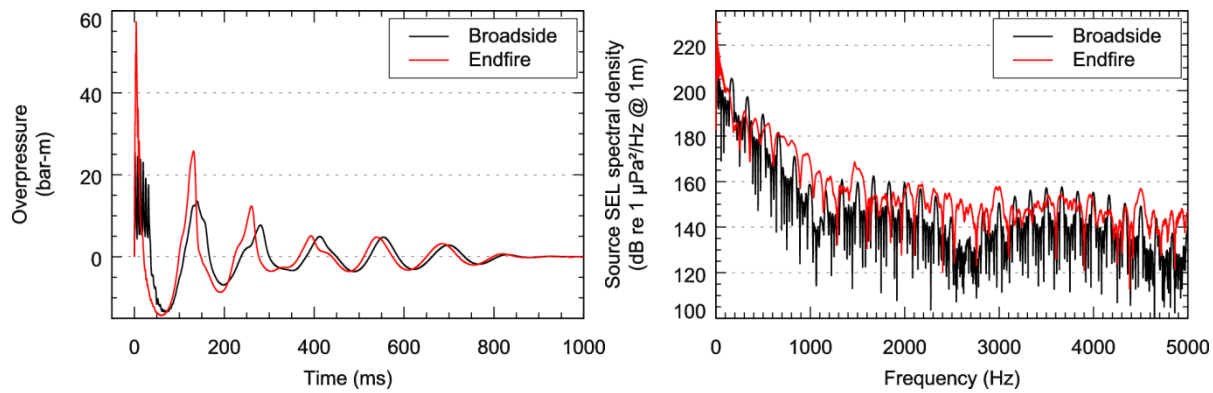

(a) (b)

Figure 117. Predicted (a) overpressure signature and (b) power spectrum in the broadside and endfire (horizontal) directions, for a generic 8000 in^3 airgun array towed at a depth of 8 m.

Table 69. Horizontal source level specifications for a generic 8000 in^3 airgun array.

Direction	Zero-to-peak SPL (dB re 1 µPa @ 1 m)	SEL (dB re 1 µPa^2 @ 1 m) 10 Hz to 5 kHz
Broadside	248.1	225.7
Endfire	255.2	231.8

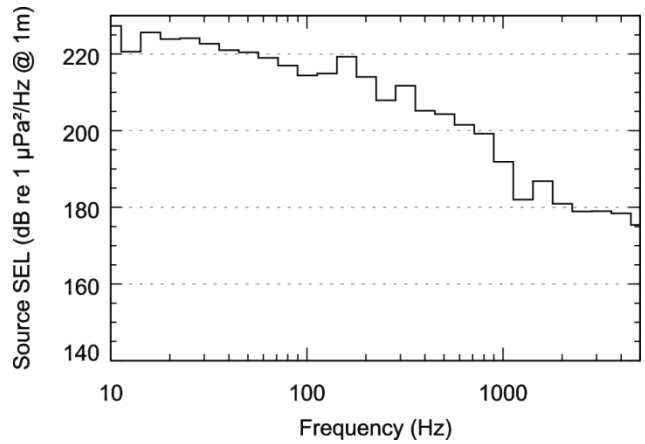

Figure 118. Maximum 1/3-octave-band source level in the horizontal plane for a generic 8000 in³ airgun array. The maximum over all modeled azimuths is shown for each 1/3-octave-band.

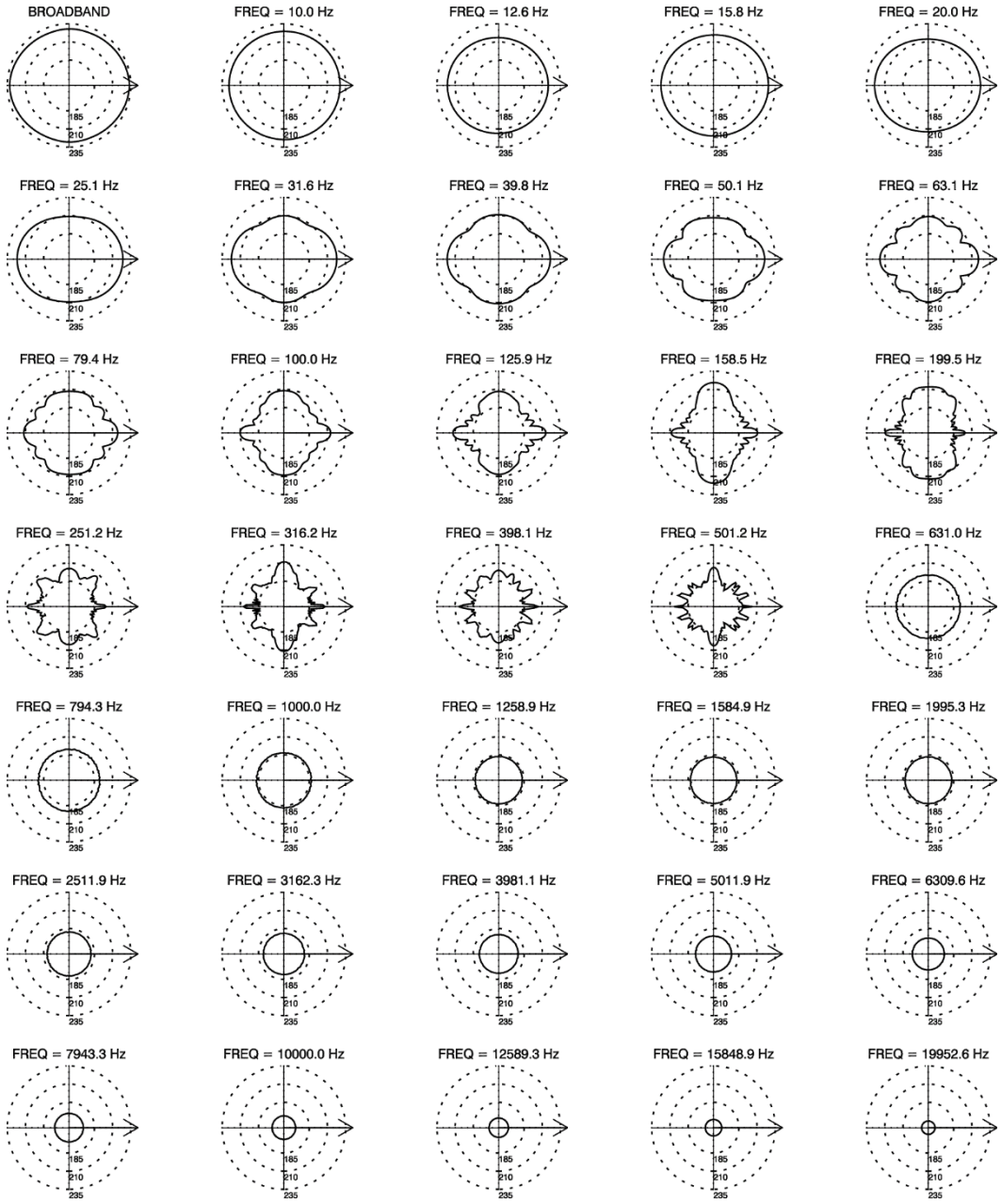

Figure 119. Directionality of predicted horizontal source levels for a generic 8000 in^3 airgun array. Source levels in dB re 1 µPa^2·s are shown as a function of azimuth for the center frequencies of the 1/3-octave-bands modeled; frequencies are indicated above the plots. Tow direction was to the right.

7.3.1.1.2. Single Airgun—90 in³

Since the source consists of one gun, the acoustic wave is omnidirectional and has virtually the same characteristics in all directions. The overpressure for a single 90 in^3 airgun towed at a depth of 6 m is shown in Figure 120. The overpressure signature (Figure 120a) consist of a strong primary peak, related to the initial firing of the airguns, followed by a series of pulses associated with the bubble oscillations. Most energy is produced at frequencies below 600 Hz (Figure 121). Zero-to-peak SPL is 227.7 dB re 1 µPa @ 1 m and source SEL is 207.8 dB re 1 µPa2 @ 1 m.

Maximum (horizontal) 1/3-octave-band source levels over all azimuths are shown in Figure 121.

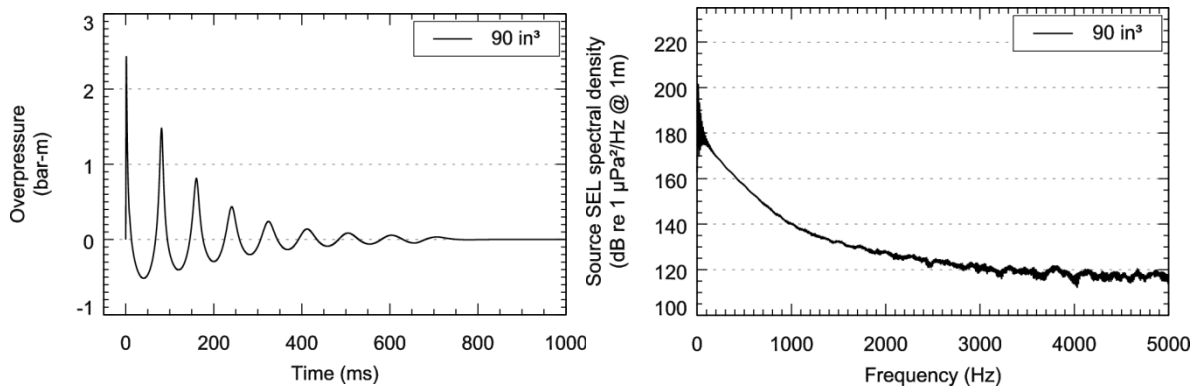

(a) (b)

Figure 120. Predicted (a) overpressure signature and (b) power spectrum in the broadside and endfire (horizontal) directions for a single 90 in^3 airgun.

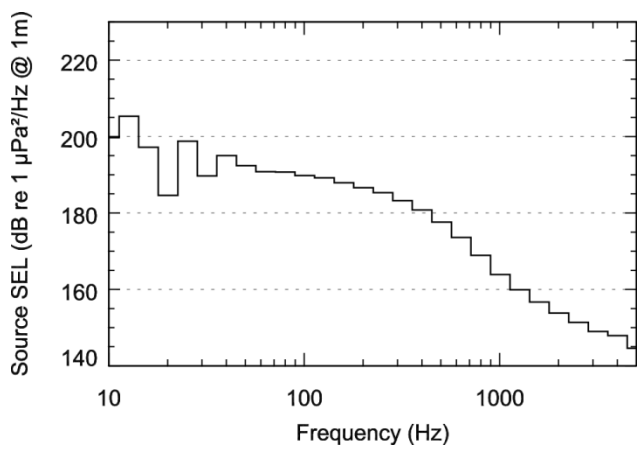

Figure 121. Maximum 1/3-octave-band source level in the horizontal plane for a single 90 in³ airgun. The maximum over all modeled azimuths is shown for each 1/3-octave-band.

7.3.1.2. Boomer

To estimate the broadband source level for the AA301 boomer (350 J input energy) from the source level for AP3000 system (1000 J input energy), we applied a −4.6 dB correction factor. The estimated source levels for the boomer plate—198.4 dB 1 µPa @ 1 m rms SPL and 168.0 dB re 1 µPa^2·s @ 1 m SEL—were significantly lower than those provided by the manufacturer because the manufacturer's level is estimated based only on the input energy. When electrical signals are converted into acoustic waves, output source levels are reduced.

The power spectrum of the boomer signal and the beamwidth at different frequencies were estimated based on Simpkin's (2005) study of the Huntec'70 Deep Tow Boomer, a typical boomer plate of comparable dimensions. The source level in each 1/3-octave-band was calculated based on the broadband source level and relative power spectrum data (Table 70).

The parameters of the AA301 boomer used for modeling were:

- Operating frequency (wide band): 100 Hz–10 kHz
- Beam width: omnidirectional –11°

- Beams: 1
- Beam direction: vertically down
- Maximum energy input (per shot): 350 J
- rms SPL: 198.4 dB re 1 µPa @ 1 m T_{rmsSPL}=0.2 ms (estimated from field measurements; Martin et al. 2012)
- Per pulse SEL: 171.0 dB re 1 µPa²·s @ 1 m (estimated from field measurements; Martin et al. 2012)

Table 70. Estimated source levels (SELs) and beamwidths from the AA301 boomer plate at 350 J per pulse distributed into twenty 1/3-octave-bands.

1/3-octave-band center frequency (Hz)	Band SEL (dB re 1 µPa²·s @ 1 m)	Beam width
100	152.0	Omnidirectional
125	153.0	Omnidirectional
160	154.0	Omnidirectional
200	155.0	Omnidirectional
250	155.4	Omnidirectional
315	156.1	Omnidirectional
400	156.7	Omnidirectional
500	157.5	Omnidirectional
630	158.4	Omnidirectional
800	159.0	Omnidirectional
1,000	159.8	Omnidirectional
1,250	160.5	105°
1,600	160.6	78°
2,000	160.9	60°
2,500	160.4	47°
3,150	159.8	37°
4,000	159.1	29°
5,000	157.9	23°
6,300	156.8	18°
8,000	155.1	14°
10,000	151.8	11°
Broadband	171.0	Omnidirectional

We compared the boomer source with the 90 in³ airgun to confirm if acoustic field modeling results for the airgun were adequate to approximate the ones for the boomer. The broadband source levels for the airgun and the boomer were calculated after the set of M-weighted filters were applied (Table 71). As indicated in the Table 71, the broadband source level for the boomer is lower than for the airgun after application of all applicable M-weighting filters. Considering the negligible fraction of the surveys conducted using boomers and that the estimated impact from the 90 in³ is always greater than for the boomer, the 90 in³ airgun results were proposed as a conservative substitute for the boomer. Therefore, the source level modeling results presented in this section were not used in any acoustic field results or exposure estimates.

Table 71. Boomer and 90 in³ airgun broadband source levels after M-weighting filters were applied.

Source	FLAT	Type I LFC	Type I MFC	Type I HFC	Type II MFC	Type II HFC
90 in³	207.8	206.0	190.7	188.6	174.3	169.2
Boomer	171.2	171.0	170.7	170.5	158.0	155.6

LFC=low-frequency cetaceans, MFC= mid-frequency cetaceans, HFC=high-frequency cetaceans

7.3.1.3. High-resolution Acoustic Sources

7.3.1.3.1. Multibeam Echosounder—Simrad EM2000

For the multibeam echosounder, the operational parameters producing the greatest acoustic impact were modeled. The Simrad EM2000 multibeam echosounder was modeled at the operational frequency of 200 kHz, maximum source level of 203 dB re 1 µPa @ 1 m, the pulse length of 1.3 ms. The source beam pattern was modeled using rectangular transducer theory (Section 5.1.2.2).

The estimated beam pattern from the transmitter of Simrad EM2000 is provided in Figure 122 as vertical slices along- and across-track directions.

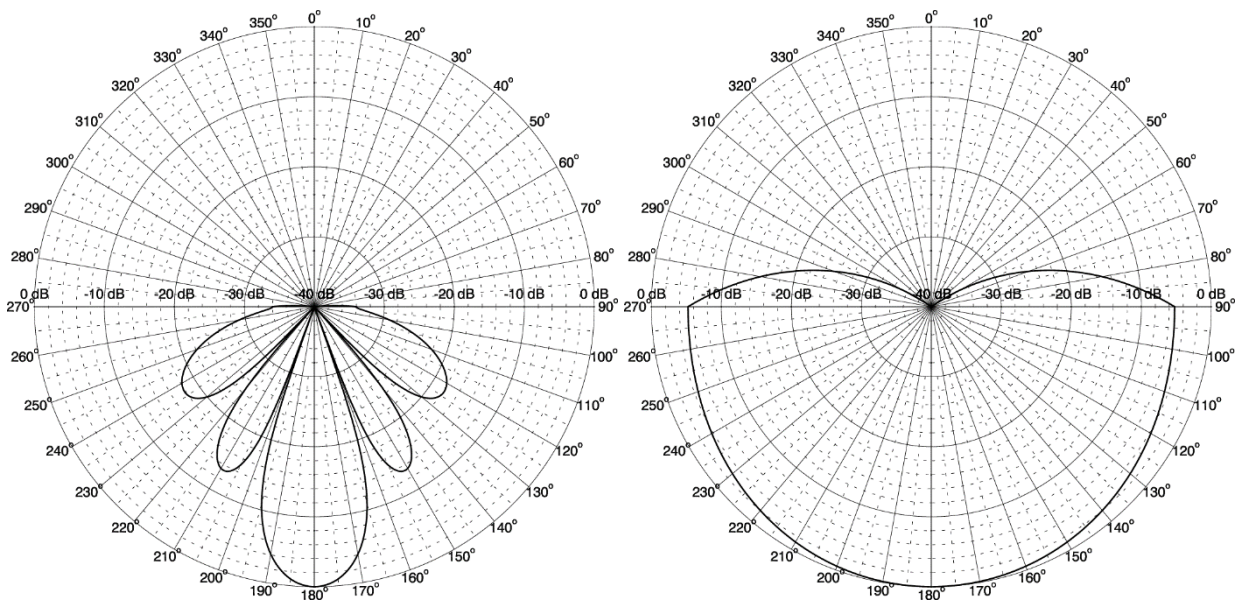

Figure 122. Vertical beam pattern calculated for the Simrad EM2000 multibeam 88° × 17° width in the (left) along- and (right) across-track directions.

7.3.1.3.2. Side-scan Sonar—EdgeTech 2200 IM

The side-scan sonar EdgeTech 2200 IM was modeled at two operational frequencies, 120 and 410 kHz. The rms SPL source level was estimated based on the peak source levels at 207 and 213 dB re 1 µPa @ 1 m for 120 and 410 kHz center frequencies. The SEL source level was estimated based on the rms SPL source level values and the pulse lengths at 186.2 and 186.8 dB re 1 µPa²·s for 120 and 410 kHz center frequencies.

The source beam pattern was modeled using rectangular transducer theory (Section 5.1.2.2). The estimated beam pattern from the transmitter of the EdgeTech 2200 IM side-scan sonar is provided in

Figure 123 as slices at 20° declination angle (through beam maximums) and vertical across-track directions.

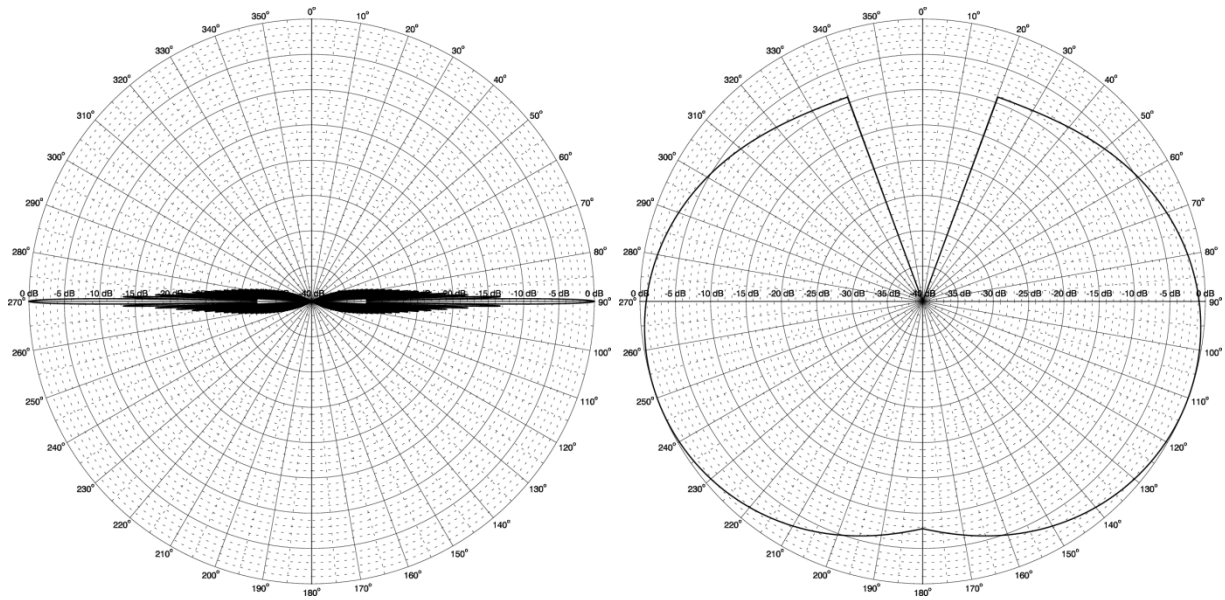

Figure 123. Vertical beam pattern calculated for the EdgeTech 2200 IM side-scan sonar 70° × 0.8° width and 20° declination angle. Slices (left) at 20° declination angle and (right) across-track directions.

7.3.1.3.3. Sub-bottom Profiler—EdgeTech 2200 IM, DW−424

The chirp sub-bottom profiler emits a pulse, with a frequency constantly changing over time from the lower frequency of the working band at the beginning of the pulse to the higher frequency at the end of the pulse. The amplitude of the pulse also changes. Field measurements on a similar chirp system (Zykov and MacDonnell 2013) showed that the maximum amplitude of the pulse is achieved at the center frequency of the range, approximately. The pulse amplitude holds this maximum in the two 1/3-octave-bands closest to the center frequency of the operational band and drops by about 10 dB for the 1/3-octave-bands on either side of the maximum, dropping farther by 30 dB from the maximum at either end of the operational band. As a result, the chirp sub-bottom profiler can be modeled with sufficient accuracy using only the center frequency of the operational band.

The chirp sub-bottom profiler of EdgeTech 2200 IM system was modeled at single frequency of 14 kHz. The rms SPL source level was considered at 200 dB re 1 µPa @ 1 m. The SEL source level was estimated based on the rms SPL source level and the pulse length at 180 dB re 1 µPa²·s. The beamwidth was estimated at 20° at the center frequency.

The source beam pattern was modeled using circular transducer beam theory (Section 5.1.2.1). The estimated beam pattern from the transmitter of the EdgeTech 2200 IM chirp sub-bottom profiler is provided in Figure 124 as a vertical slice. The beam is omnidirectional in the horizontal plain.

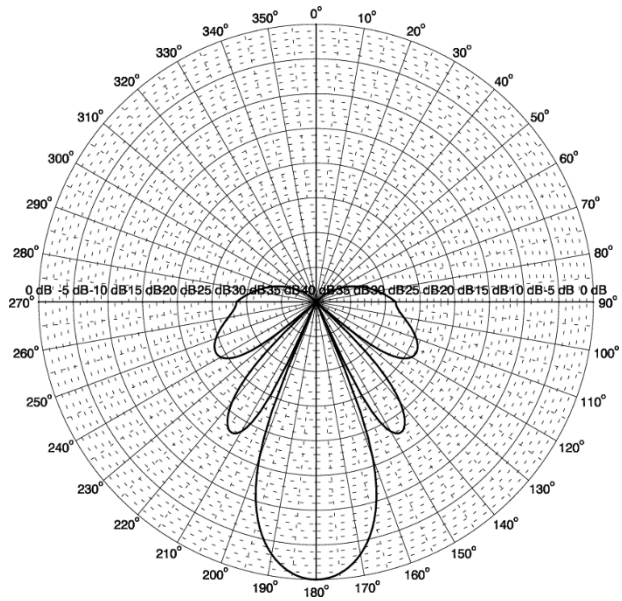

Figure 124. Vertical beam pattern calculated for the EdgeTech 2200 IM sub-bottom with 20° beamwidth.

7.3.2. Per-Pulse Acoustic Field

7.3.2.1. Per-Pulse Acoustic Field for Input to JEMS

Acoustic propagation modeling was performed for of all sources at the modeling sites. The per-pulse acoustic fields were used as input for the exposure simulation using JEMS (Section 7.2.7). The acoustic fields were passed as 3-D cylindrical grids (range-depth-azimuth) of received levels.

7.3.2.1.1. Seismic Survey (8000 in³ Airgun Array)

The acoustic field from 8000 in³ airgun array was modeled at 10 sites in each of the regions (East, Central, and West) for a total of 30 sites in the Gulf of Mexico (see Figure 110, Tables 48–51). At each site a towing azimuth of 0° or 90° was used based on the orientation of the survey box. Special consideration was given to the simulation of the Coil survey (Section 7.2.2.4) because of its continuously changing towing direction as the survey vessel follows a circular path. To accommodate the changing tow direction, additional acoustic fields were created using 9 different towing azimuths from 0° to 160° with a 20° step. The towing directions from 180° to 340° were represented by the same fields assuming source geometry symmetry for the towing axis. Considering the directivity pattern of the array, it was assumed that 20° towing azimuth step was optimal for exposure modeling.

Transmission loss was modeled along 15 radial profiles (angular step 22.5°) to the range of up to 50 km from the source location. The horizontal step along the radials was 10 m. At each surface sampling location, the sound field was sampled at multiple depths:

- 2 m
- Every 5 m from 5 to 20 m
- Every 10 m from 20 to 100 m
- Every 25 m from 100 to 200 m
- Every 50 m from 200 to 300 m

- Every 100 m from 300 to 1200 m
- Every 200 m from 1200 to 3000 m

The frequencies up to 5 kHz for the airgun array source were considered in the calculations of the broadband received levels. All 1/3-octave-band frequencies from 10 Hz to 5 kHz were used for the airgun array source level modeling (Section 7.3.1). For the transmission loss calculations, frequencies higher than 2 kHz were computationally intensive, so it was assumed that the transmission loss field for higher frequencies (up to 5 kHz) is identical to that at 2 kHz.

For each modeling scenario, the acoustic fields were calculated in SEL and rms SPL metrics. The rms SPL field was estimated from SEL field by applying range/depth/azimuth dependent conversion factor, which was obtained with full waveform modeling (Section 5.2.4). In addition to the unweighted acoustic fields, a set of filtered acoustic fields were calculated by applying M-weighting filters: Type I (low, medium, and high frequency) for rms SPL and Type II (medium and high frequency) for SEL. The total number of precomputed acoustic field grids prepared for the exposure simulation with JEMS was more than 1600.

7.3.2.1.2. Geotechnical Surveys with High-resolution sources

The acoustic field from the high-resolution sources (90 in³ airgun, sub-bottom profiler, side-scan sonar, and multibeam sonar) was modeled at 7 sites: center of each survey box (see Figure 110 and Table 51). At each site, a towing azimuth of 0° or 90° was used based on the orientation of the survey box.

The high-frequency geotechnical sources have significantly finer structure to the beam pattern in the horizontal plane compared to the large airgun array. The geometry of the profiles along which the acoustic propagation was modeled was individually adjusted for each source based on the beam pattern (Table 72).

At each surface sampling location along the modeled profiles, the sound field was sampled at multiple depths:

- 2 m
- Every 5 m from 5 to 20 m
- Every 10 m from 20 to 100 m
- Every 25 m from 100 to 200 m
- Every 50 m from 200 to 300 m
- Every 100 m from 300 to 1200 m
- Every 200 m from 1200 to 3000 m

For each modeling scenario, the acoustic fields were calculated in SEL and rms SPL metrics. The rms SPL field was estimated from SEL field by applying constant conversion factor of +10 dB (see Section 5.2.4). In addition to the unweighted acoustic fields, a set of filtered acoustic fields were created by applying M-weighting filters: Type I (low, medium, and high frequency) for rms SPL and Type II (medium and high frequency) for SEL.

Table 72. Modeling parameters for the geotechnical sources.

Source	Frequencies modeled	Profiles	Range modeled (km)	Grid size (m)
90 in³ airgun	10–2000 Hz	72 (5° angle step)	50	10
Multibeam	200 kHz	130 (3° angle step)	3	5
Side-scan sonar	120 kHz, 410 kHz	236 (see Table 73 for angle steps)		
Sub-bottom profiler	14 kHz	90 (4° angle step)		

Table 73. Angle step configuration of profiles around side-scan sonar. In total, 236 profiles were modeled.

Horizontal range, in degrees, around source	Angle step, in degrees, for profiles
0–45	3
45–75	2
75–84	1
84–88	0.4
88–92	0.2
92–96	0.4
96–105	1
105–135	2
135–225	3
225−255	2
255–264	1
264–268	0.4
268–272	0.2
272–276	0.4
276–285	1
285–315	2
315–360	3

7.3.2.2. Range to Zero-to-Peak SPL Isopleths

To evaluate the risk of acoustic injury, the range to the unweighted, zero-to-peak SPL (dB re 1µPa) is needed for the 200 dB isopleth (high frequency cetaceans) and 230 dB isopleth (low and medium frequency cetaceans). The spherical spreading law:

$$L_{pk}(R) = L_{pkSL} - 20 \cdot \log(R),$$

where L_{pkSL} is the peak SPL source level of the source and R is the range, was assumed as the propagation model for peak SPL. The ranges to the thresholds were calculated for each source (Table 74).

Table 74. Ranges to specific threshold levels for all sources.

Source	Source level (peak SPL; dB)	Range (m)	
		230 dB peak SPL	200 dB peak SPL
8000 in³ airgun array	255.2	18	575
90 in³ airgun array	227.7	–	24
Side-scan sonar	213	–	4.5
Sub-bottom profiler	203	–	–
Multibeam echosounder	206	–	–

7.3.2.3. Per-Pulse Acoustic Field for Threshold Ranges

The per-pulse acoustic fields were processed to provide two products:

- Tables of ranges to specific thresholds from 210 dB down to 110 dB with a 10 dB step
- Maps of the acoustic field around the sources

The tables of threshold ranges can help to determine at what range from each source a potential exposure can occur. The maps provide the view of azimuthal variability of the received acoustic field. Appendix E provides a sample of the tables of threshold ranges and maps for Site CM3 (Central-Slope zone, 750 m water depth). Appendix E provides results for all sources in Box 4 for Seasons 1 and 3 and in SEL and rms SPL metric. The threshold ranges were calculated for all applicable M-weighting filters.

7.3.3. 24-hour Exposure Estimates

Simulations were run in the 3MB survey areas (Section 7.2.5) and, using JEMS, were convolved with the per-pulse acoustic fields (Section 7.3.2). The result is the time history of acoustic exposure (received levels) for the animats in the simulation. There were many animats in the simulations and together their received levels represent the probability, or risk, of exposure for each survey. This can be seen by plotting the received levels as a histogram. Figure 125 shows the received-level SEL in a 24 h window for *Kogia* species. The frequency of occurrence of the received levels is plotted as a function of the received level, so the histogram is a discretized representation of the exposure probability density function (PDF). PDFs are often normalized so that the area under the curve is equal to 1. That can be accomplished by dividing by the modeling animat density to get the probability of occurrence for the operation. It is the number of animals exposed to levels exceeding threshold that we are interested in, so the probability can be multiplied by the real-world density of animals in the simulation area. Therefore, the number of individual animals expected to exceed threshold is the number of animats exposed to levels exceeding threshold multiplied by the real-world animal density/model animat density.

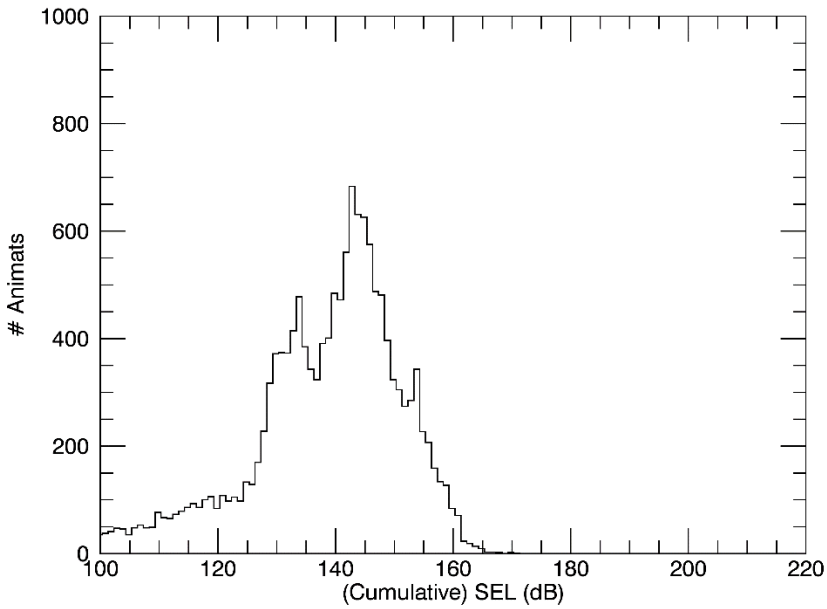

Figure 125. Probability density function of received levels shown as a histogram. Cumulative SEL for Kogia species using short-finned pilot whales as the surrogate and high-frequency weighting in Box 3 for a 2-D survey. The SEL threshold for injury is 161 dB re 1 $\mu Pa^2 \cdot s$. 91 animats exceeded the threshold in this 24 h window.

Seven-day simulations were run and the number of animats exposed to levels exceeding threshold were determined in 24 h windows within the seven days. In a sliding-window approach, the first 24 h window begins at the start of the simulation and each subsequent window is advanced by 4 h. This gave 42 samples for each survey, and the mean value was used as the 24 h estimate for that survey. The number of individuals exposed to levels exceeding the NMFS criteria, 180 and 160 dB rms SPL, respectively for injury and behavior, were found. Additional metrics were used to evaluate potential injury, cumulative SEL and zero-to-peak SPL. SEL was determined by summing acoustic energy received from each source integrated over 24 h. Range was used to determine the zero-to-peak SPL for each animat relative to each source. The number of animats within the range where the received level could exceed threshold were found. A graded function was also used as an additional metric to evaluate potential behavioral response. SEL used Type I weighting for low-frequency species (Bryde's whales) and Type II weighting for the mid- and high-frequency species. Type I weighting was used for rms SPL sound fields with the graded function to evaluate potential behavioral response. The remaining metrics (NMFS criteria and zero-to-peak SPL) were not weighted.

The exposure estimates are compiled in Microsoft Excel workbooks and provided on BOEM's webpage for the GOM G&G Activities Programmatic EIS. The modeled exposure estimates can be found in the workbooks: *Box1.xlxs to Box7.xlxs*. The box numbers correspond to the 3MB simulation areas (Section 7.2.5), and the results were the average ± standard deviation 24 h number of animats exposed to levels exceeding the various threshold criteria. Modeled exposure estimates are shown for each species and for the two modeled seasons (S1 and S3). The number of model iterations for animats exposed to levels that exceed 160 dB rms SPL, is also shown for the 10th, 50th, and 90th percentiles of a cumulative distribution. Each tab contains the results from one source.

The number of real-world individual animals expected to exceed the various thresholds are shown in the exposure estimate workbooks: *TakeEstimates_Zone1.Flat.xlxs* to *TakeEstimates_Zone7.Flat.xlxs*. The zones correspond to our Gulf of Mexico modeling zones (Section 7.2.3). To get the real-world individual exposure estimates, the modeled exposure estimates from the appropriate *Box1.xlxs* to *Box7.xlxs*

workbooks were scaled by the ratio of the mean real-world density estimate from the zone to the modeled density. The mean real-world density estimates were obtained from the Marine Geospatial Ecology Laboratory (Duke University) model (Roberts et al. In preparation; Section 7.2.6, and Tables 62–68). The layout of the exposure estimate workbooks is identical to the "Box" workbooks, except that the values represent the number of real-world individual animals exposed to levels exceeding the various threshold criteria instead of animats. In the "TakeEstimate" workbooks, the amount of time (in minutes) that animates exceed 160 dB rms SPL is shown for the percentiles of a cumulative distribution.

7.3.4. Annual Exposure Estimates

The overall goal of this analysis was to estimate the number of exposures for each species for each year for the entire Gulf. Projections of survey level of effort for the different survey types for the Gulf Planning Areas (Eastern, Central, and Western; divided into shallow and deep zones) were provided by BOEM (Table 75). Our modeling zones and survey locations were chosen, in part, to coincide with the Planning Areas so that the survey projections could be easily used for scaling. The shallow portion of the east, central, and western Planning Areas were the same as our modeling zones 1–3. A portion of each of the deep parts of Planning Areas maps directly to our modeling zones 4–6. The remainder of the deep parts of the Planning Areas were combined as modeling zone 7. The 24 h exposure estimates were scaled by the projected number of survey days to get the annual aggregate exposure estimates. The annual aggregate results are shown in Appendix F. Tables 76–82 show the sum of the annual results representing the 2016–2025 decade exposure estimates. The exposure estimates are the number of individual animals with the potential to exceed each of the criteria used to evaluate potential injury (SEL, peak SPL, and 180 dB rms SPL) and potential behavioral disruption (the step function, and 160 dB rms SPL). The estimates are for each type of survey and for each marine mammal species.

Table 75. Projected level of effort in days (24 h) for survey types in years 2016 to 2025. 2-D seismic survey is an 8000 in^3 airgun array with 1 vessel. 3-D seismic survey is an 8000 in^3 airgun array with two vessels. The WAZ seismic survey is an 8000 in^3 airgun array with four vessels. Coil seismic survey is an 8000 in^3 airgun array with four vessels. Shallow hazards seismic survey is a 90 in^3 airgun. The high resolution sources include for side-scan sonar, multibeam, and sub-bottom profiler. VSP is an 8000 in^3 airgun array with one vessel.

Year	Zone	2-D	3-D	WAZ	Coil	Shallow hazards	Boomer	High resolution sources	VSP
2016	1	0	0	0	0	0	0	1	0
	2	0	243	0	0	2	0	19	0
	3	0	30	0	0	0	0	4	0
	4	0	0	0	0	0	0	0	0
	5	56	389	192	82	0	0	26	2
	6	0	186	49	21	0	0	10	0
	7	69	515	248	106	0	0	34	2
2017	1	0	0	0	0	0	0	1	0
	2	0	364	43	19	2	0	19	0
	3	0	0	0	0	0	0	4	0
	4	33	0	0	0	0	0	0	0
	5	0	389	192	82	0	0	26	2
	6	0	99	0	0	0	0	11	0
	7	30	502	241	103	0	0	34	2

Year	Zone	2-D	3-D	WAZ	Coil	Shallow hazards	Boomer	High resolution sources	VSP
2018	1	0	0	0	0	0	0	1	0
	2	0	243	0	0	2	0	18	0
	3	0	0	0	0	0	0	4	0
	4	0	0	0	0	0	0	1	0
	5	0	342	160	69	0	0	27	2
	6	0	186	49	21	0	0	12	0
	7	0	456	208	89	0	0	36	2
2019	1	0	0	0	0	0	0	0	0
	2	0	364	43	19	2	1	16	0
	3	0	30	0	0	0	0	3	0
	4	66	61	21	9	0	0	1	0
	5	28	247	96	41	0	0	27	2
	6	0	99	0	0	0	0	12	0
	7	94	380	140	60	0	0	36	2
2020	1	0	0	0	0	0	0	0	0
	2	0	243	0	0	0	0	20	0
	3	0	0	0	0	0	0	3	0
	4	0	92	0	0	0	0	0	0
	5	0	295	192	82	2	1	25	2
	6	0	99	0	0	0	0	13	0
	7	0	467	241	103	3	2	34	3
2021	1	0	0	0	0	0	0	0	0
	2	0	364	43	19	0	0	18	0
	3	0	0	0	0	0	0	2	0
	4	0	92	0	0	0	0	1	0
	5	0	247	160	69	0	0	30	2
	6	0	186	49	21	0	0	13	0
	7	0	421	208	89	0	0	40	3
2022	1	0	0	0	0	0	0	0	0
	2	0	243	0	0	0	0	16	0
	3	0	30	0	0	0	0	2	0
	4	33	61	21	9	0	0	1	0
	5	28	247	160	69	0	0	32	2
	6	0	99	0	0	0	0	13	0
	7	64	380	220	94	0	0	43	3
2023	1	0	0	0	0	0	0	0	0
	2	0	364	43	19	0	0	16	0
	3	0	0	0	0	0	0	2	0
	4	11	61	0	0	0	0	1	0

Year	Zone	2-D	3-D	WAZ	Coil	Shallow hazards	Boomer	High resolution sources	VSP
	5	9	247	128	55	0	0	35	2
	6	0	99	0	0	0	0	13	0
	7	21	380	160	69	0	0	46	3
2024	1	0	0	0	0	0	0	0	0
	2	0	243	0	0	0	0	16	0
	3	0	0	0	0	0	0	2	0
	4	0	61	0	0	0	0	1	0
	5	0	200	192	82	0	0	35	2
	6	0	99	0	0	0	0	14	0
	7	0	321	241	103	0	0	47	3
2025	1	0	0	0	0	0	0	0	0
	2	0	364	43	19	0	0	13	0
	3	0	30	0	0	0	0	2	0
	4	5	61	0	0	0	0	1	0
	5	0	200	160	69	0	0	37	2
	6	0	99	0	0	0	0	14	0
	7	5	321	200	86	0	0	49	3

Table 76. Decade exposure estimates totals for 2-D survey (8000 in3 airgun array, 1 vessel).

Species	Number of Level A exposures			Number of Level B exposures	
	peak SPL	SEL	180 rms SPL	Step fxn	160 rms SPL
Atlantic spotted dolphins	15.4	0.4	799.2	11119.4	25677.0
Beaked whales	8.6	0.2	817.5	63149.9	14473.3
Common bottlenose dolphins	38.3	2.7	1537.0	28167.1	62589.2
Bryde's whales	0.1	1.6	10.6	170.7	206.9
Clymene dolphins	53.3	4.1	1323.7	24009.2	44719.5
False killer whales	11.4	0.3	357.1	5674.4	10068.6
Fraser's dolphins	5.3	0.1	434.5	3293.6	5461.2
Killer whales	0.6	0.0	51.3	356.0	513.9
Kogia	695.3	54.8	562.3	4109.2	9529.1
Melon-headed whales	27.5	0.5	2042.3	16758.4	30165.0
Pantropical spotted dolphins	392.2	32.9	9484.5	147959.4	233759.0
Pygmy killer whales	8.8	0.2	271.9	4103.6	6791.7
Risso's dolphins	14.4	1.6	386.5	6152.2	11897.9
Rough-toothed dolphins	14.1	0.5	445.9	7404.2	13861.5
Short-finned pilot whales	6.4	0.1	373.6	3756.0	7949.1
Sperm whales	5.3	0.5	1155.7	8440.7	17049.9
Spinner dolphins	37.5	2.4	975.3	22080.0	48754.6
Striped dolphins	24.4	2.0	600.2	10310.2	18203.5

Table 77. Decade exposure estimates totals for 3-D NAZ survey (8000 in^3 airgun array, 2 vessels).

Species	Number of Level A exposures			Number of Level B exposures	
	peak SPL	SEL	180 rms SPL	Step fxn	160 rms SPL
Atlantic spotted dolphins	3058.8	291.8	425998.1	1228034.9	1667456.2
Beaked whales	280.9	14.8	26069.3	1110419.9	278440.7
Common bottlenose dolphins	20841.3	987.6	2473207.9	6923848.5	8897488.1
Bryde's whales	1.9	80.1	290.4	3445.4	4136.5
Clymene dolphins	2178.8	188.1	42251.2	511975.3	958233.2
False killer whales	608.9	63.7	14073.8	123229.2	222375.7
Fraser's dolphins	287.4	20.1	11851.7	66174.0	110436.2
Killer whales	26.4	3.0	1464.6	6780.5	9922.1
Kogia	13737.4	3033.6	14719.0	76595.1	170808.1
Melon-headed whales	1378.5	103.4	54084.8	324416.8	577869.6
Pantropical spotted dolphins	12361.1	633.0	263990.9	2766953.3	4444346.7
Pygmy killer whales	449.7	43.4	9594.2	85023.0	147507.7
Risso's dolphins	554.3	80.1	11917.9	124421.0	230226.7
Rough-toothed dolphins	899.8	96.1	34970.6	212341.8	367525.5
Short-finned pilot whales	372.7	47.3	13308.4	92144.7	188732.9
Sperm whales	209.8	9.9	39711.3	200875.5	440333.7
Spinner dolphins	1326.5	52.8	26421.5	379755.9	755780.9
Striped dolphins	864.9	57.0	17617.0	202165.4	356206.0

Table 78. Decade exposure estimates totals for 3-D WAZ survey (8000 in^3 airgun array, 4 vessels).

Species	Number of Level A exposures			Number of Level B exposures	
	peak SPL	SEL	180 rms SPL	Step fxn	160 rms SPL
Atlantic spotted dolphins	200.0	7.7	46492.0	176331.1	297393.7
Beaked whales	35.7	0.4	18840.3	509016.2	122280.5
Common bottlenose dolphins	731.6	23.9	214892.9	740252.6	1266979.2
Bryde's whales	0.4	8.0	232.1	1537.8	1778.4
Clymene dolphins	382.2	9.9	24392.2	242870.1	423953.6
False killer whales	90.8	7.8	6945.0	52221.3	88802.1
Fraser's dolphins	38.8	0.4	9055.6	30624.1	46756.5
Killer whales	3.8	0.6	984.1	3607.6	4493.7
Kogia	17564.6	328.7	11860.7	36823.3	78907.1
Melon-headed whales	192.9	1.9	42915.7	153249.3	254568.5
Pantropical spotted dolphins	2530.6	23.2	168480.7	1463671.7	2233856.1
Pygmy killer whales	70.6	6.8	5232.3	37762.1	60391.3
Risso's dolphins	95.7	11.8	5304.4	61686.3	107841.1
Rough-toothed dolphins	114.8	8.7	9990.9	71087.6	124947.1
Short-finned pilot whales	45.2	1.3	8862.5	35979.0	71216.1
Sperm whales	70.2	0.5	31667.8	88325.5	182929.6
Spinner dolphins	268.6	0.7	17124.8	208893.6	410523.8
Striped dolphins	165.7	2.6	10805.2	102441.1	170483.2

Table 79. Decade exposure estimates totals for Coil survey (8000 in^3 airgun array, 4 vessels).

Species	Number of Level A exposures			Number of Level B exposures	
	peak SPL	SEL	180 rms SPL	Step fxn	160 rms SPL
Atlantic spotted dolphins	289.2	9.1	13749.8	43206.0	61621.2
Beaked whales	99.3	4.0	5927.4	126419.5	25788.4
Common bottlenose dolphins	1408.5	72.1	53895.2	168113.4	206461.0
Bryde's whales	0.7	28.1	55.8	339.3	365.1
Clymene dolphins	705.8	36.8	11518.1	60515.5	86456.1
False killer whales	172.4	7.0	4008.4	17015.2	26092.4
Fraser's dolphins	78.7	1.8	2626.7	7884.0	9747.0
Killer whales	8.0	0.4	372.4	937.4	1085.9
Kogia	3430.4	925.4	3477.7	9621.9	16570.1
Melon-headed whales	380.8	9.2	12526.0	39889.1	53267.6
Pantropical spotted dolphins	5027.9	288.9	78535.6	363843.5	473365.5
Pygmy killer whales	130.8	5.0	3032.9	12322.3	18068.9
Risso's dolphins	193.1	16.9	2913.9	15014.2	20920.1
Rough-toothed dolphins	220.8	9.5	5459.9	22950.9	35966.9
Short-finned pilot whales	81.3	2.3	2637.2	9621.6	14859.6
Sperm whales	65.3	5.5	8703.0	24374.2	40181.5
Spinner dolphins	473.7	21.0	8156.9	51218.3	81117.5
Striped dolphins	316.6	17.2	5071.9	25453.3	35226.2

Table 80. Decade exposure estimates totals for 90 in^3 airgun.

Species	Number of Level A exposures			Number of Level B exposures	
	peak SPL	SEL	180 rms SPL	Step fxn	160 rms SPL
Atlantic spotted dolphins	0.0	0.0	7.0	50.1	104.1
Beaked whales	0.0	0.0	0.0	34.8	1.8
Common bottlenose dolphins	0.0	0.0	57.7	228.8	353.6
Bryde's whales	0.0	0.0	0.0	0.0	0.0
Clymene dolphins	0.0	0.0	1.0	2.9	3.4
False killer whales	0.0	0.0	0.2	0.9	1.4
Fraser's dolphins	0.0	0.0	0.2	0.5	0.7
Killer whales	0.0	0.0	0.0	0.1	0.1
Kogia	0.1	0.0	0.3	0.5	0.9
Melon-headed whales	0.0	0.0	1.1	2.0	3.1
Pantropical spotted dolphins	0.0	0.0	6.1	20.0	25.3
Pygmy killer whales	0.0	0.0	0.2	0.5	0.7
Risso's dolphins	0.0	0.0	0.2	0.7	1.1
Rough-toothed dolphins	0.0	0.0	0.5	4.6	7.7
Short-finned pilot whales	0.0	0.0	0.2	0.4	0.7
Sperm whales	0.0	0.0	0.4	2.1	4.6
Spinner dolphins	0.0	0.0	1.0	2.3	2.3
Striped dolphins	0.0	0.0	0.4	1.3	1.6

Table 81. Decade exposure estimates totals for boomer.

Species	Number of Level A exposures			Number of Level B exposures	
	peak SPL	SEL	180 rms SPL	Step fxn	160 rms SPL
Atlantic spotted dolphins	0.0	0.0	1.3	7.5	15.0
Beaked whales	0.0	0.0	0.0	23.2	1.2
Common bottlenose dolphins	0.0	0.0	9.0	33.3	51.0
Bryde's whales	0.0	0.0	0.0	0.0	0.0
Clymene dolphins	0.0	0.0	0.7	1.9	2.3
False killer whales	0.0	0.0	0.1	0.5	0.7
Fraser's dolphins	0.0	0.0	0.2	0.3	0.4
Killer whales	0.0	0.0	0.0	0.0	0.1
Kogia	0.1	0.0	0.2	0.4	0.6
Melon-headed whales	0.0	0.0	0.7	1.3	2.0
Pantropical spotted dolphins	0.0	0.0	4.1	13.3	16.8
Pygmy killer whales	0.0	0.0	0.1	0.3	0.5
Risso's dolphins	0.0	0.0	0.1	0.5	0.8
Rough-toothed dolphins	0.0	0.0	0.2	1.1	1.7
Short-finned pilot whales	0.0	0.0	0.1	0.3	0.4
Sperm whales	0.0	0.0	0.3	1.4	3.1
Spinner dolphins	0.0	0.0	0.6	1.5	1.5
Striped dolphins	0.0	0.0	0.3	0.9	1.0

Table 82. Decade exposure estimate totals for the high resolution sources (side-scan sonar, sub-bottom profiler, and multibeam scanner).

Species	Number of Level A exposures			Number of Level B exposures	
	peak SPL	SEL	180 rms SPL	Step fxn	160 rms SPL
Atlantic spotted dolphins	0.0	8.2	9.0	34.3	11.4
Beaked whales	0.0	0.7	0.7	45.6	0.0
Common bottlenose dolphins	0.0	95.2	122.8	245.3	68.5
Bryde's whales	0.0	0.0	0.0	0.0	0.0
Clymene dolphins	0.0	0.1	0.1	0.1	0.0
False killer whales	0.0	0.0	0.0	0.1	0.0
Fraser's dolphins	0.0	0.0	0.0	0.1	0.0
Killer whales	0.0	0.0	0.0	0.0	0.0
Kogia	0.0	0.0	0.0	0.0	0.0
Melon-headed whales	0.0	0.1	0.1	0.1	0.0
Pantropical spotted dolphins	0.0	0.4	0.4	0.4	0.0
Pygmy killer whales	0.0	0.0	0.0	0.0	0.0
Risso's dolphins	0.0	0.0	0.0	0.0	0.0
Rough-toothed dolphins	0.0	0.4	0.4	1.6	0.7
Short-finned pilot whales	0.0	0.0	0.0	0.0	0.0
Sperm whales	0.0	0.3	0.4	0.5	0.0
Spinner dolphins	0.0	0.1	0.1	0.1	0.0
Striped dolphins	0.0	0.0	0.0	0.0	0.0

8. Discussion

This study provides estimates of annual marine mammal acoustic exposure due to geological and geophysical exploration activity in the Gulf of Mexico for years 2016 to 2025. Exposure estimates were computed from modeled sound levels received by simulated animals for several types of geophysical surveying. Because animals and sources move relative to the environment and each other, and the sound fields generated by the sources are shaped by various physical parameters, the sound levels received by an animal are a complex function of location and time. The basic modeling approach was to use acoustic models to compute the three-dimensional (3-D) sound fields and their variations in time. Simulated animals (animats) were modeled moving through these fields to sample the sound levels in a manner similar to how real animals would experience these sounds. From the time histories of the received sound levels of all animats, the numbers of animals exposed to levels exceeding effects threshold criteria were determined and then adjusted by the number of animals expected in the area, based on density information, to estimate the potential number of animals impacted.

In the preliminary Phase I component of this study (Section 6.3), a Test Case simulating a typical 3-D WAZ survey at two locations was performed to demonstrate and test the basic modeling approach and, importantly, to evaluate its limitations and accuracy of results prior to employing the methods in the main Phase II study (Section 7.2). A series of Test Scenarios were examined using, primarily, the results of the Test Case to investigate the effects of methodological choices on exposure estimates. With the overall modeling goal to estimate exposure levels from future survey activity whose individual details such as exact location and duration are unknown, a primary concern was how to scale results to account for different survey types, locations and spatial extents, and durations.

In Test Scenario 1 (Section 6.5.1), issues arising when estimating impacts during long-duration surveys were investigated and a method was suggested. In this study, a 24 h reset period was used, meaning that received levels for all animats were reset to zero after any 24 h evaluation period. For time-based, SEL metrics, energy accumulation was restarted at zero after 24 h, and the time-independent SPL metrics maximum values were reset to zero. After each reset, animals were again available to be taken (counted as exposed above the effects threshold). A reset period creates a scaling time-basis for impact analysis, and 24 h is short relative to most surveys. It was shown in Test Scenario 1 that scaling (multiplying) the average 24 h exposure estimate by the number of days of survey was more conservative (produced lower number of animats exposed to levels exceeding threshold) than evaluating exposure for longer periods because individual animats could be counted multiple times. The parameters governing animal movement were obtained from short-duration events, such as several dives, and for this modeling project did not include long-duration behavior like migration or periodically revisiting an area as part of a circulation pattern. These behaviors could be modeled, but there are no data available currently to support detailed modeling of this type of behavior in the Gulf of Mexico.

It was also found in Test Scenario 1 that the location-specific details of the survey had the greatest impact on exposure estimates—that is, whether the survey is conducted in shallow or deep water has a greater influence on exposure estimates than trends due to short-duration movement of the animats. Because specific location details for future surveys were not know, the modeling goal was to determine accurate 24 h exposure estimates from representative surveys in the areas where future surveys may be conducted. The simulations should cover relevant acoustic environments, including areas with different sound velocity profiles, depths, and geoacoustic properties. Seven day simulations were chosen to ensure differing environments would be sampled.

Sound velocity profiles change continuously, but it was shown in Test Scenario 2 (Section 6.5.2) that the primary difference in acoustic propagation due to changes in the sound velocity profile was the presence or absence of a sound conducting channel near the surface. In the Gulf, a surface duct only occurs in the winter season. To account for this difference in acoustic propagation, simulations were performed in

winter and summer (with summer also representing spring and fall). The seven day simulations were analyzed in 24 h periods using a sliding window approach to get the average 24 h estimate for each survey type in each modeling zone. Future surveys of unknown duration may be conducted during any portion of the year and in any location within a specified Planning Area, so the aim of the modeling and analysis was to determine accurate 24 h exposure estimates to be scaled by the projected level of effort for the different survey types in order to provide yearly exposure estimates.

With any modeling exercise, uncertainty in the input parameters results in uncertainty in the output. Sources of uncertainty and their effects on exposure estimates were investigated in Test Scenario 2. The primary source of uncertainty in this project was the location of the animals at the times of the surveys, which drives the choice of using an agent-based modeling approach and Monte Carlo sampling. Uncertainty in the density estimates of the animals is related to the uncertainty in the location of the animals. For the Phase II assessment we used density estimates from the Marine Geospatial Ecology Laboratory (Duke University) model (Roberts et al. In preparation) (Section 7.2.6.1). The model does not include seasonal variations of densities in the Gulf, and because surveys could occur at any location within a Planning Area, the density estimates were taken over an entire modeling zone. Similarly, the density was assumed to be uniform and static over the area covered by each survey. Real world animal densities can fluctuate significantly, but assuming many surveys will be conducted in many locations the variations in density are expected to average toward the mean. Sources of uncertainty in the other modeling parameters were found to affect the variance of the modeling results, as opposed to their mean. Our common use of mean input parameters is therefore justified by the same argument as using mean animal densities. For example, the nominal pressure of an operating airgun array may be specified as 2000 psi, but in practice the pressure will sometimes be higher or lower; therefore, the source level will be somewhat higher or lower. Again, over many surveys the average source level, and therefore received sound levels, will tend toward the specified nominal values. The effects of the variability in many of the modeling parameters on exposure estimates were quantified using a resampling technique (Bootstrap resampling). It was found that uncertainty in parameters such as animal density and social group size had a profound effect on the distribution of the exposure estimates, but not on the mean exposure. That is, the distribution shape and range of the number of animals above threshold changed, but the mean number of animals above threshold remained the same. Though a relatively minor effect, a small variability in the source level could increase the number of animals above threshold because the numbers of animals just below threshold is usually greater than the number of animats just above threshold.

Some modeling options do affect the mean of the exposure estimates. Mitigation procedures, such as shutting down the airgun array when animals were detected within an established exclusion zone, could reduce the injury exposure estimates. Mitigation effectiveness, (Test Case 3, Section 6.5.3), was found to be influenced by several factors, such as the density of the animals in the survey area and detection probability. Some species are more easily detected than others, and detection probability varies with weather and observational set up. Weather during any seismic survey is unknown beforehand and detection probabilities are difficult to predict. As a conservative measure, the potential effects of mitigation were not included in the exposure estimates.

Likewise, aversion, or animals avoiding loud or annoying sounds, could lead to reduced numbers of injury exposure estimates (Test Case 4, Section 6.5.4). Aversion is a behavioral response and depends on the context in which the sound is received and on biological factors, such as energetic and reproductive state, sociality, and health status of individual animals. Currently, too little is known about the factors that could influence aversion, including the thresholds for received sound levels that might elicit an aversion response, or movement of averting animals to justify decreasing the exposure estimates by assuming aversion.

In summary, the choice of a 24 h resetting period separated the analysis of a survey into portions typically much shorter duration than the survey itself. The average 24 h exposure estimate scaled by the duration of the survey in days gives the exposure estimate for the total survey. There is variance associated with 24 h

exposure estimates due to sampling, movement of the survey, and uncertainty in modeling parameters. Variance, in general, affects the distribution shape of the number of animals above exposure criteria, but it did not significantly affect the mean number of animals above the criteria. When many surveys are pooled the effects of uncertainty are decreased. The aim of Phase II components of this study was to estimate the exposure distributions for each species, for each year, and over the entire gulf that result from many surveys. The resulting exposure estimates of Phase II represent the aggregate average exposure risk from future surveys given the specified levels of effort for each survey type in each year.

9. Literature Cited

[DoN] Department of the Navy. 2007. *Navy OPAREA Density Estimate (NODE) for the Gulf of Mexico*. Prepared for the Department of the Navy, U.S. Fleet Forces Command, Norfolk, VA. Contract #N62470-02 D-9997, CTO 0030. Prepared by Geo-Marine, Inc., Hampton, VA. . http://seamap.env.duke.edu/seamap2/downloads/resources/serdp/Gulf%20of%20Mexico%20NODE%20Final%20Report.pdf.

[ITC] International Transducer Corporation. 1993. *Application Equations for Underwater Sound Transducers* (pamphlet). International Transducer Corporation, Santa Barbara, CA.

[IWC] International Whaling Commission. 2007. Report of the Scientific Committee. Annex K. Report of the Standing Working Group on Environmental Concerns. *Journal of Cetacean Research and Management (Suppl.)* 9: 227-296.

[MMC] Marine Mammal Commission. 2007. *Marine mammals and noise: A sound approach to research and management*. A Report to Congress from the Marine Mammal Commission. http://www.mmc.gov/reports/workshop/pdf/fullsoundreport.pdf.

[MMPA] Marine Mammal Protection Act of 1972 as Amended. 2007. United States Pub. L. No. 92-522, 16 U.S.C. 1361 (Oct. 21, 1972). http://www.nmfs.noaa.gov/pr/laws/mmpa/text.htm.

[NGDC] National Geophysical Data Center. 2014. U.S. Coastal Relief Model, Vol. 3 Florida and Eastern Gulf of Mexico, Vol. 4 Central Gulf of Mexico, Vol. 5 Western Gulf of Mexico. National Geophysical Data Center, National Oceanic and Atmospheric Administration, U.S. Department of Commerce. http://www.ngdc.noaa.gov/mgg/coastal/crm.html (Accessed Dec 2014).

[NMFS] National Marine Fisheries Service (US) and [NOAA] National Oceanic and Atmospheric Administration. 1995. Small takes of marine mammals incidental to specified activities; offshore seismic activities in southern California: Notice of issuance of an incidental harassment authorization. *Federal Register* 60(200): 53753-53760.

[NMFS] National Marine Fisheries Service (US). 2000. Small takes of marine mammals incidental to specified activities; Marine seismic-reflection data collection in southern California. *Federal Register* 65(60): 16374-16379.

[NOS] National Ocean Service. 2013. *NOAA/NOS and USCGS Seabed Descriptions from Hydrographic Surveys* National Geophysical Data Center, NOAA.

Aerts, L., M. Blees, S. Blackwell, C. Greene, K. Kim, D. Hannay, and M. Austin. 2008. *Marine mammal monitoring and mitigation during BP Liberty OBC seismic survey in Foggy Island Bay, Beaufort Sea, July-August 2008: 90-day report*. Document Number LGL Report P1011-1. Report by LGL Alaska Research Associates Inc., LGL Ltd., Greeneridge Sciences Inc. and JASCO Applied Sciences for BP Exploration Alaska. 199 pp. http://www.nmfs.noaa.gov/pr/pdfs/permits/bp_liberty_monitoring.pdf.

Aguilar Soto, N., M. Johnson, P.T. Madsen, P.L. Tyack, A. Bocconcelli, and J. Fabrizio Borsani. 2006. Does intense ship noise disrupt foraging in deep-diving Cuvier's beaked whales (*Ziphius cavirostris*) ? *Marine Mammal Science* 22(3): 690-699.

Aguilar Soto, N., M.P. Johnson, P.T. Madsen, F. Diaz, I. Dominguez, A. Brito, and P. Tyack. 2009. Cheetahs of the deep sea: deep foraging sprints in short-finned pilot whales off Tenerife (Canary Islands). *Journal of Animal Ecology* 77: 936-947.

Alves, F., A. Dinis, I. Cascao, and L. Freitas. 2010. Bryde's whale (*Balaenoptera brydei*) stable associations and dive profiles: new insights into foraging behavior. *Marine Mammal Science* 26(1): 202-212.

Amano, M. and M. Yoshioka. 2003. Sperm whale diving behavior monitored using a suction-cup-attached TDR tag. *Marine Ecology Progress Series* 258: 291-295.

Amos, B., C. Schlotterer, and D. Tautz. 1993. Social structure of pilot whales revealed by analytical DNA profiling. *Science* 260(5108): 670-672.

Aoki, K., M. Amano, M. Yoshioka, K. Mori, D. Tokuda, and N. Miyazaki. 2007. Diel diving behavior of sperm whales off Japan. *Marine Ecology Progress Series* 349: 277-287.

Arveson, P.T. and D.J. Vendittis. 2000. Radiated noise characteristics of a modern cargo ship. *Journal of the Acoustical Society of America* 107(1): 118-129.

Au, D. and W. Perryman. 1982. Movement and speed of dolphin schools responding to an approaching ship. *Fishery Bulletin, US* 80: 371-379.

Au, W.W.L., A.A. Pack, M.O. Lammers, L.M. Herman, M.H. Deakos, and K. Andrews. 2006. Acoustic properties of humpback whale songs. *Journal of the Acoustical Society of America* 120(2): 1103-1110.

Austin, M., A. MacGillivray, D. Hannay, and M. Zykov. 2010. *Marine Acoustics (Enbridge Northern Gateway Project 2006)*. Technical Data Report. Technical Data Report by JASCO Applied Sciences for Stantec Inc.

Austin, M., A.O. MacGillivray, and N.R. Chapman. 2012. Acoustic transmission loss measurements in Queen Charlotte Basin. *Canadian Acoustics* 40(1): 27-31.

Baird, R.W. 1994. *Foraging behaviour and ecology of transient killer whales (Orcinus orca)*. Ph.D. Thesis. Simon Fraser University, Burnaby, BC.

Baird, R.W., D.J. McSweeney, D.L. Webster, A.M. Gorgone, and A.D. Ligon. 2003. *Studies of Odontocete Population Structure in Hawaiian Waters: Results of a Survey Through the Main Hawaiian Islands in May and June 2003*. Report prepared under contract# AB133F-02-CN-0106 to the Southwest Fisheries Science Center, National Marine Fisheries Service 8604. http://www.researchgate.net/profile/Robin_Baird/publication/228363974_Studies_of_odontocete_population_structure_in_Hawaiian_waters_Results_of_a_survey_through_the_main_Hawaiian_Islands_in_May_and_June_2003/links/02bfe5122cacb495a9000000.pdf.

Baird, R.W. 2005. Sightings of Dwarf (*Kogia sima*) and Pygmy (*K. breviceps*) sperm whales from the main Hawaiian Islands. *Pacific Science* 59(3): 461-466.

Baird, R.W., G.S. Shorr, D.J. Websater, D.J. McSweeney, and S.D. Mahaffy. 2006a. *Studies of beaked whale diving behavior and odontocete stock structure in Hawai'i in March/April 2006*. Report to Cascadia Research Collective, Olympia, WA from the Southwest Fisheries Science Center, National Marine Fisheries Service. 30 pp.

Baird, R.W., D.L. Webster, D.J. McSweeney, A.D. Ligon, G.S. Schorr, and J. Barlow. 2006b. Diving behaviour of Cuvier's (*Ziphius cavirostris*) and Blainville's (*Mesoplodon densirostris*) beaked whales in Hawai‘i. *Canadian Journal of Zoology* 84(8): 1120-1128.

Baird, R.W., G.S. Schorr, D.L. Webster, D.J. McSweeney, M.B. Hanson, and R.D. Andrews. 2010. Movements and habitat use of satellite-tagged false killer whales around the main Hawaiian Islands. *Endangered Species Research* 10: 107-121.

Baird, R.W., G.S. Schorr, D.L. Webster, D.J. McSweeney, M.B. Hanson, and R.D. Andrews. 2011. Movements of two satellite-tagged pygmy killer whales (*Feresa attenuata*) off the Island of Hawai'i. *Marine Mammal Science* 27(4): E332-E337.

Barlow, J. 1988. Harbor porpoise, *Phocoena phocoena*, abundance estimation for California, Oregon, and Washington. I: Ship surveys. *Fishery Bulletin* 86: 417-432.

Barlow, J. 1995. Abundance of cetaceans in California waters: I. Ship surveys in summer/fall 1991. *Fishery Bulletin (Seattle)* 93: 1-14.

Barlow, J. 1999. Trackline detection probability for long-diving whales. *In* Garner, G.W., S.C. Amstrup, I.L. Laake, B.E.I. Manly, L.L. McDonald, and D.G. Robertson (eds.). *Marine mammal survey and assessment methods*. Balkema Press, Netherlands. 209-221 pp.

Barlow, J. 2006. Cetacean abundance in Hawaiian waters estimated from a summer/fall survey in 2002. *Marine Mammal Science* 22(2): 446−464. http://digitalcommons.unl.edu/cgi/viewcontent.cgi?article=1237&context=usdeptcommercepub.

Barros, N.B. and D.K. Odell. 1990. Food Habits of Common bottlenose Dolphins in the Southeastern United States. *In* Leatherwood, S. and R. Reeves (eds.). *The common bottlenose dolphin*. Academic Press. 309-328 pp.

Barros, N.B. and R.S. Wells. 1998. Prey and feeding patterns of resident common bottlenose dolphins (*Tursiops truncatus*) in Sarasota Bay, Florida. *Journal of Mammologyology* 79(3): 1045-1059.

Bateson, M. 2007. Environmental noise and decision making possible implications of increases in anthropogenic noise for information processing in marine mammals. *International Journal of Comparative Psychology* 20(2).

Bearzi, G., R.R. Reeves, E. Remonato, N. Pierantonio, and S. Airoldi. 2011. Risso's dolphin *Grampus griseus* in the Mediterranean Sea. *Mammalian Biology* 76: 385-400.

Bearzi, M. 2005. Aspects of the ecology and behaviour of common bottlenose dolphins (*Tursiops truncatus*) in Santa Monica Bay, California. *Journal of the Cetacean Research Management* 7(1): 75-83.

Blackwell, S.B., R.G. Norman, C.R. Greene, Jr., and W.J. Richardson. 2007. *Acoustic measurements*. Marine Mammal Monitoring and Mitigation during Open Water Seismic Exploration by Shell Offshore Inc. in the Chukchi and Beaufort Seas, July–September 2006: 90-Day Report. LGL Report P891-1. Report by LGL Alaska Research Associates Inc. and Greeneridge Sciences Inc. for Shell Offshore Inc., National Marine Fisheries Service (US), and US Fish and Wildlife Service. 4-1 to 4-52 pp.

Brandt, M.J., A. Diederichs, K. Betke, and G. Nehls. 2011. Responses of harbour porpoises to pile driving at the Horns Rev II offshore wind farm in the Danish North Sea. *Marine Ecology Progress Series* 421: 205-216.

Buckingham, M.J. 2005. Compressional and shear wave properties of marine sediments: Comparisons between theory and data. *Journal of the Acoustical Society of America* 117(1): 137-152. http://link.aip.org/link/?JAS/117/137/1.

Buckland, S.T., D.R. Anderson, K.P. Burnham, J.L. Laake, D.L. Borchers, and L. Thomas. 2001. *Introduction to Distance Sampling*. Oxford University Press, Oxford.

Buckstaff, K.C. 2004. Effects of watercraft noise on the acoustic behavior of common bottlenose dolphins, *Tursiops truncatus*, in Sarasota Bay, Florida. *Marine Mammal Science* 20(4): 709-725.

Burdic, W.S. 2003. *Underwater acoustic system analysis*. 2nd edition. Peninsula Publishing, Los Altos, CA. 489.

Burkhardt, E. and C. Lanfredi. 2012. Fall feeding aggregations of fin whales off Elephant Island (Antarctica). *Paper SC/64/SH9 presented to the IWC Scientific Committee (unpublished). 6 pp. [Available from the Office of this Journal]*. http://epic.awi.de/30452/1/SC-64-SH9_corrected_may22.pdf.

Carnes, M.R. 2009. *Description and Evaluation of GDEM-V 3.0*. Document Number NRL Memorandum Report 7330-09-9165. US Naval Research Laboratory, Stennis Space Center, MS. 21 pp.

Castellote, M., C.W. Clark, and M.O. Lammers. 2012. Acoustic and behavioural changes by fin whales (*Balaenaptera physalus*) in response to shipping and airgun noise. *Biological Conservation* 147: 115-122.

Christal, J., H. Whitehead, and E. Lettevall. 1998. Sperm whale social units: Variation and change. *Canadian Journal of Zoology* 76(8): 1431-1440.

Christal, J. and H. Whitehead. 2001. Social affiliations within sperm whale (*Physeter macrocephalus*) groups. *Ethology* 107(4): 323-340.

Collins, M.D. 1993. A split-step Padé solution for the parabolic equation method. *Journal of the Acoustical Society of America* 93: 1736-1742.

Collins, M.D., R.J. Cederberg, D.B. King, and S. Chin-Bing. 1996. Comparison of algorithms for solving parabolic wave equations. *Journal of the Acoustical Society of America* 100(1): 178-182.

Connor, R.C., J. Mann, P.L. Tyack, and H. Whitehead. 1998. Social evolution in toothed whales. *Trends in Ecology & Evolution* 13(6): 228-232.

Cook, M.L.H. 2006. *Behavioral and auditory evoked potential (AEP) hearing measurements in odontocete cetaceans*. PhD Thesis. University of South Florida, St. Petersburg. 123 pp.

Coppens, A.B. 1981. Simple equations for the speed of sound in Neptunian waters. *Journal of the Acoustical Society of America* 69(3): 862-863. http://link.aip.org/link/?JAS/69/862/1.

Cox, T.M., T. Ragen, A. Read, E. Vos, R. Baird, K. Balcomb, J. Barlow, J. Caldwell, T. Cranford, et al. 2006. Understanding the impacts of anthropogenic sound on beaked whales. *Journal of Cetacean Research and Management* 7(3): 177-187. http://www.researchgate.net/publication/224554761_Understanding_the_impacts_of_anthropogenic_sound_on_beaked_whales/file/60b7d51e46006d38ae.pdf.

Cranford, T.W. and P. Krysl. 2015. Fin whale sound reception mechanisms: Skull vibration enables low-frequency hearing. *PLoS ONE* 10(1): e0116222.

Croll, D.A., A. Acevedo-Gutiérrez, B.R. Tershy, and J. Urbán-Ramírez. 2001. The diving behavior of blue and fin whales: is dive duration shorter than expected based on oxygen stores? *Comparative Biochemistry and Physiology, Part A: Molecular & Integrative Physiology* 129(4): 797-809.

Crum, L.A. and Y. Mao. 1996. Acoustically enhanced bubble growth at low frequencies and its implications for human diver and marine mammal safety. *Journal of the Acoustical Society of America* 99(5): 2898-2907. http://link.aip.org/link/?JAS/99/2898/1.

D'Amico, A., R. Gisiner, D. Ketten, J. Hammock, C. Johnson, P. Tyack, and J. Mead. 2009. Beaked whale strandings and naval exercises. *Aquatic Mammals* 35(4): 452-472.

Dahlheim, M.E. and P.A. White. 2010. Ecological aspects of transient killer whales *Orcinus orca* as predators in southeastern Alaska. *Wildlife Biology* 16: 308-322.

Dähne, M., A. Gilles, K. Lucke, V. Peschko, S. Adler, K. Krügel, J. Sundermeyer, and U. Siebert. 2013. Effects of pile-driving on harbour porpoises (*Phocoena phocoena*) at the first offshore wind farm in Germany. *Environmental Research Letters* 8(2): 025002.

Davis, R.W., G.A.J. Worthy, B. Wursig, and S.K. Lynn. 1996. Diving behavior and at-sea movements of an Atlantic spotted dolphin in the Gulf of Mexico. *Marine Mammal Science* 12(4): 569-581.

Davis, R.W., J.G. Ortega-Ortiz, C.A. Ribic, W.E. Evans, D.C. Biggs, P.H. Ressler, R.B. Cady, R.R. Leben, K.D. Mullin, et al. 2001. Cetacean habitat in the northern oceanic Gulf of Mexico. *Deep-Sea Research* 49: 1-22. http://www.researchgate.net/profile/Robert_Leben/publication/223834810_Cetacean_habitat_in_the_northern_oceanic_Gulf_of_Mexico/links/02bfe510d374ed262d000000.pdf.

Di Iorio, L. and C.W. Clark. 2010. Exposure to seismic survey alters blue whale acoustic communication. *Biology Letters* 6(1): 51-54.

Di Sciara, G.N. 1983. *Bryde's whales (Balaenoptera edeni Anderson 1878) off eastern Venezuela (Cetacea, Balaenopteridae)*. Technical Report 83-153. Hubbs-Sea World Research Institute, San Diego, CA. 27 pp.

Dragoset, W.H. 1984. A comprehensive method for evaluating the design of airguns and airgun arrays. *Proceedings, 16th Annual Offshore Technology Conference* Volume 3, May 7-9, 1984. OTC 4747, Houston, Houston. 75–84 pp.

EdgeTech. 2007. *Hull Mount Sub-bottom Profiler 3300-HM* (pamphlet).

Ellison, W.T., C.W. Clark, and G.C. Bishop. 1987. *Potential use of surface reverberation by bowhead whales, Balaena mysticetus, in under-ice navigation: Preliminary considerations*. Report of the International Whaling Commission. Volume 37. 329-332 pp.

Ellison, W.T., B.L. Southall, C.W. Clark, and A.S. Frankel. 2012. A new context-based approach to assess marine mammal behavioral responses to anthropogenic sounds. *Conservation Biology* 26(1): 21-28.

Engås, A., S. Løkkeborg, E. Ona, and A.V. Soldal. 1996. Effects of seismic shooting on local abundance and catch rates of cod (*Gadus morhua*) and haddock (*Melanogrammus aeglefinus*). *Canadian Journal of Fisheries and Aquatic Sciences* 53(10): 2238-2249. http://www.nrcresearchpress.com/doi/abs/10.1139/f96-177.

Fernández, A., J.F. Edwards, F. Rodriguez, A.E. De Los Monteros, P. Herraez, P. Castro, J.R. Jaber, V. Martin, and M. Arbelo. 2005. Gas and fat embolic syndrome involving a mass stranding of beaked whales (Family Ziphiidae) exposed to anthropogenic sonar signals. *Veterinary Pathology* 42(4): 446-457.

Finneran, J.J., C.E. Schlundt, R. Dear, D.A. Carder, and S.H. Ridgway. 2002. Temporary shift in masked hearing thresholds in odontocetes after exposure to single underwater impulses from a seismic watergun. *Journal of the Acoustical Society of America* 111(6): 2929-2940.

Finneran, J.J., D.A. Carder, C.E. Schlundt, and S.H. Ridgway. 2005. Temporary threshold shift in common bottlenose dolphins (*Tursiops truncatus*) exposed to mid-frequency tones. *Journal of the Acoustical Society of America* 119(4): 2696-2705.

Finneran, J.J. and C.E. Schlundt. 2010. Frequency-dependent and longitudinal changes in noise-induced hearing loss in a common bottlenose dolphin (*Tursiops truncatus*). *Journal of the Acoustical Society of America* 128(2): 567-570.

Finneran, J.J. and C.E. Schlundt. 2011. Subjective loudness level measurements and equal loudness contours in a common bottlenose dolphin (*Tursiops truncatus*). *Journal of the Acoustical Society of America* 130(5): 3124-3136.

Finneran, J.J. and A.K. Jenkins. 2012. *Criteria and thresholds for U.S. Navy acoustic and explosive effects analysis*. SPAWAR Systems Center Pacific, San Diego, California.

Fisher, F.H. and V.P. Simmons. 1977. Sound absorption in sea water. *Journal of the Acoustical Society of America* 62(3): 558-564. http://link.aip.org/link/?JAS/62/558/1.

Fletcher, J.L. and R.G. Busnel. 1978. *Effects of noise on wildlife*. Academic Press, New York.

Foote, A.D., R.W. Osborne, and A. Rus Hoelzel. 2004. Whale-call response to masking boat noise. *Nature* 428: 910.

Frankel, A.S., W.T. Ellison, and J. Buchanan. 2002. Application of the acoustic integration model (AIM) to predict and minimize environmental impacts. *OCEANS'02 MTS/IEEE*. 1438-1443 pp.

Funk, D., D. Hannay, D. Ireland, R. Rodrigues, and W. Koski (eds.). 2008. *Marine mammal monitoring and mitigation during open water seismic exploration by Shell Offshore Inc. in the Chukchi and Beaufort Seas, July–November 2007: 90-day report*. LGL Report P969-1. Prepared by LGL

Alaska Research Associates Inc., LGL Ltd., and JASCO Research Ltd. for Shell Offshore Inc., National Marine Fisheries Service (US), and US Fish and Wildlife Service. 218 pp.

Gentry, R., A. Bowles, W. Ellison, J. Finneran, C.R. Greene, Jr, D. Kastak, D. Ketten, J. Miller, P. Nachtigall, et al. 2004. *Noise exposure criteria*. Presentation to the Second Plenary Meeting of the Advisory Committee on Acoustic Impacts on Marine Animals, Arlington, VA. http://mmc.gov/sound/plenary2/pdf/gentryetal.pdf.

Gordon, J., D. Gillespie, J. Potter, A. Frantzis, M.P. Simmonds, R. Swift, and D. Thompson. 2003. A review of the effects of seismic surveys on marine mammals. *Marine Technology Society Journal* 37(4): 16-34. http://www.ingentaconnect.com/content/mts/mtsj/2003/00000037/00000004/art00003.

Greene, C.R., Jr and W.J. Richardson. 1988. Characteristics of marine seismic survey sounds in the Beaufort Sea. *Journal of the Acoustical Society of America* 83(6): 2246-2254.

Greene, C.R., Jr. 1997. *Physical acoustics measurements*. *In*: Richardson, W.J. (ed.). *Northstar Marine Mammal Monitoring Program, 1996: Marine Mammal and Acoustical Monitoring of a Seismic Program in the Alaskan Beaufort Sea*. LGL Rep. 2121-2. Report from LGL Ltd., King City, ON, and Greeneridge Sciences Inc., Santa Barbara, CA, for BP Exploration (Alaska) Inc., Anchorage, AK, and National Marine Fisheries Services, Anchorage, AK, and Silver Spring, MD. 3-1 to 3-63 pp.

Griffin, R.B., R.W. Baird, and C. Hu. 2005. *Movement patterns and diving behavior of Atlantic spotted dolphins (Stenella frontalis) in relation to oceanographic features: a study using remotely-deployed suction-cup attached tags. Project Number HBOI2003-09.* Mote Marine Laboratory Technical Report. Document Number Number 1005. Mote Marine Laboratory.

Hannay, D. and R. Racca. 2005. *Acoustic Model Validation*. Document Number 0000-S-90-04-T-7006-00-E, Revision 02. Technical report for Sakhalin Energy Investment Company Ltd. by JASCO Research Ltd. 34 pp.

Harris, C.M. 1998. *Handbook of acoustical measurements and noise control*. 3rd edition. Acoustical Society of America, Huntington, NY.

Hassel, A., T. Knutsen, J. Dalen, K. Skaar, S. Løkkeborg, O.A. Misund, Ø. Østensen, M. Fonn, and E.K. Haugland. 2004. Influence of seismic shooting on the lesser sandeel (Ammodytes marinus). *ICES Journal of Marine Science: Journal du Conseil* 61(7): 1165-1173. http://icesjms.oxfordjournals.org/content/61/7/1165.abstract.

Hastie, G.D., B. Wilson, L.J. Wilson, K.M. Parsons, and P.M. Thompson. 2004. Functional mechanisms underlying cetacean distribution patterns: Hotspots for common bottlenose dolphins are linked to foraging. *Marine Biology* 144(2): 397-403. http://www.beamreach.org/data/091/science/processing/erica/Articles/hot%20spots%20for%20dolphins.pdf.

Hastie, G.D., B. Wilson, and P.M. Thompson. 2006. Diving deep in a foraging hotspot: Acoustic insights into common bottlenose dolphin dive depths and feeding behaviour. *Marine Biology* 148: 1181-1188.

Hatch, L.T. and A.J. Wright. 2007. A brief review of anthropogenic sound in the oceans. *International Journal of Comparative Psychology* 20: 121-133.

Hatch, L.T., C.W. Clark, S.M. Van Parijs, A.S. Frankel, and D.W. Ponirakis. 2012. Quantifying loss of acoustic communication space for right whales in and around a U.S. National Marine Sanctuary. *Conservation Biology* 26(5): 983-994.

Heimlich-Boran, J.R. 1993. *Social organisation of the short-finned pilot whale, Globicephala macrorhynchus, with special reference to the comparative social ecology of delphinids*. University of Cambridge.

Henderson, D. and R.P. Hamernik. 1986. Impulse noise: Critical review. *Journal of the Acoustical Society of America* 80(2): 569-584. http://link.aip.org/link/?JAS/80/569/1.

Hildebrand, J.A. 2009. Anthropogenic and natural sources of ambient noise in the ocean. *Marine Ecology Progress Series* 395: 5-20.

Hill, H.M. and C. Campbell. 2014. The frequency and nature of allocare by a group of belugas (*Delphinapterus leucas*) in human care. *International Journal of Comparative Psychology* 27(3).

Holt, M.M., D.P. Noren, V. Veirs, C.K. Emmons, and S. Veirs. 2009. Speaking up: Killer whales (*Orcinus orca*) increase their call amplitude in response to vessel noise. *Journal of the Acoustical Society of America* 125(1): EL27-EL32.

Hooker, S.K. and R.W. Baird. 1999. Deep–diving behaviour of the northern common bottlenose whale, *Hyperoodon ampullatus* (Cetacea: Ziphiidae). *Proceedings of the Royal Society of London B: Biological Sciences* 266(1420): 671-676. http://rspb.royalsocietypublishing.org/royprsb/266/1420/671.full.pdf.

Hotchkin, C. and S. Parks. 2013. The Lombard effect and other noise-induced vocal modifications: insight from mammalian communication systems. *Biological Reviews* 88(4): 809-824.

Houser, D.S., R. Howard, and S. Ridgway. 2001. Can diving-induced tissue nitrogen supersaturation increase the chance of acoustically driven bubble growth in marine mammals? *Journal of Theoretical Biology* 213(2): 183-195.

Houser, D.S. 2006. A method for modeling marine mammal movement and behavior for environmental impact assessment. *IEEE Journal of Oceanic Engineering* 31(1): 76-81.

Houser, D.S., L.A. Dankiewicz -Talmadge, T.K. Stockard, and P.J. Ponganis. 2010. Investigation of the potential for vascular bubble formation in a repetitively diving dolphin. *Journal of Experimental Biology* 213: 52-62. http://jeb.biologists.org/content/213/1/52.full.pdf+html.

Houser, D.S. and M.J. Cross. 2014. *Marine Mammal Movement and Behavior (3MB): A Component of the Effects of Sound on the Marine Environment (ESME) Distributed Model*. Version 10.14, by BIOMIMETICA.

Ireland, D.S., R. Rodrigues, D. Funk, W. Koski, and D. Hannay. 2009. *Marine mammal monitoring and mitigation during open water seismic exploration by Shell Offshore Inc. in the Chukchi and Beaufort Seas, July–October 2008: 90-Day Report*. Document Number LGL Report P1049-1. 277 pp.

Jaquet, N. and D. Gendron. 2002. Distribution and relative abundance of sperm whales in relation to key environmental features, squid landings and the distribution of other cetacean species in the Gulf of California, Mexico. *Marine Biology* 141(3): 591-601.

Jepson, P.D., R. Deaville, K. Acevedo-Whitehouse, J. Barnett, A. Brownlow, R.L. Brownell Jr, F.C. Clare, N. Davison, R.J. Law, et al. 2013. What caused the UK's largest common dolphin (*Delphinus delphis*) mass stranding event? *PLoS ONE* 8(4): e60953. http://www.plosone.org/article/info%3Adoi%2F10.1371%2Fjournal.pone.0060953#pone-0060953-g009.

Kasuya, T. and H. Marsh. 1984. Life history and reproductive biology of the short-finned pilot whale, *Globicephala macrorhynchus*, off the Pacific coast of Japan. *Report of the International Whaling Commission, Special* 6: 259-310.

Kasuya, T., R. Brownell, Jr, and K. Balcomb, III. 1997. Life history of Baird's beaked whales off the Pacific coast of Japan. *Report of the International Whaling Commission* 47: 969-979.

Kato, H. and W. Perrin. 2009. *Bryde's whale*. *In*: Perrin, W., B. Wursig, and J.G.M. Thewissen (eds.). *Encyclopedia of marine mammals*. Academic Press.

Kingsley, M.C.S. and I. Stirling. 1991. Haul-out behaviour of ringed and bearded seals in relation to defence against surface predators. *Canadian Journal of Zoology* 69: 1857-1861.

Kinsler, L.E., A.R. Frey, A.B. Coppens, and J.V. Sanders. 2000. *Fundamentals of acoustics*. 4th edition. John Wiley & Sons Inc., New York.

Kongsberg. 2004. *SM 2000 200 kHz Multibeam Echosounder Sonar. P/N 920-20210000* (pamphlet).

Kremser, U., P. Klemm, and W.-D. Kötz. 2005. Estimating the risk of temporary acoustic threshold shift, caused by hydroacoustic devices, in whales in the Southern Ocean. *Antarctic Science* 17(1): 3-10

Kryter, K.D., W.D. Ward, J.D. Miller, and D.H. Eldredge. 1966. Hazardous Exposure to Intermittent and Steady-State Noise. *Journal of the Acoustical Society of America* 39(3): 451-464. http://link.aip.org/link/?JAS/39/451/1.

Landro, M. 1992. Modeling of GI gun signatures. *Geophysical Prospecting* 40: 721–747.

Laws, M., L. Hatton, and M. Haartsen. 1990. Computer modeling of clustered airguns. *First Break* 8: 331–338.

Lin, H.W., A.C. Furman, S.G. Kujawa, and M.C. Liberman. 2011. Primary neural degeneration in the guinea pig cochlea after reversible noise-induced threshold shift. *Journal of the Association for Research in Otolarynology* 12(5): 605-616.

Long, T.M., R.T. Hanlon, A. Ter Maat, and H.M. Pinsker. 1989. Non-associative learning in the squid *lolliguncula brevis* (Mollusca, Cephalopoda). *Marine Behaviour and Physiology* 16: 1-9.

Lopez, B.D. 2009. The common bottlenose dolphin *Tursiops truncatus* foraging around a fish farm: Effects of prey abundance on dolphin's behavior. *Current Zoology* 55(4): 243-248.

Lucke, K., U. Siebert, P. Lepper, A., and M.-A. Blanchet. 2009. Temporary shift in masked hearing thresholds in a harbor porpoise (*Phocoena phocoena*) after exposure to seismic airgun stimuli. *Journal of the Acoustical Society of America* 125(6): 4060-4070.

Lurton, X. 2002. *An Introduction to Underwater Acoustics: Principles and Applications*. Springer, Chichester, U.K. 347.

Lurton, X. and S. DeRuiter. 2011. Sound radiation of seafloor-mapping echosounders in the water column, in relation to the risks posed to marine mammals. *International Hydrographic Review*, (November), 7-17.

Lydersen, C. and K.M. Kovacs. 1999. Behaviour and energetics of ice-breeding, North Atlantic phocid seals during the lactation period. *Marine Ecology Progress Series* 187: 265-281.

MacGillivray, A., M. Zykov, and D. Hannay. 2007. Summary of Noise Assessment. (Chapter 3) *In Marine Mammal Monitoring and Mitigation During Open Water Seismic Exploration by ConocoPhillips Alaska, Inc. in the Chukchi Sea July-October 2006*. Report by LGL Alaska Research Associates and JASCO Research Ltd. for ConocoPhillips Alaska, Inc.

MacGillivray, A.O. 2006. *Acoustic Modelling Study of Seismic Airgun Noise in Queen Charlotte Basin*. M. Sc. Thesis. University of Victoria, Victoria, BC.

MacGillivray, A.O., R. Racca, and Z. Li. 2014. Marine mammal audibility of selected shallow-water survey sources. *Journal of the Acoustical Society of America* 135(1): EL35-EL40. http://scitation.aip.org/content/asa/journal/jasa/135/1/10.1121/1.4838296.

MacIntyre, K.Q., K.M. Stafford, C.L. Berchok, and P.L. Boveng. 2013. Year-round acoustic detection of bearded seals (*Erignathus barbatus*) in the Beaufort Sea relative to changing environmental conditions, 2008-2010. *Polar Biology* 36(8): 1161-1173.

MacIntyre, K.Q., K.M. Stafford, P. Conn, K.L. Laidre, and P.L. Boveng. In Press. The relationship between sea ice concentration and the spatio-temporal distribution of vocalizing bearded seals

(*Erignathus barbatus*) in the Bering, Chukchi, and Beaufort Seas from 2008-2011. *Progress of Oceanography*.

Madsen, P.T., M. Wahlberg, J. Tougaard, K. Lucke, and P.L. Tyack. 2006. Wind turbine underwater noise and marine mammals: implications of current knowledge and data needs.

Malme, C.I., P.R. Miles, C.W. Clark, P. Tyack, and J.E. Bird. 1984. *Investigations of the potential effects of underwater noise from petroleum industry activities on migrating gray whale behavior. Phase II: January 1984 migration*. BBN Report 5586. Bolt Beranek and Newman Inc. 357 pp.

Malme, C.I., P.W. Smith, and P.R. Miles. 1986. *Characterisation of Geophysical Acoustic Survey Sounds*. Report by BBN Laboratories Inc. for Battelle Memorial Institute to the Minerals Management Service, Pacific Outer Continental Shelf Region.

Malme, C.I., B. Würsig, J.E. Bird, and P.L. Tyack. 1988. Observations of feeding gray whale responses to controlled industrial noise exposure. *In* Sackinger, W.M., M.O. Jeffries, J.L. Imm, and S.D. Treacy (eds.). *Port and ocean engineering under Arctic conditions*. Volume 2. University of Alaska, Geophysical Institute, Fairbanks.

Marques, F.F.C. and S.T. Buckland. 2004. Covariate models for the detection function. *In* Buckland, S.T., D.R. Anderson, K.P. Burnham, J.L. Laake, D.L. Borchers, and L. Thomas (eds.). *Advanced Distance Sampling*. Oxford University Press, Oxford. 31-47 pp.

Martin, B., J. MacDonnell, N.E. Chorney, and D. Zeddies. 2012. Appendix A: Sound Source Verification of Fugro Geotechnical Sources. *In ESS Group, Inc. Renewal Application for Incidental Harassment Authorization for the Non-Lethal Taking of Marine Mammals Resulting from Pre-Construction High Resolution Geophysical Survey*. For Cape Wind Associates, LLC. http://www.nmfs.noaa.gov/pr/pdfs/permits/capewind_iha_application_renewal.pdf.

Massa, D.P. 2003. Acoustic transducers. *In Wiley Encyclopedia of Telecommunications*. John Wiley & Sons, Inc.

Matthews, M.-N.R. and A.O. MacGillivray. 2013. Comparing modeled and measured sound levels from a seismic survey in the Canadian Beaufort Sea. *Proceedings of Meetings on Acoustics* 19(1): 1-8. http://scitation.aip.org/content/asa/journal/poma/19/1/10.1121/1.4800553.

Mattsson, A. and M. Jenkerson. 2008. *Single Airgun and Cluster Measurement Project*. *Joint Industry Programme (JIP) on Exploration and Production Sound and Marine Life Proramme Review*, October 28-30. International Association of Oil and Gas Producers, Houston, TX.

Maze-Foley, K. and K.D. Mullin. 2006. Cetaceans of the oceanic northern Gulf of Mexico: Distributions, group sizes and interspecific associations. *Journal of Cetacean Research and Management* 8(2): 203-213.

McCauley, R.D., M. Jenner, C. Jenner, K. McCabe, and J. Murdoch. 1998. The response of humpback whales (*Megaptera novaeangliae*) to offshore seismic survey noise: Preliminary results of observations about a working seismic vessel and experimental exposures. *Australian Petroleum Production Exploration Association (APPEA) Journal* 38(1): 692-707.

McCauley, R.D., J. Fewtrell, A.J. Duncan, C. Jenner, M.-N. Jenner, J.D. Penrose, R.I.T. Prince, A. Adihyta, J. Murdoch, et al. 2000a. *Marine seismic surveys: Analysis and propagation of air gun signals, and effects of exposure on humpback whales, sea turtles, fishes and squid*. Volume CMST R99-15. Prepared for the Australian Petroleum Exploration and Production Association from the Centre for Marine Science and Technology, Curtin University, Perth. 185 pp.

McCauley, R.D., J. Fewtrell, A.J. Duncan, C. Jenner, M.-N. Jenner, J.D. Penrose, R.I.T. Prince, A. Adihyta, J. Murdoch, et al. 2000b. Marine seismic surveys: A study of environmental implications. *Australian Petroleum Production Exploration Association (APPEA) Journal* 40: 692-708.

McCauley, R.D., J. Fewtrell, and A.N. Popper. 2003. High intensity anthropogenic sound damages fish ears. *Journal of the Acoustical Society of America* 113: 638-642.

McDonald, M.A., J.A. Hildebrand, and S.C. Webb. 1995. Blue and fin whales observed on a seafloor array in the Northeast Pacific. *Journal of the Acoustical Society of America* 98(2): 712-721.

McDonald, M.A., J.A. Hildebrand, S.M. Wiggins, and D. Ross. 2008. A 50 year comparison of ambient ocean noise near San Clemente Island: a bathymetrically complex coastal region off southern California. *Journal of the Acoustical Society of America* 124: 1985-1992.

McPherson, G.R., C.I. Clague, C.R. McPherson, P. Turner, O. Kenny, A. Madry, I. Bedwell, D.H. Cato, and D. Kreutz. 2005. Mitigation of toothed whale depredation in the eastern Australian Fishing Zone. *Presentation to Discussion Group on cetacean interactions with longlines. International Tuna Fishers Conference on Responsible Fisheries, in association with the Third International Fishers Forum*. July 24-29, Yokohama.

McSweeney, D., J, R.W. Baird, and S. Mahaffy, D. 2007. Site fidelity, associations, and movements of Cuvier's (*Ziphius cavirostris*) and Blainville's (*Mesoplodon densirostris*) beaked whales off the island of Hawai'i. *Marine Mammal Science* 23(3): 666-687.

Melcon, M.L., A.J. Cummins, S.M. Kerosky, L.K. Roche, S.M. Wiggins, and J.A. Hildebrand. 2012. Blue whales respond to anthropogenic noise. *PLoS ONE* 7(2): 1-6. http://www.plosone.org/article/info%3Adoi%2F10.1371%2Fjournal.pone.0032681.

Miksis, J.L., M.D. Grund, D.P. Nowacek, A.R. Solow, R.C. Connor, and P.L. Tyack. 2001. Cardiac response to acoustic playback experiments in the captive common bottlenose dolphin (*Tursiops truncatus*). *Journal of Comparative Psychology* 115(3): 227.

Miller, D.L., M.L. Burt, E.A. Rexstad, and L. Thomas. 2013. Spatial models for distance sampling data: Recent developments and future directions. *Methods in Ecology and Evolution* 4(11): 1001-1010.

Miller, J.D. 1963. Audibility curve of chinchilla. *Journal of the Acoustical Society of America* 35(11): 1907-1907.

Miller, P.J., M. Johnson, P.T. Madsen, N. Biassoni, M. Quero, and P. Tyack. 2009. Using at-sea experiments to study the effects of airguns on the foraging behavior of sperm whales in the Gulf of Mexico. *Deep Sea Research Part I: Oceanographic Research Papers* 56(7): 1168-1181.

Miller, P.J.O., N. Biassoni, A. Samuels, and P.L. Tyack. 2000. Whale songs lengthen in response to sonar. *Nature* 405(6789): 903-903. http://dx.doi.org/10.1038/35016148.

Miller, P.J.O., M.P. Johnson, P.L. Tyack, and E.A. Terray. 2004. Swimming gaits, passive drag and buoynacy of diving sperm whales *Physeter macrocephalus*. *Journal of Experimental Biology* 207: 1953-1967.

Miller, P.J.O., K. Aoki, L.E. Rendell, and M. Amano. 2008. Stereotypical resting behavior of the sperm whale. *Current Biology* 18(1): 21-23.

Miller, P.J.O., A.D. Shapiro, and V.B. Deecke. 2010. The diving behaviour of mammal-eating killer whales (*Orcinus orca*): variations with ecological not physiological factors. *Canadian Journal of Zoology* 88: 1103-1112.

Minamikawa, S., T. Iwasaki, Y. Tanaka, A. Ryono, S. Noji, H. Soto, S. Kurosawa, and H. Kato. 2003. Diurnal pattern of diving behavior in striped dolphins, *Stenella coeruleoalba*. *International Symposium on Bio-logging Science*. 17-21 March 2003. National Institute of Polar Research, Tokyo, Japan. 23-24 pp.

Minamikawa, S., H. Watanabe, and T. Iwasaki. 2013. Diving behavior of a false killer whale, *Pseudorca crassidens*, in the Kuroshio-Oyashio transition region and the Kuroshio front region of the western North Pacific. *Marine Mammal Science* 29(1): 177-185.

Mooney, T.A., M. Yamato, and B.K. Branstetter. 2012. Hearing in cetaceans: From natural history to experimental biology. *Advances in Marine Biology* 63: 197-246.

Moore, J.E. and J.P. Barlow. 2013. Declining abundance of beaked whales (Family Ziphiidae) in the California current large marine ecosystem. *PLoS ONE* 8(1): e52770. http://www.plosone.org/article/fetchObject.action?uri=info:doi/10.1371/journal.pone.0052770&representation=PDF.

Mullin, K.D. and G.L. Fulling. 2004. Abundance of cetaceans in the oceanic northern Gulf of Mexico, 1996-2001. *Marine Mammal Science* 20(4): 787-807.

Nachtigall, P.E., J. Pawloski, W.W.L. Au. 2003. Temporary threshold shifts and recovery following noise exposure in the Atlantic bottlenosed dolphin (*Tursiops truncatus*). *Journal of the Acoustical Society of America* 113(6): 3425-3429.

Nachtigall, P.E., A. Supin, J. Pawloski, W.W.L. Au. 2004. Temporary threshold shifts after noise exposure in the Atlantic common bottlenose dolphin (*Tursiops truncatus*) measured using evoked auditory potentials. *Marine Mammal Science* 20: 673-687.

Nieukirk, S.L., K.M. Stafford, D.K. Mellinger, R.P. Dziak, and C.G. Fox. 2004. Low-frequency whale and seismic airgun sounds recorded in the mid-Atlantic Ocean. *Journal of the Acoustical Society of America* 115(4): 1832-1843.

NOAA Fisheries. 2012a. *Short-finned Pilot Whale (Globicephala macrorhynchus)* (webpage). Office of Protected Resources, December 12, 2012. http://www.nmfs.noaa.gov/pr/species/mammals/cetaceans/pilotwhale_shortfinned.htm.

NOAA Fisheries. 2012b. *Dwarf Sperm Whale (Kogia sima)* (webpage). Office of Protected Resources, December 12, 2012. http://www.nmfs.noaa.gov/pr/species/mammals/cetaceans/dwarfspermwhale.htm.

NOAA Fisheries. 2012c. *Cuvier's Beaked Whale (Ziphius cavirostris)* (webpage). Office of Protected Resources, December 12, 2012. http://www.nmfs.noaa.gov/pr/species/mammals/cetaceans/beakedwhale_cuviers.htm.

NOAA Fisheries. 2014. *Bryde's Whale (Balaenoptera edeni)* (webpage). Office of Protected Resources, September 30, 2014. http://www.nmfs.noaa.gov/pr/species/mammals/cetaceans/brydeswhale.htm.

NOAA Fisheries. 2015a. *Common bottlenose Dolphin (Tursiops truncatus)* (webpage). Office of Protected Resources, January 16, 2015. http://www.nmfs.noaa.gov/pr/species/mammals/cetaceans/bottlenosedolphin.htm.

NOAA Fisheries. 2015b. *Sperm Whale (Physeter macrocephalus)* (webpage). Office of Protected Resources, January 15, 2015. http://www.fisheries.noaa.gov/pr/species/mammals/whales/sperm-whale.html.

Norris, K.S., H.A. Baldwin, and D.J. Samson. 1965. Open ocean diving test with a trained porpoise, *Steno bredanensis* (Lesson). *Deep-Sea Research* 12: 505-509.

Nowacek, D., M. Johnson, and P.L. Tyack. 2004. North Atlantic right whales (*Eubalaena glacialis*) ignore ships but respond to alarm stimuli. *Proceedings of the Royal Society of London B* 271: 227-231.

Nowacek, D.P., L.H. Thorne, D.W. Johnston, and P.L. Tyack. 2007. Responses of cetaceans to anthropogenic noise. *Mammal Review* 37(2): 81-115.

O'Neill, C., D. Leary, and A. McCrodan. 2010. Sound Source Verification. (Chapter 3) *In* Blees, M.K., K.G. Hartin, D.S. Ireland, and D. Hannay (eds.). *Marine mammal monitoring and mitigation during open water seismic exploration by Statoil USA E&P Inc. in the Chukchi Sea, August-October 2010: 90-day report*. LGL Report P1119. Prepared by LGL Alaska Research Associates

Inc., LGL Ltd., and JASCO Applied Sciences Ltd. for Statoil USA E&P Inc., National Marine Fisheries Service (US), and US Fish and Wildlife Service. 1-34 pp.

Parks, S.E., C.W. Clark, and P.L. Tyack. 2007. Short-and long-term changes in right whale calling behavior: The potential effects of noise on acoustic communication. *Journal of the Acoustical Society of America* 122(6): 3725-3731.

Parks, S.E., I. Urazghildiiev, and C.W. Clark. 2009. Variability in ambient noise levels and call parameters of North Atlantic right whales in three habitat areas. *Journal of the Acoustical Society of America* 125(2): 1230-1239.

Parks, S.E., M. Johnson, D. Nowacek, and P.L. Tyack. 2010. Individual right whales call louder in increased environmental noise. *Biology Letters* 7: 33-35.

Payne, R. and D. Webb. 1971. Orientation by means of long range acoustic signaling in baleen whales. *Annals of the New York Academy of Sciences* 188: 110-142.

Ridgway, S. and D. Carder. 1997. Hearing deficits measured in some *Tursiops truncatus*, and discovery of a deaf/mute dolphin. *Journal of the Acoustical Society of America* 101(1): 590-594.

Pirotta, E., R. Milor, N. Quick, D. Moretti, N. Di Marzio, P. Tyack, I. Boyd, and G. Hastie. 2012. Vessel noise affects beaked whale behavior: Results of a dedicated acoustic response study. *PLoS ONE* 7(8): e42535. http://www.plosone.org/article/info%3Adoi%2F10.1371%2Fjournal.pone.0042535#pone-0042535-g004.

Plomp, R. and M.A. Bouman. 1959. Relation between hearing threshold and duration for tone pulses. *Journal of the Acoustical Society of America* 31(6): 749-758. http://link.aip.org/link/?JAS/31/749/1.

Polacheck, T. and L. Thorpe. 1990. The swimming direction of harbor porpoise in relationship to a survey vessel. *Report for the International Whaling Commission* 40: 463-470.

Popper, A.N. and M.C. Hastings. 2009. The effects of human-generated sound on fish. *Integrative Zoology* 4: 43-52.

Porter, M.B. and Y.-C. Liu. 1994. Finite-element ray tracing. *In*: Lee, D. and M.H. Schultz (eds.). *Proceedings of the International Conference on Theoretical and Computational Acoustics*. Volume 2. World Scientific Publishing Co. 947-956 pp.

Purser, J. and A.N. Radford. 2011. Acoustic noise induces attention shifts and reduces foraging performance in three-spined sticklebacks (*Gasterosteus aculeatus*). *PLoS ONE* 6(2): e17478. http://www.plosone.org/article/info%3Adoi%2F10.1371%2Fjournal.pone.0017478#pone-0017478-g005.

Racca, R., A. Rutenko, K. Bröker, and M. Austin. 2012a. A line in the water - design and enactment of a closed loop, model based sound level boundary estimation strategy for mitigation of behavioural impacts from a seismic survey. *11th European Conference on Underwater Acoustics 2012*. Volume 34(3), Edinburgh, United Kingdom.

Racca, R., A. Rutenko, K. Bröker, and G. Gailey. 2012b. *Model based sound level estimation and in-field adjustment for real-time mitigation of behavioural impacts from a seismic survey and post-event evaluation of sound exposure for individual whales*. *Acoustics 2012 Fremantle: Acoustics, Development and the Environment*, Fremantle, Australia. http://www.acoustics.asn.au/conference_proceedings/AAS2012/papers/p92.pdf.

Racca, R.G. and J.A. Scrimger. 1986. *Underwater Acoustic Source Characteristics of Air and Water Guns*. Document Number DREP Tech. Rep. 06SB 97708-5-7055. Report by JASCO Research Ltd. for Defence Research Establishment Pacific (Canada), Victoria, BC.

Rankin, S. and W.E. Evans. 1998. Effect of low-frequency seismic exploration signals on the cetaceans of the Gulf of Mexico. *Journal of the Acoustical Society of America* 103(5): 2908-2908.

Rendell, L. and J. Gordon. 1999. Vocal Response of Long-Finned Pilot Whales (*Globicephala melas*) to Military Sonar in the Ligurian Sea. *Marine Mammal Science* 15(1): 198-204.

Richardson, W.J., C.R. Greene, Jr., C.I. Malme, and D.H. Thomson. 1995. *Marine Mammals and Noise*. Academic Press, San Diego, California. 576.

Richardson, W.J., G.W. Miller, and C.R. Greene, Jr. 1999. Displacement of migrating bowhead whales by sounds from seismic surveys in shallow waters of the Beaufort Sea. *Journal of the Acoustical Society of America* 106(4): 2281-2281. http://link.aip.org/link/?JAS/106/2281/3.

Richter, C., G. Jonathan, N. Jaquet, and B. Würsig. 2008. Social structure of sperm whales in the Northern Gulf of Mexico. *Gulf of Mexico Science* 2: 118-123.

Ridgway, S. and D. Carder. 1997. Hearing deficits measured in some *Tursiops truncatus*, and discovery of a deaf/mute dolphin. *Journal of the Acoustical Society of America* 101(1): 590-594.

Risch, D., P.J. Corkeron, W.T. Ellison, and S.M. Van Parijs. 2012. Changes in humpback whale song occurrence in response to an acoustic source 200 km away. *PLoS ONE* 7(1): e29741. http://www.plosone.org/article/info%3Adoi%2F10.1371%2Fjournal.pone.0029741#pone-0029741-g003.

Ritter, F. 2002. Behavioural observations of rough-toothed dolphins (*Steno bredanensis*) off La Gomera, Canary Islands (1995-2000), with special reference to their interactions with humans. *Aquatic Mammals* 28(1): 46-59.

Roberts, J.J., B.D. Best, L. Mannocci, P.N. Halpin, D.L. Palka, L.P. Garrison, K.D. Mullin, T.V.N. Cole, and W.M. McLellan. In preparation. *Habitat-based cetacean density models for the Northwest Atlantic and Northern Gulf of Mexico*.

Rolland, R.M., S.E. Parks, K.E. Hunt, M. Castellote, P.J. Corkeron, D.P. Nowacek, S.K. Wasser, and S.D. Kraus. 2012. Evidence that ship noise increases stress in right whales. *Proceedings of the Royal Society B: Biological Sciences*. http://rspb.royalsocietypublishing.org/content/early/2012/02/01/rspb.2011.2429.abstract.

Romano, T.A., M.J. Keogh, C. Kelly, P. Feng, L. Berk, C.E. Schlundt, D.A. Carder, and J.J. Finneran. 2004. Anthropogenic sound and marine mammal health: Measures of the nervous and immune systems before and after intense sound exposure. *Canadian Journal of Fisheries and Aquatic Sciences* 61(7): 1124-1134. http://www.nrcresearchpress.com/doi/abs/10.1139/f04-055.

Sakai, M., K. Aoki, K. Sato, M. Amano, R.W. Baird, D. Webster, G.S. Schorr, and N. Miyazaki. 2011. Swim speed and acceleration measurements of short-finned pilot whales (*Globicephala macrorhynchus*) in Hawai'i. *Mammal Study* 36: 55-59.

Schlundt, C.E., J.J. Finneran, D.A. Carder, and S.H. Ridgway. 2000. Temporary shift in masked hearing thresholds of common bottlenose dolphins, *Tursiops truncatus*, and white whales, *Delphinapterus leucas*, after exposure to intense tones. *Journal of the Acoustical Society of America* 107(6): 3496-3508.

Schorr, G.S., R.W. Baird, M.B. Hanson, D.L. Webster, D.J. McSweeney, and R.D. Andrews. 2009. Movements of satellite-tagged Blainville's beaked whales off the island of Hawai'i. *Endangered Species Research* 10: 203-213.

Scott, M.D. and S.J. Chivers. 2009. Movements and diving behavior of pelagic spotted dolphins. *Marine Mammal Science* 25(1): 137-160.

Shane, S.H., R.S. Wells, and B. Würsig. 1986. Ecology, behavior and social organization of the common bottlenose dolphin: A review. *Marine Mammal Science* 2(1): 34-63.

Simpkin, P.G. 2005. The Boomer sound source as a tool for shallow water geophysical exploration. *Marine Geophysical Researches* 26(2-4): 171-181.

Slabbekoorn, H., N. Bouton, I. van Opzeeland, A. Coers, C. ten Cate, and A.N. Popper. 2010. A noisy spring: the impact of globally rising underwater sound levels on fish. *Trends in ecology & evolution (Personal edition)* 25(7): 419-427. http://linkinghub.elsevier.com/retrieve/pii/S0169534710000832.

Slotte, A., K. Hansen, J. Dalen, and E. Ona. 2004. Acoustic mapping of pelagic fish distribution and abundance in relation to a seismic shooting area off the Norwegian west coast. *Fisheries Research* 67(2): 143-150. http://www.sciencedirect.com/science/article/pii/S016578360300290X.

Southall, B.L., A.E. Bowles, W.T. Ellison, J.J. Finneran, R.L. Gentry, C.R. Greene, Jr., D. Kastak, D.R. Ketten, J.H. Miller, et al. 2007. Marine mammal noise exposure criteria: Initial scientific recommendations. *Aquatic Mammals* 33(4): 411-521.

Southall, B.L., R. Braun, A.D.Gulland, , R.W.Baird, S.M. Wilkin, and T.K. Rowles 2006. Hawaiian Melon-headed whale (*Peponocephala electra*) mass stranding event of July 3–4, 2004. *NOAA Technical Memorandum NMFS-OPR-31* April 2006, 73 pp

Southall, B.L., T.K. Rowles, F. Gulland, R.W. Baird, and P.D. Jepson. 2013. *Final report of the Independent Scientific Review Panel investigating potential contributing factors to a 2008 mass stranding of melonheaded whales (*Peponocephala electra*) in Antsohihy, Madagascar*. 75 pp.

Stansfield, S.A. and M.P. Matheson. 2003. Noise pollution: Non-auditory effects on health. *British Medical Bulletin* 68: 243-257.

Stone, C.J. and M.L. Tasker. 2006. The effects of seismic airguns on cetaceans in UK waters. *Journal of Cetacean Research and Management* 8(3): 255.

Taylor, B.L., R. Baird, J. Barlow, S. Dawson, J. Ford, J. Mead, G. Notarbartolo di Sciara, P. Wade, and R.L. Pitman. 2008a. *Physeter macrocephalus*. Accessed Dec 11 2014. www.iucnredlist.org.

Taylor, B.L., R. Baird, J. Barlow, S.M. Dawson, J. Ford, J.G. Mead, G. Notarbartolo di Sciara, P. Wade, and R.L. Pitman. 2008b. *Ziphius cavirostris*. Downloaded on 11 Dec 2014. www.iucnredlist.org.

Taylor, B.L., R. Baird, J. Barlow, S.M. Dawson, J. Ford, J.G. Mead, G. Notarbartolo di Sciara, P. Wade, and R.L. Pitman. 2011. *Globicephala macrorhynchus*. Downloaded on 11 Dec 2014. www.iucnredlist.org.

Teague, W.J., M.J. Carron, and P.J. Hogan. 1990. A comparison between the Generalized Digital Environmental Model and Levitus climatologies. *Journal of Geophysical Research* 95(C5): 7167-7183.

Tershy, B.R. 1992. Body size, diet, habitat use, and social behavior of Balaenoptera whales in the Gulf of California. *Journal of Mammalogy*: 477-486.

Thomas, J.A., R.A. Kastelein, and F.T. Awbrey. 1990. Behavior and blood catecholamines of captive belugas during playbacks of noise from an oil drilling platform. *Zoo Biology* 9(5): 393-402.

Toth, J.L., A.A. Hohn, K.W. Able, and A.M. Gorgone. 2012. Defining common bottlenose dolphin (*Tursiops truncatus*) stocks based on environmental, physical, and behavioral characteristics. *Marine Mammal Science* 28(3): 461-478.

Tubelli, A., A. Zosuls, D. Ketten, and D.C. Mountain. 2012. *Prediction of a mysticete audiogram via finite element analysis of the middle ear*. *The effects of noise on aquatic life*.

Tyack, P., M. Johnson, N. Aguilar Soto, A. Sturlese, and P.T. Madsen. 2006. Extreme diving of beaked whales. *The Journal of Experimental Biology* 209: 4238-4253.

Tyack, P.L. 2008. Implications for marine mammals of large-scale changes in the marine acoustic environment. *Journal of Mammalogy* 89(3): 549-558.

Van Parijs, S.M. and P.J. Corkeron. 2001. Boat traffic affects the acoustic behaviour of Pacific humpback dolphins, *Sousa chinensis*. *Marine Mammal Science* 17(4): 944-949.

Verbeek, N.H. and T.M. McGee. 1995. Characteristics of high-resolution marine reflection profiling sources. *Journal of Applied Geophysics* 33(4): 251-269.

Ward, W.D., A. Glorig, and D.L. Sklar. 1958. Dependence of Temporary Threshold Shift at 4 kc on Intensity and Time. *Journal of the Acoustical Society of America* 30(10): 944-954. http://link.aip.org/link/?JAS/30/944/1.

Ward, W.D., A. Glorig, and D.L. Sklar. 1959. Temporary threshold shift from octave-band noise: Applications to damage-risk criteria. *Journal of the Acoustical Society of America* 31(4): 522-528. http://link.aip.org/link/?JAS/31/522/1.

Ward, W.D. 1960. Recovery from high values of temporary threshold shift. *Journal of the Acoustical Society of America* 32(4): 497-500.

Wardle, C., T. Carter, G. Urquhart, A. Johnstone, A. Ziolkowski, G. Hampson, and D. Mackie. 2001. Effects of seismic air guns on marine fish. *Continental Shelf Research* 21(8): 1005-1027.

Waring, G.T., E. Josephson, K. Maze-Foley, and P.E. Rosel (eds.). 2013. *U.S. Atlantic and Gulf of Mexico Marine Mammal Stock Assessments -- 2012*. NOAA Tech Memo NMFS NE 223. National Marine Fisheries Service, Woods Hole, MA. 419 pp. http://www.nefsc.noaa.gov/nefsc/publications/.

Warner, G., C. Erbe, and D. Hannay. 2010. Underwater Sound Measurements. (Chapter 3) *In* Reiser, C.M., D.W. Funk, R. Rodrigues, and D. Hannay (eds.). *Marine Mammal Monitoring and Mitigation during Open Water Shallow Hazards and Site Clearance Surveys by Shell Offshore Inc. in the Alaskan Chukchi Sea, July-October 2009: 90-Day Report*. LGL Report P1112-1. Report by LGL Alaska Research Associates Inc. and JASCO Applied Sciences for Shell Offshore Inc., National Marine Fisheries Service (US), and US Fish and Wildlife Service. 1-54 pp.

Wartzok, D. and D.E. Ketten. 1999. Marine Mammal Sensory Systems. *In* Reynolds, J. and S. Rommel (eds.). *Biology of Marine Mammals*. Smithsonian Institution Press, Washington DC. 117-175 pp.

Watwood, S.L., P.J.O. Miller, M.P. Johnson, P.T. Madsen, and P.L. Tyack. 2006. Deep-diving foraging behaviour of sperm whales (*Physeter macrocephalus*). *Journal of Animal Ecology* 75: 814-825.

Weilgart, L.S. 2007. The impacts of anthropogenic ocean noise on cetaceans and implications for management. *Canadian Journal of Zoology* 85: 1091-1116.

Wells, R.S., G.A. Early, J.G. Gannon, R.G. Lingenfelser, and P. Sweenay. 2008. *Tagging and tracking of rough-toothed dolphins (Steno bredanensis) from the March 2005 mass strandind in the Florida keys*. NOAA Technical Memorandum NMFS-SEFSC-574.

Wells, R.S., C.A. Manire, L. Byrd, D. Smith, J.G. Gannon, D. Fauquier, and K.D. Mullin. 2009. Movements and dive patterns of a rehabilitated Risso's dolphin, Grampus griseus, in the Gulf of Mexico and Atlantic Ocean. *Marine Mammal Science* 25(2): 420-429.

Wells, R.S., E.M. Fougeres, A.G. Cooper, R.O. Stevens, M. Brodsky, R. Lingenfelser, C. Dold, and D.C. Douglas. 2013. Movements and dive patterns of short-finned pilot whales (*Globicepha macrorhynchus*) released from a mass stranding in the Florid Keys. *Aquatic Mammals* 39(1): 61-72.

Whitehead, H. and T. Arnbom. 1987. Social organization of sperm whales off the Galapagos Islands, February-April 1985. *Canadian Journal of Zoology* 65(4): 913-919.

Whitehead, H. 1996. Babysitting, dive synchrony, and indications of alloparental care in sperm whales. *Behavioral Ecology and Sociobiology* 38(4): 237-244.

Whitlock, M.C. and D. Schluter. 2009. *The analysis of biological data*. Roberts and Company Publishers Greenwood Village, Colorado.

Wood, J., B.L. Southall, and D.J. Tollit. 2012. *PG&E offshore 3 D Seismic Survey Project EIR-Marine Mammal Technical Draft Report*. SMRU Ltd.

Wood, S.N. 2006. *Generalized additive models: An introduction with R*. Chapman and Hall. Boca Raton.

Wursig, B. and M. Wursing. 1979. Behavior an ecology of the common bottlenose dolphin, *Tursiops truncatus* in the South Atlantic. *Fisheries Bulletin* 77: 399-412.

Würsig, B., R.S. Wells, K.S. Norris, and M. Würsig. 1994. A spinner dolphin's day. *In* Norris, K.S., B. Würsig, R.S. Wells, and M. Würsig (eds.). *The Hawaiian spinner dolphin*. University of California Press, Berkeley and Los Angeles, CA. 65-102 pp.

Würsig, B., S.K. Lynn, T.A. Jefferson, and K.D. Mullin. 1998. Behavior of cetaceans in the northern Gulf of Mexico relative to survey ships and aircraft. *Aquatic Mammals* 24(1): 41-50. http://www.aquaticmammalsjournal.org/share/AquaticMammalsIssueArchives/1998/AquaticMammals_24-01/24-01_Wursig.pdf.

Zhang, Y. and C. Tindle. 1995. Improved equivalent fluid approximations for a low shear speed ocean bottom. *Journal of the Acoustical Society of America* 98(6): 3391-3396.

Ziolkowski, A. 1970. A method for calculating the output pressure waveform from an air gun. *Geophysical Journal of the Royal Astronomical Society* 21(2): 137-161.

Zykov, M. and J. MacDonnell. 2013. *Sound Source Characterizations for the Collaborative Baseline Survey Offshore Massachusetts Final Report: Side Scan Sonar, Sub-Bottom Profiler, and the R/V Small Research Vessel experimental*. Document Number 00413, Version 2.0. Technical report by JASCO Applied Sciences for Fugro GeoServices, Inc. and the (US) Bureau of Ocean Energy Management.

Appendix A. Per-Pulse Acoustic Field Example Radii Tables and Maps

As with the per-pulse acoustic field input to ESME (Section 6.3.1.2), the per-pulse acoustic field for exclusion zone radii were computed for the Survey sites A and B modeling locations. Transmission loss was modeled along 72 radial profiles (angular step 5°) to the range of up to 130 km from the source location. The horizontal step along the radials was 10 m. At each surface sampling location, the sound field was sampled at multiple depths:

- 2 m
- Every 5 m from 5 to 25 m
- Every 25 m from 50 to 100 m
- Every 50 m from 150 to 300 m
- Every 100 m from 400 to 1200 m
- Every 200 m from 1400 to 3000 m

At each sampling range along the surface, the sound field was sampled at various depths. The received SEL at a surface sampling location was taken as the maximum value that occurs over all samples within the water column below, i.e., the maximum-over-depth received SEL. This provided a conservative prediction of the received sound level around the source, independent of depth. These maximum-over-depth per-pulse SELs were also converted to rms SPL estimates and are presented as color contours around the source in the shaded maps in Figures 126–128. For each sound level threshold, two statistical estimates of the safety radii are provided: (1) the maximum range (R_{max}, in meters) and (2) the 95% range ($R_{95\%}$, in meters). Given a regularly gridded spatial distribution of sound levels, the $R_{95\%}$ for a given sound level was defined as the radius of the circle, centered on the source, encompassing 95% of the grid points with sound levels at or above the given value. This definition is meaningful in terms of potential impact to animals because, regardless of the shape of the contour for a given sound level, $R_{95\%}$ is the range from the source beyond which less than 5% of a uniformly distributed population would be exposed to sound at or above that level. The R_{max} for a given sound level is simply the distance to the farthest occurrence of the threshold level (equivalent to $R_{100\%}$). It is more conservative than $R_{95\%}$, but may overestimate the effective exposure zone. For cases where the volume ensonified to a specific level is discontinuous and small pockets of higher received levels occur far beyond the main ensonified volume (e.g., due to convergence), R_{max} would be much larger than $R_{95\%}$ and could therefore be misleading if not given along with $R_{95\%}$.

The per-pulse threshold radii for the 8000 in³ airgun array, with August sound speed profile, are presented at three modeling sites. Radii for the two Survey site A provinces, S01 and S02, are presented in Tables 83 and 84; and for the Survey site B province, D01, in Table 85. The maps of maximum-over-depth sound pressure levels around the sources are also provided in Figures 126, 127, and 128, respectively.

Table 83. 8000 in³ airgun array at the Survey site A, S01 modeling province: maximum (R_{max}, m) and 95% ($R_{95\%}$, m) horizontal distance from the source to modeled broadband (10–5000 Hz) maximum-over-depth sound level thresholds, for August, without and with auditory frequency weighting applied for low-frequency cetaceans (LFC), mid-frequency cetaceans (MFC), and high-frequency cetaceans (HFC).

Type I M-Weighting									
SEL (dB re 1 µPa²·s)	SPL_{rms} (dB re 1 µPa)	Un-weighted		LFC		MFC		HFC	
		R_{max}	$R_{95\%}$	R_{max}	$R_{95\%}$	R_{max}	$R_{95\%}$	R_{max}	$R_{95\%}$
200	210	40	40	40	32	10	10	< 10	< 10
190	200	150	130	140	120	50	50	30	30
180	190	500	410	480	390	150	132	120	110
170	180	1800	1460	1680	1370	510	455	390	351
160	170	4240	3680	4160	3580	1740	1560	1320	1160
150	160	10700	8690	10400	8580	5190	4470	4660	4160
140	150	34400	23700	31100	21400	14600	10300	11600	5240
130	140	> 130000	> 130000	> 130000	> 130000	57400	21100	21700	18600
120	130					> 130000	> 130000	> 130000	> 130000

Type II M-Weighting					
SEL (dB re 1 µPa²·s)	SPL_{rms} (dB re 1 µPa)	MFC		HFC	
		R_{max}	$R_{95\%}$	R_{max}	$R_{95\%}$
200	210 †				
190	200 †	< 10	< 10	< 10	< 10
180	190 †	20	20	10	10
170	180 †	70	61	40	40
160	170 †	250	230	130	120
150	160 †	780	700	420	380
140	150 †	3800	2520	1430	1250
130	140 †	5630	4860	4940	4310
120	130 †	19900	13600	11800	5360
110	120 †	107000	56400	21900	18900
100	110 †	> 130000	> 130000	> 130000	> 130000

† rms levels computed by adding 10 dB to per-shot SEL levels.

Table 84. 8000 in³ airgun array at the Survey site A, S02 modeling province: maximum (R_{max}, m) and 95% ($R_{95\%}$, m) horizontal distance from the source to modeled broadband (10–5000 Hz) maximum-over-depth sound level thresholds, for August, without and with auditory frequency weighting applied for low-frequency cetaceans (LFC), mid-frequency cetaceans (MFC), and high-frequency cetaceans (HFC).

Type I M-Weighting									
SEL (dB re 1 µPa²·s)	SPL_{rms} (dB re 1 µPa)	Un-weighted		LFC		MFC		HFC	
		R_{max}	$R_{95\%}$	R_{max}	$R_{95\%}$	R_{max}	$R_{95\%}$	R_{max}	$R_{95\%}$
200	210 †	40	40	40	32	10	10	< 10	< 10
190	200 †	160	130	150	120	50	50	30	30
180	190 †	560	461	530	434	150	132	120	110
170	180 †	1580	1330	1540	1300	520	462	400	354
160	170 †	6490	4670	5770	4310	1870	1640	1690	1490
150	160 †	16500	12100	16500	11100	7370	6620	6950	4910
140	150 †	44500	32000	44400	29200	29600	16100	16700	15300
130	140 †	99300	80300	97900	75500	67000	49800	54500	40800
120	130 †	> 100000	> 100000	> 100000	> 100000	> 100000	> 100000	> 100000	> 100000

† rms levels computed by adding 10 dB to per-shot SEL levels.

Type II M-Weighting					
SEL (dB re 1 µPa²·s)	SPL_{rms} (dB re 1 µPa)	MFC		HFC	
		R_{max}	$R_{95\%}$	R_{max}	$R_{95\%}$
200	210 †				
190	200 †	< 10	< 10	< 10	< 10
180	190 †	20	20	10	10
170	180 †	70	61	40	40
160	170 †	250	230	130	120
150	160 †	810	711	430	381
140	150 †	3920	2080	1730	1530
130	140 †	15800	7010	7010	5380
120	130 †	41900	27800	17100	15600
110	120 †	80900	62100	54600	41800
100	110 †	> 100000	> 100000	> 100000	> 100000

Table 85. 8000 in³ airgun array at the Survey site B, D01 modeling province: maximum (R_{max}, m) and 95% ($R_{95\%}$, m) horizontal distance from the source to modeled broadband (10–5000 Hz) maximum-over-depth sound level thresholds, for August, without and with auditory frequency weighting applied for low-frequency cetaceans (LFC), mid-frequency cetaceans (MFC), and high-frequency cetaceans (HFC).

Type I M-Weighting									
SEL (dB re 1 µPa²·s)	SPL_{rms} (dB re 1 µPa)	Un-weighted		LFC		MFC		HFC	
		R_{max}	$R_{95\%}$	R_{max}	$R_{95\%}$	R_{max}	$R_{95\%}$	R_{max}	$R_{95\%}$
200	210 †	40	40	40	32	10	10	< 10	< 10
190	200 †	150	130	140	120	50	50	30	30
180	190 †	500	404	470	383	150	132	120	110
170	180 †	1620	1310	1540	1240	510	454	390	352
160	170 †	5700	4270	5020	4070	1690	1500	1280	1120
150	160 †	19800	12700	14900	12700	6320	5620	4740	4140
140	150 †	47600	35100	43400	32100	15500	8970	9690	8810
130	140 †	101000	77300	100000	65900	20700	16800	18000	15600
120	130 †	> 130000	> 130000	> 130000	> 130000	34900	24300	26300	22000
110	120 †					71100	50300	53600	38900
100	110 †					> 130000	> 130000	128000	94300

† rms levels computed by adding 10 dB to per-shot SEL levels.

Type II M-Weighting					
SEL (dB re 1 µPa²·s)	SPL_{rms} (dB re 1 µPa)	MFC		HFC	
		R_{max}	$R_{95\%}$	R_{max}	$R_{95\%}$
200	210 †				
190	200 †	< 10	< 10	< 10	< 10
180	190 †	20	20	10	10
170	180 †	70	61	40	40
160	170 †	250	230	130	120
150	160 †	770	683	420	373
140	150 †	2680	2370	1380	1210
130	140 †	8760	7820	5190	4500
120	130 †	16800	9530	9750	8870
110	120 †	23800	20100	18300	15700
100	110 †	43800	32200	26400	22200

† rms levels computed by adding 10 dB to per-shot SEL levels.

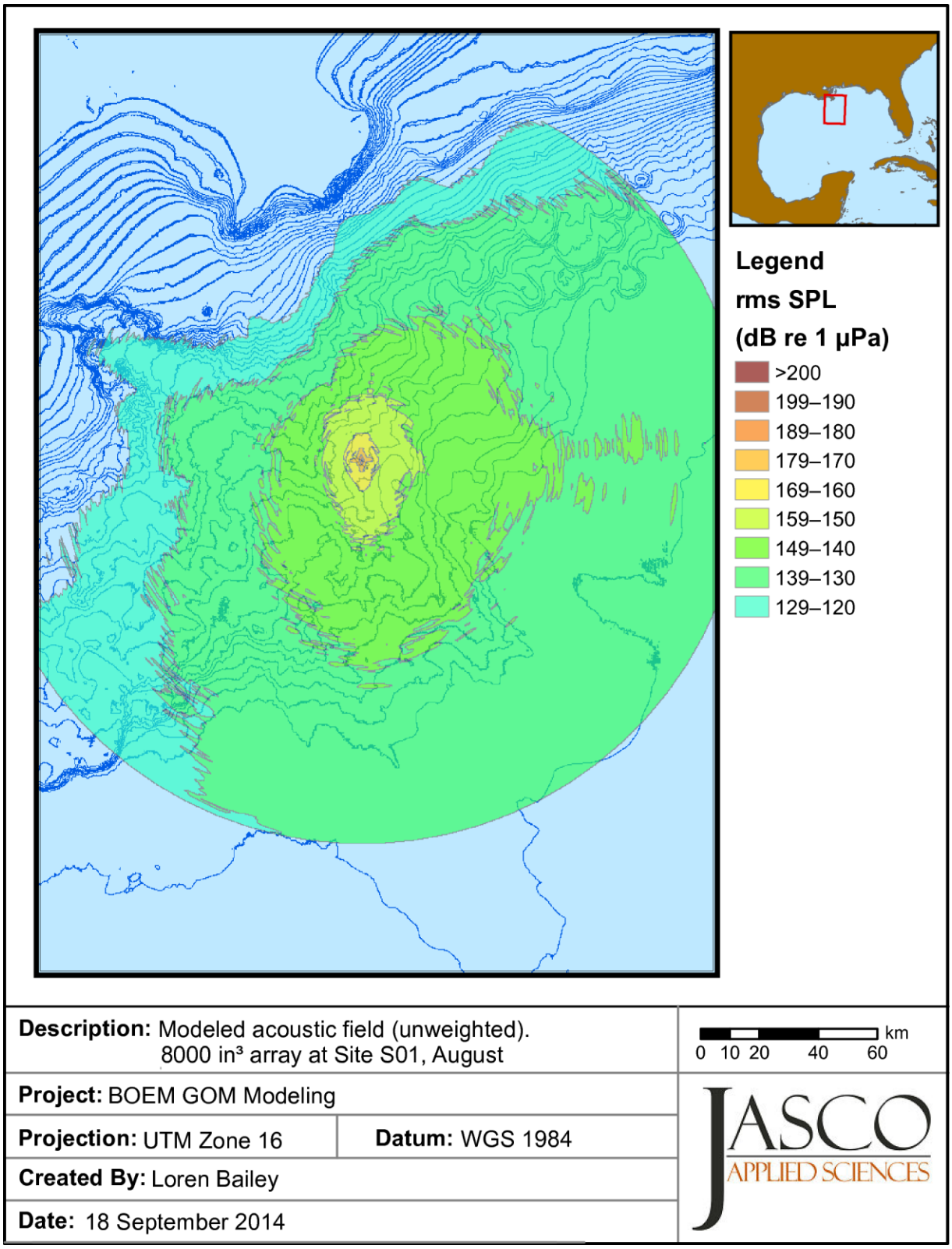

Figure 126. Broadband (10–5000 Hz) maximum-over-depth sound pressure levels for 8000 in³ airgun array, in August at the Survey site A, S01 modeling province. Blue contours indicate water depth in meters.

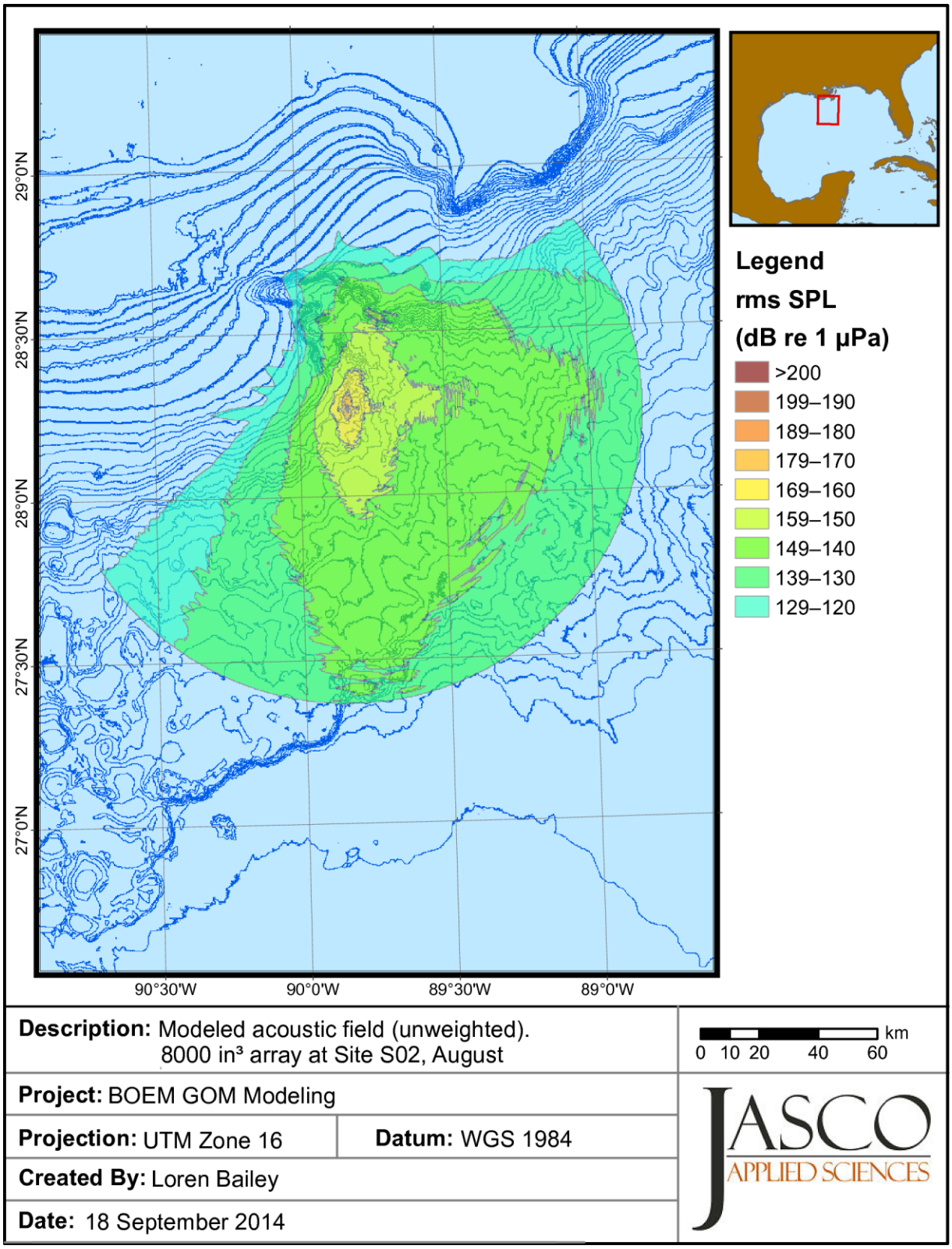

Figure 127. Broadband (10–5000 Hz) maximum-over-depth sound pressure levels for 8000 in³ airgun array, in August at the Survey site A, S02 modeling province. Blue contours indicate water depth in meters.

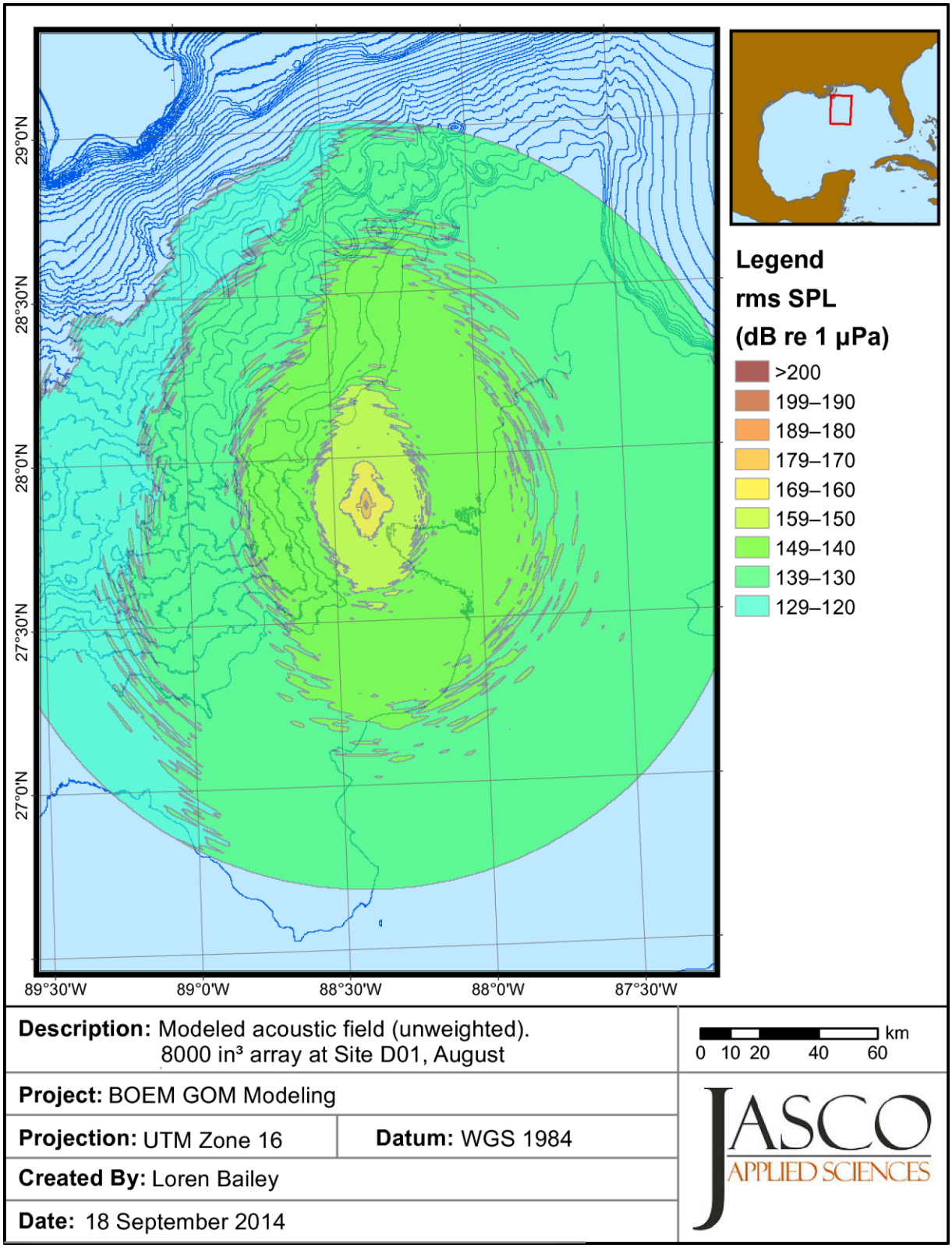

Figure 128. Broadband (10–5000 Hz) maximum-over-depth sound pressure levels for 8000 in³ airgun array, in August at the Survey site B, D01 modeling province. Blue contours indicate water depth in meters.

Appendix B. Test Case Simulation Received Levels

Figure B-1 to Figure B-6 show the occurrence frequency of cumulative SEL for all of the animats in the simulations for the combined acoustic energy of the airgun arrays during the five day simulation, panel A is Survey site A and panel C is Survey site B. The occurrence frequency of the maximum rms SPLs that animats received during the thirty-day simulation are shown in panel B for Survey site A and panel D for Survey site B

B.1. Bryde's Whales

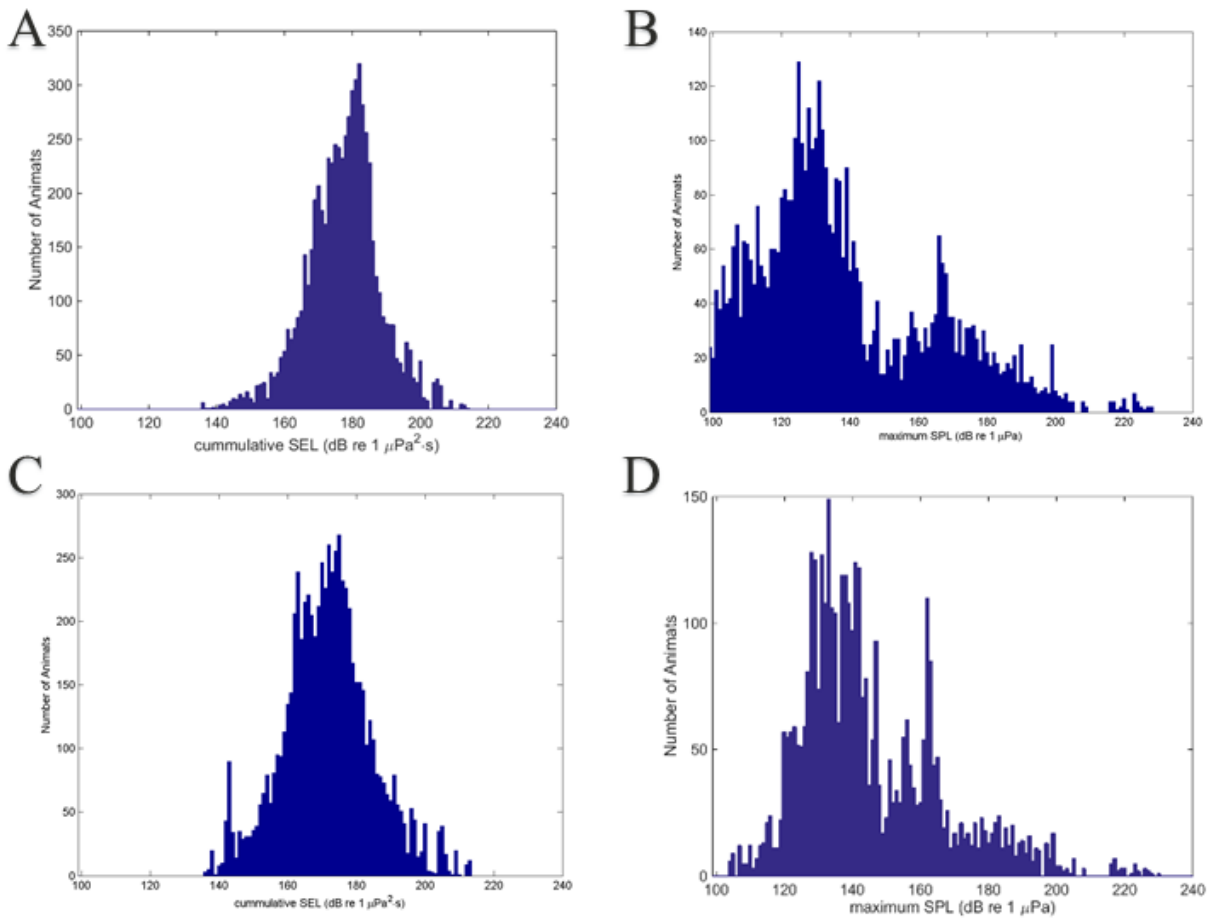

Figure B-1. Bryde's whale exposure frequency for injury (5 day) and behavior (30 day) simulations. (A) cumulative sound exposure level (SEL) for Survey site A; (B) maximum root-mean-square (rms) sound pressure level (SPL) for Survey site A; (C) cumulative sound exposure level (SEL) for Survey site B; and (D) maximum root-mean-square (rms) sound pressure level (SPL) for Survey site B.

B.2. Cuvier's Beaked Whales

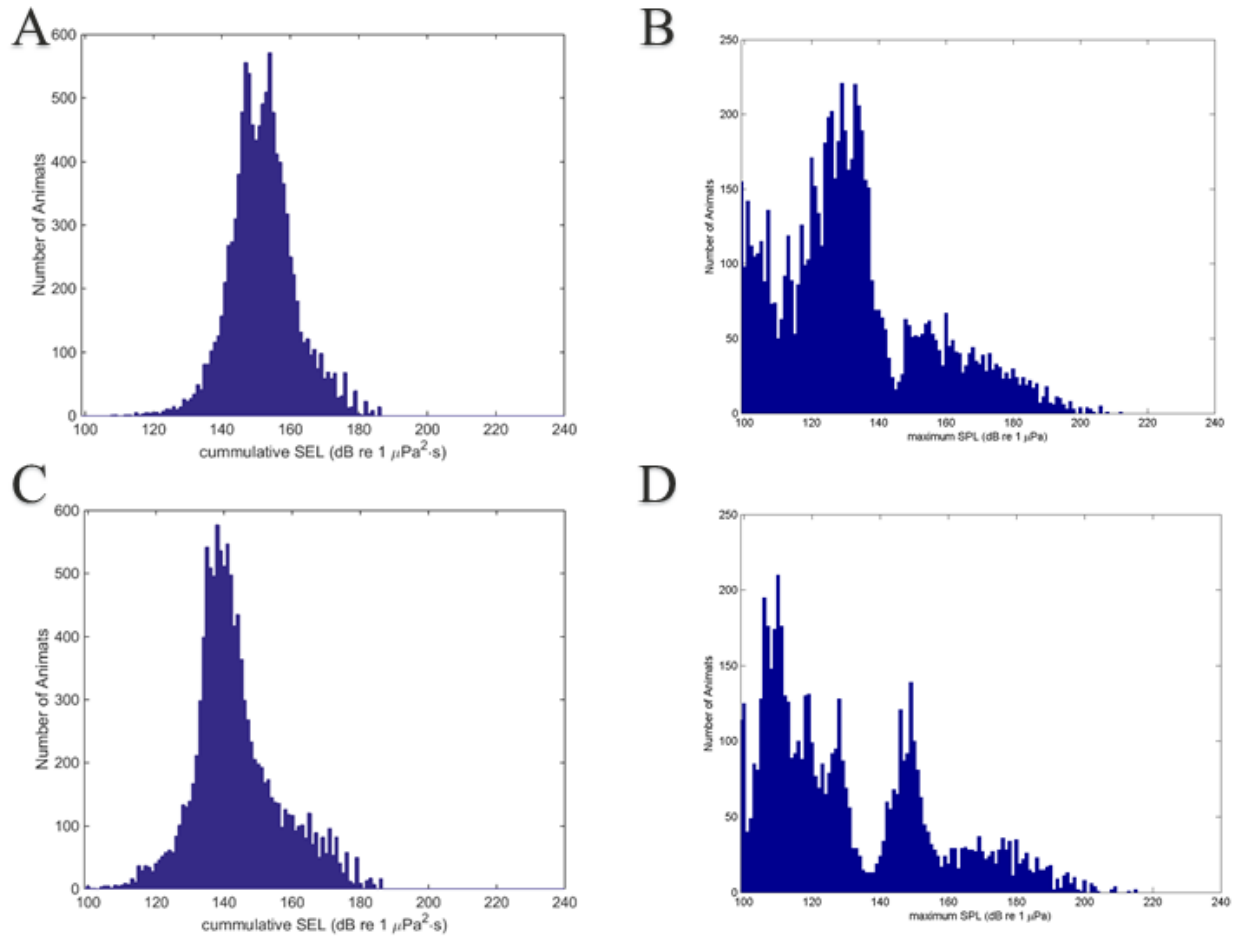

Figure B-2. Cuvier's beaked whale exposure frequency for injury (5 day) and behavior (30 day) simulations. (A) cumulative sound exposure level (SEL) for Survey site A; (B) maximum root-mean-square (rms) sound pressure level (SPL) for Survey site A; (C) cumulative sound exposure level (SEL) for Survey site B; and (D) maximum root-mean-square (rms) sound pressure level (SPL) for Survey site B.

B.3. Common bottlenose Dolphins

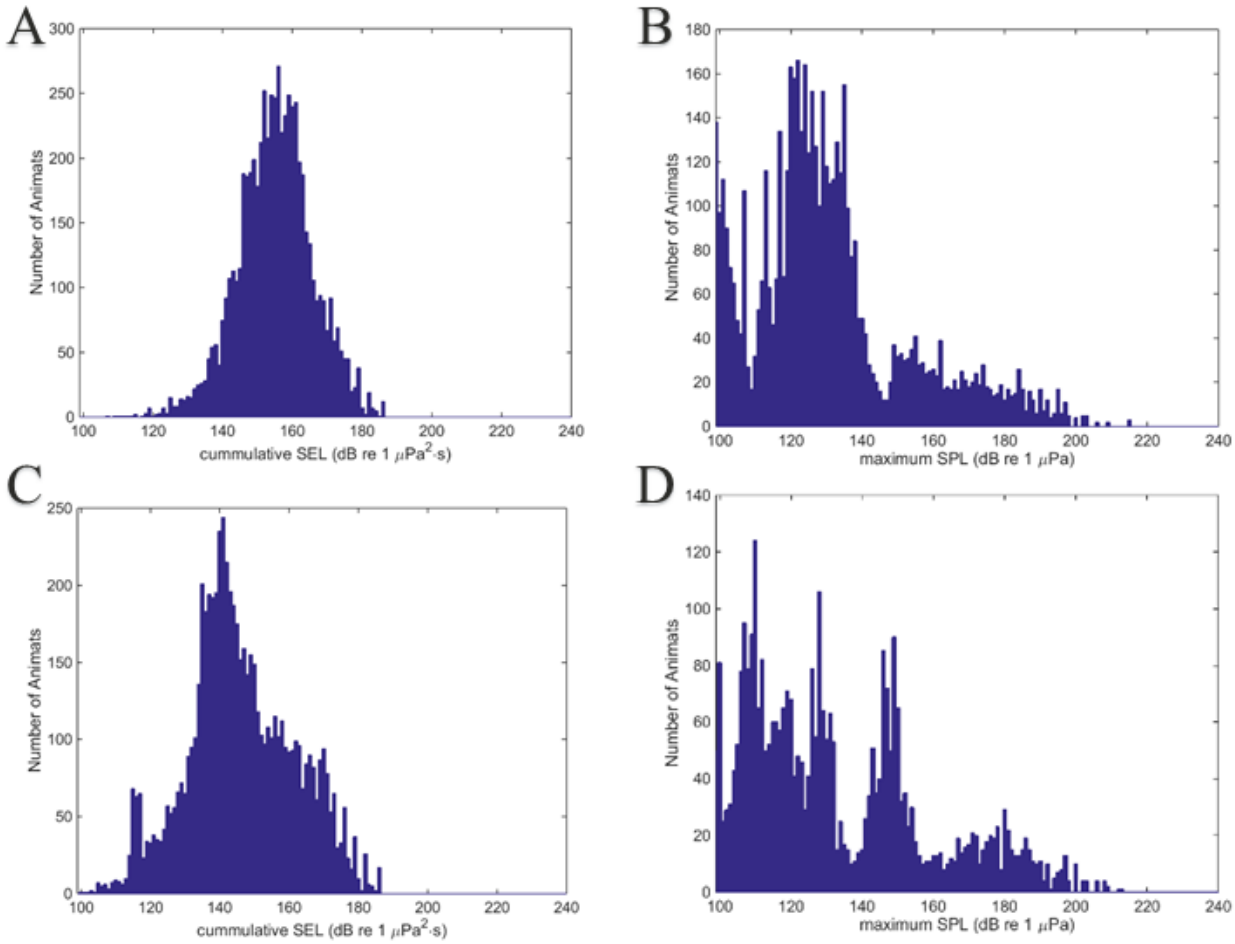

Figure B-3. Common bottlenose dolphin exposure frequency for injury (5 day) and behavior (30 day) simulations. (A) cumulative sound exposure level (SEL) for Survey site A; (B) maximum root-mean-square (rms) sound pressure level (SPL) for Survey site A; (C) cumulative sound exposure level (SEL) for Survey site B; and (D) maximum root-mean-square (rms) sound pressure level (SPL) for Survey site B.

B.4. Short-Finned Pilot Whales

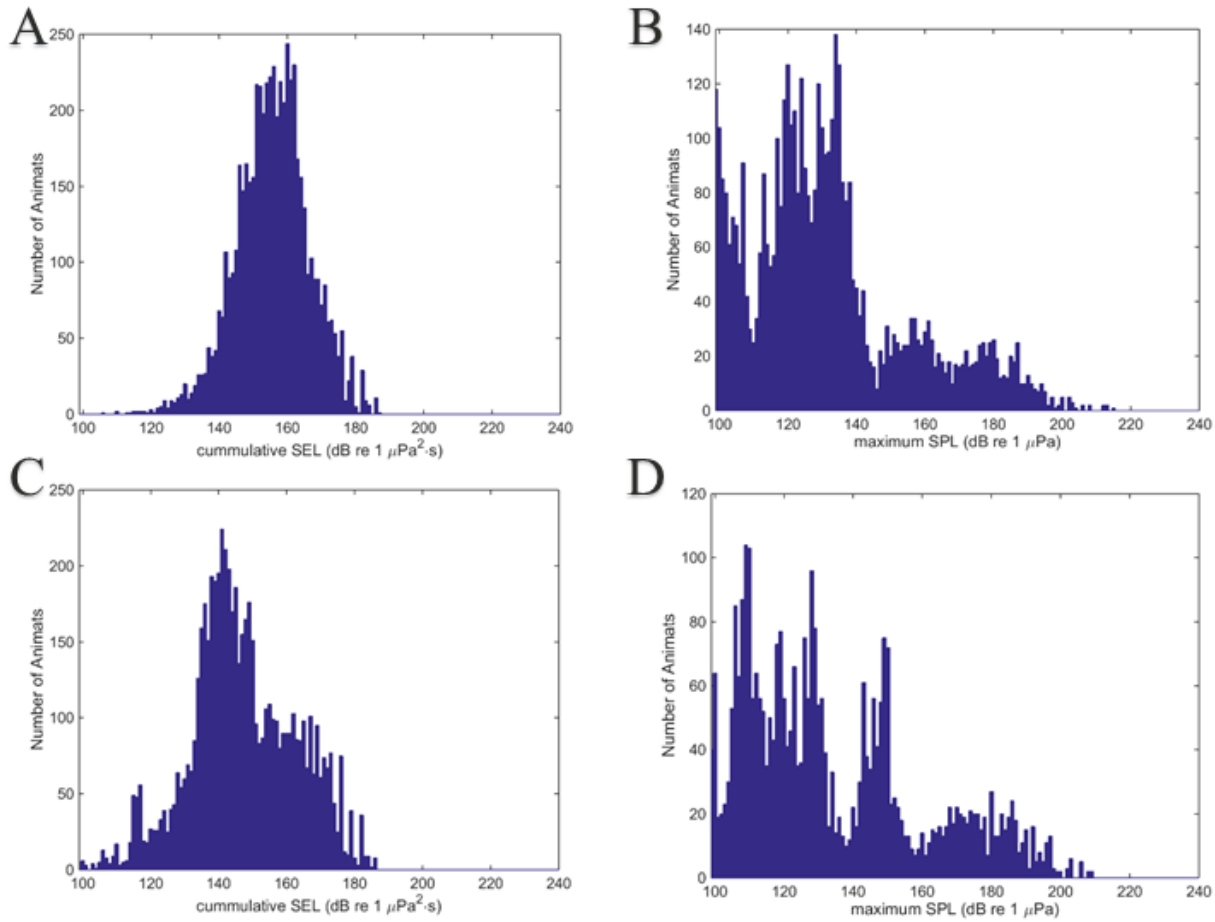

Figure B-4. Short-finned pilot whale exposure frequency for injury (5 day) and behavior (30 day) simulations. (A) cumulative sound exposure level (SEL) for Survey site A; (B) maximum root-mean-square (rms) sound pressure level (SPL) for Survey site A; (C) cumulative sound exposure level (SEL) for Survey site B; and (D) maximum root-mean-square (rms) sound pressure level (SPL) for Survey site B.

B.5. Sperm Whales

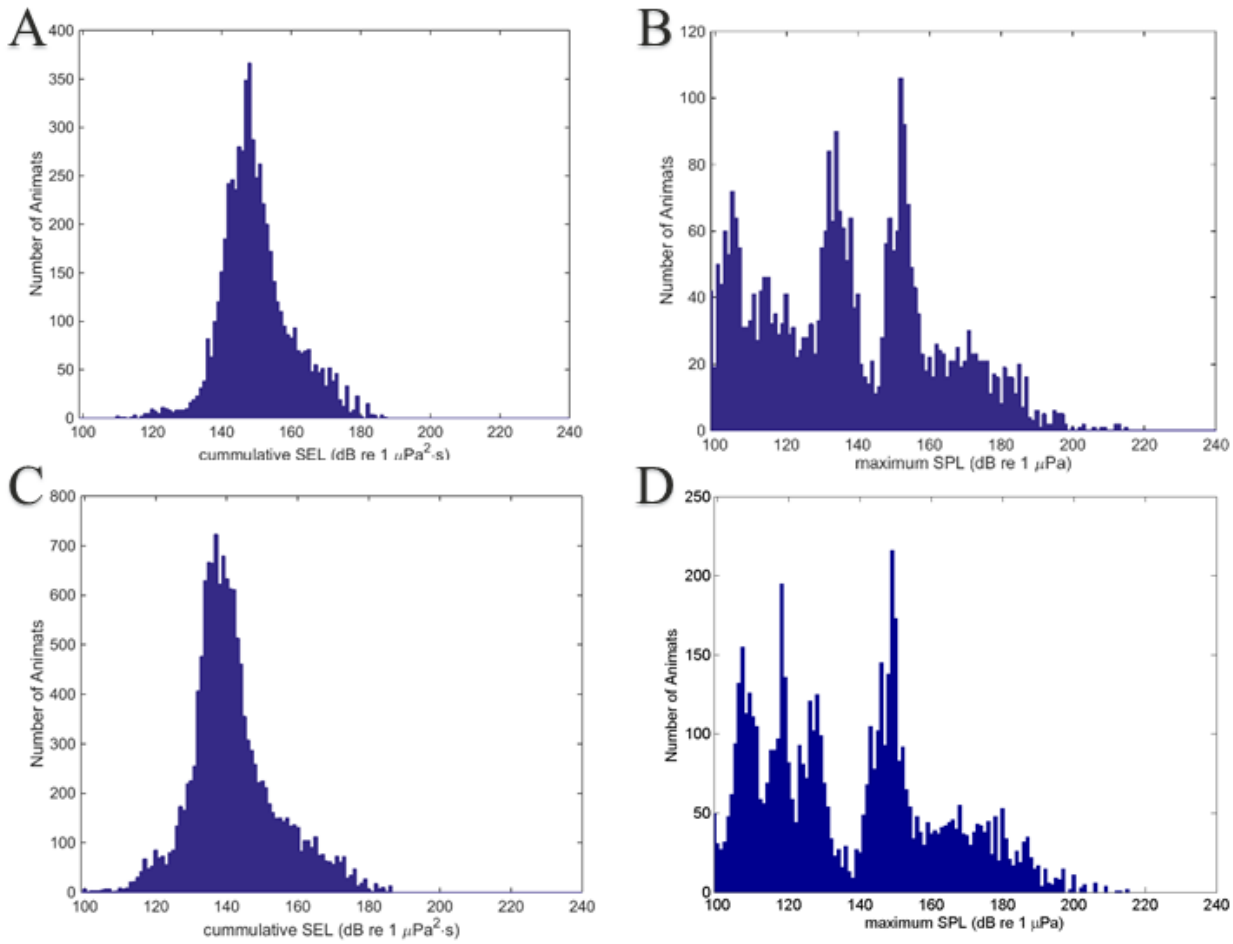

Figure B-5. Sperm whale exposure frequency for injury (5 day) and behavior (30 day) simulations. (A) cumulative sound exposure level (SEL) for Survey site A; (B) maximum root-mean-square (rms) sound pressure level (SPL) for Survey site A; (C) cumulative sound exposure level (SEL) for Survey site B; and (D) maximum root-mean-square (rms) sound pressure level (SPL) for Survey site B.

B.6. Dwarf Sperm Whales

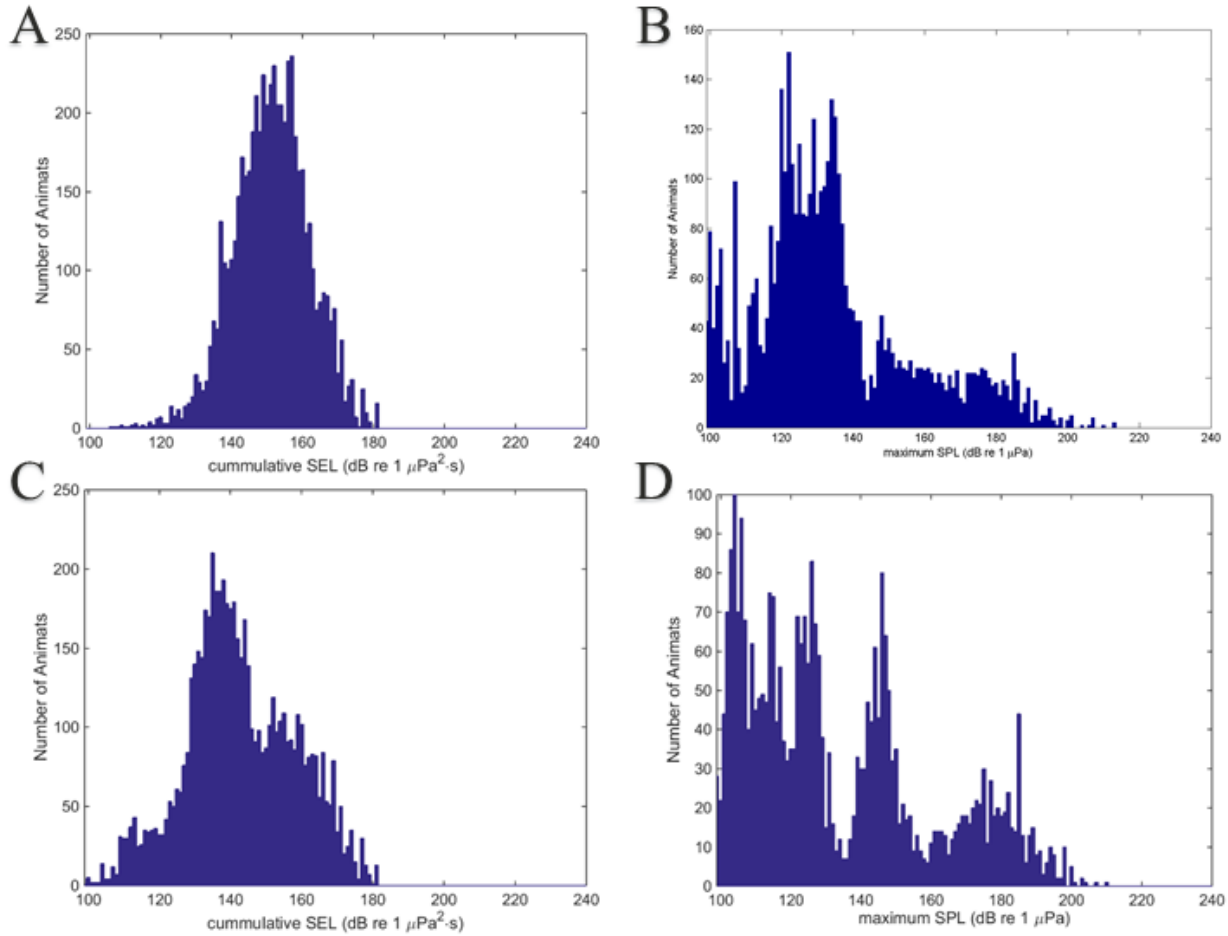

Figure B-6. Dwarf sperm whale exposure frequency for injury (5 day) and behavior (30 day) simulations. (A) cumulative sound exposure level (SEL) for Survey site A; (B) maximum root-mean-square (rms) sound pressure level (SPL) for Survey site A; (C) cumulative sound exposure level (SEL) for Survey site B; and (D) maximum root-mean-square (rms) sound pressure level (SPL) for Survey site B.

Appendix C. Marine Mammal Distribution in the Gulf of Mexico

This appendix contains distribution maps for the marine mammal species likely to be affected by geological and geophysical exploration surveys. The distributions were obtained from the Marine Geospatial Ecology Laboratory (Duke University) model (Roberts et al. In preparation) as GIS-compatible rasters of density estimates in 100 km^2 areas. These animal distributions guided our selection of modeling zones, which were also patterned on BOEM's planning areas, and to maintain acoustic uniformity throughout zones. The zone boundaries are shown as overlays in the figures.

The minimum, maximum, and mean density values and standard deviations of the means were obtained for each species in each zone (Table 62–Table 68).

C.1. Atlantic Spotted Dolphins

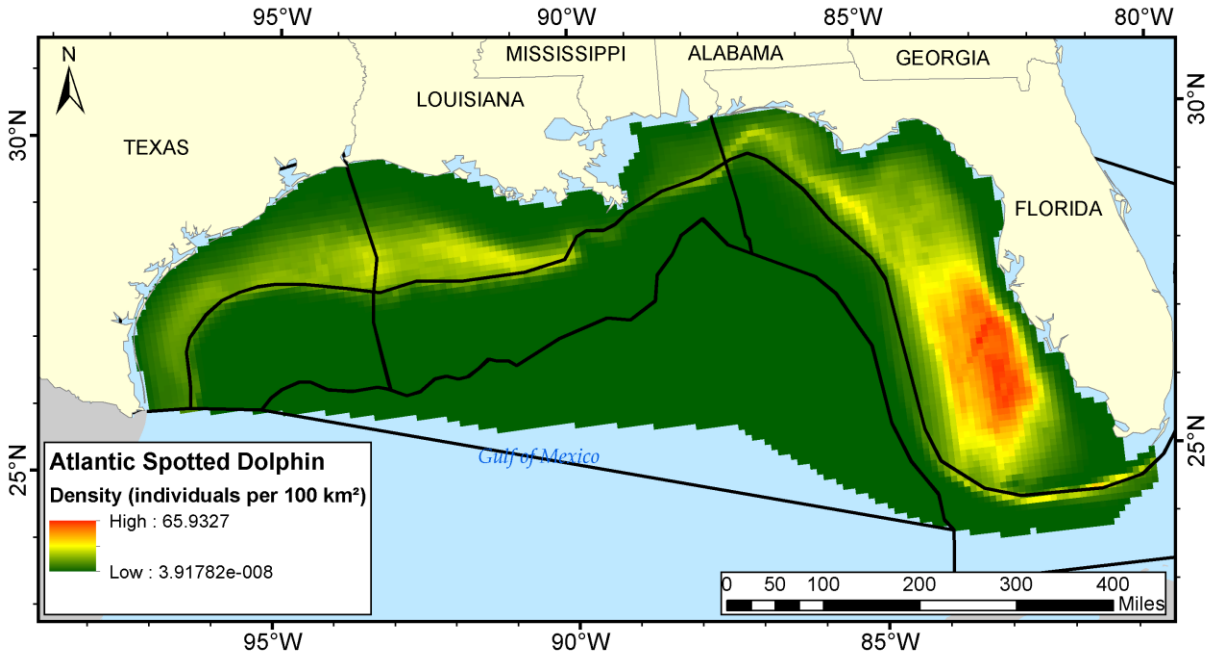

Figure C-1. Atlantic spotted dolphin distribution in the Gulf of Mexico project area. Density estimates were obtained from the Marine Geospatial Ecology Laboratory (Duke University) model (Roberts et al. In preparation), black lines depict the boundaries of the modeling zones.

C.2. Beaked Whales

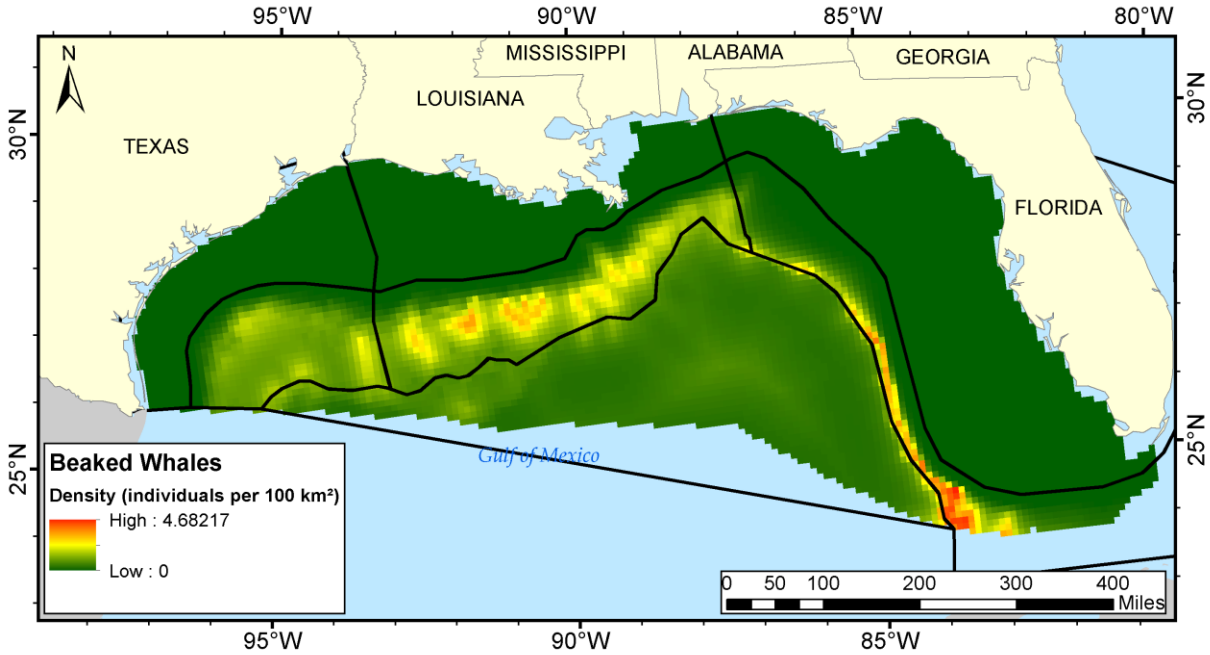

Figure C-2. Beaked whale distribution in the Gulf of Mexico project area. Density estimates were obtained from the Marine Geospatial Ecology Laboratory (Duke University) model (Roberts et al. In preparation), black lines depict the boundaries of the modeling zones.

C.3. Common Bottlenose Dolphins

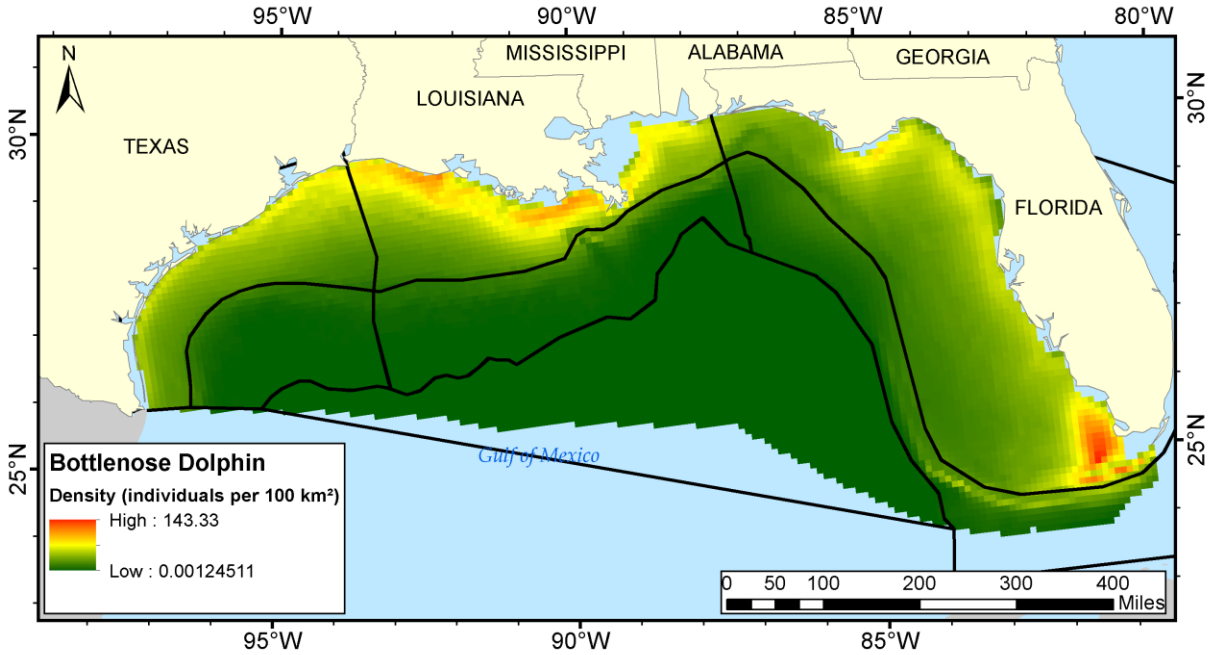

Figure C-3. Common bottlenose dolphin distribution in the Gulf of Mexico project area. Density estimates were obtained from the Marine Geospatial Ecology Laboratory (Duke University) model (Roberts et al. In preparation), black lines depict the boundaries of the modeling zones.

C.4. Bryde's Whales

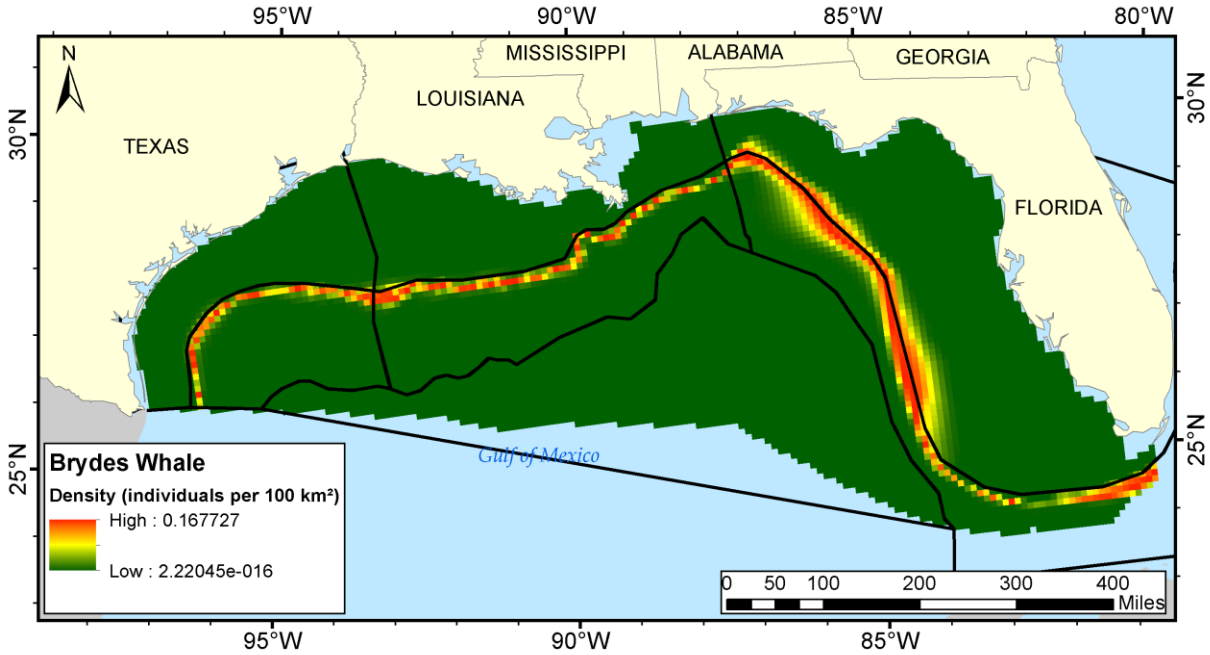

Figure C-4. Bryde's whale distribution in the Gulf of Mexico project area. Density estimates were obtained from the Marine Geospatial Ecology Laboratory (Duke University) model (Roberts et al. In preparation), black lines depict the boundaries of the modeling zones.

C.5. Clymene Dolphins

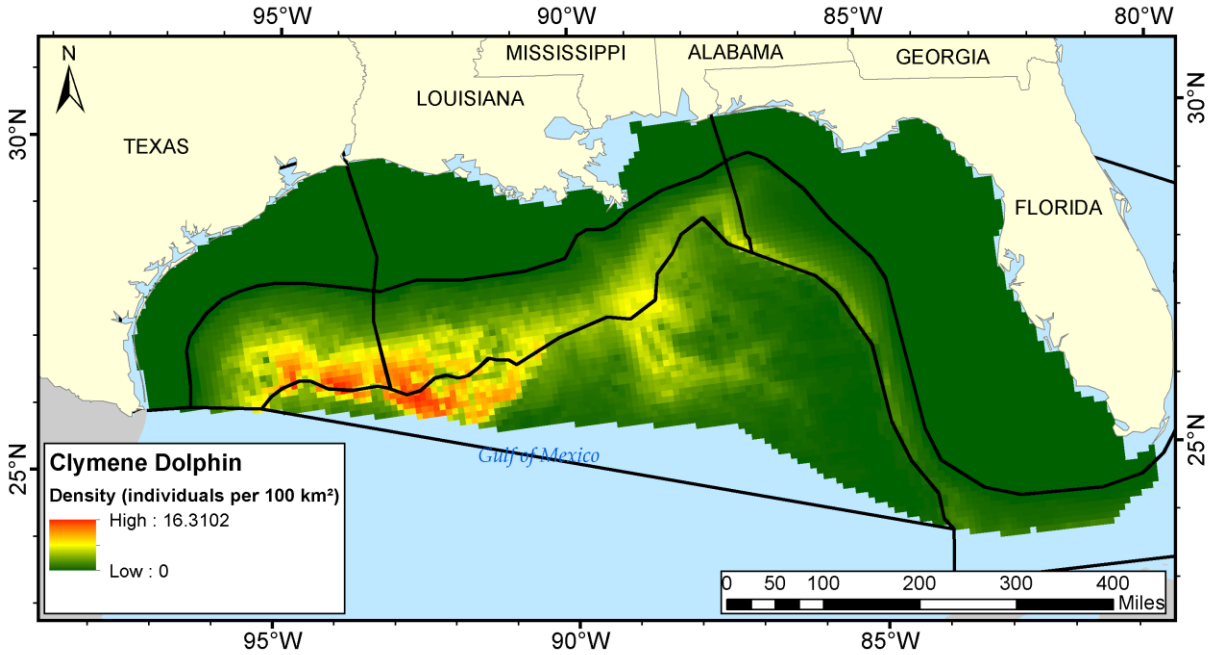

Figure C-5. Clymene dolphin distribution in the Gulf of Mexico project area. Density estimates were obtained from the Marine Geospatial Ecology Laboratory (Duke University) model (Roberts et al. In preparation), black lines depict the boundaries of the modeling zones.

C.6. False Killer Whales

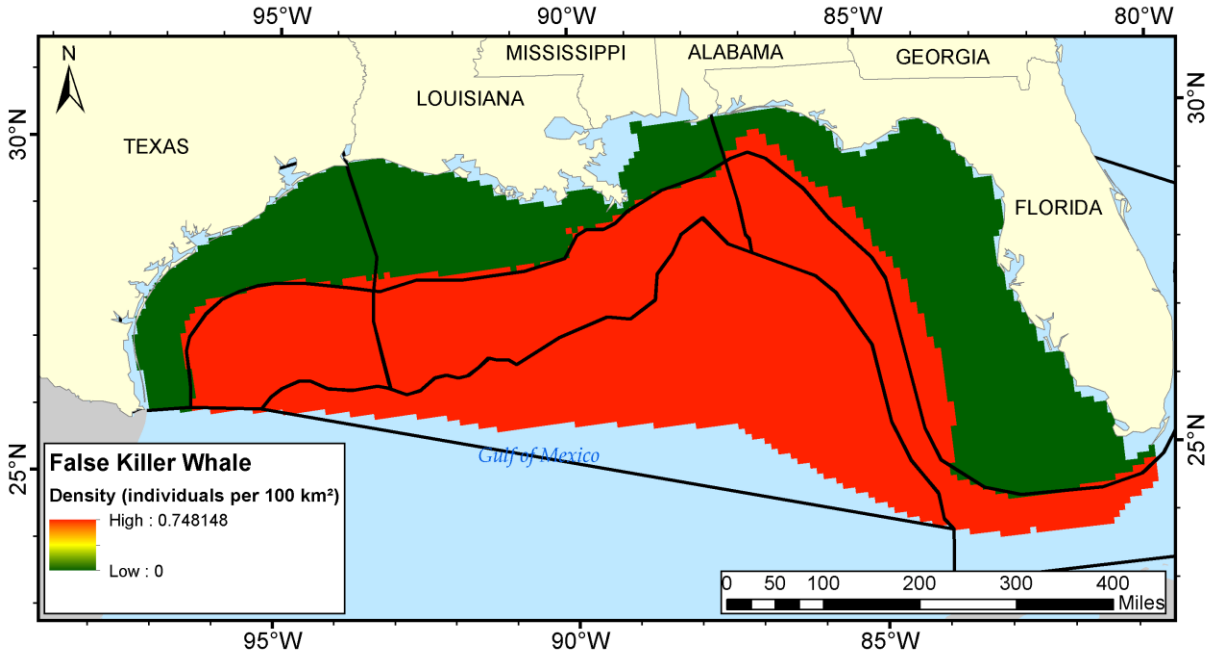

Figure C-6. False killer whale distribution in the Gulf of Mexico project area. Density estimates were obtained from the Marine Geospatial Ecology Laboratory (Duke University) model (Roberts et al. In preparation), black lines depict the boundaries of the modeling zones.

C.7. Fraser's Dolphins

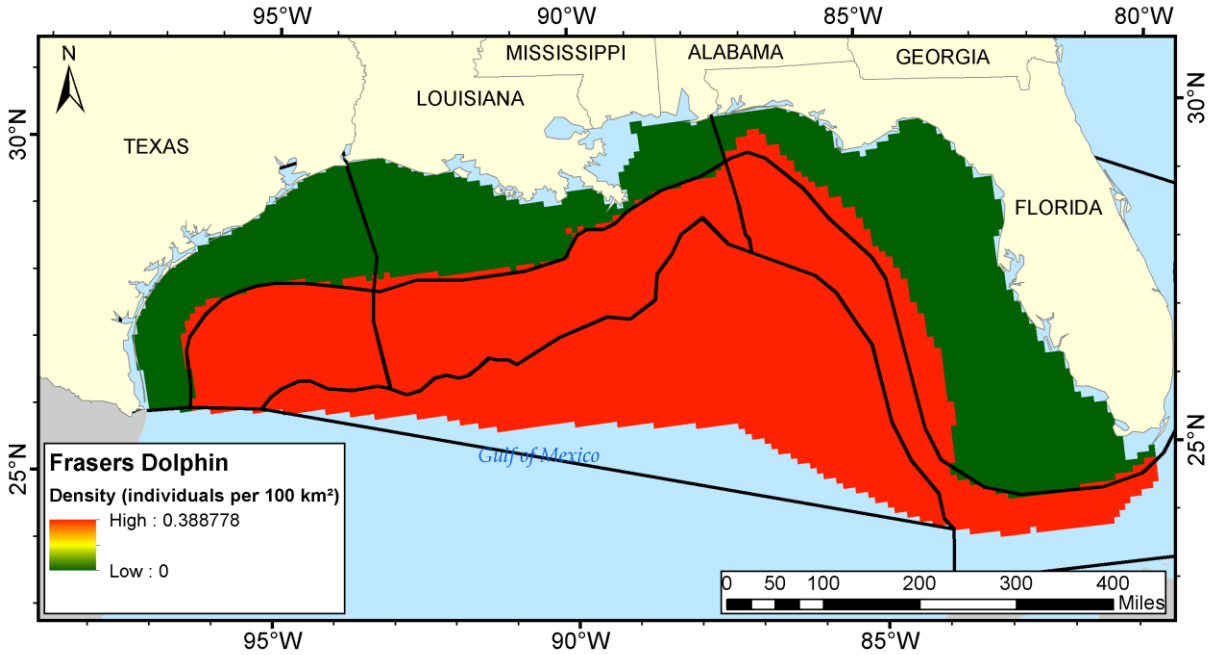

Figure C-7. Fraser's dolphin distribution in the Gulf of Mexico project area. Density estimates were obtained from the Marine Geospatial Ecology Laboratory (Duke University) model (Roberts et al. In preparation), black lines depict the boundaries of the modeling zones.

C.8. Killer Whales

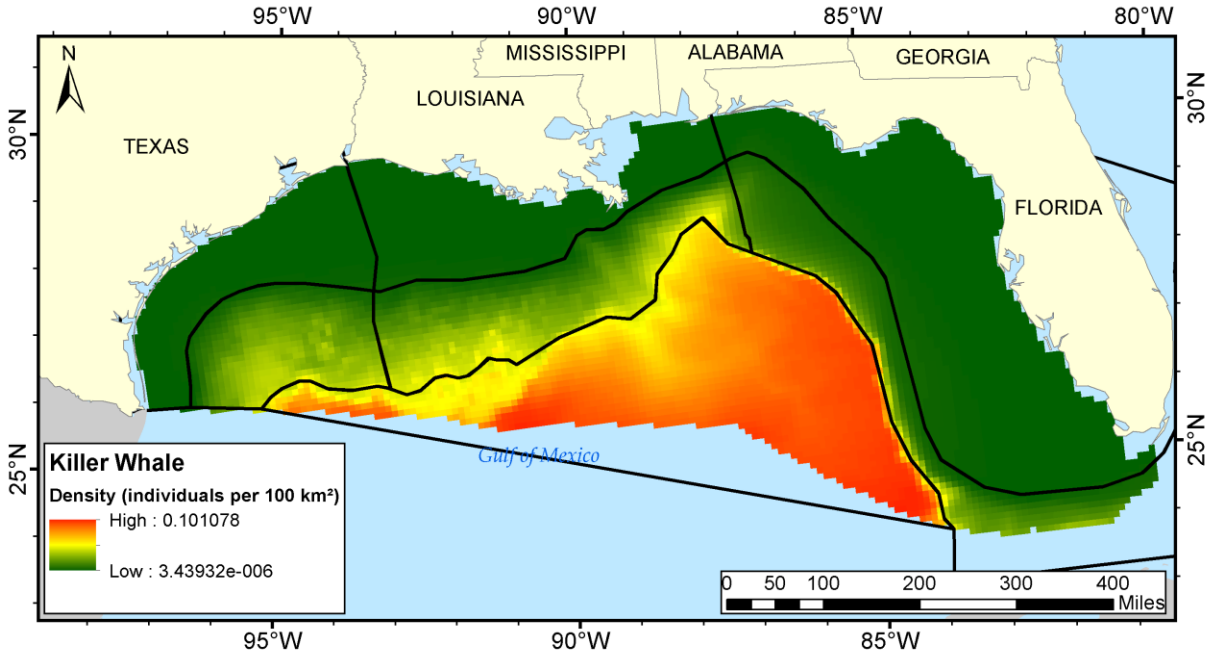

Figure C-8. Killer whale distribution in the Gulf of Mexico project area. Density estimates were obtained from the Marine Geospatial Ecology Laboratory (Duke University) model (Roberts et al. In preparation), black lines depict the boundaries of the modeling zones.

C.9. Kogia Species

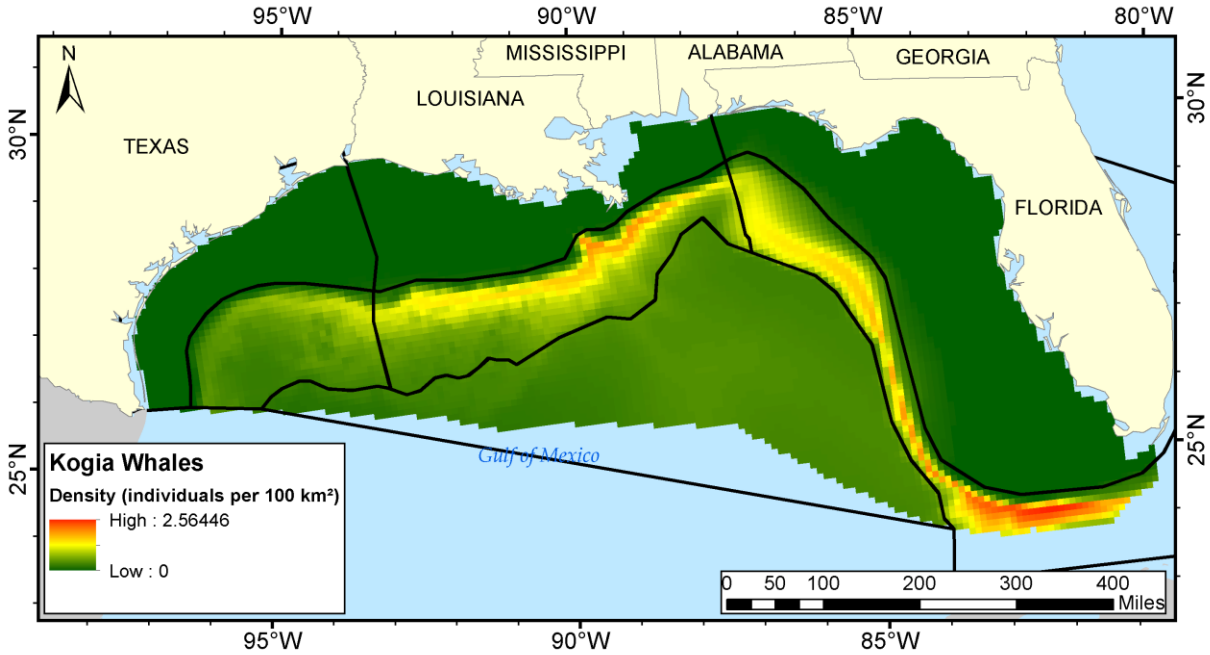

Figure C-9. *Kogia* distribution in the Gulf of Mexico project area. Density estimates were obtained from the Marine Geospatial Ecology Laboratory (Duke University) model (Roberts et al. In preparation), black lines depict the boundaries of the modeling zones.

C.10. Melon-headed Whales

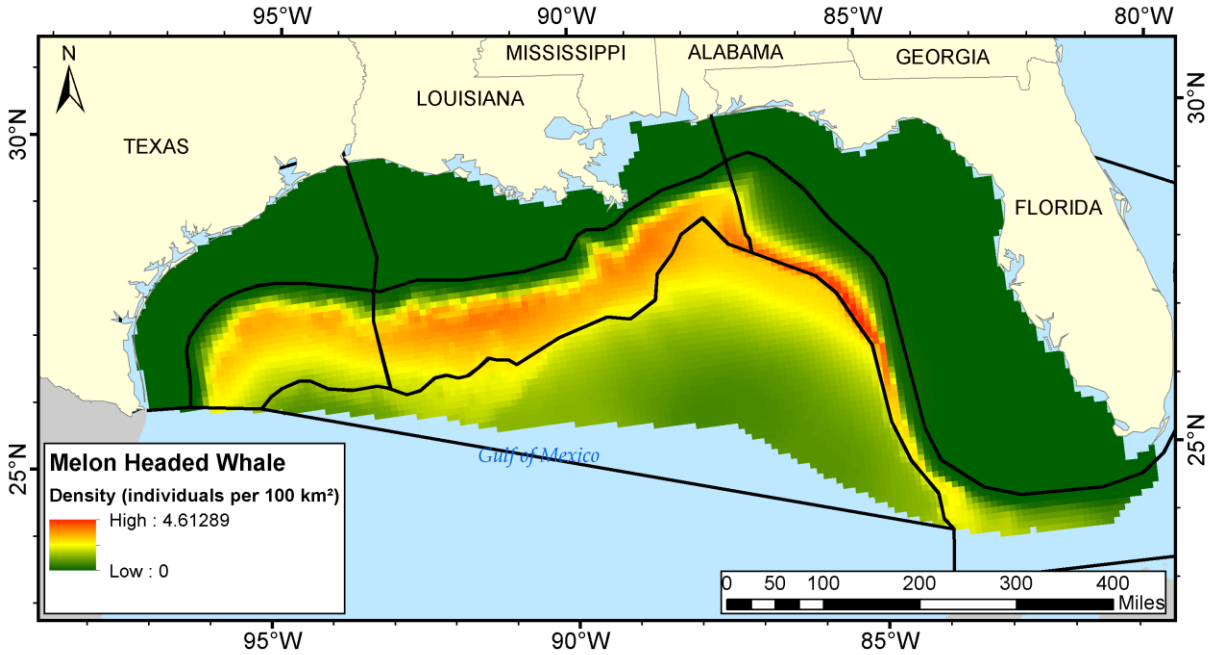

Figure C-10. Melon-headed whale distribution in the Gulf of Mexico project area. Density estimates were obtained from the Marine Geospatial Ecology Laboratory (Duke University) model (Roberts et al. In preparation), black lines depict the boundaries of the modeling zones.

C.11. Pantropical Spotted Dolphins

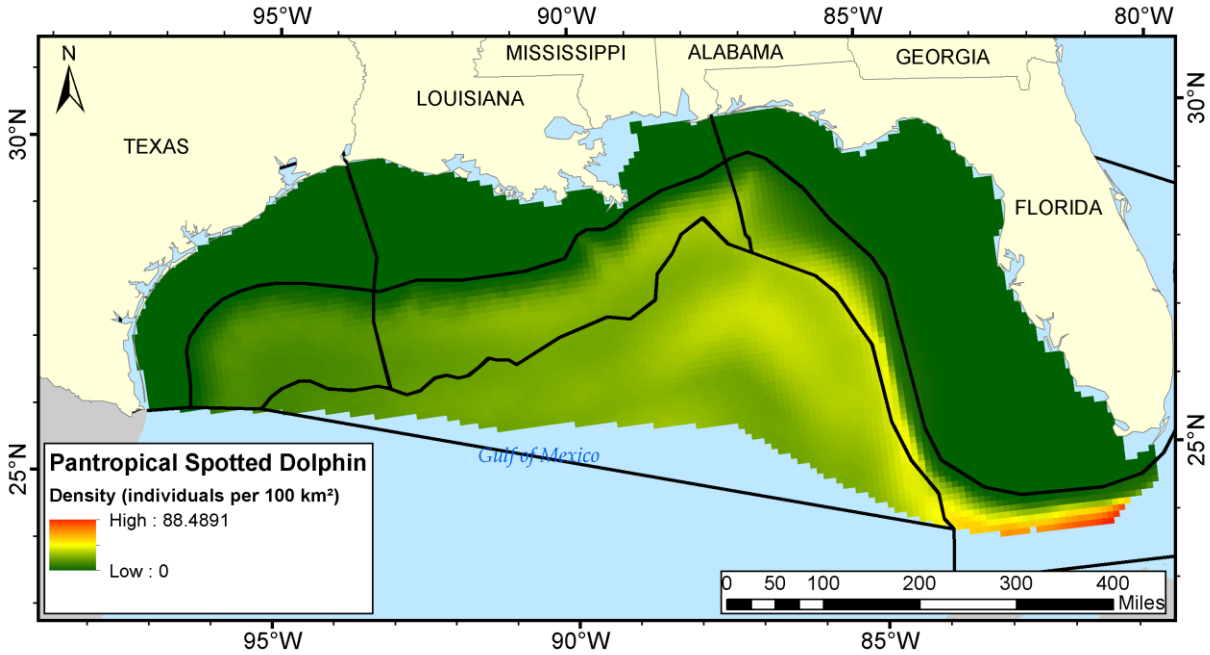

Figure C-11. Pantropical spotted dolphin distribution in the Gulf of Mexico project area. Density estimates were obtained from the Marine Geospatial Ecology Laboratory (Duke University) model (Roberts et al. In preparation), black lines depict the boundaries of the modeling zones.

C.12. Pygmy Killer Whales

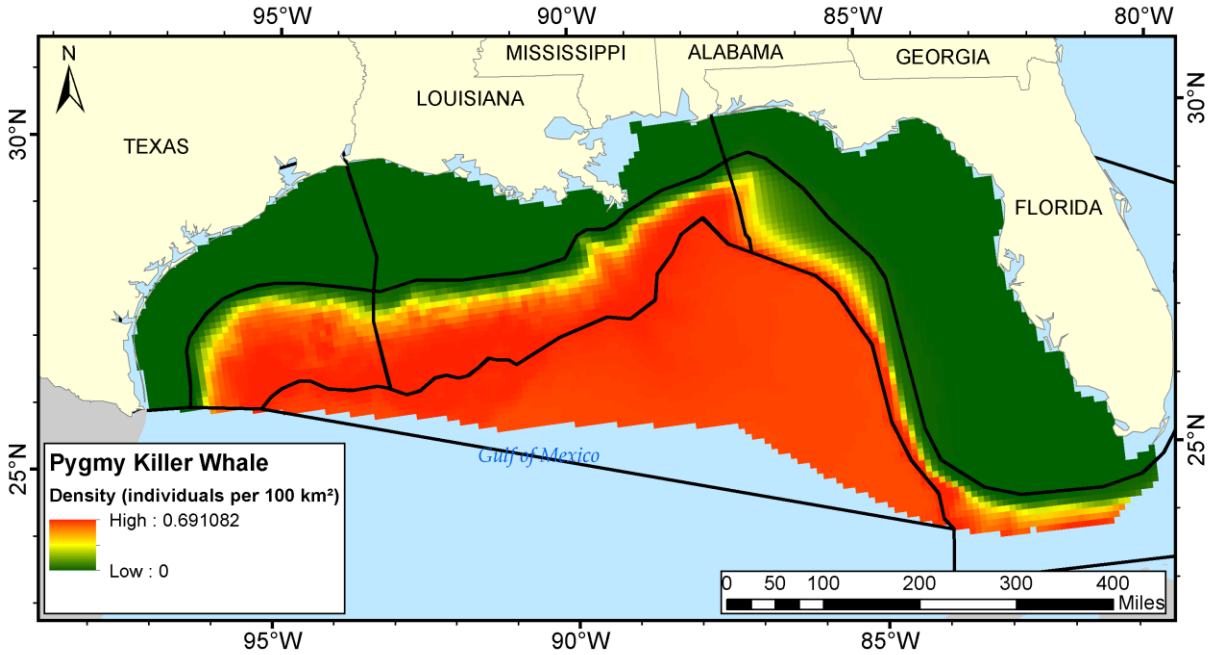

Figure C-12. Pygmy killer whale distribution in the Gulf of Mexico project area. Density estimates were obtained from the Marine Geospatial Ecology Laboratory (Duke University) model (Roberts et al. In preparation), black lines depict the boundaries of the modeling zones.

C.13. Risso's Dolphins

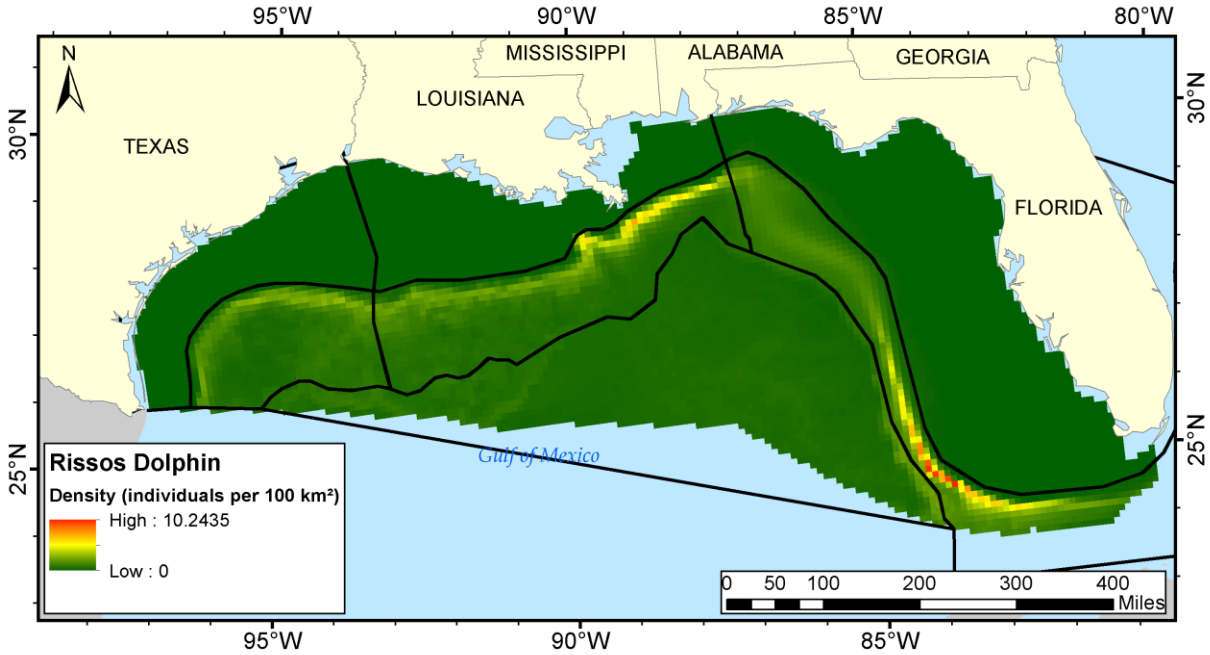

Figure C-13. Risso's dolphin distribution in the Gulf of Mexico project area. Density estimates were obtained from the Marine Geospatial Ecology Laboratory (Duke University) model (Roberts et al. In preparation), black lines depict the boundaries of the modeling zones.

C.14. Rough-toothed Dolphins

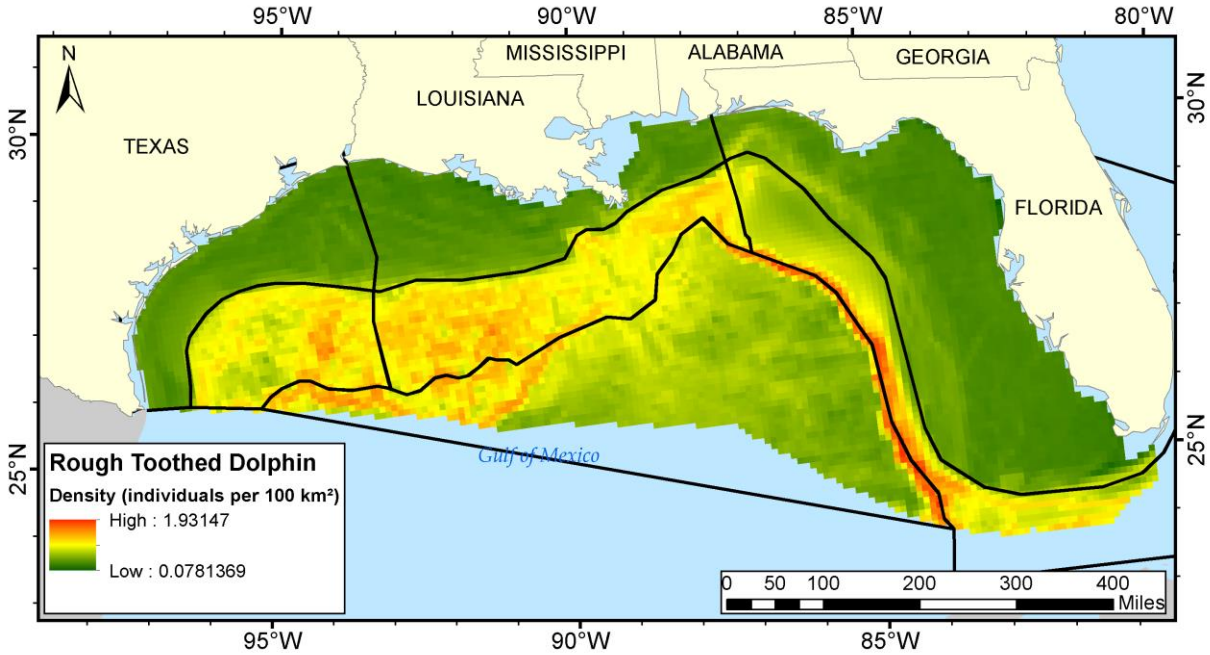

Figure C-14. Rough-toothed dolphin distribution in the Gulf of Mexico project area. Density estimates were obtained from the Marine Geospatial Ecology Laboratory (Duke University) model (Roberts et al. In preparation), black lines depict the boundaries of the modeling zones.

C.15. Short-finned Pilot Whales

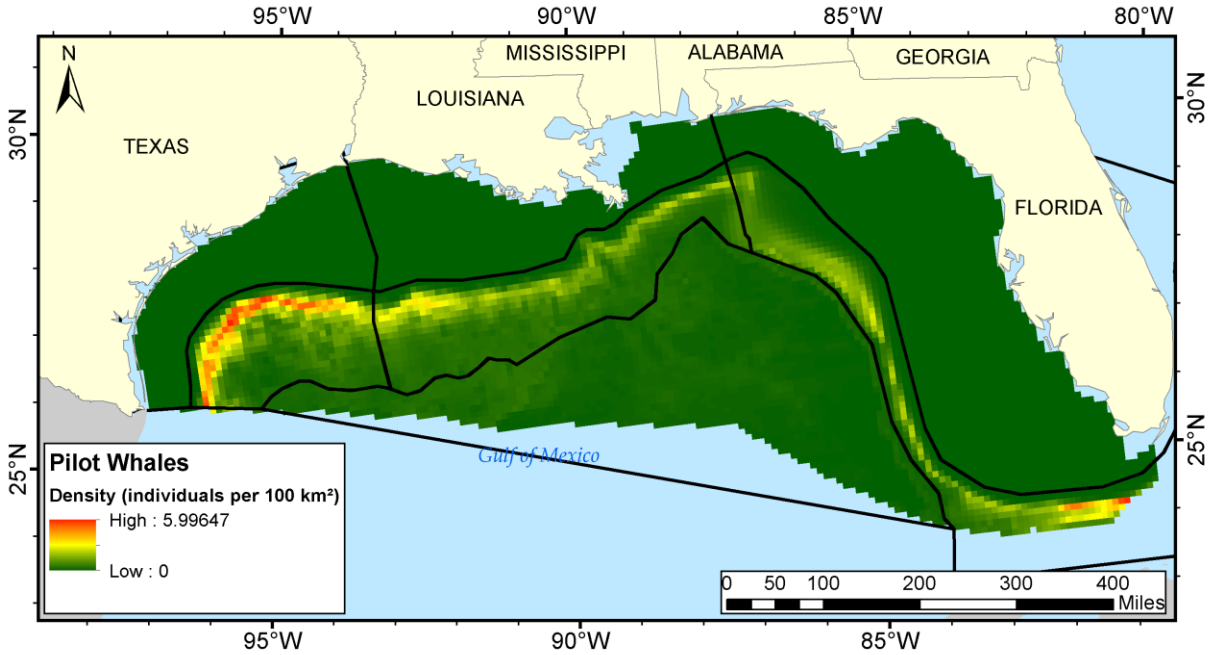

Figure C-15. Short-finned pilot whale distribution in the Gulf of Mexico project area. Density estimates were obtained from the Marine Geospatial Ecology Laboratory (Duke University) model (Roberts et al. In preparation), black lines depict the boundaries of the modeling zones.

C.16. Sperm Whales

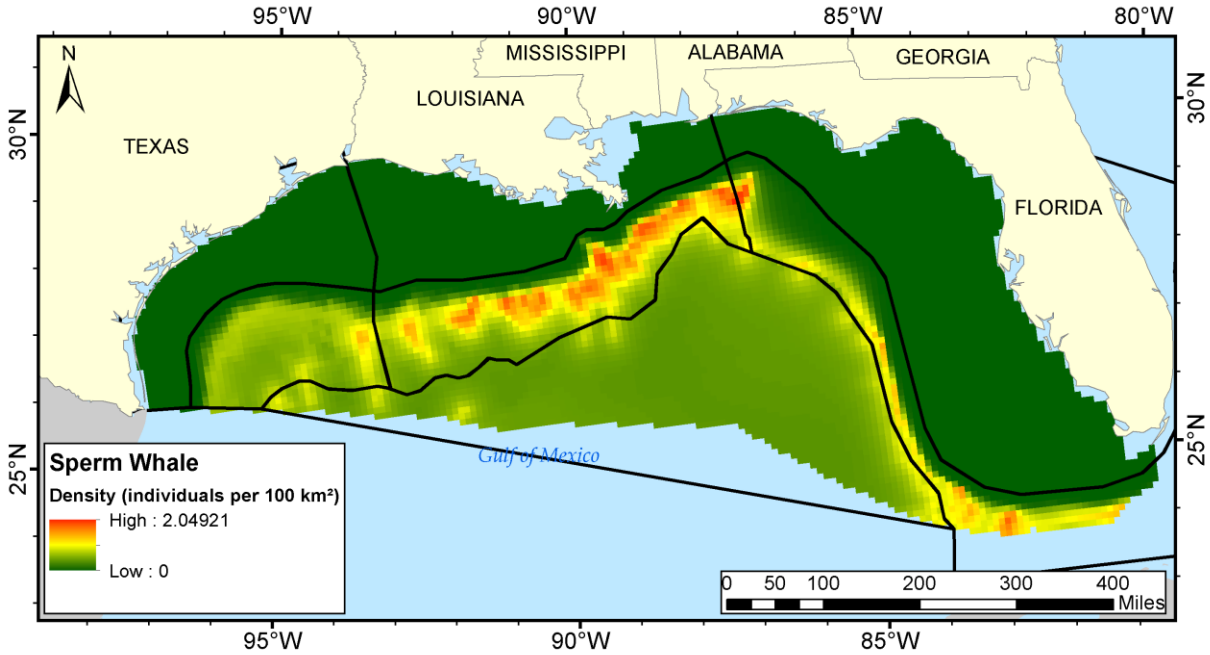

Figure C-16. Sperm whale distribution in the Gulf of Mexico project area. Density estimates were obtained from the Marine Geospatial Ecology Laboratory (Duke University) model (Roberts et al. In preparation), black lines depict the boundaries of the modeling zones.

C.17. Spinner Dolphins

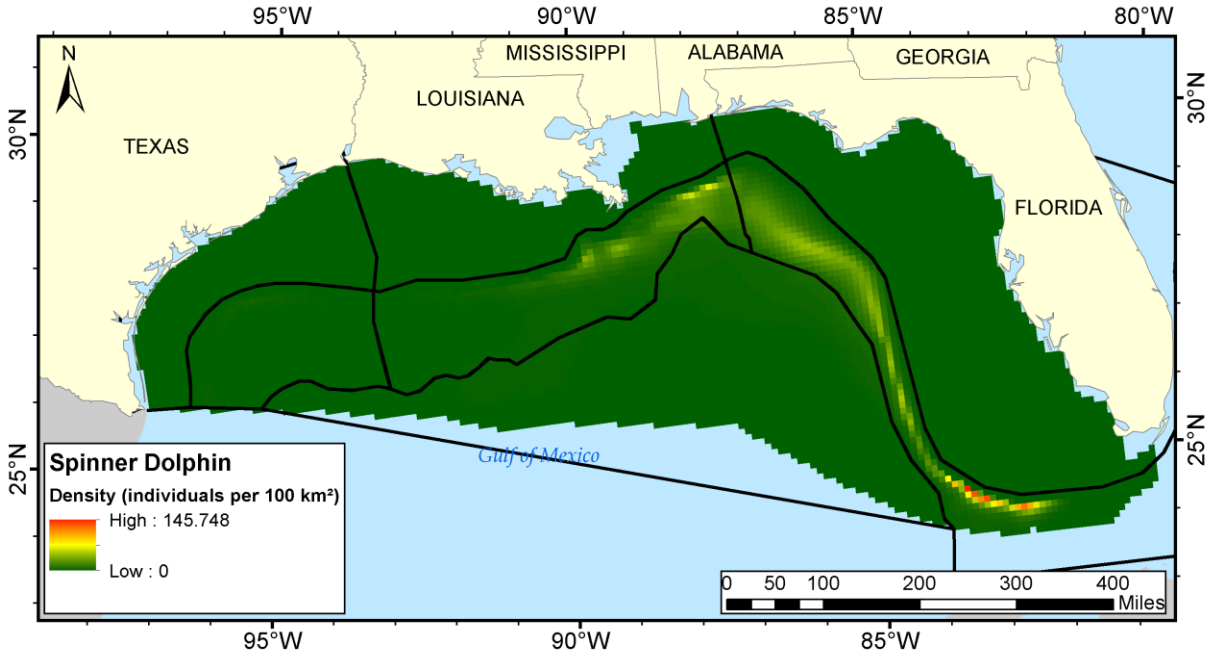

Figure C-17. Spinner dolphin distribution in the Gulf of Mexico project area. Density estimates were obtained from the Marine Geospatial Ecology Laboratory (Duke University) model (Roberts et al. In preparation), black lines depict the boundaries of the modeling zones.

C.18. Striped Dolphins

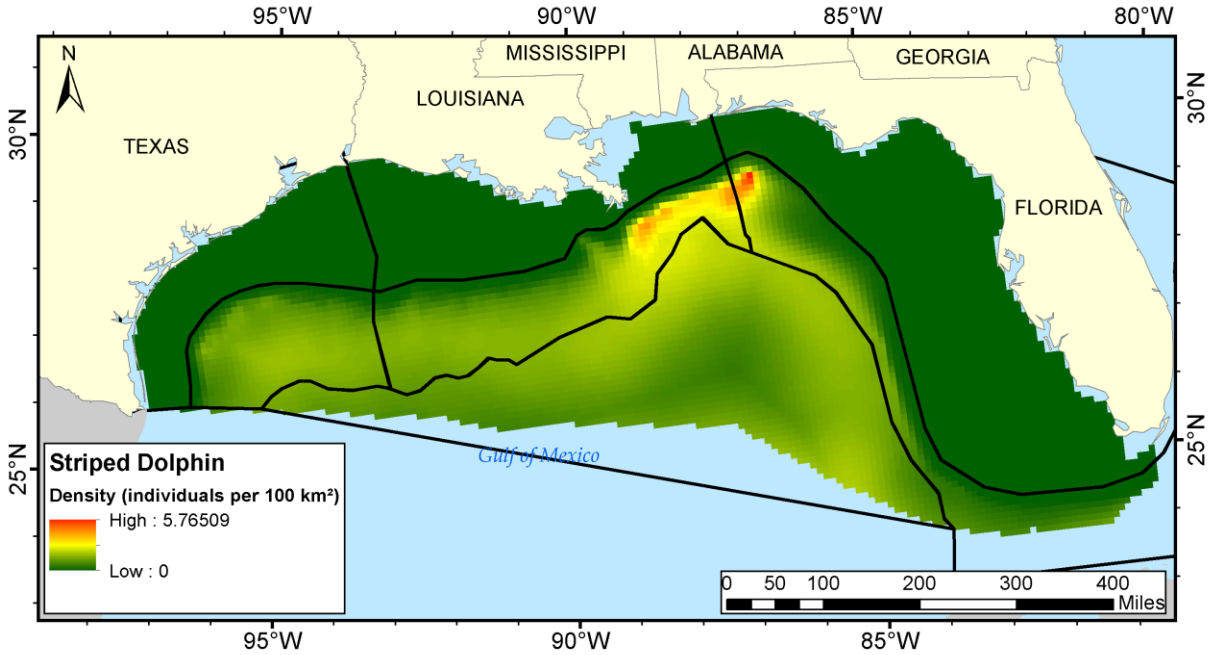

Figure C-18. Striped dolphin distribution in the Gulf of Mexico project area. Density estimates were obtained from the Marine Geospatial Ecology Laboratory (Duke University) model (Roberts et al. In preparation), black lines depict the boundaries of the modeling zones.

Appendix D. 3MB Animal Movement Parameters

The marine mammal movement and behavior (3MB) model uses previously measured animal movements to forecast how animals move in new situations and locations. 3MB creates simulated animals, referred to as animats, which are used to populate a simulation area. The animats are receivers; the sound levels they receive are logged as they move through the simulation.

3MB controls animat movement in horizontal and vertical directions using sub-models (see Houser and Cross 2014). Travel sub-models determine horizontal movement, including sub-models for the animats' travel direction and the travel rate (speed of horizontal movement). Dive sub-models determine vertical movement. Diving behavior sub-models include ascent and descent rates, maximum dive depth, bottom following, reversals, and surface interval. Bottom following describes the animat's behavior when it reaches the seafloor, for example during a foraging dive. If the bottom-following option is selected, the animat will continue along the same bathymetric contour line instead of the horizontal direction determined by another sub-model. Reversals simulate foraging behavior by defining the number of vertical excursions the animat makes after it reaches its maximum dive depth. The surface interval is the amount of time an animat spends at the surface before diving again.

Species-specific, realistic movement is simulated by supplying the sub-models with appropriate input parameters for each species. Parameter values are determined by visually observing species and reviewing tagging studies. For most sub-models, the input parameter is a probability distribution. When detailed information about a species' movements and behaviors are available, a user-created distribution vector should be used. When there is little to no information, either Gaussian or uniform distributions are used in the model. The user determines the appropriate mean and standard deviation for Gaussian distribution or the range if uniform distributions are being used. For behaviors with no directional preference, such as, perhaps, feeding and playing, a random walk model is used to define the bearing of an animats' travel direction. In a random walk model, at each parameter transition time step all bearings are equally likely choices. A variation of the random walk model, the correlated random walk, includes a directional bias. This variant should be used when animals have a preferred absolute direction, such as migration. The correlated random walk option smooths the changes in bearing by using the current bearing as the mean of the distribution from which the next heading is selected. Another option to control travel direction allows the user to create a vector of directional probabilities. In addition to the input distribution, parameters have a termination function that governs how long the parameter persists in a simulation. Houser (2006) and Houser and Cross (2014) discuss these input parameters in more detail.

3MB allows a user to define multiple behavioral states, which distinguish between specific subsets of behaviors like shallow and deep dives, or more general behavioral states such as foraging, resting, and socializing. The transition probability between these states can be defined as a probability value and related to the time of day. The level of detail included depends on the amount of data available for the species, and on the temporal and spatial framework of the simulation.

The animal movement parameters developed for each species are in the following sections. There is little or no data available for some species included in this study. In these cases we used a surrogate, which reflects values for a similar species: Pantropical spotted dolphins were used as a surrogate for Clymene, spinner, and striped dolphins; short-finned pilot whales were a surrogate for Fraser's dolphin, the *Kogia* species, and melon-headed whales; and rough-toothed dolphin as the surrogate for false killer whales and pygmy killer whales. Table D-19 lists the groups used for animal movement modeling.

D.1. Atlantic Spotted Dolphins

Table D-1. Distribution data for Atlantic spotted dolphins. Unless otherwise indicated, numbers in the Value column represent means with their standard deviations in brackets after.

Behavior	Variable	Value	Reference
Dive	Travel direction	Random walk	Best estimate
	Termination coefficient	0.2	Best estimate
	Travel rate (m/s)	Random Max: 5.69, Min: 0.08)	Davis et al. 1996
	Ascent rate (m/s)	Gaussian 1.15 (0.8)	Griffin et al. 2005
	Descent rate (m/s)	Gaussian 1.23 (0.48)	Griffin et al. 2005
	Average depth (m)	Random Max: 60	Davis et al. 1996
	Bottom following	Yes	Griffin et al. 2005
	Reversals	Gaussian	Best estimate
	Probability of reversal	0.5	Best estimate
	Number of reversals	2 (2)	Griffin et al. 2005
	Time in reversal log (s)	20.81 (21.5)	Griffin et al. 2005
	Surface interval (s)	Gaussian 63.59 (52.66)	Griffin et al. 2005

D.2. Beaked Whale spp.

This category includes Cuvier's, Blainville's, and Gervais' whales. Diving behavior for Blainville's and Cuvier's beaked whales (Baird et al. 2006b) is similar to the diving behavior documented for northern common bottlenose whales (Hooker and Baird 1999).

Table D-2. Distribution data for beaked whale spp. are based on Cuvier's beaked whale data. Unless otherwise indicated, numbers in the Value column represent means with their standard deviations in brackets after.

Behavior	Variable	Value	Reference
Deep dive	Travel direction	Correlated random walk	Best estimate
	Perturbation value	10	Best estimate
	Termination coefficient	0.2	Best estimate
	Travel rate (m/s)	Gaussian 0.508 (0.392)	Schorr et al. 2009
	Ascent rate (m/s)	Gaussian 0.7 (0.2)	Baird et al. 2006b, Tyack et al. 2006
	Descent rate (m/s)	Gaussian 1.39 (0.19)	Baird et al. 2006b, Tyack et al. 2006
	Average depth (m)	Gaussian 1070 (317)	Tyack et al. 2006
	Bottom following	No	Best estimate
	Reversals	Gaussian	Best estimate
	Probability of reversal	0.5	Best estimate
	Number of reversals	5 (3)	Baird et al. 2006a
	Time in reversal log (s)	696 (228)	Baird et al. 2006a
	Surface interval (s)	Gaussian 486 (1035)	Baird et al. 2006b
	Bout duration (s)	3480 (684)	Best estimate
Shallow dive	Travel direction	Correlated random walk	Best estimate
	Perturbation value	10	Best estimate
	Termination coefficient	0.2	Best estimate
	Travel rate (m/s)	Gaussian 0.508 (0.392)	Schorr et al. 2009
	Ascent rate (m/s)	Gaussian 0.66 (0.2)	Baird et al. 2006b, Tyack et al. 2006
	Descent rate (m/s)	Gaussian 0.7 (0.46)	Baird et al. 2006b, Tyack et al. 2006
	Average depth (m)	Gaussian 221 (100)	Tyack et al. 2006
	Bottom following	No	Best estimate
	Reversals	Gaussian	Best estimate
	Probability of reversal	0.5	Best estimate
	Number of reversals	3 (2)	Baird et al. 2006a
	Time in reversal log (s)	304 (156)	Baird et al. 2006a
	Surface interval (s)	Gaussian 486 (1035)	Baird et al. 2006b
	Bout duration (s)	912 (312)	Best estimate

D.3. Common Bottlenose Dolphins

Table D-3. Distribution data for common bottlenose dolphins. Unless otherwise indicated, numbers in the Value column represent means with their standard deviations in brackets after.

Behavior	Variable	Value	Reference
Foraging	Travel direction	Random walk	Best estimate
	Termination coefficient	0.2	Best estimate
	Travel rate (m/s)	Gaussian 1.19 (0.71)	Bearzi 2005
	Ascent rate (m/s)	Gaussian 2.1 (0.3)	Houser et al. 2010
	Descent rate (m/s)	Gaussian 1.6 (0.2)	Houser et al. 2010
	Average depth (m)	Gaussian 25 (5)	Hastie et al. 2006
	Bottom following	Yes	Best estimate
	Reversals	Gaussian 18 (1.1)	Best estimate
	Probability of reversal	0.09	Best estimate
	Reversal dive rate	Gaussian 1.0 (0.2)	Best estimate
	Time in reversal (s)	Gaussian 1 (0.1)	Best estimate
	Surface interval (s)	Gaussian 46.4 (2.5)	Lopez 2009
Playing	Travel Direction	Random walk	Best estimate
	Termination coefficient	0.2	Best estimate
	Travel rate (m/s)	Gaussian 1.19 (0.71)	Bearzi 2005
	Ascent rate (m/s)	Gaussian 2.1 (0.3)	Houser et al. 2010
	Descent rate (m/s)	Gaussian 1.6 (0.2)	Houser et al. 2010
	Average depth (m)	Gaussian 7 (3)	Wursig and Wursing 1979, Hastie et al. 2006
	Bottom following	Yes	Best estimate
	Reversals	No	Best estimate
	Surface interval (s)	Gaussian 3 (2)	Best estimate
Resting	Travel Direction	Random walk	Best estimate
	Termination coefficient	0.2	Best estimate
	Travel rate (m/s)	Gaussian 1.19 (0.71)	Bearzi 2005
	Ascent rate (m/s)	Gaussian 0.5 (0.1)	Best estimate
	Descent rate (m/s)	Gaussian 0.5 (0.1)	Best estimate
	Average depth (m)	Random Max: 2	Best estimate
	Bottom following	No	Best estimate
	Reversals	No	Best estimate
	Surface interval (s)	Gaussian 3 (2)	Best estimate
Socializing	Travel Direction	Random walk	Best estimate
	Termination coefficient	0.2	Best estimate
	Travel rate (m/s)	Gaussian 1.19 (0.71)	Bearzi 2005
	Ascent rate (m/s)	Gaussian 2.1 (0.3)	Houser et al. 2010
	Descent rate (m/s)	Gaussian 1.6 (0.2)	Houser et al. 2010

Behavior	Variable	Value	Reference
	Average depth (m)	Random Max: 10	Wursig and Wursing 1979, Hastie et al. 2006
	Bottom following	Yes	Best estimate
	Reversals	No	Best estimate
	Surface interval (s)	Gaussian 3 (2)	Best estimate
Travel	Travel Direction	Random walk	Best estimate
	Termination coefficient	0.2	Best estimate
	Travel rate (m/s)	Gaussian 1.19 (0.71)	Bearzi 2005
	Ascent rate (m/s)	Gaussian 2.1 (0.3)	Houser et al. 2010
	Descent rate (m/s)	Gaussian 1.6 (0.2)	Houser et al. 2010
	Average depth (m)	Gaussian 7 (3)	Wursig and Wursing 1979, Hastie et al. 2006
	Bottom following	Yes	Best estimate
	Reversals	No	Best estimate
	Surface interval (s)	Gaussian 3 (2)	Best estimate

D.4. Bryde's Whales

Table D-4. Distribution data for Bryde's whales. Unless otherwise indicated, numbers in the Value column represent means with their standard deviations in brackets after.

Behavior	Variable	Value	Reference
Dive	Travel direction	Random walk	Best estimate
	Termination coefficient	0.2	Best estimate
	Travel rate (m/s)	Gaussian 1.39 (0.83)	Kato and Perrin 2009
	Ascent rate (m/s)	Gaussian 0.95 (0.55)	Alves et al. 2010
	Descent rate (m/s)	Gaussian 1.25 (0.4)	Alves et al. 2010
	Average depth (m)	Random Max: 292	Alves et al. 2010
	Bottom following	No	Best estimate
	Reversals	Gaussian	Best estimate
	Probability of reversal	0.5	Best estimate
	Number of reversals	4 (3)	Alves et al. 2010
	Time in reversal log (s)	72 (21.2)	Alves et al. 2010
	Surface interval (s)	Gaussian 188 (48)	Di Sciara 1983
	Bout duration (s)	288 (63.6)	Best estimate

D.5. Clymene Dolphins

Table D-5. Distribution data for Clymene dolphins based on Pantropical spotted dolphin data. Unless otherwise indicated, numbers in the Value column represent means with their standard deviations in brackets after.

Behavior	Variable	Value	Reference
Day dive	Travel direction	Random walk	Best estimate
	Termination coefficient	0.2	Best estimate
	Travel rate (m/s)	Gaussian 2.39 (1.22)	Pantropical spotted dolphins
	Ascent rate (m/s)	Gaussian 0.42 (0.24)	Pantropical spotted dolphins
	Descent rate (m/s)	Gaussian 0.58 (0.34)	Pantropical spotted dolphins
	Average depth (m)	Gaussian 22.1 (15.71)	Pantropical spotted dolphins
	Bottom following	No	Pantropical spotted dolphins
	Reversals	No	Pantropical spotted dolphins
	Surface interval (s)	Gaussian 59.4 (293.4)	Pantropical spotted dolphins
Night dive	Travel direction	Correlated random walk	Best estimate
	Perturbation value	10	Best estimate
	Termination coefficient	0.2	Best estimate
	Travel rate (m/s)	Gaussian 1.83 (1.54)	Pantropical spotted dolphins
	Ascent rate (m/s)	Gaussian 0.74 (0.41)	Pantropical spotted dolphins
	Descent rate (m/s)	Gaussian 0.93 (0.54)	Pantropical spotted dolphins
	Average depth (m)	Gaussian 24 (27.1)	Pantropical spotted dolphins
	Bottom following	No	Pantropical spotted dolphins
	Reversals	Gaussian	Pantropical spotted dolphins
	Probability of reversal	0.5	Pantropical spotted dolphins
	Number of reversals	3 (1)	Pantropical spotted dolphins
	Time in reversal log (s)	39 (55.2)	Pantropical spotted dolphins
	Surface interval (s)	Gaussian 47.4 (106.8)	Pantropical spotted dolphins

D.6. False Killer Whales

Table D-6. Distribution data for false killer whales. Unless otherwise indicated, numbers in the Value column represent means with their standard deviations in brackets after.

Behavior	Variable	Value	Reference
Day dive	Travel direction	Random walk	Best estimate
	Termination coefficient	0.2	Best estimate
	Travel rate (m/s)	Random Min: 1.18; Max: 1.59	Baird et al. 2010
	Ascent rate (m/s)	Gaussian 0.77 (0.61)	Minamikawa et al. 2013
	Descent rate (m/s)	Gaussian 0.74 (0.72)	Minamikawa et al. 2013
	Average depth (m)	Gaussian 63.3 (131.5)	Minamikawa et al. 2013
	Bottom following	No	Best estimate
	Reversals	Gaussian	Best estimate
	Probability of reversal	0.5	Minamikawa et al. 2013
	Number of reversals	2 (1)	Minamikawa et al. 2013
	Time in reversal log (s)	65.76 (73.84)	Minamikawa et al. 2013
	Surface interval (s)	Gaussian 569.69 (630.68)	Minamikawa et al. 2013
Night dive	Travel direction	Random walk	Best estimate
	Termination coefficient	0.2	Best estimate
	Travel rate (m/s)	Random Min: 1.18; Max: 1.59	Baird et al. 2010
	Ascent rate (m/s)	Gaussian 0.51 (0.42)	Minamikawa et al. 2013
	Descent rate (m/s)	Gaussian 0.43 (0.4)	Minamikawa et al. 2013
	Average depth (m)	Gaussian 26.4 (46.5)	Minamikawa et al. 2013
	Bottom following	No	Best estimate
	Reversals	Gaussian	Best estimate
	Probability of reversal	0.5	Minamikawa et al. 2013
	Number of reversals	2 (1)	Minamikawa et al. 2013
	Time in reversal log (s)	127.68 (63.84)	Minamikawa et al. 2013
	Surface interval (s)	Gaussian 299.4 (345.98)	Minamikawa et al. 2013

D.7. Fraser's Dolphins

Table D-7. Distribution data for Fraser's dolphins based on Short-finned pilot whale data. Unless otherwise indicated, numbers in the Value column represent means with their standard deviations in brackets after.

Behavior	Variable	Value	Reference
Day dive	Travel direction	Random walk	Best estimate
	Termination coefficient	0.2	Best estimate
	Travel rate (m/s)	Gaussian 0.875 (0.572)	Short-finned pilot whales
	Ascent rate (m/s)	Gaussian 2.2 (0.2)	Short-finned pilot whales
	Descent rate (m/s)	Gaussian 2 (0.2)	Short-finned pilot whales
	Average depth (m)	Gaussian 30 (20)	Short-finned pilot whales
	Bottom following	No	Best estimate
	Reversals	No	Best estimate
	Surface interval (s)	Gaussian 165 (69)	Short-finned pilot whales
Night dive	Travel direction	Random walk	Best estimate
	Termination coefficient	0.2	Best estimate
	Travel rate (m/s)	Gaussian 0.875 (0.572)	Short-finned pilot whales
	Ascent rate (m/s)	Gaussian 3.2 (0.4)	Short-finned pilot whales
	Descent rate (m/s)	Gaussian 3 (0.4)	Short-finned pilot whales
	Average depth (m)	Gaussian 300 (100)	Short-finned pilot whales
	Bottom following	No	Best estimate
	Reversals	No	Best estimate
	Surface interval (s)	Gaussian 165 (69)	Short-finned pilot whales

D.8. Killer Whales

Table D-8. Distribution data for killer whales. Unless otherwise indicated, numbers in the Value column represent means with their standard deviations in brackets after.

Behavior	Variable	Value	Reference
Shallow dive	Travel direction	Random walk	Best estimate
	Termination coefficient	0.2	Best estimate
	Travel rate (m/s)	Gaussian 2 (1.61)	Dahlheim and White 2010
	Ascent rate (m/s)	Gaussian 1.832 (1.448)	Baird 1994
	Descent rate (m/s)	Gaussian 1.822 (1.51)	Baird 1994
	Average depth (m)	Gaussian 8 (2)	Miller et al. 2010
	Bottom following	No	Best estimate
	Reversals	No	Best estimate
	Surface interval (s)	Gaussian 3 (2)	Miller et al. 2010
Deep dive	Travel direction	Random walk	Best estimate
	Termination coefficient	0.2	Best estimate
	Travel rate (m/s)	Gaussian 2 (1.61)	Dahlheim and White 2010
	Ascent rate (m/s)	Gaussian 1.832 (1.448)	Baird 1994
	Descent rate (m/s)	Gaussian 1.822 (1.51)	Baird 1994
	Average depth (m)	Gaussian 40 (20)	Miller et al. 2010
	Bottom following	No	Best estimate
	Reversals	Random	Best estimate
	Probability of reversal	1	Best estimate
	Number of reversals	Min: 2, Max: 5	Best estimate
	Time in reversal log (s)	10 (1)	Best estimate
	Surface interval (s)	Gaussian 3 (2)	Miller et al. 2010

D.9. *Kogia spp.* including Dwarf Sperm Whales and Pygmy Sperm Whales (*Kogia sima* and *K. breviceps*)

Table D-9. Distribution data for Kogia spp. based on short-finned pilot whale data. Unless otherwise indicated, numbers in the Value column represent means with their standard deviations in brackets after.

Behavior	Variable	Value	Reference
Day dive	Travel direction	Random walk	Best estimate
	Termination coefficient	0.2	Best estimate
	Travel rate (m/s)	Gaussian 0.875 (0.572)	Short-finned pilot whales
	Ascent rate (m/s)	Gaussian 2.2 (0.2)	Short-finned pilot whales
	Descent rate (m/s)	Gaussian 2 (0.2)	Short-finned pilot whales
	Average depth (m)	Gaussian 30 (20)	Short-finned pilot whales
	Bottom following	No	Best estimate
	Reversals	No	Best estimate
	Surface interval (s)	Gaussian 165 (69)	Short-finned pilot whales
Night dive	Travel direction	Random walk	Best estimate
	Termination coefficient	0.2	Best estimate
	Travel rate (m/s)	Gaussian 0.875 (0.572)	Short-finned pilot whales
	Ascent rate (m/s)	Gaussian 3.2 (0.4)	Short-finned pilot whales
	Descent rate (m/s)	Gaussian 3 (0.4)	Short-finned pilot whales
	Average depth (m)	Gaussian 300 (100)	Short-finned pilot whales
	Bottom following	No	Best estimate
	Reversals	No	Best estimate
	Surface interval (s)	Gaussian 165 (69)	Short-finned pilot whales

D.10. Melon-headed Whales

Table D-10. Distribution data for melon-headed whales based on short-finned pilot whale data. Unless otherwise indicated, numbers in the Value column represent means with their standard deviations in brackets after.

Behavior	Variable	Value	Reference
Day dive	Travel direction	Random walk	Best estimate
	Termination coefficient	0.2	Best estimate
	Travel rate (m/s)	Gaussian 0.875 (0.572)	Short-finned pilot whales
	Ascent rate (m/s)	Gaussian 2.2 (0.2)	Short-finned pilot whales
	Descent rate (m/s)	Gaussian 2 (0.2)	Short-finned pilot whales
	Average depth (m)	Gaussian 30 (20)	Short-finned pilot whales
	Bottom following	No	Best estimate
	Reversals	No	Best estimate
	Surface interval (s)	Gaussian 165 (69)	Short-finned pilot whales
Night dive	Travel direction	Random walk	Best estimate
	Termination coefficient	0.2	Best estimate
	Travel rate (m/s)	Gaussian 0.875 (0.572)	Short-finned pilot whales
	Ascent rate (m/s)	Gaussian 3.2 (0.4)	Short-finned pilot whales
	Descent rate (m/s)	Gaussian 3 (0.4)	Short-finned pilot whales
	Average depth (m)	Gaussian 300 (100)	Short-finned pilot whales
	Bottom following	No	Best estimate
	Reversals	No	Best estimate
	Surface interval (s)	Gaussian 165 (69)	Short-finned pilot whales

D.11. Pantropical Spotted Dolphins

Table D-11. Distribution data for pantropical spotted dolphins. Unless otherwise indicated, numbers in the Value column represent means with their standard deviations in brackets after.

Behavior	Variable	Value	Reference
Day dive	Travel direction	Random walk	Best estimate
	Termination coefficient	0.2	Best estimate
	Travel rate (m/s)	Gaussian 2.39 (1.22)	Scott and Chivers 2009
	Ascent rate (m/s)	Gaussian 0.42 (0.24)	Scott and Chivers 2009
	Descent rate (m/s)	Gaussian 0.58 (0.34)	Scott and Chivers 2009
	Average depth (m)	Gaussian 22.1 (15.71)	Scott and Chivers 2009
	Bottom following	No	Best estimate
	Reversals	No	Best estimate
	Surface interval (s)	Gaussian 59.4 (293.4)	Scott and Chivers 2009
Night dive	Travel direction	Correlated random walk	Best estimate
	Perturbation value	10	Best estimate
	Termination coefficient	0.2	Best estimate
	Travel rate (m/s)	Gaussian 1.83 (1.54)	Scott and Chivers 2009
	Ascent rate (m/s)	Gaussian 0.74 (0.41)	Scott and Chivers 2009
	Descent rate (m/s)	Gaussian 0.93 (0.54)	Scott and Chivers 2009
	Average depth (m)	Gaussian 24 (27.1)	Scott and Chivers 2009
	Bottom following	No	Best estimate
	Reversals	Gaussian	Best estimate
	Probability of reversal	0.5	Best estimate
	Number of reversals	3 (1)	Best estimate
	Time in reversal log (s)	39 (55.2)	Best estimate
	Surface interval (s)	Gaussian 47.4 (106.8)	Scott and Chivers 2009

D.12. Pygmy Killer Whales

Table D-12. Distribution data for pygmy killer whales based on pantropical spotted and rough-toothed dolphin data. Unless otherwise indicated, numbers in the Value column represent means with their standard deviations in brackets after.

Behavior	Variable	Value	Reference
Travel dive	Travel direction	Random walk	Best estimate
	Termination coefficient	0.2	Best estimate
	Travel rate (m/s)	Gaussian 0.805 (0.05)	Baird et al. 2011
	Ascent rate (m/s)	Gaussian 0.42 (0.24)	Pantropical spotted dolphins
	Descent rate (m/s)	Gaussian 0.58 (0.34)	Pantropical spotted dolphins
	Average depth (m)	Gaussian 6 (4)	Rough-toothed dolphins
	Bottom following	No	Best estimate
	Reversals	No	Best estimate
	Surface interval (s)	Gaussian 59.4 (293.4)	Pantropical spotted dolphins
Forage dive	Travel direction	Correlated random walk	Best estimate
	Perturbation value	10	Best estimate
	Termination coefficient	0.2	Best estimate
	Travel rate (m/s)	Gaussian 0.805 (0.05)	Baird et al. 2011
	Ascent rate (m/s)	Gaussian 0.74 (0.41)	Pantropical spotted dolphins
	Descent rate (m/s)	Gaussian 0.93 (0.54)	Pantropical spotted dolphins
	Average depth (m)	Gaussian 25 (20)	Rough-toothed dolphins
	Bottom following	No	Best estimate
	Reversals	Gaussian	Best estimate
	Probability of reversal	0.5	Best estimate
	Number of reversals	3 (1)	Best estimate
	Time in reversal log (s)	23.3 (50)	Rough-toothed dolphins
	Surface interval (s)	Gaussian 47.4 (106.8)	Pantropical spotted dolphins

D.13. Risso's Dolphins

Table D-13. Distribution data for Risso's dolphins based on short-finned pilot whale data. Unless otherwise indicated, numbers in the Value column represent means with their standard deviations in brackets after.

Behavior	Variable	Value	Reference
Dive	Travel direction	Random walk	Best estimate
	Termination coefficient	0.2	Best estimate
	Travel rate (m/s)	Gaussian 1.997 (1.058)	Wells et al. 2009
	Ascent rate (m/s)	Gaussian 2.2 (0.2)	Short-finned pilot whales
	Descent rate (m/s)	Gaussian 2 (0.2)	Short-finned pilot whales
	Average depth (m)	Gaussian 11 (10)	Wells et al. 2009
	Bottom following	No	Best estimate
	Reversals	No	Best estimate
	Surface interval (s)	Gaussian 11 (4)	Bearzi et al. 2011

D.14. Rough-toothed Dolphins

Table D-14. Distribution data for rough-toothed dolphins based on pantropical spotted dolphin data. Unless otherwise indicated, numbers in the Value column represent means with their standard deviations in brackets after.

Behavior	Variable	Value	Reference
Travel dive	Travel direction	Random walk	Best estimate
	Termination coefficient	0.2	Best estimate
	Travel rate (m/s)	Gaussian 1.25 (0.5)	Ritter 2002
	Ascent rate (m/s)	Gaussian 0.42 (0.24)	Pantropical spotted dolphins
	Descent rate (m/s)	Gaussian 0.58 (0.34)	Pantropical spotted dolphins
	Average depth (m)	Gaussian 6 (4)	Wells et al. 2008
	Bottom following	No	Best estimate
	Reversals	No	Best estimate
	Surface interval (s)	Gaussian 59.4 (293.4)	Pantropical spotted dolphins
Forage dive	Travel direction	Correlated random walk	Best estimate
	Perturbation value	10	Best estimate
	Termination coefficient	0.2	Best estimate
	Travel rate (m/s)	Gaussian 2 (0.8)	Wells et al. 2008
	Ascent rate (m/s)	Gaussian 0.74 (0.41)	Pantropical spotted dolphins
	Descent rate (m/s)	Gaussian 0.93 (0.54)	Pantropical spotted dolphins
	Average depth (m)	Gaussian 25 (20)	Best estimate
	Bottom following	No	Best estimate
	Reversals	Gaussian	Best estimate
	Probability of reversal	0.5	Best estimate
	Number of reversals	3 (1)	Best estimate
	Time in reversal log (s)	23.3 (50)	Norris et al. 1965
	Surface interval (s)	Gaussian 47.4 (106.8)	Pantropical spotted dolphins

D.15. Short-finned Pilot Whales

Table D-15. Distribution data for short-finned pilot whales. Unless otherwise indicated, numbers in the Value column represent means with their standard deviations in brackets after.

Behavior	Variable	Value	Reference
Day dive	Travel direction	Random walk	Best estimate
	Termination coefficient	0.2	Best estimate
	Travel rate (m/s)	Gaussian 0.875 (0.572)	Wells et al. 2013
	Ascent rate (m/s)	Gaussian 2.2 (0.2)	Aguilar Soto et al. 2009
	Descent rate (m/s)	Gaussian 2 (0.2)	Aguilar Soto et al. 2009
	Average depth (m)	Gaussian 30 (20)	Wells et al. 2013
	Bottom following	No	Best estimate
	Reversals	No	Best estimate
	Surface interval (s)	Gaussian 165 (69)	Sakai et al. 2011
Night dive	Travel direction	Correlated random walk	Best estimate
	Perturbation value	10	Best estimate
	Termination coefficient	0.2	Best estimate
	Travel rate (m/s)	Gaussian 0.875 (0.572)	Wells et al. 2013
	Ascent rate (m/s)	Gaussian 3.2 (0.4)	Aguilar Soto et al. 2009
	Descent rate (m/s)	Gaussian 3 (0.4)	Aguilar Soto et al. 2009
	Average depth (m)	Gaussian 300 (100)	Wells et al. 2013
	Bottom following	No	Best estimate
	Reversals	No	Best estimate
	Surface interval (s)	Gaussian 165 (69)	Best estimate

D.16. Sperm Whales

Table D-16. Distribution data for sperm whales. Unless otherwise indicated, numbers in the Value column represent means with their standard deviations in brackets after.

Behavior	Variable	Value	Reference
Deep foraging dive	Travel direction	Correlated random walk	Best estimate
	Perturbation value	10	Best estimate
	Termination coefficient	0.2	Best estimate
	Travel rate (m/s)	Gaussian 0.88 (0.27)	Miller et al. 2004
	Ascent rate (m/s)	Gaussian 1.3 (0.2)	Watwood et al. 2006
	Descent rate (m/s)	Gaussian 1.1 (0.2)	Watwood et al. 2006
	Average depth (m)	Gaussian 546.9 (130)	Watwood et al. 2006
	Bottom following	No	Best estimate
	Reversals	Gaussian 8.2 (4.2)	Aoki et al. 2007
	Reversal dive rate (m/s)	Gaussian 1.8 (0.5)	Aoki et al. 2007
	Time in reversal (s)	Gaussian 141 (82.7)	Amano and Yoshioka 2003, Aoki et al. 2007
	Surface interval (s)	Gaussian 486 (156)	Watwood et al. 2006
Inactive bottom time	Travel Direction	Correlated random walk	Best estimate
	Perturbation value	10	Best estimate
	Termination coefficient	0.2	Best estimate
	Travel rate (m/s)	Gaussian 0.88 (0.27)	Miller et al. 2004
	Ascent rate (m/s)	Gaussian 1.13 (0.07)	Amano and Yoshioka 2003
	Descent rate (m/s)	Gaussian 1.4 (0.13)	Amano and Yoshioka 2003
	Average depth (m)	Gaussian 490 (74.6)	Amano and Yoshioka 2003
	Bottom following	No	Best estimate
	Reversals	Gaussian 1.0 (0)	Best estimate
	Reversal dive rate (m/s)	Gaussian 0.1 (0.1)	Best estimate
	Time in reversal (s)	Gaussian 1188 (174.6)	Amano and Yoshioka 2003
	Surface interval (s)	Gaussian 546 (354)	Amano and Yoshioka 2003
V dive	Travel Direction	Correlated random walk	Best estimate
	Perturbation value	10	Best estimate
	Termination coefficient	0.2	Best estimate
	Travel rate (m/s)	Gaussian 0.88 (0.27)	Miller et al. 2004
	Ascent rate (m/s)	Gaussian 0.67 (0.43)	Amano and Yoshioka 2003
	Descent rate (m/s)	Gaussian 0.85 (0.05)	Amano and Yoshioka 2003
	Average depth (m)	Gaussian 282.7 (69.9)	Amano and Yoshioka 2003
	Bottom following	No	Best estimate
	Reversals	No	Best estimate
	Surface interval (s)	Gaussian 408 (114)	Amano and Yoshioka 2003
Surface inactive (head down)	Travel Direction	Correlated random walk	Best estimate
	Perturbation value	10	Best estimate
	Termination coefficient	0.2	Best estimate
	Travel rate (m/s)	Gaussian 0.0 (0.0)	Best estimate

Behavior	Variable	Value	Reference
	Ascent rate (m/s)	Gaussian 0.1 (0.1)	Miller et al. 2008
	Descent rate (m/s)	Gaussian 0.1 (0.1)	Miller et al. 2008
	Average depth (m)	Gaussian 16.5 (4.9)	Miller et al. 2008
	Bottom following	No	Best estimate
	Reversals	Gaussian 1.0 (0)	Best estimate
	Reversal dive rate (m/s)	Gaussian 0.0 (0.0)	Best estimate
	Time in reversal (s)	Gaussian 804 (522)	Miller et al. 2008
	Surface interval (s)	Gaussian 462 (360)	Miller et al. 2008
	Bout duration*	T50 = 8.1, K = 0.9	Best estimate
Surface inactive (head up)	Travel Direction	Correlated random walk	Best estimate
	Perturbation value	10	Best estimate
	Termination coefficient	0.2	Best estimate
	Travel rate (m/s)	Gaussian 0.0 (0.0)	Best estimate
	Ascent rate (m/s)	Gaussian 0.1 (0.1)	Miller et al. 2008
	Descent rate (m/s)	Gaussian 0.1 (0.1)	Miller et al. 2008
	Average depth (m)	Gaussian 8.6 (4.8)	Miller et al. 2008
	Bottom following	No	Best estimate
	Reversals	Gaussian 1.0 (0)	Best estimate
	Reversal dive rate (m/s)	Gaussian 0.0 (0.0)	Best estimate
	Time in reversal (s)	Gaussian 708 (552)	Miller et al. 2008
	Surface interval (s)	Gaussian 462 (360)	Miller et al. 2008
	Bout duration*	T50 = 8.1, K = 0.9	Best estimate
Surface active	Travel Direction	Correlated random walk	Best estimate
	Perturbation value	10	Best estimate
	Termination coefficient	0.2	Best estimate
	Travel rate (m/s)	Gaussian 0.88 (0.27)	Miller et al. 2004
	Ascent rate (m/s)	Gaussian 0.67 (0.43)	Amano and Yoshioka 2003
	Descent rate (m/s)	Gaussian 0.85 (0.05)	Amano and Yoshioka 2003
	Average depth (m)	Gaussian 25.0 (25.0)	Amano and Yoshioka 2003
	Bottom following	No	Best estimate
	Reversals	No	Best estimate
	Surface interval (s)	Gaussian 408 (114)	Amano and Yoshioka 2003

* Sigmoidal function: T50 is the midpoint in minutes, K is the steepness

D.17. Spinner Dolphins

Table D-17. Distribution data for spinner dolphins based on pantropical spotted dolphin data. Unless otherwise indicated, numbers in the Value column represent means with their standard deviations in brackets after.

Behavior	Variable	Value	Reference
Day dive	Travel direction	Correlated random walk	Best estimate
	Perturbation value	10	Best estimate
	Termination coefficient	0.2	Best estimate
	Travel rate (m/s)	Gaussian 0.72 (0.83)	Würsig et al. 1994
	Ascent rate (m/s)	Gaussian 0.42 (0.24)	Pantropical spotted dolphins
	Descent rate (m/s)	Gaussian 0.58 (0.34)	Pantropical spotted dolphins
	Average depth (m)	Gaussian 22.1 (15.71)	Pantropical spotted dolphins
	Bottom following	No	Best estimate
	Reversals	No	Best estimate
	Surface interval (s)	Gaussian 59.4 (293.4)	Pantropical spotted dolphins
Night dive	Travel direction	Correlated random walk	Best estimate
	Perturbation value	10	Best estimate
	Termination coefficient	0.2	Best estimate
	Travel rate (m/s)	Gaussian 1.36 (0.83)	Würsig et al. 1994
	Ascent rate (m/s)	Gaussian 0.74 (0.41)	Pantropical spotted dolphins
	Descent rate (m/s)	Gaussian 0.93 (0.54)	Pantropical spotted dolphins
	Average depth (m)	Gaussian 24 (27.1)	Pantropical spotted dolphins
	Bottom following	No	Best estimate
	Reversals	Gaussian	Best estimate
	Probability of reversal	0.5	Pantropical spotted dolphins
	Number of reversals	3 (1)	Pantropical spotted dolphins
	Time in reversal log (s)	39 (55.2)	Pantropical spotted dolphins
	Surface interval (s)	Gaussian 47.4 (106.8)	Pantropical spotted dolphins

D.18. Striped Dolphins

Table D-18. Distribution data for striped dolphins based on pantropical spotted dolphin data. Unless otherwise indicated, numbers in the Value column represent means with their standard deviations in brackets after.

Behavior	Variable	Value	Reference
Day dive	Travel direction	Random walk	Best estimate
	Termination coefficient	0.2	Best estimate
	Travel rate (m/s)	Gaussian 3.035 (1.22)	Au and Perryman 1982
	Ascent rate (m/s)	Gaussian 0.6 (0.37)	Minamikawa et al. 2003
	Descent rate (m/s)	Gaussian 0.538 (0.343)	Minamikawa et al. 2003
	Average depth (m)	Gaussian 22.6 (17.5)	Minamikawa et al. 2003
	Bottom following	No	Best estimate
	Reversals	No	Best estimate
	Surface interval (s)	Gaussian 55.7 (32.1)	Minamikawa et al. 2003
Night dive	Travel direction	Random walk	Best estimate
	Termination coefficient	0.2	Best estimate
	Travel rate (m/s)	Gaussian 3.035 (1.22)	Au and Perryman 1982
	Ascent rate (m/s)	Gaussian 1.542 (0.709)	Minamikawa et al. 2003
	Descent rate (m/s)	Gaussian 1.463 (0.668)	Minamikawa et al. 2003
	Average depth (m)	Gaussian 126.7 (120.9)	Minamikawa et al. 2003
	Bottom following	No	Best estimate
	Reversals	Gaussian	Best estimate
	Probability of reversal	0.5	Pantropical spotted dolphins
	Number of reversals	3 (1)	Pantropical spotted dolphins
	Time in reversal log (s)	39 (55.2)	Pantropical spotted dolphins
	Surface interval (s)	Gaussian 65.8 (32)	Minamikawa et al. 2003

D.19. Animal Movement Modeling Species and Groups

Table D-19. Group name and species in each animal movement modeling group.

Group name	Species represented
Atlantic spotted dolphins	Atlantic spotted dolphins
Beaked whales	Cuvier's beaked whales, Blainville's beaked whales, Gervais' beaked whales
Common bottlenose dolphins	Common bottlenose dolphins
Bryde's whales	Bryde's whales
Killer whales	Killer whales
Pantropical spotted dolphins	Pantropical spotted dolphins, Clymene dolphins, Spinner dolphins, Striped dolphins
Risso's dolphins	Risso's dolphins
Rough-toothed dolphins	Rough-toothed dolphins, False killer whales, Pygmy killer whales
Short-finned pilot whales	Short-finned pilot whales, Fraser's dolphins, *Kogia spp.* (dwarf sperm whales, pygmy sperm whales), Melon-headed whales
Sperm whales	Sperm whales

Appendix E. Per-Pulse Acoustic Field Maps and Radii

The 3-D per-pulse acoustic fields used as inputs for acoustic exposure analysis were also processed to provide two other products:

- Plan-view maps of the acoustic field around the sources
- Tables of ranges to various isopleths (radii tables) for each source

The maps and radii tables are, respectively, 2-D and 1-D projections of the 3-D sound fields, which serve as quality assurance checkpoints to verify the acoustic modeling output and control the results of the exposure simulation.

Maps were created from the 3-D grid of the acoustic pressure levels by taking the maximum-over-depth value at each horizontal sampling location. The maps therefore represent the maximum received acoustic level over all depths at each location.

The ranges to isopleths in the radii tables are provided as two statistical estimates:

- The maximum range (R_{max}, in meters)
- The 95% range ($R_{95\%}$, in meters)

Given a regularly gridded spatial distribution of sound levels, the $R_{95\%}$ for a given sound level is defined as the radius of the circle, centered on the source, encompassing 95% of the grid points with sound levels at or above the given value. This definition is meaningful in terms of potential effects on animals because, regardless of the shape of the contour for a given sound level, $R_{95\%}$ is the range from the source beyond which only 5% of a uniformly distributed population would be exposed to sounds at or above that level.

The R_{max} for a given sound level is the maximum distance at which the specified received level occurs (equivalent to $R_{100\%}$). It is more conservative than $R_{95\%}$, but could be relevant for defining exclusion zones to avoid any chance of exposures above the specified level. For cases where the volume ensonified to a specific level is discontinuous and small pockets of higher received levels occur far beyond the main ensonified volume (e.g., due to convergence), the R_{max} can be much larger than $R_{95\%}$. Interpretation of these cases can be difficult if R_{max} if not presented with $R_{95\%}$.

Example modeling results the 8000 in^3 airgun array at site CM3, located in the Central-Slope zone at 750 m water depth, are presented below as maps of unweighted, per-pulse SEL, and SPL fields (Figure E-1 to Figure E-4). Site CM3 results are present as example results because that site is centrally located within the Gulf (see Tables 48–50 for all modeling site locations). The corresponding radii tables for the site are shown in Table E-1 to Table E-4 for Seasons 1 (January to March) and 3 (July to September) in SEL and rms SPL metrics with all applicable M-weighted filtering.

Example modeling results for the geotechnical survey sources at Box 4, an animat movement simulation box, are presented below as maps of unweighted, per-pulse SEL and SPL fields (Figure E-5 to Figure E-6, Table E-6 to Table E-12). Box 4 results are present as example results because that box is centrally located within the Gulf (See Table 51 for all box locations.) Radii tables for each site and season, and for all sources are provided in the Microsoft Excel workbooks: *_Radii.P001253_BOEM-PH2_8000in_array.xlsx and _Radii.P001253_BOEM-PH2_eng_sources.xlsx*, as provided on BOEM's webpage for the GOM G&G Activities Programmatic EIS.

E.1. 8000 in³ Airgun Array

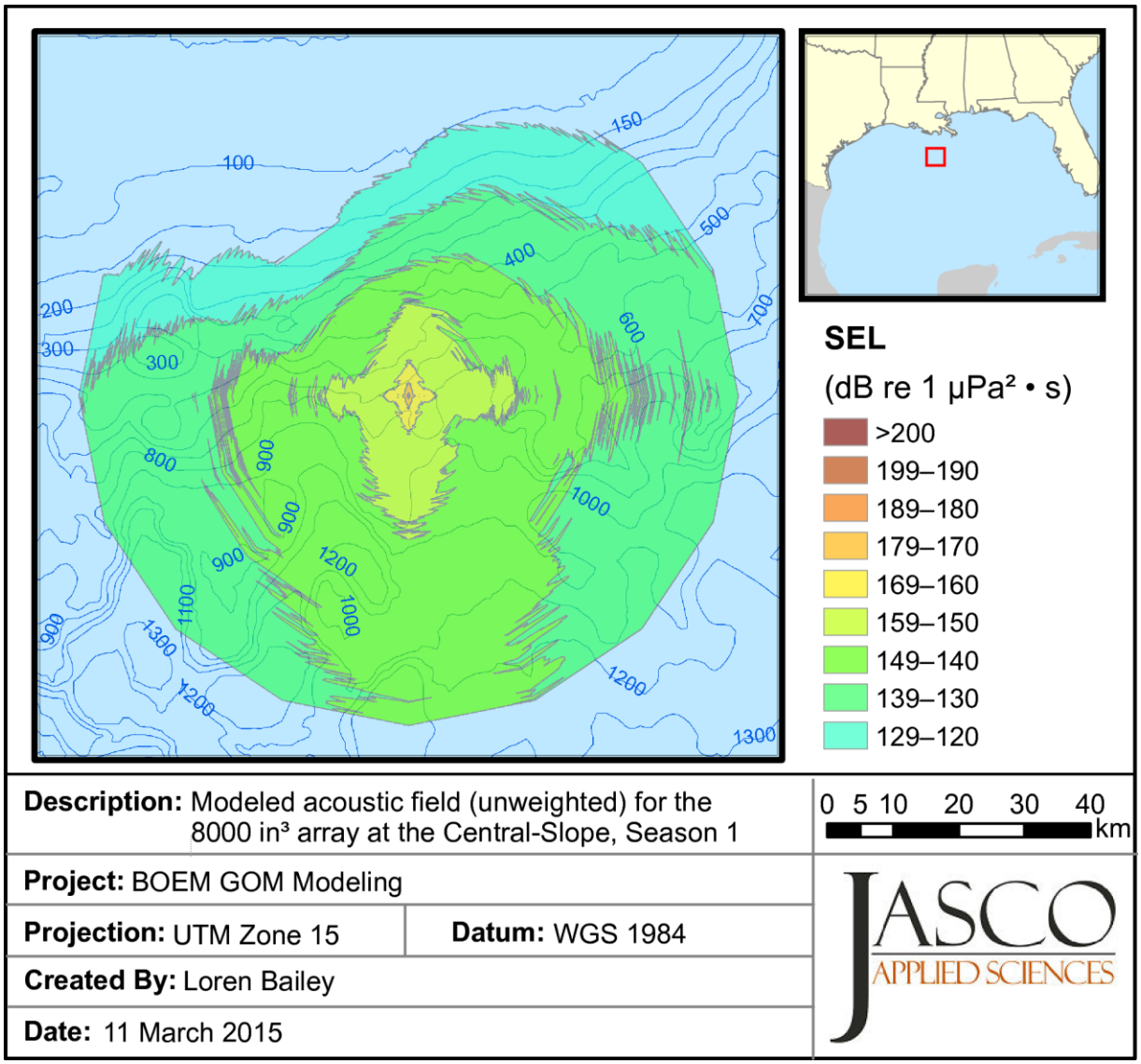

Figure E-1. 8000 in³ airgun array at the Central-Slope region (Site CM3), Season 1 (February): Broadband (10–5,000 Hz) maximum-over-depth per-pulse SEL field. Blue contours indicate water depth in meters.

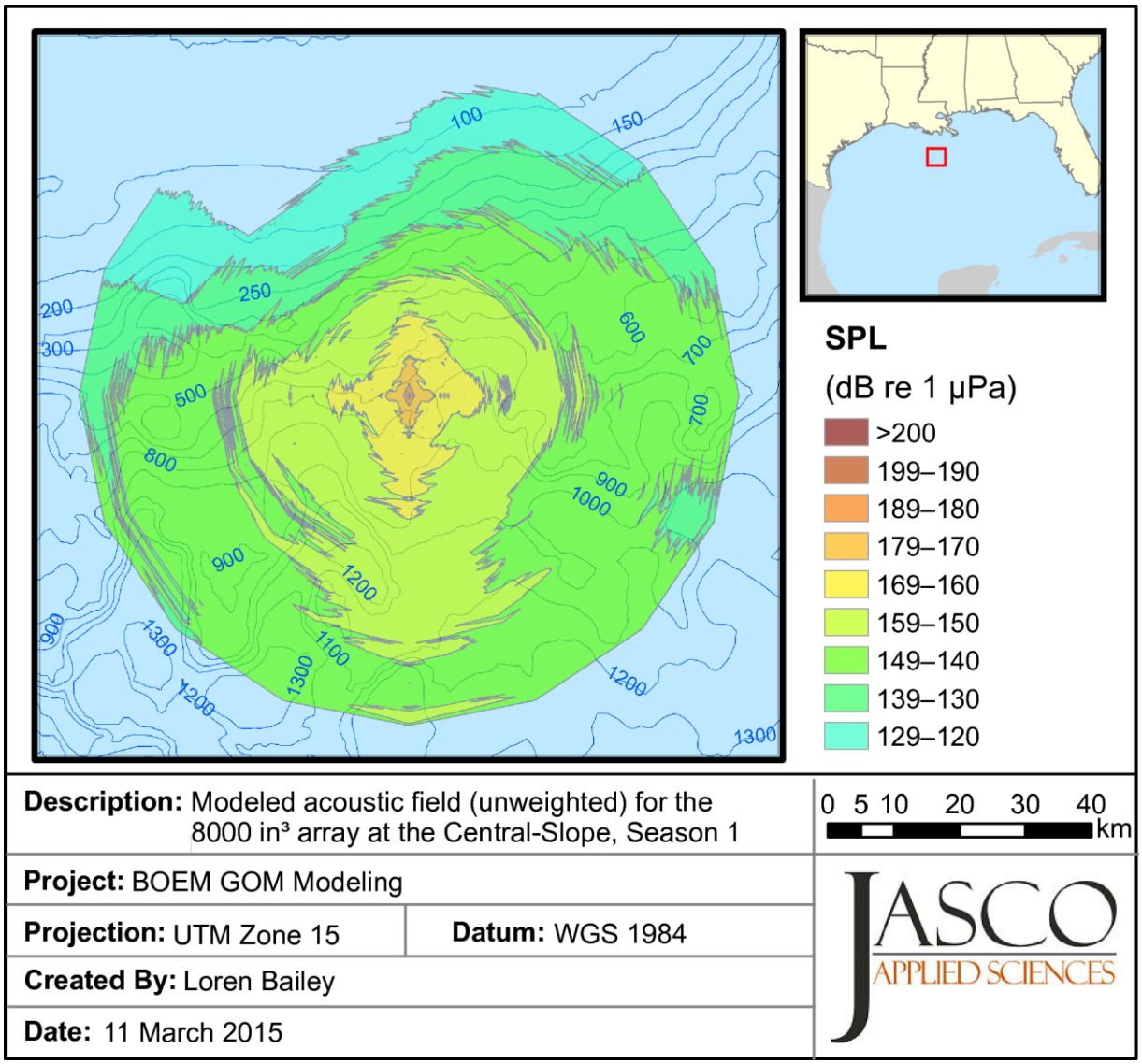

Figure E-2. 8000 in³ airgun array at the Central-Slope region (Site CM3), Season 1 (February): Broadband (10–5,000 Hz) maximum-over-depth rms SPL field. Blue contours indicate water depth in meters.

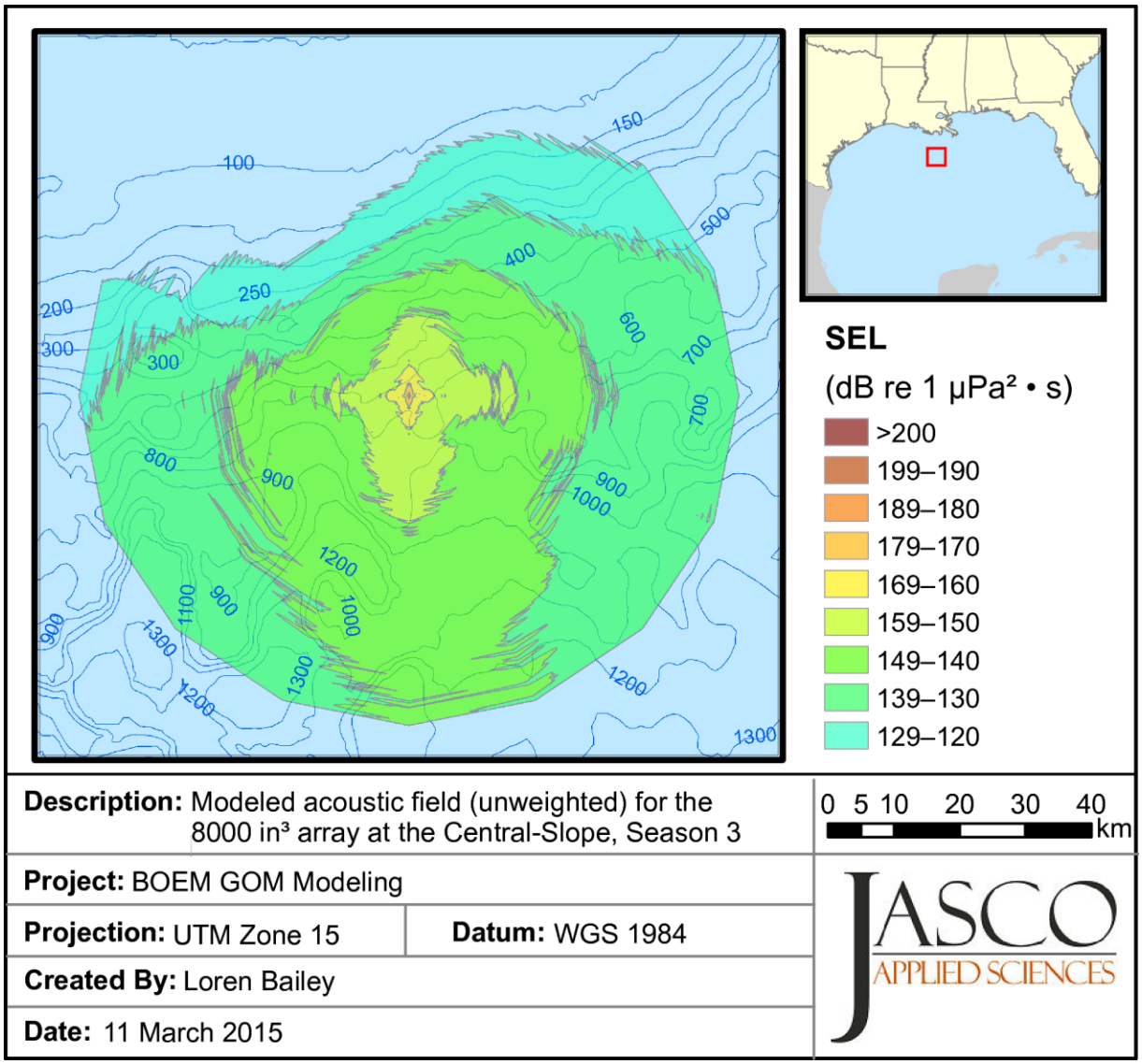

Figure E-3. 8000 in³ airgun array at the Central-Slope region (Site CM3), Season 3 (September) (February): Broadband (10–5,000 Hz) maximum-over-depth per-pulse SEL field. Blue contours indicate water depth in meters.

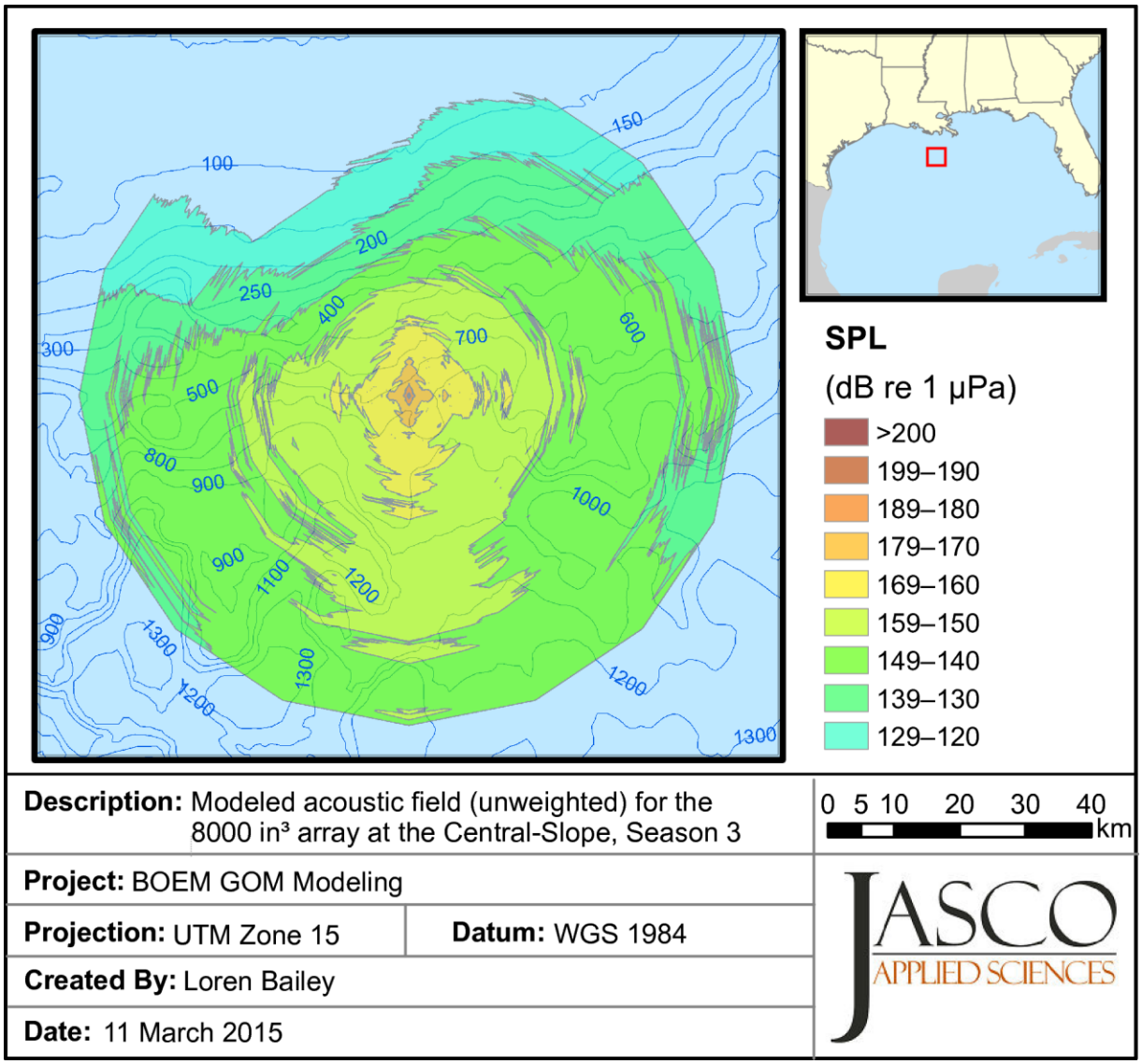

Figure E-4. 8000 in³ airgun array at the Central-Slope region (Site CM3), Season 3 (September) (February): Broadband (10–5,000 Hz) maximum-over-depth rms SPL field. Blue contours indicate water depth in meters.

Table E-1. 8000 in³ airgun array at Site CM3, Season 1 (February): Ranges to specific threshold levels (SEL).

SEL	Unweighted		Type I M-Weighting					
			LFC		MFC		HFC	
	R_{max}	$R_{95\%}$	R_{max}	$R_{95\%}$	R_{max}	$R_{95\%}$	R_{max}	$R_{95\%}$
210	10	10	10	10	< 10	< 10		
200	50	40	40	40	10	10	< 10	< 10
190	150	120	140	120	50	50	30	30
180	500	400	470	380	160	140	120	100
170	2100	1800	2000	1400	520	440	400	330
160	5900	4400	5400	4000	2900	1500	1300	1100
150	23000	17000	23000	16000	14000	9700	10000	9300
140	> 50000	> 50000	> 50000	> 50000	32000	21000	25000	18000
130					> 50000	> 50000	50000	36000
120							> 50000	> 50000
110								

Maximum (R_{max}, m) and 95% ($R_{95\%}$, m) horizontal distance from the source to modeled broadband maximum-over-depth sound level thresholds, with and
without auditory frequency weighting applied for low-frequency cetaceans (LFC), mid-frequency cetaceans (MFC), and high-frequency cetaceans (HFC).
Units: rms SPL (dB re 1 µPa²·s).

Table E-2. 8000 in³ airgun array at Site CM3, Season 1 (February): Ranges to specific threshold levels (rms SPL).

rms SPL	Unweighted		Type I M-Weighting					
			LFC		MFC		HFC	
	R_{max}	$R_{95\%}$	R_{max}	$R_{95\%}$	R_{max}	$R_{95\%}$	R_{max}	$R_{95\%}$
210	50	41	50	40	10	10	10	10
200	170	140	160	130	60	50	40	30
190	470	390	470	370	180	150	120	100
180	1900	1300	1500	1200	590	480	460	370
170	6700	5300	6400	4700	2400	1100	1200	900
160	19000	15000	18000	14000	11000	8500	9800	7200
150	50000	36000	50000	35000	26000	17000	23000	15000
140	> 50000	> 50000	> 50000	> 50000	47000	32000	43000	27000
130					> 50000	> 50000	> 50000	> 50000
120								
110								

Maximum (R_{max}, m) and 95% ($R_{95\%}$, m) horizontal distance from the source to modeled broadband maximum-over-depth sound level thresholds, with and without
auditory frequency weighting applied for low-frequency cetaceans (LFC), mid-frequency cetaceans (MFC), and high-frequency cetaceans (HFC). Units: rms SPL (dB re 1 µPa).

Table E-3. 8000 in³ airgun array at Site CM3, Season 3 (September): Ranges to specific threshold levels (SEL).

SEL	Unweighted		Type I M-Weighting					
			LFC		MFC		HFC	
	R_{max}	$R_{95\%}$	R_{max}	$R_{95\%}$	R_{max}	$R_{95\%}$	R_{max}	$R_{95\%}$
210	10	10	10	10	< 10	< 10		
200	50	40	40	40	10	10	< 10	< 10
190	150	120	140	120	50	50	30	30
180	490	400	470	380	160	140	120	100
170	2000	1700	1900	1400	510	430	390	330
160	5900	4200	5600	3900	2900	1700	1300	1100
150	21000	16000	19000	16000	15000	9300	9900	9100
140	> 50000	> 50000	> 50000	> 50000	23000	19000	23000	16000
130					48000	33000	40000	29000
120					> 50000	> 50000	> 50000	> 50000
110								

Maximum (R_{max}, m) and 95% ($R_{95\%}$, m) horizontal distance from the source to modeled broadband maximum-over-depth sound level thresholds, with and
without auditory frequency weighting applied for low-frequency cetaceans (LFC), mid-frequency cetaceans (MFC), and high-frequency cetaceans (HFC).
Units: rms SPL (dB re 1 µPa²·s).

Table E-4. 8000 in³ airgun array at Site CM3, Season 3 (September): Ranges to specific threshold levels (rms SPL).

rms SPL	Unweighted		Type I M-Weighting					
			LFC		MFC		HFC	
	R_{max}	$R_{95\%}$	R_{max}	$R_{95\%}$	R_{max}	$R_{95\%}$	R_{max}	$R_{95\%}$
210	50	41	50	40	10	10	10	10
200	170	140	160	130	60	50	40	30
190	470	390	470	370	180	150	120	100
180	1900	1300	1500	1200	590	470	460	370
170	6500	5300	6400	5000	2600	1200	1200	910
160	19000	15000	19000	14000	12000	9100	9700	7200
150	49000	35000	49000	34000	21000	16000	18000	15000
140	> 50000	> 50000	> 50000	> 50000	37000	28000	32000	26000
130					> 50000	> 50000	> 50000	> 50000
120								
110								

Maximum (R_{max}, m) and 95% ($R_{95\%}$, m) horizontal distance from the source to modeled broadband maximum-over-depth sound level thresholds, with and without
auditory frequency weighting applied for low-frequency cetaceans (LFC), mid-frequency cetaceans (MFC), and high-frequency cetaceans (HFC). Units: rms SPL (dB re 1 µPa).

E.2. High-resolution Sources

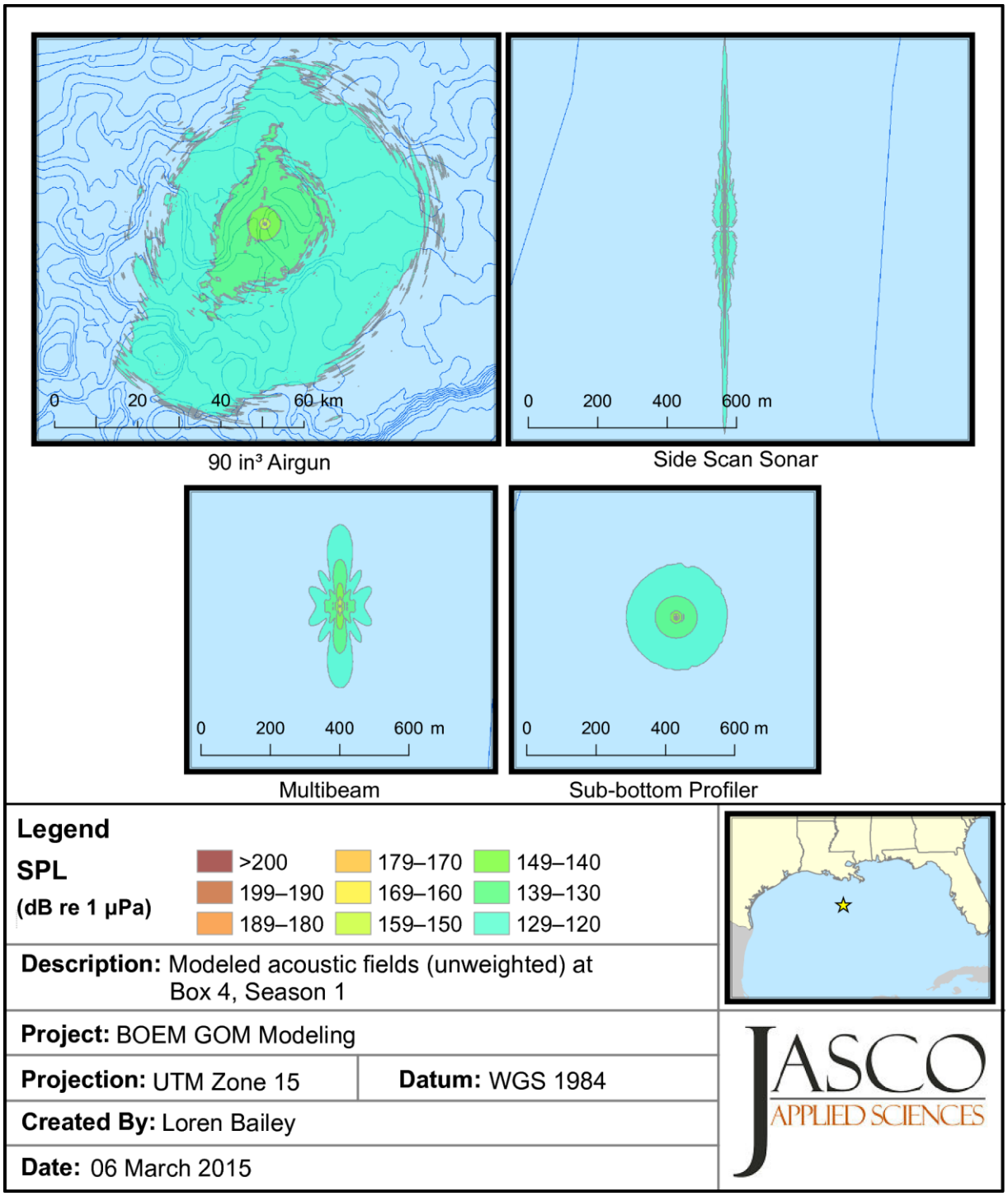

Figure E-5. Box 4 geotechnical sources: Maximum-over-depth sound pressure levels during Season 1 (February).

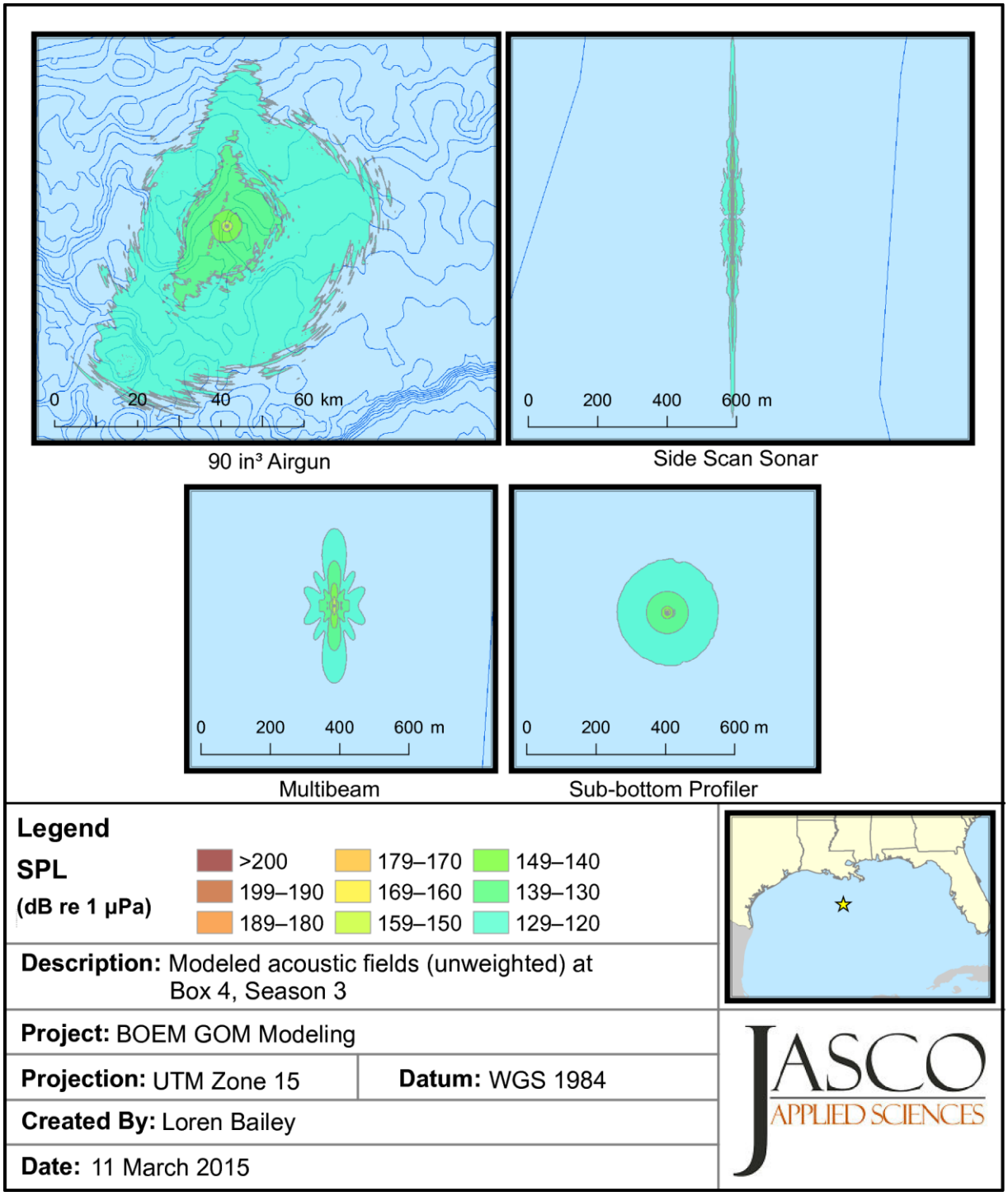

Figure E-6. Box 4 geotechnical sources: Maximum-over-depth sound pressure levels during Season 3 (September).

E.2.1. 90 in^3 Airgun/Boomer

Table E-5. Box 4, Season 1 (February), ranges to specific threshold levels for a 90 in³ single airgun.

SEL	rms SPL	Unweighted		Type I M-Weighting					
				LFC		MFC		HFC	
		R_{max}	$R_{95\%}$	R_{max}	$R_{95\%}$	R_{max}	$R_{95\%}$	R_{max}	$R_{95\%}$
190	200	< 10	< 10	< 10	< 10				
180	190	14	14	14	14	< 10	< 10	< 10	< 10
170	180	45	42	42	42	14	14	14	14
160	170	120	110	110	110	54	54	45	45
150	160	370	360	360	350	160	160	130	130
140	150	1300	1300	1300	1200	500	490	410	390
130	140	8900	4800	8900	4200	1800	1700	1300	1300
120	130	28000	19000	28000	18000	17000	9400	17000	8300
110	120	> 50000	> 50000	> 50000	> 50000	35000	25000	35000	23000
100	110					> 50000	> 50000	> 50000	> 50000

Maximum (R_{max}, m) and 95% ($R_{95\%}$, m) horizontal distance from the source to modeled broadband maximum-over-depth sound level thresholds, with and without
auditory frequency weighting applied for low-frequency cetaceans (LFC), mid-frequency cetaceans (MFC), and high-frequency cetaceans (HFC). Units: SEL (dB re 1 µPa^2·s);
rms SPL (dB re 1 µPa).

Table E-6. Box 4, Season 3 (September), ranges to specific threshold levels for a 90 in³ single airgun.

SEL	rms SPL	Unweighted		Type I M-Weighting					
				LFC		MFC		HFC	
		R_{max}	$R_{95\%}$	R_{max}	$R_{95\%}$	R_{max}	$R_{95\%}$	R_{max}	$R_{95\%}$
190	200	< 10	< 10	< 10	< 10				
180	190	14	14	14	14	< 10	< 10	< 10	< 10
170	180	42	42	41	41	14	14	14	14
160	170	120	110	110	110	54	54	45	45
150	160	370	360	360	350	160	160	130	130
140	150	1300	1300	1300	1200	500	490	410	400
130	140	8400	5200	8300	4000	1900	1700	1400	1300
120	130	27000	18000	25000	18000	14000	9100	13000	8300
110	120	> 50000	> 50000	50000	37000	35000	24000	35000	21000
100	110			> 50000	> 50000	> 50000	> 50000	> 50000	> 50000

Maximum (R_{max}, m) and 95% ($R_{95\%}$, m) horizontal distance from the source to modeled broadband maximum-over-depth sound level thresholds, with and without
auditory frequency weighting applied for low-frequency cetaceans (LFC), mid-frequency cetaceans (MFC), and high-frequency cetaceans (HFC). Units: SEL (dB re 1 µPa^2·s);
rms SPL (dB re 1 µPa).

E.2.2. Multibeam Sonar

Table E-7. Box 4, Season 1 (February), ranges to specific threshold levels for a multibeam sonar.

SEL	rms SPL	Unweighted		Type I M-Weighting					
				LFC		MFC		HFC	
		R_{max}	$R_{95\%}$	R_{max}	$R_{95\%}$	R_{max}	$R_{95\%}$	R_{max}	$R_{95\%}$
150	160	< 5	< 5			< 5	< 5	< 5	< 5
140	150	25	25			5	5	5	5
130	140	65	60			30	25	35	30
120	130	140	120	< 5	< 5	75	70	80	75
110	120	240	210	5	5	150	140	160	150
100	110	380	330	30	25	260	230	280	240

Maximum (R_{max}, m) and 95% ($R_{95\%}$, m) horizontal distance from the source to modeled broadband maximum-over-depth sound level thresholds, with and without auditory
frequency weighting applied for low-frequency cetaceans (LFC), mid-frequency cetaceans (MFC), and high-frequency cetaceans (HFC). Units: SEL (dB re 1 µPa^2·s);
rms SPL (dB re 1 µPa).

Table E-8. Box 4, Season 3 (September), ranges to specific threshold levels for a multibeam sonar.

SEL	rms SPL	Unweighted		Type I M-Weighting					
				LFC		MFC		HFC	
		R_{max}	$R_{95\%}$	R_{max}	$R_{95\%}$	R_{max}	$R_{95\%}$	R_{max}	$R_{95\%}$
150	160	< 5	< 5			< 5	< 5	< 5	< 5
140	150	25	25			5	5	5	5
130	140	65	60			30	25	35	30
120	130	130	120	< 5	< 5	75	70	80	70
110	120	220	200	5	5	150	130	160	140
100	110	350	300	30	30	240	220	260	230

Maximum (R_{max}, m) and 95% ($R_{95\%}$, m) horizontal distance from the source to modeled broadband maximum-over-depth sound level thresholds, with and without auditory
frequency weighting applied for low-frequency cetaceans (LFC), mid-frequency cetaceans (MFC), and high-frequency cetaceans (HFC). Units: SEL (dB re 1 µPa^2·s);
rms SPL (dB re 1 µPa).

E.2.3. Side-scan Sonar

Table E-9. Box 4, Season 1 (February), ranges to specific threshold levels for a side-scan sonar.

SEL	rms SPL	Unweighted		Type I M-Weighting					
				LFC		MFC		HFC	
		R_{max}	$R_{95\%}$	R_{max}	$R_{95\%}$	R_{max}	$R_{95\%}$	R_{max}	$R_{95\%}$
160	170	< 5	< 5			< 5	< 5	< 5	< 5
150	160	65	65			30	30	35	35
140	150	140	140			90	85	95	90
130	140	260	250	< 5	< 5	190	180	200	190
120	130	420	370	55	55	340	320	360	330
110	120	590	500	130	120	530	440	540	460
100	110	790	600	240	230	700	580	710	580

Maximum (R_{max}, m) and 95% ($R_{95\%}$, m) horizontal distance from the source to modeled broadband maximum-over-depth sound level thresholds, with and without auditory
frequency weighting applied for low-frequency cetaceans (LFC), mid-frequency cetaceans (MFC), and high-frequency cetaceans (HFC). Units: SEL (dB re 1 µPa^2·s);
rms SPL (dB re 1 µPa).

Table E-10. Box 4, Season 3 (September), ranges to specific threshold levels for a side-scan sonar.

SEL	rms SPL	Unweighted		Type I M-Weighting					
				LFC		MFC		HFC	
		R_{max}	$R_{95\%}$	R_{max}	$R_{95\%}$	R_{max}	$R_{95\%}$	R_{max}	$R_{95\%}$
160	170	< 5	< 5			< 5	< 5	< 5	< 5
150	160	65	65			30	30	35	35
140	150	140	130			90	85	95	90
130	140	240	230	< 5	< 5	190	180	190	180
120	130	410	350	55	50	330	310	350	330
110	120	580	480	130	120	520	430	520	430
100	110	760	580	240	230	680	560	700	570

Maximum (R_{max}, m) and 95% ($R_{95\%}$, m) horizontal distance from the source to modeled broadband maximum-over-depth sound level thresholds, with and without auditory
frequency weighting applied for low-frequency cetaceans (LFC), mid-frequency cetaceans (MFC), and high-frequency cetaceans (HFC). Units: SEL (dB re 1 µPa^2·s);
rms SPL (dB re 1 µPa).

E.2.4. Sub-bottom Profiler

Table E-11. Box 4, Season 1 (February), ranges to specific threshold levels for a sub-bottom profiler.

SEL	rms SPL	Unweighted		Type I M-Weighting					
				LFC		MFC		HFC	
		R_{max}	$R_{95\%}$	R_{max}	$R_{95\%}$	R_{max}	$R_{95\%}$	R_{max}	$R_{95\%}$
150	160	< 5	< 5	< 5	< 5	< 5	< 5	< 5	< 5
140	150	8	8	8	8	8	8	8	8
130	140	17	17	16	15	17	17	17	17
120	130	61	59	45	44	61	59	61	59
110	120	150	150	110	110	150	140	150	140
100	110	750	600	440	370	750	600	750	600

Maximum (R_{max}, m) and 95% ($R_{95\%}$, m) horizontal distance from the source to modeled broadband maximum-over-depth sound level thresholds, with and without auditory
frequency weighting applied for low-frequency cetaceans (LFC), mid-frequency cetaceans (MFC), and high-frequency cetaceans (HFC). Units: SEL (dB re 1 µPa^2·s);
rms SPL (dB re 1 µPa).

Table E-12. Box 4, Season 3 (September), ranges to specific threshold levels for a sub-bottom profiler.

SEL	rms SPL	Unweighted		Type I M-Weighting					
				LFC		MFC		HFC	
		R_{max}	$R_{95\%}$	R_{max}	$R_{95\%}$	R_{max}	$R_{95\%}$	R_{max}	$R_{95\%}$
150	160	< 5	< 5	< 5	< 5	< 5	< 5	< 5	< 5
140	150	8	8	8	8	8	8	8	8
130	140	17	17	16	15	17	17	17	17
120	130	61	59	45	44	61	59	61	59
110	120	160	150	110	110	150	140	150	140
100	110	770	610	440	370	750	600	750	600

Maximum (R_{max}, m) and 95% ($R_{95\%}$, m) horizontal distance from the source to modeled broadband maximum-over-depth sound level thresholds, with and without auditory
frequency weighting applied for low-frequency cetaceans (LFC), mid-frequency cetaceans (MFC), and high-frequency cetaceans (HFC). Units: SEL (dB re 1 µPa^2·s);
rms SPL (dB re 1 µPa).

Appendix F. Annual Exposure Estimates

F.1. Annual Totals for All Sources

Table F-1. 2016 annual exposure estimate totals for all sources.

Species	Number of Level A exposures			Number of Level B exposures	
	peak SPL	SEL	180 rms SPL	Step fxn	160 rms SPL
Atlantic spotted dolphins	331.1	33.5	40080.2	133426.8	201356.3
Beaked whales	51.7	2.9	6563.7	235614.8	57492.8
Common bottlenose dolphins	1974.6	151.7	212385.2	653404.8	891037.8
Bryde's whales	0.4	15.1	77.4	731.8	860.9
Clymene dolphins	431.5	35.0	10240.0	110741.8	201187.1
False killer whales	111.4	10.7	3130.6	25510.6	45216.7
Fraser's dolphins	52.0	3.2	3006.9	13858.3	22507.8
Killer whales	4.8	0.5	357.6	1492.9	2069.3
Kogia	4426.8	541.4	3824.5	16188.5	35585.5
Melon-headed whales	252.4	16.5	14115.5	68899.5	119722.0
Pantropical spotted dolphins	2550.3	134.2	64870.6	606728.6	947527.9
Pygmy killer whales	83.4	7.5	2281.5	18029.1	30429.7
Risso's dolphins	105.9	14.5	2608.6	27061.9	48495.8
Rough-toothed dolphins	150.8	15.1	5401.8	37666.3	67023.8
Short-finned pilot whales	68.1	7.6	3426.8	19258.3	38823.6
Sperm whales	44.8	2.4	10872.7	43503.7	93979.5
Spinner dolphins	253.1	9.4	6328.8	82778.6	160968.7
Striped dolphins	174.2	11.1	4295.8	44037.5	75388.5

Table F-2. 2017 annual exposure estimate totals for all sources.

Species	Number of Level A exposures			Number of Level B exposures	
	peak SPL	SEL	180 rms SPL	Step fxn	160 rms SPL
Atlantic spotted dolphins	425.1	33.7	59630.6	175824.7	244098.4
Beaked whales	45.1	1.8	5870.3	204860.9	50231.7
Common bottlenose dolphins	2757.9	111.3	341522.1	966790.3	1283476.0
Bryde's whales	0.3	12.6	62.7	605.0	724.2
Clymene dolphins	360.6	21.3	8795.2	93767.5	165628.8
False killer whales	99.9	8.0	2879.5	22516.7	38959.8
Fraser's dolphins	47.1	2.3	2719.2	12240.7	19386.6
Killer whales	4.5	0.5	332.0	1351.6	1833.6
Kogia	3991.0	493.2	3488.7	14520.1	31629.3
Melon-headed whales	227.5	12.2	12607.0	60546.5	103396.1
Pantropical spotted dolphins	2319.6	98.6	59828.3	548764.4	843785.8
Pygmy killer whales	75.1	5.7	2055.5	15845.3	26126.8
Risso's dolphins	95.0	12.3	2309.0	23594.5	41516.2
Rough-toothed dolphins	142.0	11.8	5959.5	36133.7	61548.4
Short-finned pilot whales	54.0	4.8	2635.1	14972.4	29918.0
Sperm whales	40.4	1.4	9213.3	36832.3	79611.9
Spinner dolphins	244.7	8.5	6129.9	78708.7	153523.0
Striped dolphins	153.6	7.5	3862.8	38903.9	65281.2

Table F-3. 2018 annual exposure estimate totals for all sources.

Species	Number of Level A exposures			Number of Level B exposures	
	peak SPL	SEL	180 rms SPL	Step fxn	160 rms SPL
Atlantic spotted dolphins	290.2	25.5	36272.0	117295.4	173452.2
Beaked whales	44.4	2.7	5585.4	195022.1	47714.9
Common bottlenose dolphins	1784.9	90.3	198079.4	598127.8	804687.8
Bryde's whales	0.3	13.3	67.0	618.4	723.4
Clymene dolphins	376.4	32.7	8786.2	93293.4	171405.6
False killer whales	96.3	10.0	2687.6	21389.7	38221.2
Fraser's dolphins	45.3	3.0	2549.0	11575.0	18847.7
Killer whales	4.1	0.4	299.9	1229.9	1715.8
Kogia	3710.5	468.1	3226.1	13379.4	29285.6
Melon-headed whales	219.1	15.5	11957.0	57389.9	99683.7
Pantropical spotted dolphins	2157.9	116.7	54470.9	499090.9	786512.4
Pygmy killer whales	71.8	6.9	1945.2	15048.9	25668.9
Risso's dolphins	91.6	12.9	2226.9	22558.6	40690.5
Rough-toothed dolphins	131.1	13.9	4703.2	31907.1	56928.3
Short-finned pilot whales	61.3	7.4	3024.1	16718.6	33605.6
Sperm whales	38.1	2.1	9330.0	36576.4	78417.3
Spinner dolphins	212.1	7.9	5254.2	66746.3	129459.8
Striped dolphins	149.3	10.1	3637.0	36541.7	63137.2

Table F-4. 2019 annual exposure estimate totals for all sources.

Species	Number of Level A exposures			Number of Level B exposures	
	peak SPL	SEL	180 rms SPL	Step fxn	160 rms SPL
Atlantic spotted dolphins	423.0	40.2	61334.2	174705.4	237351.8
Beaked whales	38.0	1.6	4259.4	162134.0	39332.0
Common bottlenose dolphins	2833.4	161.0	352798.8	977108.3	1286763.9
Bryde's whales	0.3	10.2	48.2	481.3	571.5
Clymene dolphins	282.8	19.7	6587.0	72912.8	132307.6
False killer whales	76.6	6.5	2175.1	17631.1	30853.9
Fraser's dolphins	35.6	1.9	2010.0	9654.3	15405.2
Killer whales	3.4	0.4	240.9	1031.1	1429.7
Kogia	2889.2	380.6	2554.4	11427.6	24827.9
Melon-headed whales	171.2	9.5	9239.0	47547.6	81651.0
Pantropical spotted dolphins	1759.0	86.0	43742.7	419737.6	657701.8
Pygmy killer whales	56.9	4.5	1505.4	12277.6	20528.0
Risso's dolphins	75.2	9.5	1761.0	18123.5	32923.3
Rough-toothed dolphins	114.5	10.2	5244.4	30192.3	51110.5
Short-finned pilot whales	42.6	4.1	2005.0	12154.5	24322.1
Sperm whales	28.9	1.3	6248.9	27270.6	56706.5
Spinner dolphins	188.1	7.5	4550.8	59622.5	119366.8
Striped dolphins	118.2	6.7	2855.3	29936.2	51432.8

Table F-5. 2020 annual exposure estimate totals for all sources.

Species	Number of Level A exposures			Number of Level B exposures	
	peak SPL	SEL	180 rms SPL	Step fxn	160 rms SPL
Atlantic spotted dolphins	290.5	23.4	36255.0	116698.1	171995.1
Beaked whales	46.7	1.7	5591.0	190777.4	46608.9
Common bottlenose dolphins	1788.3	81.9	198182.1	596824.1	801708.1
Bryde's whales	0.3	12.4	61.3	565.8	672.5
Clymene dolphins	348.1	20.9	8468.2	87614.7	155501.5
False killer whales	95.4	7.6	2700.3	20828.4	36168.0
Fraser's dolphins	43.9	2.1	2572.2	11393.8	17978.9
Killer whales	4.3	0.4	316.2	1258.4	1703.8
Kogia	3857.7	475.2	3346.4	13664.1	29421.3
Melon-headed whales	212.9	10.6	12084.1	56791.0	96371.0
Pantropical spotted dolphins	2215.8	94.3	57221.4	511036.9	789057.3
Pygmy killer whales	71.8	5.4	1975.1	14787.7	24406.7
Risso's dolphins	93.7	11.4	2202.9	21914.2	38821.7
Rough-toothed dolphins	129.5	10.6	4704.1	31102.5	54226.7
Short-finned pilot whales	50.8	4.3	2546.7	14163.3	28103.6
Sperm whales	38.1	1.5	8517.9	33340.0	70032.5
Spinner dolphins	238.2	8.3	5935.9	73012.9	142804.9
Striped dolphins	147.6	7.3	3708.3	36266.5	61116.2

Table F-6. 2021 annual exposure estimate totals for all sources.

Species	Number of Level A exposures			Number of Level B exposures	
	peak SPL	SEL	180 rms SPL	Step fxn	160 rms SPL
Atlantic spotted dolphins	417.0	35.4	59474.2	171905.7	236363.4
Beaked whales	47.1	2.7	5398.0	187604.0	45590.3
Common bottlenose dolphins	2763.1	115.9	341320.6	955742.1	1266130.0
Bryde's whales	0.3	13.3	66.8	597.2	693.3
Clymene dolphins	369.8	32.7	8603.4	89618.0	166262.4
False killer whales	94.1	9.6	2708.4	20760.0	37075.3
Fraser's dolphins	43.3	2.8	2516.9	11279.5	18255.5
Killer whales	4.0	0.4	290.5	1176.3	1643.8
Kogia	3659.4	457.5	3153.7	12984.2	28092.0
Melon-headed whales	208.1	14.0	11669.4	55474.4	95823.2
Pantropical spotted dolphins	2096.5	116.1	52890.5	476698.9	757643.4
Pygmy killer whales	69.4	6.7	1895.4	14427.9	24697.5
Risso's dolphins	92.5	12.2	2171.1	21521.7	39337.2
Rough-toothed dolphins	136.0	14.0	5774.8	33915.3	58878.2
Short-finned pilot whales	58.9	7.0	2981.0	16327.5	32625.2
Sperm whales	36.3	2.3	8733.4	33804.8	69850.9
Spinner dolphins	209.9	8.1	5169.9	63322.2	124218.1
Striped dolphins	146.0	10.0	3547.6	34969.4	60995.9

Table F-7. 2022 annual exposure estimate totals for all sources.

Species	Number of Level A exposures			Number of Level B exposures	
	peak SPL	SEL	180 rms SPL	Step fxn	160 rms SPL
Atlantic spotted dolphins	302.4	30.4	38803.6	122141.9	177946.6
Beaked whales	41.9	1.7	5076.4	178787.5	43303.5
Common bottlenose dolphins	1890.0	134.3	210451.4	624454.4	835161.0
Bryde's whales	0.3	11.2	57.0	530.3	627.5
Clymene dolphins	315.9	20.6	7735.4	81413.5	145490.2
False killer whales	84.5	6.9	2452.5	19325.5	33630.0
Fraser's dolphins	39.0	1.9	2355.5	10607.9	16763.3
Killer whales	3.8	0.4	285.9	1162.9	1580.0
Kogia	3585.0	419.9	3054.8	12695.9	27371.7
Melon-headed whales	188.9	9.8	11040.9	52809.2	89767.1
Pantropical spotted dolphins	1998.7	93.2	51950.6	472822.4	732288.9
Pygmy killer whales	63.5	4.9	1780.6	13685.7	22634.5
Risso's dolphins	83.6	10.3	2012.3	20305.1	36265.7
Rough-toothed dolphins	117.1	10.1	4547.2	29545.9	51348.7
Short-finned pilot whales	46.0	4.1	2347.1	13294.3	26435.6
Sperm whales	33.6	1.5	7627.1	30668.4	63959.6
Spinner dolphins	212.0	8.0	5399.8	67309.9	132699.6
Striped dolphins	133.3	7.2	3375.6	33603.6	56934.9

Table F-8. 2023 annual exposure estimate totals for all sources.

Species	Number of Level A exposures			Number of Level B exposures	
	peak SPL	SEL	180 rms SPL	Step fxn	160 rms SPL
Atlantic spotted dolphins	397.5	32.7	58303.6	164824.3	221780.8
Beaked whales	36.5	1.6	4243.7	151708.3	37134.2
Common bottlenose dolphins	2687.0	102.8	339639.6	938321.5	1229214.3
Bryde's whales	0.3	9.9	47.0	454.3	540.4
Clymene dolphins	276.7	18.7	6501.2	69608.5	125034.2
False killer whales	75.9	6.5	2164.3	16774.1	29231.5
Fraser's dolphins	35.2	1.8	1991.4	9126.7	14537.6
Killer whales	3.4	0.4	240.0	984.3	1351.0
Kogia	2861.0	373.8	2526.2	10742.9	23321.6
Melon-headed whales	168.6	9.4	9148.2	44841.9	76892.5
Pantropical spotted dolphins	1719.9	78.8	43334.2	399580.5	621470.2
Pygmy killer whales	56.4	4.6	1504.2	11676.8	19464.7
Risso's dolphins	73.1	9.3	1710.1	17308.8	30955.1
Rough-toothed dolphins	112.5	9.9	5076.5	28662.8	48301.8
Short-finned pilot whales	41.8	4.0	1982.0	11522.5	23062.6
Sperm whales	29.6	1.3	6530.7	26650.9	56439.5
Spinner dolphins	182.7	6.6	4450.0	56546.1	111110.8
Striped dolphins	115.6	6.3	2821.3	28522.2	48514.8

Table F-9. 2024 annual exposure estimate totals for all sources.

Species	Number of Level A exposures			Number of Level B exposures	
	peak SPL	SEL	180 rms SPL	Step fxn	160 rms SPL
Atlantic spotted dolphins	269.3	22.6	35542.4	109856.5	157436.0
Beaked whales	37.7	1.7	4753.2	156583.6	38031.8
Common bottlenose dolphins	1721.5	74.9	196862.6	579403.1	766053.4
Bryde's whales	0.3	10.2	53.2	469.8	554.3
Clymene dolphins	288.4	19.0	7196.6	72741.3	129402.6
False killer whales	76.7	6.6	2296.8	17163.3	29795.7
Fraser's dolphins	35.3	1.7	2209.3	9391.4	14760.2
Killer whales	3.4	0.3	266.7	1035.8	1390.7
Kogia	3410.8	377.2	2858.4	11164.7	23941.2
Melon-headed whales	170.4	8.9	10344.7	46630.5	78841.0
Pantropical spotted dolphins	1814.1	82.8	48318.0	419823.7	647642.4
Pygmy killer whales	57.6	4.7	1668.1	12140.9	20053.1
Risso's dolphins	76.0	9.3	1830.2	18091.8	31995.2
Rough-toothed dolphins	106.3	9.4	4200.0	26314.7	45535.6
Short-finned pilot whales	42.0	3.9	2210.3	11900.0	23598.7
Sperm whales	31.6	1.5	7443.5	27656.6	57735.6
Spinner dolphins	189.4	6.6	4961.2	59253.3	115261.0
Striped dolphins	121.1	6.4	3136.7	29890.1	50373.1

Table F-10. 2025 annual exposure estimate totals for all sources.

Species	Number of Level A exposures			Number of Level B exposures	
	peak SPL	SEL	180 rms SPL	Step fxn	160 rms SPL
Atlantic spotted dolphins	417.5	39.8	61360.8	172104.3	230498.1
Beaked whales	35.4	1.6	4314.1	146016.7	35545.7
Common bottlenose dolphins	2819.0	157.5	352480.7	970712.7	1269758.3
Bryde's whales	0.2	9.6	48.4	439.4	519.1
Clymene dolphins	269.9	18.4	6573.7	67663.6	121148.0
False killer whales	72.7	6.4	2189.7	16242.2	28188.8
Fraser's dolphins	33.5	1.7	2038.4	8848.8	13959.3
Killer whales	3.2	0.3	242.8	958.5	1298.3
Kogia	3036.5	355.7	2587.1	10383.1	22339.9
Melon-headed whales	160.4	8.7	9365.2	43386.6	73728.2
Pantropical spotted dolphins	1680.1	77.9	43875.2	388177.6	601739.4
Pygmy killer whales	54.0	4.5	1520.5	11291.9	18750.8
Risso's dolphins	71.0	8.8	1691.1	16794.8	29887.1
Rough-toothed dolphins	109.6	10.0	5256.8	28351.1	47408.9
Short-finned pilot whales	40.0	3.9	2024.0	11190.6	22263.7
Sperm whales	29.1	1.4	6721.2	25716.3	53768.8
Spinner dolphins	176.1	6.3	4499.6	54651.1	106767.8
Striped dolphins	112.7	6.2	2854.7	27700.9	46946.9

Table F-11. Decade annual exposure estimate totals for all sources.

Species	Number of Level A exposures			Number of Level B exposures	
	peak SPL	SEL	180 rms SPL	Step fxn	160 rms SPL
Atlantic spotted dolphins	3563.5	317.2	487056.5	1458783.3	2052278.6
Beaked whales	424.6	20.1	51655.2	1809109.2	440985.8
Common bottlenose dolphins	23019.7	1181.6	2743722.5	7860889.1	10433990.6
Bryde's whales	3.0	117.8	588.8	5493.2	6487.0
Clymene dolphins	3320.1	239.0	79487.0	839375.0	1513368.0
False killer whales	883.5	78.8	25384.9	198141.7	347341.0
Fraser's dolphins	410.3	22.4	23968.9	107976.5	172402.1
Killer whales	38.8	4.1	2872.4	11681.7	16015.8
Kogia	35427.9	4342.6	30620.3	127150.4	275815.8
Melon-headed whales	1979.7	115.1	111570.8	534317.0	915875.8
Pantropical spotted dolphins	20311.8	978.5	520502.4	4742461.5	7385369.4
Pygmy killer whales	659.8	55.4	18131.6	139211.8	232760.7
Risso's dolphins	857.6	110.4	20523.1	207274.9	370887.7
Rough-toothed dolphins	1249.5	115.1	50868.4	313791.7	542311.0
Short-finned pilot whales	505.5	51.1	25182.1	141502.0	282758.8
Sperm whales	350.6	16.7	81238.9	322020.0	680502.4
Spinner dolphins	2106.2	77.1	52680.2	661951.7	1296180.6
Striped dolphins	1371.6	78.7	34095.0	340372.2	580121.5

F.2. Annual Exposure Estimates for Each Source

F.2.1. 2016

Table F-12. 2016 annual exposure estimate totals for 2-D survey (8000 in^3 airgun array, 1 vessel).

Species	Number of Level A exposures			Number of Level B exposures	
	peak SPL	SEL	180 rms SPL	Step fxn	160 rms SPL
Atlantic spotted dolphins	3.4	0.2	164.7	2667.7	6011.5
Beaked whales	1.8	0.1	186.4	15183.3	3562.4
Common bottlenose dolphins	7.3	0.6	396.6	7010.8	13939.6
Bryde's whales	0.0	0.3	2.4	41.2	50.6
Clymene dolphins	12.4	0.9	307.8	5925.8	10276.6
False killer whales	2.9	0.1	80.4	1363.4	2334.0
Fraser's dolphins	1.1	0.0	98.1	773.5	1330.2
Killer whales	0.1	0.0	12.4	87.5	123.4
Kogia	153.7	12.1	121.8	960.1	2319.9
Melon-headed whales	5.3	0.0	451.8	3911.0	7345.2
Pantropical spotted dolphins	93.0	7.7	2247.7	36435.7	54177.4
Pygmy killer whales	2.2	0.0	62.1	988.3	1580.3
Risso's dolphins	2.4	0.2	85.1	1530.8	2738.8
Rough-toothed dolphins	3.6	0.1	99.0	1775.4	3204.4
Short-finned pilot whales	1.1	0.0	77.6	864.2	1934.7
Sperm whales	1.4	0.2	327.0	2391.4	5749.3
Spinner dolphins	8.4	0.5	219.1	5464.7	11120.2
Striped dolphins	5.7	0.4	140.6	2542.7	4194.2

Table F-13. 2016 annual exposure estimate totals for 3-D NAZ survey (8000 in^3 airgun array, 2 vessels).

Species	Number of Level A exposures			Number of Level B exposures	
	peak SPL	SEL	180 rms SPL	Step fxn	160 rms SPL
Atlantic spotted dolphins	290.5	30.6	37123.8	114136.0	163006.9
Beaked whales	33.0	2.1	3289.8	141081.3	35503.2
Common bottlenose dolphins	1852.8	133.0	208355.1	603788.8	796124.2
Bryde's whales	0.2	10.1	36.7	444.8	534.2
Clymene dolphins	278.5	26.4	5339.5	65882.6	123800.0
False killer whales	76.0	8.8	1710.2	15509.1	28278.4
Fraser's dolphins	36.4	2.9	1463.8	8294.8	14018.2
Killer whales	3.3	0.4	182.0	853.8	1256.3
Kogia	1704.3	376.1	1827.1	9551.2	21540.5
Melon-headed whales	176.0	14.7	6772.6	40937.4	73612.3
Pantropical spotted dolphins	1541.9	84.9	32815.2	348649.0	560399.0
Pygmy killer whales	56.4	6.0	1202.0	10803.8	18880.2
Risso's dolphins	67.4	10.6	1495.2	15913.9	29352.4
Rough-toothed dolphins	106.9	12.8	3633.2	24669.3	44010.9
Short-finned pilot whales	49.5	6.9	1725.8	12049.3	24878.6
Sperm whales	26.8	1.3	5337.1	26668.0	59889.8
Spinner dolphins	158.6	6.4	3179.1	47035.2	92654.6
Striped dolphins	108.7	7.8	2199.9	25673.0	45301.4

Table F-14. 2016 annual exposure estimate totals for 3-D WAZ survey (8000 in^3 airgun array, 4 vessels).

Species	Number of Level A exposures			Number of Level B exposures	
	peak SPL	SEL	180 rms SPL	Step fxn	160 rms SPL
Atlantic spotted dolphins	15.4	1.2	1948.8	13153.1	26634.9
Beaked whales	4.7	0.1	2347.0	63466.0	15214.7
Common bottlenose dolphins	34.7	0.9	2284.2	34068.7	68051.1
Bryde's whales	0.1	1.1	30.9	200.9	229.3
Clymene dolphins	51.5	3.2	3108.5	31042.9	55785.4
False killer whales	11.2	1.0	847.6	6504.1	11321.1
Fraser's dolphins	4.9	0.1	1119.1	3800.5	5931.0
Killer whales	0.5	0.1	118.3	437.5	556.7
Kogia	2149.2	40.1	1449.9	4496.0	9696.3
Melon-headed whales	24.3	0.6	5331.1	19034.4	32091.0
Pantropical spotted dolphins	311.8	7.5	20302.3	177190.6	274838.2
Pygmy killer whales	8.7	0.8	644.0	4698.6	7698.9
Risso's dolphins	12.1	1.7	658.9	7710.5	13746.5
Rough-toothed dolphins	13.7	1.1	1055.3	8450.8	15393.5
Short-finned pilot whales	6.4	0.4	1249.2	4986.4	9964.0
Sperm whales	8.4	0.2	4068.0	11273.2	23183.1
Spinner dolphins	31.3	0.2	1984.1	24292.3	47726.1
Striped dolphins	21.1	0.8	1327.7	12638.6	21468.6

Table F-15. 2016 annual exposure estimate totals for Coil survey (8000 in^3 airgun array, 4 vessels).

Species	Number of Level A exposures			Number of Level B exposures	
	peak SPL	SEL	180 rms SPL	Step fxn	160 rms SPL
Atlantic spotted dolphins	21.8	0.4	840.3	3454.1	5677.3
Beaked whales	12.3	0.5	740.4	15880.5	3212.4
Common bottlenose dolphins	79.9	6.4	1322.0	8454.5	12832.0
Bryde's whales	0.1	3.7	7.5	44.8	46.9
Clymene dolphins	89.1	4.5	1484.1	7890.5	11325.0
False killer whales	21.3	0.9	492.4	2134.0	3283.1
Fraser's dolphins	9.7	0.2	325.8	989.4	1228.4
Killer whales	1.0	0.1	44.8	114.1	132.8
Kogia	419.6	113.2	425.6	1181.3	2028.8
Melon-headed whales	46.8	1.1	1560.0	5016.7	6673.5
Pantropical spotted dolphins	603.6	34.1	9505.3	44453.4	58113.2
Pygmy killer whales	16.1	0.6	373.4	1538.5	2270.2
Risso's dolphins	24.0	2.0	369.4	1906.7	2658.2
Rough-toothed dolphins	26.7	1.1	614.3	2769.6	4413.4
Short-finned pilot whales	11.1	0.3	374.2	1358.4	2046.4
Sperm whales	8.2	0.7	1140.7	3171.0	5157.4
Spinner dolphins	54.8	2.4	946.6	5986.4	9468.0
Striped dolphins	38.7	2.0	627.6	3183.2	4424.3

Table F-16. 2016 annual exposure estimate totals for 90 in^3 airgun.

Species	Number of Level A exposures			Number of Level B exposures	
	peak SPL	SEL	180 rms SPL	Step fxn	160 rms SPL
Atlantic spotted dolphins	0.0	0.0	1.5	11.6	24.3
Beaked whales	0.0	0.0	0.0	0.0	0.0
Common bottlenose dolphins	0.0	0.0	13.2	53.3	82.5
Bryde's whales	0.0	0.0	0.0	0.0	0.0
Clymene dolphins	0.0	0.0	0.0	0.0	0.0
False killer whales	0.0	0.0	0.0	0.1	0.1
Fraser's dolphins	0.0	0.0	0.0	0.0	0.0
Killer whales	0.0	0.0	0.0	0.0	0.0
Kogia	0.0	0.0	0.0	0.0	0.0
Melon-headed whales	0.0	0.0	0.0	0.0	0.0
Pantropical spotted dolphins	0.0	0.0	0.0	0.0	0.0
Pygmy killer whales	0.0	0.0	0.0	0.0	0.0
Risso's dolphins	0.0	0.0	0.0	0.0	0.0
Rough-toothed dolphins	0.0	0.0	0.1	0.9	1.6
Short-finned pilot whales	0.0	0.0	0.0	0.0	0.0
Sperm whales	0.0	0.0	0.0	0.0	0.0
Spinner dolphins	0.0	0.0	0.0	0.0	0.0
Striped dolphins	0.0	0.0	0.0	0.0	0.0

Table F-17. 2016 annual exposure estimate totals for boomer.

Species	Number of Level A exposures			Number of Level B exposures	
	peak SPL	SEL	180 rms SPL	Step fxn	160 rms SPL
Atlantic spotted dolphins	0.0	0.0	0.0	0.0	0.0
Beaked whales	0.0	0.0	0.0	0.0	0.0
Common bottlenose dolphins	0.0	0.0	0.0	0.0	0.0
Bryde's whales	0.0	0.0	0.0	0.0	0.0
Clymene dolphins	0.0	0.0	0.0	0.0	0.0
False killer whales	0.0	0.0	0.0	0.0	0.0
Fraser's dolphins	0.0	0.0	0.0	0.0	0.0
Killer whales	0.0	0.0	0.0	0.0	0.0
Kogia	0.0	0.0	0.0	0.0	0.0
Melon-headed whales	0.0	0.0	0.0	0.0	0.0
Pantropical spotted dolphins	0.0	0.0	0.0	0.0	0.0
Pygmy killer whales	0.0	0.0	0.0	0.0	0.0
Risso's dolphins	0.0	0.0	0.0	0.0	0.0
Rough-toothed dolphins	0.0	0.0	0.0	0.0	0.0
Short-finned pilot whales	0.0	0.0	0.0	0.0	0.0
Sperm whales	0.0	0.0	0.0	0.0	0.0
Spinner dolphins	0.0	0.0	0.0	0.0	0.0
Striped dolphins	0.0	0.0	0.0	0.0	0.0

Table F-18. 2016 annual exposure estimate totals for side-scan sonar, sub-bottom profiler, and multibeam scanner).

Species	Number of Level A exposures			Number of Level B exposures	
	peak SPL	SEL	180 rms SPL	Step fxn	160 rms SPL
Atlantic spotted dolphins	0.0	1.0	1.1	4.3	1.4
Beaked whales	0.0	0.1	0.1	3.7	0.0
Common bottlenose dolphins	0.0	10.9	14.1	28.7	8.3
Bryde's whales	0.0	0.0	0.0	0.0	0.0
Clymene dolphins	0.0	0.0	0.0	0.0	0.0
False killer whales	0.0	0.0	0.0	0.0	0.0
Fraser's dolphins	0.0	0.0	0.0	0.0	0.0
Killer whales	0.0	0.0	0.0	0.0	0.0
Kogia	0.0	0.0	0.0	0.0	0.0
Melon-headed whales	0.0	0.0	0.0	0.0	0.0
Pantropical spotted dolphins	0.0	0.0	0.0	0.0	0.0
Pygmy killer whales	0.0	0.0	0.0	0.0	0.0
Risso's dolphins	0.0	0.0	0.0	0.0	0.0
Rough-toothed dolphins	0.0	0.0	0.0	0.2	0.1
Short-finned pilot whales	0.0	0.0	0.0	0.0	0.0
Sperm whales	0.0	0.0	0.0	0.0	0.0
Spinner dolphins	0.0	0.0	0.0	0.0	0.0
Striped dolphins	0.0	0.0	0.0	0.0	0.0

F.2.2. 2017

Table F-19. 2017 annual exposure estimate totals for 2-D survey (8000 in^3 airgun array, 1 vessel).

Species	Number of Level A exposures			Number of Level B exposures	
	peak SPL	SEL	180 rms SPL	Step fxn	160 rms SPL
Atlantic spotted dolphins	1.8	0.0	98.3	1186.5	2811.6
Beaked whales	1.1	0.0	91.9	6722.8	1501.1
Common bottlenose dolphins	5.0	0.3	150.6	2883.8	7197.1
Bryde's whales	0.0	0.2	1.2	18.1	21.6
Clymene dolphins	5.9	0.5	146.0	2482.2	4989.7
False killer whales	1.1	0.0	40.7	604.5	1113.7
Fraser's dolphins	0.7	0.0	49.3	359.5	573.1
Killer whales	0.1	0.0	5.4	37.0	54.8
Kogia	80.5	6.3	66.3	450.9	1000.6
Melon-headed whales	3.5	0.1	236.3	1841.0	3166.7
Pantropical spotted dolphins	42.4	3.6	1025.4	15336.8	25861.0
Pygmy killer whales	0.9	0.0	30.5	436.0	748.4
Risso's dolphins	2.1	0.3	44.9	630.1	1325.3
Rough-toothed dolphins	1.4	0.1	51.4	790.5	1537.5
Short-finned pilot whales	0.9	0.0	45.7	418.6	834.9
Sperm whales	0.5	0.0	99.4	724.3	1020.7
Spinner dolphins	4.3	0.3	111.3	2275.5	5480.2
Striped dolphins	2.7	0.2	65.7	1066.9	2025.8

Table F-20. 2017 annual exposure estimate totals for 3-D NAZ survey (8000 in^3 airgun array, 2 vessels).

Species	Number of Level A exposures			Number of Level B exposures	
	peak SPL	SEL	180 rms SPL	Step fxn	160 rms SPL
Atlantic spotted dolphins	352.4	30.5	49497.1	142643.3	192650.5
Beaked whales	29.3	1.2	3051.9	128007.2	32312.8
Common bottlenose dolphins	2407.7	86.1	290214.0	812697.3	1039664.0
Bryde's whales	0.2	8.6	31.3	385.7	469.7
Clymene dolphins	237.8	16.8	4766.0	58336.4	106122.3
False killer whales	69.6	6.4	1615.6	14263.3	25295.6
Fraser's dolphins	33.4	2.1	1375.0	7624.2	12619.0
Killer whales	3.1	0.4	173.7	804.0	1158.3
Kogia	1578.4	348.0	1715.3	8894.0	19970.3
Melon-headed whales	160.5	11.1	6254.8	37393.8	66375.9
Pantropical spotted dolphins	1430.8	62.3	31083.7	328109.8	516513.5
Pygmy killer whales	51.8	4.4	1107.2	9874.8	16811.3
Risso's dolphins	61.2	9.0	1365.9	14505.6	26158.1
Rough-toothed dolphins	102.6	9.7	4022.8	24583.6	41975.2
Short-finned pilot whales	40.1	4.5	1425.8	9878.3	20237.6
Sperm whales	24.6	0.7	4681.1	23741.8	53770.0
Spinner dolphins	156.0	5.8	3137.8	46544.4	91603.8
Striped dolphins	97.7	5.3	2038.9	23633.7	40670.8

Table F-21. 2017 annual exposure estimate totals for 3-D WAZ survey (8000 in^3 airgun array, 4 vessels).

Species	Number of Level A exposures			Number of Level B exposures	
	peak SPL	SEL	180 rms SPL	Step fxn	160 rms SPL
Atlantic spotted dolphins	29.0	0.7	7890.2	25800.2	40335.2
Beaked whales	3.8	0.0	2074.1	56206.0	13558.4
Common bottlenose dolphins	121.1	4.3	41316.0	123526.4	204394.8
Bryde's whales	0.0	0.8	24.3	165.0	193.0
Clymene dolphins	40.0	0.0	2643.0	26420.6	45219.4
False killer whales	10.1	0.9	776.3	5771.4	9674.7
Fraser's dolphins	4.3	0.0	1004.7	3388.2	5118.5
Killer whales	0.4	0.1	110.9	405.4	498.7
Kogia	1950.8	36.6	1321.2	4103.9	8797.9
Melon-headed whales	21.2	0.0	4738.6	16924.7	27954.6
Pantropical spotted dolphins	280.9	0.0	18918.8	164513.4	248467.6
Pygmy killer whales	7.9	0.7	580.5	4172.5	6575.4
Risso's dolphins	10.4	1.2	582.4	6809.4	11737.3
Rough-toothed dolphins	13.1	1.0	1235.3	8147.1	13989.8
Short-finned pilot whales	4.6	0.0	898.6	3696.0	7297.5
Sperm whales	8.0	0.0	3481.2	9698.1	20342.7
Spinner dolphins	30.6	0.0	1951.1	23989.5	47094.8
Striped dolphins	18.0	0.0	1197.9	11386.2	18696.2

Table F-22. 2017 annual exposure estimate totals for Coil survey (8000 in^3 airgun array, 4 vessels).

Species	Number of Level A exposures			Number of Level B exposures	
	peak SPL	SEL	180 rms SPL	Step fxn	160 rms SPL
Atlantic spotted dolphins	41.9	1.5	2142.5	6178.9	8275.4
Beaked whales	10.9	0.5	652.4	13921.0	2859.4
Common bottlenose dolphins	224.1	9.8	9814.4	27601.1	32129.4
Bryde's whales	0.1	3.0	5.8	36.3	39.9
Clymene dolphins	76.8	4.1	1240.3	6528.2	9297.4
False killer whales	19.1	0.8	447.1	1877.4	2875.7
Fraser's dolphins	8.8	0.2	290.1	868.8	1075.8
Killer whales	0.9	0.0	42.0	105.2	121.8
Kogia	381.2	102.3	385.9	1071.3	1860.5
Melon-headed whales	42.3	1.0	1377.3	4386.9	5898.9
Pantropical spotted dolphins	565.5	32.6	8800.4	40804.4	52943.6
Pygmy killer whales	14.5	0.6	337.3	1361.9	1991.7
Risso's dolphins	21.3	1.9	315.8	1649.3	2295.4
Rough-toothed dolphins	24.9	1.1	649.9	2611.4	4044.3
Short-finned pilot whales	8.4	0.2	265.0	979.6	1548.0
Sperm whales	7.4	0.6	951.6	2668.1	4478.6
Spinner dolphins	53.9	2.3	929.8	5899.2	9344.3
Striped dolphins	35.2	1.9	560.3	2817.1	3888.5

Table F-23. 2017 annual exposure estimate totals for 90 in^3 airgun.

Species	Number of Level A exposures			Number of Level B exposures	
	peak SPL	SEL	180 rms SPL	Step fxn	160 rms SPL
Atlantic spotted dolphins	0.0	0.0	1.5	11.6	24.3
Beaked whales	0.0	0.0	0.0	0.0	0.0
Common bottlenose dolphins	0.0	0.0	13.2	53.3	82.5
Bryde's whales	0.0	0.0	0.0	0.0	0.0
Clymene dolphins	0.0	0.0	0.0	0.0	0.0
False killer whales	0.0	0.0	0.0	0.1	0.1
Fraser's dolphins	0.0	0.0	0.0	0.0	0.0
Killer whales	0.0	0.0	0.0	0.0	0.0
Kogia	0.0	0.0	0.0	0.0	0.0
Melon-headed whales	0.0	0.0	0.0	0.0	0.0
Pantropical spotted dolphins	0.0	0.0	0.0	0.0	0.0
Pygmy killer whales	0.0	0.0	0.0	0.0	0.0
Risso's dolphins	0.0	0.0	0.0	0.0	0.0
Rough-toothed dolphins	0.0	0.0	0.1	0.9	1.6
Short-finned pilot whales	0.0	0.0	0.0	0.0	0.0
Sperm whales	0.0	0.0	0.0	0.0	0.0
Spinner dolphins	0.0	0.0	0.0	0.0	0.0
Striped dolphins	0.0	0.0	0.0	0.0	0.0

Table F-24. 2017 annual exposure estimate totals for boomer.

Species	Number of Level A exposures			Number of Level B exposures	
	peak SPL	SEL	180 rms SPL	Step fxn	160 rms SPL
Atlantic spotted dolphins	0.0	0.0	0.0	0.0	0.0
Beaked whales	0.0	0.0	0.0	0.0	0.0
Common bottlenose dolphins	0.0	0.0	0.0	0.0	0.0
Bryde's whales	0.0	0.0	0.0	0.0	0.0
Clymene dolphins	0.0	0.0	0.0	0.0	0.0
False killer whales	0.0	0.0	0.0	0.0	0.0
Fraser's dolphins	0.0	0.0	0.0	0.0	0.0
Killer whales	0.0	0.0	0.0	0.0	0.0
Kogia	0.0	0.0	0.0	0.0	0.0
Melon-headed whales	0.0	0.0	0.0	0.0	0.0
Pantropical spotted dolphins	0.0	0.0	0.0	0.0	0.0
Pygmy killer whales	0.0	0.0	0.0	0.0	0.0
Risso's dolphins	0.0	0.0	0.0	0.0	0.0
Rough-toothed dolphins	0.0	0.0	0.0	0.0	0.0
Short-finned pilot whales	0.0	0.0	0.0	0.0	0.0
Sperm whales	0.0	0.0	0.0	0.0	0.0
Spinner dolphins	0.0	0.0	0.0	0.0	0.0
Striped dolphins	0.0	0.0	0.0	0.0	0.0

Table F-25. 2017 annual exposure estimate totals for side-scan sonar, sub-bottom profiler, and multibeam scanner).

Species	Number of Level A exposures			Number of Level B exposures	
	peak SPL	SEL	180 rms SPL	Step fxn	160 rms SPL
Atlantic spotted dolphins	0.0	1.0	1.1	4.2	1.4
Beaked whales	0.0	0.1	0.1	3.9	0.0
Common bottlenose dolphins	0.0	10.8	14.0	28.3	8.1
Bryde's whales	0.0	0.0	0.0	0.0	0.0
Clymene dolphins	0.0	0.0	0.0	0.0	0.0
False killer whales	0.0	0.0	0.0	0.0	0.0
Fraser's dolphins	0.0	0.0	0.0	0.0	0.0
Killer whales	0.0	0.0	0.0	0.0	0.0
Kogia	0.0	0.0	0.0	0.0	0.0
Melon-headed whales	0.0	0.0	0.0	0.0	0.0
Pantropical spotted dolphins	0.0	0.0	0.0	0.0	0.0
Pygmy killer whales	0.0	0.0	0.0	0.0	0.0
Risso's dolphins	0.0	0.0	0.0	0.0	0.0
Rough-toothed dolphins	0.0	0.0	0.0	0.2	0.1
Short-finned pilot whales	0.0	0.0	0.0	0.0	0.0
Sperm whales	0.0	0.0	0.0	0.0	0.0
Spinner dolphins	0.0	0.0	0.0	0.0	0.0
Striped dolphins	0.0	0.0	0.0	0.0	0.0

F.2.3. 2018

Table F-26. 2018 annual exposure estimate totals for 2-D survey (8000 in^3 airgun array, 1 vessel).

Species	Number of Level A exposures			Number of Level B exposures	
	peak SPL	SEL	180 rms SPL	Step fxn	160 rms SPL
Atlantic spotted dolphins	0.0	0.0	0.0	0.0	0.0
Beaked whales	0.0	0.0	0.0	0.0	0.0
Common bottlenose dolphins	0.0	0.0	0.0	0.0	0.0
Bryde's whales	0.0	0.0	0.0	0.0	0.0
Clymene dolphins	0.0	0.0	0.0	0.0	0.0
False killer whales	0.0	0.0	0.0	0.0	0.0
Fraser's dolphins	0.0	0.0	0.0	0.0	0.0
Killer whales	0.0	0.0	0.0	0.0	0.0
Kogia	0.0	0.0	0.0	0.0	0.0
Melon-headed whales	0.0	0.0	0.0	0.0	0.0
Pantropical spotted dolphins	0.0	0.0	0.0	0.0	0.0
Pygmy killer whales	0.0	0.0	0.0	0.0	0.0
Risso's dolphins	0.0	0.0	0.0	0.0	0.0
Rough-toothed dolphins	0.0	0.0	0.0	0.0	0.0
Short-finned pilot whales	0.0	0.0	0.0	0.0	0.0
Sperm whales	0.0	0.0	0.0	0.0	0.0
Spinner dolphins	0.0	0.0	0.0	0.0	0.0
Striped dolphins	0.0	0.0	0.0	0.0	0.0

Table F-27. 2018 annual exposure estimate totals for 3-D NAZ survey (8000 in^3 airgun array, 2 vessels).

Species	Number of Level A exposures			Number of Level B exposures	
	peak SPL	SEL	180 rms SPL	Step fxn	160 rms SPL
Atlantic spotted dolphins	258.5	23.0	33885.6	103132.0	145888.8
Beaked whales	30.0	2.1	2952.3	127359.3	32024.0
Common bottlenose dolphins	1686.8	73.7	194968.1	561859.9	735584.6
Bryde's whales	0.2	9.2	33.6	406.2	486.1
Clymene dolphins	255.3	25.7	4840.8	59851.4	113381.4
False killer whales	68.6	8.4	1546.5	14014.8	25695.4
Fraser's dolphins	32.9	2.7	1318.0	7489.7	12714.7
Killer whales	2.9	0.3	162.2	763.3	1129.6
Kogia	1530.4	337.9	1635.0	8564.4	19336.5
Melon-headed whales	158.7	13.9	6085.2	36890.6	66561.4
Pantropical spotted dolphins	1383.6	80.5	29282.7	311665.6	503795.1
Pygmy killer whales	50.8	5.7	1080.8	9734.3	17127.6
Risso's dolphins	60.9	9.7	1348.2	14350.8	26624.2
Rough-toothed dolphins	96.7	12.0	3279.7	22320.9	39942.9
Short-finned pilot whales	45.9	6.7	1594.6	11153.1	23069.5
Sperm whales	24.1	1.3	4860.1	24193.1	54213.7
Spinner dolphins	140.0	5.7	2803.7	41449.0	81672.3
Striped dolphins	98.4	7.5	1974.7	23087.2	41008.4

Table F-28. 2018 annual exposure estimate totals for 3-D WAZ survey (8000 in^3 airgun array, 4 vessels).

Species	Number of Level A exposures			Number of Level B exposures	
	peak SPL	SEL	180 rms SPL	Step fxn	160 rms SPL
Atlantic spotted dolphins	13.1	1.1	1666.3	11199.8	22710.5
Beaked whales	4.0	0.1	2001.4	54098.3	12955.0
Common bottlenose dolphins	29.5	0.9	1952.6	28973.5	58068.6
Bryde's whales	0.0	0.9	26.8	173.5	197.1
Clymene dolphins	44.8	3.2	2668.0	26639.5	48248.8
False killer whales	9.5	0.8	721.9	5551.2	9719.5
Fraser's dolphins	4.2	0.1	953.1	3239.8	5082.9
Killer whales	0.4	0.1	99.8	370.0	473.7
Kogia	1824.1	34.0	1229.8	3812.2	8230.3
Melon-headed whales	20.7	0.6	4541.3	16213.6	27431.9
Pantropical spotted dolphins	265.0	7.5	17149.5	149772.4	233427.8
Pygmy killer whales	7.3	0.7	547.3	4003.2	6603.0
Risso's dolphins	10.4	1.5	562.0	6575.9	11790.6
Rough-toothed dolphins	11.6	0.9	899.9	7216.7	13211.7
Short-finned pilot whales	5.7	0.4	1099.4	4370.4	8747.7
Sperm whales	7.1	0.2	3487.8	9656.9	19792.6
Spinner dolphins	26.2	0.2	1658.9	20294.1	39876.9
Striped dolphins	18.1	0.8	1128.1	10740.9	18352.6

Table F-29. 2018 annual exposure estimate totals for Coil survey (8000 in^3 airgun array, 4 vessels).

Species	Number of Level A exposures			Number of Level B exposures	
	peak SPL	SEL	180 rms SPL	Step fxn	160 rms SPL
Atlantic spotted dolphins	18.6	0.4	717.5	2947.3	4825.6
Beaked whales	10.4	0.4	631.7	13560.3	2735.9
Common bottlenose dolphins	68.6	5.4	1131.1	7210.2	10938.4
Bryde's whales	0.1	3.2	6.5	38.7	40.2
Clymene dolphins	76.3	3.8	1277.4	6802.5	9775.5
False killer whales	18.1	0.7	419.2	1823.6	2806.2
Fraser's dolphins	8.2	0.2	277.9	845.5	1050.0
Killer whales	0.8	0.0	37.8	96.6	112.5
Kogia	356.1	96.1	361.3	1002.8	1718.7
Melon-headed whales	39.8	1.0	1330.5	4285.6	5690.4
Pantropical spotted dolphins	509.3	28.7	8038.6	37652.8	49289.5
Pygmy killer whales	13.7	0.5	317.2	1311.5	1938.3
Risso's dolphins	20.4	1.7	316.8	1631.9	2275.7
Rough-toothed dolphins	22.7	1.0	523.5	2368.3	3772.0
Short-finned pilot whales	9.7	0.3	330.1	1195.1	1788.4
Sperm whales	7.0	0.6	982.1	2726.3	4411.0
Spinner dolphins	45.8	2.0	791.6	5003.2	7910.6
Striped dolphins	32.8	1.7	534.2	2713.7	3776.2

Table F-30. 2018 annual exposure estimate totals for 90 in^3 airgun.

Species	Number of Level A exposures			Number of Level B exposures	
	peak SPL	SEL	180 rms SPL	Step fxn	160 rms SPL
Atlantic spotted dolphins	0.0	0.0	1.6	12.4	26.0
Beaked whales	0.0	0.0	0.0	0.0	0.0
Common bottlenose dolphins	0.0	0.0	14.1	57.1	88.4
Bryde's whales	0.0	0.0	0.0	0.0	0.0
Clymene dolphins	0.0	0.0	0.0	0.0	0.0
False killer whales	0.0	0.0	0.0	0.1	0.1
Fraser's dolphins	0.0	0.0	0.0	0.0	0.0
Killer whales	0.0	0.0	0.0	0.0	0.0
Kogia	0.0	0.0	0.0	0.0	0.0
Melon-headed whales	0.0	0.0	0.0	0.0	0.0
Pantropical spotted dolphins	0.0	0.0	0.0	0.0	0.0
Pygmy killer whales	0.0	0.0	0.0	0.0	0.0
Risso's dolphins	0.0	0.0	0.0	0.0	0.0
Rough-toothed dolphins	0.0	0.0	0.1	1.0	1.7
Short-finned pilot whales	0.0	0.0	0.0	0.0	0.0
Sperm whales	0.0	0.0	0.0	0.0	0.0
Spinner dolphins	0.0	0.0	0.0	0.0	0.0
Striped dolphins	0.0	0.0	0.0	0.0	0.0

Table F-31. 2018 annual exposure estimate totals for boomer.

Species	Number of Level A exposures			Number of Level B exposures	
	peak SPL	SEL	180 rms SPL	Step fxn	160 rms SPL
Atlantic spotted dolphins	0.0	0.0	0.0	0.0	0.0
Beaked whales	0.0	0.0	0.0	0.0	0.0
Common bottlenose dolphins	0.0	0.0	0.0	0.0	0.0
Bryde's whales	0.0	0.0	0.0	0.0	0.0
Clymene dolphins	0.0	0.0	0.0	0.0	0.0
False killer whales	0.0	0.0	0.0	0.0	0.0
Fraser's dolphins	0.0	0.0	0.0	0.0	0.0
Killer whales	0.0	0.0	0.0	0.0	0.0
Kogia	0.0	0.0	0.0	0.0	0.0
Melon-headed whales	0.0	0.0	0.0	0.0	0.0
Pantropical spotted dolphins	0.0	0.0	0.0	0.0	0.0
Pygmy killer whales	0.0	0.0	0.0	0.0	0.0
Risso's dolphins	0.0	0.0	0.0	0.0	0.0
Rough-toothed dolphins	0.0	0.0	0.0	0.0	0.0
Short-finned pilot whales	0.0	0.0	0.0	0.0	0.0
Sperm whales	0.0	0.0	0.0	0.0	0.0
Spinner dolphins	0.0	0.0	0.0	0.0	0.0
Striped dolphins	0.0	0.0	0.0	0.0	0.0

Table F-32. 2018 annual exposure estimate totals for side-scan sonar, sub-bottom profiler, and multibeam scanner).

Species	Number of Level A exposures			Number of Level B exposures	
	peak SPL	SEL	180 rms SPL	Step fxn	160 rms SPL
Atlantic spotted dolphins	0.0	0.9	1.0	3.9	1.3
Beaked whales	0.0	0.1	0.1	4.1	0.0
Common bottlenose dolphins	0.0	10.4	13.4	27.1	7.7
Bryde's whales	0.0	0.0	0.0	0.0	0.0
Clymene dolphins	0.0	0.0	0.0	0.0	0.0
False killer whales	0.0	0.0	0.0	0.0	0.0
Fraser's dolphins	0.0	0.0	0.0	0.0	0.0
Killer whales	0.0	0.0	0.0	0.0	0.0
Kogia	0.0	0.0	0.0	0.0	0.0
Melon-headed whales	0.0	0.0	0.0	0.0	0.0
Pantropical spotted dolphins	0.0	0.0	0.0	0.0	0.0
Pygmy killer whales	0.0	0.0	0.0	0.0	0.0
Risso's dolphins	0.0	0.0	0.0	0.0	0.0
Rough-toothed dolphins	0.0	0.0	0.0	0.2	0.1
Short-finned pilot whales	0.0	0.0	0.0	0.0	0.0
Sperm whales	0.0	0.0	0.0	0.0	0.0
Spinner dolphins	0.0	0.0	0.0	0.0	0.0
Striped dolphins	0.0	0.0	0.0	0.0	0.0

F.2.4. 2019

Table F-33. 2019 annual exposure estimate totals for 2-D survey (8000 in^3 airgun array, 1 vessel).

Species	Number of Level A exposures			Number of Level B exposures	
	peak SPL	SEL	180 rms SPL	Step fxn	160 rms SPL
Atlantic spotted dolphins	5.3	0.1	278.9	3706.9	8628.9
Beaked whales	3.0	0.1	277.0	21037.3	4783.3
Common bottlenose dolphins	13.7	0.9	499.5	9273.0	21363.9
Bryde's whales	0.0	0.5	3.6	56.8	68.5
Clymene dolphins	18.0	1.4	445.8	7927.3	15117.6
False killer whales	3.7	0.1	121.5	1890.8	3394.4
Fraser's dolphins	1.9	0.0	147.7	1105.7	1811.4
Killer whales	0.2	0.0	17.0	117.7	171.2
Kogia	237.9	18.8	193.5	1381.8	3161.1
Melon-headed whales	9.7	0.2	698.5	5637.5	10006.1
Pantropical spotted dolphins	131.2	11.1	3174.7	48891.3	78810.7
Pygmy killer whales	2.9	0.1	92.1	1366.3	2286.9
Risso's dolphins	5.3	0.6	132.4	2025.6	4020.0
Rough-toothed dolphins	4.6	0.2	152.4	2468.8	4677.2
Short-finned pilot whales	2.3	0.1	130.2	1269.2	2637.2
Sperm whales	1.7	0.1	362.3	2644.3	4916.0
Spinner dolphins	12.8	0.9	332.1	7283.4	16520.5
Striped dolphins	8.2	0.7	201.7	3405.1	6148.7

Table F-34. 2019 annual exposure estimate totals for 3-D NAZ survey (8000 in^3 airgun array, 2 vessels).

Species	Number of Level A exposures			Number of Level B exposures	
	peak SPL	SEL	180 rms SPL	Step fxn	160 rms SPL
Atlantic spotted dolphins	360.2	37.5	51987.7	145156.3	192048.7
Beaked whales	26.0	1.2	2364.2	100180.1	25095.0
Common bottlenose dolphins	2513.7	139.3	302326.3	832539.5	1058082.9
Bryde's whales	0.2	7.2	26.1	307.3	369.5
Clymene dolphins	194.7	15.6	3812.4	45827.6	85313.6
False killer whales	55.5	5.4	1317.1	11237.1	20096.9
Fraser's dolphins	26.1	1.7	1093.4	6036.2	9991.7
Killer whales	2.4	0.3	134.2	617.0	898.6
Kogia	1253.7	277.0	1345.5	6982.0	15495.4
Melon-headed whales	124.2	8.7	4916.8	29368.5	52043.7
Pantropical spotted dolphins	1126.0	54.5	24137.8	251515.9	402878.2
Pygmy killer whales	40.8	3.7	871.8	7677.1	13240.5
Risso's dolphins	50.8	7.1	1082.0	11204.0	20701.3
Rough-toothed dolphins	86.5	8.7	3806.3	21030.5	35439.8
Short-finned pilot whales	32.6	3.9	1178.1	8121.9	16564.8
Sperm whales	18.9	0.8	3487.9	17766.7	38593.6
Spinner dolphins	123.5	4.9	2455.8	34951.0	69804.6
Striped dolphins	78.3	4.8	1603.9	18273.9	32084.1

Table F-35. 2019 annual exposure estimate totals for 3-D WAZ survey (8000 in^3 airgun array, 4 vessels).

Species	Number of Level A exposures			Number of Level B exposures	
	peak SPL	SEL	180 rms SPL	Step fxn	160 rms SPL
Atlantic spotted dolphins	23.0	0.4	7216.1	20946.0	30581.8
Beaked whales	2.3	0.0	1232.9	32845.5	7811.7
Common bottlenose dolphins	108.7	4.3	40554.0	110805.1	179899.5
Bryde's whales	0.0	0.5	14.9	96.3	110.9
Clymene dolphins	23.8	0.1	1586.7	15424.4	26555.0
False killer whales	6.0	0.5	471.0	3409.5	5700.4
Fraser's dolphins	2.5	0.0	595.4	2005.5	2987.9
Killer whales	0.2	0.0	65.1	235.6	290.0
Kogia	1169.6	22.0	783.2	2434.9	5115.3
Melon-headed whales	12.3	0.0	2799.5	9992.7	16250.3
Pantropical spotted dolphins	165.5	0.4	11220.9	95897.8	145622.4
Pygmy killer whales	4.7	0.4	344.0	2445.2	3852.8
Risso's dolphins	6.3	0.7	354.0	3957.5	6893.5
Rough-toothed dolphins	8.2	0.6	860.3	5093.7	8580.2
Short-finned pilot whales	2.6	0.0	535.7	2194.0	4242.7
Sperm whales	4.5	0.0	1899.3	5432.1	10919.1
Spinner dolphins	18.4	0.1	1196.3	14031.9	27709.5
Striped dolphins	10.7	0.0	715.8	6643.8	10972.3

Table F-36. 2019 annual exposure estimate totals for Coil survey (8000 in^3 airgun array, 4 vessels).

Species	Number of Level A exposures			Number of Level B exposures	
	peak SPL	SEL	180 rms SPL	Step fxn	160 rms SPL
Atlantic spotted dolphins	34.5	1.5	1848.0	4872.8	6049.0
Beaked whales	6.7	0.3	385.2	8066.9	1642.0
Common bottlenose dolphins	197.3	7.2	9384.0	24373.8	27267.1
Bryde's whales	0.0	1.9	3.6	20.9	22.6
Clymene dolphins	46.3	2.6	742.1	3733.5	5321.4
False killer whales	11.3	0.4	265.4	1093.6	1662.0
Fraser's dolphins	5.2	0.1	173.6	506.9	614.2
Killer whales	0.5	0.0	24.6	60.8	69.8
Kogia	228.1	62.9	232.2	628.9	1056.0
Melon-headed whales	25.0	0.6	824.1	2548.9	3351.0
Pantropical spotted dolphins	336.2	19.9	5209.2	23432.5	30390.4
Pygmy killer whales	8.6	0.3	197.5	789.1	1147.8
Risso's dolphins	12.7	1.1	192.6	936.4	1308.4
Rough-toothed dolphins	15.3	0.7	425.4	1597.6	2410.7
Short-finned pilot whales	5.0	0.1	161.0	569.3	877.4
Sperm whales	3.8	0.3	499.4	1427.4	2277.9
Spinner dolphins	33.4	1.6	566.6	3356.2	5332.2
Striped dolphins	21.1	1.2	333.9	1613.4	2227.7

Table F-37. 2019 annual exposure estimate totals for 90 in^3 airgun.

Species	Number of Level A exposures			Number of Level B exposures	
	peak SPL	SEL	180 rms SPL	Step fxn	160 rms SPL
Atlantic spotted dolphins	0.0	0.0	1.7	13.4	28.2
Beaked whales	0.0	0.0	0.0	0.0	0.0
Common bottlenose dolphins	0.0	0.0	15.3	61.7	95.7
Bryde's whales	0.0	0.0	0.0	0.0	0.0
Clymene dolphins	0.0	0.0	0.0	0.0	0.0
False killer whales	0.0	0.0	0.0	0.1	0.1
Fraser's dolphins	0.0	0.0	0.0	0.0	0.0
Killer whales	0.0	0.0	0.0	0.0	0.0
Kogia	0.0	0.0	0.0	0.0	0.0
Melon-headed whales	0.0	0.0	0.0	0.0	0.0
Pantropical spotted dolphins	0.0	0.0	0.0	0.0	0.0
Pygmy killer whales	0.0	0.0	0.0	0.0	0.0
Risso's dolphins	0.0	0.0	0.0	0.0	0.0
Rough-toothed dolphins	0.0	0.0	0.1	1.0	1.8
Short-finned pilot whales	0.0	0.0	0.0	0.0	0.0
Sperm whales	0.0	0.0	0.0	0.0	0.0
Spinner dolphins	0.0	0.0	0.0	0.0	0.0
Striped dolphins	0.0	0.0	0.0	0.0	0.0

Table F-38. 2019 annual exposure estimate totals for boomer.

Species	Number of Level A exposures			Number of Level B exposures	
	peak SPL	SEL	180 rms SPL	Step fxn	160 rms SPL
Atlantic spotted dolphins	0.0	0.0	0.9	6.7	14.1
Beaked whales	0.0	0.0	0.0	0.0	0.0
Common bottlenose dolphins	0.0	0.0	7.7	31.0	48.1
Bryde's whales	0.0	0.0	0.0	0.0	0.0
Clymene dolphins	0.0	0.0	0.0	0.0	0.0
False killer whales	0.0	0.0	0.0	0.0	0.1
Fraser's dolphins	0.0	0.0	0.0	0.0	0.0
Killer whales	0.0	0.0	0.0	0.0	0.0
Kogia	0.0	0.0	0.0	0.0	0.0
Melon-headed whales	0.0	0.0	0.0	0.0	0.0
Pantropical spotted dolphins	0.0	0.0	0.0	0.0	0.0
Pygmy killer whales	0.0	0.0	0.0	0.0	0.0
Risso's dolphins	0.0	0.0	0.0	0.0	0.0
Rough-toothed dolphins	0.0	0.0	0.0	0.5	0.9
Short-finned pilot whales	0.0	0.0	0.0	0.0	0.0
Sperm whales	0.0	0.0	0.0	0.0	0.0
Spinner dolphins	0.0	0.0	0.0	0.0	0.0
Striped dolphins	0.0	0.0	0.0	0.0	0.0

Table F-39. 2019 annual exposure estimate totals for side-scan sonar, sub-bottom profiler, and multibeam scanner).

Species	Number of Level A exposures			Number of Level B exposures	
	peak SPL	SEL	180 rms SPL	Step fxn	160 rms SPL
Atlantic spotted dolphins	0.0	0.8	0.9	3.3	1.1
Beaked whales	0.0	0.1	0.1	4.1	0.0
Common bottlenose dolphins	0.0	9.3	12.0	24.1	6.8
Bryde's whales	0.0	0.0	0.0	0.0	0.0
Clymene dolphins	0.0	0.0	0.0	0.0	0.0
False killer whales	0.0	0.0	0.0	0.0	0.0
Fraser's dolphins	0.0	0.0	0.0	0.0	0.0
Killer whales	0.0	0.0	0.0	0.0	0.0
Kogia	0.0	0.0	0.0	0.0	0.0
Melon-headed whales	0.0	0.0	0.0	0.0	0.0
Pantropical spotted dolphins	0.0	0.0	0.0	0.0	0.0
Pygmy killer whales	0.0	0.0	0.0	0.0	0.0
Risso's dolphins	0.0	0.0	0.0	0.0	0.0
Rough-toothed dolphins	0.0	0.0	0.0	0.2	0.1
Short-finned pilot whales	0.0	0.0	0.0	0.0	0.0
Sperm whales	0.0	0.0	0.0	0.0	0.0
Spinner dolphins	0.0	0.0	0.0	0.0	0.0
Striped dolphins	0.0	0.0	0.0	0.0	0.0

F.2.5. 2020

Table F-40. 2020 annual exposure estimate totals for 2-D survey (8000 in^3 airgun array, 1 vessel).

Species	Number of Level A exposures			Number of Level B exposures	
	peak SPL	SEL	180 rms SPL	Step fxn	160 rms SPL
Atlantic spotted dolphins	0.0	0.0	0.0	0.0	0.0
Beaked whales	0.0	0.0	0.0	0.0	0.0
Common bottlenose dolphins	0.0	0.0	0.0	0.0	0.0
Bryde's whales	0.0	0.0	0.0	0.0	0.0
Clymene dolphins	0.0	0.0	0.0	0.0	0.0
False killer whales	0.0	0.0	0.0	0.0	0.0
Fraser's dolphins	0.0	0.0	0.0	0.0	0.0
Killer whales	0.0	0.0	0.0	0.0	0.0
Kogia	0.0	0.0	0.0	0.0	0.0
Melon-headed whales	0.0	0.0	0.0	0.0	0.0
Pantropical spotted dolphins	0.0	0.0	0.0	0.0	0.0
Pygmy killer whales	0.0	0.0	0.0	0.0	0.0
Risso's dolphins	0.0	0.0	0.0	0.0	0.0
Rough-toothed dolphins	0.0	0.0	0.0	0.0	0.0
Short-finned pilot whales	0.0	0.0	0.0	0.0	0.0
Sperm whales	0.0	0.0	0.0	0.0	0.0
Spinner dolphins	0.0	0.0	0.0	0.0	0.0
Striped dolphins	0.0	0.0	0.0	0.0	0.0

Table F-41. 2020 annual exposure estimate totals for 3-D NAZ survey (8000 in^3 airgun array, 2 vessels).

Species	Number of Level A exposures			Number of Level B exposures	
	peak SPL	SEL	180 rms SPL	Step fxn	160 rms SPL
Atlantic spotted dolphins	257.3	21.5	33820.5	101931.8	143334.9
Beaked whales	32.0	1.2	2864.4	120588.4	30188.2
Common bottlenose dolphins	1689.3	64.7	195029.7	558752.9	730436.3
Bryde's whales	0.2	8.6	31.1	364.5	439.5
Clymene dolphins	231.2	16.8	4583.2	54661.0	100979.0
False killer whales	66.4	5.9	1506.3	13247.4	23695.8
Fraser's dolphins	31.0	1.9	1288.4	7165.0	11819.3
Killer whales	3.0	0.3	163.4	748.1	1083.6
Kogia	1526.0	336.4	1639.5	8489.6	18763.7
Melon-headed whales	149.4	9.6	5966.5	35476.4	62512.8
Pantropical spotted dolphins	1369.3	61.7	29494.0	305690.7	487609.9
Pygmy killer whales	49.4	4.1	1057.1	9252.6	15838.7
Risso's dolphins	62.0	8.3	1305.4	13456.6	24789.6
Rough-toothed dolphins	93.7	8.7	3226.7	21288.3	37285.2
Short-finned pilot whales	37.8	4.1	1382.8	9487.1	19257.1
Sperm whales	22.8	0.9	4084.4	20970.2	45203.6
Spinner dolphins	153.7	6.0	3053.5	43120.3	86362.0
Striped dolphins	94.4	5.3	1949.4	22061.1	38529.1

Table F-42. 2020 annual exposure estimate totals for 3-D WAZ survey (8000 in^3 airgun array, 4 vessels).

Species	Number of Level A exposures			Number of Level B exposures	
	peak SPL	SEL	180 rms SPL	Step fxn	160 rms SPL
Atlantic spotted dolphins	13.8	0.7	1695.3	11719.6	23546.6
Beaked whales	3.8	0.0	2074.1	56206.0	13558.4
Common bottlenose dolphins	31.1	0.0	1989.5	30571.2	59895.0
Bryde's whales	0.0	0.8	24.3	165.0	193.0
Clymene dolphins	40.0	0.0	2643.0	26420.6	45219.4
False killer whales	10.0	0.8	754.2	5717.3	9609.3
Fraser's dolphins	4.2	0.0	995.6	3364.5	5088.1
Killer whales	0.4	0.1	110.8	405.1	498.3
Kogia	1950.4	36.6	1320.6	4102.6	8796.0
Melon-headed whales	21.2	0.0	4738.5	16924.4	27954.2
Pantropical spotted dolphins	280.9	0.0	18917.1	164509.3	248462.5
Pygmy killer whales	7.9	0.7	580.5	4172.4	6575.2
Risso's dolphins	10.4	1.2	581.6	6807.6	11735.1
Rough-toothed dolphins	12.1	0.9	932.4	7404.4	13091.1
Short-finned pilot whales	4.6	0.0	898.5	3695.9	7297.5
Sperm whales	8.0	0.0	3481.2	9698.1	20342.7
Spinner dolphins	30.6	0.0	1951.1	23989.5	47094.8
Striped dolphins	18.0	0.0	1197.9	11386.1	18696.1

Table F-43. 2020 annual exposure estimate totals for Coil survey (8000 in^3 airgun array, 4 vessels).

Species	Number of Level A exposures			Number of Level B exposures	
	peak SPL	SEL	180 rms SPL	Step fxn	160 rms SPL
Atlantic spotted dolphins	19.4	0.3	737.0	3041.0	5110.1
Beaked whales	10.9	0.5	652.4	13921.0	2859.3
Common bottlenose dolphins	68.0	6.1	1145.4	7466.0	11361.6
Bryde's whales	0.1	3.0	5.8	36.3	39.9
Clymene dolphins	76.8	4.1	1240.3	6528.2	9297.4
False killer whales	19.0	0.8	439.4	1862.6	2861.4
Fraser's dolphins	8.7	0.2	287.8	863.6	1070.5
Killer whales	0.9	0.0	41.9	105.2	121.7
Kogia	381.1	102.2	385.8	1071.0	1860.2
Melon-headed whales	42.3	1.0	1377.3	4386.9	5898.9
Pantropical spotted dolphins	565.5	32.6	8800.1	40803.5	52942.7
Pygmy killer whales	14.5	0.6	337.3	1361.9	1991.7
Risso's dolphins	21.3	1.9	315.6	1648.9	2295.0
Rough-toothed dolphins	23.7	1.0	544.5	2408.3	3848.4
Short-finned pilot whales	8.4	0.2	265.0	979.6	1548.0
Sperm whales	7.4	0.6	951.6	2668.1	4478.6
Spinner dolphins	53.9	2.3	929.8	5899.2	9344.3
Striped dolphins	35.2	1.9	560.3	2817.1	3888.4

Table F-44. 2020 annual exposure estimate totals for 90 in^3 airgun.

Species	Number of Level A exposures			Number of Level B exposures	
	peak SPL	SEL	180 rms SPL	Step fxn	160 rms SPL
Atlantic spotted dolphins	0.0	0.0	0.7	1.2	1.3
Beaked whales	0.0	0.0	0.0	34.8	1.8
Common bottlenose dolphins	0.0	0.0	2.0	3.5	4.4
Bryde's whales	0.0	0.0	0.0	0.0	0.0
Clymene dolphins	0.0	0.0	1.0	2.9	3.4
False killer whales	0.0	0.0	0.2	0.7	0.9
Fraser's dolphins	0.0	0.0	0.2	0.4	0.6
Killer whales	0.0	0.0	0.0	0.1	0.1
Kogia	0.1	0.0	0.3	0.5	0.9
Melon-headed whales	0.0	0.0	1.1	2.0	3.1
Pantropical spotted dolphins	0.0	0.0	6.1	20.0	25.3
Pygmy killer whales	0.0	0.0	0.1	0.5	0.7
Risso's dolphins	0.0	0.0	0.2	0.7	1.1
Rough-toothed dolphins	0.0	0.0	0.2	0.8	1.2
Short-finned pilot whales	0.0	0.0	0.6	0.4	0.7
Sperm whales	0.0	0.0	0.4	2.1	4.6
Spinner dolphins	0.0	0.0	1.0	2.3	2.3
Striped dolphins	0.0	0.0	0.4	1.3	1.6

Table F-45. 2020 annual exposure estimate totals for boomer.

Species	Number of Level A exposures			Number of Level B exposures	
	peak SPL	SEL	180 rms SPL	Step fxn	160 rms SPL
Atlantic spotted dolphins	0.0	0.0	0.5	0.8	0.9
Beaked whales	0.0	0.0	0.0	23.2	1.2
Common bottlenose dolphins	0.0	0.0	1.3	2.3	2.9
Bryde's whales	0.0	0.0	0.0	0.0	0.0
Clymene dolphins	0.0	0.0	0.7	1.9	2.3
False killer whales	0.0	0.0	0.1	0.4	0.6
Fraser's dolphins	0.0	0.0	0.2	0.3	0.4
Killer whales	0.0	0.0	0.0	0.0	0.1
Kogia	0.1	0.0	0.2	0.4	0.6
Melon-headed whales	0.0	0.0	0.7	1.3	2.0
Pantropical spotted dolphins	0.0	0.0	4.1	13.3	16.8
Pygmy killer whales	0.0	0.0	0.1	0.3	0.5
Risso's dolphins	0.0	0.0	0.1	0.5	0.8
Rough-toothed dolphins	0.0	0.0	0.2	0.6	0.8
Short-finned pilot whales	0.0	0.0	0.1	0.3	0.4
Sperm whales	0.0	0.0	0.3	1.4	3.1
Spinner dolphins	0.0	0.0	0.6	1.5	1.5
Striped dolphins	0.0	0.0	0.3	0.9	1.0

Table F-46. 2020 annual exposure estimate totals for side-scan sonar, sub-bottom profiler, and multibeam scanner).

Species	Number of Level A exposures			Number of Level B exposures	
	peak SPL	SEL	180 rms SPL	Step fxn	160 rms SPL
Atlantic spotted dolphins	0.0	0.9	1.0	3.8	1.3
Beaked whales	0.0	0.1	0.1	3.9	0.0
Common bottlenose dolphins	0.0	11.0	14.2	28.2	7.8
Bryde's whales	0.0	0.0	0.0	0.0	0.0
Clymene dolphins	0.0	0.0	0.0	0.0	0.0
False killer whales	0.0	0.0	0.0	0.0	0.0
Fraser's dolphins	0.0	0.0	0.0	0.0	0.0
Killer whales	0.0	0.0	0.0	0.0	0.0
Kogia	0.0	0.0	0.0	0.0	0.0
Melon-headed whales	0.0	0.0	0.0	0.0	0.0
Pantropical spotted dolphins	0.0	0.0	0.0	0.0	0.0
Pygmy killer whales	0.0	0.0	0.0	0.0	0.0
Risso's dolphins	0.0	0.0	0.0	0.0	0.0
Rough-toothed dolphins	0.0	0.0	0.0	0.2	0.1
Short-finned pilot whales	0.0	0.0	0.0	0.0	0.0
Sperm whales	0.0	0.0	0.0	0.0	0.0
Spinner dolphins	0.0	0.0	0.0	0.0	0.0
Striped dolphins	0.0	0.0	0.0	0.0	0.0

F.2.6. 2021

Table F-47. 2021 annual exposure estimate totals for 2-D survey (8000 in^3 airgun array, 1 vessel).

Species	Number of Level A exposures			Number of Level B exposures	
	peak SPL	SEL	180 rms SPL	Step fxn	160 rms SPL
Atlantic spotted dolphins	0.0	0.0	0.0	0.0	0.0
Beaked whales	0.0	0.0	0.0	0.0	0.0
Common bottlenose dolphins	0.0	0.0	0.0	0.0	0.0
Bryde's whales	0.0	0.0	0.0	0.0	0.0
Clymene dolphins	0.0	0.0	0.0	0.0	0.0
False killer whales	0.0	0.0	0.0	0.0	0.0
Fraser's dolphins	0.0	0.0	0.0	0.0	0.0
Killer whales	0.0	0.0	0.0	0.0	0.0
Kogia	0.0	0.0	0.0	0.0	0.0
Melon-headed whales	0.0	0.0	0.0	0.0	0.0
Pantropical spotted dolphins	0.0	0.0	0.0	0.0	0.0
Pygmy killer whales	0.0	0.0	0.0	0.0	0.0
Risso's dolphins	0.0	0.0	0.0	0.0	0.0
Rough-toothed dolphins	0.0	0.0	0.0	0.0	0.0
Short-finned pilot whales	0.0	0.0	0.0	0.0	0.0
Sperm whales	0.0	0.0	0.0	0.0	0.0
Spinner dolphins	0.0	0.0	0.0	0.0	0.0
Striped dolphins	0.0	0.0	0.0	0.0	0.0

Table F-48. 2021 annual exposure estimate totals for 3-D NAZ survey (8000 in^3 airgun array, 2 vessels).

Species	Number of Level A exposures			Number of Level B exposures	
	peak SPL	SEL	180 rms SPL	Step fxn	160 rms SPL
Atlantic spotted dolphins	347.6	31.8	49489.2	140536.8	188872.3
Beaked whales	32.7	2.1	2764.9	119940.7	29899.4
Common bottlenose dolphins	2418.9	92.0	290228.9	806443.3	1031848.6
Bryde's whales	0.2	9.2	33.4	385.0	455.9
Clymene dolphins	248.7	25.7	4658.0	56176.1	108238.1
False killer whales	66.3	8.0	1537.5	13316.3	24469.9
Fraser's dolphins	30.9	2.4	1274.5	7165.3	12086.8
Killer whales	2.8	0.3	152.7	709.2	1057.1
Kogia	1478.7	327.3	1561.8	8167.6	18140.7
Melon-headed whales	147.6	12.4	5797.4	34974.8	62700.4
Pantropical spotted dolphins	1322.3	79.8	27700.2	289268.8	474920.2
Pygmy killer whales	48.4	5.4	1030.9	9113.0	16156.0
Risso's dolphins	61.7	9.0	1291.4	13311.6	25268.3
Rough-toothed dolphins	99.4	12.0	3943.0	23384.3	40799.8
Short-finned pilot whales	43.6	6.3	1551.5	10762.0	22089.1
Sperm whales	22.3	1.5	4263.5	21421.5	45647.3
Spinner dolphins	137.8	5.9	2719.4	38024.9	76430.6
Striped dolphins	95.1	7.5	1885.3	21514.8	38867.0

Table F-49. 2021 annual exposure estimate totals for 3-D WAZ survey (8000 in^3 airgun array, 4 vessels).

Species	Number of Level A exposures			Number of Level B exposures	
	peak SPL	SEL	180 rms SPL	Step fxn	160 rms SPL
Atlantic spotted dolphins	28.4	1.1	7861.1	25280.4	39499.1
Beaked whales	4.0	0.1	2001.4	54098.4	12955.0
Common bottlenose dolphins	119.5	5.1	41279.1	121928.8	202568.4
Bryde's whales	0.0	0.9	26.8	173.5	197.1
Clymene dolphins	44.8	3.2	2668.0	26639.5	48248.8
False killer whales	9.6	0.8	744.0	5605.3	9785.0
Fraser's dolphins	4.2	0.1	962.3	3263.5	5113.4
Killer whales	0.4	0.1	100.0	370.4	474.1
Kogia	1824.5	34.0	1230.4	3813.5	8232.2
Melon-headed whales	20.7	0.6	4541.4	16213.9	27432.3
Pantropical spotted dolphins	265.0	7.5	17151.2	149776.5	233432.8
Pygmy killer whales	7.3	0.7	547.3	4003.3	6603.2
Risso's dolphins	10.4	1.5	562.7	6577.7	11792.8
Rough-toothed dolphins	12.6	1.0	1202.8	7959.4	14110.5
Short-finned pilot whales	5.7	0.4	1099.4	4370.4	8747.7
Sperm whales	7.1	0.2	3487.8	9656.9	19792.6
Spinner dolphins	26.2	0.2	1658.9	20294.1	39876.9
Striped dolphins	18.1	0.8	1128.1	10740.9	18352.7

Table F-50. 2021 annual exposure estimate totals for Coil survey (8000 in^3 airgun array, 4 vessels).

Species	Number of Level A exposures			Number of Level B exposures	
	peak SPL	SEL	180 rms SPL	Step fxn	160 rms SPL
Atlantic spotted dolphins	41.1	1.6	2122.9	6085.2	7990.8
Beaked whales	10.4	0.4	631.7	13560.3	2735.9
Common bottlenose dolphins	224.7	9.0	9800.1	27345.3	31706.3
Bryde's whales	0.1	3.2	6.5	38.7	40.2
Clymene dolphins	76.3	3.8	1277.4	6802.5	9775.5
False killer whales	18.2	0.7	426.9	1838.4	2820.4
Fraser's dolphins	8.3	0.2	280.1	850.7	1055.3
Killer whales	0.8	0.0	37.8	96.7	112.6
Kogia	356.2	96.2	361.5	1003.1	1719.1
Melon-headed whales	39.8	1.0	1330.5	4285.7	5690.4
Pantropical spotted dolphins	509.3	28.7	8039.0	37653.7	49290.4
Pygmy killer whales	13.7	0.5	317.2	1311.5	1938.3
Risso's dolphins	20.4	1.7	317.0	1632.3	2276.1
Rough-toothed dolphins	24.0	1.0	628.9	2571.4	3967.8
Short-finned pilot whales	9.7	0.3	330.1	1195.1	1788.4
Sperm whales	7.0	0.6	982.1	2726.3	4411.0
Spinner dolphins	45.8	2.0	791.6	5003.2	7910.6
Striped dolphins	32.8	1.7	534.2	2713.7	3776.2

Table F-51. 2021 annual exposure estimate totals for 90 in^3 airgun.

Species	Number of Level A exposures			Number of Level B exposures	
	peak SPL	SEL	180 rms SPL	Step fxn	160 rms SPL
Atlantic spotted dolphins	0.0	0.0	0.0	0.0	0.0
Beaked whales	0.0	0.0	0.0	0.0	0.0
Common bottlenose dolphins	0.0	0.0	0.0	0.0	0.0
Bryde's whales	0.0	0.0	0.0	0.0	0.0
Clymene dolphins	0.0	0.0	0.0	0.0	0.0
False killer whales	0.0	0.0	0.0	0.0	0.0
Fraser's dolphins	0.0	0.0	0.0	0.0	0.0
Killer whales	0.0	0.0	0.0	0.0	0.0
Kogia	0.0	0.0	0.0	0.0	0.0
Melon-headed whales	0.0	0.0	0.0	0.0	0.0
Pantropical spotted dolphins	0.0	0.0	0.0	0.0	0.0
Pygmy killer whales	0.0	0.0	0.0	0.0	0.0
Risso's dolphins	0.0	0.0	0.0	0.0	0.0
Rough-toothed dolphins	0.0	0.0	0.0	0.0	0.0
Short-finned pilot whales	0.0	0.0	0.0	0.0	0.0
Sperm whales	0.0	0.0	0.0	0.0	0.0
Spinner dolphins	0.0	0.0	0.0	0.0	0.0
Striped dolphins	0.0	0.0	0.0	0.0	0.0

Table F-52. 2021 annual exposure estimate totals for boomer.

Species	Number of Level A exposures			Number of Level B exposures	
	peak SPL	SEL	180 rms SPL	Step fxn	160 rms SPL
Atlantic spotted dolphins	0.0	0.0	0.0	0.0	0.0
Beaked whales	0.0	0.0	0.0	0.0	0.0
Common bottlenose dolphins	0.0	0.0	0.0	0.0	0.0
Bryde's whales	0.0	0.0	0.0	0.0	0.0
Clymene dolphins	0.0	0.0	0.0	0.0	0.0
False killer whales	0.0	0.0	0.0	0.0	0.0
Fraser's dolphins	0.0	0.0	0.0	0.0	0.0
Killer whales	0.0	0.0	0.0	0.0	0.0
Kogia	0.0	0.0	0.0	0.0	0.0
Melon-headed whales	0.0	0.0	0.0	0.0	0.0
Pantropical spotted dolphins	0.0	0.0	0.0	0.0	0.0
Pygmy killer whales	0.0	0.0	0.0	0.0	0.0
Risso's dolphins	0.0	0.0	0.0	0.0	0.0
Rough-toothed dolphins	0.0	0.0	0.0	0.0	0.0
Short-finned pilot whales	0.0	0.0	0.0	0.0	0.0
Sperm whales	0.0	0.0	0.0	0.0	0.0
Spinner dolphins	0.0	0.0	0.0	0.0	0.0
Striped dolphins	0.0	0.0	0.0	0.0	0.0

Table F-53. 2021 annual exposure estimate totals for side-scan sonar, sub-bottom profiler, and multibeam scanner).

Species	Number of Level A exposures			Number of Level B exposures	
	peak SPL	SEL	180 rms SPL	Step fxn	160 rms SPL
Atlantic spotted dolphins	0.0	0.8	0.9	3.3	1.1
Beaked whales	0.0	0.1	0.1	4.6	0.0
Common bottlenose dolphins	0.0	9.8	12.6	24.7	6.7
Bryde's whales	0.0	0.0	0.0	0.0	0.0
Clymene dolphins	0.0	0.0	0.0	0.0	0.0
False killer whales	0.0	0.0	0.0	0.0	0.0
Fraser's dolphins	0.0	0.0	0.0	0.0	0.0
Killer whales	0.0	0.0	0.0	0.0	0.0
Kogia	0.0	0.0	0.0	0.0	0.0
Melon-headed whales	0.0	0.0	0.0	0.0	0.0
Pantropical spotted dolphins	0.0	0.0	0.0	0.0	0.0
Pygmy killer whales	0.0	0.0	0.0	0.0	0.0
Risso's dolphins	0.0	0.0	0.0	0.0	0.0
Rough-toothed dolphins	0.0	0.0	0.0	0.2	0.1
Short-finned pilot whales	0.0	0.0	0.0	0.0	0.0
Sperm whales	0.0	0.0	0.0	0.1	0.0
Spinner dolphins	0.0	0.0	0.0	0.0	0.0
Striped dolphins	0.0	0.0	0.0	0.0	0.0

F.2.7. 2022

Table F-54. 2022 annual exposure estimate totals for 2-D survey (8000 in^3 airgun array, 1 vessel).

Species	Number of Level A exposures			Number of Level B exposures	
	peak SPL	SEL	180 rms SPL	Step fxn	160 rms SPL
Atlantic spotted dolphins	3.5	0.1	180.6	2520.4	5817.3
Beaked whales	1.9	0.1	185.1	14314.5	3282.3
Common bottlenose dolphins	8.7	0.6	348.9	6389.2	14166.9
Bryde's whales	0.0	0.4	2.4	38.7	46.9
Clymene dolphins	12.1	0.9	299.9	5445.1	10128.0
False killer whales	2.6	0.1	80.9	1286.2	2280.7
Fraser's dolphins	1.2	0.0	98.4	746.2	1238.2
Killer whales	0.1	0.0	11.6	80.7	116.5
Kogia	157.3	12.4	127.2	930.9	2160.5
Melon-headed whales	6.2	0.1	462.2	3796.5	6839.3
Pantropical spotted dolphins	88.9	7.5	2149.3	33554.6	52949.7
Pygmy killer whales	2.0	0.0	61.6	930.2	1538.5
Risso's dolphins	3.3	0.4	87.5	1395.5	2694.7
Rough-toothed dolphins	3.2	0.1	100.9	1678.2	3139.7
Short-finned pilot whales	1.4	0.0	84.5	850.7	1802.3
Sperm whales	1.2	0.1	262.9	1920.0	3895.3
Spinner dolphins	8.5	0.5	220.8	5007.9	11040.3
Striped dolphins	5.5	0.4	136.0	2338.2	4122.9

Table F-55. 2022 annual exposure estimate totals for 3-D NAZ survey (8000 in^3 airgun array, 2 vessels).

Species	Number of Level A exposures			Number of Level B exposures	
	peak SPL	SEL	180 rms SPL	Step fxn	160 rms SPL
Atlantic spotted dolphins	268.1	28.5	36347.7	106098.2	145899.1
Beaked whales	26.0	1.2	2364.2	100180.1	25094.9
Common bottlenose dolphins	1788.4	119.4	207103.8	583275.6	755337.1
Bryde's whales	0.2	7.2	26.1	307.3	369.5
Clymene dolphins	194.7	15.6	3812.4	45827.6	85313.6
False killer whales	55.1	5.4	1267.0	11078.4	19909.7
Fraser's dolphins	25.8	1.7	1071.8	5968.8	9905.8
Killer whales	2.4	0.3	133.9	616.1	897.5
Kogia	1253.3	276.6	1344.1	6978.2	15490.0
Melon-headed whales	124.2	8.7	4916.5	29367.7	52042.6
Pantropical spotted dolphins	1126.0	54.5	24134.2	251504.8	402863.9
Pygmy killer whales	40.8	3.7	871.7	7676.6	13240.0
Risso's dolphins	50.8	7.1	1080.1	11199.1	20695.0
Rough-toothed dolphins	80.7	8.2	3076.6	18851.2	32666.3
Short-finned pilot whales	32.6	3.9	1178.1	8121.9	16564.8
Sperm whales	18.9	0.8	3487.9	17766.7	38593.6
Spinner dolphins	123.5	4.9	2455.8	34951.0	69804.6
Striped dolphins	78.3	4.8	1603.8	18273.8	32084.0

Table F-56. 2022 annual exposure estimate totals for 3-D WAZ survey (8000 in^3 airgun array, 4 vessels).

Species	Number of Level A exposures			Number of Level B exposures	
	peak SPL	SEL	180 rms SPL	Step fxn	160 rms SPL
Atlantic spotted dolphins	12.3	0.7	1586.3	10771.9	21642.0
Beaked whales	3.6	0.0	1924.3	51580.8	12331.2
Common bottlenose dolphins	29.1	0.0	1890.8	28040.3	55364.6
Bryde's whales	0.0	0.8	23.1	151.3	175.3
Clymene dolphins	37.1	0.1	2467.6	24231.2	41628.1
False killer whales	9.3	0.8	700.4	5261.2	8838.1
Fraser's dolphins	3.9	0.0	918.1	3103.3	4653.5
Killer whales	0.4	0.1	101.9	370.3	455.7
Kogia	1819.3	34.1	1222.9	3801.1	8045.4
Melon-headed whales	19.4	0.0	4378.9	15633.9	25568.0
Pantropical spotted dolphins	259.2	0.4	17524.9	150730.2	228438.3
Pygmy killer whales	7.3	0.7	537.4	3835.8	6044.4
Risso's dolphins	9.8	1.1	547.2	6224.9	10803.0
Rough-toothed dolphins	11.3	0.8	868.1	6819.1	12045.1
Short-finned pilot whales	4.2	0.0	835.2	3426.0	6675.2
Sperm whales	7.1	0.0	3059.7	8664.8	17700.0
Spinner dolphins	28.6	0.1	1846.7	22028.4	43407.8
Striped dolphins	16.7	0.0	1115.1	10439.1	17204.3

Table F-57. 2022 annual exposure estimate totals for Coil survey (8000 in^3 airgun array, 4 vessels).

Species	Number of Level A exposures			Number of Level B exposures	
	peak SPL	SEL	180 rms SPL	Step fxn	160 rms SPL
Atlantic spotted dolphins	18.5	0.4	688.1	2748.5	4587.1
Beaked whales	10.3	0.4	602.7	12707.2	2595.1
Common bottlenose dolphins	63.8	5.6	1096.8	6727.3	10286.4
Bryde's whales	0.1	2.9	5.5	33.0	35.8
Clymene dolphins	72.0	3.9	1155.6	5909.5	8420.5
False killer whales	17.6	0.7	404.2	1699.6	2601.6
Fraser's dolphins	8.0	0.2	267.3	789.6	965.7
Killer whales	0.8	0.0	38.5	95.8	110.3
Kogia	355.1	96.8	360.6	985.6	1675.8
Melon-headed whales	39.1	1.0	1283.2	4011.1	5317.2
Pantropical spotted dolphins	524.7	30.8	8142.2	37032.7	48037.0
Pygmy killer whales	13.4	0.5	309.9	1243.0	1811.7
Risso's dolphins	19.8	1.8	297.6	1485.6	2073.0
Rough-toothed dolphins	21.9	0.9	501.5	2197.3	3497.6
Short-finned pilot whales	7.8	0.2	249.3	895.8	1393.4
Sperm whales	6.3	0.5	816.6	2316.8	3770.7
Spinner dolphins	51.4	2.4	876.5	5322.6	8447.0
Striped dolphins	32.8	1.8	520.6	2552.4	3523.8

Table F-58. 2022 annual exposure estimate totals for 90 in^3 airgun.

Species	Number of Level A exposures			Number of Level B exposures	
	peak SPL	SEL	180 rms SPL	Step fxn	160 rms SPL
Atlantic spotted dolphins	0.0	0.0	0.0	0.0	0.0
Beaked whales	0.0	0.0	0.0	0.0	0.0
Common bottlenose dolphins	0.0	0.0	0.0	0.0	0.0
Bryde's whales	0.0	0.0	0.0	0.0	0.0
Clymene dolphins	0.0	0.0	0.0	0.0	0.0
False killer whales	0.0	0.0	0.0	0.0	0.0
Fraser's dolphins	0.0	0.0	0.0	0.0	0.0
Killer whales	0.0	0.0	0.0	0.0	0.0
Kogia	0.0	0.0	0.0	0.0	0.0
Melon-headed whales	0.0	0.0	0.0	0.0	0.0
Pantropical spotted dolphins	0.0	0.0	0.0	0.0	0.0
Pygmy killer whales	0.0	0.0	0.0	0.0	0.0
Risso's dolphins	0.0	0.0	0.0	0.0	0.0
Rough-toothed dolphins	0.0	0.0	0.0	0.0	0.0
Short-finned pilot whales	0.0	0.0	0.0	0.0	0.0
Sperm whales	0.0	0.0	0.0	0.0	0.0
Spinner dolphins	0.0	0.0	0.0	0.0	0.0
Striped dolphins	0.0	0.0	0.0	0.0	0.0

Table F-59. 2022 annual exposure estimate totals for boomer.

Species	Number of Level A exposures			Number of Level B exposures	
	peak SPL	SEL	180 rms SPL	Step fxn	160 rms SPL
Atlantic spotted dolphins	0.0	0.0	0.0	0.0	0.0
Beaked whales	0.0	0.0	0.0	0.0	0.0
Common bottlenose dolphins	0.0	0.0	0.0	0.0	0.0
Bryde's whales	0.0	0.0	0.0	0.0	0.0
Clymene dolphins	0.0	0.0	0.0	0.0	0.0
False killer whales	0.0	0.0	0.0	0.0	0.0
Fraser's dolphins	0.0	0.0	0.0	0.0	0.0
Killer whales	0.0	0.0	0.0	0.0	0.0
Kogia	0.0	0.0	0.0	0.0	0.0
Melon-headed whales	0.0	0.0	0.0	0.0	0.0
Pantropical spotted dolphins	0.0	0.0	0.0	0.0	0.0
Pygmy killer whales	0.0	0.0	0.0	0.0	0.0
Risso's dolphins	0.0	0.0	0.0	0.0	0.0
Rough-toothed dolphins	0.0	0.0	0.0	0.0	0.0
Short-finned pilot whales	0.0	0.0	0.0	0.0	0.0
Sperm whales	0.0	0.0	0.0	0.0	0.0
Spinner dolphins	0.0	0.0	0.0	0.0	0.0
Striped dolphins	0.0	0.0	0.0	0.0	0.0

Table F-60. 2022 annual exposure estimate totals for side-scan sonar, sub-bottom profiler, and multibeam scanner).

Species	Number of Level A exposures			Number of Level B exposures	
	peak SPL	SEL	180 rms SPL	Step fxn	160 rms SPL
Atlantic spotted dolphins	0.0	0.7	0.8	3.0	1.0
Beaked whales	0.0	0.1	0.1	5.0	0.0
Common bottlenose dolphins	0.0	8.7	11.1	22.0	6.0
Bryde's whales	0.0	0.0	0.0	0.0	0.0
Clymene dolphins	0.0	0.0	0.0	0.0	0.0
False killer whales	0.0	0.0	0.0	0.0	0.0
Fraser's dolphins	0.0	0.0	0.0	0.0	0.0
Killer whales	0.0	0.0	0.0	0.0	0.0
Kogia	0.0	0.0	0.0	0.0	0.0
Melon-headed whales	0.0	0.0	0.0	0.0	0.0
Pantropical spotted dolphins	0.0	0.1	0.1	0.0	0.0
Pygmy killer whales	0.0	0.0	0.0	0.0	0.0
Risso's dolphins	0.0	0.0	0.0	0.0	0.0
Rough-toothed dolphins	0.0	0.0	0.0	0.1	0.1
Short-finned pilot whales	0.0	0.0	0.0	0.0	0.0
Sperm whales	0.0	0.0	0.0	0.1	0.0
Spinner dolphins	0.0	0.0	0.0	0.0	0.0
Striped dolphins	0.0	0.0	0.0	0.0	0.0

F.2.8. 2023

Table F-61. 2023 annual exposure estimate totals for 2-D survey (8000 in^3 airgun array, 1 vessel).

Species	Number of Level A exposures			Number of Level B exposures	
	peak SPL	SEL	180 rms SPL	Step fxn	160 rms SPL
Atlantic spotted dolphins	1.2	0.0	60.2	840.1	1939.1
Beaked whales	0.6	0.0	61.7	4771.5	1094.1
Common bottlenose dolphins	2.9	0.2	116.3	2129.7	4722.3
Bryde's whales	0.0	0.1	0.8	12.9	15.6
Clymene dolphins	4.0	0.3	100.0	1815.0	3376.0
False killer whales	0.9	0.0	27.0	428.7	760.2
Fraser's dolphins	0.4	0.0	32.8	248.7	412.7
Killer whales	0.0	0.0	3.9	26.9	38.8
Kogia	52.4	4.1	42.4	310.3	720.2
Melon-headed whales	2.1	0.0	154.1	1265.5	2279.8
Pantropical spotted dolphins	29.6	2.5	716.4	11184.9	17649.9
Pygmy killer whales	0.7	0.0	20.5	310.1	512.8
Risso's dolphins	1.1	0.1	29.2	465.2	898.2
Rough-toothed dolphins	1.1	0.0	33.6	559.4	1046.6
Short-finned pilot whales	0.5	0.0	28.2	283.6	600.8
Sperm whales	0.4	0.0	87.6	640.0	1298.4
Spinner dolphins	2.8	0.2	73.6	1669.3	3680.1
Striped dolphins	1.8	0.1	45.3	779.4	1374.3

Table F-62. 2023 annual exposure estimate totals for 3-D NAZ survey (8000 in^3 airgun array, 2 vessels).

Species	Number of Level A exposures			Number of Level B exposures	
	peak SPL	SEL	180 rms SPL	Step fxn	160 rms SPL
Atlantic spotted dolphins	336.5	30.1	49020.7	136922.4	180782.4
Beaked whales	26.0	1.2	2364.2	100180.1	25095.0
Common bottlenose dolphins	2371.9	81.9	289426.7	797721.2	1011713.9
Bryde's whales	0.2	7.2	26.1	307.2	369.5
Clymene dolphins	194.7	15.6	3812.4	45827.6	85313.6
False killer whales	55.5	5.4	1311.9	11223.3	20077.8
Fraser's dolphins	26.1	1.7	1091.6	6030.3	9983.3
Killer whales	2.4	0.3	134.1	616.8	898.3
Kogia	1253.7	277.0	1345.4	6981.9	15495.1
Melon-headed whales	124.2	8.7	4916.8	29368.5	52043.6
Pantropical spotted dolphins	1126.0	54.5	24137.6	251515.4	402877.4
Pygmy killer whales	40.8	3.7	871.8	7677.0	13240.4
Risso's dolphins	50.8	7.1	1081.8	11203.7	20700.8
Rough-toothed dolphins	85.4	8.4	3649.9	20615.6	34867.5
Short-finned pilot whales	32.6	3.9	1178.1	8121.9	16564.8
Sperm whales	18.9	0.8	3487.9	17766.7	38593.6
Spinner dolphins	123.5	4.9	2455.8	34951.0	69804.6
Striped dolphins	78.3	4.8	1603.9	18273.9	32084.1

Table F-63. 2023 annual exposure estimate totals for 3-D WAZ survey (8000 in^3 airgun array, 4 vessels).

Species	Number of Level A exposures			Number of Level B exposures	
	peak SPL	SEL	180 rms SPL	Step fxn	160 rms SPL
Atlantic spotted dolphins	24.4	0.5	7325.1	21893.7	32486.3
Beaked whales	2.5	0.0	1382.7	37470.7	9039.0
Common bottlenose dolphins	110.7	4.3	40652.8	113336.0	184429.8
Bryde's whales	0.0	0.6	16.2	110.0	128.7
Clymene dolphins	26.7	0.0	1762.0	17613.7	30146.3
False killer whales	6.7	0.6	524.9	3865.6	6471.6
Fraser's dolphins	2.9	0.0	672.9	2266.7	3422.5
Killer whales	0.3	0.0	74.0	270.4	332.6
Kogia	1300.7	24.4	881.0	2736.4	5865.9
Melon-headed whales	14.2	0.0	3159.1	11283.2	18636.5
Pantropical spotted dolphins	187.3	0.0	12613.1	109677.0	165646.7
Pygmy killer whales	5.2	0.5	387.0	2781.7	4383.7
Risso's dolphins	6.9	0.8	388.5	4540.2	7825.6
Rough-toothed dolphins	9.0	0.7	924.5	5679.0	9626.2
Short-finned pilot whales	3.0	0.0	599.0	2464.0	4865.0
Sperm whales	5.3	0.0	2320.8	6465.4	13561.8
Spinner dolphins	20.4	0.0	1300.7	15993.0	31396.5
Striped dolphins	12.0	0.0	798.6	7590.8	12464.1

Table F-64. 2023 annual exposure estimate totals for Coil survey (8000 in^3 airgun array, 4 vessels).

Species	Number of Level A exposures			Number of Level B exposures	
	peak SPL	SEL	180 rms SPL	Step fxn	160 rms SPL
Atlantic spotted dolphins	35.4	1.4	1896.8	5165.2	6572.0
Beaked whales	7.3	0.3	434.9	9280.7	1906.2
Common bottlenose dolphins	201.4	7.7	9432.6	25112.5	28342.2
Bryde's whales	0.1	2.0	3.9	24.2	26.6
Clymene dolphins	51.2	2.7	826.9	4352.2	6198.3
False killer whales	12.8	0.5	300.6	1256.5	1921.9
Fraser's dolphins	5.9	0.1	194.2	580.9	719.0
Killer whales	0.6	0.0	28.0	70.2	81.2
Kogia	254.2	68.2	257.3	714.3	1240.4
Melon-headed whales	28.2	0.7	918.2	2924.6	3932.6
Pantropical spotted dolphins	377.0	21.7	5867.1	27203.2	35296.1
Pygmy killer whales	9.7	0.4	224.9	908.0	1327.8
Risso's dolphins	14.2	1.3	210.6	1099.7	1530.4
Rough-toothed dolphins	17.0	0.8	468.4	1808.7	2761.5
Short-finned pilot whales	5.6	0.2	176.7	653.0	1032.0
Sperm whales	4.9	0.4	634.4	1778.7	2985.7
Spinner dolphins	35.9	1.6	619.8	3932.8	6229.5
Striped dolphins	23.5	1.3	373.5	1878.1	2592.3

Table F-65. 2023 annual exposure estimate totals for 90 in^3 airgun.

Species	Number of Level A exposures			Number of Level B exposures	
	peak SPL	SEL	180 rms SPL	Step fxn	160 rms SPL
Atlantic spotted dolphins	0.0	0.0	0.0	0.0	0.0
Beaked whales	0.0	0.0	0.0	0.0	0.0
Common bottlenose dolphins	0.0	0.0	0.0	0.0	0.0
Bryde's whales	0.0	0.0	0.0	0.0	0.0
Clymene dolphins	0.0	0.0	0.0	0.0	0.0
False killer whales	0.0	0.0	0.0	0.0	0.0
Fraser's dolphins	0.0	0.0	0.0	0.0	0.0
Killer whales	0.0	0.0	0.0	0.0	0.0
Kogia	0.0	0.0	0.0	0.0	0.0
Melon-headed whales	0.0	0.0	0.0	0.0	0.0
Pantropical spotted dolphins	0.0	0.0	0.0	0.0	0.0
Pygmy killer whales	0.0	0.0	0.0	0.0	0.0
Risso's dolphins	0.0	0.0	0.0	0.0	0.0
Rough-toothed dolphins	0.0	0.0	0.0	0.0	0.0
Short-finned pilot whales	0.0	0.0	0.0	0.0	0.0
Sperm whales	0.0	0.0	0.0	0.0	0.0
Spinner dolphins	0.0	0.0	0.0	0.0	0.0
Striped dolphins	0.0	0.0	0.0	0.0	0.0

Table F-66. 2023 annual exposure estimate totals for boomer.

Species	Number of Level A exposures			Number of Level B exposures	
	peak SPL	SEL	180 rms SPL	Step fxn	160 rms SPL
Atlantic spotted dolphins	0.0	0.0	0.0	0.0	0.0
Beaked whales	0.0	0.0	0.0	0.0	0.0
Common bottlenose dolphins	0.0	0.0	0.0	0.0	0.0
Bryde’s whales	0.0	0.0	0.0	0.0	0.0
Clymene dolphins	0.0	0.0	0.0	0.0	0.0
False killer whales	0.0	0.0	0.0	0.0	0.0
Fraser’s dolphins	0.0	0.0	0.0	0.0	0.0
Killer whales	0.0	0.0	0.0	0.0	0.0
Kogia	0.0	0.0	0.0	0.0	0.0
Melon-headed whales	0.0	0.0	0.0	0.0	0.0
Pantropical spotted dolphins	0.0	0.0	0.0	0.0	0.0
Pygmy killer whales	0.0	0.0	0.0	0.0	0.0
Risso’s dolphins	0.0	0.0	0.0	0.0	0.0
Rough-toothed dolphins	0.0	0.0	0.0	0.0	0.0
Short-finned pilot whales	0.0	0.0	0.0	0.0	0.0
Sperm whales	0.0	0.0	0.0	0.0	0.0
Spinner dolphins	0.0	0.0	0.0	0.0	0.0
Striped dolphins	0.0	0.0	0.0	0.0	0.0

Table F-67. 2023 annual exposure estimate totals for side-scan sonar, sub-bottom profiler, and multibeam scanner).

Species	Number of Level A exposures			Number of Level B exposures	
	peak SPL	SEL	180 rms SPL	Step fxn	160 rms SPL
Atlantic spotted dolphins	0.0	0.7	0.8	3.0	1.0
Beaked whales	0.0	0.1	0.1	5.3	0.0
Common bottlenose dolphins	0.0	8.7	11.1	22.0	6.0
Bryde's whales	0.0	0.0	0.0	0.0	0.0
Clymene dolphins	0.0	0.0	0.0	0.0	0.0
False killer whales	0.0	0.0	0.0	0.0	0.0
Fraser's dolphins	0.0	0.0	0.0	0.0	0.0
Killer whales	0.0	0.0	0.0	0.0	0.0
Kogia	0.0	0.0	0.0	0.0	0.0
Melon-headed whales	0.0	0.0	0.0	0.0	0.0
Pantropical spotted dolphins	0.0	0.1	0.1	0.1	0.0
Pygmy killer whales	0.0	0.0	0.0	0.0	0.0
Risso's dolphins	0.0	0.0	0.0	0.0	0.0
Rough-toothed dolphins	0.0	0.0	0.0	0.1	0.1
Short-finned pilot whales	0.0	0.0	0.0	0.0	0.0
Sperm whales	0.0	0.0	0.0	0.1	0.0
Spinner dolphins	0.0	0.0	0.0	0.0	0.0
Striped dolphins	0.0	0.0	0.0	0.0	0.0

F.2.9. 2024

Table F-68. 2024 annual exposure estimate totals for 2-D survey (8000 in^3 airgun array, 1 vessel).

Species	Number of Level A exposures			Number of Level B exposures	
	peak SPL	SEL	180 rms SPL	Step fxn	160 rms SPL
Atlantic spotted dolphins	0.0	0.0	0.0	0.0	0.0
Beaked whales	0.0	0.0	0.0	0.0	0.0
Common bottlenose dolphins	0.0	0.0	0.0	0.0	0.0
Bryde's whales	0.0	0.0	0.0	0.0	0.0
Clymene dolphins	0.0	0.0	0.0	0.0	0.0
False killer whales	0.0	0.0	0.0	0.0	0.0
Fraser's dolphins	0.0	0.0	0.0	0.0	0.0
Killer whales	0.0	0.0	0.0	0.0	0.0
Kogia	0.0	0.0	0.0	0.0	0.0
Melon-headed whales	0.0	0.0	0.0	0.0	0.0
Pantropical spotted dolphins	0.0	0.0	0.0	0.0	0.0
Pygmy killer whales	0.0	0.0	0.0	0.0	0.0
Risso's dolphins	0.0	0.0	0.0	0.0	0.0
Rough-toothed dolphins	0.0	0.0	0.0	0.0	0.0
Short-finned pilot whales	0.0	0.0	0.0	0.0	0.0
Sperm whales	0.0	0.0	0.0	0.0	0.0
Spinner dolphins	0.0	0.0	0.0	0.0	0.0
Striped dolphins	0.0	0.0	0.0	0.0	0.0

Table F-69. 2024 annual exposure estimate totals for 3-D NAZ survey (8000 in^3 airgun array, 2 vessels).

Species	Number of Level A exposures			Number of Level B exposures	
	peak SPL	SEL	180 rms SPL	Step fxn	160 rms SPL
Atlantic spotted dolphins	236.1	20.9	33109.3	95093.0	128778.3
Beaked whales	23.0	1.2	2026.6	86451.3	21614.1
Common bottlenose dolphins	1622.5	60.1	193716.6	541343.9	694790.8
Bryde's whales	0.2	6.4	23.0	268.6	321.4
Clymene dolphins	171.5	14.9	3313.3	39792.5	74885.7
False killer whales	47.7	5.0	1103.2	9583.5	17325.0
Fraser's dolphins	22.3	1.5	925.9	5163.3	8601.5
Killer whales	2.1	0.2	114.0	525.6	770.7
Kogia	1079.3	238.4	1151.9	5991.1	13285.1
Melon-headed whales	106.9	7.8	4228.9	25319.1	44988.0
Pantropical spotted dolphins	967.6	50.1	20600.8	214510.8	346237.1
Pygmy killer whales	35.2	3.4	750.4	6606.7	11486.2
Risso's dolphins	44.3	6.2	933.0	9635.2	17965.1
Rough-toothed dolphins	70.5	7.4	2723.1	16501.8	28596.1
Short-finned pilot whales	29.0	3.7	1046.7	7224.5	14753.3
Sperm whales	16.2	0.8	3010.7	15290.3	32914.3
Spinner dolphins	104.9	4.2	2080.4	29364.5	58821.9
Striped dolphins	67.9	4.5	1378.6	15686.9	27788.5

Table F-70. 2024 annual exposure estimate totals for 3-D WAZ survey (8000 in^3 airgun array, 4 vessels).

Species	Number of Level A exposures			Number of Level B exposures	
	peak SPL	SEL	180 rms SPL	Step fxn	160 rms SPL
Atlantic spotted dolphins	13.8	0.7	1695.3	11719.6	23546.6
Beaked whales	3.8	0.0	2074.1	56206.0	13558.4
Common bottlenose dolphins	31.1	0.0	1989.5	30571.2	59895.0
Bryde's whales	0.0	0.8	24.3	165.0	193.0
Clymene dolphins	40.0	0.0	2643.0	26420.6	45219.4
False killer whales	10.0	0.8	754.2	5717.3	9609.3
Fraser's dolphins	4.2	0.0	995.6	3364.5	5088.1
Killer whales	0.4	0.1	110.8	405.1	498.3
Kogia	1950.4	36.6	1320.6	4102.6	8796.0
Melon-headed whales	21.2	0.0	4738.5	16924.4	27954.2
Pantropical spotted dolphins	280.9	0.0	18917.1	164509.3	248462.5
Pygmy killer whales	7.9	0.7	580.5	4172.4	6575.2
Risso's dolphins	10.4	1.2	581.6	6807.6	11735.1
Rough-toothed dolphins	12.1	0.9	932.4	7404.4	13091.1
Short-finned pilot whales	4.6	0.0	898.5	3695.9	7297.5
Sperm whales	8.0	0.0	3481.2	9698.1	20342.7
Spinner dolphins	30.6	0.0	1951.1	23989.5	47094.8
Striped dolphins	18.0	0.0	1197.9	11386.1	18696.1

Table F-71. 2024 annual exposure estimate totals for Coil survey (8000 in^3 airgun array, 4 vessels).

Species	Number of Level A exposures			Number of Level B exposures	
	peak SPL	SEL	180 rms SPL	Step fxn	160 rms SPL
Atlantic spotted dolphins	19.4	0.3	737.0	3041.0	5110.1
Beaked whales	10.9	0.5	652.4	13921.0	2859.3
Common bottlenose dolphins	68.0	6.1	1145.4	7466.0	11361.6
Bryde's whales	0.1	3.0	5.8	36.3	39.9
Clymene dolphins	76.8	4.1	1240.3	6528.2	9297.4
False killer whales	19.0	0.8	439.4	1862.6	2861.4
Fraser's dolphins	8.7	0.2	287.8	863.6	1070.5
Killer whales	0.9	0.0	41.9	105.2	121.7
Kogia	381.1	102.2	385.8	1071.0	1860.2
Melon-headed whales	42.3	1.0	1377.3	4386.9	5898.9
Pantropical spotted dolphins	565.5	32.6	8800.1	40803.5	52942.7
Pygmy killer whales	14.5	0.6	337.3	1361.9	1991.7
Risso's dolphins	21.3	1.9	315.6	1648.9	2295.0
Rough-toothed dolphins	23.7	1.0	544.5	2408.3	3848.4
Short-finned pilot whales	8.4	0.2	265.0	979.6	1548.0
Sperm whales	7.4	0.6	951.6	2668.1	4478.6
Spinner dolphins	53.9	2.3	929.8	5899.2	9344.3
Striped dolphins	35.2	1.9	560.3	2817.1	3888.4

Table F-72. 2024 annual exposure estimate totals for 90 in^3 airgun.

Species	Number of Level A exposures			Number of Level B exposures	
	peak SPL	SEL	180 rms SPL	Step fxn	160 rms SPL
Atlantic spotted dolphins	0.0	0.0	0.0	0.0	0.0
Beaked whales	0.0	0.0	0.0	0.0	0.0
Common bottlenose dolphins	0.0	0.0	0.0	0.0	0.0
Bryde's whales	0.0	0.0	0.0	0.0	0.0
Clymene dolphins	0.0	0.0	0.0	0.0	0.0
False killer whales	0.0	0.0	0.0	0.0	0.0
Fraser's dolphins	0.0	0.0	0.0	0.0	0.0
Killer whales	0.0	0.0	0.0	0.0	0.0
Kogia	0.0	0.0	0.0	0.0	0.0
Melon-headed whales	0.0	0.0	0.0	0.0	0.0
Pantropical spotted dolphins	0.0	0.0	0.0	0.0	0.0
Pygmy killer whales	0.0	0.0	0.0	0.0	0.0
Risso's dolphins	0.0	0.0	0.0	0.0	0.0
Rough-toothed dolphins	0.0	0.0	0.0	0.0	0.0
Short-finned pilot whales	0.0	0.0	0.0	0.0	0.0
Sperm whales	0.0	0.0	0.0	0.0	0.0
Spinner dolphins	0.0	0.0	0.0	0.0	0.0
Striped dolphins	0.0	0.0	0.0	0.0	0.0

Table F-73. 2024 annual exposure estimate totals for boomer.

Species	Number of Level A exposures			Number of Level B exposures	
	peak SPL	SEL	180 rms SPL	Step fxn	160 rms SPL
Atlantic spotted dolphins	0.0	0.0	0.0	0.0	0.0
Beaked whales	0.0	0.0	0.0	0.0	0.0
Common bottlenose dolphins	0.0	0.0	0.0	0.0	0.0
Bryde's whales	0.0	0.0	0.0	0.0	0.0
Clymene dolphins	0.0	0.0	0.0	0.0	0.0
False killer whales	0.0	0.0	0.0	0.0	0.0
Fraser's dolphins	0.0	0.0	0.0	0.0	0.0
Killer whales	0.0	0.0	0.0	0.0	0.0
Kogia	0.0	0.0	0.0	0.0	0.0
Melon-headed whales	0.0	0.0	0.0	0.0	0.0
Pantropical spotted dolphins	0.0	0.0	0.0	0.0	0.0
Pygmy killer whales	0.0	0.0	0.0	0.0	0.0
Risso's dolphins	0.0	0.0	0.0	0.0	0.0
Rough-toothed dolphins	0.0	0.0	0.0	0.0	0.0
Short-finned pilot whales	0.0	0.0	0.0	0.0	0.0
Sperm whales	0.0	0.0	0.0	0.0	0.0
Spinner dolphins	0.0	0.0	0.0	0.0	0.0
Striped dolphins	0.0	0.0	0.0	0.0	0.0

Table F-74. 2024 annual exposure estimate totals for side-scan sonar, sub-bottom profiler, and multibeam scanner).

Species	Number of Level A exposures			Number of Level B exposures	
	peak SPL	SEL	180 rms SPL	Step fxn	160 rms SPL
Atlantic spotted dolphins	0.0	0.7	0.8	3.0	1.0
Beaked whales	0.0	0.1	0.1	5.3	0.0
Common bottlenose dolphins	0.0	8.7	11.1	22.0	6.0
Bryde's whales	0.0	0.0	0.0	0.0	0.0
Clymene dolphins	0.0	0.0	0.0	0.0	0.0
False killer whales	0.0	0.0	0.0	0.0	0.0
Fraser's dolphins	0.0	0.0	0.0	0.0	0.0
Killer whales	0.0	0.0	0.0	0.0	0.0
Kogia	0.0	0.0	0.0	0.0	0.0
Melon-headed whales	0.0	0.0	0.0	0.0	0.0
Pantropical spotted dolphins	0.0	0.1	0.1	0.1	0.0
Pygmy killer whales	0.0	0.0	0.0	0.0	0.0
Risso's dolphins	0.0	0.0	0.0	0.0	0.0
Rough-toothed dolphins	0.0	0.0	0.0	0.1	0.1
Short-finned pilot whales	0.0	0.0	0.0	0.0	0.0
Sperm whales	0.0	0.0	0.0	0.1	0.0
Spinner dolphins	0.0	0.0	0.0	0.0	0.0
Striped dolphins	0.0	0.0	0.0	0.0	0.0

F.2.10. 2025

Table F-75. 2025 annual exposure estimate totals for 2-D survey (8000 in^3 airgun array, 1 vessel).

Species	Number of Level A exposures			Number of Level B exposures	
	peak SPL	SEL	180 rms SPL	Step fxn	160 rms SPL
Atlantic spotted dolphins	0.3	0.0	16.4	197.8	468.6
Beaked whales	0.2	0.0	15.3	1120.5	250.2
Common bottlenose dolphins	0.8	0.1	25.1	480.6	1199.5
Bryde's whales	0.0	0.0	0.2	3.0	3.6
Clymene dolphins	1.0	0.1	24.3	413.7	831.6
False killer whales	0.2	0.0	6.8	100.8	185.6
Fraser's dolphins	0.1	0.0	8.2	59.9	95.5
Killer whales	0.0	0.0	0.9	6.2	9.1
Kogia	13.4	1.1	11.0	75.1	166.8
Melon-headed whales	0.6	0.0	39.4	306.8	527.8
Pantropical spotted dolphins	7.1	0.6	170.9	2556.1	4310.2
Pygmy killer whales	0.1	0.0	5.1	72.7	124.7
Risso's dolphins	0.3	0.0	7.5	105.0	220.9
Rough-toothed dolphins	0.2	0.0	8.6	131.8	256.2
Short-finned pilot whales	0.1	0.0	7.6	69.8	139.2
Sperm whales	0.1	0.0	16.6	120.7	170.1
Spinner dolphins	0.7	0.1	18.5	379.3	913.4
Striped dolphins	0.4	0.0	10.9	177.8	337.6

Table F-76. 2025 annual exposure estimate totals for 3-D NAZ survey (8000 in^3 airgun array, 2 vessels).

Species	Number of Level A exposures			Number of Level B exposures	
	peak SPL	SEL	180 rms SPL	Step fxn	160 rms SPL
Atlantic spotted dolphins	351.8	37.2	51716.5	142385.1	186194.2
Beaked whales	23.0	1.2	2026.6	86451.4	21614.1
Common bottlenose dolphins	2489.5	137.4	301838.7	825426.1	1043905.6
Bryde's whales	0.2	6.4	23.0	268.6	321.4
Clymene dolphins	171.5	14.9	3313.3	39792.5	74885.7
False killer whales	48.2	5.0	1158.6	9756.0	17531.3
Fraser's dolphins	22.5	1.5	949.3	5236.5	8695.8
Killer whales	2.1	0.2	114.4	526.7	772.1
Kogia	1079.7	238.9	1153.3	5995.0	13290.8
Melon-headed whales	106.9	7.8	4229.2	25320.0	44989.1
Pantropical spotted dolphins	967.7	50.1	20604.6	214522.5	346252.3
Pygmy killer whales	35.2	3.4	750.6	6607.1	11486.8
Risso's dolphins	44.3	6.2	935.0	9640.5	17971.8
Rough-toothed dolphins	77.4	8.2	3609.2	19096.1	31941.8
Short-finned pilot whales	29.0	3.7	1046.8	7224.6	14753.3
Sperm whales	16.2	0.8	3010.7	15290.3	32914.3
Spinner dolphins	104.9	4.2	2080.4	29364.5	58821.9
Striped dolphins	67.9	4.5	1378.6	15687.0	27788.7

Table F-77. 2025 annual exposure estimate totals for 3-D WAZ survey (8000 in^3 airgun array, 4 vessels).

Species	Number of Level A exposures			Number of Level B exposures	
	peak SPL	SEL	180 rms SPL	Step fxn	160 rms SPL
Atlantic spotted dolphins	26.7	0.6	7607.6	23846.9	36410.8
Beaked whales	3.2	0.0	1728.4	46838.4	11298.7
Common bottlenose dolphins	115.9	4.3	40984.4	118431.2	194412.3
Bryde's whales	0.0	0.7	20.3	137.5	160.9
Clymene dolphins	33.4	0.0	2202.5	22017.2	37682.9
False killer whales	8.4	0.7	650.6	4818.5	8073.2
Fraser's dolphins	3.6	0.0	838.8	2827.5	4270.5
Killer whales	0.4	0.1	92.5	337.9	415.6
Kogia	1625.7	30.5	1101.1	3420.2	7331.9
Melon-headed whales	17.7	0.0	3948.8	14104.0	23295.6
Pantropical spotted dolphins	234.1	0.0	15765.9	137095.2	207057.2
Pygmy killer whales	6.5	0.6	483.8	3477.1	5479.5
Risso's dolphins	8.7	1.0	485.5	5674.8	9781.5
Rough-toothed dolphins	11.0	0.8	1079.9	6913.0	11808.0
Short-finned pilot whales	3.8	0.0	748.8	3080.0	6081.3
Sperm whales	6.7	0.0	2901.0	8081.8	16952.3
Spinner dolphins	25.5	0.0	1625.9	19991.3	39245.7
Striped dolphins	15.0	0.0	998.2	9488.5	15580.1

Table F-78. 2025 annual exposure estimate totals for Coil survey (8000 in^3 airgun array, 4 vessels).

Species	Number of Level A exposures			Number of Level B exposures	
	peak SPL	SEL	180 rms SPL	Step fxn	160 rms SPL
Atlantic spotted dolphins	38.7	1.4	2019.7	5672.1	7423.7
Beaked whales	9.1	0.4	543.7	11600.8	2382.8
Common bottlenose dolphins	212.8	8.8	9623.5	26356.8	30235.8
Bryde's whales	0.1	2.5	4.8	30.2	33.2
Clymene dolphins	64.0	3.4	1033.6	5440.2	7747.8
False killer whales	15.9	0.7	373.8	1566.9	2398.8
Fraser's dolphins	7.3	0.2	242.1	724.9	897.4
Killer whales	0.8	0.0	35.0	87.7	101.5
Kogia	317.7	85.3	321.6	892.8	1550.5
Melon-headed whales	35.3	0.8	1147.7	3655.8	4915.8
Pantropical spotted dolphins	471.3	27.2	7333.7	34003.8	44119.9
Pygmy killer whales	12.1	0.5	281.1	1135.0	1659.7
Risso's dolphins	17.8	1.6	263.2	1374.5	1912.9
Rough-toothed dolphins	21.0	0.9	559.1	2210.0	3402.9
Short-finned pilot whales	7.0	0.2	220.9	816.3	1290.0
Sperm whales	6.1	0.5	793.0	2223.4	3732.1
Spinner dolphins	44.9	2.0	774.8	4916.0	7786.9
Striped dolphins	29.3	1.6	466.9	2347.6	3240.4

Table F-79. 2025 annual exposure estimate totals for 90 in^3 airgun.

Species	Number of Level A exposures			Number of Level B exposures	
	peak SPL	SEL	180 rms SPL	Step fxn	160 rms SPL
Atlantic spotted dolphins	0.0	0.0	0.0	0.0	0.0
Beaked whales	0.0	0.0	0.0	0.0	0.0
Common bottlenose dolphins	0.0	0.0	0.0	0.0	0.0
Bryde's whales	0.0	0.0	0.0	0.0	0.0
Clymene dolphins	0.0	0.0	0.0	0.0	0.0
False killer whales	0.0	0.0	0.0	0.0	0.0
Fraser's dolphins	0.0	0.0	0.0	0.0	0.0
Killer whales	0.0	0.0	0.0	0.0	0.0
Kogia	0.0	0.0	0.0	0.0	0.0
Melon-headed whales	0.0	0.0	0.0	0.0	0.0
Pantropical spotted dolphins	0.0	0.0	0.0	0.0	0.0
Pygmy killer whales	0.0	0.0	0.0	0.0	0.0
Risso's dolphins	0.0	0.0	0.0	0.0	0.0
Rough-toothed dolphins	0.0	0.0	0.0	0.0	0.0
Short-finned pilot whales	0.0	0.0	0.0	0.0	0.0
Sperm whales	0.0	0.0	0.0	0.0	0.0
Spinner dolphins	0.0	0.0	0.0	0.0	0.0
Striped dolphins	0.0	0.0	0.0	0.0	0.0

Table F-80. 2025 annual exposure estimate totals for boomer.

Species	Number of Level A exposures			Number of Level B exposures	
	peak SPL	SEL	180 rms SPL	Step fxn	160 rms SPL
Atlantic spotted dolphins	0.0	0.0	0.0	0.0	0.0
Beaked whales	0.0	0.0	0.0	0.0	0.0
Common bottlenose dolphins	0.0	0.0	0.0	0.0	0.0
Bryde's whales	0.0	0.0	0.0	0.0	0.0
Clymene dolphins	0.0	0.0	0.0	0.0	0.0
False killer whales	0.0	0.0	0.0	0.0	0.0
Fraser's dolphins	0.0	0.0	0.0	0.0	0.0
Killer whales	0.0	0.0	0.0	0.0	0.0
Kogia	0.0	0.0	0.0	0.0	0.0
Melon-headed whales	0.0	0.0	0.0	0.0	0.0
Pantropical spotted dolphins	0.0	0.0	0.0	0.0	0.0
Pygmy killer whales	0.0	0.0	0.0	0.0	0.0
Risso's dolphins	0.0	0.0	0.0	0.0	0.0
Rough-toothed dolphins	0.0	0.0	0.0	0.0	0.0
Short-finned pilot whales	0.0	0.0	0.0	0.0	0.0
Sperm whales	0.0	0.0	0.0	0.0	0.0
Spinner dolphins	0.0	0.0	0.0	0.0	0.0
Striped dolphins	0.0	0.0	0.0	0.0	0.0

Table F-81. 2025 annual exposure estimate totals for side-scan sonar, sub-bottom profiler, and multibeam scanner).

Species	Number of Level A exposures			Number of Level B exposures	
	peak SPL	SEL	180 rms SPL	Step fxn	160 rms SPL
Atlantic spotted dolphins	0.0	0.6	0.7	2.4	0.8
Beaked whales	0.0	0.1	0.1	5.6	0.0
Common bottlenose dolphins	0.0	7.0	9.0	17.9	5.0
Bryde's whales	0.0	0.0	0.0	0.0	0.0
Clymene dolphins	0.0	0.0	0.0	0.0	0.0
False killer whales	0.0	0.0	0.0	0.0	0.0
Fraser's dolphins	0.0	0.0	0.0	0.0	0.0
Killer whales	0.0	0.0	0.0	0.0	0.0
Kogia	0.0	0.0	0.0	0.0	0.0
Melon-headed whales	0.0	0.0	0.0	0.0	0.0
Pantropical spotted dolphins	0.0	0.1	0.1	0.1	0.0
Pygmy killer whales	0.0	0.0	0.0	0.0	0.0
Risso's dolphins	0.0	0.0	0.0	0.0	0.0
Rough-toothed dolphins	0.0	0.0	0.0	0.1	0.0
Short-finned pilot whales	0.0	0.0	0.0	0.0	0.0
Sperm whales	0.0	0.0	0.0	0.1	0.0
Spinner dolphins	0.0	0.0	0.0	0.0	0.0
Striped dolphins	0.0	0.0	0.0	0.0	0.0